ISSN 1018-5593

Commission of the European Communities

technical steel research

Practical design tools for unprotected steel columns submitted to ISO-Fire — Refao III

Report

EUR 14348 EN

Commission of the European Communities

technical steel research

Practical design tools for unprotected steel columns submitted to ISO-Fire — Refao III

Arbed-Recherches
66, rue de Luxembourg
L-4221 Esch/Alzette

Contract No 7210-SA/505 (1.7.1986–31.12.1989)

Final report

Directorate-General
Science, Research and Development

1993

EUR 14348 EN

Published by the
COMMISSION OF THE EUROPEAN COMMUNITIES

Directorate-General XIII
Information Technologies and Industries, and Telecommunications

L-2920 Luxembourg

LEGAL NOTICE

Neither the Commission of the European Communities nor any person acting on behalf of the Commission is responsible for the use which might be made of the following information

Cataloguing data can be found at the end of this publication

Luxembourg: Office for Official Publications of the European Communities, 1993

ISBN 92-826-4938-5

Printed in Luxembourg

C.E.C. Agreement N° 7210-SA/505

PRACTICAL DESIGN TOOLS FOR UNPROTECTED STEEL COLUMNS SUBMITTED TO ISO-FIRE

REFAO - III

Period from 01.07.1986 to 31.12.1989

FINAL REPORT

Parts I - II - II

RPS Report N° 11/91

ARBED-Recherches
66, rue de Luxembourg

L - 4221 ESCH/ALZETTE

C.E.C. Agreement N° 7210-SA/505

PRACTICAL DESIGN TOOLS FOR UNPROTECTED STEEL COLUMNS SUBMITTED TO ISO-FIRE

REFAO - III

Period from 01.07.1986 to 31.12.1989

FINAL REPORT

RPS Report N° 11/91

DEPARTMENT MANAGER
J.B. SCHLEICH
Ingénieur Civil des Constructions
Ingénieur principal

PROJECT MANAGER
J. MATHIEU
Ingénieur Civil des Constructions
P. CHANTRAIN
Ingénieur Civil des Constructions
L.-G. CAJOT
Ingénieur Civil des Constructions

Service Recherches et
Promotion technique
Structures (RPS)
ARBED-Recherches
66, rue de Luxembourg
L-4002 ESCH/ALZETTE
LUXEMBOURG

05.06.1991

CONFIDENTIAL

TITLE OF RESEARCH:	*Practical design tools for unprotected columns submitted to ISO-Fire*
AGREEMENT:	*N° 7210-SA/505*
EXECUTIVE COMMITTEE:	*F 8*
COMMENCEMENT OF RESEARCH:	*01.07.1986*
SCHEDULED COMPLETION DATE:	*31.12.1988*
BENEFICIARY:	*ARBED-Luxembourg*

ACKNOWLEDGEMENTS

This research consisting in the setting up of tables for the design of thick flanged steel columns submitted to ISO-fire exposure with any fire protection has been performed by ARBED S.A. during the years 1986 to 1988 and sponsored by C.E.C., the Commission of the European Community (C.E.C. Agreement N° 7210-SA/505).

We want to acknowledge first of all the important financial support from the COMMISSION OF THE EUROPEAN COMMUNITY, as well as the moral support given this research by all the members of the C.E.C. EXECUTIVE COMMITTEE F8 "LIGHT WEIGHT STRUCTURES".

Special thanks are due to the collaborators of Professor Dr.Ir. R. MINNE, Director of the Fire Laboratory of Gent University (Belgium), as well as to the collaborators of Professor Dr.Ir. K. KORDINA, Director of the Fire Laboratory of Braunschweig University (Federal Republic of Germany). The six full scale fire tests on steel columns could all be executed successfully, thanks to the knowledge and the experience of the technical staff of these two laboratories.

We wish to record our appreciation of the efforts and cooperation of the specialists of Professor Dr.Ir. R. BAUS, Director of the Department for Bridges and Structural Engineering of Liège University (Belgium), and especially of Dr. Ing. J-M. FRANSSEN, for the improvement of the computer code CEFICOSS.

Thanks are finally due to all, who by any means may have contributed to this research programme, as for instance people of company GST in Essen (Germany), who performed the transient state beam tests described in Part III.

"Practical design tools for unprotected steel columns submitted to ISO-fire"

Agreement N° 7210 - SA/505 C.E.C. - ARBED

SUMMARY

The main parameters to be considered in this research programme, i.e. geometrical factors (shapes, buckling lengths), steel qualities and coefficients governing the heat exchanges are presented first.

The temperature dependent stress-strain relationships of steel as initially existing in the program CEFICOSS have been tested by simulation of bending tests described in the litterature. It has shown a necessity to improve these laws when pure steel elements have to be calculated.

New improved stress-strain relationships of steel have been carried out and calibrated thanks to transient state beam tests performed on small simply supported steel beams, subjected to a concentrated constant load, and submitted to a controlled temperature increase. These new laws have been established as well for commonly used construction steels as for high strength steel FeE 460.

The validity of these improved relationships has been next verified by simulating very well six full scale fire tests performed on unprotected steel columns in the laboratories of Braunschweig and Gent.

The possibility to take into account a distribution of residual stresses has been introduced in CEFICOSS. The simulation of the six column tests showed that residual stresses have a quite small influence of the fire resistance time of columns. It has been decided, however, to consider systematically a distribution of residual stresses in the calculations.

Practical design tools have been finally carried out and are proposed in form of tables as well as diagrams.

"Outils pratiques de dimensionnement pour poutrelles-colonnes en acier non protégé soumises à l'incendie".

Contrat N° 7210 - SA/505 C.C.E. - ARBED

RESUME

Dans une première phase sont définis les paramètres essentiels à introduire dans cette recherche, tels que les facteurs géométriques (sections, longueurs) et mécaniques (qualités d'acier), ainsi que les coefficients relatifs aux échanges thermiques par radiation et convection. Les lois de comportement thermomécanique de l'acier à haute température existant initialement dans le programme CEFICOSS ont été éprouvées par des simulations d'essais décrits dans la littérature, ce qui a montré la nécessité de les affiner dans le cas où des éléments purement métalliques doivent être simulés.

Des tests de flexion sur des petites poutres métalliques soumises à une charge constante et à une élévation de température (uniforme) régulière à vitesse contrôlée, ont permis de calibrer de nouvelles lois d'évolution des propriétés métalliques de l'acier en fonction de la température, aussi bien pour les aciers courants de construction que pour l'acier FeE 460 à haute limite élastique.

La validité de ces nouvelles lois a pu être ensuite vérifiée grâce à la simulation de six essais au feu en grandeur réelle réalisés sur des colonnes nues à Braunschweig et à Gand, et ensuite parfaitement simulés par CEFICOSS.

Ensuite, la possibilité de prendre en compte une répartition de contraintes résiduelles a été introduite dans CEFICOSS. Les simulations des six tests ont démontré que ces contraintes résiduelles n'ont pas une très grande importance sur le temps de ruine final, mais il a été néanmoins décidé de les prendre en compte dans tous les calculs.

Enfin, des outils pratiques de dimensionnement ont été établis par calcul et sont proposés sous forme de diagrammes aussi bien que de tables.

Praktische Bemessungshilfen für die Interaktion von Normalkräften (N) und Biegemomenten (M) für Stahl-Beton Verbundelemente unter Feuerbeanspruchung (ISO - Kurve)

Vertrag N° 7210-SA/505 KEG-ARBED

ZUSAMMENFASSUNG

Die erste Phase dieser Forschungsarbeit behandelt die Bestimmung der wesentlichen einzugebenden Parameter. Diese Parameter bestehen aus geometrischen Faktoren (Querschnitt, Länge) und mechanischen Faktoren (Stahlgüte), sowie aus den relativen thermischen Austauschkoeffizienten verursacht durch die Wärmeausstrahlung und Konvektion.

Die thermomechanischen Gesetze von Stahl bei hoher Temperatur, welche anfänglich im Programm CEFICOSS enthalten waren, wurden durch Simulationsversuche gemäss Beschreibung in Literatur überprüft. Diese ergaben die Notwendigkeit die Gesetze zu verfeinern im Falle der Simulation von ungeschützten Stahlelementen.

Biegeversuche von kleinen Stahlprofilträgern beansprucht durch eine konstante Einzellast und einer gleichmässig ansteigenden Temperatur haben es erlaubt, neue Gesetze über die metallischen Eigenschaften von Stahl unter Temperatureinfluss zu entwickeln, welche für geläufige Stahlgüten in der Baukonstruktion und ebenso für Stahl FeE 460 mit hoher Streckgrenze anwendbar sind.

Die Gültigkeit dieser neuen Gesetze kann auf Grund der Simulation von sechs Versuchen (Massstab 1:1) unter Feuerbeanspruchung an ungeschützten Stahlstützen in Braunschweig und in Gent bestätigt werden und konnten nachträglich mit CEFICOSS simuliert werden.

Ausserdem wurde im Programm CEFICOSS die Möglichkeit gegeben Eigenspannungen zu berücksichtigen. Die Simulation der sechs Versuche hat bewiesen, dass diese keinen grossen Einfluss auf das Endergebnis haben, sie wurden jedoch in allen Berechnungen berücksichtigt.

Schliesslich wurden praktische Bemessungshilfen, auf Grund von CEFICOSS-Simulation, in Form von Diagrammen und Tafeln erstellt.

CONTENTS

SUMMARY	Page
PART I: REPORT	
1. INTRODUCTION	
1.1. Thermo-mechanical computer model CEFICOSS	1
1.2. Aim of research	1
1.3. General scope on the parameters	2
2. FACTORS GOVERNING THE HEAT TRANSFER	
2.1. Heating-curve	3
2.2. Coefficient of convection	3
2.3. Resultant emissivity	3
2.4. Thermal properties of steel	4
3. THERMO-MECHANICAL MATERIAL PROPERTIES	
3.1. Initial stress-strain relationships of steel	5
3.2. KRUPP test	5
3.3. Simulation of four tests by CEFICOSS	6
3.4. Comparison with test results	7
3.5. Conclusion	7
4. BEHAVIOUR OF STEEL BEAMS UNDER TRANSIENT STATE BEAMS TESTS	
4.1. Description of the new tests (S1 to S10)	8
4.2. Results of these tests	9
4.3. Simulation with CEFICOSS using the known Fe360 steel RS-LAW	10
4.4. Conclusion of the simulations	12
4.5. Improvements of steel laws	12
4.6. Additional tests (S11, S12, V1 to V7)	13
5. IMPROVED QL-LAWS	
5.1. Definition of the new QL-laws	14
5.2. Simulation of KRUPP tests with the new QL-laws	14
5.3. Comparison of the CEFICOSS results with the measures	15
5.4. Conclusion of the simulations	18

	Pages
6. ***FULL-SCALE TESTS OF COLUMNS***	
6.1. Description of the columns	18
6.2. Results of the tests	19
6.3. Simulation of the six full scale tests with CEFICOSS	20
6.4. Conclusions	20
7. ***PARAMETERS***	
7.1. Selection of steel shapes	21
7.2. Bending moment distribution	21
7.3. Buckling lengths	21
7.4. Design strength of steel	22
7.5. Calculation with CEFICOSS in normal service conditions	22
7.6. Initial imperfection introduced in CEFICOSS	23
7.7. Failure criterion	24
7.8. Influence of residual stresses	25
8. ***DIAGRAMS***	
8.1. Calculation process	26
8.2. Diagrams	26
8.3. Interpolation on buckling lengths	27
8.4. Transformation method for non uniform moment distribution	27
9. ***CONCLUSIONS***	28
10. ***BIBLIOGRAPHY***	30
PART II: DIAGRAMS AND TABLES	85
PART III: TESTS	
APPENDIX A: Transient state beam tests	145
APPENDIX B: Six full scale steel colums fire tests	211

PART I

REPORT

1. *INTRODUCTION*

1.1. *Thermo-mechanical computer model CEFICOSS*

During the C.E.C. research, agreement N° 7210-SA/502 **[1]**, a computer program for the analysis of steel as well as composite structures under fire conditions has been developed. It is based on the finite element method using beam elements with subdivision of the cross section in a rectangular mesh. The structure submitted to increasing loads or temperatures is analysed step-by-step using the Newton-Raphson procedure. The thermal problem is solved by a finite difference method based on the heat balance between adjacent elements.

The numerical simulation of several full scale fire tests performed during various research projects **([1], [2], [3], [4])** has demonstrated that this numerical software CEFICOSS is able to simulate in a correct way the structural behaviour of elements submitted to fire and provides a pretty good estimation of the fire resistance times. CEFICOSS is a tool which allows most credible prediction of the fire resistance of structural elements, and which can be used particularly for steel columns, with or without fire protection.

1.2. *Aim of research*

Tests performed at the University of Gent **[1]** on thick flanged steel columns made clear that a high massivity - the section factor F/V of the steel profile was 27 m^{-1} - provides a good fire resistance even to bare steel profiles. Only numerical models giving the temperature gradient through profile section are able to predict correctly the behaviour of such thick bare steel elements.

Indeed during the test of an unprotected column a fire resistance time of 45 minutes was measured while the simulation by CEFICOSS gives 46 minutes. This column was loaded at a level corresponding practically to the maximum allowable in normal service conditions, and would not have reached the fire resistance class F30 according to the usual simple calculation method based on the assumption of an uniform temperature inside of the steel section and on the conservative stress-strain-relationships of the ECCS-Recommendations **[5]**.

In order to make the results of this computer code available for everybody, it has been decided to establish N-M interaction diagrams for unprotected steel columns made of massive steel H-shapes.

The research programme has been based on six fire tests performed in the furnaces of Gent and Braunschweig and, from the other hand, on the intensive use of the thermomechanical numerical code CEFICOSS to calculate massive shapes (HD and HEM series) in a parametrical way.

This Final Report summarizes the works performed during the previous research periods and described in the Technical Reports N° 1 to 5 ([6], [7], [8], [9], [10]).

1.3. *General scope on the parameters*

The parameters to be introduced in this research are summarized as follows:

Section: The profiles from HEM and HD series with a flange thickness of at least 40 mm

Finally the following sections are concerned in this programme:

HEM 320 up to 1000
HD 210x210x198 to 249
HD 260x260x219 to 329
HD 310x310x283 to 500
HD 400x400x314 to 1086

Steel grades: Fe 510 and FeE 460

However sections with flange thickness higher than 40 mm are not actually usual in quality FeE 460 and therefore this steel quality will be reserved for HEM series.

Buckling lengths: from 2.00 m up to 8.00 m

Fire resistance classes: F30 and F60

Eccentricity of the load defined from first order bending moments:

- constant in a first step
- a simplified method will be proposed in a second step to cover other distributions.

2. *FACTORS GOVERNING THE HEAT TRANSFER*

2.1. *Heating curve*

All the calculations performed in this research have been made with the ISO-834 **[11]** standard heating curve, giving a gas temperature varying as follows around the heated element:

$$Tg = 20 + 345 \log_{10} (8t + 1)$$

With t = fire time in minutes.

2.2. *Coefficient of convection*

Following the recommendations of Technical Committee 3 of the ECCS **[5]** it was decided to make all the calculations in this research programme with a value $\alpha = 25$ W/m².K for the convection heat transfer.

2.3. *Resultant emissivity*

The value of the resultant relative emissivity ε^* to be introduced in CEFICOSS can usually vary between 0.45 and 0.7 depending of fire test conditions, and also normally varies during a test with temperature.

As suggested in the recommendations of the ECCS **[5]**, one constant value $\varepsilon^* = 0.5$ could be used for steel surfaces.

However the full scale test done at the University of Gent **[1]** showed that the temperature in the middle of the web can only be satisfactorily calculated by choosing a resultant emissivity ε^* smaller for the inner surfaces in chambers as for the outer ones, thus simulating the radiative shadow effect (see figure 2.1).

The resultant relative emissivity ε^* in the concave part of a H-section can be calculated as follows according to **[12]**:

$$\varepsilon^*_{web} = \varepsilon^* \cdot Fweb$$
$$\varepsilon^*_{flanged} = \varepsilon^* \cdot Fflange$$

The coefficients Fweb and Fflange are given by:

$$Fweb = \frac{-(b/2-a/2) + \sqrt{(h-2e)^2 + (b/2-a/2)^2}}{(h-2e)}$$

$$Fflange = \frac{(h-2e) + (b/2-a/2) - \sqrt{(h-2e)^2 + (b/2-a/2)^2}}{(b-a)}$$

where h, b, a and e are dimensions of the steel shape height, width, thickness of the web and thickness of the flange.

The values of ε^* for the web and for the inside part of the flanges, and corresponding to $\varepsilon^* = 0.5$ for the outside face of the flanges, have been calculated for each shape concerned in this research.
For HD sections ε^* varies from 0.182 up to 0.188 for the inside face of the flange, whereas ε^* varies from 0.286 up to 0.301 for the web.

For HEM sections ε^* of the inside face of the flange increases regularly from 0.189 to 0.231 for shape increasing from 320 up to 1000, and an average value of 0.2 is not far away from the reality.
As concerns the web, the value of ε^* increases regularly from 0.305 to 0.43.

Therefore it seems reasonable as simplification to adopt for any section the following resultant relative emissivity:

$\varepsilon^* = 0.5$ for outside faces of the flanges
$\varepsilon^* = 0.2$ for inside faces of the flanges
$\varepsilon^* = 0.3$ for the web.

and all the calculations have been performed according to figure 2.1.

2.4. *Thermal properties of steel*

In order to compute the time dependent temperature field in structural elements, the thermal conductivity λ (W/m.k) and the specific heat C (J/kg.K) of steel must be known as functions of temperature. These functions are presented in figure 2.2 for the thermal conductivity and in figure 2.3 for the specific heat, while the thermal expansion for steel is given in figure 2.4. These laws are the original ones introduced in the program CEFICOSS [1].

3. *THERMO-MECHANICAL STEEL PROPERTIES*

3.1. *Initial stress-strain relationships for steel*

The laws describing the temperature dependent stress-strain relationships of steel are given in figure 3.1 to 3.6 as existing initially in CEFICOSS (see [1]). These laws have been established for usual construction steels like Fe 360 and Fe 510 and mainly for calculation of composite sections. It was to be examined, whether these temperature-dependent stress-strain relationships are too much simplified for simulating unprotected bare steel columns.

Furthermore the behaviour at high temperatures of steel FeE 460 had not yet been calibrated before, and it was reasonable to fear a different behaviour of this steel in fire owing to the fact that his properties are obtained by a thermomechanical treatment.

3.2. *KRUPP tests*

First of all it was interesting to try to find in the litterature some reports over tests performed on pure steel elements and covering as far as possible the field of strains interesting in this research. This possibility was given by bending tests performed by Rubert and Schaumann [13] in KRUPP Research Centre in order to investigate the properties of steel in fire, and it has been decided to simulate some of these tests with CEFICOSS.

These bending tests on profiles IPE 80 are schematically explained in figure 3.7. The beam with a span of 114 cm is situated inside of an electrical furnace, and subjected to a external point load F which is kept constantly during the test. After loading, the temperature inside of the small electrical furnace increases continuously with a given velocity. Because of the small thickness of the profile IPE 80, the temperatures can be considered as uniform inside of the steel section, and the thermal expansion of steel has practically no influence on the vertical deflection, which is registred at mid-span of the beam during the test. This type of test has been performed in KRUPP Research Centre for different loading rates F/Fplastic, and for different heating velocities. Process and results of these tests are described in [13] and [14].

3.3. *Simulation of four tests by CEFICOSS*

Four tests, called WK1 to WK4 and described in the reports **[13]** and **[14]** have been simulated with CEFICOSS with the existing stress-strain relationships, and with the following assumptions:

1) The dimensions of sections have been assumed to be constant and equal to the theoretical dimensions of an IPE 80. This assumption is justified by the very small differences measured by Rubert & Schaumann in tests and presented in the report **[14]**:

   - Average of differences on the inertia: 0.93 %
   - Average of differences on the plastic moment: 0.88 %

2) The curves giving the actual measured variation of temperature during tests are not given in **[13]**. The authors give just for each test a mean value of the heating velocities which are very close to the theoretical one (the highest difference for tests WK 1 to WK 4 reaches 5 %). Moreover, a conclusion of all the tests presented by the authors is that the heating velocity doesn't play an important role on results. Therefore the tests may logically be simulated with the theoretical temperature curve presented in figure 3.8.

3) All the temperatures mentioned in [13] are steel temperatures and not gas temperatures. Therefore, the statical calculations in CEFICOSS have been performed with effectively given steel temperatures.

4) The mechanical properties of steel used in CEFICOSS were taken from the report and are measured values:

   σ_y = 35.2 KN/cm^2 for the test WK1
   σ_y = 39.9 KN/cm^2 for the test WK2
   σ_y = 39.9 KN/cm^2 for the test WK3
   σ_y = 40.1 KN/cm^2 for the test WK4

   As the actual tensile strengths σ_t have not been measured, the coefficient K of figure 3.1 was taken as a constant value 1.5 in these present CEFICOSS calculations.

3.4. *Comparison with test results*

The curves D=f(t) given by CEFICOSS in the four simulations have been transformed into the form D=f(T) using the relation T=f(t) defined earlier in figure 3.8. These curves D=f(T) are given in figure 3.9 together with the actual measured displacements.

For tests WK1 to WK3, CEFICOSS gives smaller displacements than measured up to a certain temperature. Over this critical point, the displacements given by CEFICOSS are larger than the measured ones. This critical temperature (for D=40 mm) increases when the rate of loading decreases, and the differences between CEFICOSS and tests go down progressively. For test WK4, which has the lowest load, CEFICOSS gives lower displacements for any temperature.

To sum up, the pseudo-vertical (assymptotic) curves given by CEFICOSS for high displacements go progessively from the left side of the measured curves to the right side when the rate of loading decreases. The crossing point can be roughly defined by T ~ 600°C or F/Fp ~ 0.50.

Up to about 600°C, CEFICOSS gives results which are conservative for a design based on the plastic moment, but they seem to be unsafe for higher temperatures.

In the intermediate zone of lower temperature, where the curves turn from small to high displacements, the existing laws give deflections always smaller than measured in tests and seems to be clearly unsafe.

3.5. *Conclusion*

The last notice before is very important for the present research. As a matter of fact, the form of the (σ-ε) diagram in the intermediate zone just before to reach the plastic plateau has an important influence on the buckling behaviour of columns. The comparison done here shows that the σ-ε relationships included in CEFICOSS should be improved to perform calculation of pure steel columns.

4. BEHAVIOUR OF STEEL BEAMS UNDER TRANSIENT STATE BEAM TESTS

4.1. Structural steel qualities

Tests described in **[13]** have been performed on beams theoretically in Fe 360, but steels were rather of quality Fe 510 according to their yield strengths (see § 3.3). These tests can obviously be considered to cover the quality Fe 510, and the highest quality FeE460 was to be investigated too, in a same way, in the same testing device by KRUPP (figure 4.1).

In the previous bending tests, IPE 80 profiles were used; for steel FeE460, however, such profiles are not rolled and similar sections had to be manufactured. The test pieces have been extracted from a FeE460 steel beam W 360x410x314 in its 40 mm thick flanges (see figures 4.2). The tests take aim at measures of mechanical properties of steel at high temperatures, so that's why it was important to reduce as much as possible the heating of steel during the tooling, with adapted machine speed and cooling. The cuttings have been made preferably by sawing than with blowtorch.

The bending tests in themselves are schematically explained on the figure 4.1 and more detailed in Appendix A of part III. The simply supported beam with a span of 114.7 cm is situated inside an electrical heating furnace, and subjected to an external point load F which is applied at the middle of the span and kept constant during the test. After loading, the temperature induced by the electrical resistance increases continuously with a given velocity.

Because of the small thickness of the manufactured profile, the temperature can be considered as uniform inside the steel section and more, the thermal expansion of steel has practically no influence on the vertical displacement which is registered at the middle of the beam during the test.

To control the assumption of a uniform temperature, thermocouples have been placed on all the beams to record in different points of the steel cross section the time-temperature curves (see page A3 in Appendix A of PART III).

The next page A4 in this Appendix A shows the extrema values of steel temperatures capted by thermocouples for one of the most unfavorable tests and so proves the validity of this assumption.

The heating velocity has been chosen equal to 3.5 K/min; it has been shown in previous tests [13] that variations of velocity have no significant influence on results.

Nine tests of this type have been performed for different loading rates F/F_{pcold}, where F_{pcold} means the theoretical necessary applied force to obtain the middle-span section fully plastified (plastic hinge) with a bi-rectangular stress distribution (rigid-plastic theory). The nine transient state beam tests are called S1 to S7, S9 and S10; S8 is a cold test with loadings and unloadings up to collapse.

4.2. *Results of the tests*

The pages A5 to A13 of Appendix A, PART III, give the measured vertical displacements (mm) at the middle of the span in function of the temperature (°C), for the nine transient tests, in a decreasing order of loading levels.

The next page A14 shows the measured deflection at mid-span of the beam in function of the load F, for the cold test S8.

The ten tests are summarized in figure 4.3 as well as in the table of page A15 in Appendix A of PART III, giving the following informations:

- The yield point βs has been determined with tensile test pieces extracted from the flanges of the beam W 360x410x314 as shown on the figure 4.2 (T = specimens for tensile tests). The different values of βs appears in the column Re_H, the superior elastic limits obtained by tensile tests.
- F_{pcold}, the theoretical necessary applied forces to obtain the middle-span section fully plastified (plastic hinge) with a bi-rectangular stresses distribution (rigid-plastic theory).
- F, the applied loads
- F/F_{pcold}, the loading levels
- $\dot{\theta}_m$, the mean velocities of heating
- $\theta_{init.}$, the initial temperatures during the cold loading

- $(\theta m)_{max}$, the maximal mean temperatures of the steel reached during the test (thermocouples measures)
- $(D_{mes.})_{max}$, the maximal vertical displacements at the middle of the beam measured during the test
- $(t_{test})_{max}$, the duration of the test (not fire resistance)

4.3. *Simulation with CEFICOSS using the known Fe360 steel RS-LAW*

The performed KRUPP tests have been simulated with the following assumptions:

1) All the dimensions of the cross section have been kept constant and equal to the theoretical dimensions of the tooled beams (see figure 4.1). This assumption is justified by the very small differences (lower than 3 %) produced on geometrical and mechanical characteristics of the profile by tooling tolerances of ± 1/10 mm (see page A16 of Appendix A, PART III).

   The modelisation of a quarter of a beam section is presented on the page A17 of Appendix A.

2) Temperature-time curves issued from mean measures θ_m[°C] between thermocouples TH5 and TH12 (see page A.3), obtained for each test have been used for simulations. As explained before, differences between measured temperatures are so small that an uniform temperature can be considered everywhere through the cross section and along the beams.

   Moreover in the previous KRUPP tests, the authors showed that the heating velocity doesn't play an important role on results and so it's the same for differences between all the temperature-time curves with thermocouples for each test.

   Therefore, the statical calculations have been performed with mean measured steel temperatures from TH5 and TH12 (see pages A13 and A19 of Appendix A).

The Fe360 steel RUBERT-SCHAUMANN laws (RS-LAWS) defined in **[13]** have been used to simulate the new tests. These laws are defined in figure 4.4 showing a simplified general σ-ε_σ diagram for steel. This diagram is characterized by 3 temperature dependant parameters: the elastic modulus E_o, the proportional stress β_p and the yield point β_s. Three domains are observed:

the linear elastic, the elliptical elasto-plastic and the plastic plateau.

Figures 4.5, 4.6 and 4.7 give respectively the reduction of the elastic modulus factor $Eo(\theta)/Eo(\theta=20°C)$, the proportional stress factor $\beta_p(\theta)/\beta_p(\theta=20°C)$, and the yield point factor $\beta_s(\theta)/\beta_s(\theta=20°C)$, in function of temperature, for steel Fe 360.
Figure 4.8 shows the resultant diagram with all the RS-LAW curves at different temperatures for steel FeE460 ($\beta_s(\theta=20°C)$ = 460 N/mm², for example).

The results of the nine fire simulations S1 to S10 and the only cold one S8 are given in Appendix A, PART III, pages A20 to A89 in a decreasing loading level order. The fire simulation figures represent the curve D = f(θ), the simulated vertical displacement (—..—..—..—..) the middle of the beam in function of the temperature, compared with the measures (————).
The cold simulation figure shows W = f(F), the same type of displacement in function of the increasing load.

For the fire simulation of <u>S1</u> test (<u>loading level = 1.0</u>; that means a fully plastified middle-span section) CEFICOSS can't give any results because the cold loading ends already with problems of numerical convergence (plastic hing failure). Indeed, the RS-LAW ends with a plateau and so doesn't consider the strain-hardening (see page A20).

The same remark can be made for the <u>cold simulation of S8 test</u> because the collapse load cannot be reached without strain-hardening. The failure load obtained with CEFICOSS is 30.6 kN, different in about 2.0 % of the calculated value from the rigid-plastic theory, 31.3 kN. The difference between 30.6 kN calculated with RS-LAW and the measured real failure load 37.65 kN is about -18%.

For the other fire simulations (S2 to S7, S9 and S10) it can be observed that CEFICOSS with Fe 360 RS-LAW leads to a behaviour of the beams not too much different from reality. The results have especially good agreements in the field of usual loading level concerning this research, in other words F/F_{pcold} = 0.30 to 0.70.

For high or low loading level, for example 0.85 (S3 test) or 0.10 (S7 test) and 0.075 (S6 test), more important differences are found.

4.4. *Conclusions of the simulations*

As a matter of fact, the form of the (σ-β) diagram in the intermediate zone just before to reach the plastic plateau has an important influence on the buckling behaviour of columns. All the comparisons done show that the σ-β laws included in CEFICOSS should be improved, especially for steel FeE460, when pure steel columns are calculated.

4.5. *Improvement of steel laws*

* A first possibility to improve the existing (σ-β) laws in CEFICOSS, was to adapt the Fe360 Rubert-Schaumann law [13] to the FeE460 steel quality, because the simulations with the RS-LAW in CEFICOSS are not too bad as shown before.

* Another approach could be to take into account the strain-hardening reality, by use of a simple type of diagram, a quadrilinear law defined by the following temperature-dependent parameters (see figure 4.9):

- $E_{o,\theta}$, the elastic modulus.

  ≃0,2 %
- $\sigma_{y,\theta}$, the yield point.

- E^*_{θ}, the elastic modulus relevant for strain-hardening.

- $\sigma_{t,\theta}$, the ultimate stress.

Such a multilinear σ-ε idealization, correctly done, would have the advantage to cover conveniently all 10 tests (S1, S3, S7 and S8 included).

In other words:

* the whole range of loading levels is covered i.e. $0.075 \leq F/F_{pcold} \leq 1.0$ corresponding to the critical temperature field $461°C \leq \theta_{max} \leq 828°C$ (see fig.4.3)

* the cold test S8 could also be simulated in a correct way.

So this QUADRILINEAR LAW (QL-LAW), apparently less accurate than a curved law, would have a more general application field as ALL LOAD LEVELS and ALL TEMPERATURE SITUATIONS could be considered.

.6. *Additional tests (S11, S12, V1 to V7)*

Additional tests have been performed in the same testing device; two of them (S11 and S12) have been performed in the plastic domain for steel FeE460, while seven tests (V1 to V7) have been performed on small sections IPE80 in steel Fe360 (figure 4.10).

As mentionned before, the initial KRUPP tests [13] have been performed on steel having 386 MPa as mean value of yield strength at 20°C, while the specimens used here reach only 313 MPa. Thus the field of yield strengths has been fully covered.

These tests are reported with details in the Appendix A of PART III, pages A30 up to A40

For steel FeE460, the procedure of testing applied for S11 and S12 consisted in starting at room temperature to load the beam, with F/F_{pcold} greater than 1.0; afterwards heating until a definite temperature with a constant load and finally heating and increasing the load of the beam together until collapse.

For steel Fe360 two tests have been perfomed in the plastic domain with the same procedure as explained before (V1 and V2 tsts), while four tests have been performed in the elastic domain beginning with different F/F_{pcold} strictly smaller than 1.0 and being heated with constant load until collapse (V4, V4, V5 and V6 tests). The V7 test is a cold test with loading and unloading up to failure.

A sensitivity of beams to a well-known parasite phenomenon, the buckling (local buckling of the flanges; lateral-torsional buckling of the whole beam) has been observed, more especially for beams already fully plastified ($F/Fcold \geq 1.0$) before heating. Therefore the testing procedure has been adapted without changing its validity, in applying loads via a kind of knife edge and in welding by points some stiffeners on each side of the web, out of the middle-span of the beam (only this for V2 and S12 tests) (see details in Appendix A).

5. *IMPROVED QL-LAWS*

5.1. *Definition of the new QL-laws*

To define such a modelization, as suggested in § 4.5 by figure 4.9, steady state tensile tests (SSTT) for FeE460 steel quality have been performed in the laboratory of ARBED-Research. They consisted in tensile tests under constant high temperature induced by an electrical furnace around the specimen. Some curves (σ, ε) issued from these tests are shown in figures 5.1 and 5.2 with at the same time the QL-IDEALIZATION.

It can be seen on these figures how the four main parameters have been found, respectively for 20°C and 400°C:

$$\left[\frac{E_{o,\theta}}{E_{o,20C}}\right], \left[\frac{\sigma_{y,\theta}^{=0,2\%}}{\sigma_{y,20°C}}\right], \left[\frac{E_{\theta}^{*}}{E_{o,20°C}}\right], \left[\frac{\sigma_{t,\theta}}{\sigma_{y,20°C}}\right]$$

A more precise evolution of these parameters in function of the temperature θ[°C], for QL-law concerning steel FeE460, can be found in figures 5.3 to 5.6. The figures 5.7 and 5.8 show the diagrams (σ, ε) of QL-law for high strength steel with different curves corresponding to different given temperatures, respectively with ε increasing up to 4 % or 25 %.

5.2. *Simulation of KRUPP test with the new QL-laws*

All the KRUPP tests described in the previous chapter 4, called S1 to S12 for steel FeE460 and VI to V7 for steel Fe360, have been simulated in CEFICOSS with the new QL-laws proposed above and with the following assumptions:

1) For simulations of S1 to S10 tests (steel FeE460) the same geometrical dimensions have been taken for all the specimens because of the weak influence of the tooling tolerances on the geometrical and mechanical characteristics (see § 4.3).

   For the simulations of tests S11, S12 (steel FeE460) and V1 to V7 (steel Fe360) all the specimens have been measured and the real mechanical characteristics of each section have been introduced in the simulations.

   The modelisation of a quarter of the beam section is presented in figure 5.9, where the fillets between web and flanges are neglected.

2) For tests S1 to S10, the temperature-time curves issued from mean measures $\theta_{m[°C]}$ between thermocouples TH5 and TH12 (see Appendix A page A3), obtained for each test, have been used.

For S11, S12 and V1 to V6 tests, the used temperature-time curves are issued from mean measures $\theta_{m[°C]}$ between thermocouples TH6, TH8, TH10 and TH12 (see Appendix A page A33) obtained for each test.

As explained previously the differences of temperatures measured with thermocouples are so small that an uniform temperature can be considered all through the cross section and along the beams.

3) The yield point σ_y and the ultimate strength σ_t have been determined with tensile tests on pieces extracted from the shape W360x410x314 as shown in Appendix A of PART III, on pages A2 and A32 (T = specimens for tensile tests).

The same values σ_y and σ_t have been determined with tensile test pieces extracted from the flanges of the IPE 80 profile as shown also on that page A32 for V1 to V7 tests (P = specimens for tensile tests).

5.3. *Comparison of the CEFICOSS results with the measures*

** KRUPP tests for steel FeE460 (S1 to S10)

The comparative curves of the KRUPP tests measures and the QL simulations can be seen in Appendix A, PART III in pages A39 to A49, where the vertical middle-span deflections are given either in function of the applied load F for the cold test S8, or in function of the temperature θ in the steel profile in a decreasing order of loading level (F/F_{pcold}) for the other tests.

The cold bending test S8 can be quite well simulated, much better as with RS-law.

The bending test S1 can be simulated in a correcter way (428°C in place of 461°C measured) in spite of the fact that the load level (F/F_{pcold} = 1.0) doesn't give any result with RS-law which forgets completely strain-hardening.

The tests S3, S2, S4, S10, S5 and S9 can be simulated as well as with RS-laws.

For load levels F/F_{pcold} = 0.10 (S7 test) and 0.075 (S6 test), the simulation by QL-law is also quite acceptable, contrary to RS simulation giving always unsafe answers.

** KRUPP tests (S11 and S12)

For S11 and S12 tests, the procedure consisted in starting at room temperature to load the beam, with F/F_{pcold} equal to 1.05 (plastic domain), heating until ~ 70°C with a constant load and finally heating and increasing the load of the beam together until collapse. The variation of loading $\Delta F/\Delta\theta$ [kN/°C] was different in the two tests:

- 0.024 for S11,
- 0.009 (≃ 38% of 0.024) for S12

to pass through the plastic domain by different paths.

For a first approach with the QL-law numerical simulations we increased the load until the measured failure value and kept it constant afterwards until the simulated failure (see pages A37 and A38 in the Appendix A of PART III).

Because of the lateral-torsional buckling especially more sensitive in the plastic domain an early failure occured for S11 test; S12 specimen has better results according to the welded stiffeners and the knife edge which transmits the load, both introduced to avoid as much as possible buckling problems without changing the validity of the test.

Pages A52 and A53 of Appendix A show the comparison between the measured and the simulated mid-span vertical deflection of the beam in function of temperature and also show the influence of the parameter $(E^*/E_{0,20°C})_{20°C}$ defining the hardening in QL-law idealization. It can be seen for these particular cases (particular ranges of strains and load levels) that with the approximation of QL-law, the use of a higher coefficient $(E^*/E_{0,20°C})_{20°C}$ = 0.0172 improves the results at cold conditions, but still provides higher deflections than reality. To approach better the reality, the law would have to leave (Quadri-Linear) QL model and to follow more closely the true (σ,ε) diagram with a multilinear idealization, for example.

** KRUPP tests for steel Fe360 (V1 to V7)

For numerical simulations with QL-law, used the same evolution of the four parameters in function of temperature as for steel FeE460 has been used. Only the values at room temperature corresponding to the real characteristics of this steel quality have been changed as follows, using the measured mean values:

- $\sigma_{y,20°C}$ = 313 N/mm² (yield point)
- $\sigma_{t,20°C}$ = 505 N/mm² (tensile strength)

V1 and V2 tests are similar to tests S11 and S12 (FeE460 steel): the beam was first loaded at room temperature with F/F_{pcold} = 1.10 (plastic domain), and next heated until ~ 120°C (V1 test) or ~ 110°C (V2 test) with a constant load, and finally heated and subjected to an increasing load until collapse.

The variation of the loading $\Delta F/\Delta\theta$ [kN/°C] was different in the two tests:

- 0.030 for V1
- 0.012 (≃ 40% of 0.030) for V2

to pass through the plastic domain by different paths.

Appendix A, PART III, pages A54 and A55 show the comparison between the measured and the simulated mid-span vertical displacements of the beam in function of temperature for V1 and V2 tests.

Because of the lateral-torsional buckling an early failure occured for V1 and probably for V2 test .

More details about the performed simulations can be found in [10].

** V3 to V6 tests (see Appendix A, PART III, pages A56 to A59)

For the load levels 0.85 (V3 test), 0.60 (V4 test) and 0.50 (V5 test), a good agreement with the measures is found by using the QL-law. The calculated deflections follow quite well the evolution of the measured ones; in the ultimate conditions, the simulation is always in the safe side, and the failure temperatures are very similar.

For the low load level 0.10 (V6 test), the simulation with QL-law is also quite acceptable giving safe answer. The deflections are higher in the simulations but the failure temperature is similar.

For the cold bending test V7, similarly as made for test S8, two simulations have been performed by varying the value of QL-law parameter $(E^*_{20°C}/E_{0,20°C})$

The initial value 0.0061 leads to a quite good simulation.

5.4. *Conclusion of the simulations*

As a general conclusion, it can be said that the ARBED QL-LAW presented here allows to represent well the physical steel behaviour for COLD and for HOT conditions from 20°C to 900°C, for all load levels

$$1.21 \geq F/F_{cold} \geq 0.075$$

for FeE460 and Fe360 steel qualities (fig. 5.10 and 5.11). The undoubtful advantage of this idealization is that the calculation results are on the safe side. It's better to use the low slope of the QL-law hardening part [$(E^*_{20°C}/E_{0,20°C})$ = 0.0061] (see fig. 5.5) to stay more on the safe side.

6. *FULL-SCALE TESTS OF COLUMNS*

6.1. *Description of the columns*

The tested columns described in Appendix B of PART III have been selected in order to cover as far as possible the parameters of this research, according to the disponibility of shapes (for instance limited to a thickness of 40 mm for FeE460) and to the possibilities of testing devices (4.14 m in Gent and 5.70 m in Braunschweig).

End plates and stiffeners have been welded at both ends of unprotected steel columns, which have been loaded in the furnaces with a constant first order eccentricity. Rotations were not restrained at the ends thanks to cylindrical supports.

Details concerning the specimens are given in table 6.1 and in Appendix B, as well as in **[15]** and **[16]**.

This table 6.1 shows that column specimens cover the field of the flange thickness from 39.6 (~ 40) mm up to 125 mm, with intermediate values of 45 and 75 mm. The section factor U/A varies from 20 up to a maximum of 58.4 m^{-1}.

Five specimens were in steel Fe510, while the sixth one was in steel FeE460, and a possible direct comparison was offered with tests n° 5 and 6, in spite of different slenderness ratios and rates of loading. This table shows also that five tests have been performed with bending about the minor axis, while one has been subjected to bending about the major axis. Four tests have been carried out in the furnace of GAND in Belgium with a length of 4.14 m, while two occured with a length of 5.70 m in the furnace of Braunschweig in Germany.

Moreover, it has to be pointed out that the six specimens have various slenderness ratios (from 0.3 up to 1.3), as well as loading rates and eccentricities (or eccentricity ratios e/d).

In order to compute the ultimate load in normal service conditions, the method proposed by the German Standard DIN 18800 part 2 **[17]** has been adopted here as reference just because it was immediately available on the computer.

6.2. Results of the tests

The six full scale fire tests have been performed during September and October 1988 in the furnaces of the Universities of Gent (Belgium) and Braunschweig (Germany), and are reported in **[15]** and **[16]**. The actual parameters and the results of these tests are summarized in table 6.1, showing that these unprotected steel columns reached fire resistance times varying from 37′ up to 68′.

The following data have been measured during the tests:

- the temperatures in many points of the furnace,
- the temperature of steel measured with 32 to 40 thermocouples, located at the surface as well as inside of steel in two different cross sections of the column,
- the vertical and horizontal displacements.

The results of these measurements are given in the Appendix B of PART III on the same diagrams as the simulations made with CEFICOSS.

6.3. *Simulation of the six full scale fire tests with CEFICOSS*

The simulations have been performed with CEFICOSS under consideration of the actual sizes of cross sections, which are given in table 6.2 as well as the initial imperfections measured on the column in the buckling direction.
The fillets between web and flanges have been neglected in the simulation carried out by following the process hereafter:

1) The actual measured geometrical sizes are introduced according to table 6.2. (The sizes given in this table are the mean of many measurements).

2) The heat transfer coefficients were given by the Fire Laboratories of Gent and Braunschweig
   $\alpha = 18$ and $\varepsilon = 0,45$ for tests performed in Gent and
   $\alpha = 25$ and $\varepsilon = 0,7$ for tests performed in Braunschweig.

3) The statical calculation started only after check of the good accordance between calculated and measured temperatures.

Moreover, these values given by the laboratoires have been modified for the web and the inner side of the flanges to take into account the shadow effect which is a physical reality. The physical meaning of the shadow effect and its influence on the emissivity factor ε are given in figure 6.4.

In reality at a given time, the temperature measured in one place of the section is not unique, but there is some difference between the values given by all the thermocouples situated in a same place (see details in Appendix B).

In figure 6.3 are indicated the heating parameters of each furnace and the fire resistance times calculated by CEFICOSS with the new QL-8 steel law presented in this report, and adapted according to the actual yield point and tensile strength of steels.

6.4. *Conclusions*

It has been pointed out that the programme CECIFOSS is able to simulate correctly the behaviour of thick pure steel profiles submitted to ISO-fire. The proposed QL-8 steel law gives very good concordance with the tests, and has been adopted to perform the calculations.

7. PARAMETERS

7.1. Section of steel shapes

As noted earlier, only shapes having a flange thickness of at least 40 mm are concerned by this research. Therefore only HEM and HD series could be interesting, and a priority has been given to the HD profiles which are particularly well adapted for columns.

7.2. Bending moment distribution

Except when transverse loads are applied between columns ends - which is not usual in normal buildings - the distribution of bending moments along the column may have any form presented in figure 7.1.

As shown in figure 7.2 by means of a diagram N-e, distribution type ① (ψ = - 1, bi-triangular distribution) is the most favourable one, allowing highest eccentricity for a given axial load, or the highest axial load for a given eccentricity. The distribution type ⑤ (ψ = 1, uniform distribution) is the most unfavourable one, whereas the unsymetrical distribution ② is most usually encountered.

To go in the same way as Standards for design in normal service conditions, the columns have been calculated here with the most unfavourable distribution of moments which is uniform, having a constant eccentricity and therefore a constant first order bending moment. A transformation method is proposed next for other distributions, allowing to reduce the unfavourable effect of the uniform one.

7.3. Buckling lengths

The column buckling lengths considered in this project have been chosen between 2.00 meters and 8.00 meters by steps of 2.00 meters. Therefore, pin-ended columns of 2.00, 4.00, 6.00 and 8.00 meters have been calculated, whereas a simple linear interpolation method is sufficient for any intermediate length.

7.4. Design strength of steel

Any section considered in this program has a flange thickness equal or greater than 40 mm. This thickness is 40 mm for the HEM series, and varies between 40 and 125 mm for the HD series. Eurocode 3 **[19]**, which has to be used for the design in normal service conditions, stipulates that the yield strength σ_y should be reduced according to the thickness of steel. This rule should be applied to Fe510, but steel FeE460 is not directly mentioned in this Eurocode.

To simplify and to remain in the safe side, the decision has been taken to use in the calculations a yield strength reduced as follows for steel Fe510, in accordance with EURONORM 25 **[19]**:

Flange thickness [mm]

from	up to (≤)	σ_y [N/mm²]
16	40	345
40	63	335
63	80	325
80	100	315
100	125	305

The tensile stength has been taken everytime equal to 510 N/mm².

For steel FeE460 the following characteristic values have been used, in accordance with **[20]** for flange thickness of 40 mm:

σ_y = 450 N/mm²
σ_t = 560 N/mm²

7.5. Calculation with CEFICOSS in normal service conditions

The static modulus included in the program CEFICOSS can be used to calculate by iterations the ultimate load at ambient temperature. That is made systematically because it furnishes the highest possible load which can be progressively reduced to establish curves N-t allowing to find loads corresponding to 30 and 60 minutes of fire resistance.

In reality, however, it must be pointed out that the load given by CEFICOSS is a little different from the load calculated according to Eurocode 3 **[18]** for, mainly, the strain hardening effect is considered in the stress-strain relationships included in CEFICOSS. Of course, FIRST OF ALL, DESIGNERS HAVE TO COMPLY WITH THE STANDARDS FOR NORMAL SERVICE CONDITIONS. But for a quick and simple information, it was interesting to show together ultimate loads in normal service conditions and in fire.

From the other hand, some National Fire Codes accept clearly a load reduction in fire, and this concept will probably appear too in the final version of Eurocode 3. It is not logical indeed to consider for instance the full wind load on building together with a fire, or to have a crane in full action in an industrial building when fire occurs.

Therefore an interaction curve in fire has not to be directly compared with the interaction curve at ambient temperature where the values have been divided by 1.5. Such a comparison is not enough representative to qualify the economical interest for a construction system, and would not be sufficient for designers. It is necessary to give interaction curves in normal service conditions, as it has been made in this research.

Then, it has to be clearly noticed that results for normal service conditions given in this report are just furnished as information for scientific purpose.

7.6. *Initial imperfection introduced in CEFICOSS*

An initial column imperfection of the column has to be defined for CEFICOSS analysis, and has an influence for low bending moments. There is of course no specification in Standards to select this parameter, because a calculation in fire conditions is a quite new concept.

Eurocode 3 **[18]** defines a geometrical imperfection L/1000 to be applied with residual stresses in a second order analysis at ambient temperature. In another research **[21]** dealing with composite columns, the following initial imperfections have been adopted.

e_o = constant = L/500 for bending about the minor axis
e_o = constant = L/1000 for bending about the major axis

To have a comparison with a few National Standards, several calculations have been carried out with CEFICOSS at ambient temperature, without considering the strain hardening effect of steel [7]. Some differences could be observed between the various standards and codes, and they are particularly significant for buckling about the minor axis. It appeared, however, that CEFICOSS gives results which are in good concordance with the non-linear method of second order proposed in the German DIN 18800 [17], as well for bending about minor axis as for bending about major axis, when calculations are run with geometrical imperfections L/500 and L/1000.

In order to keep uniformity in the calculations made with CEFICOSS it has been decided to adopt here too these geometrical imperfections defined in [21], in spite of the fact that residual stresses will also be considered. The results will be a little in the safe side, especially for bending about the minor axis.

The constant initial imperfections defined above have been systematically introduced in the calculations in addition on the indicated first order eccentricities.

7.7. *Failure criterion*

The fire resistance time of a structure can be based on different criteria, usually depending on type of structure. For a column, failure corresponds practically to BUCKLING. In the program CEFICOSS, the mathematical simulation of this physical behaviour is given by the Determinant of the Structure Stiffness Matrix, which being positive becomes negative (DSSM = 0); from a practical point of view, it is sufficient to analyse the Minimum Proper Value (MPV) of the matrix, which also goes to zero.

The behaviour of the column can also be observed through horizontal displacement and displacement speed of the mid-height node, which rapidly increase when buckling occurs.

For columns many examples proved that a deflection criterion (D = L/10 for instance) has only a significant influence for very high bending moments, what means for very low axial loads N. In a practical point of view that zone of the interaction diagram is not really interesting as corresponding to a situation which never occurs in a building. Therefore it was decided to consider the equilibrium failure as single criterion for columns.

'.8. *Influence of residual stresses*

To be able to evaluate the influence of residual stresses on the fire resistance, the program CEFICOSS has been enlarged to accept a distribution of stresses in equilibrium inside of the cross section.

Using the distribution as well as the highest values suggested in Eurocode 3 **[18]**, the stresses shown in figure 7.3 have been introduced in CEFICOSS to simulate the tests n° 2 and n° 3 described in Appendix B, PART III, where:

$$\sigma_{R(max)} = 0.3\ \sigma_y = 0.3 \times 29.8 = 8.94\ kN/cm^2$$

The results of both simulations are given in figure 7.4. The observed differences are very small, particularly for test 2 when the column is buckling about the major axis ($\bar{\lambda} = 0.3$). For the column of test n° 3 having a slenderness ratio of about 0.8 the difference between the resistance times remain quite small (1 minute, about 2 %).

It was also interesting to check the influence of residual stresses on the column of test 1 having the highest slenderness ratio for a low fire resistance time. The supposed residual stresses distribution is given in figure 7.3, with a maximum of 0.3x36.4 = 10.92 kN/cm^2. The table of figure 7.4 shows that the calculated fire resistance time decreases down to 35 minutes (~ 5 %) in this case.

Of course, actual residual stresses in the beam have not been measured, but these simulations show that their influence is probably quite small for thick flanged columns in the domain considered in this research. As this influence consists in a small reduction of the fire resistance time, and in order to have conservative results, it has been decided to perform the calculations by taking into account residual stresses as proposed in Eurocode 3 **[18]** and explained on figure 7.5. The stresses will be kept constant on the whole flange or web thickness (as made in figure 7.3) and will be combined with the initial geometrical imperfection defined earlier in § 7.6 and given in figure 7.5.

8. *DIAGRAMS*

8.1. *Calculation process*

For any column cross section the calculation of temperatures in different patches of the discretized section is subordinated neither to the column length nor to the loading. Therefore the thermal analysis can be done first and the resulting time dependent temperatures can be used as data for every static calculation dealing with the same cross section.

The statical calculation process is described in figure 8.1; the first step is to find by iterations the ultimate axial load at ambient temperature (point A on vertical axis corresponding to a time t=0'). Then CEFICOSS is run by reducing progressively the load for a series of eccentricities. For instance a load corresponding to the point B applied with an eccentricity of 15 cm gives a fire resistance time $t_{B,15}$, and defines the point C in figure 8.1.

All the curves established with various eccentricities permit to read by interpolation the axial loads N for the required fire resistance times 30 and 60 minutes as shown on figure 8.1, and to create a file including pairs of values N-e for each fire resistance class.

In reality whole curves established with about 20 points as given in figure 8.1 are not necessary; it is sufficient to find points near the classified fire resistance times to allow a quite accurate interpolation. An average of not less than 3 simulations are needed, however, for each requested point.

For a practical purpose, constant relative eccentricities have been chosen: ratios e/h = 0, 0.10, 0.25, 0.50, 1.00, 2.00 and 4.00 have been used for bending about major axis, while ratios e/b = 0, 0.10, 0.25, 0.50 and 1.00 have been used for bending about minor axis. h and b are of course the height and the width of the steel shape.

8.2. *Diagrams N-e*

The presentation of results in a form N-e has been selected rather than N-M, first to have two independent variables, what leads to simplier mathematical function, and from the other hand in order to avoid the calculation of the pure bending moment corresponding to a fictitious situation.

As the number of parameters is not too high, both tables or diagrams can be convenient for designers, and both forms are presented for the examples given in **PART II** of this report.

Tables are, however, the main data base which allows to build up the diagrams by means of any spreadsheet software with integrated graphic possibilities.

8.3. *Interpolation on the buckling length*

The simple linear interpolation method is proposed to evaluate the ultimate load corresponding to a buckling length between those given in the tables.

The examples of figure 8.2 show that by performing a calculation in CEFICOSS with the interpolated load for 5.00 m, a fire resistance time of 30 minutes is practically found in both examples. Moreover, if more accuracy was needed, the users have a possibility to improve the interpolation, for four buckling lengths are given in tables allowing to see the look of the curve, as shown in figure 8.3

8.4. *Transformation method for non uniform moment distribution*

As noted before, calculation have been performed with an uniform first order bending moment (ψ = 1.00 according to figure 7.1).

At ambient temperature, Eurocode 3 **[18]** proposes to apply a corrective factor β on the moment in the interaction formula, β depending only on the form of the moment distribution.

Figure 8.4 shows a column HD260x260x329 calculated for vairous lengths and eccentricities, as well as for bending about both axes and for an uniform or a bi-triangular bending moment distribution.

In the first of the three last columns of the table, the method proposed in Eurocode 3 has been applied as defined in figure 8.5, and leads sometimes to unsafety when eccentricity increases.

The β-ψ method used in the two last columns of the table has been established in another research **[21]** using CEFICOSS to calculate steel-concrete composite columns. In this method β is not only a function of the form of the moment distribution, but also of the slenderness ratio and of the relative eccentricity e/h (or e/b). Except for the calcul of β, this method is simular to the method of Eurocode 3, presented in figure 8.5.

The differences observed in these two last columns come from two possible ways to apply the method. In the penultimate column, N_{bitr} has been calculated exactly as in figure 8.5 only from the uniform value Nu, what means:

$$K_u = \frac{\frac{N_c}{N_u} - 1}{e}$$

and

$$N_{bitr} = \frac{N_c}{1 + \beta . K_u . e} = \frac{N_c}{1 - \beta\ (N_c/N_u - 1)}$$

In the last column, however, an equivalent eccentricity has been calculated: $e_e = \beta . e$ and N'_{bitr} has been found by interpolation with this equivalent eccentricity in the table given in PART II for this section and for an uniform distribution.

The differences observed between the two possible ways to apply the β-ψ method are quite small, and depend only on the more or less good applicability of the basis formula presented first in figure 8.5.

It can be observed, however, that the values found in these last columns of figure 8.4 with this β-ψ method are more conservative that the other ones. This method could be used rather than the method of Eurocode 3.

9. CONCLUSIONS

Practical design tools for thick flanged steel columns are given here, allowing to take really benefit of the massivity of these shapes to save in some cases the costs of a fire protection. The differences of temperature existing inside of the cross section are taken into account to fully use this advantage, what could not be done by methods based on the assumption of an uniform steel temperature.

This research will finally allow to use steel elements more economically. Moreover the validity of the program CEFICOSS has been improved to simulate whole structures including as well steel-concrete composite elements as pure steel elements (**[22]**, **[23]**, **[24]**).

In a next step, to improve the convenience of the results, it should perhaps be envisaged to put them on a floppy disk with a simple program allowing on a personal computer quick interpolations as well as the transformation of the bending moment distribution.

Moreover, the results of this research can be used as a basis to establish a simplified method or to improve some existing methods. For instance it can be observed in tables given in PART II that it is difficult to define exactly when the massivity could be sufficient to reach automatically the fire resistance class F30 with a correct design in normal service conditions. As a matter of fact, that occurs for F30 when:

$$N_{F30} \geq \frac{N_{(F0,EC3)}}{1,5} = \text{maximum service load with safety factor equal to } 1,5$$

It can be observed in the tables that it depends not only on the flange thickness or on the section factor U/A, but also on the slenderness ratio of the column, and, moreover, on the eccentricity.

To simplify as far as possible, only the **flange thickness** and the **slenderness ratio** could be considered, with the minimum ratio N/N(F0,EC3) of any eccentricity. Moreover, the given ratios N/N(F0,EC3) could be multiplied by 1,5 to have a direct comparison with the maximum service load calculated according to EC3. This process leads directly to the **diagrams of figures 8.7 and 8.8** which are very easy to use and to interpretate, showing clearly what should be the **reduction of load in the worst case for the fire classes F30 and F60.**

10. BIBLIOGRAPHY

[1] SCHLEICH J.B.; REFAO-CAFIR, Computer Assisted Analysis of the Fire Resistance of Steel and Composite Concrete-Steel Structures. C.E.C. Research 7210-SA/502, Final Report EUR 10828 EN, Luxembourg 1987.

[2] CTICM, essai n° 86 - U - 052 du 22.04.1986, - Essai de résistance au feu d'un poteau en profil HE 500 AA en acier doux, rempli de béton armé.
Station d'Essais au Feu du CTICM à Maizières-les-Metz.

[3] FIRTO Technical Evaluation TE 6143
Fire resistance test in accordance with B.S. 476: Part 21 on a composite steel and reinforced concrete column (305 mm x 305 mm)
Borehamwood, January 1988.

[4] FIRTO Technical Evaluation TE 6144
Fire resistance test in accordance with B.S. 476: Part 21 on a composite steel and reinforced concrete column (356 mm x 368 mm)
Borehamwood, January 1988.

[5] ECCS-Technical Committee 3 - Fire Safety of Steel Structures - European Recommendations for the Fire Safety of Steel Structures. Elsevier Science Publishers B.V., Amsterdam 1983.

[6] Convention C.C.E. n° 7210-SA/505; Outils pratiques de dimensionnement pour poutrelles-colonnes en acier non protégé soumises à l'incendie. Rapport technique n° 1 (RT 1) March 1987.

[7] ARBED-Research Centre; Practical design tools for unprotected steel columns submitted to ISO-fire. C.E.C. Agreement n° 7210-SA/505, Technical Report n° 2, Luxembourg, October 1987.

[8] ARBED-Research Centre; Practical design tools for unprotected steel columns submitted to ISO-fire. C.E.C. Agreement n° 7210-SA/505, Technical Report n° 3, Luxembourg, March 1988.

[9] ARBED-Research Centre; Practical design tools for unprotected steel columns submitted to ISO-fire. C.E.C. Agreement n° 7210-SA/505, Technical Report n° 4, Luxembourg, September 1988.

[10] ARBED-Research Centre, Practical design tools for unprotected steel columns submitted to ISO-fire. C.E.C. Agreement n° 7210-SA/505, Technical Report n° 5, Luxembourg, February 1989.

[11] Fire resistance tests - Elements of building construction; International Standard ISO 834, first edition, 1975.

[12] FRANSSEN J.-M.; Etude du comportement au feu des structures mixtes acier-béton. Thèse de Doctorat. Université de Liège, Février 1987.

[13] RUBERT A., SCHAUMANN P.: Temperaturabhängige Werkstoffeigenschaften von Baustahl bei Brandbeanspruchung. Der Stahlbau 54, Heft 3, S. 8186, 1985.

[14] RUBERT A.: Experimentelle Untersuchungen zum Brandverhalten kompletter, ebener Rahmensysteme aus Baustahl, Forschungsbericht zur Teilaktivität 3.2 des Vorhabens Bau 6004/P86, Studiengesellschaft für Anwendungstechnik von Eisen und Stahl e.V., Düsseldorf, durchgeführt im KRUPP Forschungsinstitut Essen, 1984 (Teil 1 und Teil 2).

[15] Amtliche Materialprüfanstalt für das Bauwesen - Institut für Baustoffe, Massivbau und Brandschutz - Technische Universität Braunschweig: Untersuchungsbericht Nr 1618/8510 vom 04.12.1988.

[16] Laboratorium voor Aanwending der Brandstoffen en Warmte-overdracht - Rijkuniversiteit Gent. Rapports d'essais N^{os} 5871, 5872, 5873 et 5874.

[17] DIN 18800 Teil 2; Stahlbauten: Stabilitätsfälle, Knicken von Stäben und Stabwerken. Deutsche Norm. Entwurf Dezember 1980.

[18] C.E.C.; Industrial processes - Building and Civil Engineering EUROCODE N° 3: common unified rules for steel structures. EUR 8849, Bruxelles - Luxembourg 1984.

[19] EURONORM 25-72: Aciers de construction d'usage général. - Novembre 1972.

[20] ARBED - StE 460 FRITENAR: Hochfester Feinkornbaustahl für Profile. Luxembourg, February 1989.

[21] ARBED-Research Centre; Practical design tools for composite steel-concrete construction elements, submitted to ISO-fire, considering the interaction between axial load N and bending moment M. C.E.C. Research 7210-SA/504, Final Report, Luxembourg, August 1989.

[22] SCHLEICH J.B.; Numerische Simulation - Zukunftsorientierte Vorgehensweise zur Feuersicherheitsbeurteilung von Stahlbauten. Der Maschinenschaden 60 (1987) Heft 4. Allianz Versicherungs AG, München.

[23] SCHLEICH J.B.; Numerical simulations, the forthcoming approach in fire engineering design of steel structures. Revue Technique n° 2 1987.

[24] SCHLEICH J.B.; "Global Behaviour of Steel Structures in Fire." Building in Steel - International Symposium in Stratford-upon-Avon, September 1989.

C.E.C. AGREEMENT

N° 7210-SA/505

FIGURES

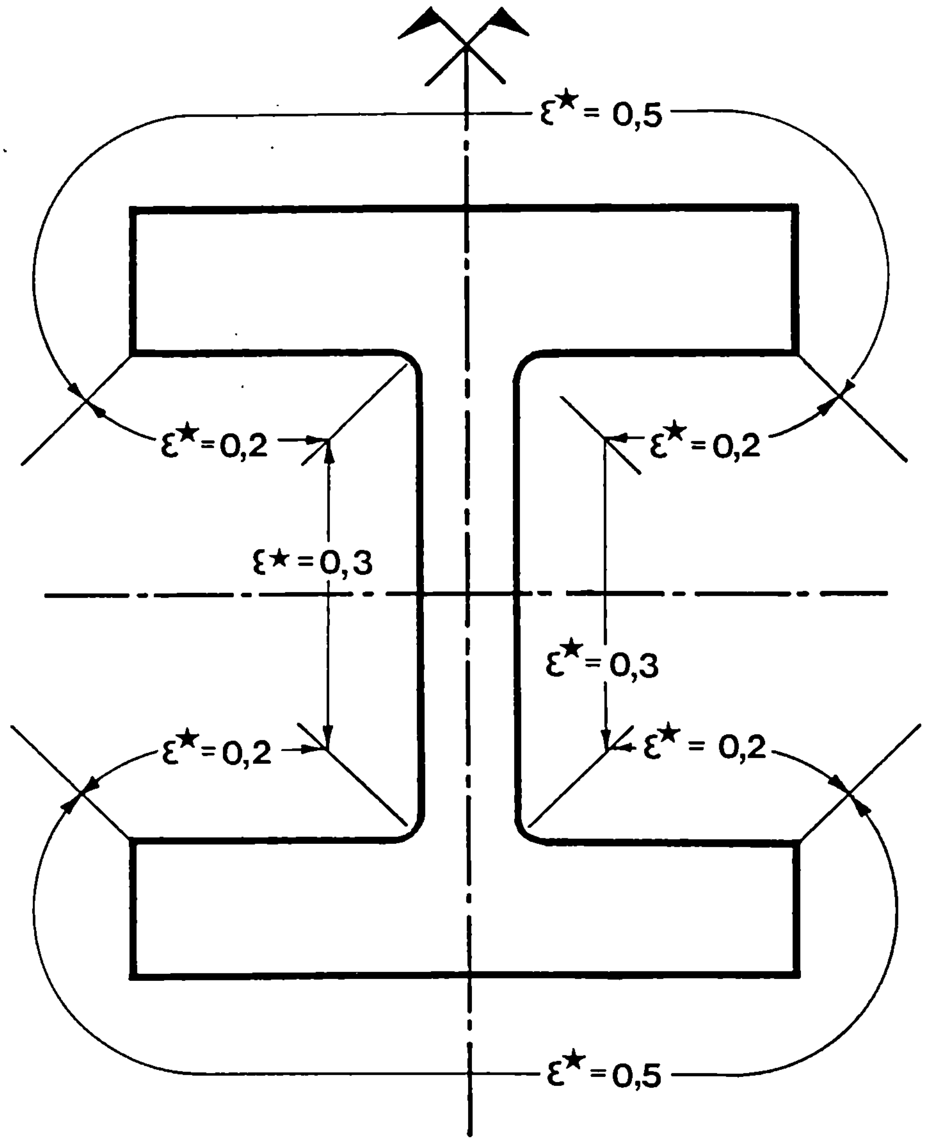

Resultant emissivity ε★ chosen for the numerical simulation of the column test 1.1.

Figure 2.1

PARAMETRIC MATERIAL LAWS

$$\begin{Bmatrix}\lambda \\ C\end{Bmatrix} = A_1 + A_2\left(\frac{\theta}{100}\right) + A_3\left(\frac{\theta}{100}\right)^2$$

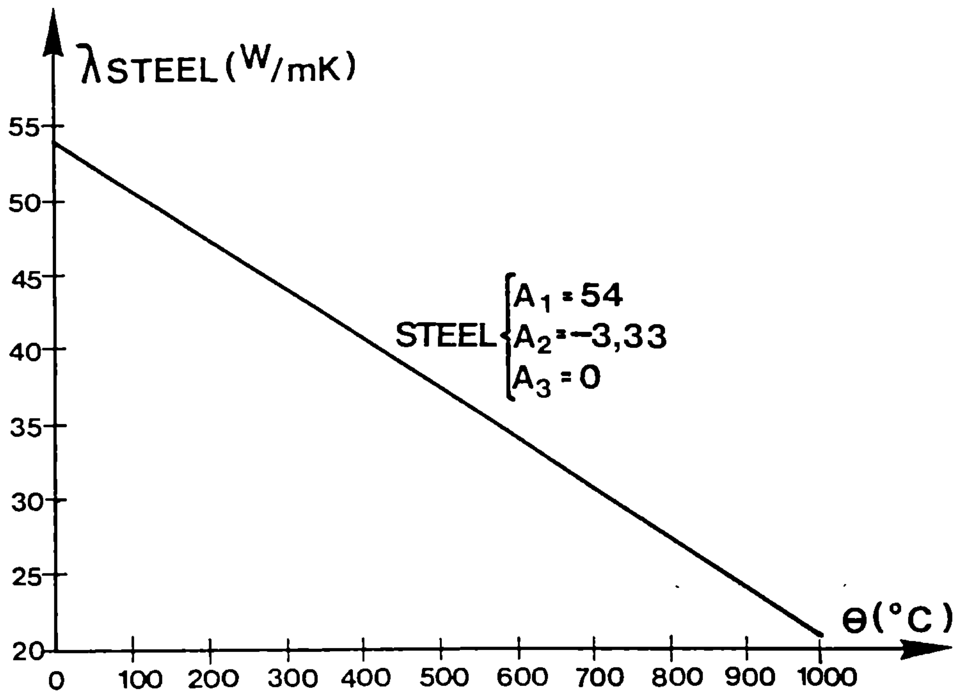

Figure 2.2 : THERMAL CONDUCTIVITY

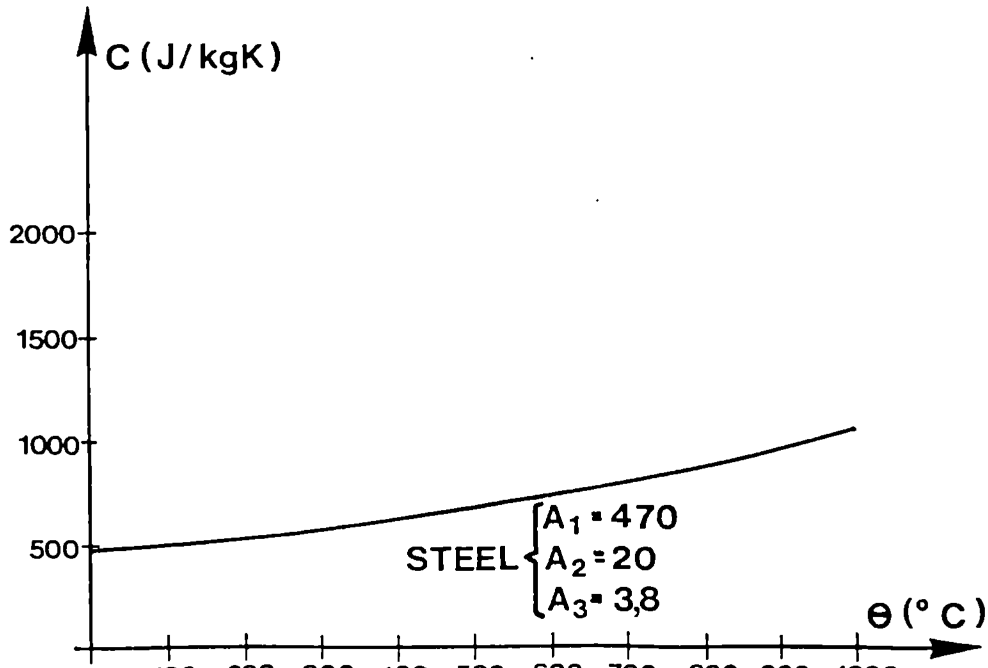

Figure 2.3 : SPECIFIC HEAT

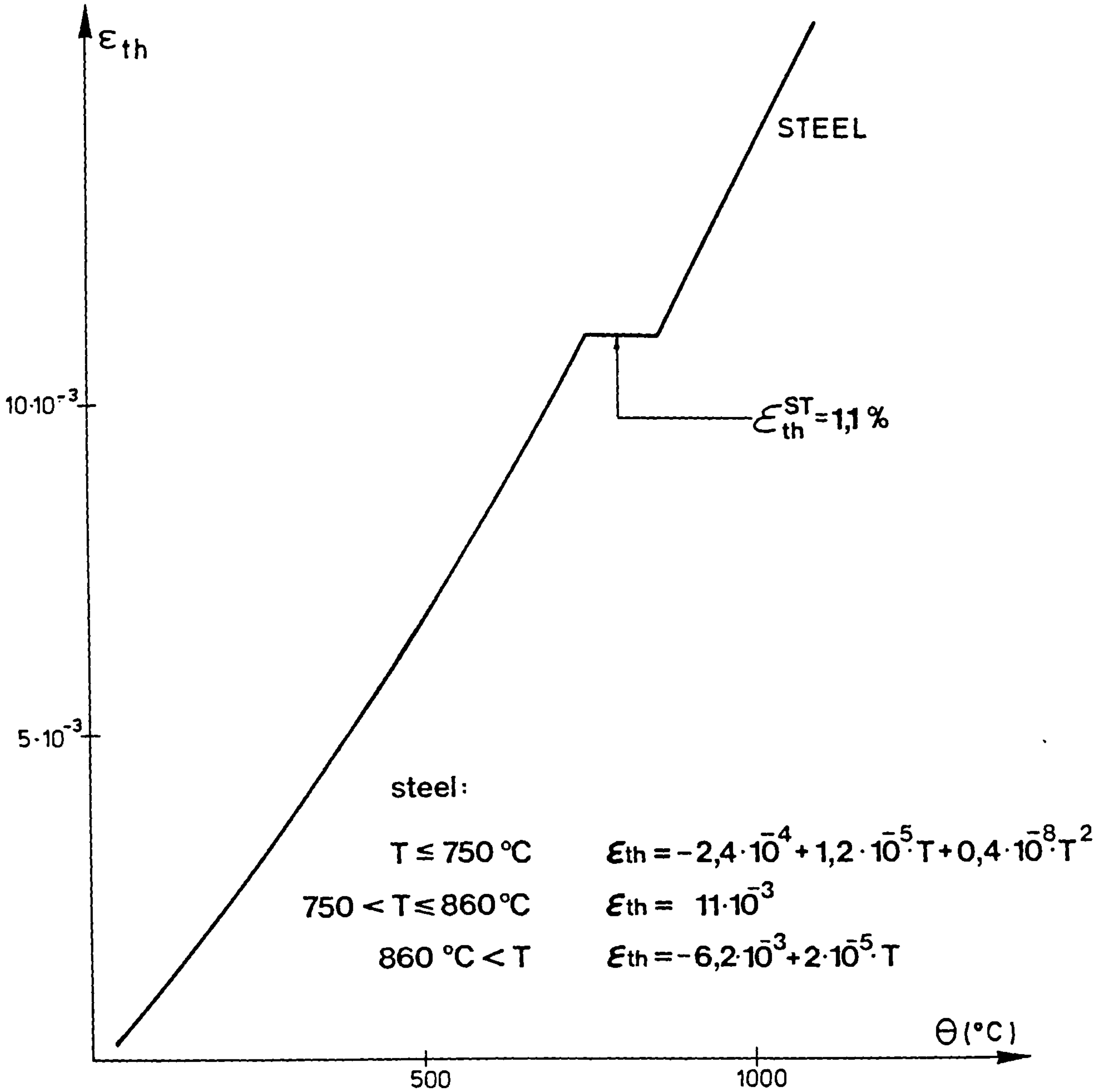

Figure 2.4 : Thermal expansion.

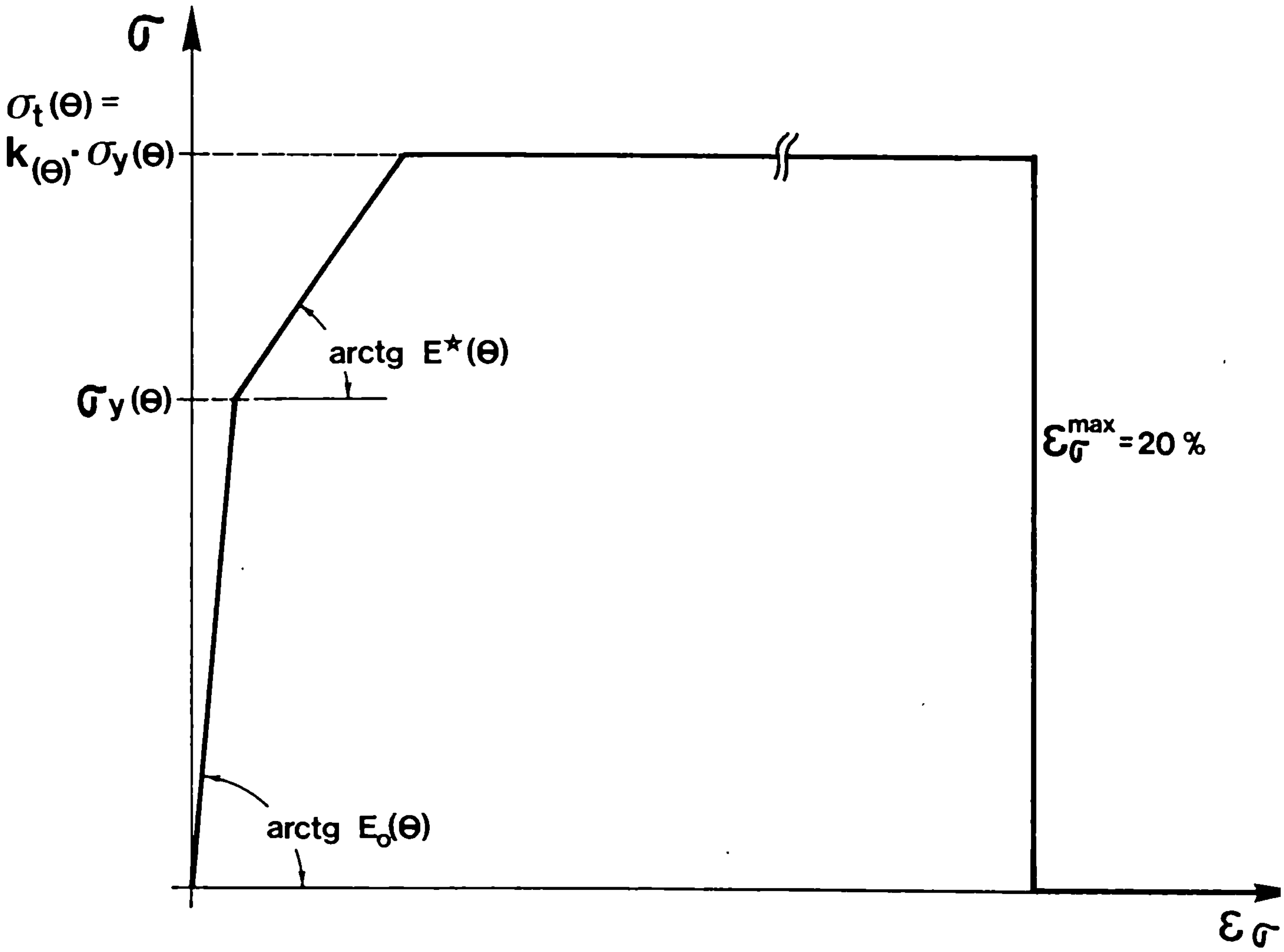

Fig. 3.1 : General σ-ε_σ diagram for steel.
Factor k has been chosen equal to 1.5
for figures 3.5 and 3.6.

$$\Theta \leq 100° ; \quad \frac{\sigma_{y,\Theta}}{\sigma_{y,20°}} = 1$$

$$100° < \Theta \leq 500° ; \quad \frac{\sigma_{y,\Theta}}{\sigma_{y,20°}} = 2{,}95 \cdot 10^{-3} \left(\frac{\Theta}{100}\right)^3 - 4{,}88 \cdot 10^{-2} \left(\frac{\Theta}{100}\right)^2 + 8{,}87 \cdot 10^{-2} \frac{\Theta}{100} + 0{,}957$$

$$500° < \Theta \leq 1200° ; \quad \frac{\sigma_{y,\Theta}}{\sigma_{y,20°}} = -4{,}21 \cdot 10^{-4} \left(\frac{\Theta}{100}\right)^3 + 2{,}344 \cdot 10^{-2} \left(\frac{\Theta}{100}\right)^2 - 0{,}3806 \frac{\Theta}{100} + 1{,}919$$

$$\Theta > 1200 °C ; \quad \frac{\sigma_{y,\Theta}}{\sigma_{y,20°}} = 0$$

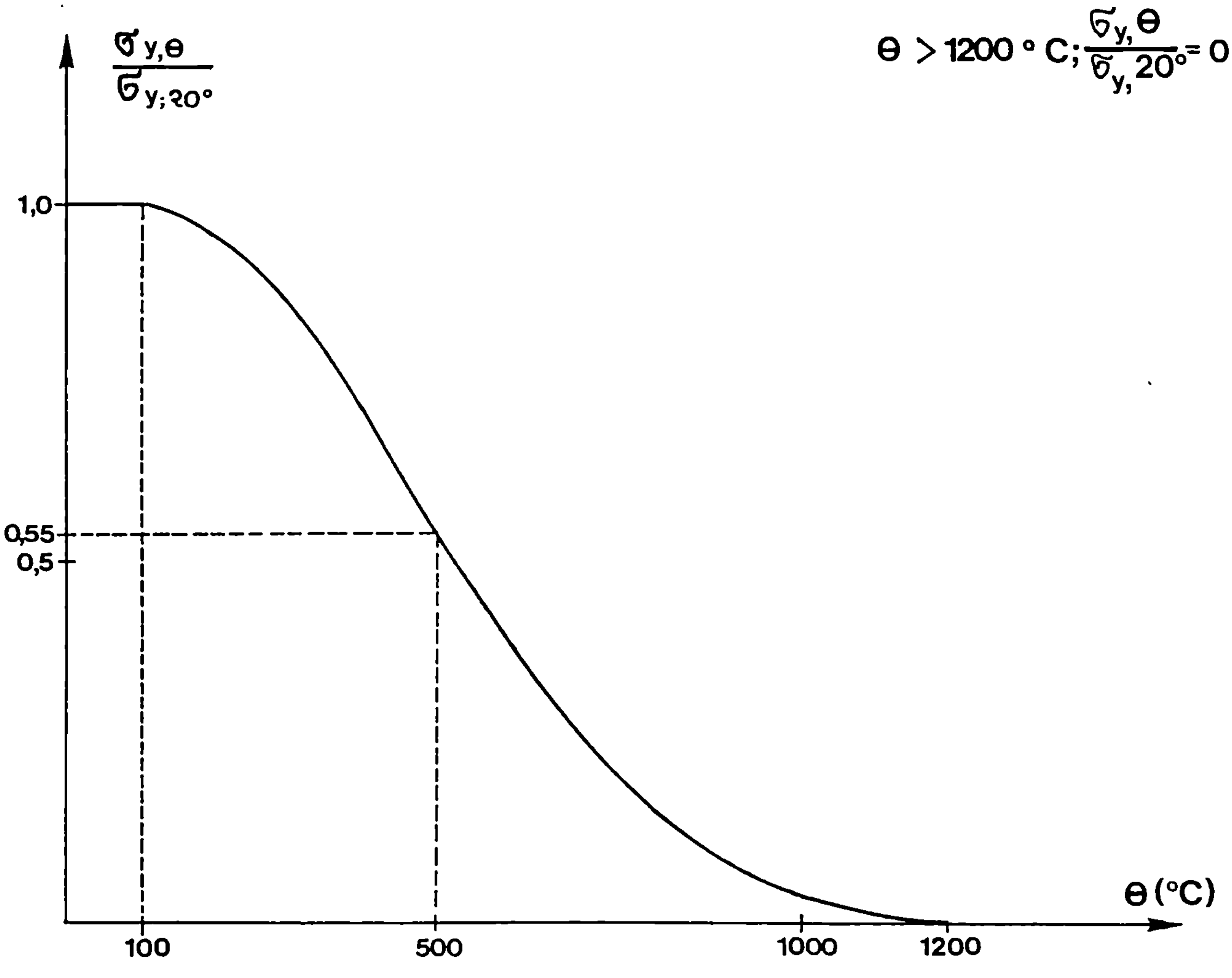

Fig.3.2 : Reduction of the yield point of steel σ_y in function of temperature Θ.

$$\theta \leqslant 100°; \quad \frac{E_{0,\theta}}{E_{0,20°}} = 1$$

$$100° < \theta < 600°; \quad \frac{E_{0,\theta}}{E_{0,20°}} = -0{,}018\left(\frac{\theta}{100}\right)^2 + 0{,}036\,\frac{\theta}{100} + 0{,}982$$

$$600° < \theta < 1200°; \quad \frac{E_{0,\theta}}{E_{0,20°}} = 9{,}25926 \cdot 10^{-5}\left(\frac{\theta}{100}\right)^3 + 0{,}0125\left(\frac{\theta}{100}\right)^2 - 0{,}34\,\frac{\theta}{100} + 2{,}12$$

$$1200° < \theta; \quad \frac{E_{0,\theta}}{E_{0,20°}} = 0$$

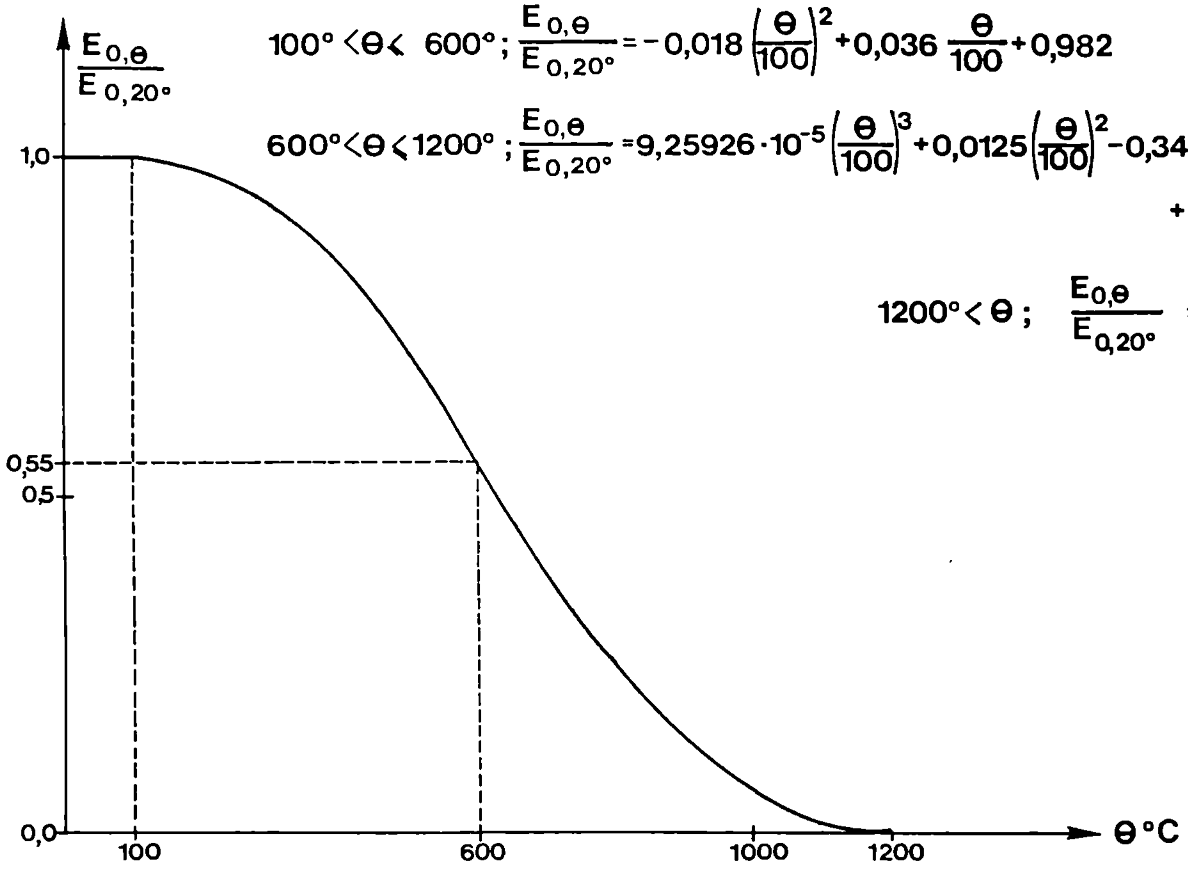

Fig. 3.3 : Reduction of the elastic modulus E_0 of steel in function of the temperature.

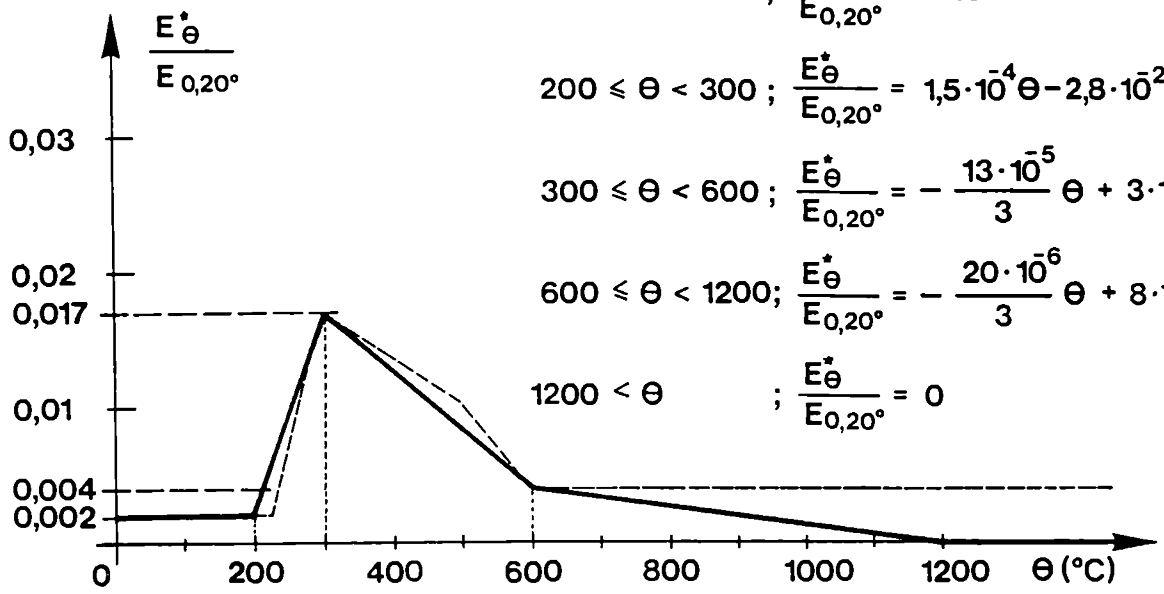

$$\Theta < 200 \; ; \; \frac{E^*_\Theta}{E_{0,20°}} = 2 \cdot 10^{-3}$$

$$200 \leq \Theta < 300 \; ; \; \frac{E^*_\Theta}{E_{0,20°}} = 1{,}5 \cdot 10^{-4}\Theta - 2{,}8 \cdot 10^{-2}$$

$$300 \leq \Theta < 600 \; ; \; \frac{E^*_\Theta}{E_{0,20°}} = -\frac{13 \cdot 10^{-5}}{3}\Theta + 3 \cdot 10^{-2}$$

$$600 \leq \Theta < 1200 \; ; \; \frac{E^*_\Theta}{E_{0,20°}} = -\frac{20 \cdot 10^{-6}}{3}\Theta + 8 \cdot 10^{-3}$$

$$1200 < \Theta \; ; \; \frac{E^*_\Theta}{E_{0,20°}} = 0$$

Fig. 3.4 : Variation of the elastic modulus E^* of steel in function of the temperature.

- - - - - - - - - "according to Anderberg"

———————— included in CEFICOSS

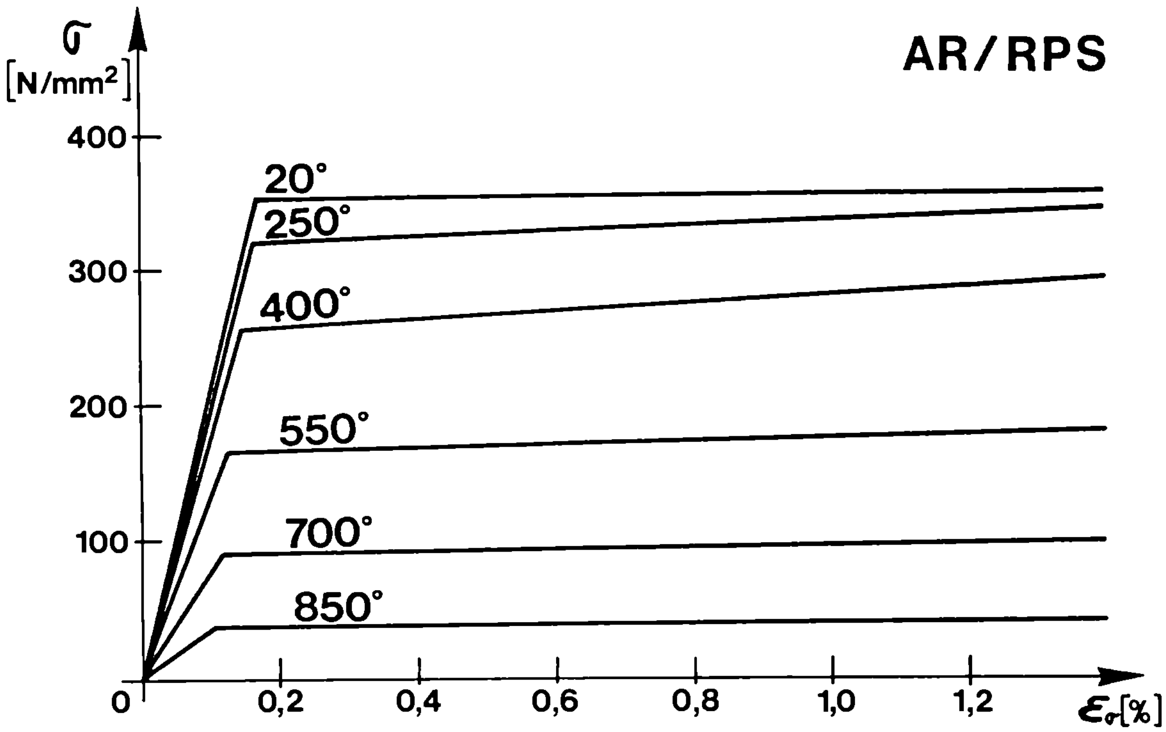

Fig. 3.5 : σ-ε_σ-diagram for Fe 510 at different temperatures.

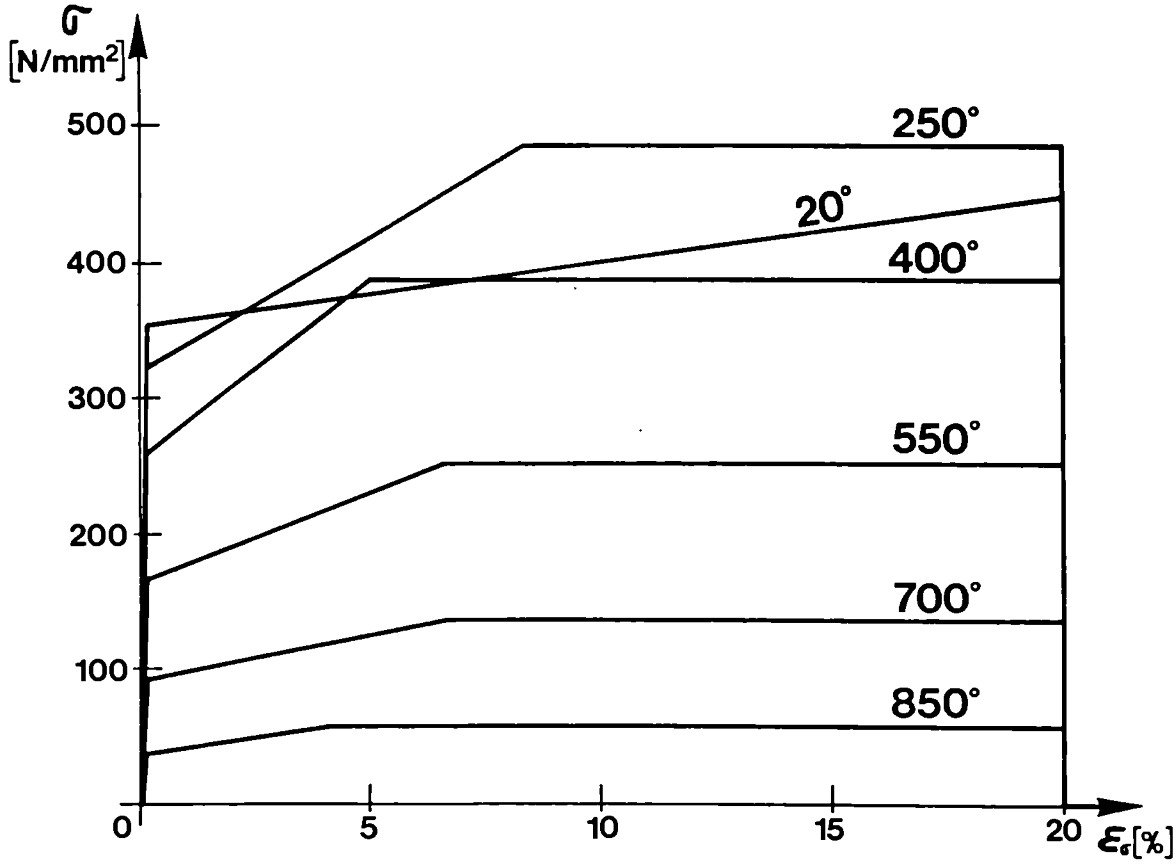

Fig. 3.6 : σ-ε_σ-diagram for Fe 510 at different temperatures with elongations ε_σ shown up to 20 %.

KRUPP TESTS 1984

REFERENCES [13] and [14]

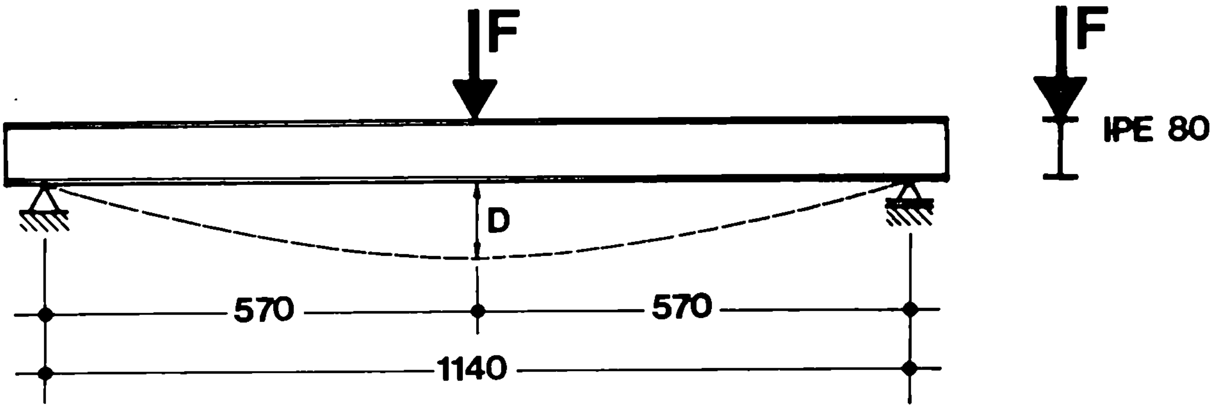

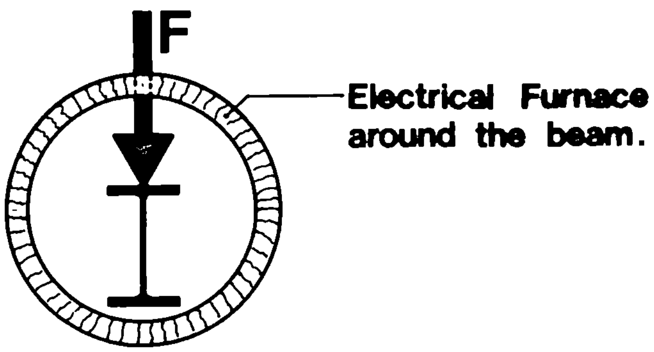

Figure 3.7

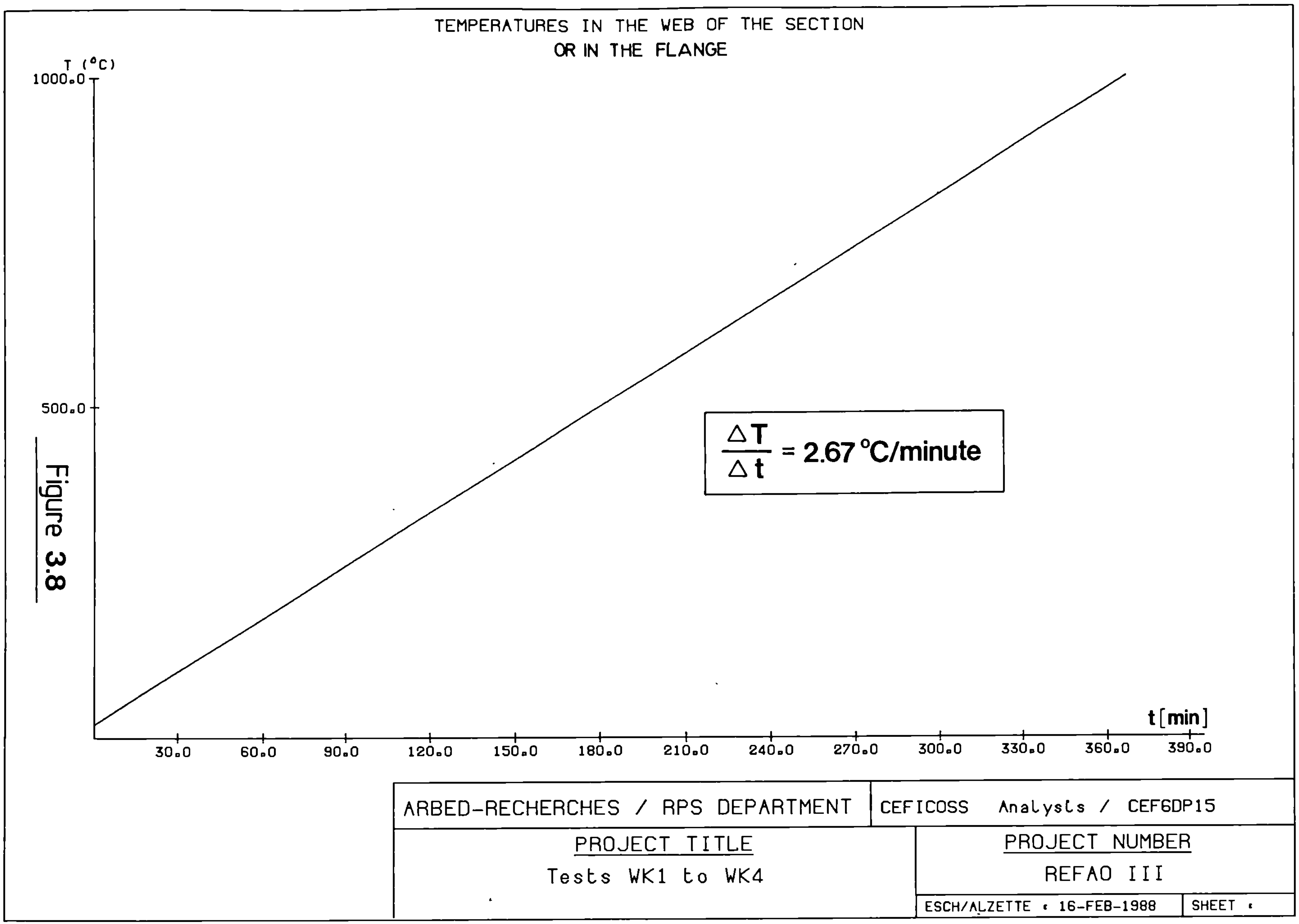
TEMPERATURES IN THE WEB OF THE SECTION
OR IN THE FLANGE
T (°C)
1000.0
500.0
$\frac{\Delta T}{\Delta t}$ = 2.67 °C/minute
t [min]
30.0
60.0
90.0
120.0
150.0
180.0
210.0
240.0
270.0
300.0
330.0
360.0
390.0
ARBED-RECHERCHES / RPS DEPARTMENT
CEFICOSS Analysis / CEF6DP15
PROJECT TITLE
Tests WK1 to WK4
PROJECT NUMBER
REFAO III
ESCH/ALZETTE : 16-FEB-1988
SHEET :

Figure 3.8

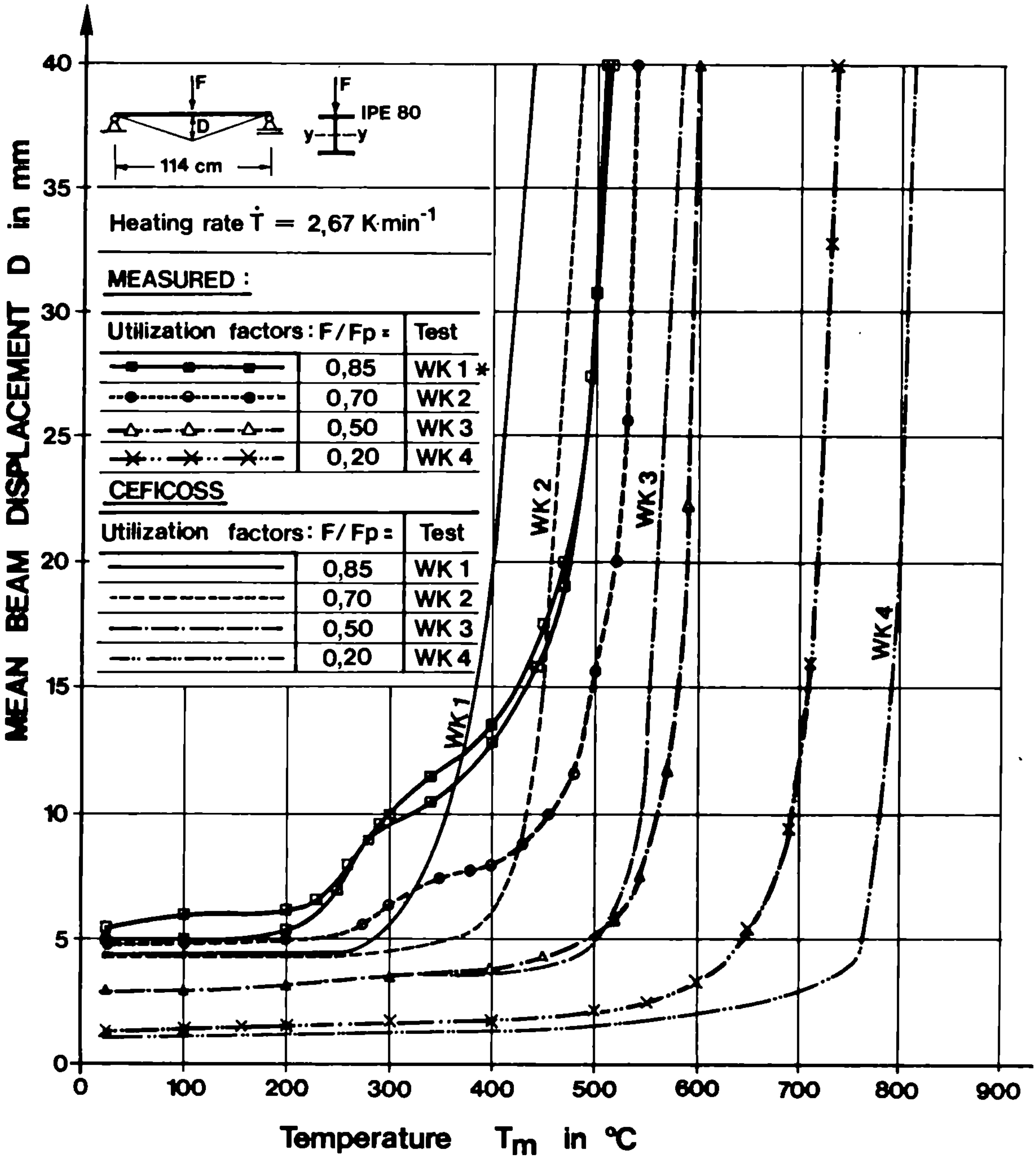

Tests : WK 1 to WK 4

Temperature dependent beam displacements as a function of utilization factor F/Fp (mean heating velocity Tm = 2,67 K/min).

* note : the test WK1 has been performed two times.

Figure 3.9

KRUPP TESTS 1988 FOR ARBED

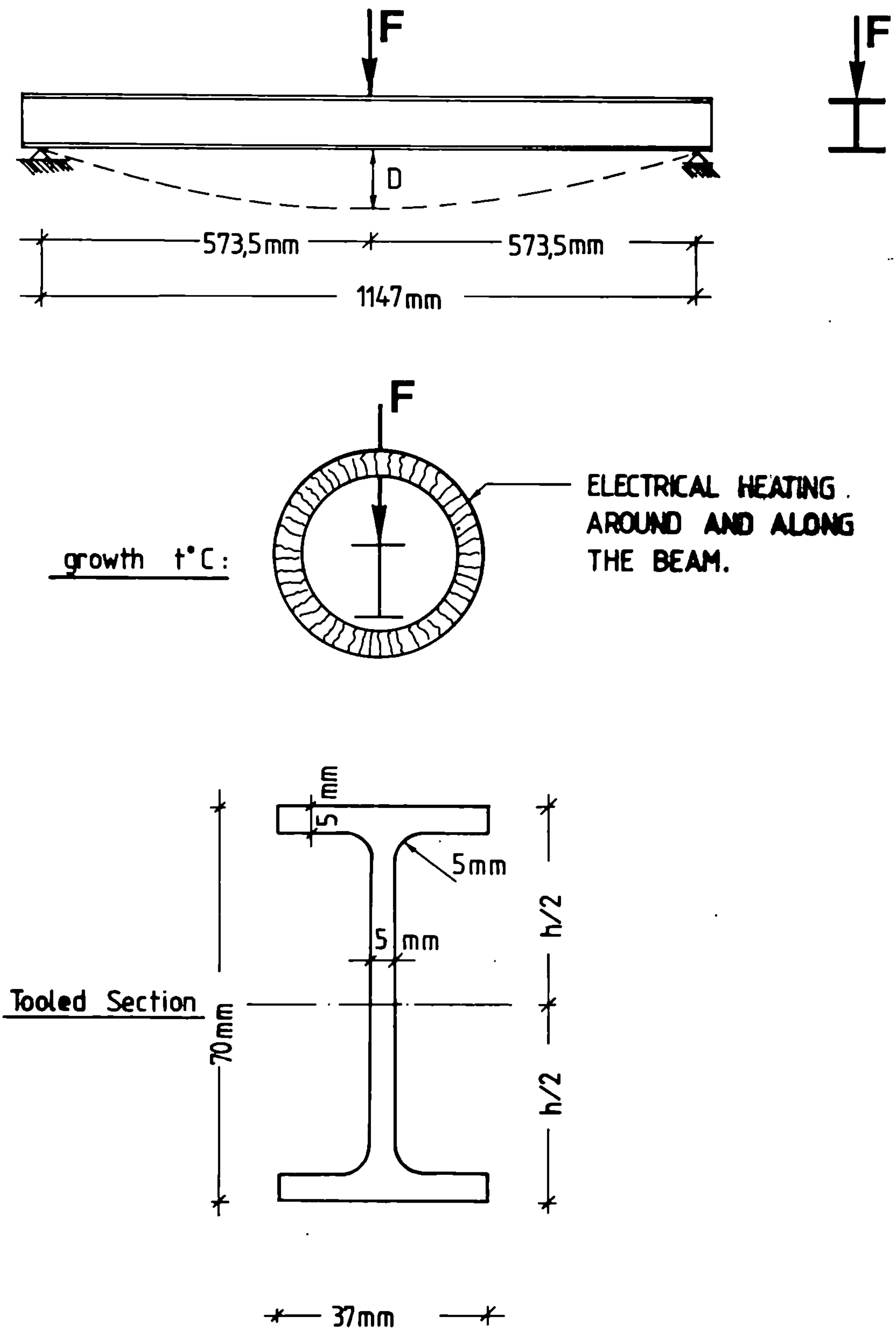

Figure 4.1

TOOLING OF I-BEAMS 70x40x5x5

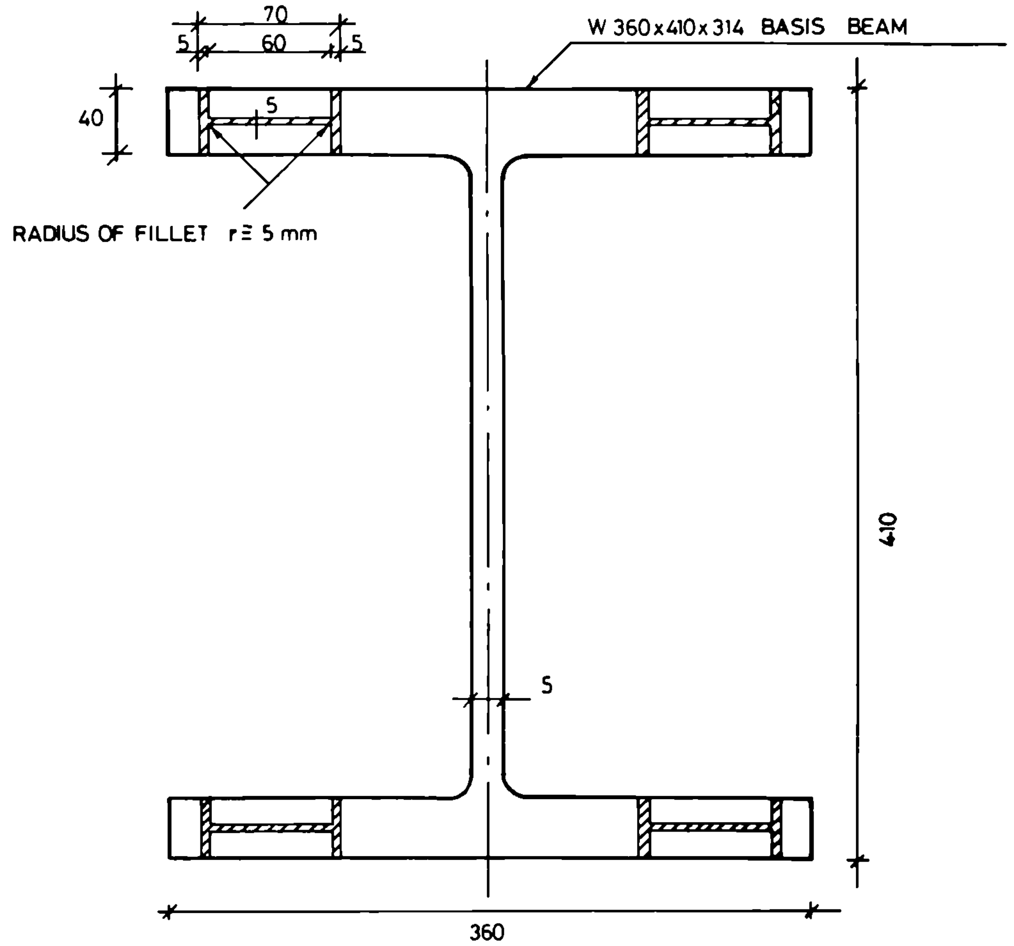

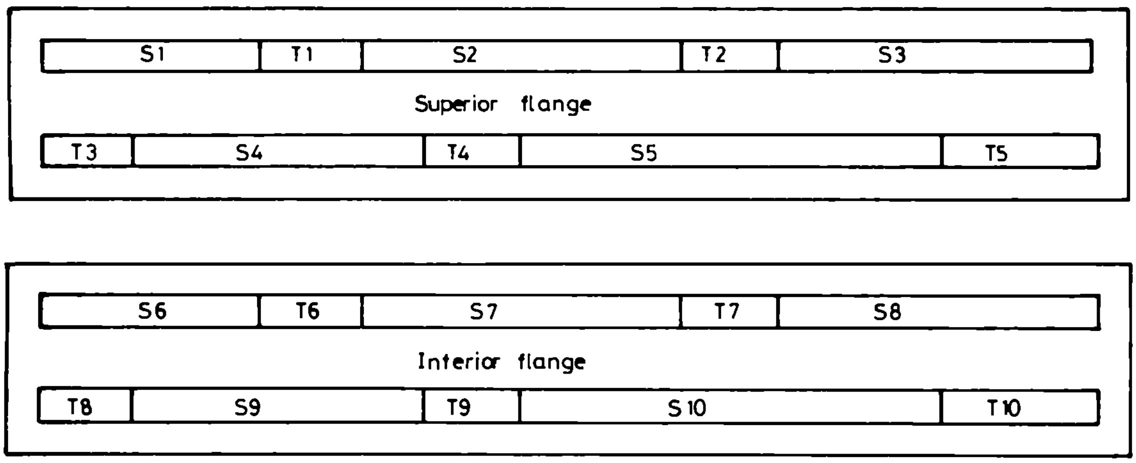

Positions of test pieces

S= beams for transient state bending tests
T= bars for tensile tests

Figure 4.2

Krupp transient state beam tests parameters (S1 to S10)

TEST	R_{eH} [N/mm^2]	F_{PCOLD} [kN]	F [kN]	F/F_{PCOLD}	$\dot{\theta}_m$ [K/min]	θ_{init} [°C]	$(\theta_m)_{max}$ [°C]	$(D_{mes})_{max}$ [mm]	$(t_{test})_{max}$ [min]	
S1	502	30.0	30.0	1.00	3.6	22.1	461	85.8	121	(1)
S2	504.5	30.2	22.7	0.75	3.4	22.5	525	53.9	146	(2)
S3	507	30.3	25.8	0.85	3.5	21.7	497	53.2	137	(2)
S4	516	30.8	18.5	0.60	3.5	21.4	566	53.1	155	(2)
S5	513	30.7	12.3	0.40	3.5	21.0	651	87.5	182	(2)
S6	529	31.6	2.4	0.075	3.4	31.2	828	87.8	235	(2)
S7	526	31.4	3.2	0.10	3.5	28	813	86.9	227	(2)
S8	523	31.3	37.65	1.2	/	/	/	75.0	/	(3)
S9	523.5	31.3	6.3	0.20	3.5	22.4	713	54.1	198	(2)
S10	522.5	31.2	15.6	0.50	3.4	20.1	605	83.2	175	(2)

REMARKS : (1) after cold loading before the heating the middle-span section is already fully plastified.

(2) after cold loading before the heating the middle-span section is partially plastified or still elastic

(3) only cold loading - unloadings.

Figure 4.3

RUBERT-SCHAUMANN LAW (RS-LAW)

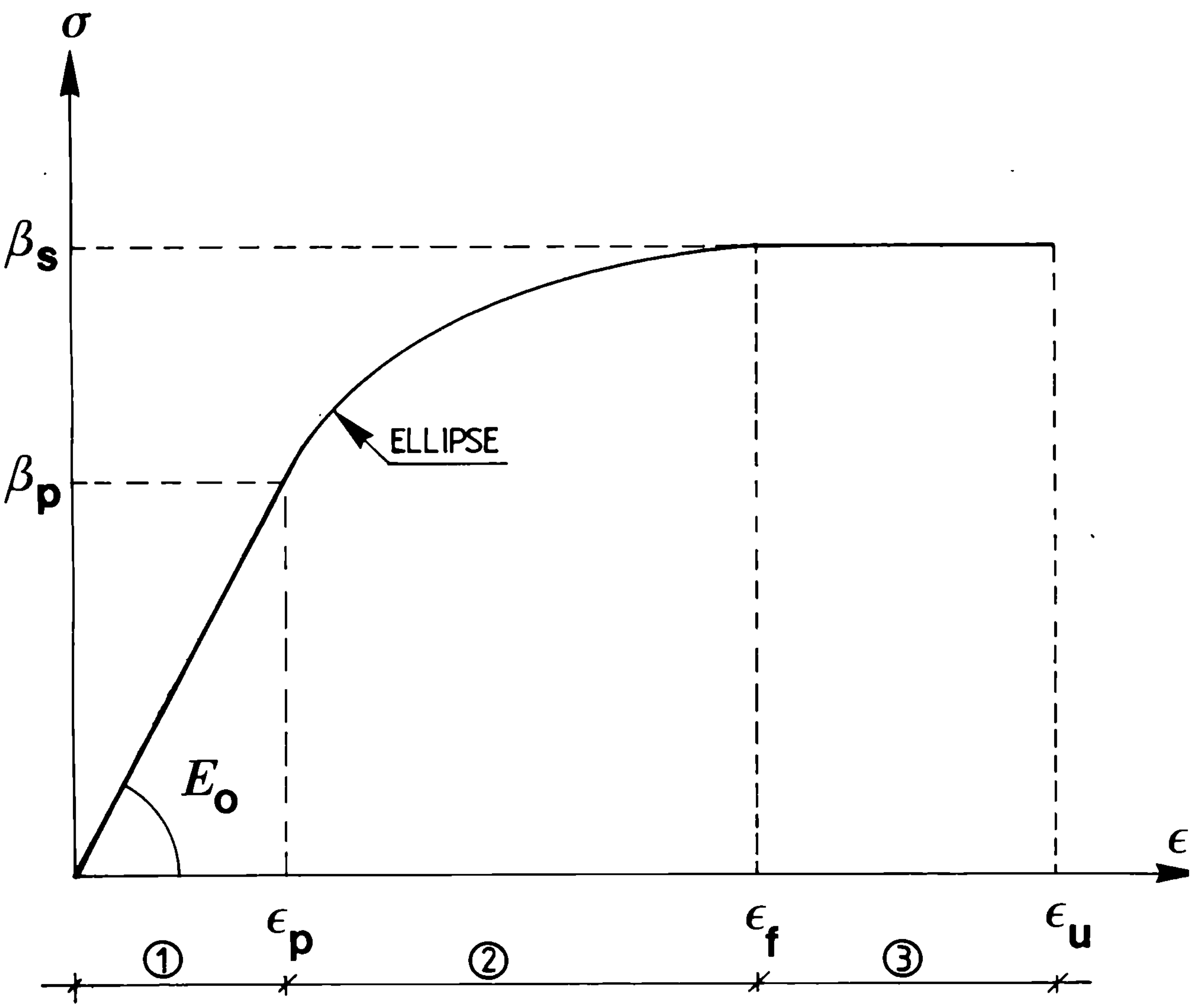

$\epsilon_p = \beta_p(\theta) / E_o(\theta)$

$\epsilon_f = 2\%$

$\epsilon_u = 20\%$

$\beta_{p(\theta=20^\circ C)} = \beta_{s(\theta=20^\circ C)}$

① ELASTIC DOMAIN

② ELASTO-PLASTIC DOMAIN

③ PLASTIC DOMAIN

Figure 4.4

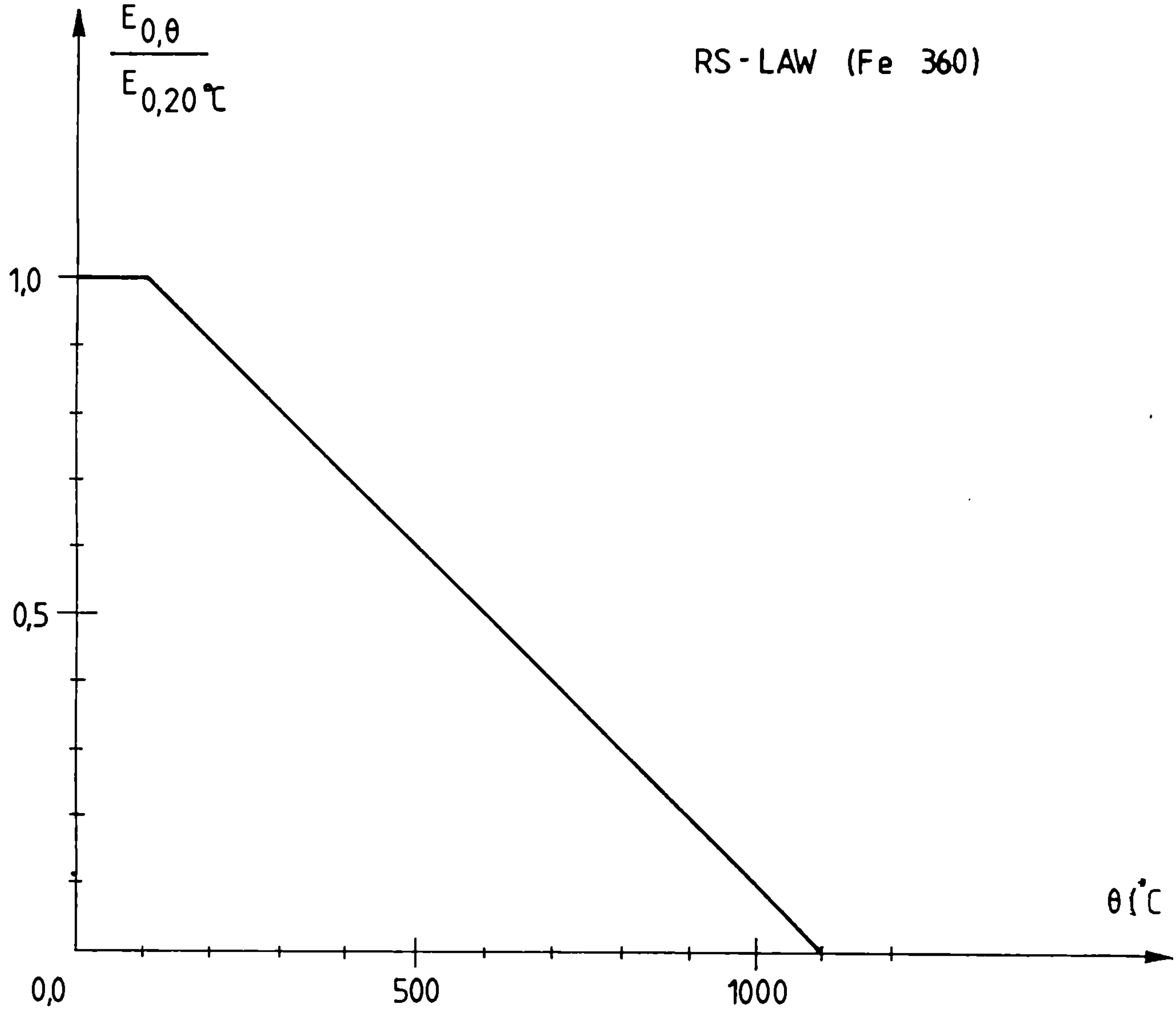

θ (°C)	20	100	200	300	400	500	600	700	800	900	1000	1100	1200
$\frac{E_{0,\theta}}{E_{0,20°C}}$	1,0	1,0	0,9	0,8	0,7	0,6	0,5	0,4	0,3	0,2	0,1	0,0	0,0

Figure 4.5

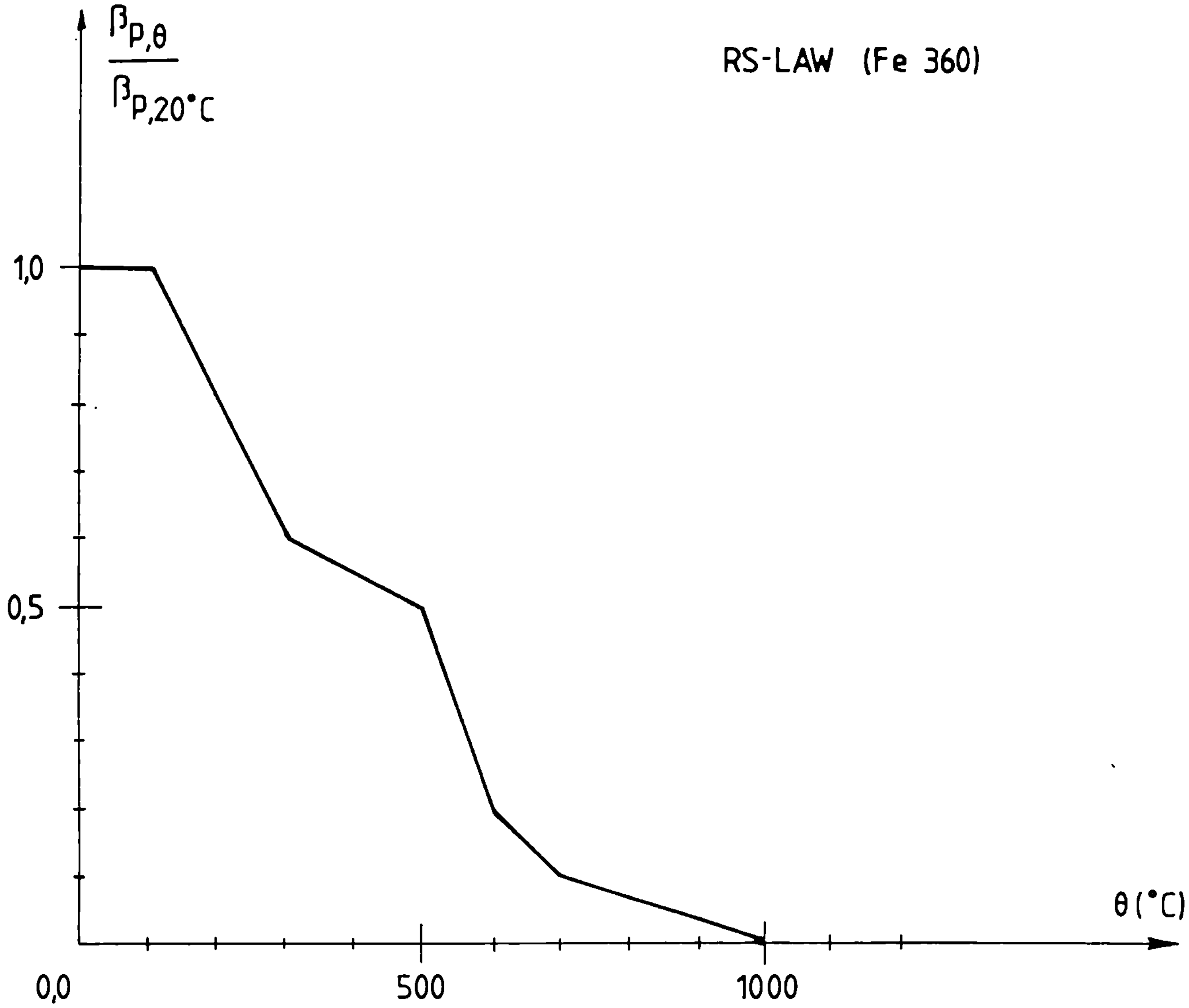

θ (°C)	20	100	200	300	400	500	600	700	800	900	1000	1100	1200
$\frac{\beta_{p,\theta}}{\beta_{p,20°C}}$	1,0	1,0	0,8	0,6	0,55	0,5	0,2	0,1	0,067	0,033	0,0	0,0	0,0

Figure 4.6

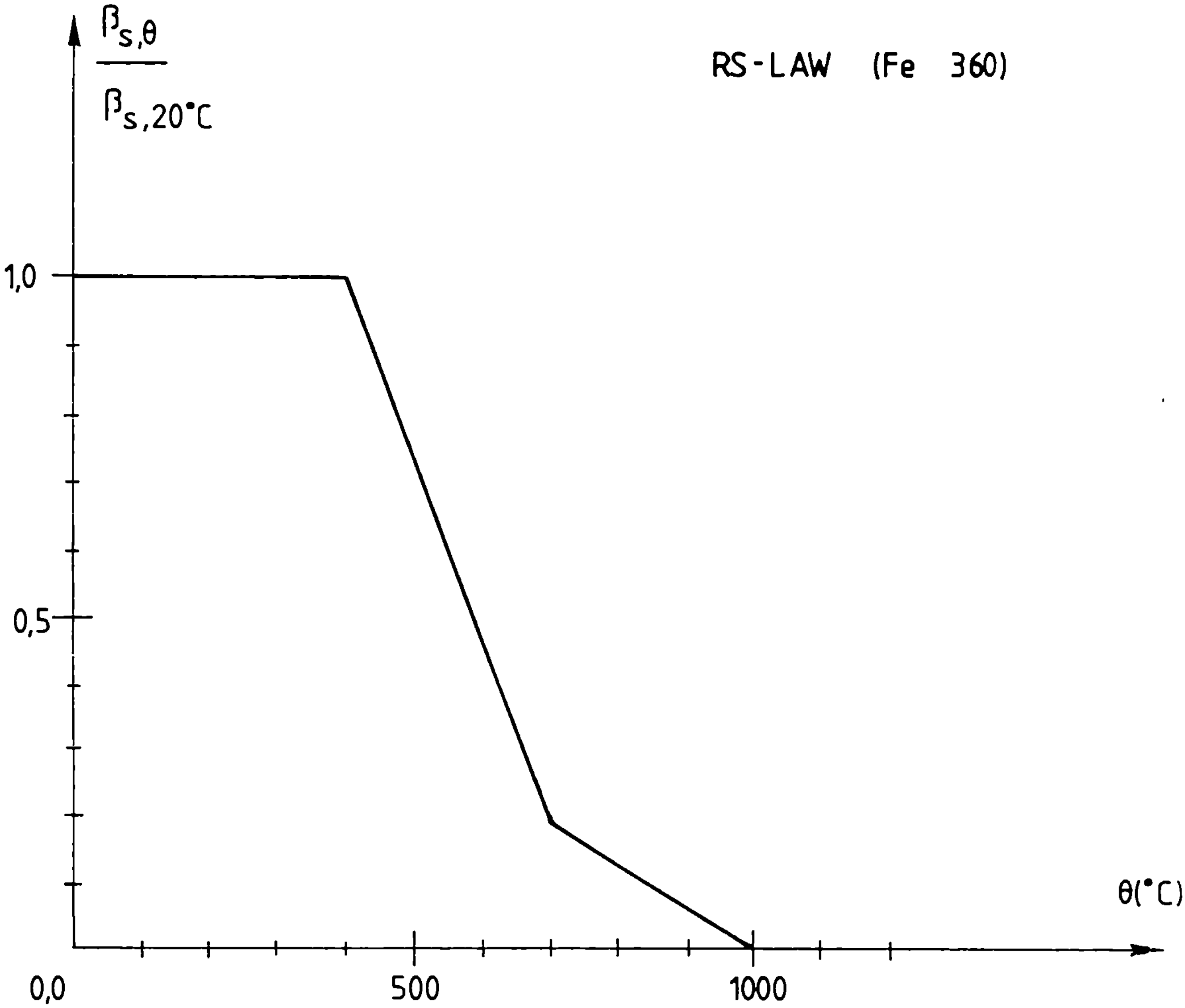

θ (°C)	20	100	200	300	400	500	600	700	800	900	1000	1100	1200
$\frac{\beta_{s,\theta}}{\beta_{s,20°C}}$	1,0	1,0	1,0	1,0	1,0	0,74	0,47	0,2	0,13	0,07	0,0	0,0	0,0

Figure 4.7

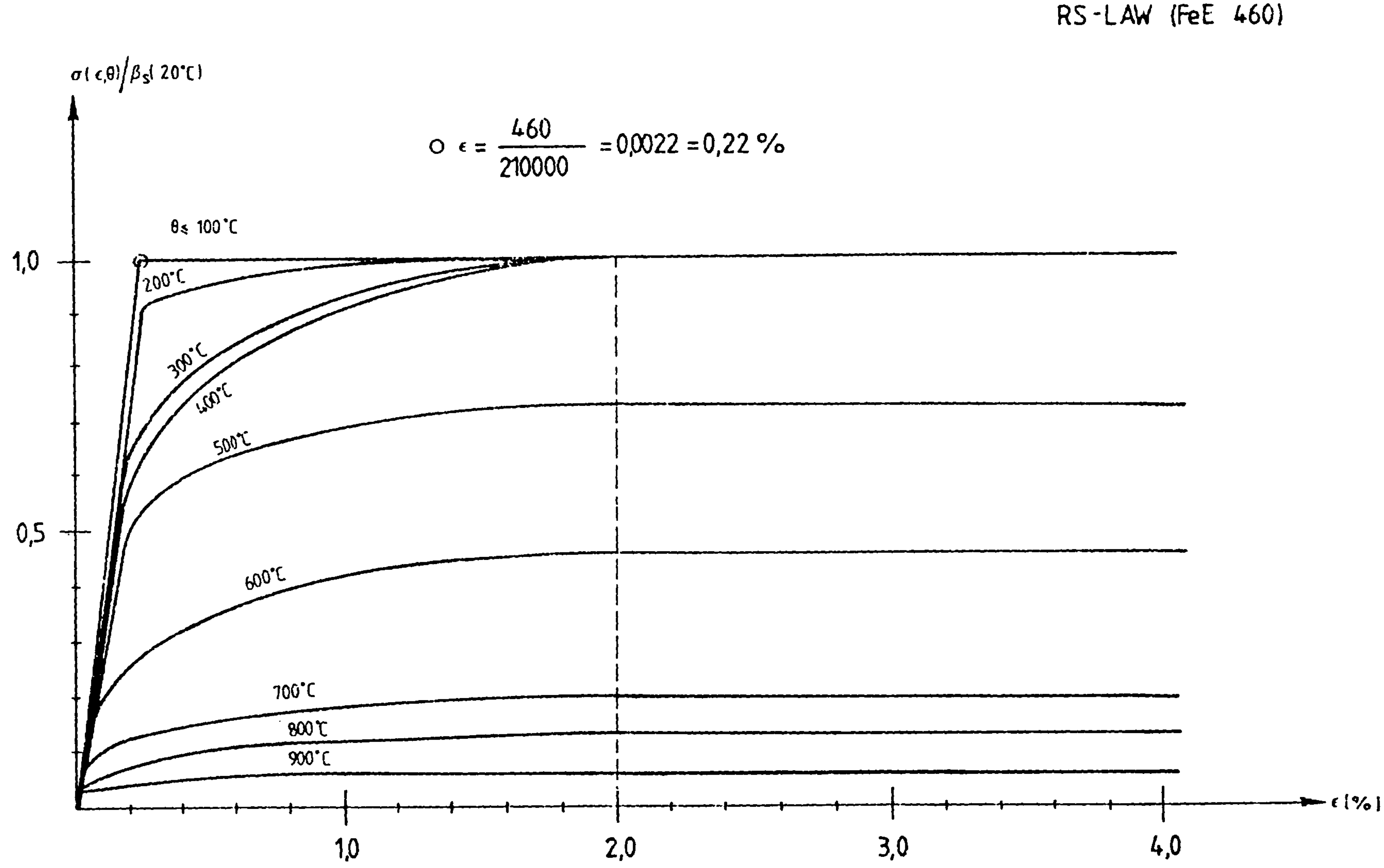
RS-LAW (FeE 460)
σ(ε,θ)/β_S(20°C)
○ ε = 460/210000 = 0,0022 = 0,22 %
θ ≤ 100°C
200°C
300°C
400°C
500°C
600°C
700°C
800°C
900°C
1,0
0,5
1,0
2,0
3,0
4,0
ε [%]

Figure 4.8

TYPE OF QUADRILINEAR LAW (Q.L)

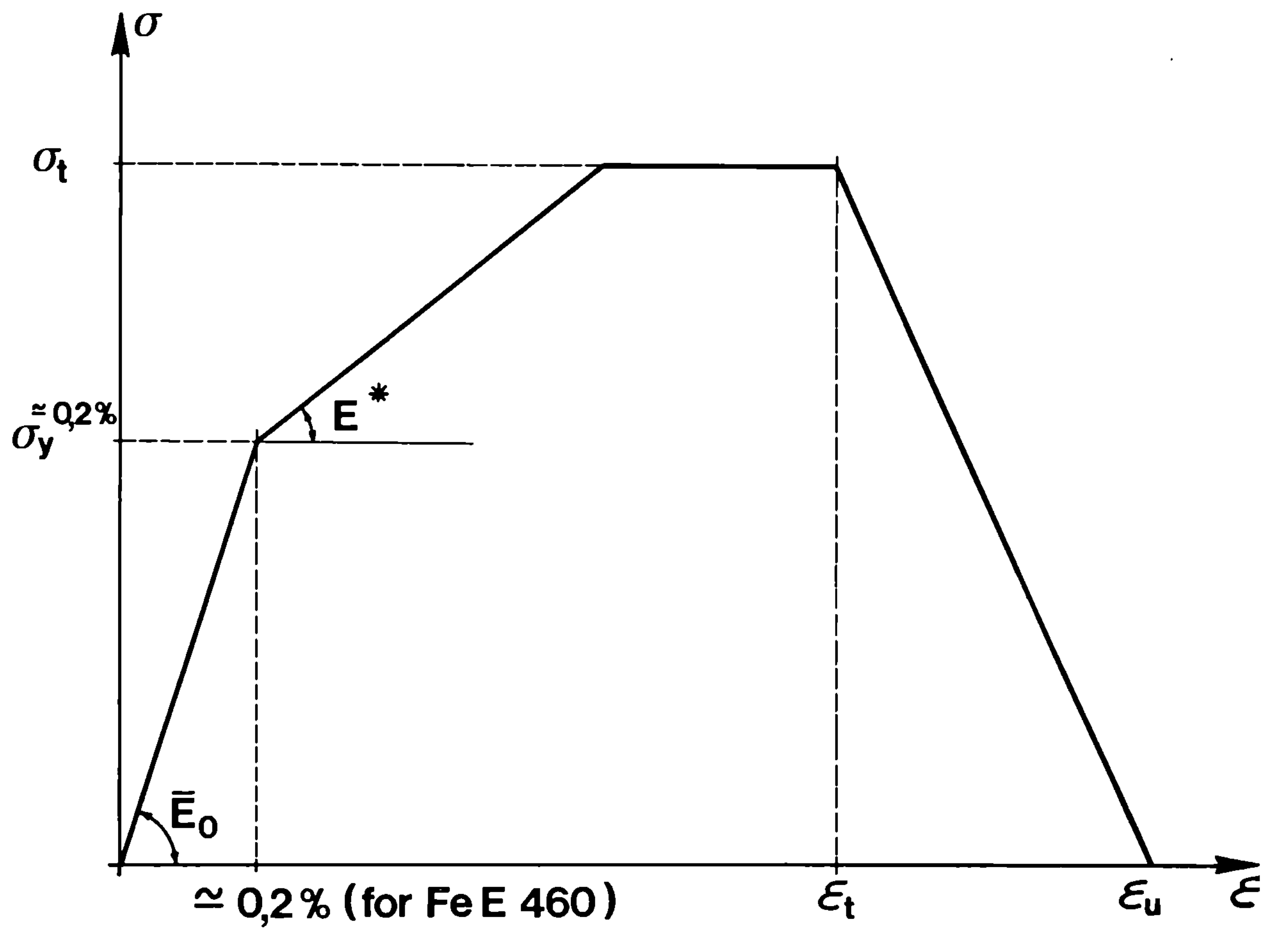

$$(\bar{E}_0\ ;\ \tilde{\sigma}_y^{0,2\%};E^*;\quad \sigma_t) \quad = \quad f(\Theta)$$

$$\varepsilon_t = 15\ \%$$

$$\varepsilon_u = 25\ \%$$

FIGURE 4.9

KRUPP TESTS 1988 FOR ARBED

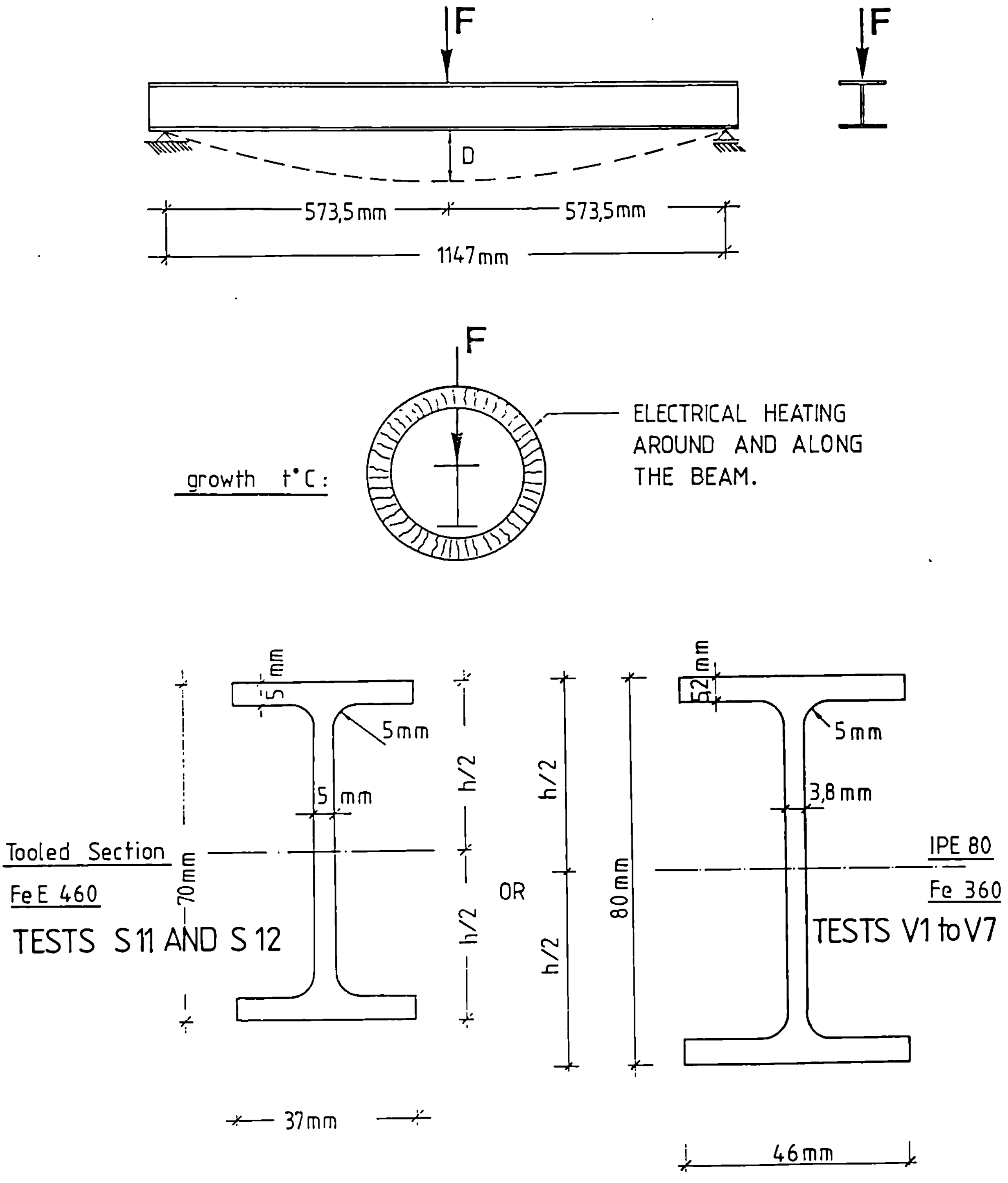

Figure 4.10

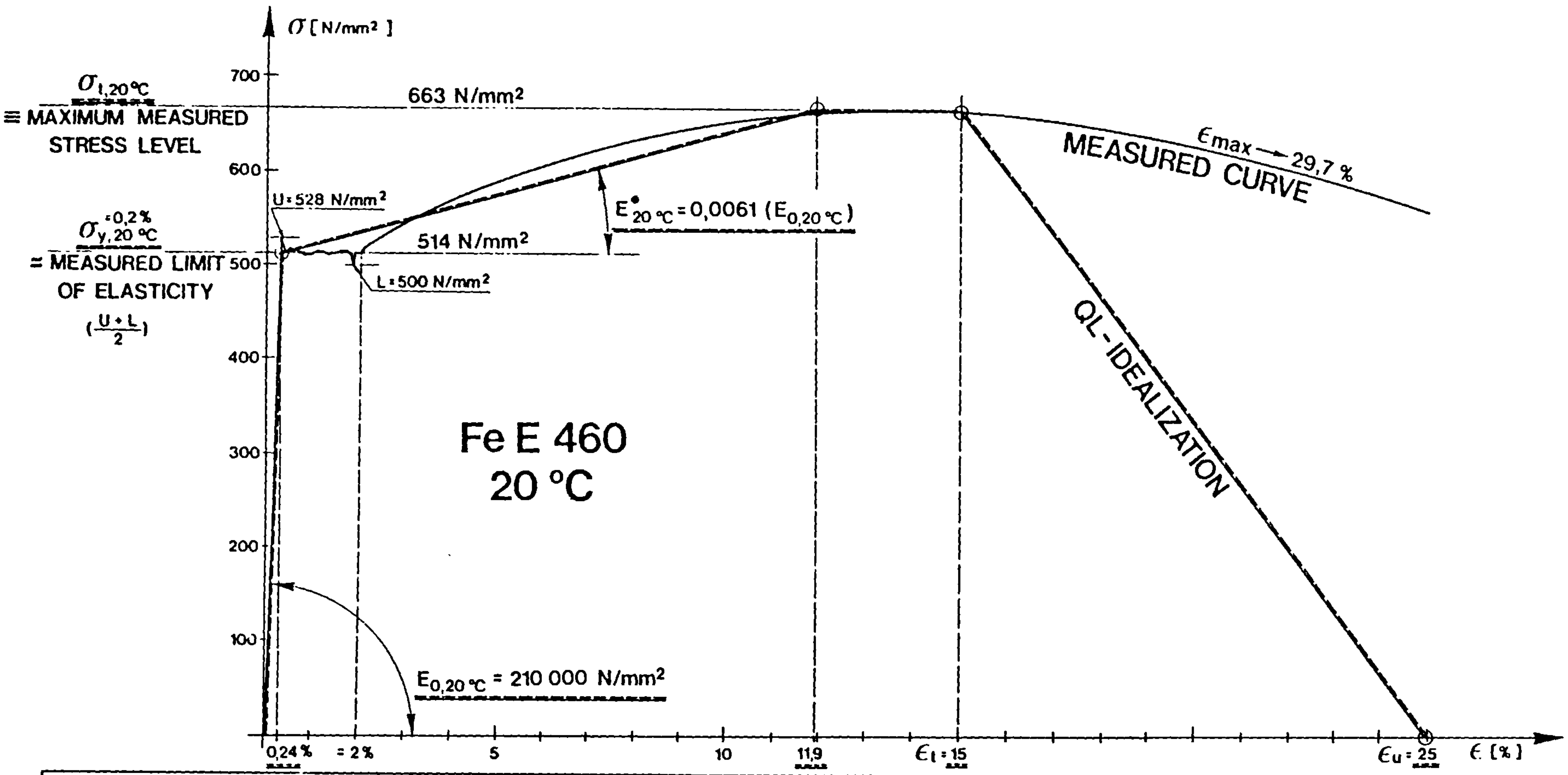

STEADY STATE TENSILE TEST at 20 °C	MULTILINEAR σ-ϵ IDEALIZATION
———— $\dot{\epsilon}$ = 0,2 % / minute up to $\epsilon \leq 2$ % $\dot{\epsilon}$ = 1 % / minute for $\epsilon > 2$ %	– – – – QUADRILINEAR LAW QL given by $E_{0,20\,°C}$ / $\sigma_{y,20\,°C}^{\pm 0,2\%}$ / $E^{\bullet}_{20\,°C}$ / $\sigma_{t,20\,°C}$

Figure 5.1

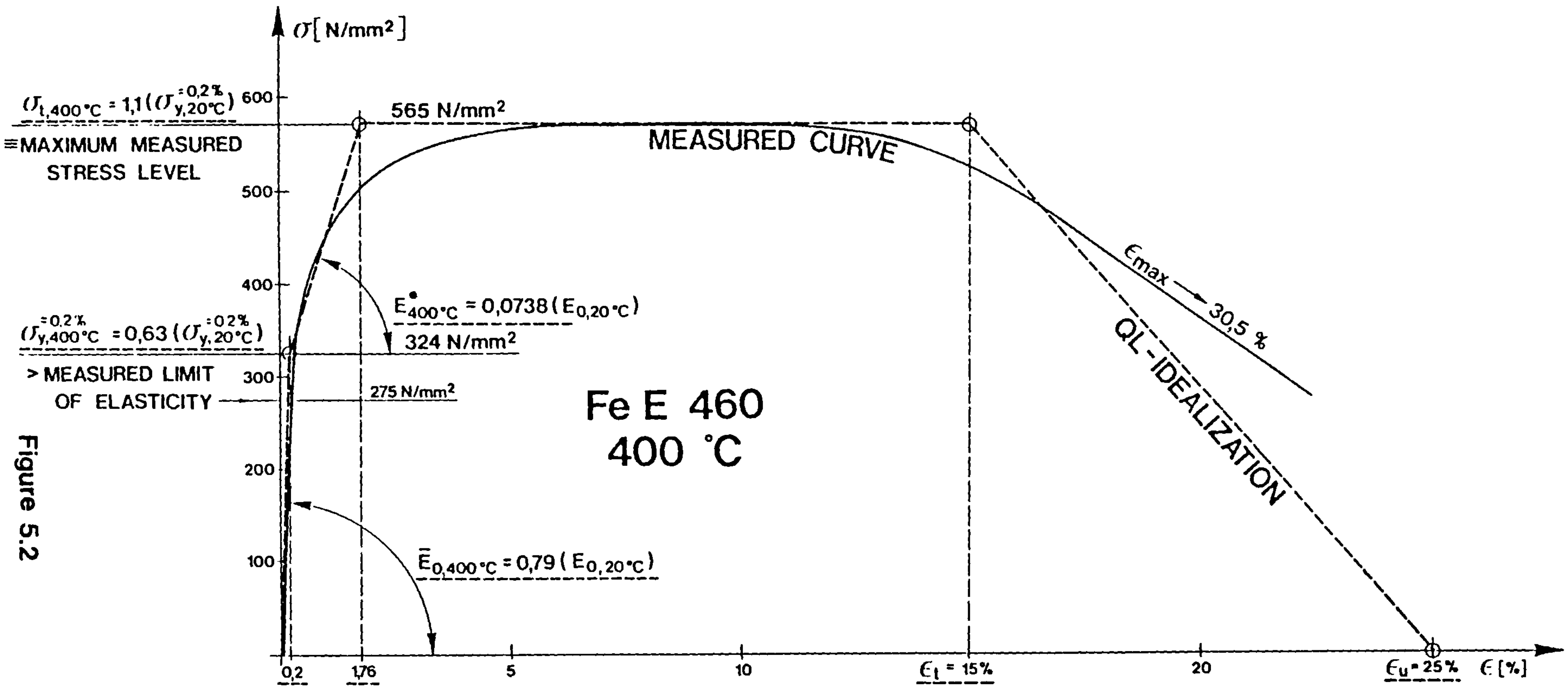

STEADY STATE TENSILE TEST at 400 °C	MULTILINEAR σ-ε IDEALIZATION
———— $\dot{\epsilon}$ = 0,2 %/minute up to $\epsilon \leq 2$ % $\dot{\epsilon}$ = 1 %/minute for $\epsilon > 2$ %	– – – – – QUADRILINEAR LAW QL given by $\bar{E}_{0,400°C}$ / $\sigma_{y,400°C}^{=0,2\%}$ / $E^{\bullet}_{400°C}$ / $\sigma_{t,400°C}$

Figure 5.2

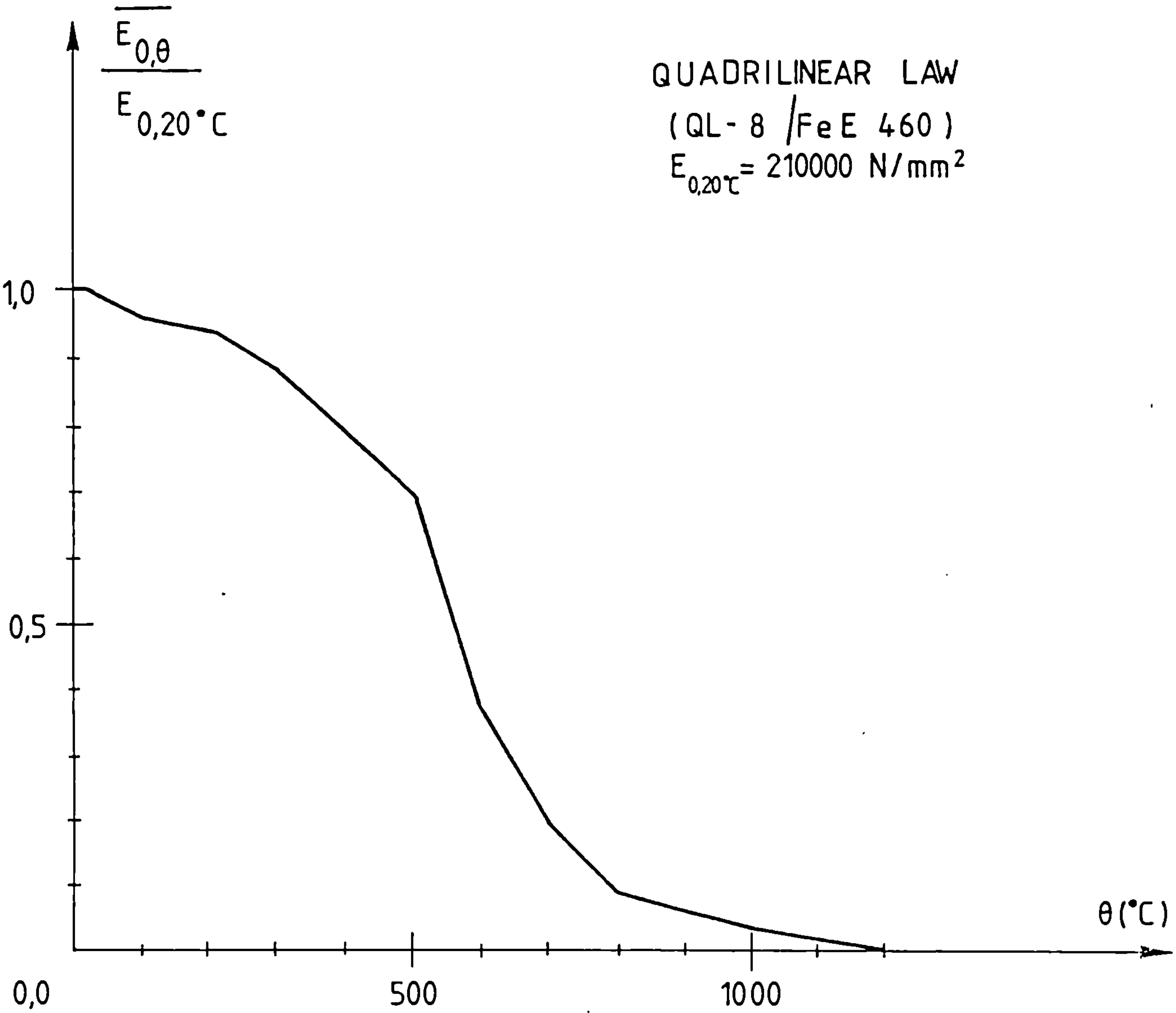

θ (°C)	20	100	200	300	400	500	600	700	800	900	1000	1100	1200
$\frac{E_{0,\theta}}{E_{0,20°C}}$	1,0	0,96	0,94	0,88	0,79	0,68	0,37	0,20	0,09	0,06	0,04	0,02	0,0

Figure 5.3

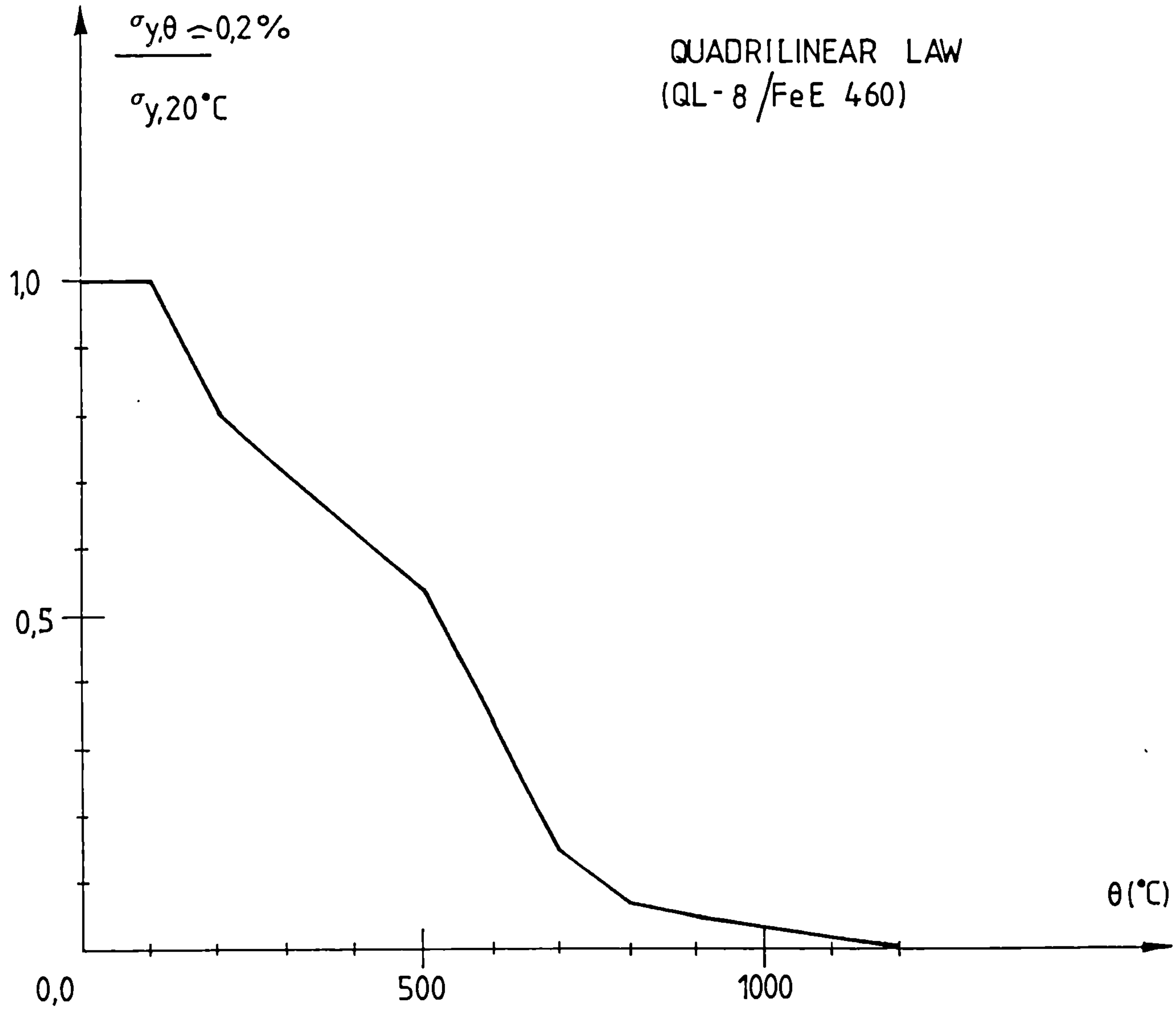

θ (°C)	20	100	200	300	400	500	600	700	800	900	1000	1100	1200
$\frac{\sigma_{y,\theta}}{\sigma_{y,20°C}}$	1,0	1,0	0,80	0,71	0,63	0,54	0,34	0,15	0,07	0,05	0,03	0,015	0,0

Figure 5.4

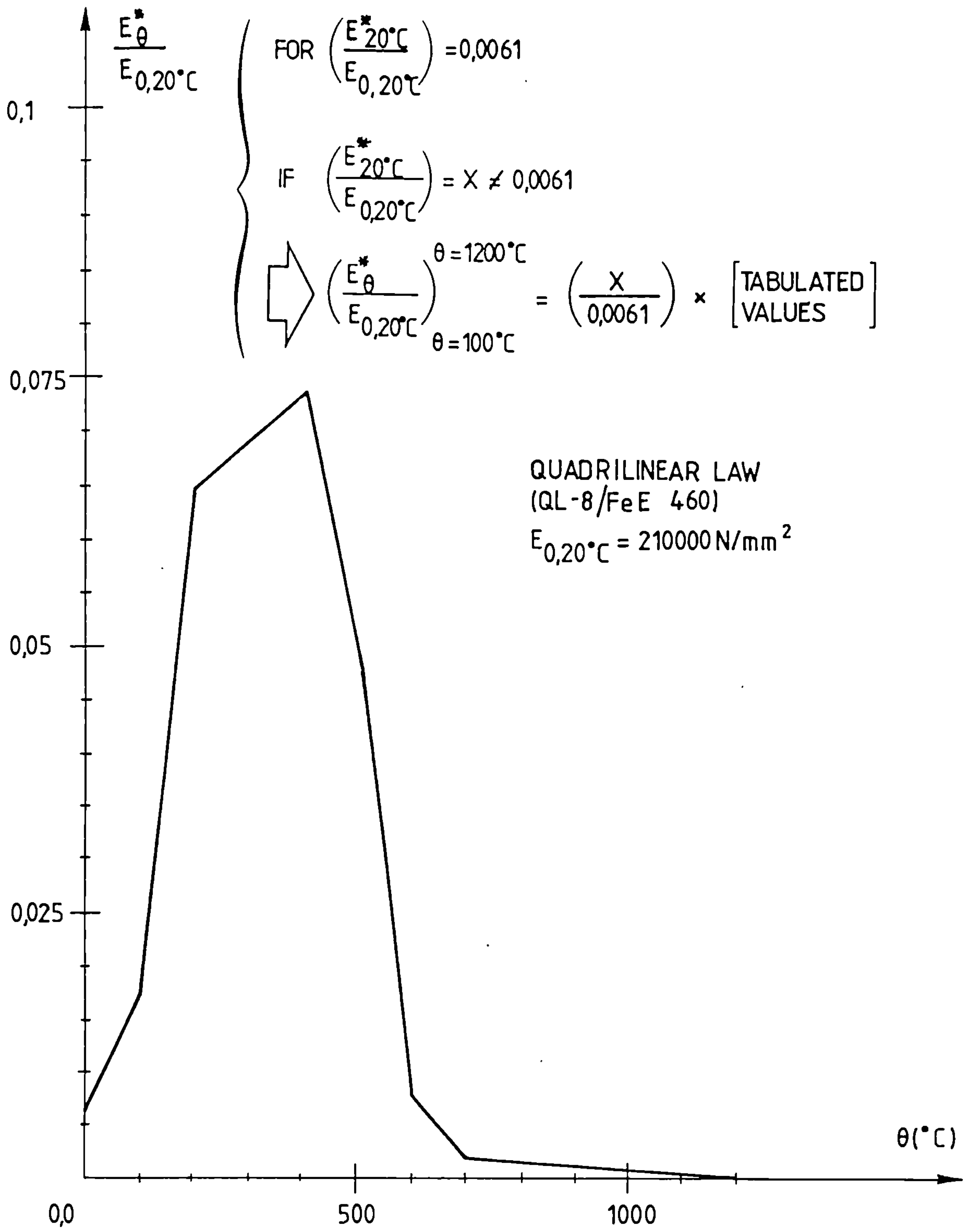

θ (°C)	20	100	200	300	400	500	600	700	800	900	1000	1100	1200
$\frac{E^*_\theta}{E_{0,20°C}}$	0,0061	0,0172	0,0646	0,0692	0,0738	0,0477	0,0078	0,0016	0,0013	0,0011	0,0008	0,0005	0,0

Figure 5.5

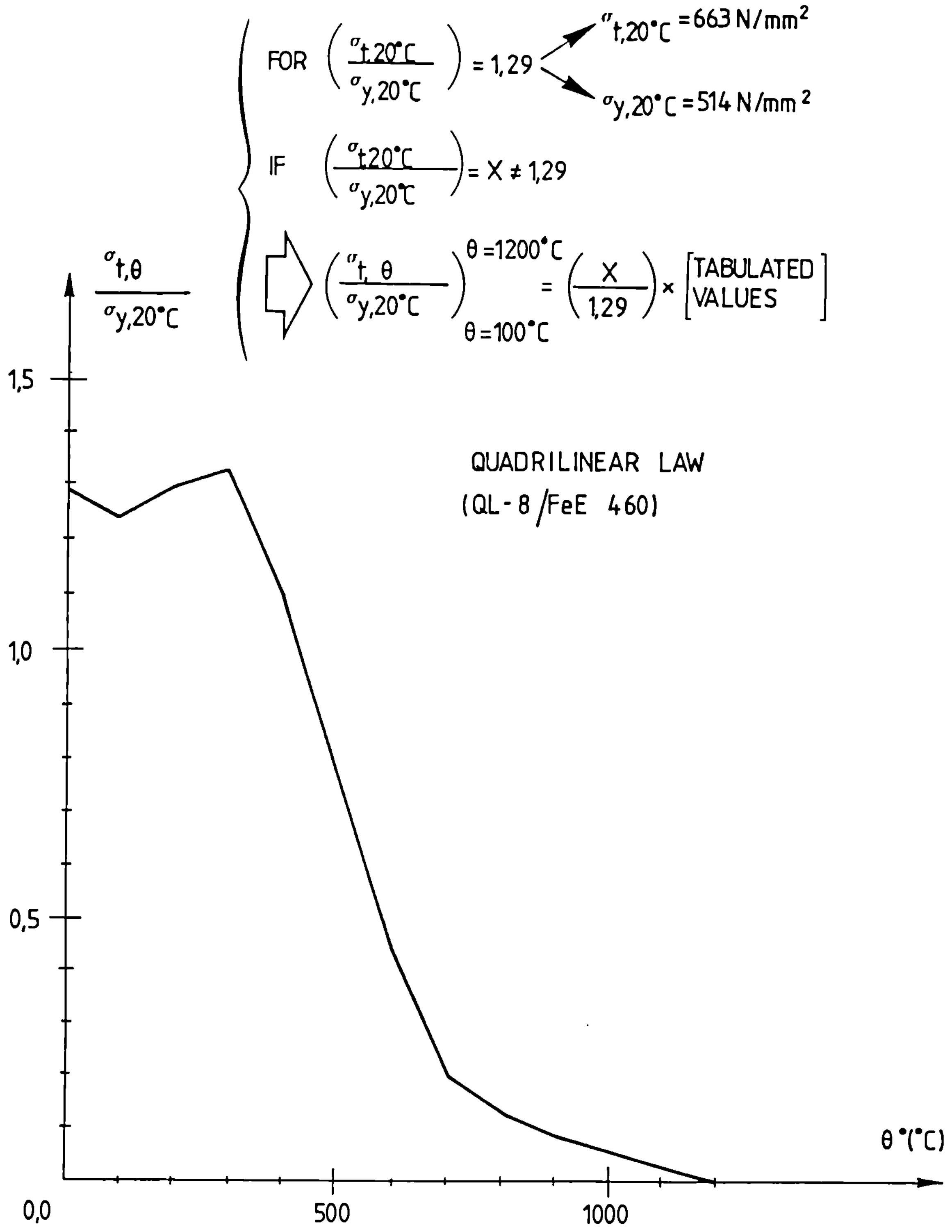

θ (°C)	20	100	200	300	400	500	600	700	800	900	1000	1100	1200
$\frac{\sigma_{t,\theta}}{\sigma_{y,20°C}}$	1,29	1,24	1,29	1,33	1,10	0,75	0,44	0,20	0,13	0,09	0,06	0,03	0,00

Figure 5.6

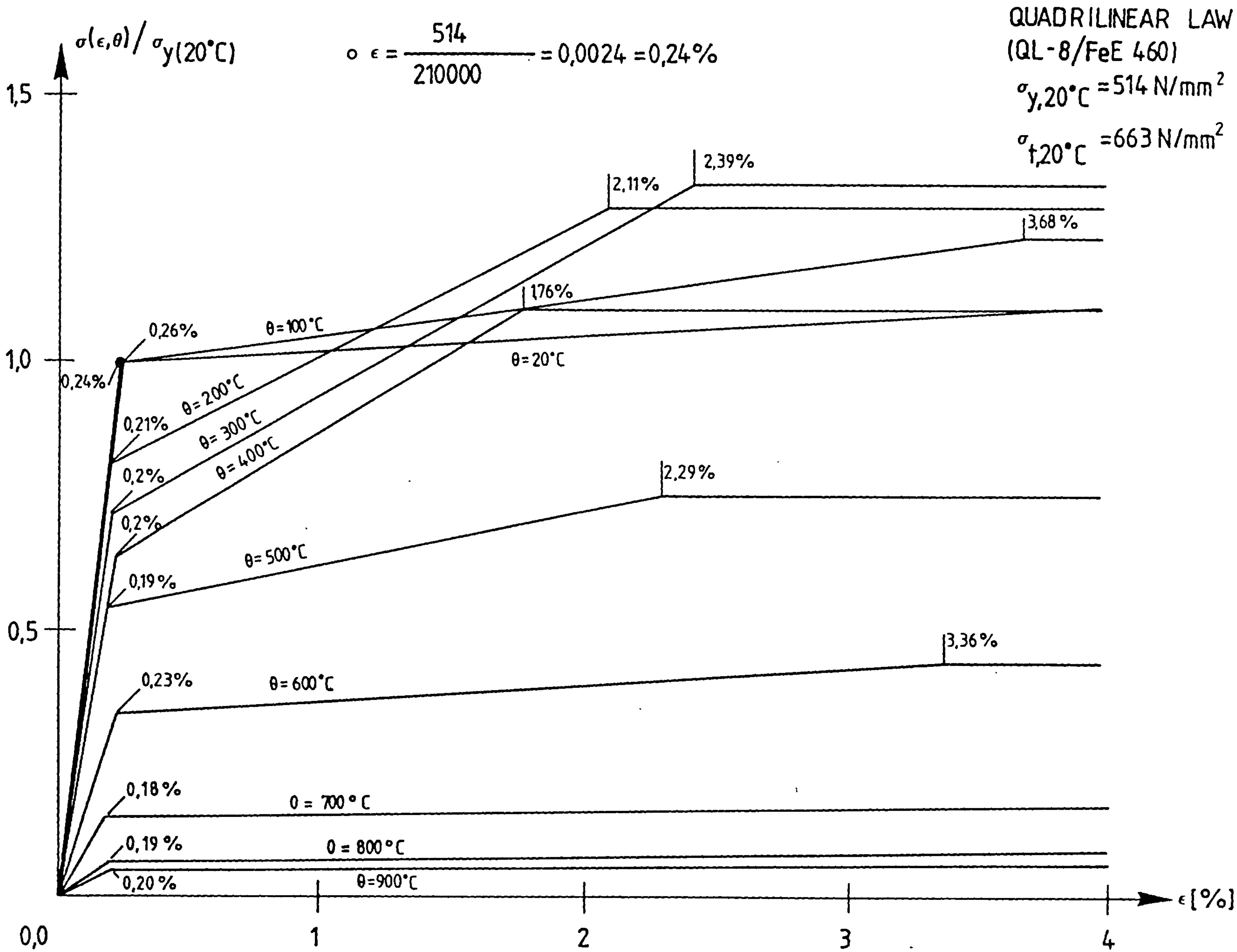

σ(ε,θ) / σy(20°C)
o ε = 514 / 210000 = 0,0024 = 0,24%
QUADRILINEAR LAW
(QL-8/FeE 460)
σy,20°C = 514 N/mm²
σt,20°C = 663 N/mm²
1,5
1,0
0,5
0,0
1
2
3
4
ε [%]
2,39%
2,11%
3,68 %
1,76%
0,26%
0,24%
θ = 100 °C
θ = 20°C
θ = 200°C
θ = 300°C
θ = 400°C
0,21%
0,2%
0,2%
2,29%
θ = 500°C
0,19 %
3,36 %
0,23%
θ = 600°C
0,18 %
0 = 700 ° C
0,19 %
0 = 800 ° C
0,20 %
θ = 900°C

Figure 5.7

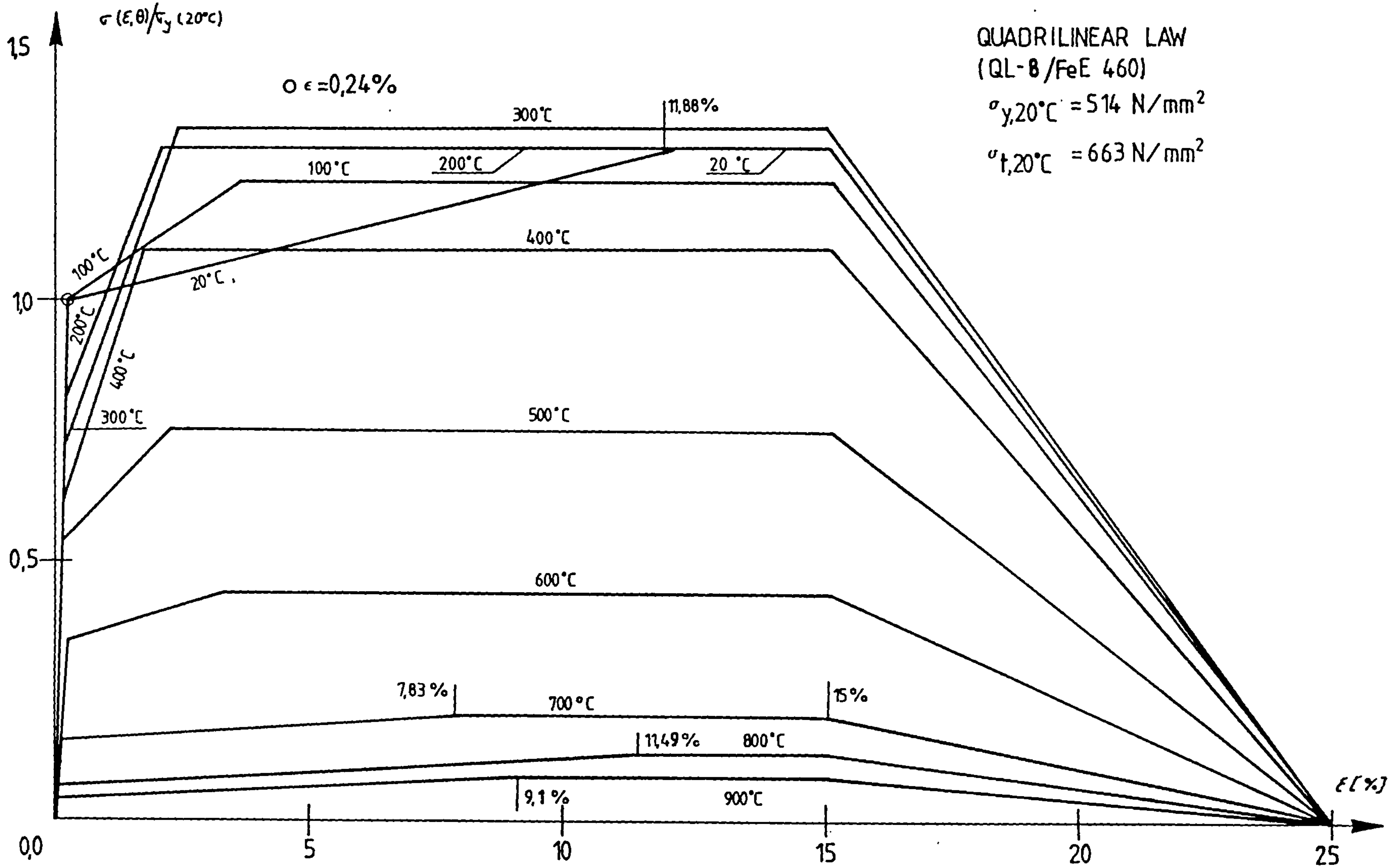
σ (ε,θ)/σy (20°C)
1,5
1,0
0,5
0,0
QUADRILINEAR LAW
(QL-B/FeE 460)
σy,20°C = 514 N/mm²
σt,20°C = 663 N/mm²
o ε =0,24%
300°C
11,88%
100°C
200°C
20 °C
400°C
100°C
20°C
200°C
400°C
300°C
500°C
600°C
7,83 %
700 °C
15%
11,49 %
800°C
9,1 %
900°C
ε [%]
5
10
15
20
25

Figure 5.8

MODELISATION OF THE SECTION
SCALE : 4/1

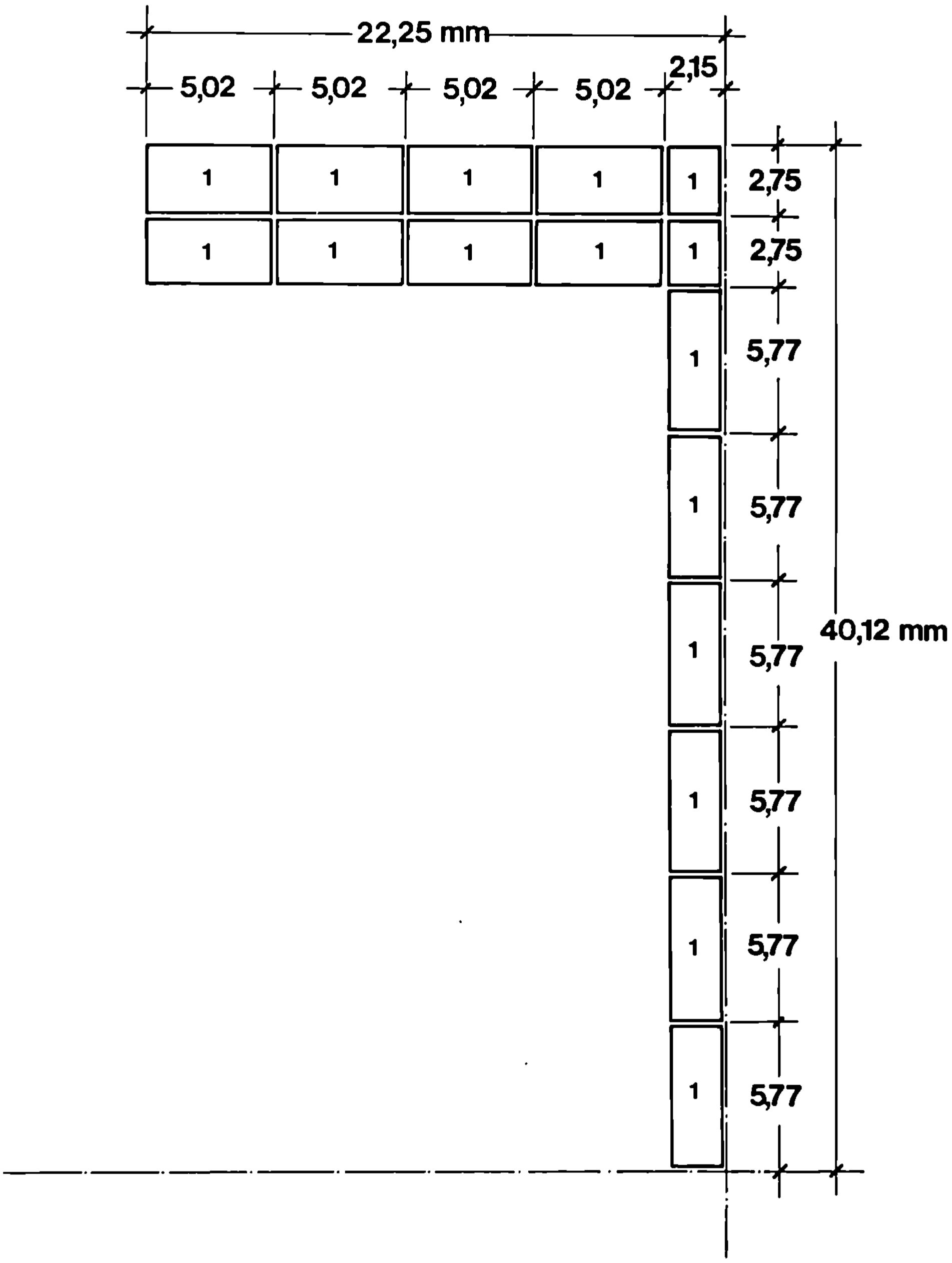

Figure 5.9

ARBED-RECHERCHES / RPS DEPARTMENT	CEFICOSS Analysis / CEF8.1
PROJECT TITLE EXAMPLE OF V 1 TEST - Fe 360 IPE 80 PROFILE	PROJECT NUMBER REFAO III ESCH/ALZETTE : 10-MAR-1989 SHEET :

FIGURE 5.10

KRUPP TRANSIENT STATE BEAM TEST PARAMETERS (S1 TO S10) COMPARED TO QL-LAW SIMULATIONS

STEEL QUALITY : Fe E 460

TEST	Sig y [N/mm2]	Sig t [N/mm2]	St/Sy	Fpcold [kN]	F [kN]	F/Fpcold	Tm [°C/min]	Tinit [°C]	(Tmeas.)max [°C]	(Tsim.)max [°C]	Dmeas.-sim. [%]	(Wmeas.)max [mm]	(Wsim.)max [mm]	(εsim.)max [%]	
S1	502.00	653.00	1.30	30.00	30.00	1.000	3.60	22.10	461.00	428.00	-7.2	85.80	64.40	4.75	(1)
S3	507.00	655.00	1.29	30.30	25.80	0.850	3.50	21.70	497.00	467.00	-6.0	53.20	44.80	2.96	(2)
S2	504.50	654.00	1.30	30.20	22.70	0.750	3.40	22.50	525.00	497.00	-5.3	53.90	39.30	2.79	(2)
S4	516.00	658.00	1.28	30.80	18.50	0.600	3.50	21.40	566.00	543.00	-4.1	53.10	39.70	2.86	(2)
S10	522.50	650.00	1.24	31.20	15.60	0.500	3.40	20.10	605.00	574.00	-5.1	83.20	73.80	7.12	(2)
S5	513.00	658.00	1.28	30.70	12.30	0.400	3.50	21.00	651.00	613.00	-5.8	87.50	89.90	7.96	(2)
S9	523.50	648.00	1.24	31.30	6.30	0.200	3.50	22.40	713.00	693.00	-2.8	54.10	108.60	10.14	(2)
S7	526.00	652.00	1.24	31.40	3.20	0.100	3.50	28.00	813.00	813.00	0.0	86.90	135.90	7.78	(2)
S6	529.00	655.00	1.24	31.60	2.40	0.075	3.40	31.20	828.00	827.00	-0.1	87.80	41.10	3.13	(2)
S8	523.00	649.00	1.24	31.30	37.65	1.200	(Fmeas.)max=37.65 kN ; (Fsim.)max = 36 kN ; Dmax = -4.3 %					75.00	74.50	7.13	(3)

Remarks :

(1) after cold loading before the heating the middle-span section is already fully plastified

(2) after cold loading before the heating the middle-span section is already partially plastified or still elastic

(3) only cold loadings - unloadings

KRUPP TRANSIENT STATE BEAM TEST PARAMETERS (S11,S12 ; V1 TO V7) COMPARED TO QL-LAW SIMULATIONS

STEEL QUALITY	TEST	PROFILES	Sig y [N/mm2]	Sig t [N/mm2]	St/Sy	Wplx [cm3]	Fpcold (1) [kN]	F [kN]	F/Fpcold	(Tmeas.)max (7) [°C]	(Tsim.)max [°C]	Dmeas.-sim. [%]	(Wmeas.)max [mm]	(Wsim.)max [mm]	(Esim.)max [%]	(Fmeas.)max [kN]	(F/Fpcold)max measured	
Fe E 460	S11	TOOLED PROFILES	496.00	758.00	1.53	17.470	30.22	31.73	1.05	120.10	460.0	(8)	21.34	135.20	12.43	32.80	1.085	(2),(6)
Fe E 460	S12	TOOLED PROFILES	489.50	744.50	1.52	17.750	30.30	31.82	1.05	422.80	440.0	4.07	54.70	98.00	7.41	35.06	1.157	(2),(5)
Fe 360	V1	IPE 80	321.80	508.30	1.58	24.150	27.10	29.81	1.10	217.80	440.0	(8)	37.90	84.00	8.67	32.41	1.196	(2),(6)
Fe 360	V2	IPE 80	315.00	505.30	1.60	25.270	27.76	30.54	1.10	336.90	440.0	(8)	58.90	63.70	5.68	33.36	1.202	(2),(5)
Fe 360	V3	IPE 80	310.00	501.50	1.62	24.780	26.79	22.77	0.85	530.00	530.0	0.00	95.30	57.10	5.27			(3)
Fe 360	V4	IPE 80	308.00	503.30	1.63	25.100	26.96	16.18	0.60	600.00	595.0	-0.83	90.66	90.10	7.75			(3)
Fe 360	V5	IPE 80	310.00	505.30	1.63	24.940	26.96	13.48	0.50	630.00	625.0	-0.79	78.60	105.20	8.22			(3)
Fe 360	V6	IPE 80	312.00	506.00	1.62	25.100	27.31	2.73	0.10	921.00	900.0	-2.28	78.40	242.10	14.66			(3)
Fe 360	V7	IPE 80	311.80	504.30	1.62	25.100	27.29	33.02	1.21	(Fmeas.)max=33.02 kN; (Fsim.)max=32.3 kN;Dmax=-2.2%			67.10	44.90	4.69	33.02	1.210	(4)

FIGURE 5.11

SUMMARY OF THE SIX FIRE TESTS

N°	WIDE FLANGE SECTION	MAX THICKNESS t (mm)	SECTION FACTOR U/A (m^{-1})	STEEL GRADE / ACTUAL σ_y (N/mm^2)	BUCKLING AXIS	Laboratorium	Column Length (m)	ACTUAL SLENDERNESS RATIO $\bar{\lambda}$	ECCENTRICITY e (cm)	e/d(1)	TEST LOAD N (kN)	ULTIMATE LOAD N_{ult} (kN) (2)	$\frac{N}{N_{ult}}$	RESISTANCE TIME (minutes)
1	HD 210x210 x198	45	54	Fe 510 / 364	WEAK	BRAUN-SCHWEIG 2.09.1988	5,70	1,303	1,0	0,045	1100	3213	0,342	**38'**
2	HD 310x310 x500	75	33	Fe 510 / 298	STRONG	GAND 6.10.1988	4,14	0,305	8,5	0,2	2000	11716	0,171	**58'**
3	HD 310x310 x500	75	33	Fe 510 / 298	WEAK	BRAUN-SCHWEIG 7.09.1988	5,70	0,777	3,4	0,1	1650	9544	0,173	**50'**
4	HD 400x400 x1086	125	20	Fe 510 / 371	WEAK	GAND 13.10.1988	4,14	0,466	22,7	0,5	4000	13824	0,289	**68'**
5	W 360x410 x314	39,6	58,4	Fe 510 / 401	WEAK	GAND 29.9.1988	4,14	0,557	12,0	0,3	1800	6086	0,296	**37'**
6	W 360x410 x314	39,6	58,4	Fe E 460 / 496	WEAK	GAND 22.09.1988	4,14	0,620	12,0	0,3	1800	7326	0,246	**39'**

(1) d = width of the section for buckling around the weak axis.
d = hight of the section for buckling around the strong axis.

(2) N_{ult} is the ultimate load in cold situation for the given eccentricity and has been calculated here according to the german DIN 18 800 (second order plastic theory) with the theoretical section sizes and the actual yield strengths.

FIGURE 6.1

ACTUAL SIZES OF SECTIONS AND MECHANICAL PROPERTIES

TEST N°	WIDE FLANGE SECTION	Measured actual sizes: Hight h (mm)	Width b (mm)	Flange-thickness e (mm)	Web-thickness a (mm)	Initial Imperfection (mm)	Yield Strength σ_y (N/mm²)	Tensile Strength σ_t (N/mm²)
1	HD 210 x 210 x 198	270,3	222,4	44,6	27,5	0	364	523
2	HD 310 x 310 x 500	427	335	73	42	0	298	490
3	HD 310 x 310 x 500	428	335	73,6	45	0	298	490
4	HD 400 x 400 x 1086	568	446	125	71	0	371	574
5	W 360 x 410 x 314	402,8	401,7	39	20,8	1	401	536
6	W 360 x 410 x 314	401	400	38,7	23	- 4	496	676

Figure 6.2

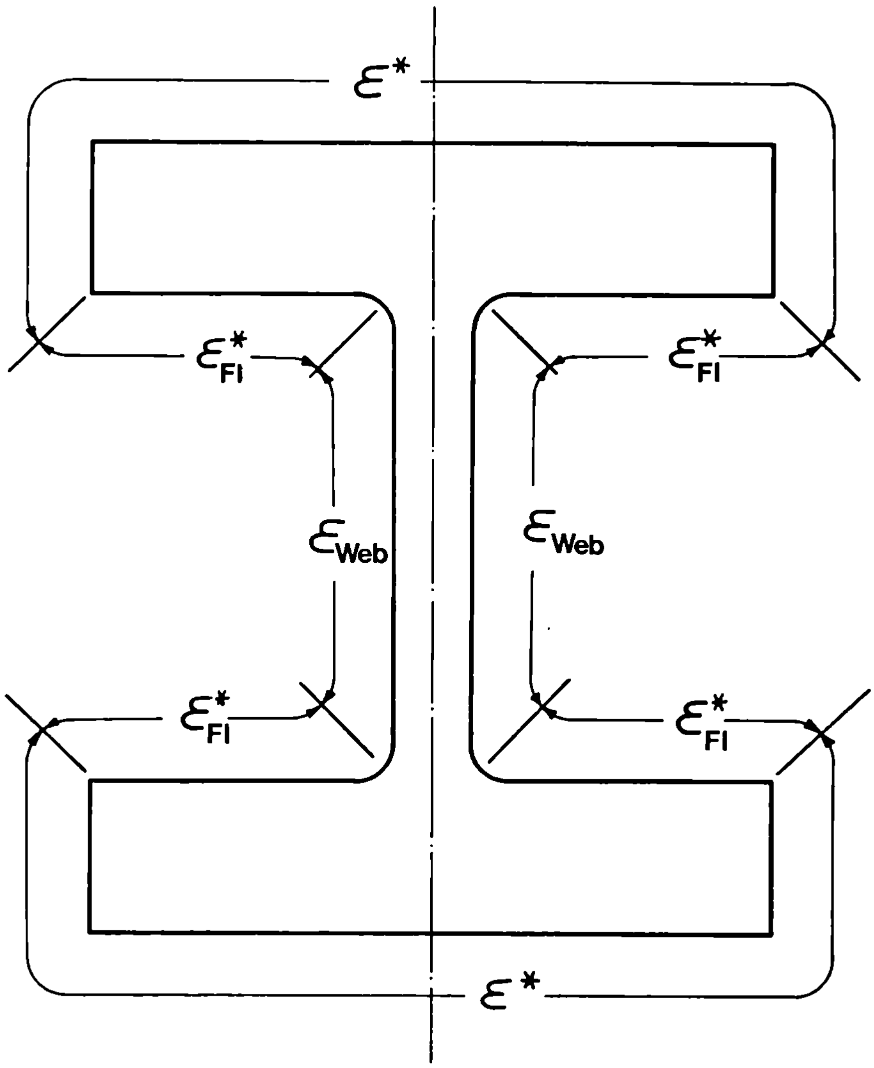

PARAMETERS FOR HEAT TRANSFER
AND CALCULATED FIRE RESISTANCE TIMES (QL-8LAW)

Furnace of	Test N°	Convection factor α (W/m^2K)	Resultant emissivity ε^*	ε^*_{Web}	ε^*_{Fl}	Fire Resistance Times in minutes TEST	CEFICOSS
Braun-schweig	1	25	0,70	0,42	0,26	38'	37'
	3	25	0,70	0,42	0,26	50'	48'
Gand	2	18	0,45	0,26	0,16	58'	58'
	4	18	0,45	0,26	0,16	68'	72'
	5	18	0,45	0,26	0,16	37'	38'
	6	18	0,45	0,26	0,16	39'	40'

FIGURE 6.3

Emissivity Coefficient affected by the Shadow Effect

$\epsilon = 0{,}5$

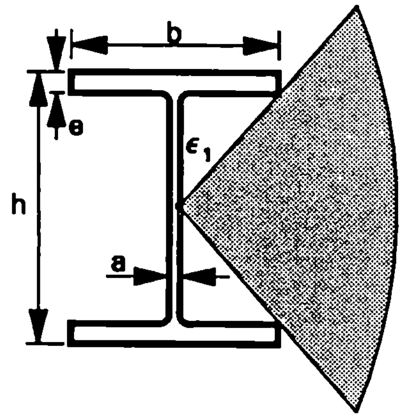

$$\epsilon_1 = \epsilon \left[\frac{\dfrac{-(b-a)}{2} + \sqrt{(h-2e)^2 + \dfrac{(b-a)^2}{4}}}{h-2e} \right]$$

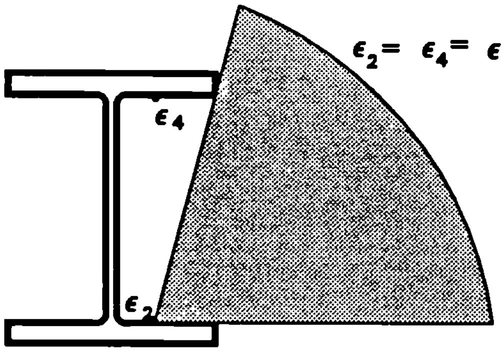

$$\epsilon_2 = \epsilon_4 = \epsilon \left[\frac{-\sqrt{(h-2e)^2 + \dfrac{(b-a)^2}{4}} + (h-2e) + \dfrac{(b-a)}{2}}{(b-a)} \right]$$

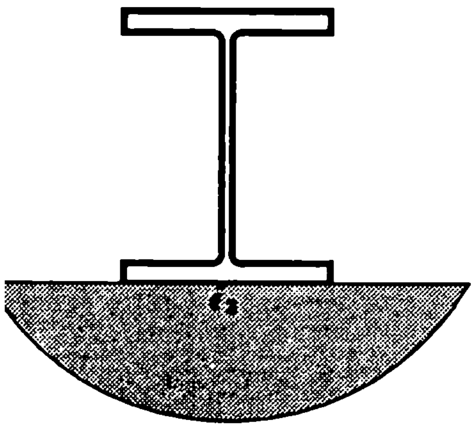

$\epsilon_3 = 0{,}5 = \epsilon$, given in EUROCODE 1, Chapter 20

Figure 6.4

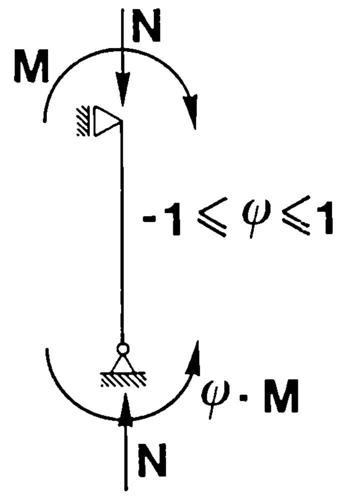

FORM OF BENDING MOMENT DISTRIBUTION

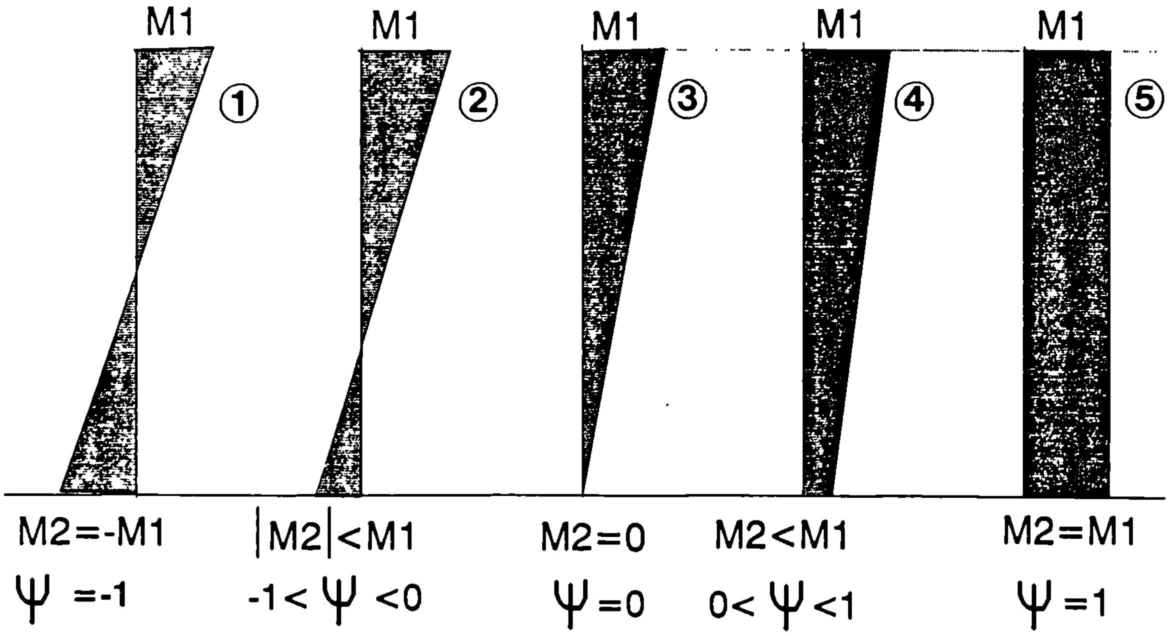

$$\Psi = \frac{M2}{M1}$$

FIGURE 7.1

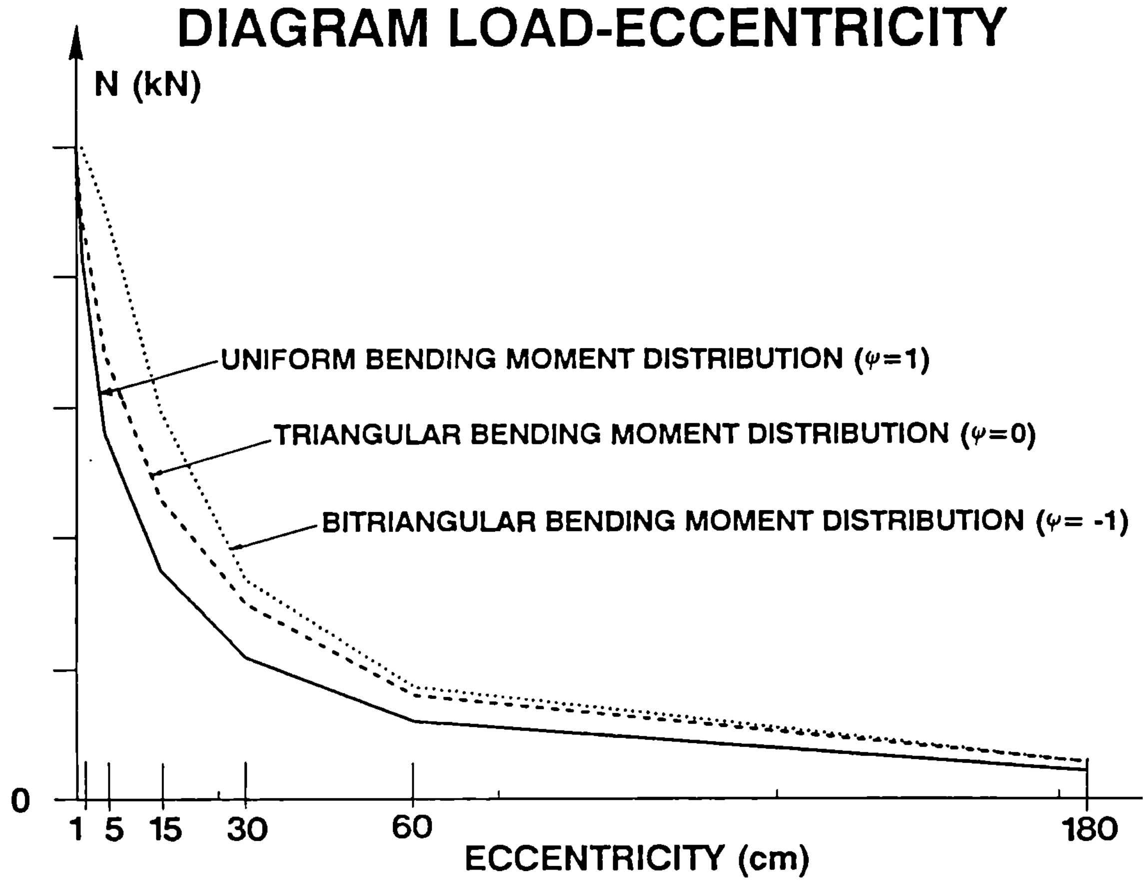
DIAGRAM LOAD-ECCENTRICITY
N (kN)
UNIFORM BENDING MOMENT DISTRIBUTION (ψ=1)
TRIANGULAR BENDING MOMENT DISTRIBUTION (ψ=0)
BITRIANGULAR BENDING MOMENT DISTRIBUTION (ψ= -1)
0
1 5 15 30 60 180
ECCENTRICITY (cm)

Figure 7.2

RESIDUAL STRESSES FOR TEST 1

-9.84	-9.84	-9.84	-9.84	-9.84							
-7.78	-7.78	-7.78	-7.78	-7.78							
-5.81	-5.81	-5.81	-5.81	-5.81							
-3.85	-3.85	-3.85	-3.85	-3.85							
-1.69	-1.69	-1.69	-1.69	-1.69							
+0.95	+0.95	+0.95	+0.95	+0.95							
+3.89	+3.89	+3.89	+3.89	+3.89							
+6.78	+6.78	+6.78	+6.78	+6.78	WEB						
+9.07	+9.07	+9.07	+9.07	+9.07	+9.11	+4.89	+0.79	-1.98	-4.27	-7.29	-10.92
+10.92	+10.92	+10.92	+10.92	+10.92	+9.11	+4.89	+0.79	-1.98	-4.27	-7.29	-10.92

RESIDUAL STRESSES FOR TEST 2

-8.40	-7.24	-5.96	-4.73	-3.69	-2.74	-1.63	-0.50	+0.56	+1.81	+3.21	+4.61	+5.99	+7.24	+8.07	+8.94
-8.40	-7.24	-5.96	-4.73	-3.69	-2.74	-1.63	-0.50	+0.56	+1.81	+3.21	+4.61	+5.99	+7.24	+8.07	+8.94
-8.40	-7.24	-5.96	-4.73	-3.69	-2.74	-1.63	-0.50	+0.56	+1.81	+3.21	+4.61	+5.99	+7.24	+8.07	+8.94
-8.40	-7.24	-5.96	-4.73	-3.69	-2.74	-1.63	-0.50	+0.56	+1.81	+3.21	+4.61	+5.99	+7.24	+8.07	+8.94
-8.40	-7.24	-5.96	-4.73	-3.69	-2.74	-1.63	-0.50	+0.56	+1.81	+3.21	+4.61	+5.99	+7.24	+8.07	+8.94
-8.40	-7.24	-5.96	-4.73	-3.69	-2.74	-1.63	-0.50	+0.56	+1.81	+3.21	+4.61	+5.99	+7.24	+8.07	+8.94
-8.40	-7.24	-5.96	-4.73	-3.69	-2.74	-1.63	-0.50	+0.56	+1.81	+3.21	+4.61	+5.99	+7.24	+8.07	+8.94
													+8.28	+8.28	+8.28
													+6.82	+6.82	+6.82
													+5.00	+5.00	+5.00
													+3.15	+3.15	+3.15
													+1.69	+1.69	+1.69
												WEB	+0.08	+0.08	+0.08
													-1.81	-1.81	-1.81
													-3.75	-3.75	-3.75
													-5.36	-5.36	-5.36
													-7.15	-7.15	-7.15
													-8.94	-8.94	-8.94

RESIDUAL STRESSES FOR TEST 3

-8.54	-8.54	-8.54	-8.54	-8.54	-8.54	-8.54											
-7.60	-7.60	-7.60	-7.60	-7.60	-7.60	-7.60											
-6.53	-6.53	-6.53	-6.53	-6.53	-6.53	-6.53											
-5.73	-5.73	-5.73	-5.73	-5.73	-5.73	-5.73											
-4.88	-4.88	-4.88	-4.88	-4.88	-4.88	-4.88											
-3.65	-3.65	-3.65	-3.65	-3.65	-3.65	-3.65											
-2.37	-2.37	-2.37	-2.37	-2.37	-2.37	-2.37											
-1.46	-1.46	-1.46	-1.46	-1.46	-1.46	-1.46											
-0.40	-0.40	-0.40	-0.40	-0.40	-0.40	-0.40											
+1.20	+1.20	+1.20	+1.20	+1.20	+1.20	+1.20											
+2.80	+2.80	+2.80	+2.80	+2.80	+2.80	+2.80											
+4.40	+4.40	+4.40	+4.40	+4.40	+4.40	+4.40											
+5.87	+5.87	+5.87	+5.87	+5.87	+5.87	+5.87				WEB							
+7.07	+7.07	+7.07	+7.07	+7.07	+7.07	+7.07	+7.66	+5.11	+3.30	+2.25	+0.72	-1.62	-3.91	-5.37	-6.52	-7.79	-8.94
+8.13	+8.13	+8.13	+8.13	+8.13	+8.13	+8.13	+7.66	+5.11	+3.30	+2.25	+0.72	-1.62	-3.91	-5.37	-6.52	-7.79	-8.94
+8.94	+8.94	+8.94	+8.94	+8.94	+8.94	+8.94	+7.66	+5.11	+3.30	+2.25	+0.72	-1.62	-3.91	-5.37	-6.52	-7.79	-8.94

FIGURE 7.3

INFLUENCE OF RESIDUAL STRESSES

ON FIRE RESISTANCE TIMES

Max. residual stresses : $\sigma_R = 0{,}3\,\sigma_y$

FIRE RESISTANCE TIMES (MINUTES)			
TEST N°	TEST	SIMULATION WITHOUT RESIDUAL STRESSES	SIMULATION with RESIDUAL STRESSES $0{,}3\,\sigma_y$
2	60'	58'	57,75'
3	50'	48,25'	47,25'
1	38'	37'	35'

FIGURE 7.4

GEOMETRICAL IMPERFECTION

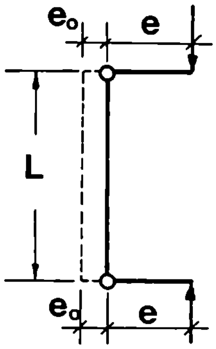

$$e_o = \text{constant} = \begin{cases} \dfrac{L}{500} & \text{(WEAK AXIS)} \\ \dfrac{L}{1000} & \text{(STRONG AXIS)} \end{cases}$$

RESIDUAL STRESSES

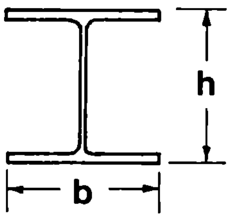

$$\begin{cases} \text{shapes with } \dfrac{h}{b} \leq 1{,}2 & \sigma_R = 0{,}5\ \sigma_y \\ \text{shapes with } \dfrac{h}{b} > 1{,}2 & \sigma_R = 0{,}3\ \sigma_y \end{cases}$$

DISTRIBUTION OF RESIDUAL STRESSES

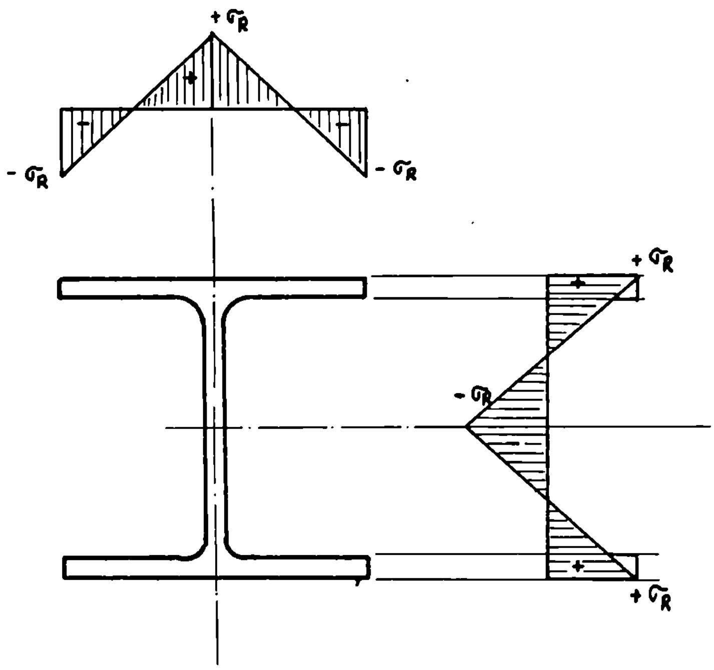

FIGURE 7.5

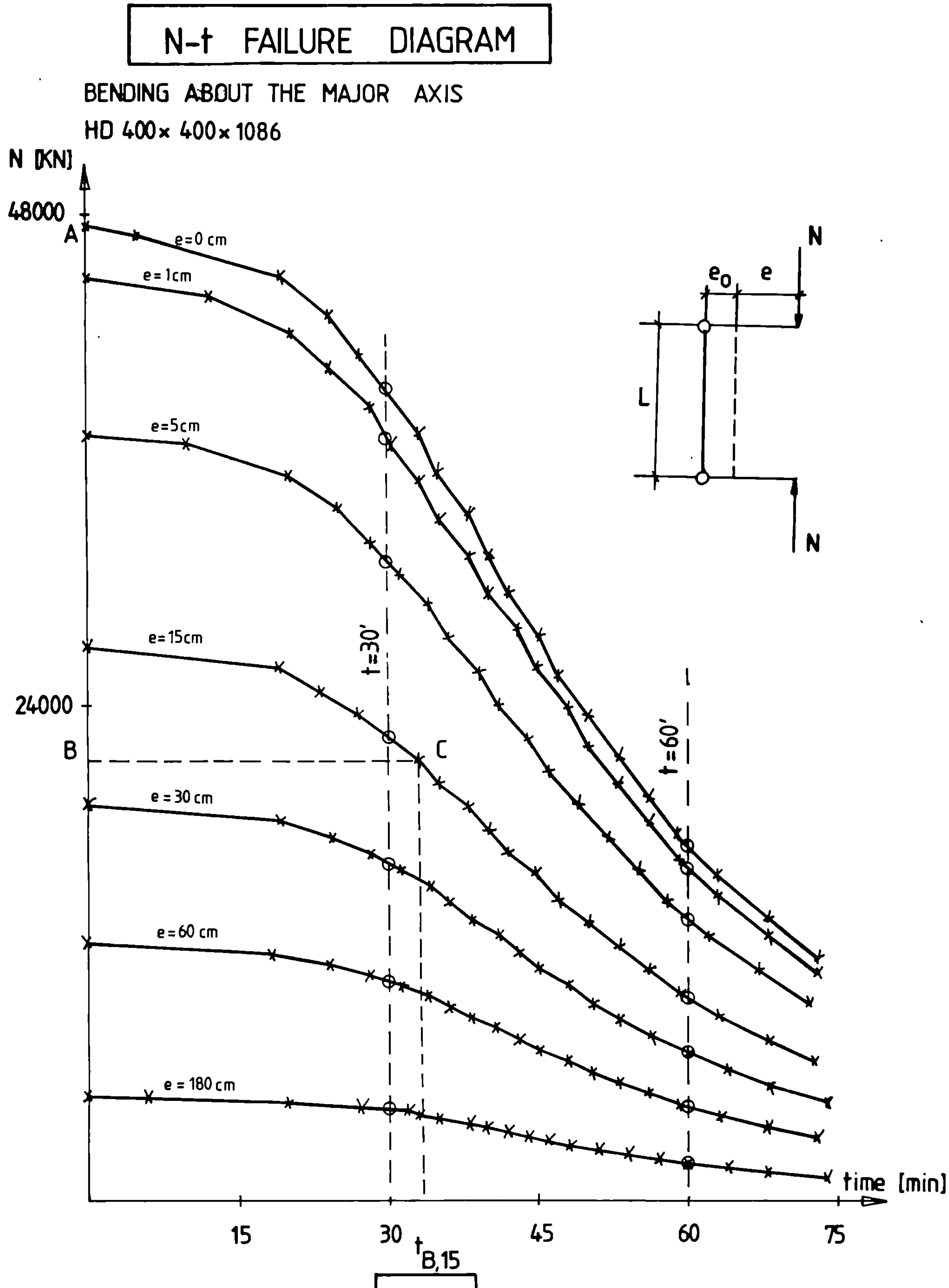
N-t FAILURE DIAGRAM
BENDING ABOUT THE MAJOR AXIS
HD 400× 400× 1086
N [KN]
48000
A
e=0 cm
e=1cm
e=5cm
e=15cm
24000
B
C
e=30 cm
e=60 cm
e=180 cm
t=30'
t=60'
N
e_0
e
L
N
15
30
45
60
75
$t_{B,15}$
time [min]

Fig. 8.1

EXAMPLE OF INTERPOLATION

SECTION : HD 260x260x329

Fire resistance class : F 30

		TABLES F 30		N [kN] interpolated for L = 5 m	t (*)
Bending axis	e/h (or e/b)	N [kN] for L = 4 m	N [kN] for L = 6 m		
Strong	0.5	3848	2996	3422	30'
Weak	0.5	1961	1487	1724	29.74'

(*) Time in minutes given by making a simulation with CEFICOSS for the interpolated load found for L = 5.00 m

Figure 8.2

VARIATION OF N [kN] WITH L [m]

HD260X260X329 e/b=0.5 F30

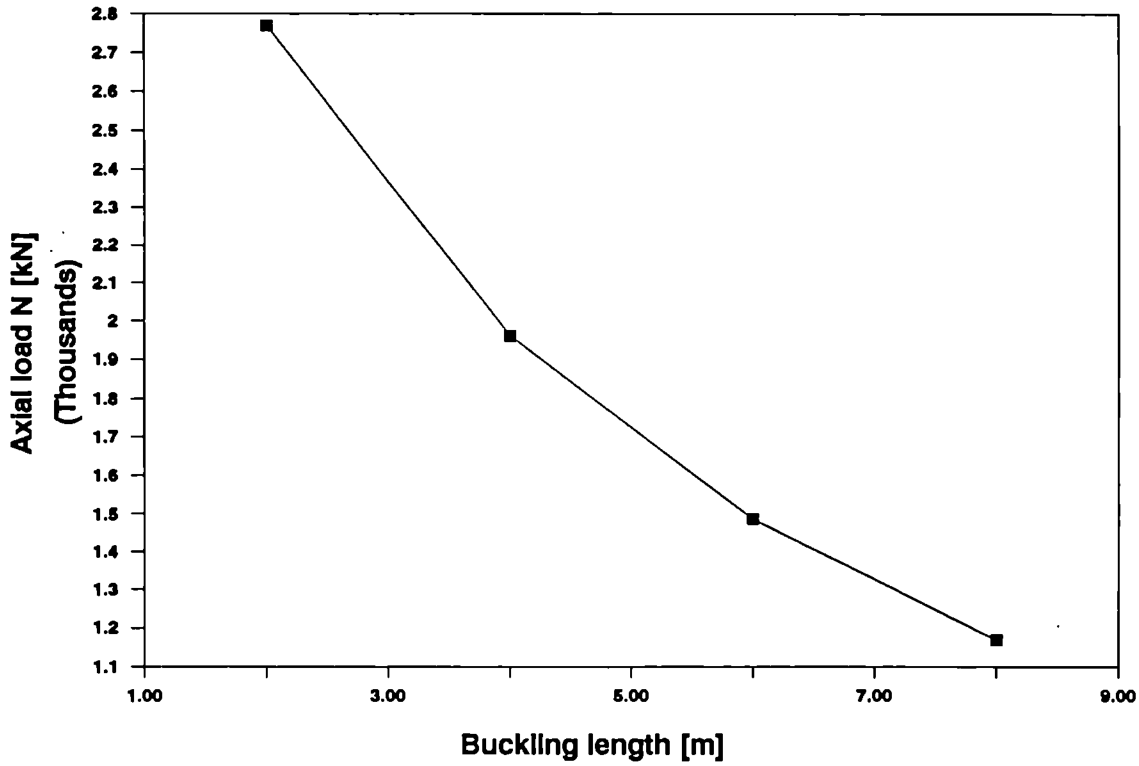

Figure 8.3

HD 260x260x329

Bi-triangular moment distribution.

BENDING AXIS	SLENDERNESS RATIO	BUCKLING LENGTH [m]	ECCENTRICITY RATIO e/H or e/B	CALCULATED BY CEFICOSS		APPROACHED METHODS FOR BITRIANGULAR DISTRIBUTION		
				N for diagr. UNIFORM	N for diagr. BITRIANGULAR	N bitr. EC3 method	N bitr. β-ψ method	N'bitr. β-ψ method
MAJOR	0.3854	4	0.5	3848	5400	5399.05	4543.80	4616
MAJOR	0.3854	4	1	2586	3660	**4238.24**	3020.95	3141
MAJOR	0.5781	6	0.5	2996	5000	4439.42	3931.31	3817
MAJOR	0.5781	6	1	2084	3390	**3525.08**	2649.45	2649
MINOR	0.6978	4	0.5	1961	3375	3061.83	2805.45	2859
MINOR	0.6978	4	1	1199	2167	**2191,85**	1654.46	1763
MINOR	1.047	6	0.5	1487	2636	2191.43	2279.65	2261
MINOR	1.047	6	1	980	1800	1679.3	1490.76	1487
				N_u	N_{bitr}			

Figure 8.4

GENERAL FORM OF INTERACTION FORMULAS FOR COLD SERVICE

$$\boxed{\frac{N}{\chi \cdot N_{pl}} + \beta \cdot \frac{M}{M_{pl}} = 1}$$

→ or $1 - \Delta$

$\frac{M}{M_{pl}} = \frac{N \cdot e}{M_{pl}}$ and we can write : $M_{pl} = \alpha \cdot N_c$

$\frac{N}{\chi \cdot N_{pl}} = \frac{N}{N_c}$ where N_c is the pure axial load (e = 0)

$\Rightarrow \left(\frac{N}{N_c}\right) + \frac{\beta}{\alpha} \cdot \left(\frac{N}{N_c}\right) \cdot e = 1$ and for $K = \frac{1}{\alpha}$

$$\Rightarrow \boxed{\frac{N}{N_c} = \frac{1}{1 + \beta \cdot K \cdot e}}$$

(Eventual correction : $1 - \Delta$ in place of 1)

Diagram uniform : $\beta = 1.1 \Rightarrow K_u = \dfrac{1 - \frac{N_u}{N_c}}{\frac{N_u}{N_c} \cdot 1.1 \cdot e} = \dfrac{\frac{N_c}{N_u} - 1}{1.1 \cdot e}$

(K_u can be calculated for each eccentricity)

Other distribution : $\beta = 0.66 + 0.44\psi > 0.44$

and particularly for a bi-triangular distribution :

$\psi = -1.00 \Rightarrow \beta = 0.44$

$$\Rightarrow N_{bitr} = \frac{N_c}{1 + 0.44 \cdot K_u \cdot e} = \frac{N_u}{0.60\frac{N_u}{N_c} + 0.4}$$

Figure 8.5

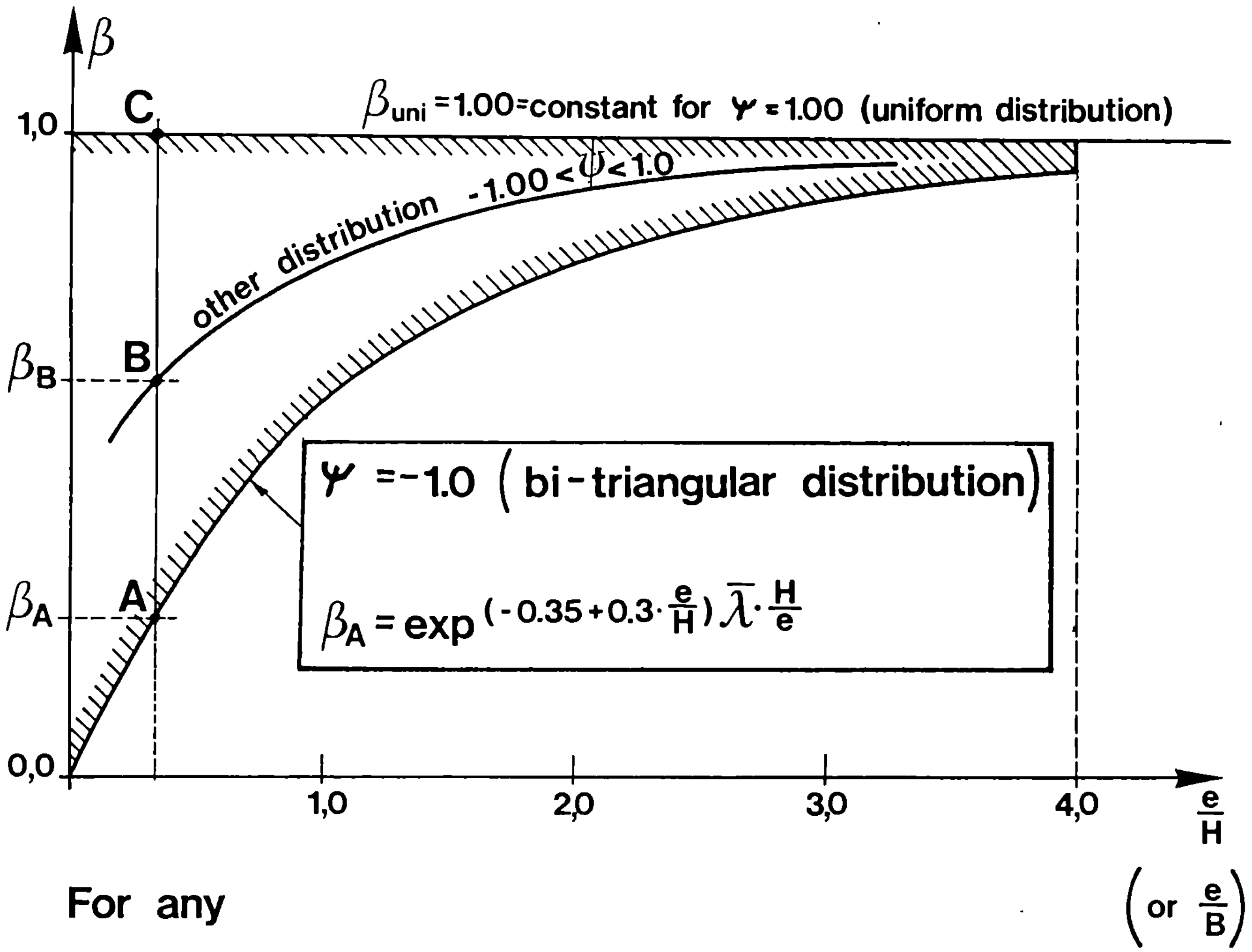

For any

$-1.0 < \Psi < 1.0$: linear interpolation :

$$\frac{\overline{AB}}{\overline{AC}} = \frac{\Psi + 1.0}{2.0}$$

$$\frac{\beta_B - \beta_A}{1.0 - \beta_A} = \frac{\Psi + 1.0}{2.0}$$

$$\Longrightarrow \beta_B = \beta_A + (1.0 - \beta_A)\,\frac{(\Psi + 1.0)}{2.0}$$

Figure 8.6

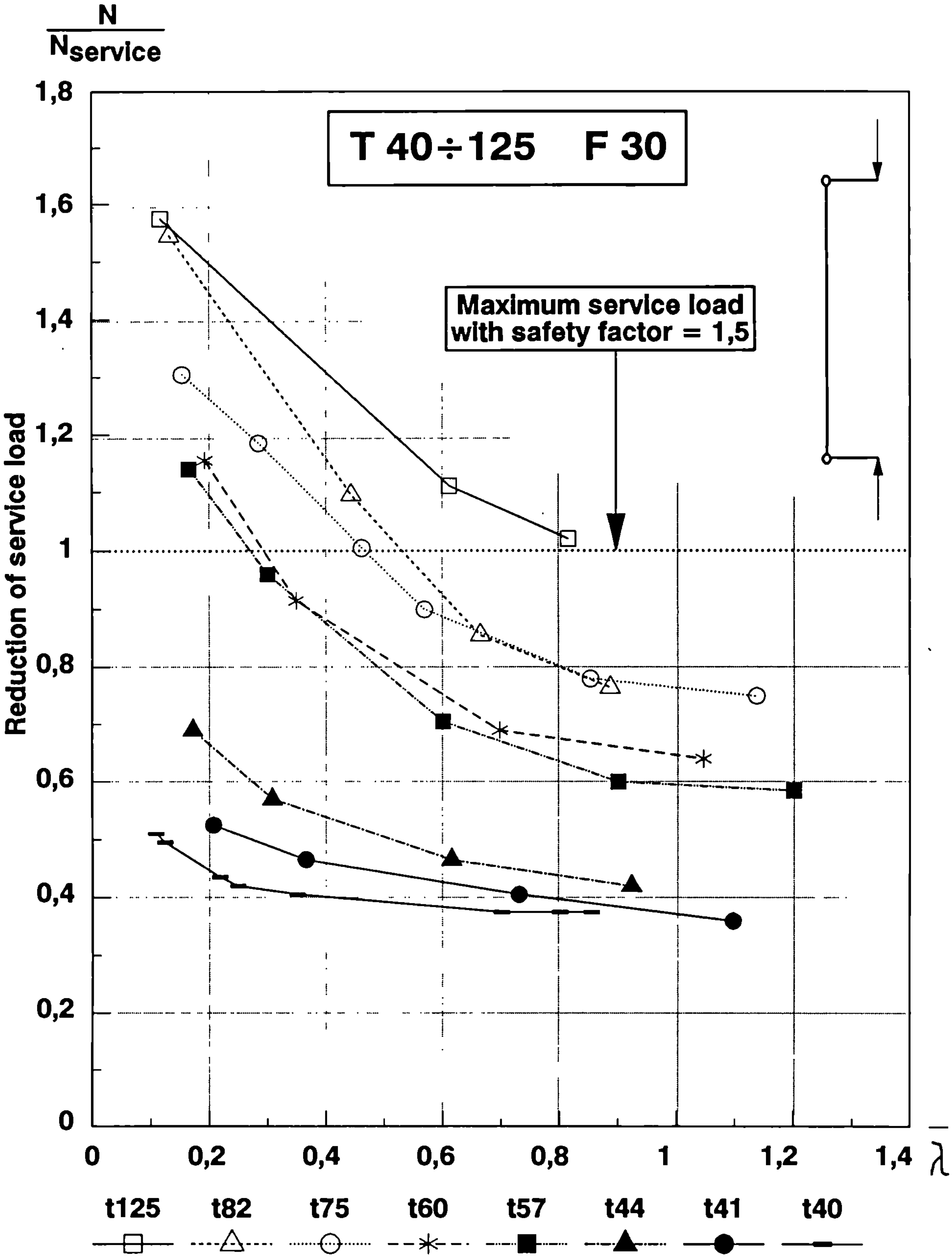
N / $N_{service}$
Reduction of service load
T 40÷125 F 30
Maximum service load with safety factor = 1,5
1,8
1,6
1,4
1,2
1
0,8
0,6
0,4
0,2
0
0
0,2
0,4
0,6
0,8
1
1,2
1,4
$\bar{\lambda}$
t125
t82
t75
t60
t57
t44
t41
t40

Figure 8.7

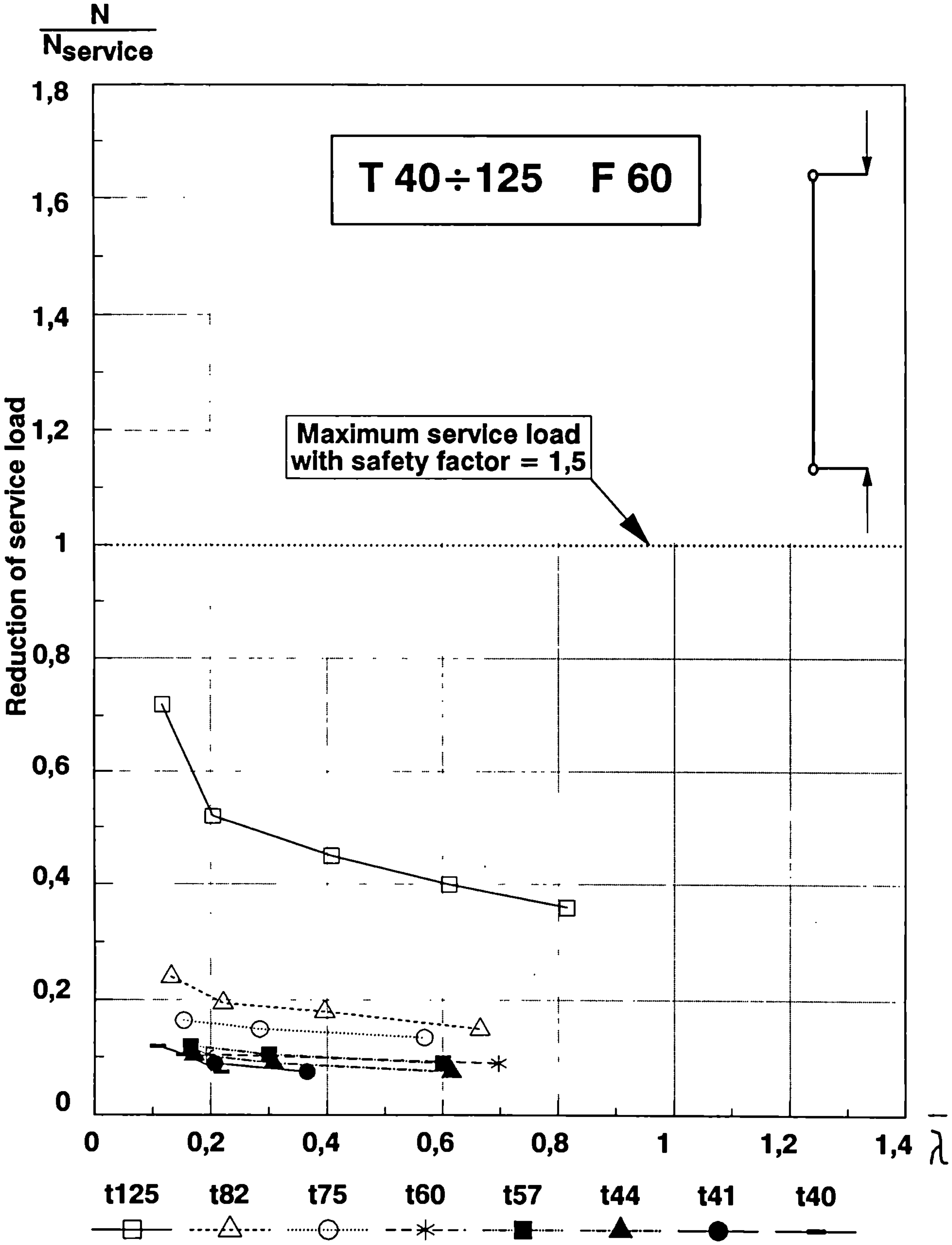

N / Nservice
Reduction of service load
1,8
1,6
1,4
1,2
1
0,8
0,6
0,4
0,2
0
T 40÷125 F 60
Maximum service load with safety factor = 1,5
0
0,2
0,4
0,6
0,8
1
1,2
1,4
λ
t125
t82
t75
t60
t57
t44
t41
t40

Figure 8.8

PART II

DIAGRAMS

and TABLES

SUMMARY OF CALCULATED SECTIONS.

Steel	PROFILE	Flange thickness [mm]	Section factor U/A [m^{-1}]	h/b	Reduced σ_y [kN/cm^2]	Max.Residual stress σ_{res}
Fe 510	HE 550 M	40	64	1.87	34.5	0.3 σ_y
	HD 210x210x198	45	54	1.21	33.5	0.3 σ_y
	HD 260x260x219	41	58	1.14	33.5	0.5 σ_y
	HD 260x260x329	60	41	1.23	33.5	0.3 σ_y
	HD 310x310x283	44	54	1.13	33.5	0.5 σ_y
	HD 310x310x375	57	42	1.18	33.5	0.5 σ_y
	HD 310x310x500	75	33	1.26	32.5	0.3 σ_y
	HD 400x400x314	40	58	1.0	34.5	0.5 σ_y
	HD 400x400x678	82	30	1.13	31.5	0.5 σ_y
	HD 400x400x1086	125	20	1.25	30.5	0.3 σ_y
FeE 460	HE 550 M	40	64	1.87	45	0.3 σ_y
	HD 400x400x314	40	58	1.0	45	0.5 σ_y

DIAGRAMS AND TABLES

FOR BENDING ABOUT

THE MAJOR AXIS

DIAGRAMS AND TABLES

FOR BENDING ABOUT

THE MAJOR AXIS

HE 550 M (Strong axis) Sigma yield = 345 N/mm2 ; U/A = 64 ; t = 40 mm

l (m)	Lambda Bar	e/h	Npl (kN)	F0				F30					F60				
				N(EC3) (kN)	N(EC3)/Npl	N(CEF) (kN)	N(CEF)/Npl	N(F30) (kN)	N/Nc	N/N(F0,EC3)	N/N(F0,CEF)	N/Npl	N(F60) (kN)	N/Nc	N/N(F0,EC3)	N/N(F0,CEF)	N/Npl
2.00	0.1092	0.00	12213	11839	0.97	11996	0.98	4082	1.00	0.34	0.34	0.33	1048	1.00	0.09	0.09	0.08
2.00	0.1092	0.10	12213	9644	0.79	9952	0.81	3255	0.80	0.34	0.33	0.26	780	0.74	0.08	0.08	0.06
2.00	0.1092	0.25	12213	7556	0.62	7964	0.65	2605	0.64	0.34	0.33	0.21	634	0.60	0.08	0.08	0.05
2.00	0.1092	0.50	12213	5553	0.45	5981	0.49	1956	0.48	0.35	0.33	0.16	480	0.46	0.09	0.08	0.03
2.00	0.1092	1.00	12213	3630	0.30	4042	0.33	1286	0.32	0.35	0.32	0.10	317	0.30	0.09	0.08	0.02
2.00	0.1092	2.00	12213	2147	0.18	2496	0.20	768	0.19	0.36	0.31	0.06	171	0.16	0.08	0.07	0.01
2.00	0.1092	4.00	12213	1182	0.10	1363	0.11	413	0.10	0.35	0.30	0.03	104	0.10	0.09	0.08	0.00
4.00	0.2183	0.00	12213	11455	0.94	11761	0.96	3353	1.00	0.29	0.29	0.27	624	1.00	0.05	0.05	0.05
4.00	0.2183	0.10	12213	9327	0.76	9510	0.78	2711	0.81	0.29	0.29	0.22	553	0.89	0.06	0.06	0.04
4.00	0.2183	0.25	12213	7319	0.60	7474	0.61	2238	0.67	0.31	0.30	0.18	472	0.76	0.06	0.06	0.03
4.00	0.2183	0.50	12213	5413	0.44	5544	0.45	1778	0.53	0.33	0.32	0.14	369	0.59	0.07	0.07	0.03
4.00	0.2183	1.00	12213	3566	0.29	3689	0.30	1183	0.35	0.33	0.32	0.09	246	0.39	0.07	0.07	0.02
4.00	0.2183	2.00	12213	2124	0.17	2173	0.18	713	0.21	0.34	0.33	0.05	153	0.25	0.07	0.07	0.01
4.00	0.2183	4.00	12213	1174	0.10	1193	0.10	391	0.12	0.33	0.33	0.03	91	0.15	0.08	0.08	0.00
6.00	0.3275	0.00	12213	11035	0.90	11583	0.95	3265	1.00	0.30	0.28	0.26	617	1.00	0.06	0.05	0.05
6.00	0.3275	0.10	12213	8976	0.73	9302	0.76	2622	0.80	0.29	0.28	0.21	499	0.81	0.06	0.05	0.04
6.00	0.3275	0.25	12213	7063	0.58	7202	0.59	2080	0.64	0.29	0.29	0.17	391	0.63	0.06	0.05	0.03
6.00	0.3275	0.50	12213	5239	0.43	5291	0.43	1555	0.48	0.30	0.29	0.12	291	0.47	0.06	0.06	0.02
6.00	0.3275	1.00	12213	3477	0.28	3529	0.29	1068	0.33	0.31	0.30	0.08	201	0.33	0.06	0.06	0.01
6.00	0.3275	2.00	12213	2089	0.17	2093	0.17	657	0.20	0.31	0.31	0.05	144	0.23	0.07	0.07	0.01
6.00	0.3275	4.00	12213	1163	0.10	1116	0.09	377	0.12	0.32	0.34	0.03	72	0.12	0.06	0.06	0.00
8.00	0.4367	0.00	12213	10578	0.87	11353	0.93	3122	1.00	0.30	0.27	0.25	604	1.00	0.06	0.05	0.04
8.00	0.4367	0.10	12213	8562	0.70	8935	0.73	2519	0.81	0.29	0.28	0.20	482	0.80	0.06	0.05	0.03
8.00	0.4367	0.25	12213	6750	0.55	6918	0.57	1998	0.64	0.30	0.29	0.16	376	0.62	0.06	0.05	0.03
8.00	0.4367	0.50	12213	5042	0.41	5092	0.42	1470	0.47	0.29	0.29	0.12	279	0.46	0.06	0.05	0.02
8.00	0.4367	1.00	12213	3376	0.28	3390	0.28	996	0.32	0.30	0.29	0.08	187	0.31	0.06	0.06	0.01
8.00	0.4367	2.00	12213	2046	0.17	2021	0.17	606	0.19	0.30	0.30	0.04	127	0.21	0.06	0.06	0.01
8.00	0.4367	4.00	12213	1149	0.09	1113	0.09	357	0.11	0.31	0.32	0.02	65	0.11	0.06	0.06	0.00

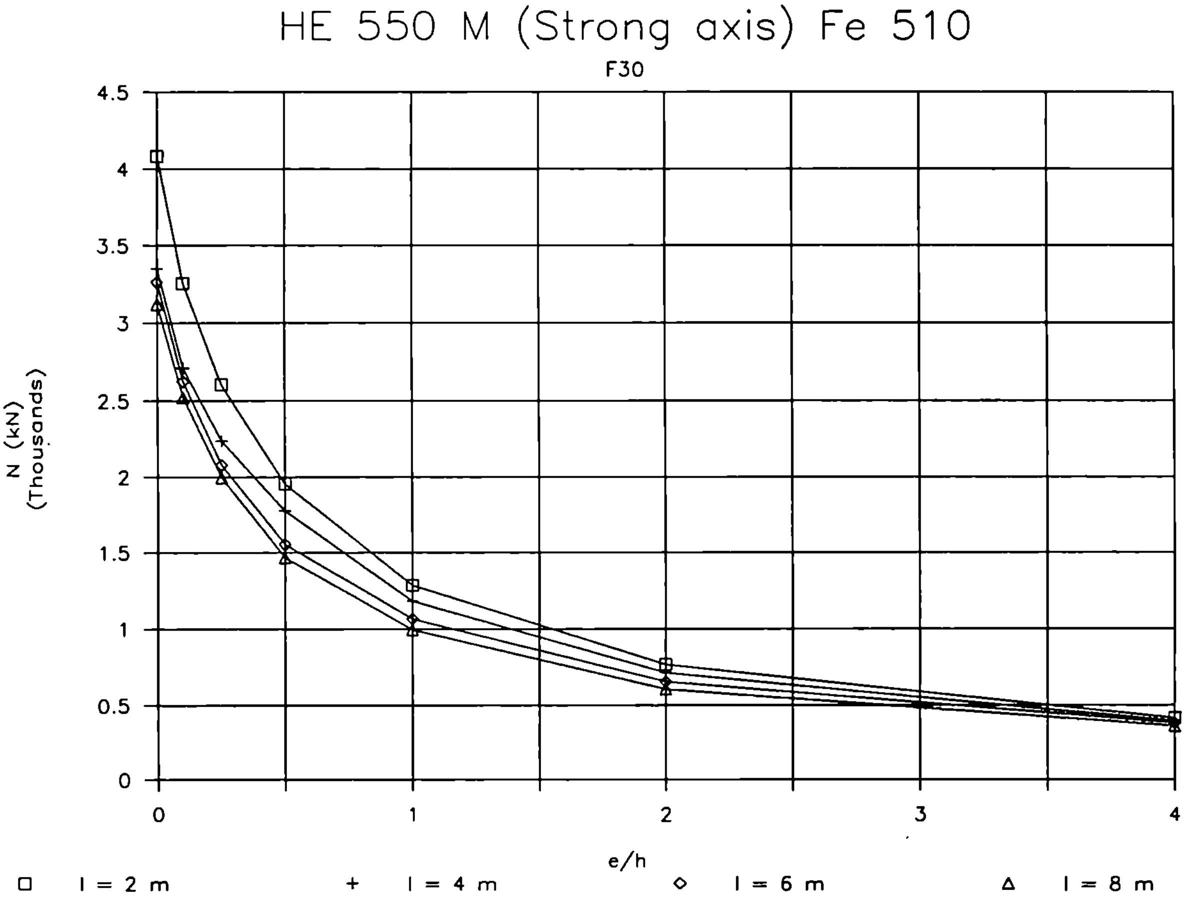

HE 550 M (Strong axis) Fe 510
F30
N (kN)
(Thousands)
4.5
4
3.5
3
2.5
2
1.5
1
0.5
0
0
1
2
3
4
e/h
□ l = 2 m
+ l = 4 m
◇ l = 6 m
Δ l = 8 m

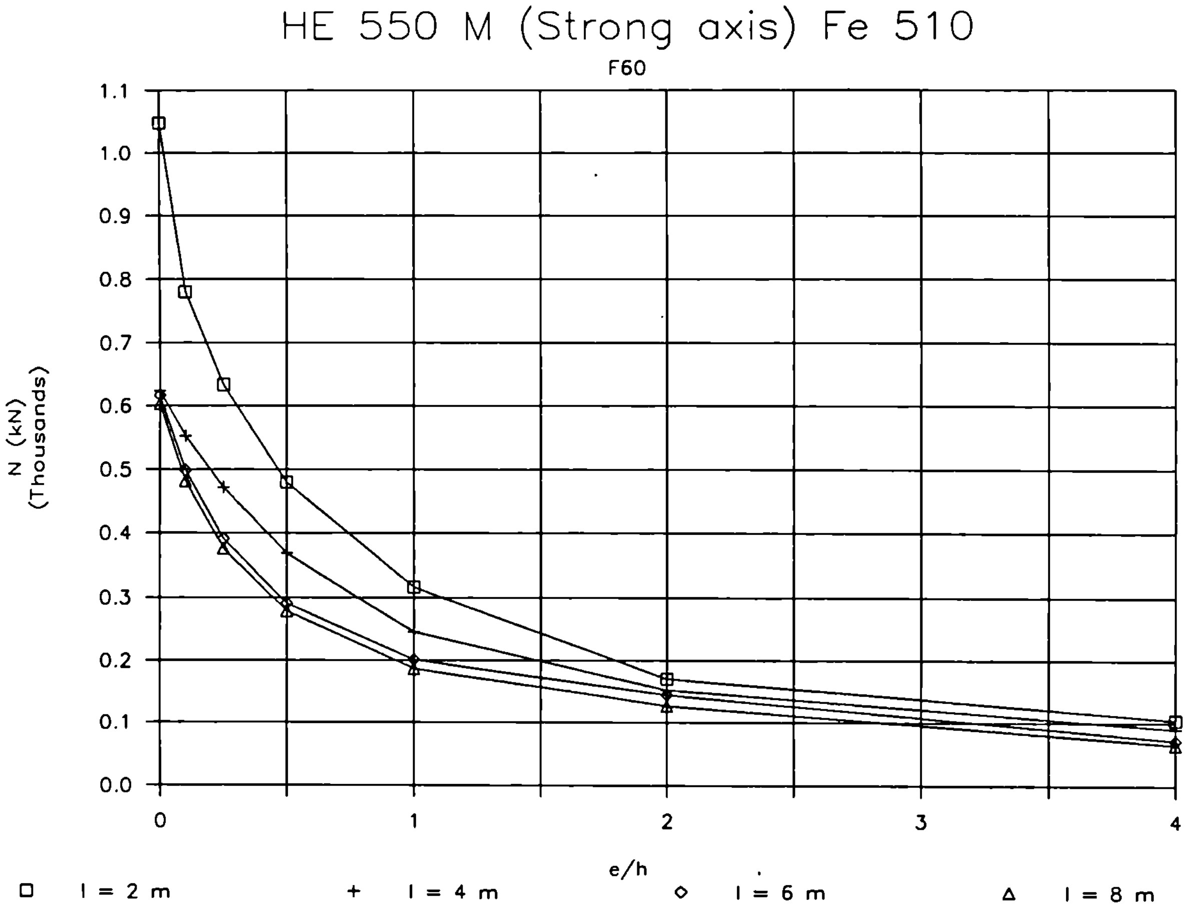

HE 550 M (Strong axis) Fe 510
F60
N (kN)
(Thousands)
1.1
1.0
0.9
0.8
0.7
0.6
0.5
0.4
0.3
0.2
0.1
0.0
0
1
2
3
4
e/h
□ l = 2 m
+ l = 4 m
◇ l = 6 m
Δ l = 8 m

HD 210X210X198 (Strong axis) Sigma yield = 335 N/mm2 ; U/A = 54 ; t = 45 mm

l (m)	Lambda Bar	e/h	Npl (kN)	F0 N(EC3) (kN)	F0 N(EC3)/Npl	F0 N(CEF) (kN)	F0 N(CEF)/Npl	F30 N(F30) (kN)	F30 N/Nc	F30 N/N(F0,EC3)	F30 N/N(F0,CEF)	F30 N/Npl	F60 N(F60) (kN)	F60 N/Nc	F60 N/N(F0,EC3)	F60 N/N(F0,CEF)	F60 N/Npl
2.00	0.2435	0.00	8442	7837	0.93	8222	0.97	2930	1.00	0.37	0.36	0.34	463	1.00	0.06	0.06	0.05
2.00	0.2435	0.10	8442	6318	0.75	6584	0.78	2542	0.87	0.40	0.39	0.30	376	0.81	0.06	0.06	0.04
2.00	0.2435	0.25	8442	4907	0.58	5049	0.60	2024	0.69	0.41	0.40	0.23	308	0.66	0.06	0.06	0.03
2.00	0.2435	0.50	8442	3592	0.43	3705	0.44	1556	0.53	0.43	0.42	0.18	242	0.52	0.07	0.07	0.02
2.00	0.2435	1.00	8442	2347	0.28	2426	0.29	1050	0.36	0.45	0.43	0.12	167	0.36	0.07	0.07	0.01
2.00	0.2435	2.00	8442	1388	0.16	1426	0.17	620	0.21	0.45	0.43	0.07	108	0.23	0.08	0.08	0.01
2.00	0.2435	4.00	8442	764	0.09	770	0.09	343	0.12	0.45	0.45	0.04	67	0.14	0.09	0.09	0.00
4.00	0.4870	0.00	8442	7144	0.85	7841	0.93	2687	1.00	0.38	0.34	0.31	439	1.00	0.06	0.06	0.05
4.00	0.4870	0.10	8442	5703	0.68	6075	0.72	2082	0.77	0.37	0.34	0.24	342	0.78	0.06	0.06	0.04
4.00	0.4870	0.25	8442	4454	0.53	4612	0.55	1610	0.60	0.36	0.35	0.19	262	0.60	0.06	0.06	0.03
4.00	0.4870	0.50	8442	3309	0.39	3362	0.40	1175	0.44	0.36	0.35	0.13	192	0.44	0.06	0.06	0.02
4.00	0.4870	1.00	8442	2206	0.26	2200	0.26	784	0.29	0.36	0.36	0.09	127	0.29	0.06	0.06	0.01
4.00	0.4870	2.00	8442	1331	0.16	1323	0.16	472	0.18	0.35	0.36	0.05	76	0.17	0.06	0.06	0.00
4.00	0.4870	4.00	8442	745	0.09	728	0.09	281	0.10	0.38	0.39	0.03	42	0.10	0.06	0.06	0.00
6.00	0.7305	0.00	8442	6190	0.73	6986	0.83	2386	1.00	0.39	0.34	0.28	395	1.00	0.06	0.06	0.04
6.00	0.7305	0.10	8442	4944	0.59	5313	0.63	1821	0.76	0.37	0.34	0.21	303	0.77	0.06	0.06	0.03
6.00	0.7305	0.25	8442	3904	0.46	4042	0.48	1413	0.59	0.36	0.35	0.16	233	0.59	0.06	0.06	0.02
6.00	0.7305	0.50	8442	2954	0.35	2996	0.35	1047	0.44	0.35	0.35	0.12	172	0.44	0.06	0.06	0.02
6.00	0.7305	1.00	8442	2022	0.24	2010	0.24	702	0.29	0.35	0.35	0.08	116	0.29	0.06	0.06	0.01
6.00	0.7305	2.00	8442	1257	0.15	1233	0.15	431	0.18	0.34	0.35	0.05	70	0.18	0.06	0.06	0.00
6.00	0.7305	4.00	8442	716	0.08	692	0.08	242	0.10	0.34	0.35	0.02	39	0.10	0.06	0.06	0.00
8.00	0.9740	0.00	8442	5024	0.60	5822	0.69	1945	1.00	0.39	0.33	0.23	332	1.00	0.07	0.06	0.03
8.00	0.9740	0.10	8442	4099	0.49	4383	0.52	1530	0.79	0.37	0.35	0.18	257	0.77	0.06	0.06	0.03
8.00	0.9740	0.25	8442	3316	0.39	3408	0.40	1191	0.61	0.36	0.35	0.14	200	0.60	0.06	0.06	0.02
8.00	0.9740	0.50	8442	2575	0.31	2584	0.31	903	0.46	0.35	0.35	0.10	151	0.46	0.06	0.06	0.01
8.00	0.9740	1.00	8442	1824	0.22	1791	0.21	626	0.32	0.34	0.35	0.07	104	0.31	0.06	0.06	0.01
8.00	0.9740	2.00	8442	1171	0.14	1130	0.13	395	0.20	0.34	0.35	0.04	65	0.20	0.06	0.06	0.00
8.00	0.9740	4.00	8442	683	0.08	655	0.08	229	0.12	0.34	0.35	0.02	37	0.11	0.05	0.06	0.00

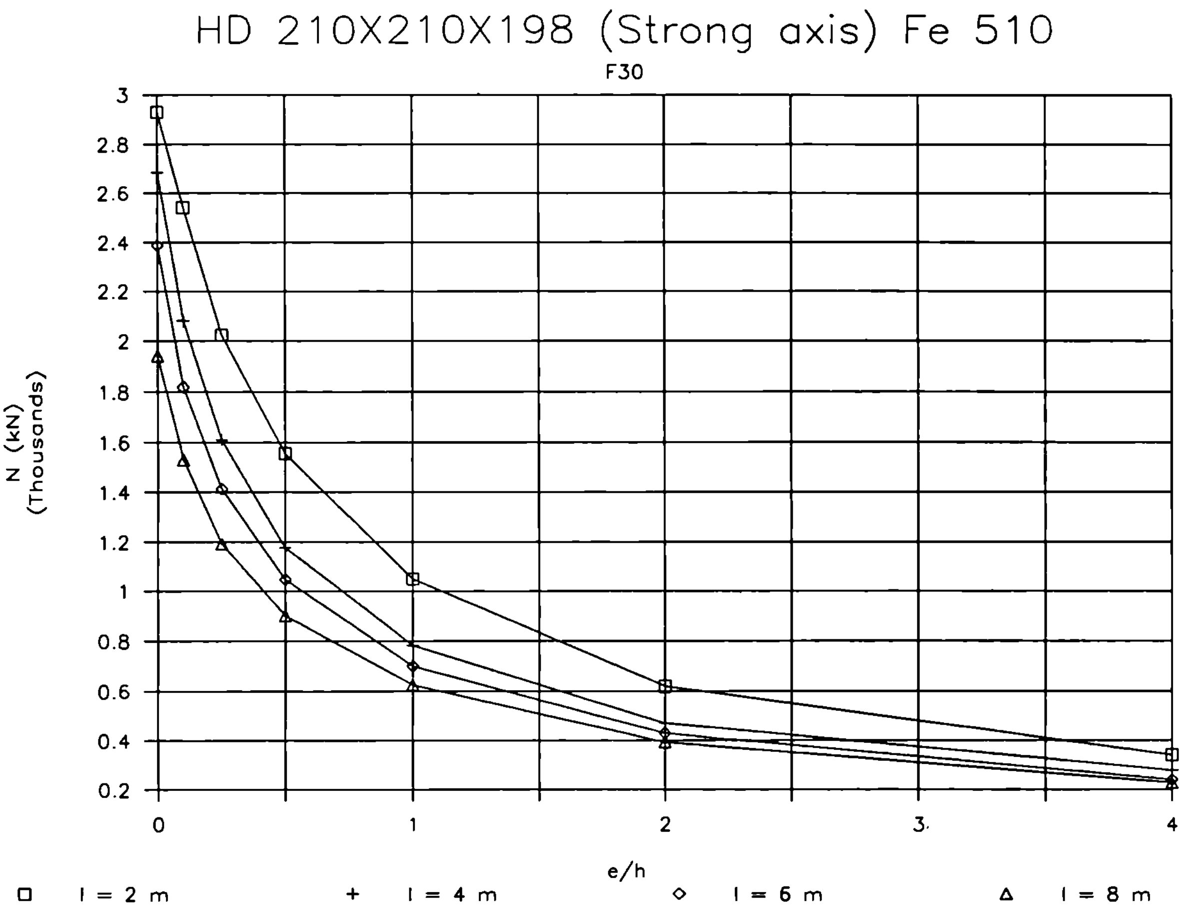
HD 210X210X198 (Strong axis) Fe 510
F30
N (kN)
(Thousands)
3
2.8
2.6
2.4
2.2
2
1.8
1.6
1.4
1.2
1
0.8
0.6
0.4
0.2
0
1
2
3
4
e/h
□ l = 2 m
+ l = 4 m
◇ l = 6 m
△ l = 8 m

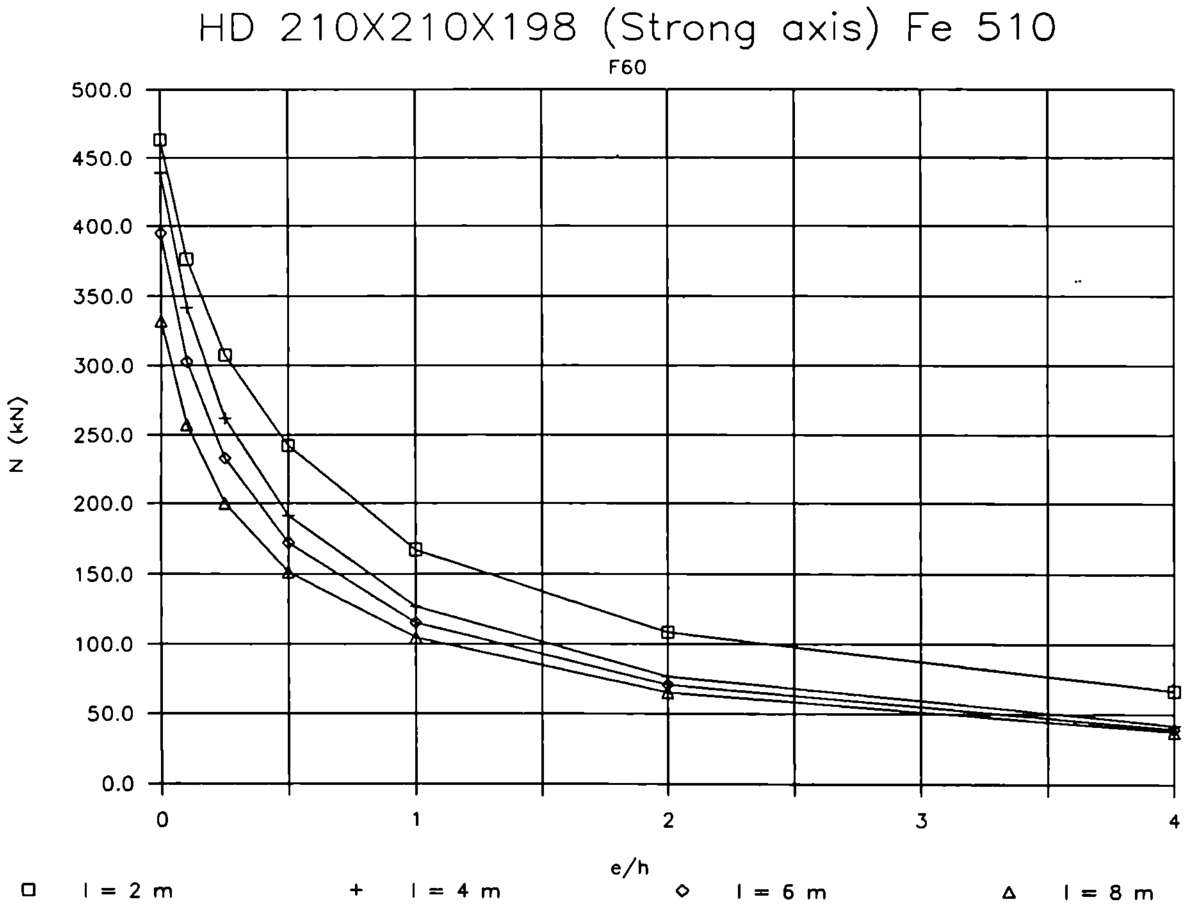
HD 210X210X198 (Strong axis) Fe 510
F60
N (kN)
500.0
450.0
400.0
350.0
300.0
250.0
200.0
150.0
100.0
50.0
0.0
0
1
2
3
4
e/h
□ l = 2 m
+ l = 4 m
◇ l = 6 m
△ l = 8 m

HD 260X260X219 (Strong axis) Sigma yield = 335 N/mm2 ; U/A = 58 ; t = 41 mm

l	Lambda Bar	e/h	Npl	F0				F30					F60				
(m)			(kN)	N(EC3) (kN)	N(EC3)/Npl	N(CEF) (kN)	N(CEF)/Npl	N(F30) (kN)	N/Nc	N/N(F0,EC3)	N/N(F0,CEF)	N/Npl	N(F60) (kN)	N/Nc	N/N(F0,EC3)	N/N(F0,CEF)	N/Npl
2.00	0.2072	0.00	9347	8784	0.94	9135	0.98	3075	1.00	0.35	0.34	0.32	524	1.00	0.06	0.06	0.05
2.00	0.2072	0.10	9347	7134	0.76	7301	0.78	2602	0.85	0.36	0.36	0.27	461	0.88	0.06	0.06	0.04
2.00	0.2072	0.25	9347	5579	0.60	5658	0.61	2161	0.70	0.39	0.38	0.23	390	0.74	0.07	0.07	0.04
2.00	0.2072	0.50	9347	4098	0.44	4158	0.44	1667	0.54	0.41	0.40	0.17	306	0.58	0.07	0.07	0.03
2.00	0.2072	1.00	9347	2689	0.29	2713	0.29	1118	0.36	0.42	0.41	0.11	209	0.40	0.08	0.08	0.02
2.00	0.2072	2.00	9347	1594	0.17	1628	0.17	671	0.22	0.42	0.41	0.07	132	0.25	0.08	0.08	0.01
2.00	0.2072	4.00	9347	881	0.09	917	0.10	372	0.12	0.42	0.41	0.03	79	0.15	0.09	0.09	0.00
4.00	0.4144	0.00	9347	8155	0.87	8733	0.93	2788	1.00	0.34	0.32	0.29	481	1.00	0.06	0.06	0.05
4.00	0.4144	0.10	9347	6591	0.71	6873	0.74	2194	0.79	0.33	0.32	0.23	379	0.79	0.06	0.06	0.04
4.00	0.4144	0.25	9347	5168	0.55	5301	0.57	1693	0.61	0.33	0.32	0.18	293	0.61	0.06	0.06	0.03
4.00	0.4144	0.50	9347	3839	0.41	3876	0.41	1266	0.45	0.33	0.33	0.13	216	0.45	0.06	0.06	0.02
4.00	0.4144	1.00	9347	2558	0.27	2563	0.27	851	0.31	0.33	0.33	0.09	144	0.30	0.06	0.06	0.01
4.00	0.4144	2.00	9347	1544	0.17	1525	0.16	519	0.19	0.34	0.34	0.05	88	0.18	0.06	0.06	0.00
4.00	0.4144	4.00	9347	863	0.09	847	0.09	302	0.11	0.35	0.36	0.03	51	0.11	0.06	0.06	0.00
6.00	0.6216	0.00	9347	7362	0.79	8000	0.86	2554	1.00	0.35	0.32	0.27	441	1.00	0.06	0.06	0.04
6.00	0.6216	0.10	9347	5914	0.63	6198	0.66	1979	0.77	0.33	0.32	0.21	342	0.78	0.06	0.06	0.03
6.00	0.6216	0.25	9347	4671	0.50	4802	0.51	1533	0.60	0.33	0.32	0.16	267	0.61	0.06	0.06	0.02
6.00	0.6216	0.50	9347	3518	0.38	3559	0.38	1146	0.45	0.33	0.32	0.12	198	0.45	0.06	0.06	0.02
6.00	0.6216	1.00	9347	2391	0.26	2377	0.25	777	0.30	0.32	0.33	0.08	133	0.30	0.06	0.06	0.01
6.00	0.6216	2.00	9347	1476	0.16	1441	0.15	471	0.18	0.32	0.33	0.05	81	0.18	0.05	0.06	0.00
6.00	0.6216	4.00	9347	839	0.09	810	0.09	265	0.10	0.32	0.33	0.02	45	0.10	0.05	0.06	0.00
8.00	0.8288	0.00	9347	6350	0.68	6861	0.73	2190	1.00	0.34	0.32	0.23	385	1.00	0.06	0.06	0.04
8.00	0.8288	0.10	9347	5135	0.55	5366	0.57	1713	0.78	0.33	0.32	0.18	301	0.78	0.06	0.06	0.03
8.00	0.8288	0.25	9347	4113	0.44	4208	0.45	1343	0.61	0.33	0.32	0.14	237	0.61	0.06	0.06	0.02
8.00	0.8288	0.50	9347	3160	0.34	3165	0.34	1034	0.47	0.33	0.33	0.11	179	0.46	0.06	0.06	0.01
8.00	0.8288	1.00	9347	2202	0.24	2178	0.23	702	0.32	0.32	0.32	0.07	122	0.32	0.06	0.06	0.01
8.00	0.8288	2.00	9347	1395	0.15	1350	0.14	441	0.20	0.32	0.33	0.04	75	0.20	0.05	0.06	0.00
8.00	0.8288	4.00	9347	809	0.09	778	0.08	251	0.11	0.31	0.32	0.02	43	0.11	0.05	0.06	0.00

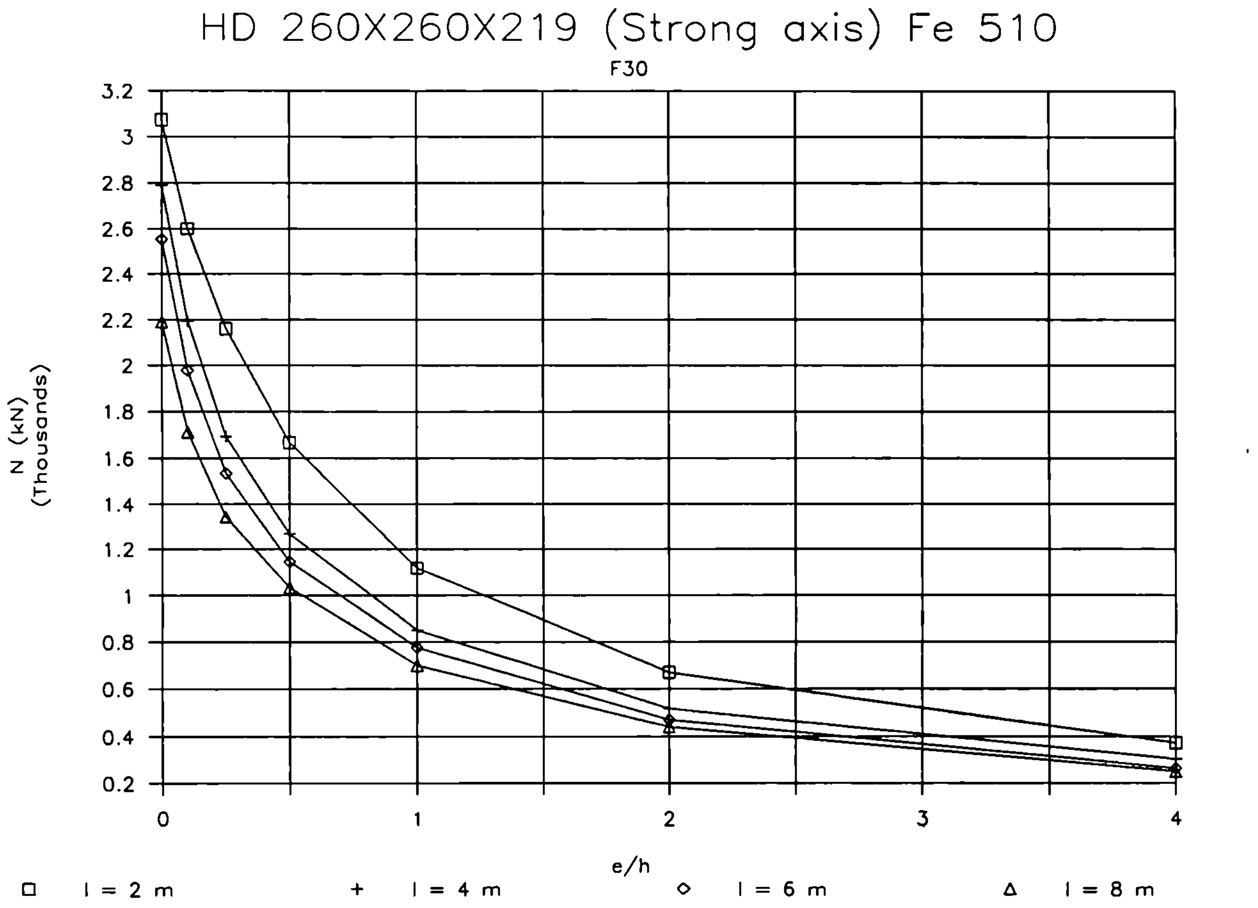

HD 260X260X219 (Strong axis) Fe 510
F30
N (kN)
(Thousands)
3.2
3
2.8
2.6
2.4
2.2
2
1.8
1.6
1.4
1.2
1
0.8
0.6
0.4
0.2
0
1
2
3
4
e/h
l = 2 m
l = 4 m
l = 6 m
l = 8 m

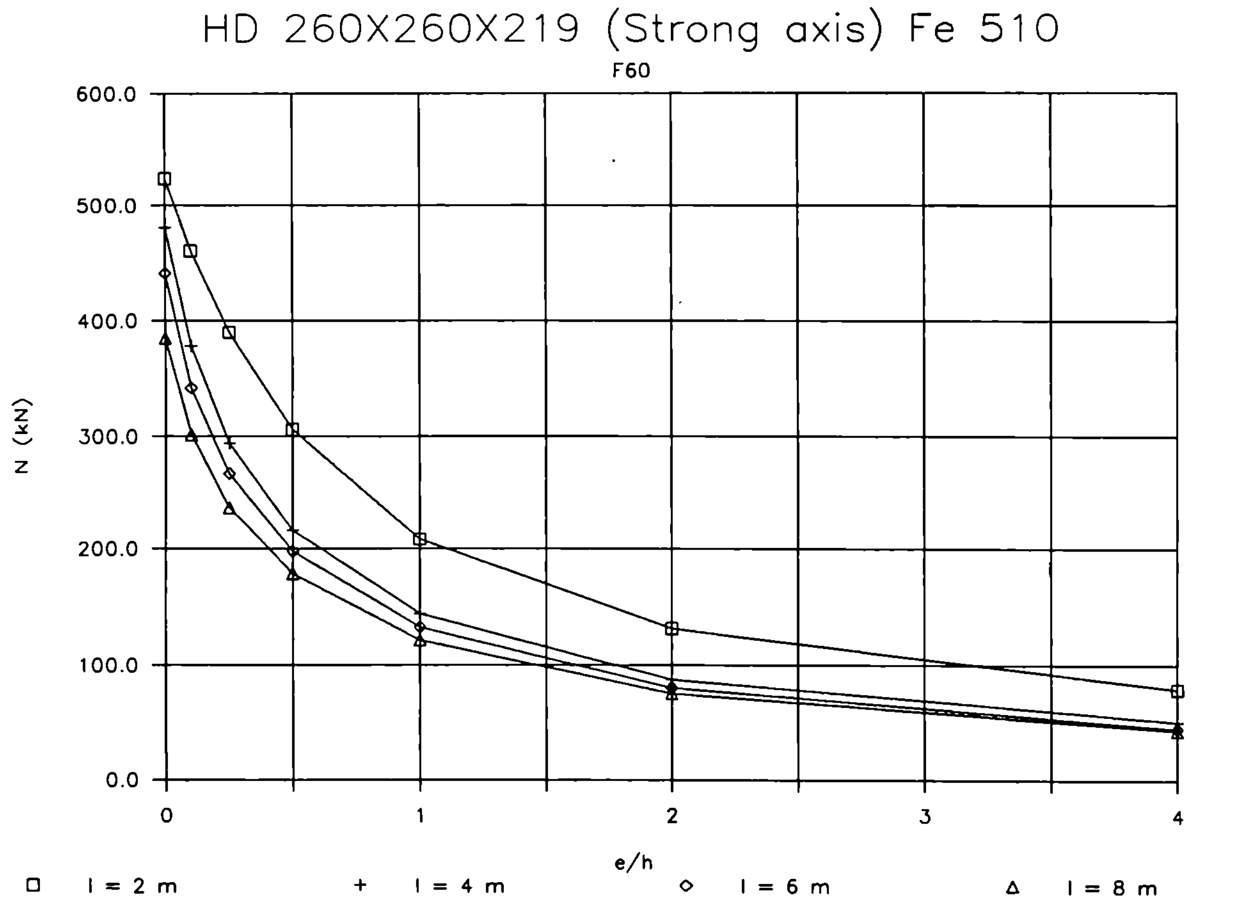

HD 260X260X219 (Strong axis) Fe 510
F60
N (kN)
600.0
500.0
400.0
300.0
200.0
100.0
0.0
0
1
2
3
4
e/h
l = 2 m
l = 4 m
l = 6 m
l = 8 m

HD 260X260X329 (Strong axis) Sigma yield = 335 N/mm2 ; U/A = 41 ; t = 60 mm

l (m)	Lambda Bar	e/h	Npl (kN)	F0				F30					F60				
				N(EC3) (kN)	N(EC3)/Npl	N(CEF) (kN)	N(CEF)/Npl	N(F30) (kN)	N/Nc	N/N(F0,EC3)	N/N(F0,CEF)	N/Npl	N(F60) (kN)	N/Nc	N/N(F0,EC3)	N/N(F0,CEF)	N/Npl
2.00	0.1927	0.00	14070	13271	0.94	13841	0.98	10853	1.00	0.82	0.78	0.77	987	1.00	0.07	0.07	0.07
2.00	0.1927	0.10	14070	10664	0.76	11061	0.79	8166	0.75	0.77	0.74	0.58	863	0.87	0.08	0.08	0.06
2.00	0.1927	0.25	14070	8267	0.59	8573	0.61	6438	0.59	0.78	0.75	0.45	722	0.73	0.09	0.08	0.05
2.00	0.1927	0.50	14070	6032	0.43	6300	0.45	4731	0.44	0.78	0.75	0.33	553	0.56	0.09	0.09	0.03
2.00	0.1927	1.00	14070	3924	0.28	4152	0.30	3066	0.28	0.78	0.74	0.21	377	0.38	0.10	0.09	0.02
2.00	0.1927	2.00	14070	2310	0.16	2466	0.18	1790	0.16	0.77	0.73	0.12	237	0.24	0.10	0.10	0.01
2.00	0.1927	4.00	14070	1268	0.09	1350	0.10	979	0.09	0.77	0.73	0.06	141	0.14	0.11	0.10	0.01
4.00	0.3854	0.00	14070	12405	0.88	13365	0.95	7383	1.00	0.60	0.55	0.52	902	1.00	0.07	0.07	0.06
4.00	0.3854	0.10	14070	9933	0.71	10414	0.74	6147	0.83	0.62	0.59	0.43	706	0.78	0.07	0.07	0.05
4.00	0.3854	0.25	14070	7727	0.55	7952	0.57	5048	0.68	0.65	0.63	0.35	542	0.60	0.07	0.07	0.03
4.00	0.3854	0.50	14070	5693	0.40	5813	0.41	3848	0.52	0.68	0.66	0.27	396	0.44	0.07	0.07	0.02
4.00	0.3854	1.00	14070	3755	0.27	3806	0.27	2586	0.35	0.69	0.68	0.18	262	0.29	0.07	0.07	0.01
4.00	0.3854	2.00	14070	2247	0.16	2250	0.16	1575	0.21	0.70	0.70	0.11	156	0.17	0.07	0.07	0.01
4.00	0.3854	4.00	14070	1245	0.09	1221	0.09	888	0.12	0.71	0.73	0.06	92	0.10	0.07	0.08	0.00
6.00	0.5781	0.00	14070	11341	0.81	12583	0.89	6540	1.00	0.58	0.52	0.46	856	1.00	0.08	0.07	0.06
6.00	0.5781	0.10	14070	9037	0.64	9679	0.69	5031	0.77	0.56	0.52	0.35	659	0.77	0.07	0.07	0.04
6.00	0.5781	0.25	14070	7070	0.50	7349	0.52	3929	0.60	0.56	0.53	0.27	502	0.59	0.07	0.07	0.03
6.00	0.5781	0.50	14070	5270	0.37	5338	0.38	2996	0.46	0.57	0.56	0.21	367	0.43	0.07	0.07	0.02
6.00	0.5781	1.00	14070	3543	0.25	3531	0.25	2084	0.32	0.59	0.59	0.14	242	0.28	0.07	0.07	0.01
6.00	0.5781	2.00	14070	2161	0.15	2140	0.15	1311	0.20	0.61	0.61	0.09	146	0.17	0.07	0.07	0.01
6.00	0.5781	4.00	14070	1214	0.09	1179	0.08	788	0.12	0.65	0.67	0.05	81	0.09	0.07	0.07	0.00
8.00	0.7708	0.00	14070	9993	0.71	11412	0.81	5788	1.00	0.58	0.51	0.41	787	1.00	0.08	0.07	0.05
8.00	0.7708	0.10	14070	7984	0.57	8550	0.61	4444	0.77	0.56	0.52	0.31	615	0.78	0.08	0.07	0.04
8.00	0.7708	0.25	14070	6325	0.45	6548	0.47	3500	0.60	0.55	0.53	0.24	455	0.58	0.07	0.07	0.03
8.00	0.7708	0.50	14070	4792	0.34	4844	0.34	2617	0.45	0.55	0.54	0.18	335	0.43	0.07	0.07	0.02
8.00	0.7708	1.00	14070	3294	0.23	3267	0.23	1791	0.31	0.54	0.55	0.12	226	0.29	0.07	0.07	0.01
8.00	0.7708	2.00	14070	2057	0.15	2005	0.14	1120	0.19	0.54	0.56	0.07	138	0.17	0.07	0.07	0.00
8.00	0.7708	4.00	14070	1177	0.08	1132	0.08	681	0.12	0.58	0.60	0.04	77	0.10	0.07	0.07	0.00

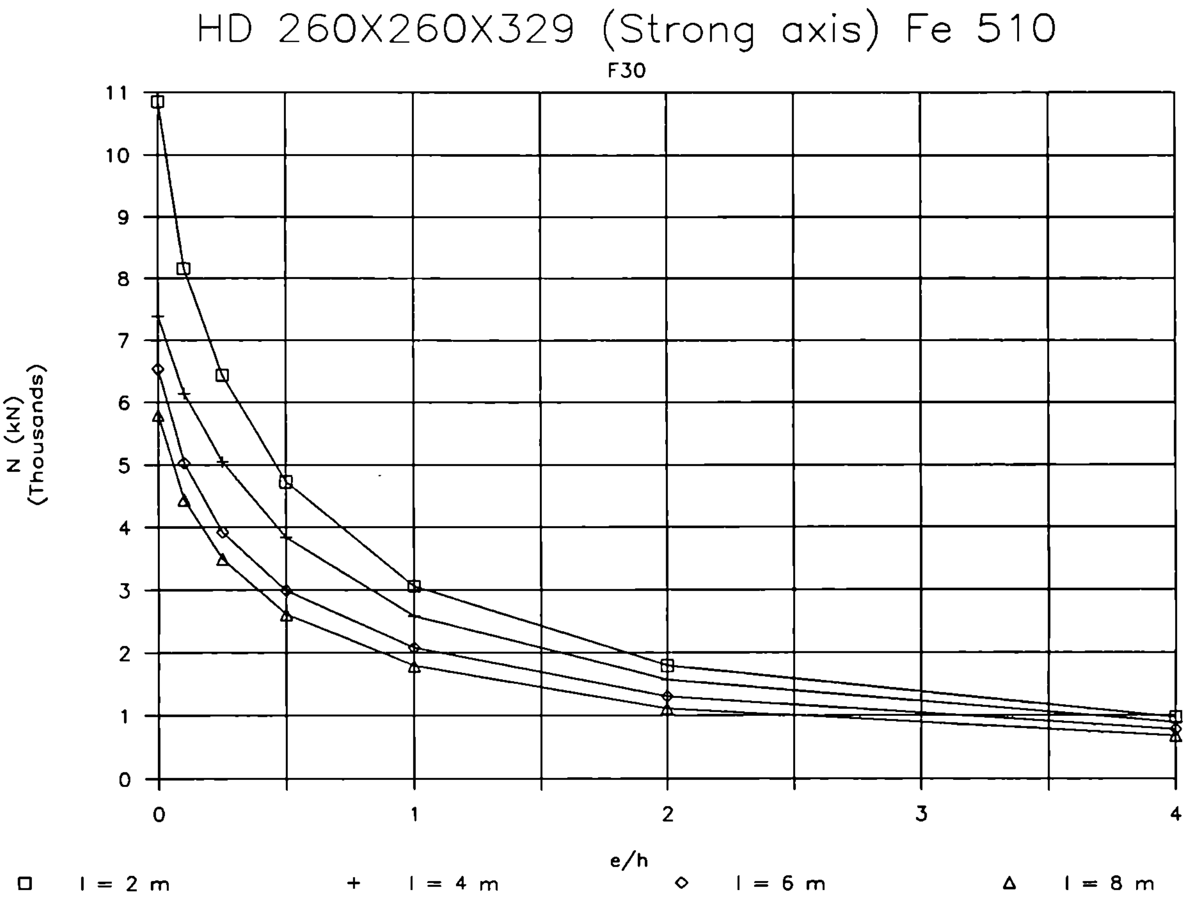
HD 260X260X329 (Strong axis) Fe 510
F30
N (kN) (Thousands)
e/h
□ l = 2 m
+ l = 4 m
◇ l = 6 m
Δ l = 8 m

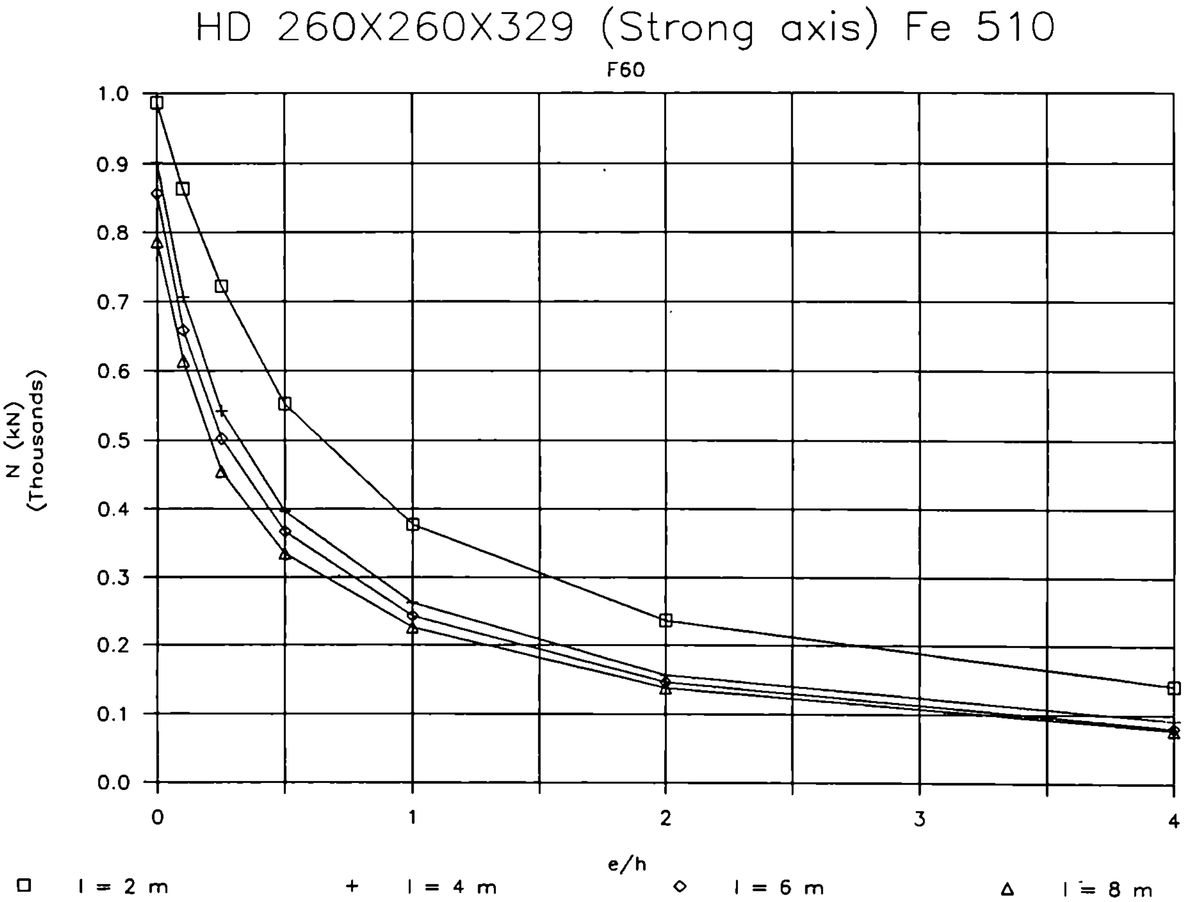
HD 260X260X329 (Strong axis) Fe 510
F60
N (kN) (Thousands)
e/h
□ l = 2 m
+ l = 4 m
◇ l = 6 m
Δ l = 8 m

HD 310X310X283 (Strong axis) Sigma yield = 335 N/mm2 ; U/A = 54 ; t = 44 mm

l (m)	Lambda Bar	e/h	Npl (kN)	F0 N(EC3) (kN)	F0 N(EC3)/Npl	F0 N(CEF) (kN)	F0 N(CEF)/Npl	F30 N(F30) (kN)	F30 N/Nc	F30 N/N(F0,EC3)	F30 N/N(F0,CEF)	F30 N/Npl	F60 N(F60) (kN)	F60 N/Nc	F60 N/N(F0,EC3)	F60 N/N(F0,CEF)	F60 N/Npl
2.00	0.1721	0.00	12060	11460	0.95	11876	0.98	5291	1.00	0.46	0.45	0.43	826	1.00	0.07	0.07	0.06
2.00	0.1721	0.10	12060	9323	0.77	9587	0.79	4413	0.83	0.47	0.46	0.36	717	0.87	0.08	0.07	0.05
2.00	0.1721	0.25	12060	7304	0.61	7430	0.62	3594	0.68	0.49	0.48	0.29	596	0.72	0.08	0.08	0.04
2.00	0.1721	0.50	12060	5370	0.45	5452	0.45	2706	0.51	0.50	0.50	0.22	468	0.57	0.09	0.09	0.03
2.00	0.1721	1.00	12060	3524	0.29	3563	0.30	1814	0.34	0.51	0.51	0.15	314	0.38	0.09	0.09	0.02
2.00	0.1721	2.00	12060	2089	0.17	2138	0.18	1061	0.20	0.51	0.50	0.08	194	0.23	0.09	0.09	0.01
2.00	0.1721	4.00	12060	1151	0.10	1247	0.10	597	0.11	0.52	0.48	0.04	114	0.14	0.10	0.09	0.00
4.00	0.3442	0.00	12060	10814	0.90	11583	0.96	4243	1.00	0.39	0.37	0.35	660	1.00	0.06	0.06	0.05
4.00	0.3442	0.10	12060	8776	0.73	9117	0.76	3452	0.81	0.39	0.38	0.28	524	0.79	0.06	0.06	0.04
4.00	0.3442	0.25	12060	6888	0.57	7066	0.59	2728	0.64	0.40	0.39	0.22	409	0.62	0.06	0.06	0.03
4.00	0.3442	0.50	12060	5115	0.42	5192	0.43	2159	0.51	0.42	0.42	0.17	303	0.46	0.06	0.06	0.02
4.00	0.3442	1.00	12060	3392	0.28	3400	0.28	1471	0.35	0.43	0.43	0.12	206	0.31	0.06	0.06	0.01
4.00	0.3442	2.00	12060	2039	0.17	2043	0.17	910	0.21	0.45	0.45	0.07	125	0.19	0.06	0.06	0.01
4.00	0.3442	4.00	12060	1135	0.09	1113	0.09	524	0.12	0.46	0.47	0.04	76	0.12	0.07	0.07	0.00
6.00	0.5163	0.00	12060	10051	0.83	10905	0.90	3984	1.00	0.40	0.37	0.33	627	1.00	0.06	0.06	0.05
6.00	0.5163	0.10	12060	8113	0.67	8473	0.70	3095	0.78	0.38	0.37	0.25	491	0.78	0.06	0.06	0.04
6.00	0.5163	0.25	12060	6395	0.53	6564	0.54	2446	0.61	0.38	0.37	0.20	382	0.61	0.06	0.06	0.03
6.00	0.5163	0.50	12060	4791	0.40	4865	0.40	1821	0.46	0.38	0.37	0.15	282	0.45	0.06	0.06	0.02
6.00	0.5163	1.00	12060	3230	0.27	3218	0.27	1229	0.31	0.38	0.38	0.10	188	0.30	0.06	0.06	0.01
6.00	0.5163	2.00	12060	1972	0.16	1950	0.16	769	0.19	0.39	0.39	0.06	114	0.18	0.06	0.06	0.00
6.00	0.5163	4.00	12060	1114	0.09	1080	0.09	449	0.11	0.40	0.42	0.03	63	0.10	0.06	0.06	0.00
8.00	0.6884	0.00	12060	9117	0.76	9791	0.81	3664	1.00	0.40	0.37	0.30	575	1.00	0.06	0.06	0.04
8.00	0.6884	0.10	12060	7330	0.61	7703	0.64	2814	0.77	0.38	0.37	0.23	449	0.78	0.06	0.06	0.03
8.00	0.6884	0.25	12060	5823	0.48	5967	0.49	2223	0.61	0.38	0.37	0.18	351	0.61	0.06	0.06	0.02
8.00	0.6884	0.50	12060	4419	0.37	4459	0.37	1669	0.46	0.38	0.37	0.13	262	0.46	0.06	0.06	0.02
8.00	0.6884	1.00	12060	3034	0.25	2999	0.25	1122	0.31	0.37	0.37	0.09	176	0.31	0.06	0.06	0.01
8.00	0.6884	2.00	12060	1890	0.16	1854	0.15	698	0.19	0.37	0.38	0.05	108	0.19	0.06	0.06	0.00
8.00	0.6884	4.00	12060	1083	0.09	1042	0.09	402	0.11	0.37	0.39	0.03	61	0.11	0.06	0.06	0.00

HD 310X310X283 (Strong axis) Fe 510

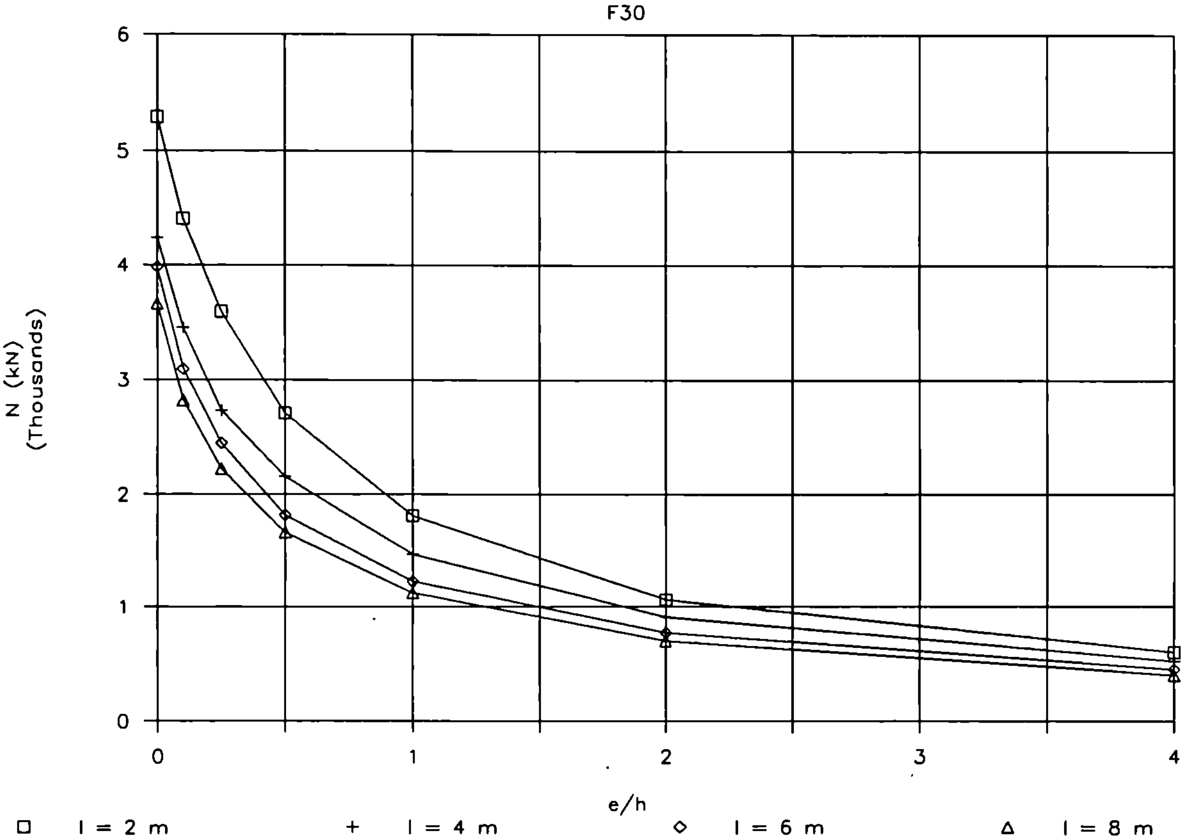

HD 310X310X283 (Strong axis) Fe 510

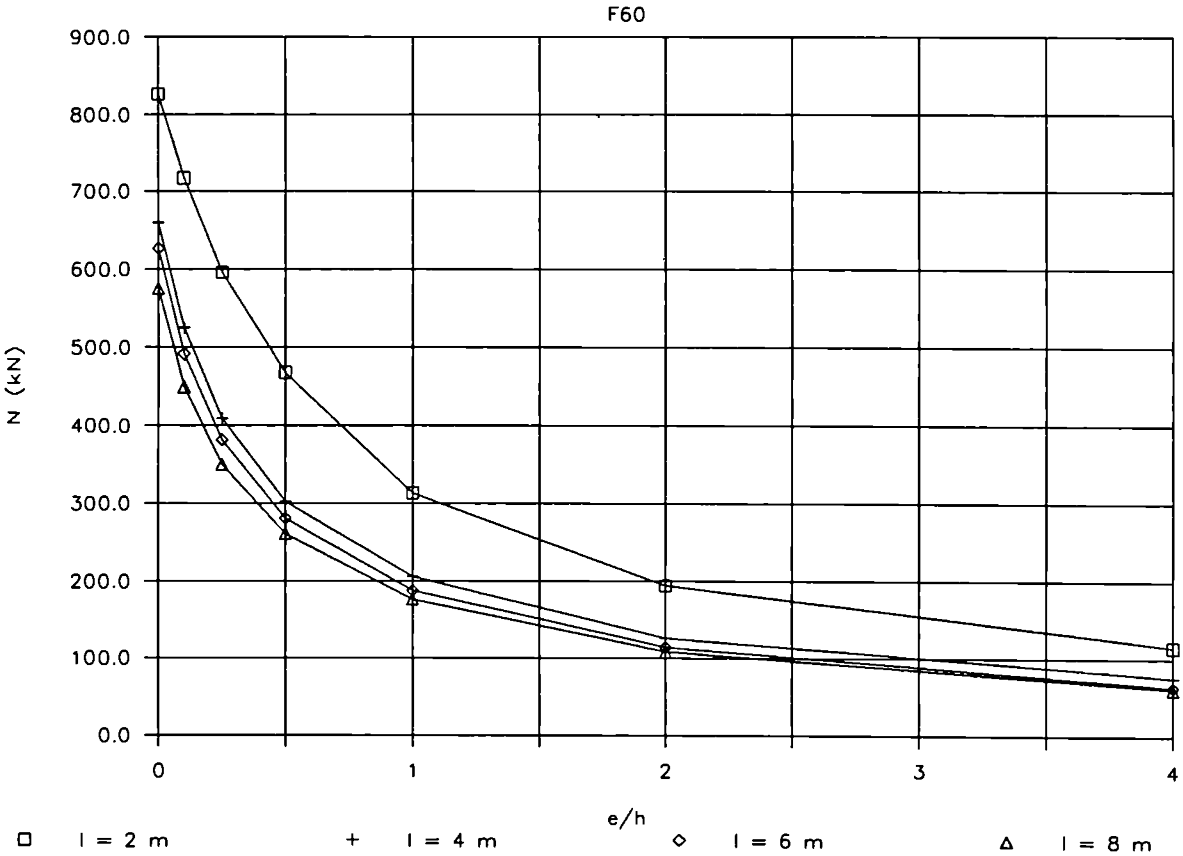

HD 310X310X375 (Strong axis) Sigma yield = 335 N/mm2 ; U/A = 42 ; t = 57 mm

l (m)	Lambda Bar	e/h	Npl (kN)	F0				F30					F60				
				N(EC3) (kN)	N(EC3)/Npl	N(CEF) (kN)	N(CEF)/Npl	N(F30) (kN)	N/Nc	N/N(F0,EC3)	N/N(F0,CEF)	N/Npl	N(F60) (kN)	N/Nc	N/N(F0,EC3)	N/N(F0,CEF)	N/Npl
2.00	0.1656	0.00	16013	15220	0.95	15640	0.98	12459	1.00	0.82	0.80	0.77	1260	1.00	0.08	0.08	0.07
2.00	0.1656	0.10	16013	12324	0.77	12663	0.79	9402	0.75	0.76	0.74	0.58	1106	0.88	0.09	0.09	0.06
2.00	0.1656	0.25	16013	9594	0.60	9914	0.62	7445	0.60	0.78	0.75	0.46	918	0.73	0.10	0.09	0.05
2.00	0.1656	0.50	16013	7019	0.44	7422	0.46	5511	0.44	0.79	0.74	0.34	709	0.56	0.10	0.10	0.04
2.00	0.1656	1.00	16013	4576	0.29	4899	0.31	3565	0.29	0.78	0.73	0.22	472	0.37	0.10	0.10	0.02
2.00	0.1656	2.00	16013	2700	0.17	2910	0.18	2111	0.17	0.78	0.73	0.13	293	0.23	0.11	0.10	0.01
2.00	0.1656	4.00	16013	1484	0.09	1664	0.10	1144	0.09	0.77	0.69	0.07	172	0.14	0.12	0.10	0.01
4.00	0.3312	0.00	16013	14406	0.90	15300	0.96	9031	1.00	0.63	0.59	0.56	1029	1.00	0.07	0.07	0.06
4.00	0.3312	0.10	16013	11626	0.73	12164	0.76	7587	0.84	0.65	0.62	0.47	815	0.79	0.07	0.07	0.05
4.00	0.3312	0.25	16013	9081	0.57	9334	0.58	6059	0.67	0.67	0.65	0.37	631	0.61	0.07	0.07	0.03
4.00	0.3312	0.50	16013	6700	0.42	6790	0.42	4667	0.52	0.70	0.69	0.29	465	0.45	0.07	0.07	0.02
4.00	0.3312	1.00	16013	4422	0.28	4491	0.28	3144	0.35	0.71	0.70	0.19	312	0.30	0.07	0.07	0.01
4.00	0.3312	2.00	16013	2638	0.16	2672	0.17	1871	0.21	0.71	0.70	0.11	188	0.18	0.07	0.07	0.01
4.00	0.3312	4.00	16013	1464	0.09	1440	0.09	1063	0.12	0.73	0.74	0.06	114	0.11	0.08	0.08	0.00
6.00	0.4968	0.00	16013	13454	0.84	14550	0.91	7661	1.00	0.57	0.53	0.47	982	1.00	0.07	0.07	0.06
6.00	0.4968	0.10	16013	10794	0.67	11305	0.71	5952	0.78	0.55	0.53	0.37	766	0.78	0.07	0.07	0.04
6.00	0.4968	0.25	16013	8457	0.53	8745	0.55	4762	0.62	0.56	0.54	0.29	591	0.60	0.07	0.07	0.03
6.00	0.4968	0.50	16013	6301	0.39	6426	0.40	3763	0.49	0.60	0.59	0.23	435	0.44	0.07	0.07	0.02
6.00	0.4968	1.00	16013	4216	0.26	4208	0.26	2624	0.34	0.62	0.62	0.16	287	0.29	0.07	0.07	0.01
6.00	0.4968	2.00	16013	2559	0.16	2525	0.16	1631	0.21	0.64	0.65	0.10	173	0.18	0.07	0.07	0.01
6.00	0.4968	4.00	16013	1435	0.09	1398	0.09	961	0.13	0.67	0.69	0.05	95	0.10	0.07	0.07	0.00
8.00	0.6624	0.00	16013	12285	0.77	13329	0.83	6928	1.00	0.56	0.52	0.43	914	1.00	0.07	0.07	0.05
8.00	0.6624	0.10	16013	9835	0.61	10327	0.64	5354	0.77	0.54	0.52	0.33	708	0.77	0.07	0.07	0.04
8.00	0.6624	0.25	16013	7750	0.48	8000	0.50	4212	0.61	0.54	0.53	0.26	546	0.60	0.07	0.07	0.03
8.00	0.6624	0.50	16013	5845	0.37	5891	0.37	3149	0.45	0.54	0.53	0.19	405	0.44	0.07	0.07	0.02
8.00	0.6624	1.00	16013	3981	0.25	3961	0.25	2188	0.32	0.55	0.55	0.13	270	0.30	0.07	0.07	0.01
8.00	0.6624	2.00	16013	2461	0.15	2425	0.15	1392	0.20	0.57	0.57	0.08	164	0.18	0.07	0.07	0.01
8.00	0.6624	4.00	16013	1400	0.09	1363	0.09	850	0.12	0.61	0.62	0.05	92	0.10	0.07	0.07	0.00

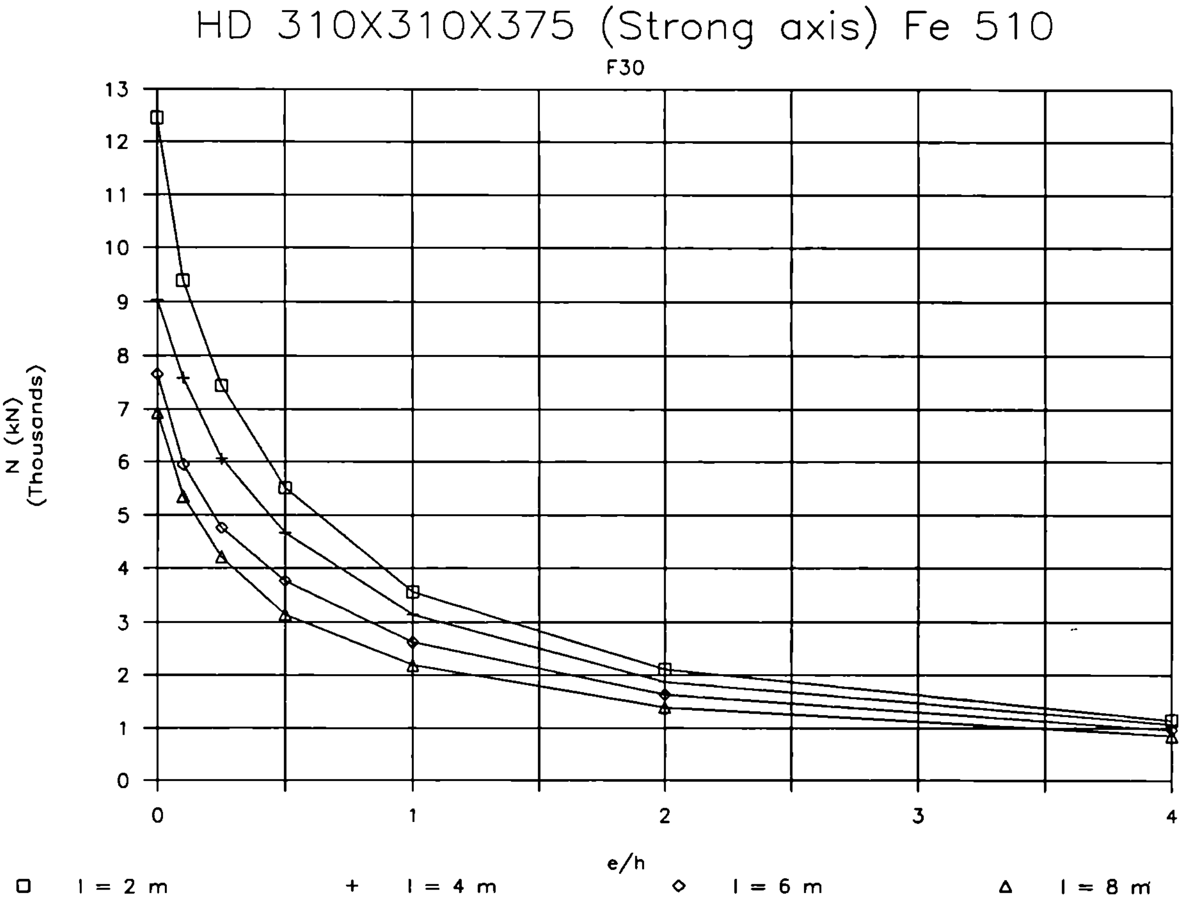

HD 310X310X375 (Strong axis) Fe 510
F30
N (kN)
(Thousands)
13
12
11
10
9
8
7
6
5
4
3
2
1
0
0
1
2
3
4
e/h
l = 2 m
l = 4 m
l = 6 m
l = 8 m

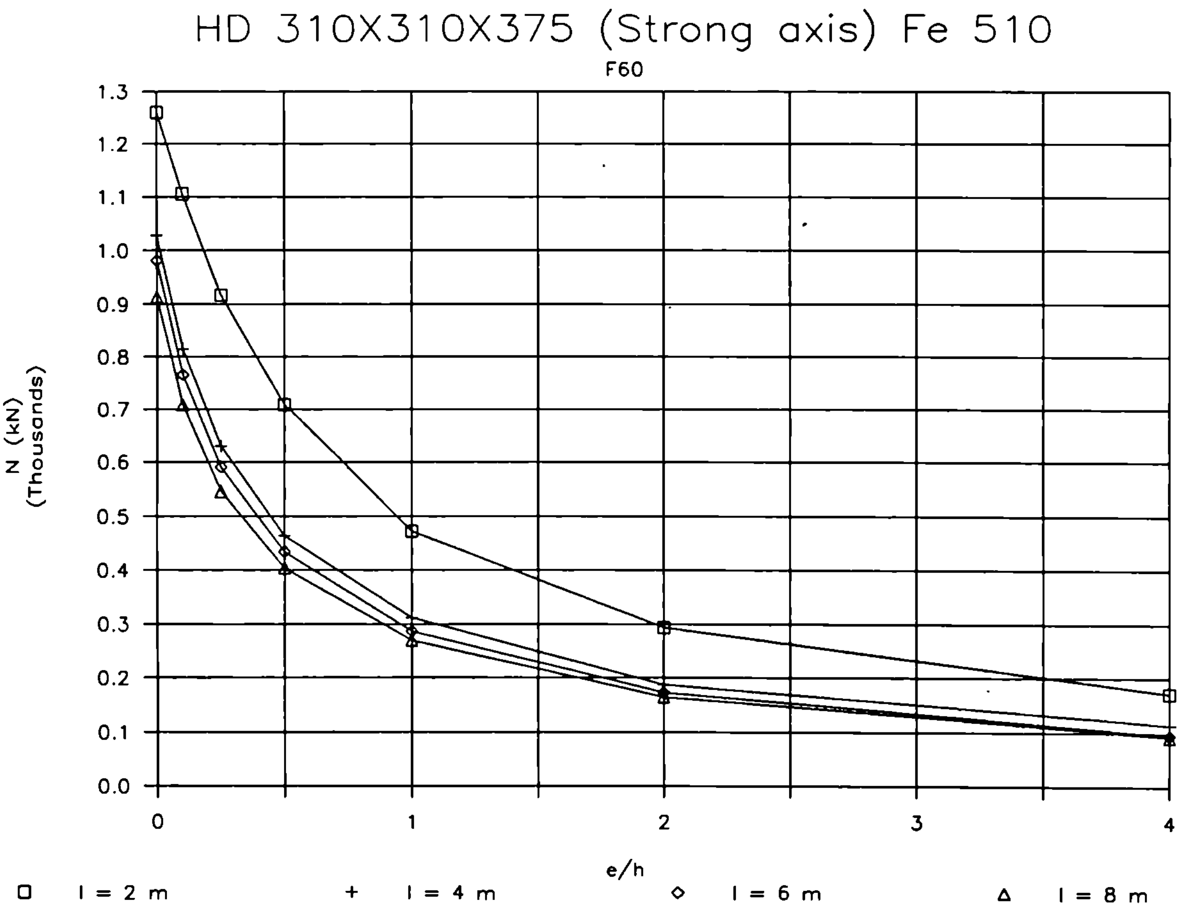

HD 310X310X375 (Strong axis) Fe 510
F60
N (kN)
(Thousands)
1.3
1.2
1.1
1.0
0.9
0.8
0.7
0.6
0.5
0.4
0.3
0.2
0.1
0.0
0
1
2
3
4
e/h
l = 2 m
l = 4 m
l = 6 m
l = 8 m

HD 310x310x500 (Strong axis) Sigma yield = 325 N/mm2 ; U/A = 33 ; t = 75 mm

l	Lambda Bar	e/h	Npl	F0				F30					F60				
(m)			(kN)	N(EC3) (kN)	N(EC3)/Npl	N(CEF) (kN)	N(CEF)/Npl	N(F30) (kN)	N/Nc	N/N(F0,EC3)	N/N(F0,CEF)	N/Npl	N(F60) (kN)	N/Nc	N/N(F0,EC3)	N/N(F0,CEF)	N/Npl
2.00	0.1538	0.00	20721	19725	0.95	20582	0.99	18041	1.00	0.91	0.88	0.87	2205	1.00	0.11	0.11	0.10
2.00	0.1538	0.10	20721	15867	0.77	16568	0.80	14181	0.79	0.89	0.86	0.68	1860	0.84	0.12	0.11	0.08
2.00	0.1538	0.25	20721	12276	0.59	13045	0.63	11166	0.62	0.91	0.86	0.53	1498	0.68	0.12	0.11	0.07
2.00	0.1538	0.50	20721	8936	0.43	9591	0.46	8209	0.46	0.92	0.86	0.39	1125	0.51	0.13	0.12	0.05
2.00	0.1538	1.00	20721	5790	0.28	6331	0.31	5092	0.28	0.88	0.80	0.24	750	0.34	0.13	0.12	0.03
2.00	0.1538	2.00	20721	3404	0.16	3798	0.18	2988	0.17	0.88	0.79	0.14	442	0.20	0.13	0.12	0.02
2.00	0.1538	4.00	20721	1864	0.09	2100	0.10	1615	0.09	0.87	0.77	0.07	247	0.11	0.13	0.12	0.01
4.00	0.3077	0.00	20721	18753	0.91	19971	0.96	15005	1.00	0.80	0.75	0.72	1957	1.00	0.10	0.10	0.09
4.00	0.3077	0.10	20721	15050	0.73	15800	0.76	12151	0.81	0.81	0.77	0.58	1539	0.79	0.10	0.10	0.07
4.00	0.3077	0.25	20721	11693	0.56	12124	0.59	9538	0.64	0.82	0.79	0.46	1191	0.61	0.10	0.10	0.05
4.00	0.3077	0.50	20721	8572	0.41	8747	0.42	7036	0.47	0.82	0.80	0.33	869	0.44	0.10	0.10	0.04
4.00	0.3077	1.00	20721	5614	0.27	5726	0.28	4606	0.31	0.82	0.80	0.22	575	0.29	0.10	0.10	0.02
4.00	0.3077	2.00	20721	3338	0.16	3370	0.16	2710	0.18	0.81	0.80	0.13	342	0.17	0.10	0.10	0.01
4.00	0.3077	4.00	20721	1841	0.09	1816	0.09	1528	0.10	0.83	0.84	0.07	198	0.10	0.11	0.11	0.00
6.00	0.4615	0.00	20721	17638	0.85	19378	0.94	11819	1.00	0.67	0.61	0.57	1880	1.00	0.11	0.10	0.09
6.00	0.4615	0.10	20721	14100	0.68	14876	0.72	9757	0.83	0.69	0.66	0.47	1458	0.78	0.10	0.10	0.07
6.00	0.4615	0.25	20721	10984	0.53	11414	0.55	8122	0.69	0.74	0.71	0.39	1120	0.60	0.10	0.10	0.05
6.00	0.4615	0.50	20721	8127	0.39	8221	0.40	6249	0.53	0.77	0.76	0.30	821	0.44	0.10	0.10	0.03
6.00	0.4615	1.00	20721	5394	0.26	5437	0.26	4229	0.36	0.78	0.78	0.20	535	0.28	0.10	0.10	0.02
6.00	0.4615	2.00	20721	3251	0.16	3228	0.16	2539	0.21	0.78	0.79	0.12	319	0.17	0.10	0.10	0.01
6.00	0.4615	4.00	20721	1808	0.09	1779	0.09	1486	0.13	0.82	0.84	0.07	176	0.09	0.10	0.10	0.00
8.00	0.6154	0.00	20721	16301	0.79	18155	0.88	11009	1.00	0.68	0.61	0.53	1804	1.00	0.11	0.10	0.08
8.00	0.6154	0.10	20721	12971	0.63	13825	0.67	8440	0.77	0.65	0.61	0.40	1374	0.76	0.11	0.10	0.06
8.00	0.6154	0.25	20721	10161	0.49	10497	0.51	6657	0.60	0.66	0.63	0.32	1055	0.58	0.10	0.10	0.05
8.00	0.6154	0.50	20721	7599	0.37	7702	0.37	5242	0.48	0.69	0.68	0.25	775	0.43	0.10	0.10	0.03
8.00	0.6154	1.00	20721	5129	0.25	5146	0.25	3608	0.33	0.70	0.70	0.17	513	0.28	0.10	0.10	0.02
8.00	0.6154	2.00	20721	3139	0.15	3100	0.15	2329	0.21	0.74	0.75	0.11	307	0.17	0.10	0.10	0.01
8.00	0.6154	4.00	20721	1769	0.09	1727	0.08	1343	0.12	0.76	0.78	0.06	171	0.09	0.10	0.10	0.00

T.14

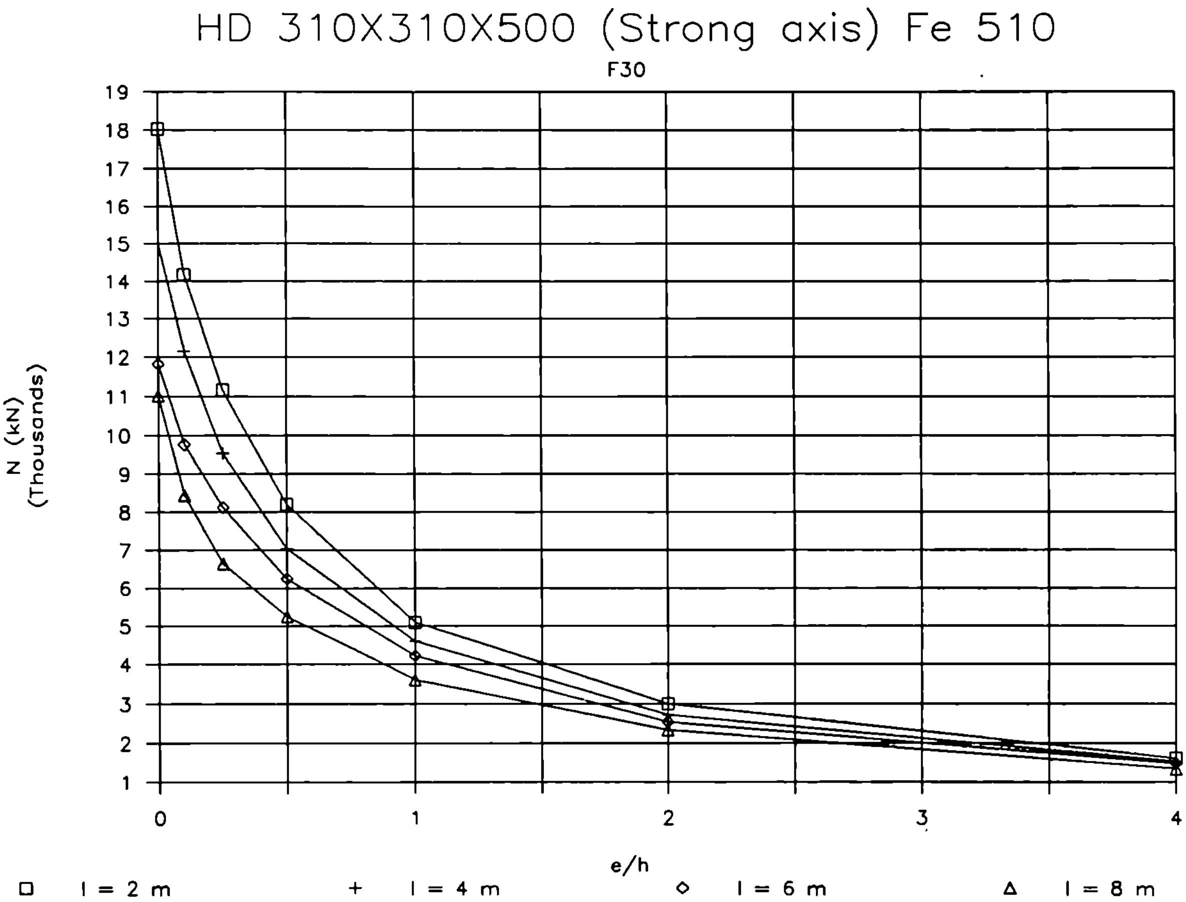
HD 310X310X500 (Strong axis) Fe 510
F30
N (kN)
(Thousands)
e/h
□ l = 2 m
+ l = 4 m
◇ l = 6 m
Δ l = 8 m

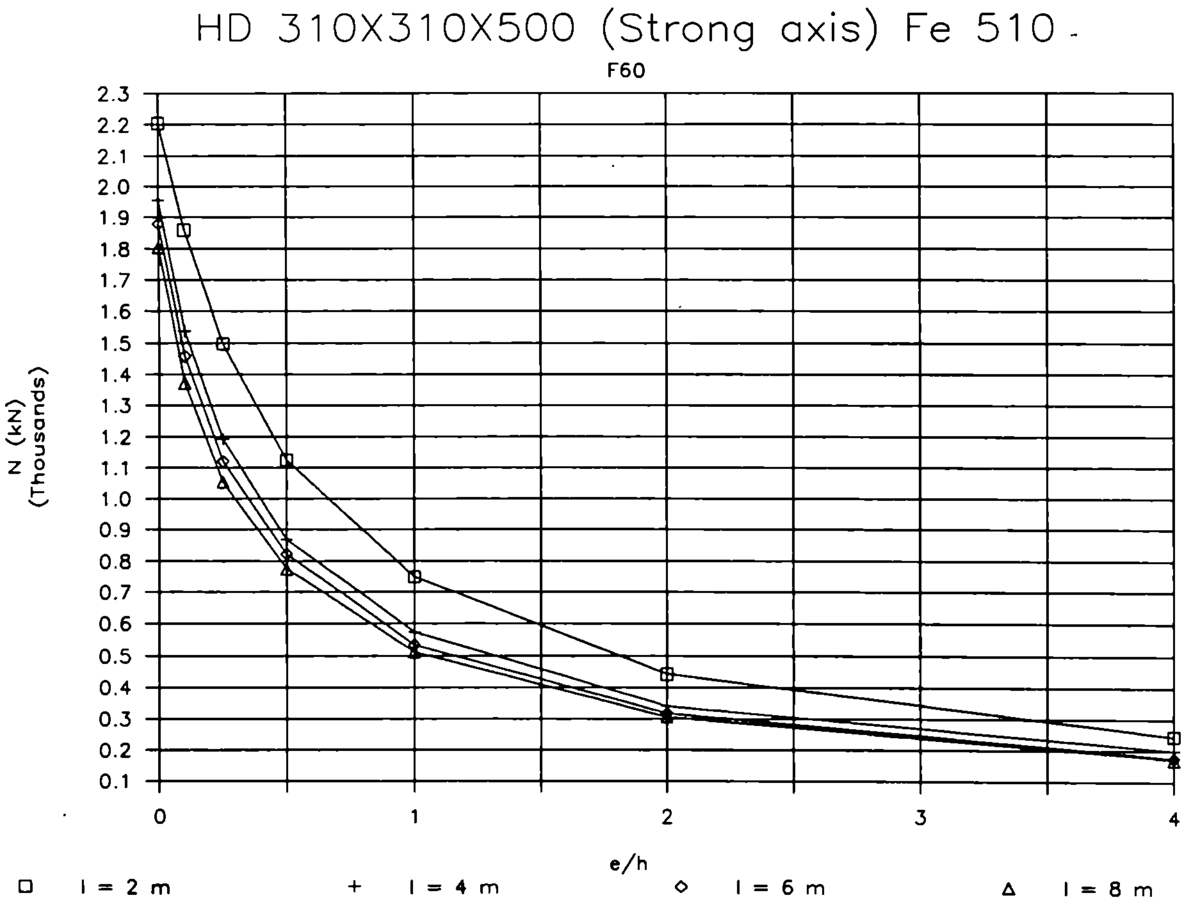
HD 310X310X500 (Strong axis) Fe 510
F60
N (kN)
(Thousands)
e/h
□ l = 2 m
+ l = 4 m
◇ l = 6 m
Δ l = 8 m

HD 400X400X314 (Strong axis) Sigma yield = 345 N/mm2 ; U/A = 58 ; t = 40 mm

l (m)	Lambda Bar	e/h	Npl (kN)	F0 N(EC3) (kN)	F0 N(EC3)/Npl	F0 N(CEF) (kN)	F0 N(CEF)/Npl	F30 N(F30) (kN)	F30 N/Nc	F30 N/N(F0,EC3)	F30 N/N(F0,CEF)	F30 N/Npl	F60 N(F60) (kN)	F60 N/Nc	F60 N/N(F0,EC3)	F60 N/N(F0,CEF)	F60 N/Npl
2.00	0.1548	0.00	13800	13209	0.96	13703	0.99	5616	1.00	0.43	0.41	0.40	985	1.00	0.07	0.07	0.07
2.00	0.1548	0.10	13800	10804	0.78	10951	0.79	4513	0.80	0.42	0.41	0.32	851	0.86	0.08	0.08	0.06
2.00	0.1548	0.25	13800	8513	0.62	8660	0.63	3665	0.65	0.43	0.42	0.26	707	0.72	0.08	0.08	0.05
2.00	0.1548	0.50	13800	6290	0.46	6321	0.46	2754	0.49	0.44	0.44	0.19	553	0.56	0.09	0.09	0.04
2.00	0.1548	1.00	13800	4143	0.30	4173	0.30	1859	0.33	0.45	0.45	0.13	372	0.38	0.09	0.09	0.02
2.00	0.1548	2.00	13800	2462	0.18	2642	0.19	1118	0.20	0.45	0.42	0.08	227	0.23	0.09	0.09	0.01
2.00	0.1548	4.00	13800	1361	0.10	1480	0.11	615	0.11	0.45	0.42	0.04	131	0.13	0.10	0.09	0.00
4.00	0.3096	0.00	13800	12554	0.91	13231	0.96	4421	1.00	0.35	0.33	0.32	739	1.00	0.06	0.06	0.05
4.00	0.3096	0.10	13800	10266	0.74	10626	0.77	3550	0.80	0.35	0.33	0.25	591	0.80	0.06	0.06	0.04
4.00	0.3096	0.25	13800	8101	0.59	8235	0.60	2862	0.65	0.35	0.35	0.20	464	0.63	0.06	0.06	0.03
4.00	0.3096	0.50	13800	6029	0.44	6113	0.44	2179	0.49	0.36	0.36	0.15	349	0.47	0.06	0.06	0.02
4.00	0.3096	1.00	13800	4010	0.29	4002	0.29	1545	0.35	0.39	0.39	0.11	244	0.33	0.06	0.06	0.01
4.00	0.3096	2.00	13800	2414	0.17	2406	0.17	949	0.21	0.39	0.39	0.06	155	0.21	0.06	0.06	0.01
4.00	0.3096	4.00	13800	1344	0.10	1323	0.10	545	0.12	0.41	0.41	0.03	92	0.12	0.07	0.07	0.00
6.00	0.4644	0.00	13800	11817	0.86	12583	0.91	4204	1.00	0.36	0.33	0.30	709	1.00	0.06	0.06	0.05
6.00	0.4644	0.10	13800	9603	0.70	10056	0.73	3360	0.80	0.35	0.33	0.24	559	0.79	0.06	0.06	0.04
6.00	0.4644	0.25	13800	7601	0.55	7794	0.56	2604	0.62	0.34	0.33	0.18	438	0.62	0.06	0.06	0.03
6.00	0.4644	0.50	13800	5709	0.41	5755	0.42	1933	0.46	0.34	0.34	0.14	324	0.46	0.06	0.06	0.02
6.00	0.4644	1.00	13800	3846	0.28	3806	0.28	1326	0.32	0.34	0.35	0.09	216	0.31	0.06	0.06	0.01
6.00	0.4644	2.00	13800	2345	0.17	2311	0.17	824	0.20	0.35	0.36	0.05	132	0.19	0.06	0.06	0.00
6.00	0.4644	4.00	13800	1321	0.10	1284	0.09	477	0.11	0.36	0.37	0.03	74	0.10	0.06	0.06	0.00
8.00	0.6192	0.00	13800	10927	0.79	11644	0.84	3977	1.00	0.36	0.34	0.28	663	1.00	0.06	0.06	0.04
8.00	0.6192	0.10	13800	8842	0.64	9204	0.67	3075	0.77	0.35	0.33	0.22	520	0.78	0.06	0.06	0.03
8.00	0.6192	0.25	13800	7025	0.51	7202	0.52	2406	0.61	0.34	0.33	0.17	408	0.62	0.06	0.06	0.02
8.00	0.6192	0.50	13800	5327	0.39	5392	0.39	1802	0.45	0.34	0.33	0.13	304	0.46	0.06	0.06	0.02
8.00	0.6192	1.00	13800	3644	0.26	3602	0.26	1230	0.31	0.34	0.34	0.08	205	0.31	0.06	0.06	0.01
8.00	0.6192	2.00	13800	2261	0.16	2205	0.16	753	0.19	0.33	0.34	0.05	125	0.19	0.06	0.06	0.00
8.00	0.6192	4.00	13800	1294	0.09	1246	0.09	434	0.11	0.34	0.35	0.03	71	0.11	0.05	0.06	0.00

HD 400X400X314 (Strong axis) Fe 510

F30

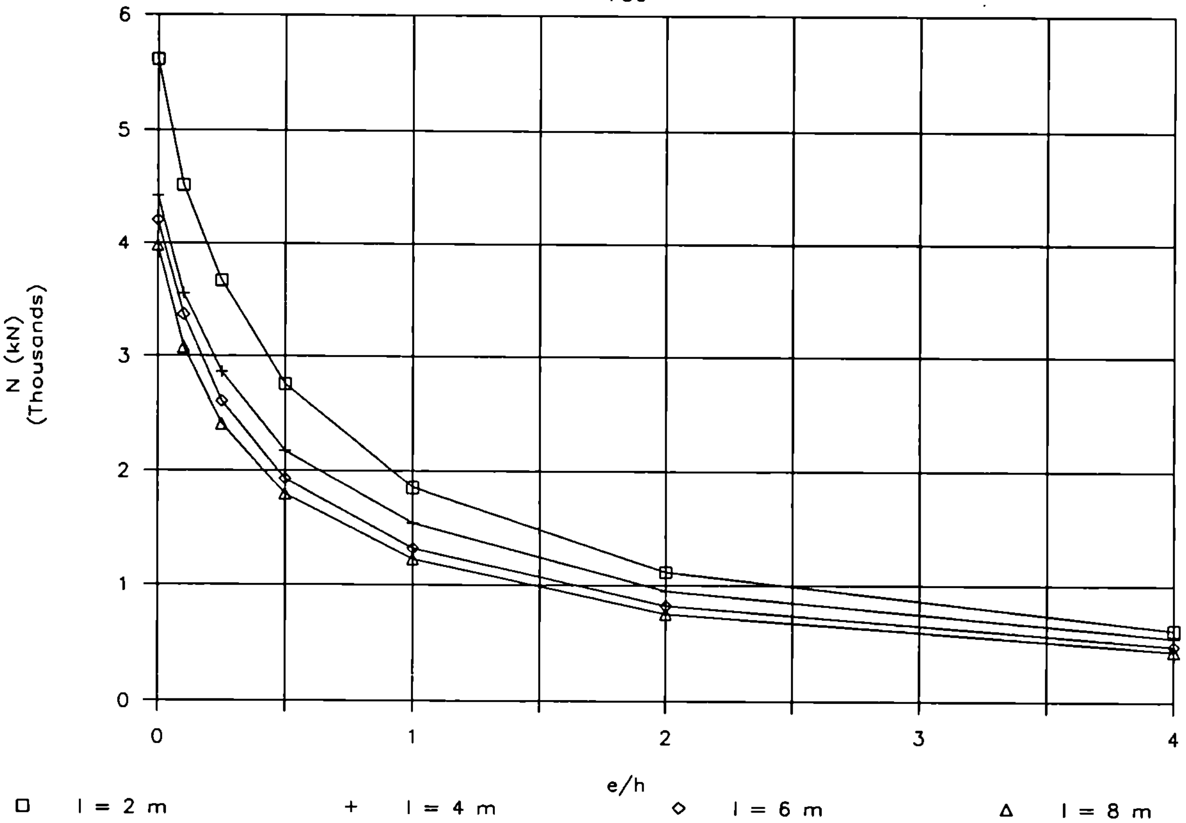

HD 400X400X314 (Strong axis) Fe 510

F60

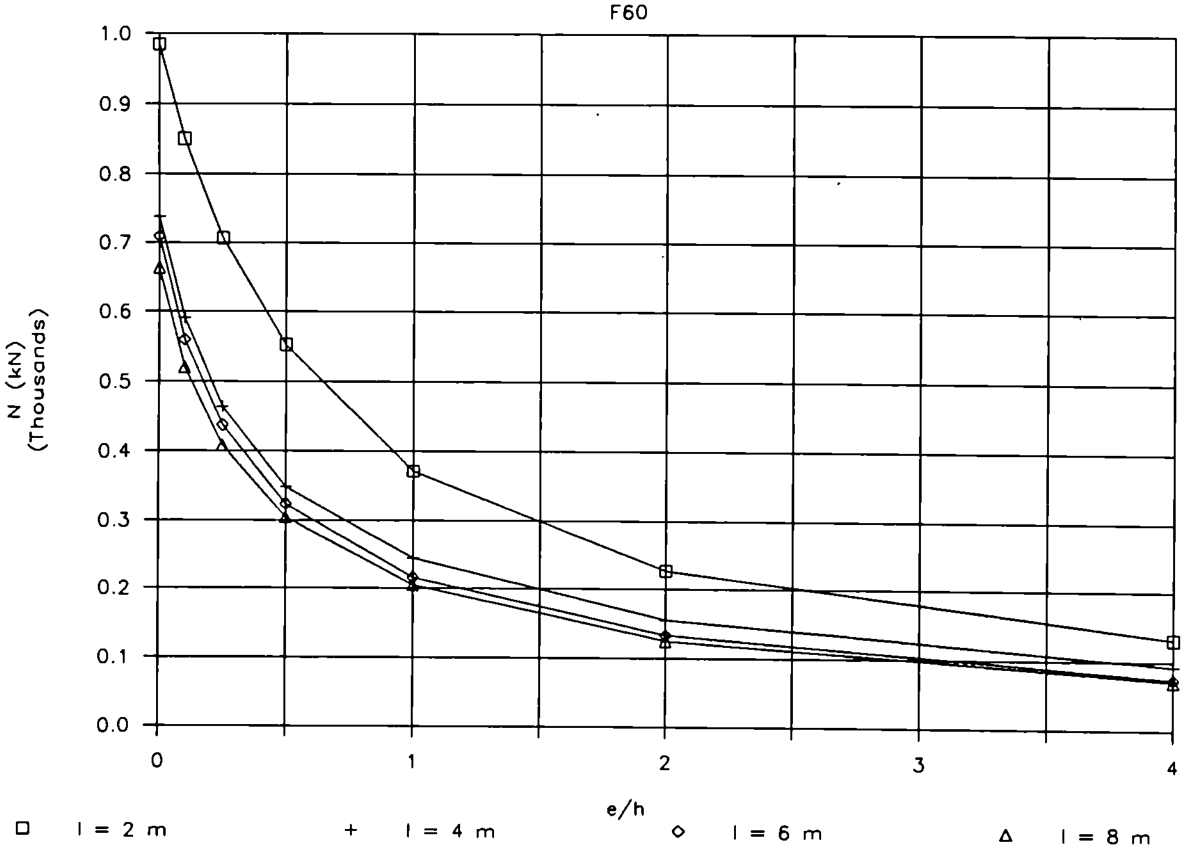

HD 400X400X678 (Strong axis) Sigma yield = 315 N/mm2 ; U/A = 30 ; t = 82 mm

l (m)	Lambda Bar	e/h	Npl (kN)	F0: N(EC3) (kN)	F0: N(EC3)/Npl	F0: N(CEF) (kN)	F0: N(CEF)/Npl	F30: N(F30) (kN)	F30: N/Nc	F30: N/N(F0,EC3)	F30: N/N(F0,CEF)	F30: N/Npl	F60: N(F60) (kN)	F60: N/Nc	F60: N/N(F0,EC3)	F60: N/N(F0,CEF)	F60: N/Npl
2.00	0.1321	0.00	27216	26112	0.96	27030	0.99	26800	1.00	1.03	0.99	0.98	4280	1.00	0.16	0.16	0.15
2.00	0.1321	0.10	27216	21071	0.77	22092	0.81	21896	0.82	1.04	0.99	0.80	3400	0.79	0.16	0.15	0.12
2.00	0.1321	0.25	27216	16343	0.60	17656	0.65	17497	0.65	1.07	0.99	0.64	2753	0.64	0.17	0.16	0.10
2.00	0.1321	0.50	27216	11903	0.44	13245	0.49	13121	0.49	1.10	0.99	0.48	2088	0.49	0.18	0.16	0.07
2.00	0.1321	1.00	27216	7717	0.28	8920	0.33	8834	0.33	1.14	0.99	0.32	1391	0.32	0.18	0.16	0.05
2.00	0.1321	2.00	27216	4535	0.17	5344	0.20	5292	0.20	1.17	0.99	0.19	828	0.19	0.18	0.15	0.03
2.00	0.1321	4.00	27216	2488	0.09	3377	0.12	3009	0.11	1.21	0.89	0.11	471	0.11	0.19	0.14	0.01
4.00	0.2642	0.00	27216	25018	0.92	26492	0.97	23880	1.00	0.95	0.90	0.87	3305	1.00	0.13	0.12	0.12
4.00	0.2642	0.10	27216	20152	0.74	20960	0.77	20754	0.87	1.03	0.99	0.76	2615	0.79	0.13	0.12	0.09
4.00	0.2642	0.25	27216	15685	0.58	16083	0.59	15931	0.67	1.02	0.99	0.58	2006	0.61	0.13	0.12	0.07
4.00	0.2642	0.50	27216	11503	0.42	11818	0.43	11708	0.49	1.02	0.99	0.43	1474	0.45	0.13	0.12	0.05
4.00	0.2642	1.00	27216	7536	0.28	7738	0.28	7667	0.32	1.02	0.99	0.28	996	0.30	0.13	0.13	0.03
4.00	0.2642	2.00	27216	4463	0.16	4558	0.17	4517	0.19	1.01	0.99	0.16	601	0.18	0.13	0.13	0.02
4.00	0.2642	4.00	27216	2465	0.09	2457	0.09	2435	0.10	0.99	0.99	0.08	350	0.11	0.14	0.14	0.01
6.00	0.3963	0.00	27216	23820	0.88	25581	0.94	19146	1.00	0.80	0.75	0.70	3191	1.00	0.13	0.12	0.11
6.00	0.3963	0.10	27216	19120	0.70	20134	0.74	16295	0.85	0.85	0.81	0.59	2482	0.78	0.13	0.12	0.09
6.00	0.3963	0.25	27216	14921	0.55	15374	0.56	13470	0.70	0.90	0.88	0.49	1918	0.60	0.13	0.12	0.07
6.00	0.3963	0.50	27216	11031	0.41	11239	0.41	10076	0.53	0.91	0.90	0.37	1411	0.44	0.13	0.13	0.05
6.00	0.3963	1.00	27216	7292	0.27	7359	0.27	7061	0.37	0.97	0.96	0.25	918	0.29	0.13	0.12	0.03
6.00	0.3963	2.00	27216	4374	0.16	4350	0.16	4308	0.23	0.98	0.99	0.15	551	0.17	0.13	0.13	0.02
6.00	0.3963	4.00	27216	2433	0.09	2384	0.09	2362	0.12	0.97	0.99	0.08	302	0.09	0.12	0.13	0.01
8.00	0.5284	0.00	27216	22437	0.82	24327	0.89	16006	1.00	0.71	0.66	0.58	3035	1.00	0.14	0.12	0.11
8.00	0.5284	0.10	27216	17921	0.66	18901	0.69	12561	0.78	0.70	0.66	0.46	2358	0.78	0.13	0.12	0.08
8.00	0.5284	0.25	27216	14047	0.52	14496	0.53	10489	0.66	0.75	0.72	0.38	1808	0.60	0.13	0.12	0.06
8.00	0.5284	0.50	27216	10457	0.38	10636	0.39	8251	0.52	0.79	0.78	0.30	1346	0.44	0.13	0.13	0.04
8.00	0.5284	1.00	27216	7006	0.26	7035	0.26	5790	0.36	0.83	0.82	0.21	878	0.29	0.13	0.12	0.03
8.00	0.5284	2.00	27216	4262	0.16	4221	0.16	3771	0.24	0.88	0.89	0.13	527	0.17	0.12	0.12	0.01
8.00	0.5284	4.00	27216	2389	0.09	2326	0.09	2226	0.14	0.93	0.96	0.08	290	0.10	0.12	0.12	0.01

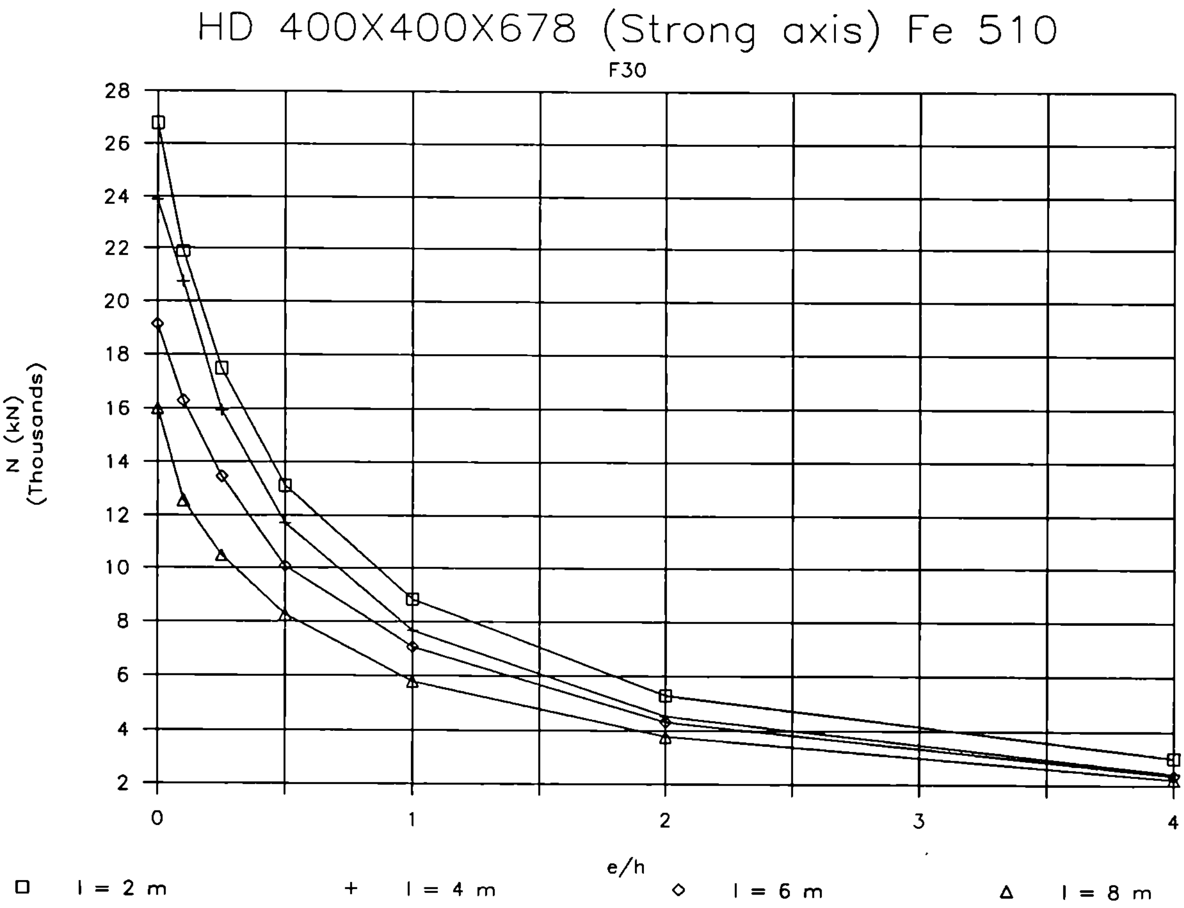

HD 400X400X678 (Strong axis) Fe 510
F30
N (kN)
(Thousands)
28
26
24
22
20
18
16
14
12
10
8
6
4
2
0
1
2
3
4
e/h
□ l = 2 m
+ l = 4 m
◇ l = 6 m
Δ l = 8 m

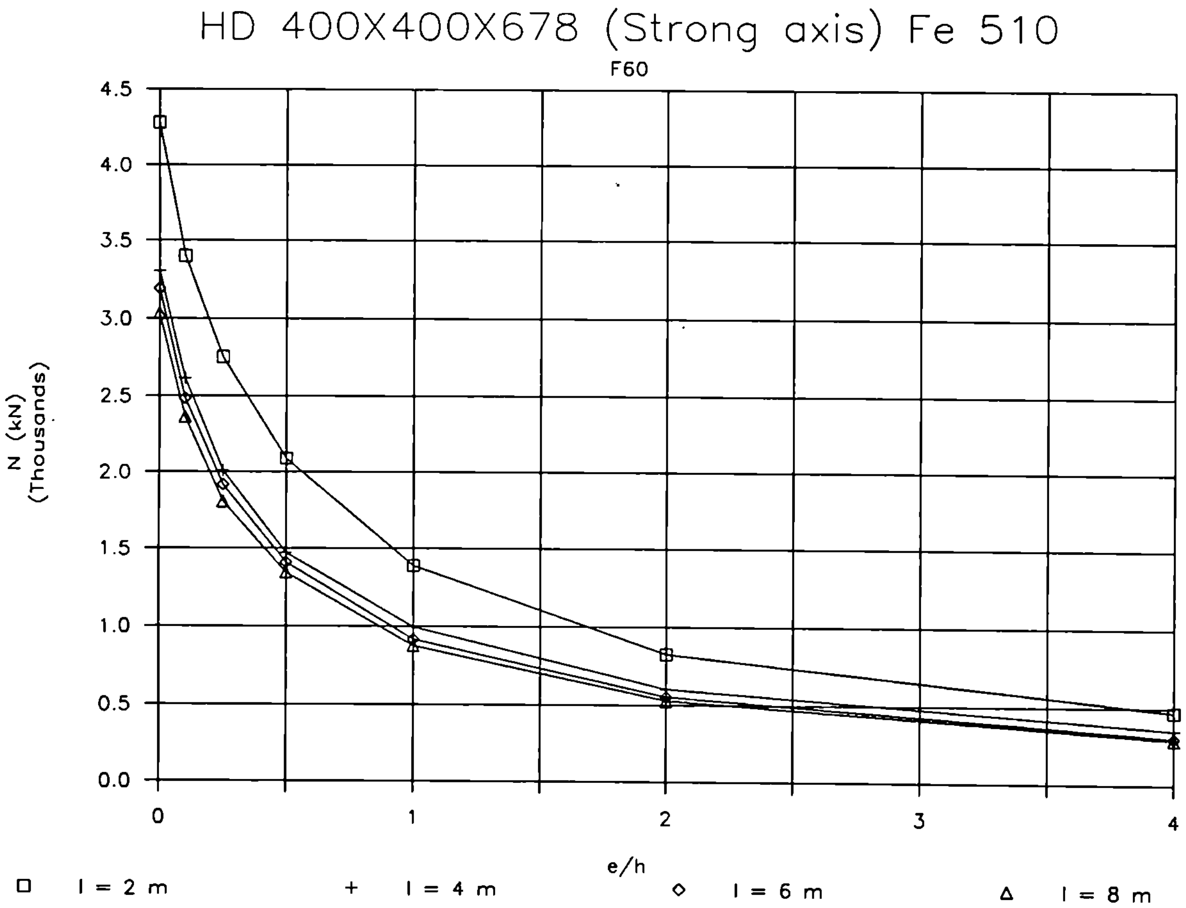

HD 400X400X678 (Strong axis) Fe 510
F60
N (kN)
(Thousands)
4.5
4.0
3.5
3.0
2.5
2.0
1.5
1.0
0.5
0.0
0
1
2
3
4
e/h
□ l = 2 m
+ l = 4 m
◇ l = 6 m
Δ l = 8 m

HD 400X400X1086 (Strong axis) Sigma yield = 305 N/mm2 ; U/A = 20 ; t = 125 mm

l (m)	Lambda Bar	e/h	Npl (kN)	F0 N(EC3) (kN)	F0 N(EC3)/Npl	F0 N(CEF) (kN)	F0 N(CEF)/Npl	F30 N(F30) (kN)	F30 N/Nc	F30 N/N(F0,EC3)	F30 N/N(F0,CEF)	F30 N/Npl	F60 N(F60) (kN)	F60 N/Nc	F60 N/N(F0,EC3)	F60 N/N(F0,CEF)	F60 N/Npl
2.00	0.1170	0.00	42273	39590	0.94	41943	0.99	41671	1.00	1.05	0.99	0.98	19365	1.00	0.49	0.46	0.45
2.00	0.1170	0.10	42273	31685	0.75	35776	0.85	35524	0.85	1.12	0.99	0.84	15088	0.78	0.48	0.42	0.35
2.00	0.1170	0.25	42273	24410	0.58	27123	0.64	26938	0.65	1.10	0.99	0.63	11761	0.61	0.48	0.43	0.27
2.00	0.1170	0.50	42273	17650	0.42	20878	0.49	20726	0.50	1.17	0.99	0.49	8557	0.44	0.48	0.41	0.20
2.00	0.1170	1.00	42273	11374	0.27	14256	0.34	13147	0.32	1.16	0.92	0.31	5504	0.28	0.48	0.39	0.13
2.00	0.1170	2.00	42273	6655	0.16	9000	0.21	7452	0.18	1.12	0.83	0.17	3195	0.16	0.48	0.36	0.07
2.00	0.1170	4.00	42273	3620	0.09	5005	0.12	4416	0.11	1.22	0.88	0.10	1725	0.09	0.48	0.34	0.04
4.00	0.2340	0.00	42273	37071	0.88	41160	0.97	40346	1.00	1.09	0.98	0.95	13765	1.00	0.37	0.33	0.32
4.00	0.2340	0.10	42273	29891	0.71	32524	0.77	32287	0.80	1.08	0.99	0.76	11410	0.83	0.38	0.35	0.26
4.00	0.2340	0.25	42273	23232	0.55	24848	0.59	24671	0.61	1.06	0.99	0.58	9225	0.67	0.40	0.37	0.21
4.00	0.2340	0.50	42273	16984	0.40	17905	0.42	17779	0.44	1.05	0.99	0.42	6872	0.50	0.40	0.38	0.16
4.00	0.2340	1.00	42273	11065	0.26	11693	0.28	11610	0.29	1.05	0.99	0.27	4568	0.33	0.41	0.39	0.10
4.00	0.2340	2.00	42273	6549	0.15	6779	0.16	6731	0.17	1.03	0.99	0.15	2741	0.20	0.42	0.40	0.06
4.00	0.2340	4.00	42273	3579	0.08	3705	0.09	3679	0.09	1.03	0.99	0.08	1556	0.11	0.43	0.42	0.03
6.00	0.3510	0.00	42273	34585	0.82	40320	0.95	36533	1.00	1.06	0.91	0.86	12600	1.00	0.36	0.31	0.29
6.00	0.3510	0.10	42273	27994	0.66	31558	0.75	28932	0.79	1.03	0.92	0.68	9774	0.78	0.35	0.31	0.23
6.00	0.3510	0.25	42273	21957	0.52	23800	0.56	22052	0.60	1.00	0.93	0.52	7589	0.60	0.35	0.32	0.17
6.00	0.3510	0.50	42273	16208	0.38	17289	0.41	17152	0.47	1.06	0.99	0.40	5709	0.45	0.35	0.33	0.13
6.00	0.3510	1.00	42273	10716	0.25	11200	0.26	11114	0.30	1.04	0.99	0.26	3992	0.32	0.37	0.36	0.09
6.00	0.3510	2.00	42273	6406	0.15	6512	0.15	6464	0.18	1.01	0.99	0.15	2321	0.18	0.36	0.36	0.05
6.00	0.3510	4.00	42273	3535	0.08	3523	0.08	3498	0.10	0.99	0.99	0.08	1360	0.11	0.38	0.39	0.03
8.00	0.4680	0.00	42273	32050	0.76	39204	0.93	28818	1.00	0.90	0.74	0.68	12067	1.00	0.38	0.31	0.28
8.00	0.4680	0.10	42273	26089	0.62	30096	0.71	23707	0.82	0.91	0.79	0.56	9142	0.76	0.35	0.30	0.21
8.00	0.4680	0.25	42273	20574	0.49	22862	0.54	19409	0.67	0.94	0.85	0.45	7037	0.58	0.34	0.31	0.16
8.00	0.4680	0.50	42273	15392	0.36	16466	0.39	14945	0.52	0.97	0.91	0.35	5170	0.43	0.34	0.31	0.12
8.00	0.4680	1.00	42273	10304	0.24	10759	0.25	9907	0.34	0.96	0.92	0.23	3403	0.28	0.33	0.32	0.08
8.00	0.4680	2.00	42273	6256	0.15	6336	0.15	6285	0.22	1.00	0.99	0.14	2050	0.17	0.33	0.32	0.04
8.00	0.4680	4.00	42273	3480	0.08	3453	0.08	3427	0.12	0.98	0.99	0.08	1158	0.10	0.33	0.34	0.02

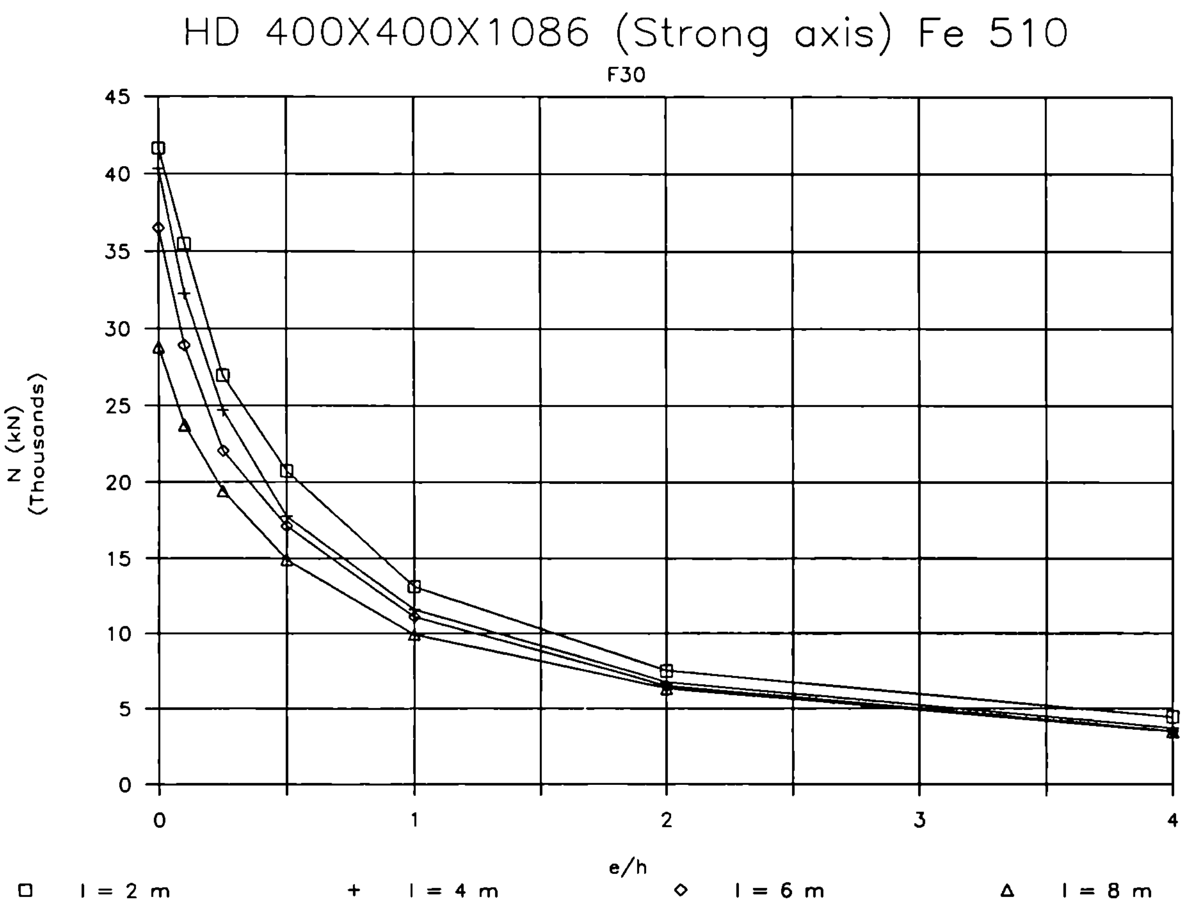

HD 400X400X1086 (Strong axis) Fe 510
F30
N (kN)
(Thousands)
45
40
35
30
25
20
15
10
5
0
0
1
2
3
4
e/h
l = 2 m
l = 4 m
l = 6 m
l = 8 m

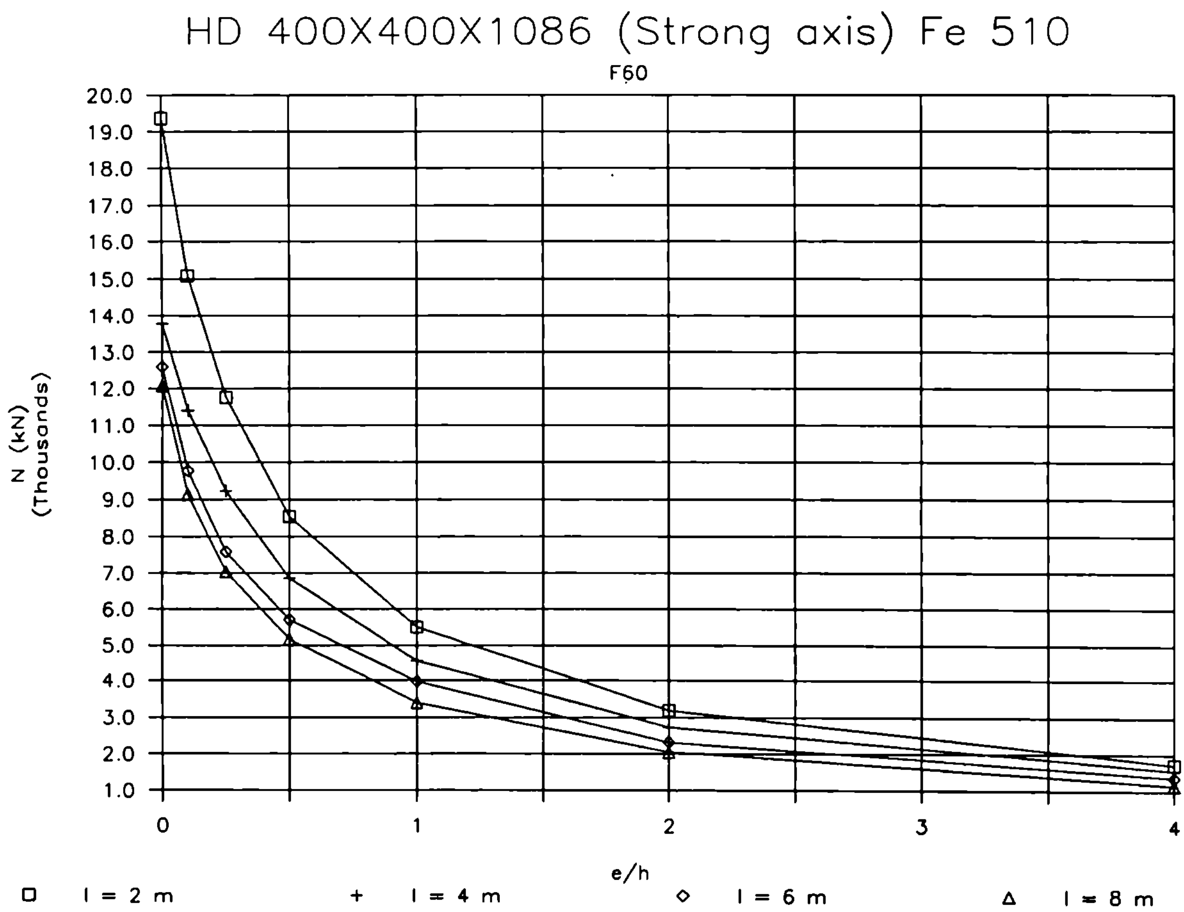

HD 400X400X1086 (Strong axis) Fe 510
F60
N (kN)
(Thousands)
20.0
19.0
18.0
17.0
16.0
15.0
14.0
13.0
12.0
11.0
10.0
9.0
8.0
7.0
6.0
5.0
4.0
3.0
2.0
1.0
0
1
2
3
4
e/h
l = 2 m
l = 4 m
l = 6 m
l = 8 m

HE 550 M (Strong axis) Sigma yield = 450 N/mm2 ; U/A = 64 ; t = 40 mm

l	Lambda Bar	e/h	Npl	F0				F30					F60				
(m)			(kN)	N(EC3) (kN)	N(EC3)/Npl	N(CEF) (kN)	N(CEF)/Npl	N(F30) (kN)	N/Nc	N/N(F0,EC3)	N/N(F0,CEF)	N/Npl	N(F60) (kN)	N/Nc	N/N(F0,EC3)	N/N(F0,CEF)	N/Npl
2.00	0.1247	0.00	15930	15442	0.97	15530	0.97	5032	1.00	0.33	0.32	0.31	1160	1.00	0.08	0.07	0.07
2.00	0.1247	0.10	15930	12569	0.79	12627	0.79	4091	0.81	0.33	0.32	0.25	956	0.82	0.08	0.08	0.06
2.00	0.1247	0.25	15930	9833	0.62	9942	0.62	3248	0.65	0.33	0.33	0.20	780	0.67	0.08	0.08	0.04
2.00	0.1247	0.50	15930	7234	0.45	7384	0.46	2452	0.49	0.34	0.33	0.15	595	0.51	0.08	0.08	0.03
2.00	0.1247	1.00	15930	4732	0.30	4833	0.30	1615	0.32	0.34	0.33	0.10	391	0.34	0.08	0.08	0.02
2.00	0.1247	2.00	15930	2798	0.18	2895	0.18	961	0.19	0.34	0.33	0.06	231	0.20	0.08	0.08	0.01
2.00	0.1247	4.00	15930	1541	0.10	1732	0.11	533	0.11	0.35	0.31	0.03	129	0.11	0.08	0.07	0.00
4.00	0.2494	0.00	15930	14912	0.94	15375	0.97	4247	1.00	0.28	0.28	0.26	816	1.00	0.05	0.05	0.05
4.00	0.2494	0.10	15930	12127	0.76	12411	0.78	3539	0.83	0.29	0.29	0.22	663	0.81	0.05	0.05	0.04
4.00	0.2494	0.25	15930	9518	0.60	9619	0.60	2857	0.67	0.30	0.30	0.17	563	0.69	0.06	0.06	0.03
4.00	0.2494	0.50	15930	7035	0.44	7069	0.44	2204	0.52	0.31	0.31	0.13	443	0.54	0.06	0.06	0.02
4.00	0.2494	1.00	15930	4629	0.29	4712	0.30	1512	0.36	0.33	0.32	0.09	303	0.37	0.07	0.06	0.01
4.00	0.2494	2.00	15930	2764	0.17	2824	0.18	915	0.22	0.33	0.32	0.05	188	0.23	0.07	0.07	0.01
4.00	0.2494	4.00	15930	1528	0.10	1497	0.09	497	0.12	0.33	0.33	0.03	110	0.13	0.07	0.07	0.00
6.00	0.3741	0.00	15930	14352	0.90	14846	0.93	4189	1.00	0.29	0.28	0.26	801	1.00	0.06	0.05	0.05
6.00	0.3741	0.10	15930	11602	0.73	12042	0.76	3398	0.81	0.29	0.28	0.21	641	0.80	0.06	0.05	0.04
6.00	0.3741	0.25	15930	9110	0.57	9240	0.58	2658	0.63	0.29	0.29	0.16	502	0.63	0.06	0.05	0.03
6.00	0.3741	0.50	15930	6771	0.43	6790	0.43	1996	0.48	0.29	0.29	0.12	372	0.46	0.05	0.05	0.02
6.00	0.3741	1.00	15930	4505	0.28	4527	0.28	1371	0.33	0.30	0.30	0.08	252	0.31	0.06	0.06	0.01
6.00	0.3741	2.00	15930	2707	0.17	2720	0.17	837	0.20	0.31	0.31	0.05	151	0.19	0.06	0.06	0.00
6.00	0.3741	4.00	15930	1512	0.09	1468	0.09	471	0.11	0.31	0.32	0.02	86	0.11	0.06	0.06	0.00
8.00	0.4988	0.00	15930	13673	0.86	14697	0.92	4038	1.00	0.30	0.27	0.25	777	1.00	0.06	0.05	0.04
8.00	0.4988	0.10	15930	11002	0.69	11512	0.72	3248	0.80	0.30	0.28	0.20	615	0.79	0.06	0.05	0.03
8.00	0.4988	0.25	15930	8655	0.54	8833	0.55	2558	0.63	0.30	0.29	0.16	482	0.62	0.06	0.05	0.03
8.00	0.4988	0.50	15930	6459	0.41	6457	0.41	1883	0.47	0.29	0.29	0.11	357	0.46	0.06	0.06	0.02
8.00	0.4988	1.00	15930	4343	0.27	4305	0.27	1290	0.32	0.30	0.30	0.08	238	0.31	0.05	0.06	0.01
8.00	0.4988	2.00	15930	2647	0.17	2613	0.16	783	0.19	0.30	0.30	0.04	144	0.19	0.05	0.06	0.00
8.00	0.4988	4.00	15930	1489	0.09	1428	0.09	440	0.11	0.30	0.31	0.02	78	0.10	0.05	0.05	0.00

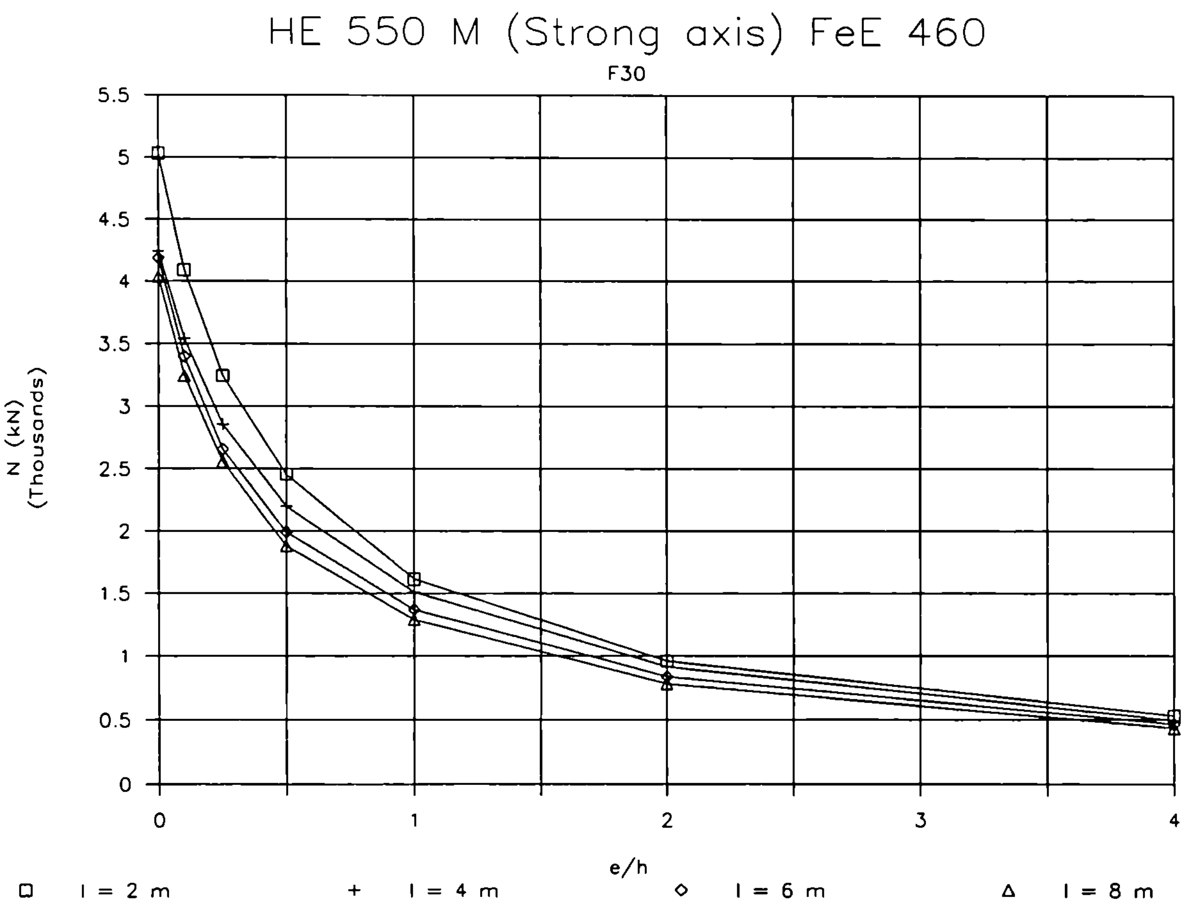

HE 550 M (Strong axis) FeE 460
F30
N (kN)
(Thousands)
e/h
l = 2 m
l = 4 m
l = 6 m
l = 8 m

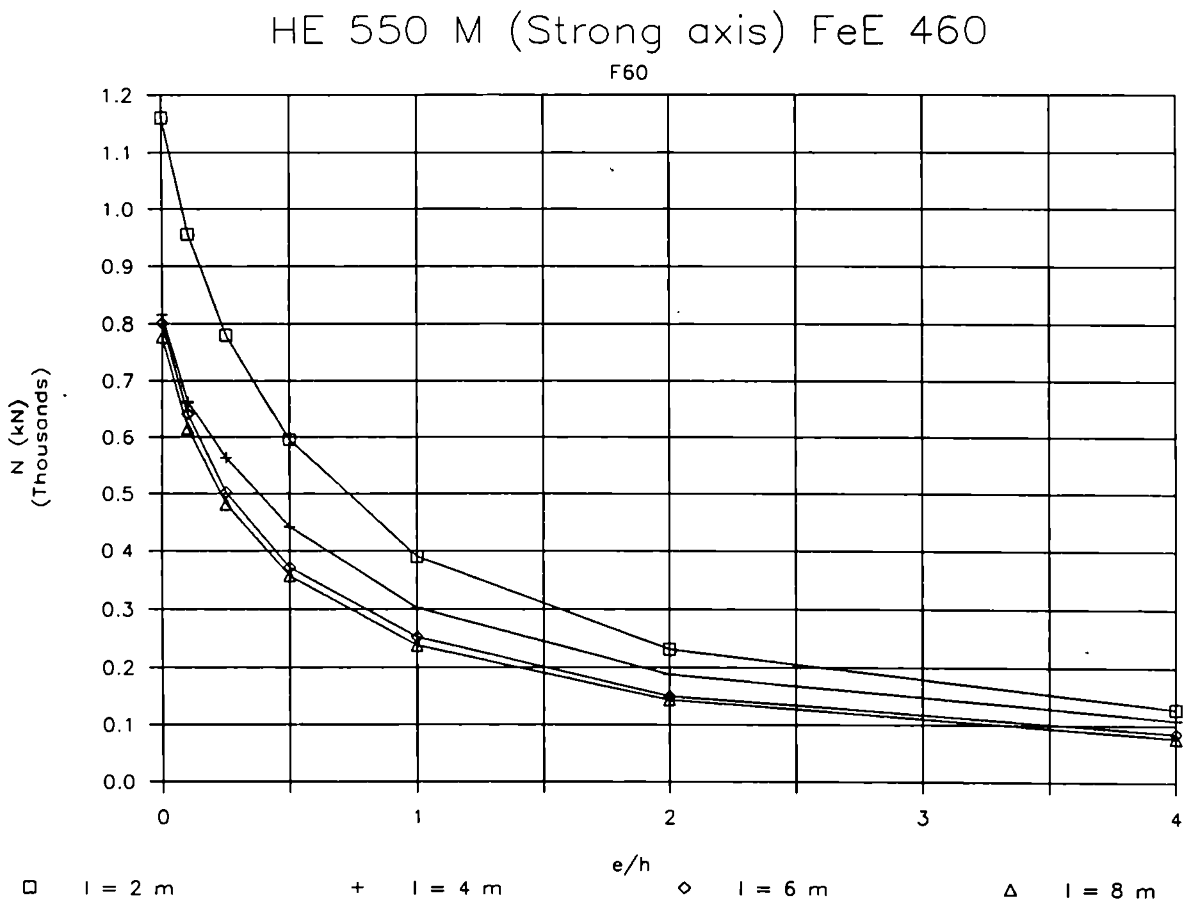

HE 550 M (Strong axis) FeE 460
F60
N (kN)
(Thousands)
e/h
l = 2 m
l = 4 m
l = 6 m
l = 8 m

HD 400X400X314 (Strong axis) Sigma yield = 450 N/mm2 ; U/A = 58 ; t = 40 mm

l (m)	Lambda Bar	e/h	Npl (kN)	F0 N(EC3) (kN)	N(EC3)/Npl	N(CEF) (kN)	N(CEF)/Npl	F30 N(F30) (kN)	N/Nc	N/N(F0,EC3)	N/N(F0,CEF)	N/Npl	F60 N(F60) (kN)	N/Nc	N/N(F0,EC3)	N/N(F0,CEF)	N/Npl
2.00	0.1768	0.00	18000	17197	0.96	17709	0.98	6312	1.00	0.37	0.36	0.35	1128	1.00	0.07	0.06	0.06
2.00	0.1768	0.10	18000	14074	0.78	14440	0.80	5307	0.84	0.38	0.37	0.29	973	0.86	0.07	0.07	0.05
2.00	0.1768	0.25	18000	11071	0.62	11192	0.62	4238	0.67	0.38	0.38	0.23	805	0.71	0.07	0.07	0.04
2.00	0.1768	0.50	18000	8188	0.45	8420	0.47	3168	0.50	0.39	0.38	0.17	627	0.56	0.08	0.07	0.03
2.00	0.1768	1.00	18000	5392	0.30	5444	0.30	2102	0.33	0.39	0.39	0.11	426	0.38	0.08	0.08	0.02
2.00	0.1768	2.00	18000	3209	0.18	3236	0.18	1281	0.20	0.40	0.40	0.07	255	0.23	0.08	0.08	0.01
2.00	0.1768	4.00	18000	1774	0.10	1916	0.11	683	0.11	0.39	0.36	0.03	147	0.13	0.08	0.08	0.00
4.00	0.3536	0.00	18000	16325	0.91	17183	0.95	5741	1.00	0.35	0.33	0.31	956	1.00	0.06	0.06	0.05
4.00	0.3536	0.10	18000	13292	0.74	13732	0.76	4588	0.80	0.35	0.33	0.25	763	0.80	0.06	0.06	0.04
4.00	0.3536	0.25	18000	10472	0.58	10643	0.59	3556	0.62	0.34	0.33	0.19	597	0.62	0.06	0.06	0.03
4.00	0.3536	0.50	18000	7797	0.43	7821	0.43	2724	0.47	0.35	0.35	0.15	442	0.46	0.06	0.06	0.02
4.00	0.3536	1.00	18000	5195	0.29	5162	0.29	1840	0.32	0.35	0.36	0.10	303	0.32	0.06	0.06	0.01
4.00	0.3536	2.00	18000	3130	0.17	3093	0.17	1137	0.20	0.36	0.37	0.06	185	0.19	0.06	0.06	0.01
4.00	0.3536	4.00	18000	1748	0.10	1725	0.10	634	0.11	0.36	0.37	0.03	111	0.12	0.06	0.06	0.00
6.00	0.5304	0.00	18000	15258	0.85	16262	0.90	5434	1.00	0.36	0.33	0.30	908	1.00	0.06	0.06	0.05
6.00	0.5304	0.10	18000	12316	0.68	12737	0.71	4256	0.78	0.35	0.33	0.23	712	0.78	0.06	0.06	0.03
6.00	0.5304	0.25	18000	9722	0.54	9872	0.55	3299	0.61	0.34	0.33	0.18	557	0.61	0.06	0.06	0.03
6.00	0.5304	0.50	18000	7299	0.41	7290	0.41	2490	0.46	0.34	0.34	0.13	413	0.45	0.06	0.06	0.02
6.00	0.5304	1.00	18000	4938	0.27	4860	0.27	1660	0.31	0.34	0.34	0.09	276	0.30	0.06	0.06	0.01
6.00	0.5304	2.00	18000	3024	0.17	2950	0.16	1027	0.19	0.34	0.35	0.05	168	0.19	0.06	0.06	0.00
6.00	0.5304	4.00	18000	1713	0.10	1657	0.09	577	0.11	0.34	0.35	0.03	94	0.10	0.05	0.06	0.00
8.00	0.7072	0.00	18000	13875	0.77	14749	0.82	4928	1.00	0.36	0.33	0.27	832	1.00	0.06	0.06	0.04
8.00	0.7072	0.10	18000	11137	0.62	11542	0.64	3857	0.78	0.35	0.33	0.21	649	0.78	0.06	0.06	0.03
8.00	0.7072	0.25	18000	8838	0.49	8941	0.50	3003	0.61	0.34	0.34	0.16	509	0.61	0.06	0.06	0.02
8.00	0.7072	0.50	18000	6718	0.37	6694	0.37	2286	0.46	0.34	0.34	0.12	382	0.46	0.06	0.06	0.02
8.00	0.7072	1.00	18000	4625	0.26	4560	0.25	1557	0.32	0.34	0.34	0.08	259	0.31	0.06	0.06	0.01
8.00	0.7072	2.00	18000	2893	0.16	2805	0.16	958	0.19	0.33	0.34	0.05	159	0.19	0.05	0.06	0.00
8.00	0.7072	4.00	18000	1665	0.09	1596	0.09	545	0.11	0.33	0.34	0.03	90	0.11	0.05	0.06	0.00

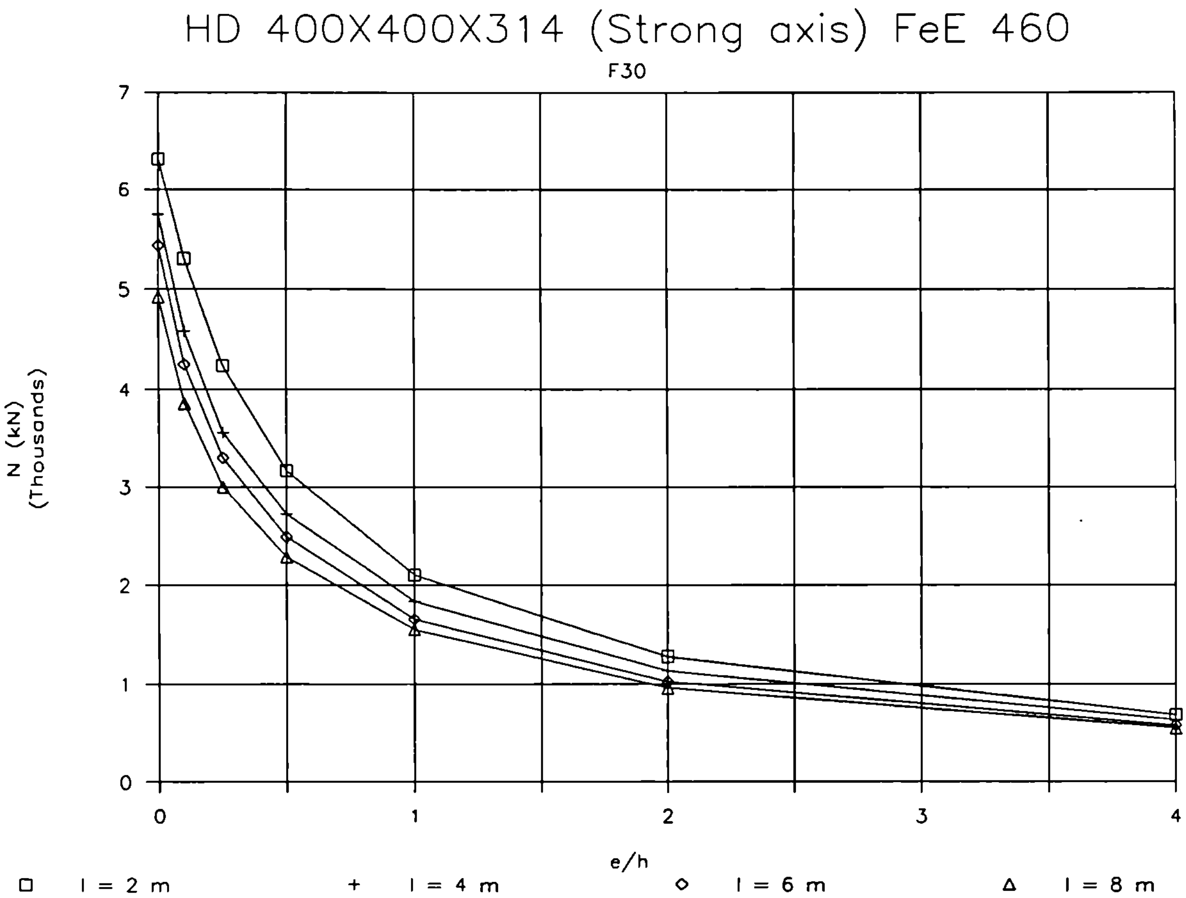
HD 400X400X314 (Strong axis) FeE 460
F30
N (kN)
(Thousands)
e/h
l = 2 m
l = 4 m
l = 6 m
l = 8 m

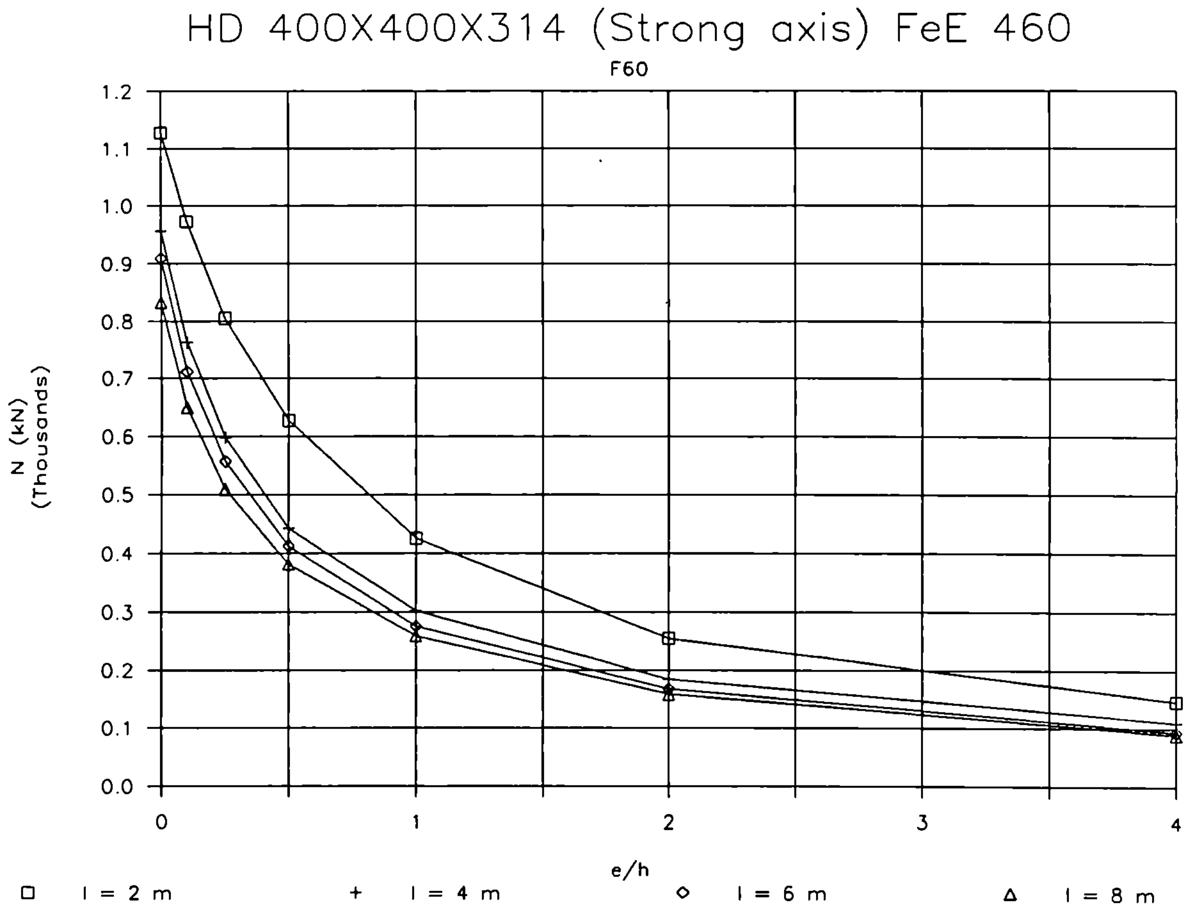
HD 400X400X314 (Strong axis) FeE 460
F60
N (kN)
(Thousands)
e/h
l = 2 m
l = 4 m
l = 6 m
l = 8 m

DIAGRAMS AND TABLES

FOR BENDING ABOUT

THE MINOR AXIS

DIAGRAMS AND TABLES

FOR BENDING ABOUT

THE MINOR AXIS

HE 550 M (Weak axis) Sigma yield = 345 N/mm2 ; U/A = 64 ; t = 40 mm

l (m)	Lambda Bar	e/h	Npl (kN)	F0 N(EC3) (kN)	F0 N(EC3)/Npl	F0 N(CEF) (kN)	F0 N(CEF)/Npl	F30 N(F30) (kN)	F30 N/Nc	F30 N/N(F0,EC3)	F30 N/N(F0,CEF)	F30 N/Npl	F60 N(F60) (kN)	F60 N/Nc	F60 N/N(F0,EC3)	F60 N/N(F0,CEF)	F60 N/Npl
2.00	0.3509	0.00	12213	11141	0.91	11127	0.91	3060	1.00	0.27	0.28	0.25	593	1.00	0.05	0.05	0.04
2.00	0.3509	0.10	12213	8291	0.68	8473	0.69	2388	0.78	0.29	0.28	0.19	459	0.77	0.06	0.05	0.03
2.00	0.3509	0.25	12213	5427	0.44	5967	0.49	1708	0.56	0.31	0.29	0.13	326	0.55	0.06	0.05	0.02
2.00	0.3509	0.50	12213	3083	0.25	3604	0.30	1087	0.36	0.35	0.30	0.08	200	0.34	0.06	0.06	0.01
2.00	0.3509	1.00	12213	1620	0.13	1959	0.16	606	0.20	0.37	0.31	0.04	110	0.19	0.07	0.06	0.00
4.00	0.7019	0.00	12213	9286	0.76	8654	0.71	2320	1.00	0.25	0.27	0.18	463	1.00	0.05	0.05	0.03
4.00	0.7019	0.10	12213	6528	0.53	6216	0.51	1752	0.76	0.27	0.28	0.14	342	0.74	0.05	0.06	0.02
4.00	0.7019	0.25	12213	4307	0.35	4376	0.36	1294	0.56	0.30	0.30	0.10	246	0.53	0.06	0.06	0.02
4.00	0.7019	0.50	12213	2638	0.22	2883	0.24	872	0.38	0.33	0.30	0.07	161	0.35	0.06	0.06	0.01
4.00	0.7019	1.00	12213	1484	0.12	1699	0.14	512	0.22	0.35	0.30	0.04	94	0.20	0.06	0.06	0.00
6.00	1.0528	0.00	12213	6430	0.53	5998	0.49	1649	1.00	0.26	0.27	0.13	326	1.00	0.05	0.05	0.02
6.00	1.0528	0.10	12213	4653	0.38	4314	0.35	1246	0.76	0.27	0.29	0.10	246	0.75	0.05	0.06	0.02
6.00	1.0528	0.25	12213	3268	0.27	3249	0.27	960	0.58	0.29	0.30	0.07	185	0.57	0.06	0.06	0.01
6.00	1.0528	0.50	12213	2195	0.18	2313	0.19	684	0.41	0.31	0.30	0.05	130	0.40	0.06	0.06	0.01
6.00	1.0528	1.00	12213	1331	0.11	1457	0.12	441	0.27	0.33	0.30	0.03	81	0.25	0.06	0.06	0.00
8.00	1.4038	0.00	12213	4174	0.34	4077	0.33	1149	1.00	0.28	0.28	0.09	227	1.00	0.05	0.06	0.01
8.00	1.4038	0.10	12213	3273	0.27	3108	0.25	897	0.78	0.27	0.29	0.07	177	0.78	0.05	0.06	0.01
8.00	1.4038	0.25	12213	2501	0.20	2447	0.20	723	0.63	0.29	0.30	0.05	141	0.62	0.06	0.06	0.01
8.00	1.4038	0.50	12213	1811	0.15	1854	0.15	551	0.48	0.30	0.30	0.04	105	0.46	0.06	0.06	0.00
8.00	1.4038	1.00	12213	1174	0.10	1249	0.10	378	0.33	0.32	0.30	0.03	70	0.31	0.06	0.06	0.00

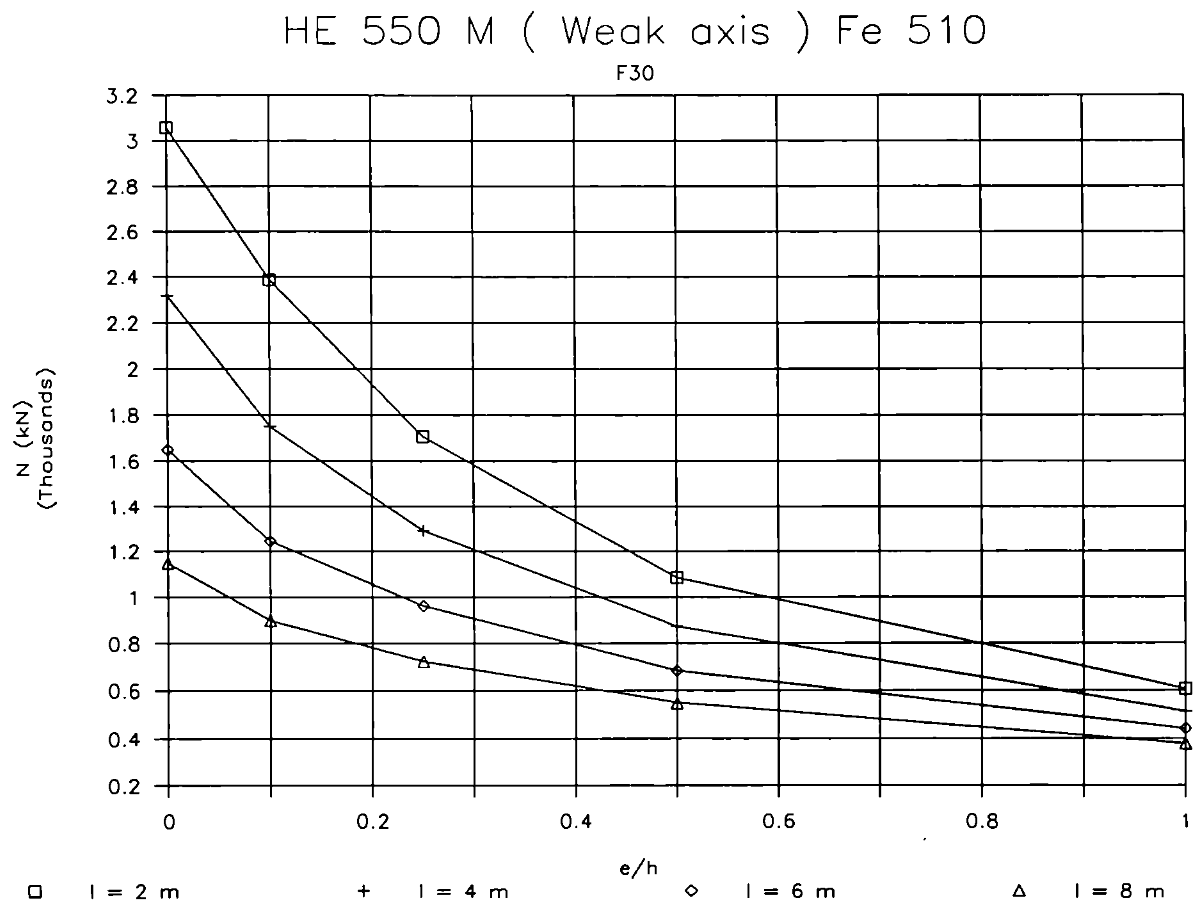
HE 550 M (Weak axis) Fe 510
F30
N (kN)
(Thousands)
3.2
3
2.8
2.6
2.4
2.2
2
1.8
1.6
1.4
1.2
1
0.8
0.6
0.4
0.2
0
0.2
0.4
0.6
0.8
1
e/h
l = 2 m
l = 4 m
l = 6 m
l = 8 m

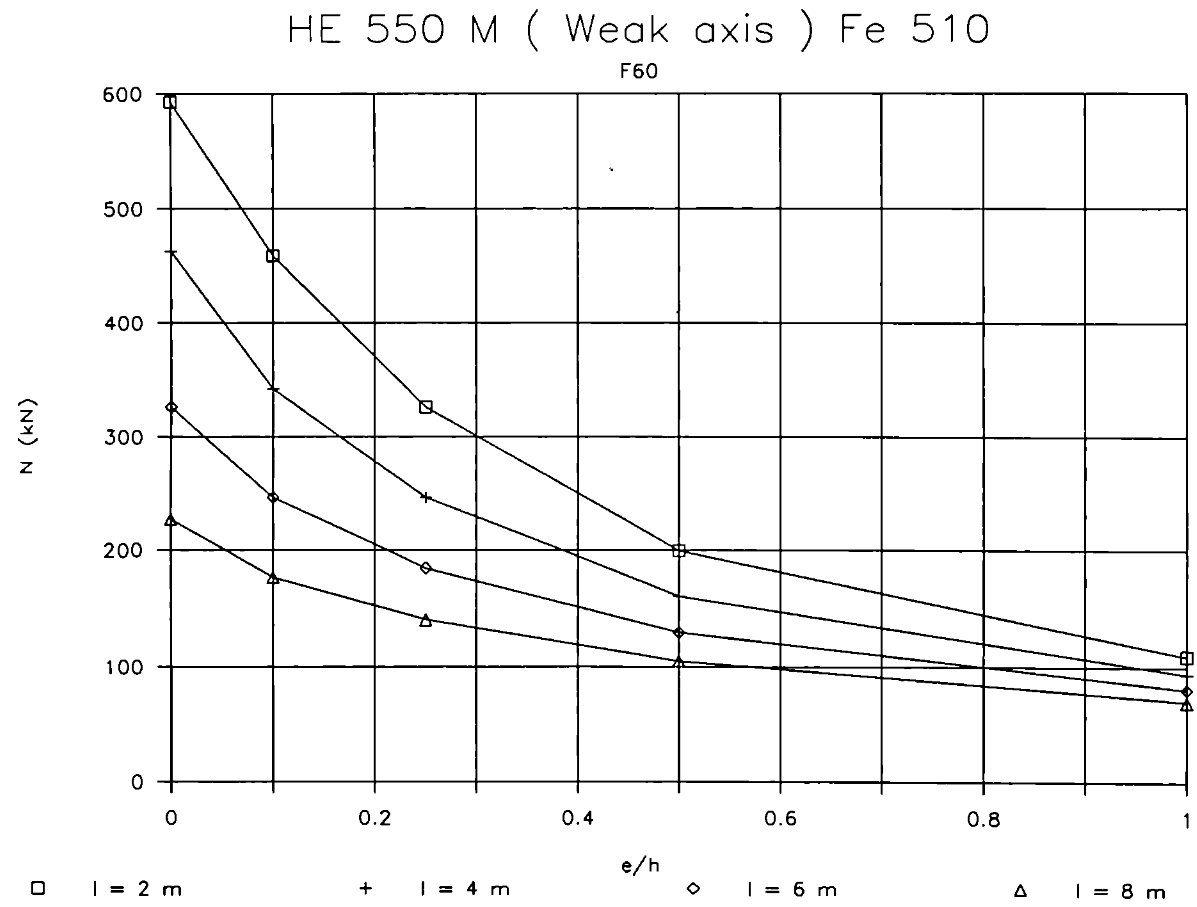
HE 550 M (Weak axis) Fe 510
F60
N (kN)
600
500
400
300
200
100
0
0
0.2
0.4
0.6
0.8
1
e/h
l = 2 m
l = 4 m
l = 6 m
l = 8 m

HD 210X210X198 (Weak axis) Sigma yield = 335 N/mm2 ; U/A = 54 ; t = 45 mm

l (m)	Lambda Bar	e/h	Npl (kN)	F0 N(EC3) (kN)	F0 N(EC3)/Npl	F0 N(CEF) (kN)	F0 N(CEF)/Npl	F30 N(F30) (kN)	F30 N/Nc	F30 N/N(F0,EC3)	F30 N/N(F0,CEF)	F30 N/Npl	F60 N(F60) (kN)	F60 N/Nc	F60 N/N(F0,EC3)	F60 N/N(F0,CEF)	F60 N/Npl
2.00	0.4390	0.00	8442	7382	0.87	7382	0.87	2479	1.00	0.34	0.34	0.29	411	1.00	0.06	0.06	0.04
2.00	0.4390	0.10	8442	5514	0.65	5531	0.66	1889	0.76	0.34	0.34	0.22	315	0.77	0.06	0.06	0.03
2.00	0.4390	0.25	8442	3775	0.45	4001	0.47	1367	0.55	0.36	0.34	0.16	230	0.56	0.06	0.06	0.02
2.00	0.4390	0.50	8442	2331	0.28	2610	0.31	891	0.36	0.38	0.34	0.10	149	0.36	0.06	0.06	0.01
2.00	0.4390	1.00	8442	1264	0.15	1485	0.18	507	0.20	0.40	0.34	0.06	84	0.21	0.07	0.06	0.01
4.00	0.8780	0.00	8442	5387	0.64	5033	0.60	1570	1.00	0.29	0.31	0.18	269	1.00	0.05	0.05	0.03
4.00	0.8780	0.10	8442	3929	0.47	3614	0.43	1181	0.75	0.30	0.33	0.13	209	0.78	0.05	0.06	0.02
4.00	0.8780	0.25	8442	2794	0.33	2754	0.33	906	0.58	0.32	0.33	0.10	158	0.59	0.06	0.06	0.01
4.00	0.8780	0.50	8442	1862	0.22	1938	0.23	647	0.41	0.35	0.33	0.07	111	0.41	0.06	0.06	0.01
4.00	0.8780	1.00	8442	1105	0.13	1218	0.14	407	0.26	0.37	0.33	0.04	69	0.26	0.06	0.06	0.00
6.00	1.3170	0.00	8442	3221	0.38	3136	0.37	931	1.00	0.29	0.30	0.11	174	1.00	0.05	0.06	0.02
6.00	1.3170	0.10	8442	2562	0.30	2391	0.28	746	0.80	0.29	0.31	0.08	137	0.79	0.05	0.06	0.01
6.00	1.3170	0.25	8442	1978	0.23	1882	0.22	606	0.65	0.31	0.32	0.07	109	0.63	0.06	0.06	0.01
6.00	1.3170	0.50	8442	1438	0.17	1441	0.17	471	0.51	0.33	0.33	0.05	83	0.48	0.06	0.06	0.00
6.00	1.3170	1.00	8442	936	0.11	990	0.12	323	0.35	0.35	0.33	0.03	56	0.32	0.06	0.06	0.00
8.00	1.7560	0.00	8442	2006	0.24	1957	0.23	610	1.00	0.30	0.31	0.07	116	1.00	0.06	0.06	0.01
8.00	1.7560	0.10	8442	1717	0.20	1643	0.19	495	0.81	0.29	0.30	0.05	95	0.82	0.06	0.06	0.01
8.00	1.7560	0.25	8442	1421	0.17	1329	0.16	424	0.70	0.30	0.32	0.05	79	0.68	0.06	0.06	0.00
8.00	1.7560	0.50	8442	1112	0.13	1076	0.13	339	0.56	0.31	0.32	0.04	64	0.55	0.06	0.06	0.00
8.00	1.7560	1.00	8442	782	0.09	796	0.09	260	0.43	0.33	0.33	0.03	46	0.40	0.06	0.06	0.00

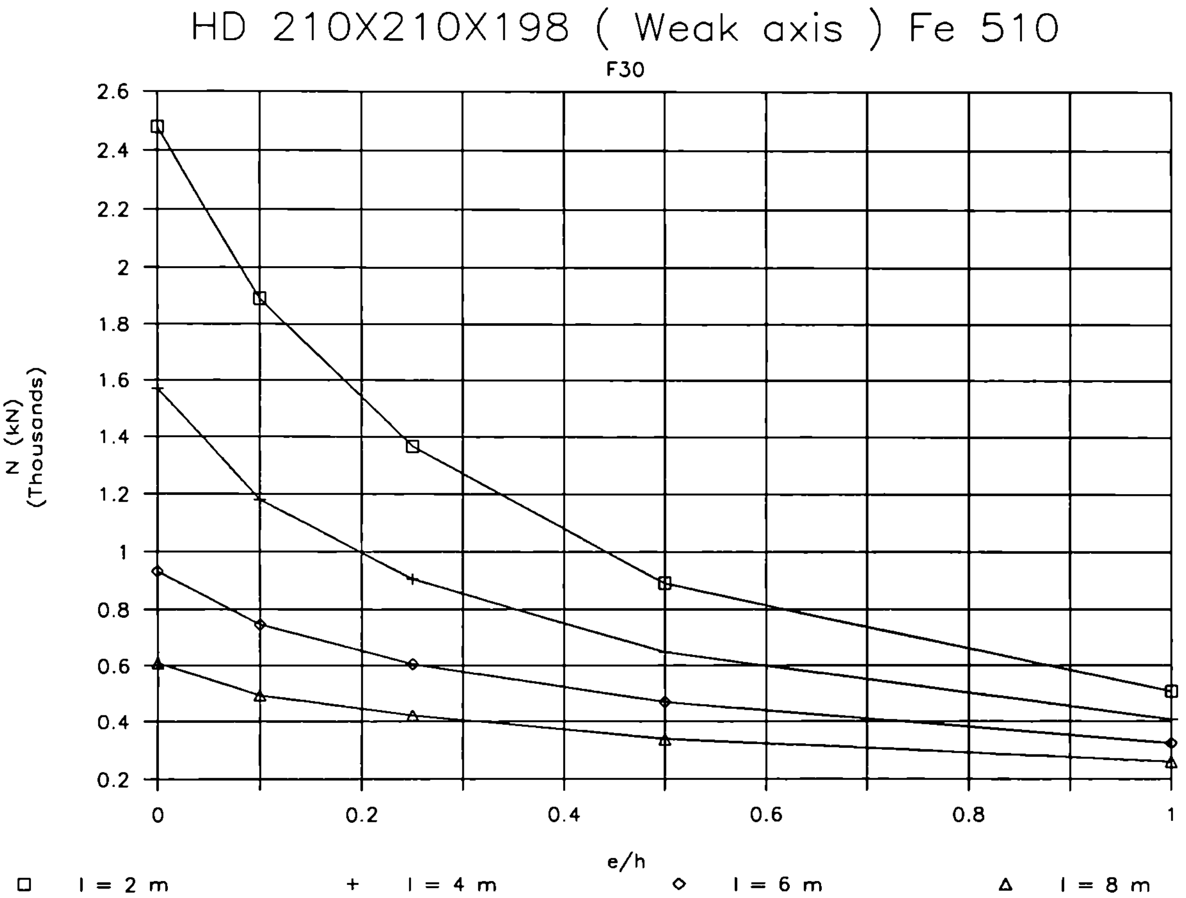
HD 210X210X198 (Weak axis) Fe 510
F30
N (kN)
(Thousands)
2.6
2.4
2.2
2
1.8
1.6
1.4
1.2
1
0.8
0.6
0.4
0.2
0
0.2
0.4
0.6
0.8
1
e/h
l = 2 m
l = 4 m
l = 6 m
l = 8 m

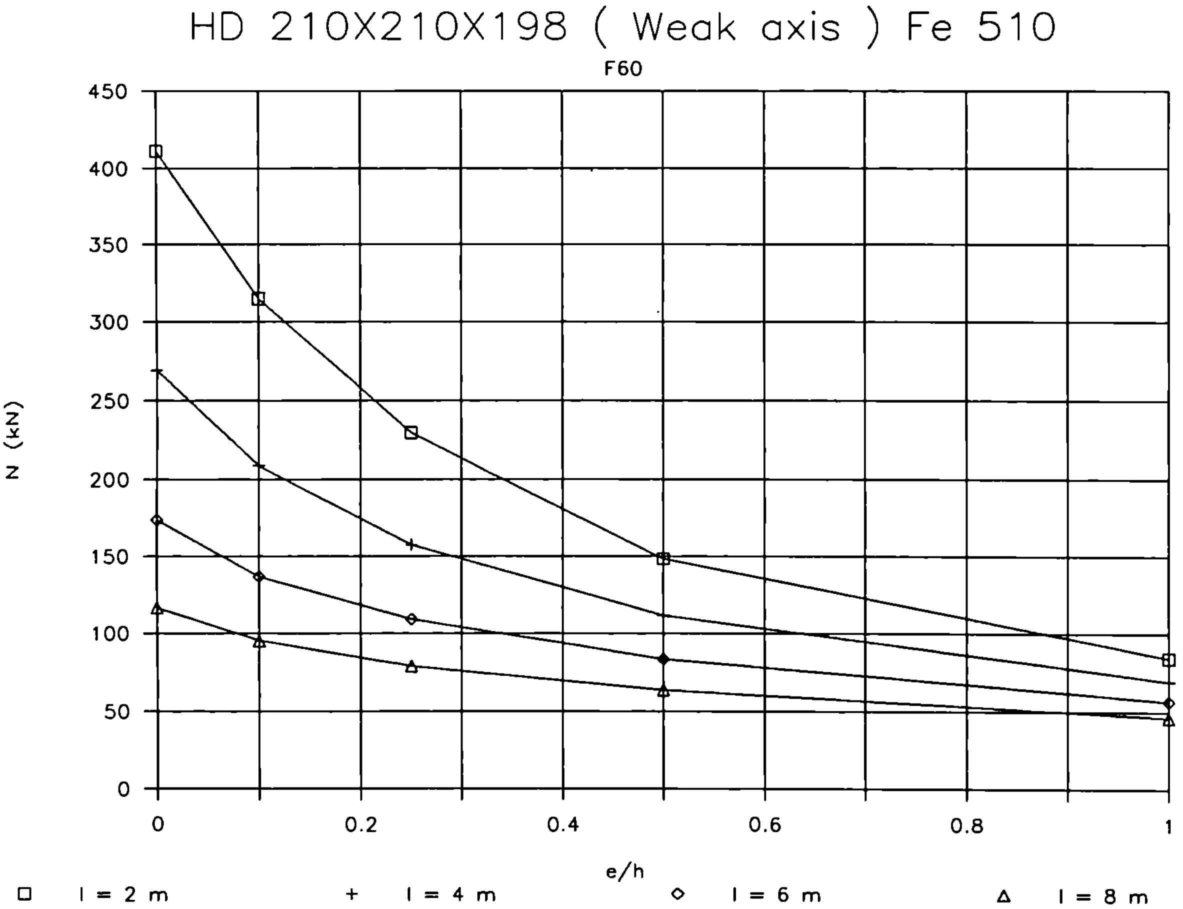
HD 210X210X198 (Weak axis) Fe 510
F60
N (kN)
450
400
350
300
250
200
150
100
50
0
0
0.2
0.4
0.6
0.8
1
e/h
l = 2 m
l = 4 m
l = 6 m
l = 8 m

HD 260X260X219 (Weak axis) Sigma yield = 335 N/mm2 ; U/A = 58 ; t = 41 mm

l	Lambda Bar	e/h	Npl	F0				F30					F60				
(m)			(kN)	N(EC3) (kN)	N(EC3)/Npl	N(CEF) (kN)	N(CEF)/Npl	N(F30) (kN)	N/Nc	N/N(F0,EC3)	N/N(F0,CEF)	N/Npl	N(F60) (kN)	N/Nc	N/N(F0,EC3)	N/N(F0,CEF)	N/Npl
2.00	0.3658	0.00	9347	8419	0.90	8305	0.89	2651	1.00	0.31	0.32	0.28	461	1.00	0.05	0.06	0.04
2.00	0.3658	0.10	9347	6359	0.68	6324	0.68	2049	0.77	0.32	0.32	0.21	357	0.77	0.06	0.06	0.03
2.00	0.3658	0.25	9347	4354	0.47	4659	0.50	1472	0.56	0.34	0.32	0.15	259	0.56	0.06	0.06	0.02
2.00	0.3658	0.50	9347	2656	0.28	2996	0.32	946	0.36	0.36	0.32	0.10	168	0.36	0.06	0.06	0.01
2.00	0.3658	1.00	9347	1420	0.15	1691	0.18	534	0.20	0.38	0.32	0.05	94	0.20	0.07	0.06	0.01
4.00	0.7316	0.00	9347	6854	0.73	6000	0.64	1894	1.00	0.28	0.32	0.20	321	1.00	0.05	0.05	0.03
4.00	0.7316	0.10	9347	4961	0.53	4472	0.48	1361	0.72	0.27	0.30	0.14	248	0.77	0.05	0.06	0.02
4.00	0.7316	0.25	9347	3453	0.37	3332	0.36	1026	0.54	0.30	0.31	0.10	187	0.58	0.05	0.06	0.01
4.00	0.7316	0.50	9347	2231	0.24	2325	0.25	725	0.38	0.33	0.31	0.07	129	0.40	0.06	0.06	0.01
4.00	0.7316	1.00	9347	1283	0.14	1426	0.15	445	0.23	0.35	0.31	0.04	79	0.25	0.06	0.06	0.00
6.00	1.0974	0.00	9347	4647	0.50	4029	0.43	1111	1.00	0.24	0.28	0.11	216	1.00	0.05	0.05	0.02
6.00	1.0974	0.10	9347	3520	0.38	3047	0.33	905	0.81	0.26	0.30	0.09	168	0.78	0.05	0.06	0.01
6.00	1.0974	0.25	9347	2603	0.28	2401	0.26	731	0.66	0.28	0.30	0.07	134	0.62	0.05	0.06	0.01
6.00	1.0974	0.50	9347	1809	0.19	1797	0.19	547	0.49	0.30	0.30	0.05	100	0.46	0.06	0.06	0.01
6.00	1.0974	1.00	9347	1127	0.12	1188	0.13	366	0.33	0.32	0.31	0.03	66	0.31	0.06	0.06	0.00
8.00	1.4632	0.00	9347	3017	0.32	2713	0.29	725	1.00	0.24	0.27	0.07	147	1.00	0.05	0.05	0.01
8.00	1.4632	0.10	9347	2466	0.26	2147	0.23	622	0.86	0.25	0.29	0.06	120	0.81	0.05	0.06	0.01
8.00	1.4632	0.25	9347	1952	0.21	1732	0.19	522	0.72	0.27	0.30	0.05	100	0.67	0.05	0.06	0.01
8.00	1.4632	0.50	9347	1457	0.16	1386	0.15	418	0.58	0.29	0.30	0.04	78	0.53	0.05	0.06	0.00
8.00	1.4632	1.00	9347	975	0.10	990	0.11	301	0.42	0.31	0.30	0.03	55	0.37	0.06	0.06	0.00

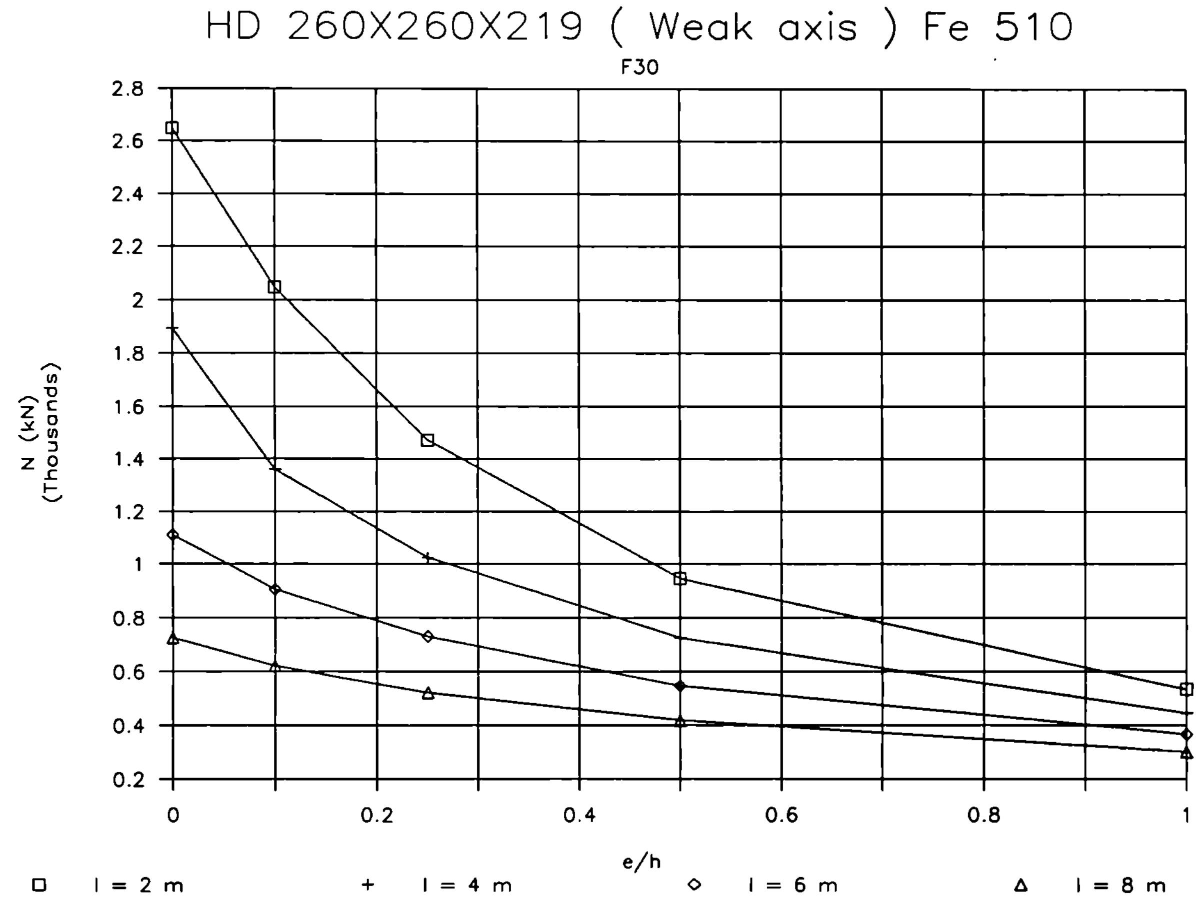
HD 260X260X219 (Weak axis) Fe 510
F30
N (kN) (Thousands)
2.8
2.6
2.4
2.2
2
1.8
1.6
1.4
1.2
1
0.8
0.6
0.4
0.2
0
0.2
0.4
0.6
0.8
1
e/h
□ l = 2 m
+ l = 4 m
◇ l = 6 m
Δ l = 8 m

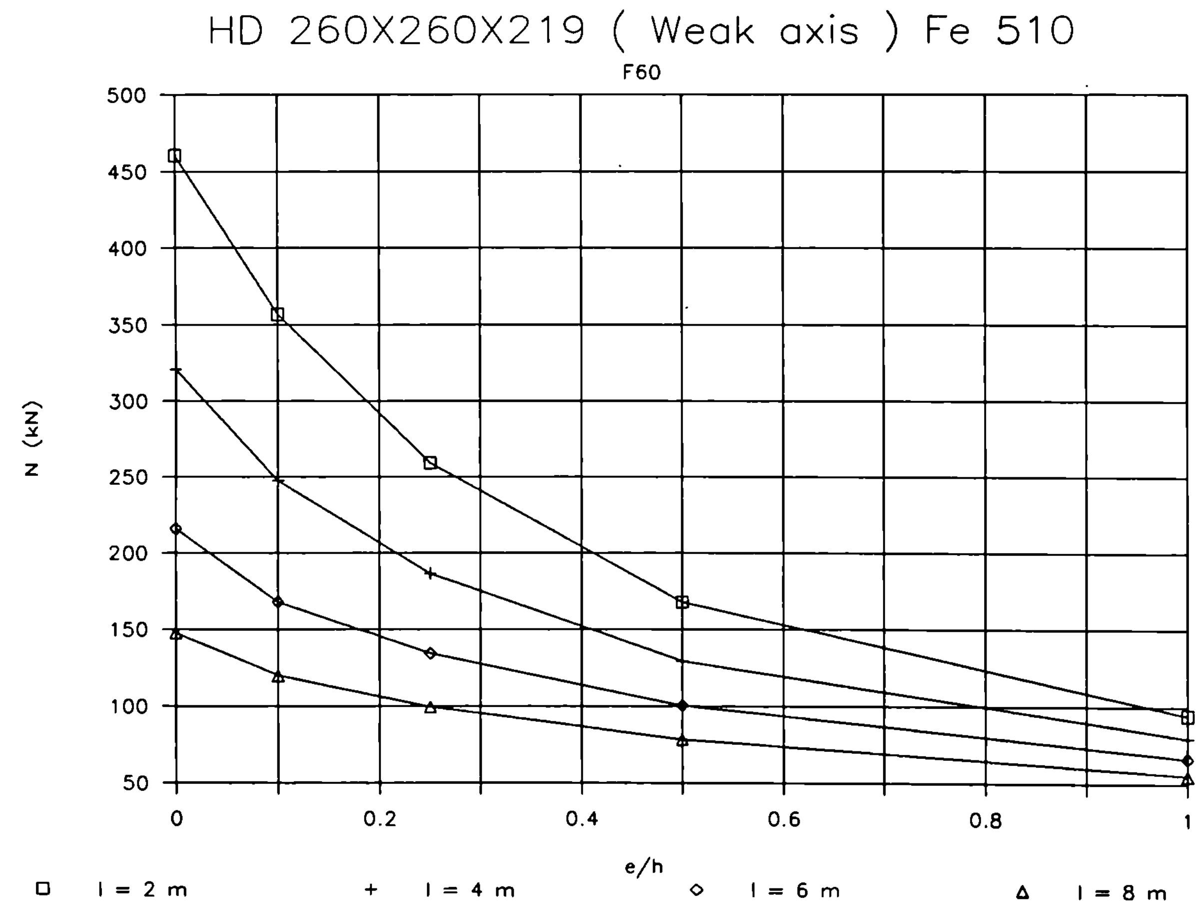
HD 260X260X219 (Weak axis) Fe 510
F60
N (kN)
500
450
400
350
300
250
200
150
100
50
0
0.2
0.4
0.6
0.8
1
e/h
□ l = 2 m
+ l = 4 m
◇ l = 6 m
Δ l = 8 m

HD 260X260X329 (Weak axis) Sigma yield = 335 N/mm2 ; U/A = 41 ; t = 60 mm

l	Lambda Bar	e/h	Npl	F0				F30					F60				
(m)			(kN)	N(EC3) (kN)	N(EC3)/Npl	N(CEF) (kN)	N(CEF)/Npl	N(F30) (kN)	N/Nc	N/N(F0,EC3)	N/N(F0,CEF)	N/Npl	N(F60) (kN)	N/Nc	N/N(F0,EC3)	N/N(F0,CEF)	N/Npl
2.00	0.3489	0.00	14070	12720	0.90	12968	0.92	7799	1.00	0.61	0.60	0.55	879	1.00	0.07	0.07	0.06
2.00	0.3489	0.10	14070	9621	0.68	9776	0.69	5973	0.77	0.62	0.61	0.42	672	0.76	0.07	0.07	0.04
2.00	0.3489	0.25	14070	6602	0.47	7202	0.51	4251	0.55	0.64	0.59	0.30	489	0.56	0.07	0.07	0.03
2.00	0.3489	0.50	14070	4041	0.29	4631	0.33	2770	0.36	0.69	0.60	0.19	311	0.35	0.08	0.07	0.02
2.00	0.3489	1.00	14070	2159	0.15	2587	0.18	1671	0.21	0.77	0.65	0.11	175	0.20	0.08	0.07	0.01
4.00	0.6978	0.00	14070	10564	0.75	9985	0.71	4893	1.00	0.46	0.49	0.34	685	1.00	0.06	0.07	0.04
4.00	0.6978	0.10	14070	7661	0.54	7245	0.51	3808	0.78	0.50	0.53	0.27	500	0.73	0.07	0.07	0.03
4.00	0.6978	0.25	14070	5323	0.38	5348	0.38	2859	0.58	0.54	0.53	0.20	368	0.54	0.07	0.07	0.02
4.00	0.6978	0.50	14070	3433	0.24	3668	0.26	1961	0.40	0.57	0.53	0.13	248	0.36	0.07	0.07	0.01
4.00	0.6978	1.00	14070	1963	0.14	2205	0.16	1199	0.24	0.61	0.54	0.08	149	0.22	0.08	0.07	0.01
6.00	1.0467	0.00	14070	7405	0.53	6990	0.50	3203	1.00	0.43	0.46	0.22	486	1.00	0.07	0.07	0.03
6.00	1.0467	0.10	14070	5563	0.40	5155	0.37	2547	0.80	0.46	0.49	0.18	357	0.73	0.06	0.07	0.02
6.00	1.0467	0.25	14070	4084	0.29	3959	0.28	2011	0.63	0.49	0.51	0.14	273	0.56	0.07	0.07	0.01
6.00	1.0467	0.50	14070	2818	0.20	2878	0.20	1487	0.46	0.53	0.52	0.10	198	0.41	0.07	0.07	0.01
6.00	1.0467	1.00	14070	1738	0.12	1864	0.13	980	0.31	0.56	0.53	0.06	127	0.26	0.07	0.07	0.00
8.00	1.3956	0.00	14070	4893	0.35	4835	0.34	2181	1.00	0.45	0.45	0.15	345	1.00	0.07	0.07	0.02
8.00	1.3956	0.10	14070	3956	0.28	3733	0.27	1774	0.81	0.45	0.48	0.12	263	0.76	0.07	0.07	0.01
8.00	1.3956	0.25	14070	3099	0.22	2969	0.21	1467	0.67	0.47	0.49	0.10	209	0.61	0.07	0.07	0.01
8.00	1.3956	0.50	14070	2289	0.16	2302	0.16	1169	0.54	0.51	0.51	0.08	159	0.46	0.07	0.07	0.01
8.00	1.3956	1.00	14070	1515	0.11	1585	0.11	819	0.38	0.54	0.52	0.05	108	0.31	0.07	0.07	0.00

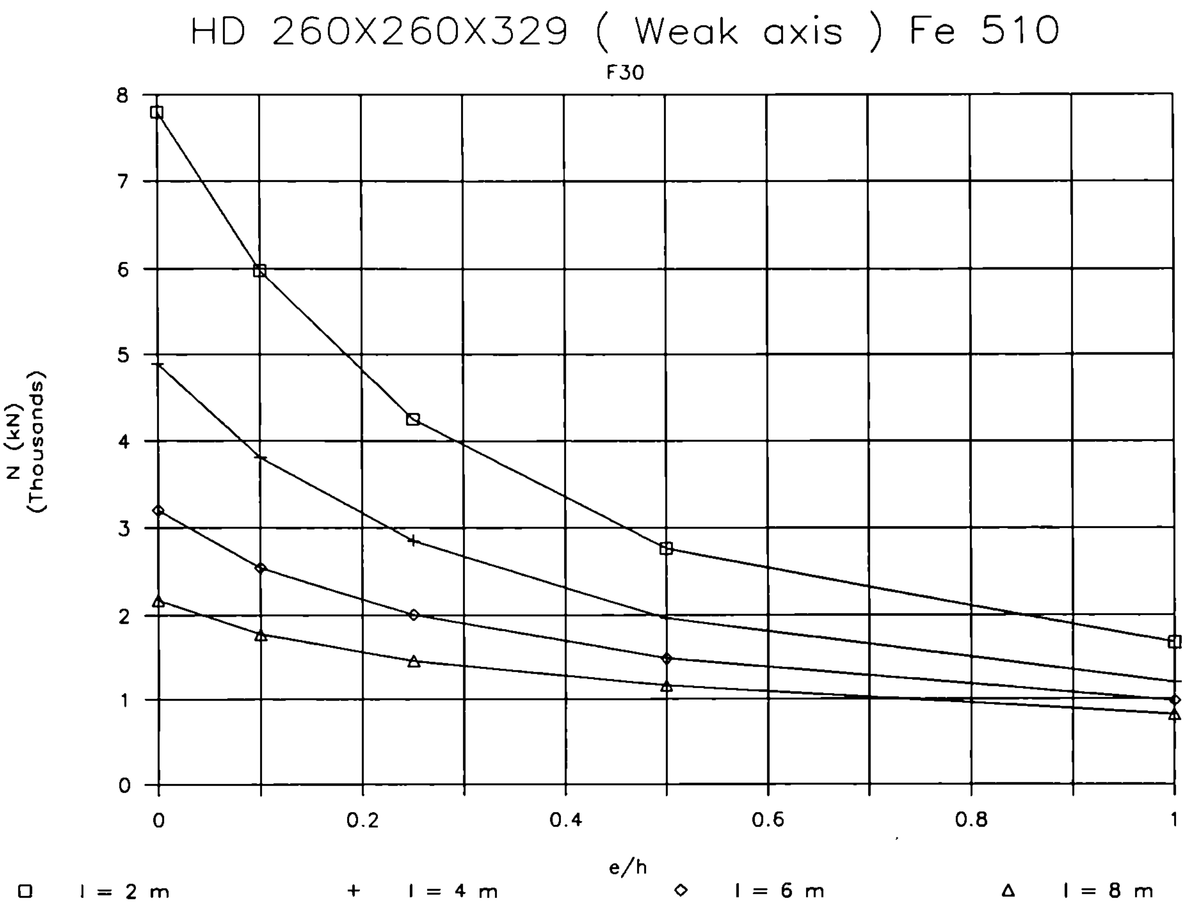
HD 260X260X329 (Weak axis) Fe 510
F30
N (kN)
(Thousands)
8
7
6
5
4
3
2
1
0
0
0.2
0.4
0.6
0.8
1
e/h
l = 2 m
l = 4 m
l = 6 m
l = 8 m

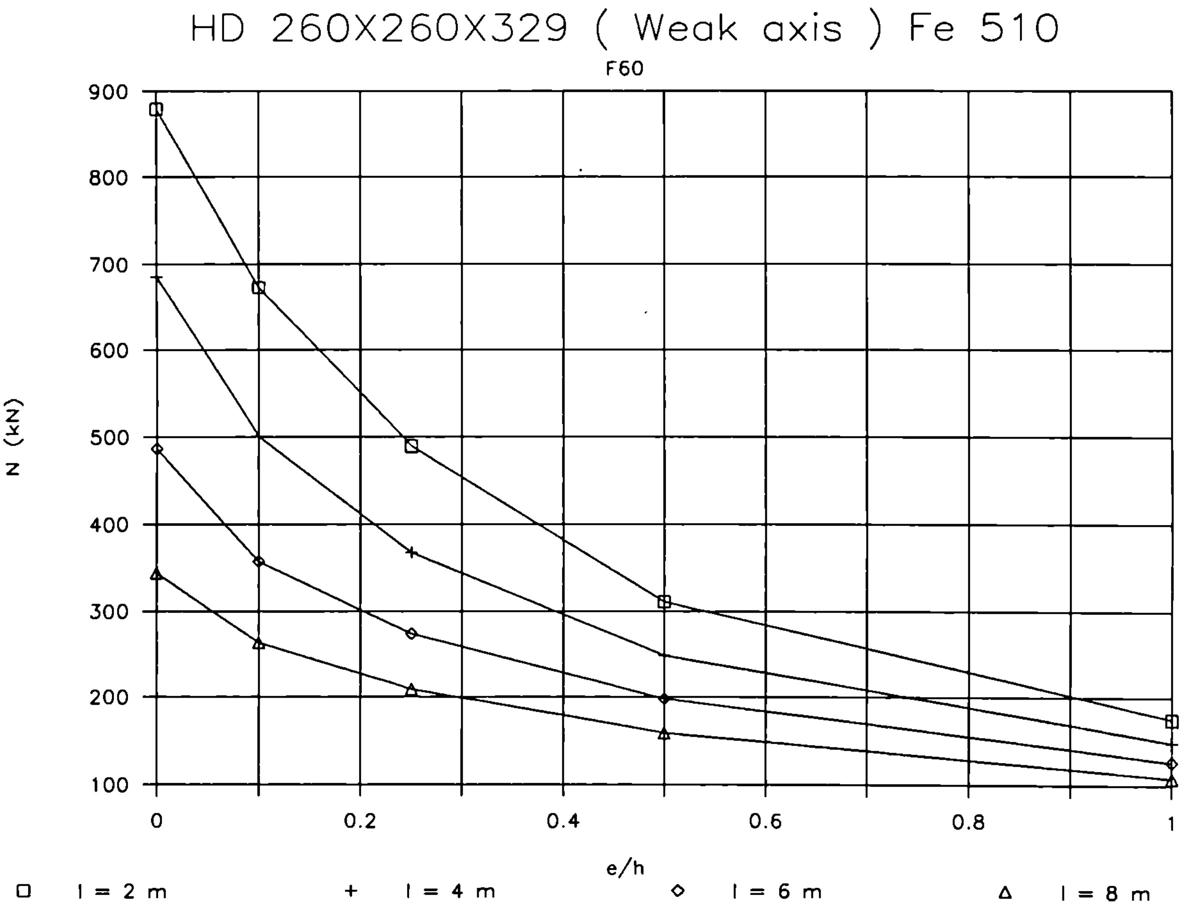
HD 260X260X329 (Weak axis) Fe 510
F60
N (kN)
900
800
700
600
500
400
300
200
100
0
0.2
0.4
0.6
0.8
1
e/h
l = 2 m
l = 4 m
l = 6 m
l = 8 m

HD 310X310X283 (Weak axis) Sigma yield = 335 N/mm2 ; U/A = 54 ; t = 44 mm

l (m)	Lambda Bar	e/h	Npl (kN)	F0				F30					F60				
				N(EC3) (kN)	N(EC3)/Npl	N(CEF) (kN)	N(CEF)/Npl	N(F30) (kN)	N/Nc	N/N(F0,EC3)	N/N(F0,CEF)	N/Npl	N(F60) (kN)	N/Nc	N/N(F0,EC3)	N/N(F0,CEF)	N/Npl
2.00	0.3080	0.00	12060	11084	0.92	11127	0.92	4249	1.00	0.38	0.38	0.35	647	1.00	0.06	0.06	0.05
2.00	0.3080	0.10	12060	8428	0.70	8559	0.71	3336	0.79	0.40	0.39	0.27	507	0.78	0.06	0.06	0.04
2.00	0.3080	0.25	12060	5768	0.48	6242	0.52	2364	0.56	0.41	0.38	0.19	366	0.57	0.06	0.06	0.03
2.00	0.3080	0.50	12060	3488	0.29	4014	0.33	1481	0.35	0.42	0.37	0.12	234	0.36	0.07	0.06	0.01
2.00	0.3080	1.00	12060	1843	0.15	2220	0.18	890	0.21	0.48	0.40	0.07	136	0.21	0.07	0.06	0.01
4.00	0.6160	0.00	12060	9624	0.80	8654	0.72	3020	1.00	0.31	0.35	0.25	500	1.00	0.05	0.06	0.04
4.00	0.6160	0.10	12060	7018	0.58	6536	0.54	2285	0.76	0.33	0.35	0.18	379	0.76	0.05	0.06	0.03
4.00	0.6160	0.25	12060	4823	0.40	4777	0.40	1702	0.56	0.35	0.36	0.14	280	0.56	0.06	0.06	0.02
4.00	0.6160	0.50	12060	3044	0.25	3243	0.27	1156	0.38	0.38	0.36	0.09	189	0.38	0.06	0.06	0.01
4.00	0.6160	1.00	12060	1704	0.14	1931	0.16	688	0.23	0.40	0.36	0.05	112	0.22	0.07	0.06	0.00
6.00	0.9240	0.00	12060	7339	0.61	6307	0.52	2087	1.00	0.28	0.33	0.17	355	1.00	0.05	0.06	0.02
6.00	0.9240	0.10	12060	5376	0.45	4698	0.39	1605	0.77	0.30	0.34	0.13	274	0.77	0.05	0.06	0.02
6.00	0.9240	0.25	12060	3843	0.32	3598	0.30	1255	0.60	0.33	0.35	0.10	211	0.59	0.05	0.06	0.01
6.00	0.9240	0.50	12060	2571	0.21	2596	0.22	925	0.44	0.36	0.36	0.07	153	0.43	0.06	0.06	0.01
6.00	0.9240	1.00	12060	1540	0.13	1665	0.14	593	0.28	0.39	0.36	0.04	97	0.27	0.06	0.06	0.00
8.00	1.2320	0.00	12060	5096	0.42	4496	0.37	1457	1.00	0.29	0.32	0.12	258	1.00	0.05	0.06	0.02
8.00	1.2320	0.10	12060	3969	0.33	3453	0.29	1160	0.80	0.29	0.34	0.09	202	0.78	0.05	0.06	0.01
8.00	1.2320	0.25	12060	3009	0.25	2753	0.23	943	0.65	0.31	0.34	0.07	163	0.63	0.05	0.06	0.01
8.00	1.2320	0.50	12060	2145	0.18	2098	0.17	732	0.50	0.34	0.35	0.06	123	0.48	0.06	0.06	0.01
8.00	1.2320	1.00	12060	1373	0.11	1430	0.12	510	0.35	0.37	0.36	0.04	83	0.32	0.06	0.06	0.00

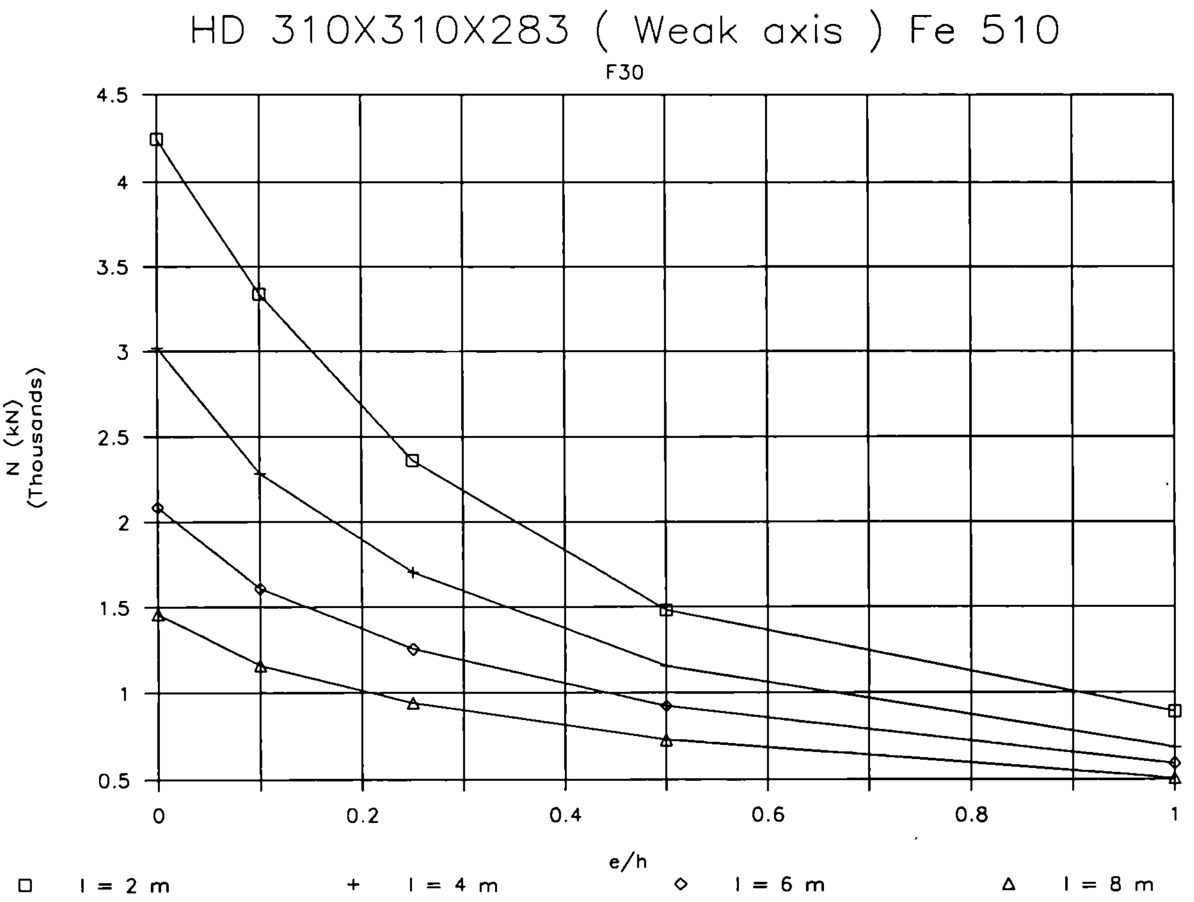
HD 310X310X283 (Weak axis) Fe 510
F30
N (kN)
(Thousands)
e/h
□ l = 2 m
+ l = 4 m
◇ l = 6 m
Δ l = 8 m

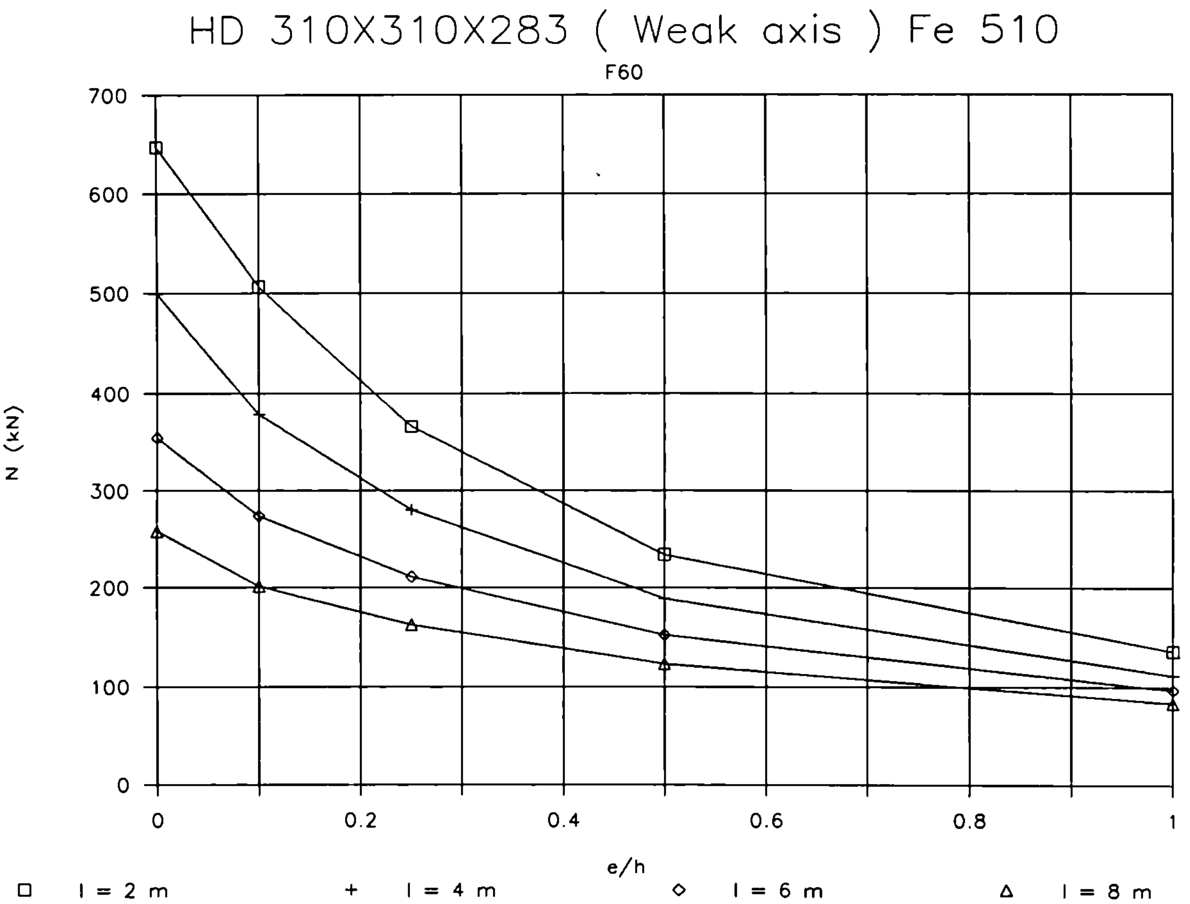
HD 310X310X283 (Weak axis) Fe 510
F60
N (kN)
e/h
□ l = 2 m
+ l = 4 m
◇ l = 6 m
Δ l = 8 m

HD 310X310X375 (Weak axis) Sigma yield = 335 N/mm2 ; U/A = 42 ; t = 57 mm

l	Lambda Bar	e/h	Npl	F0				F30					F60				
(m)			(kN)	N(EC3) (kN)	N(EC3)/Npl	N(CEF) (kN)	N(CEF)/Npl	N(F30) (kN)	N/Nc	N/N(F0,EC3)	N/N(F0,CEF)	N/Npl	N(F60) (kN)	N/Nc	N/N(F0,EC3)	N/N(F0,CEF)	N/Npl
2.00	0.3003	0.00	16013	14743	0.92	14846	0.93	9425	1.00	0.64	0.63	0.58	1012	1.00	0.07	0.07	0.06
2.00	0.3003	0.10	16013	11202	0.70	11512	0.72	7180	0.76	0.64	0.62	0.44	784	0.77	0.07	0.07	0.04
2.00	0.3003	0.25	16013	7667	0.48	8328	0.52	5088	0.54	0.66	0.61	0.31	567	0.56	0.07	0.07	0.03
2.00	0.3003	0.50	16013	4624	0.29	5355	0.33	3272	0.35	0.71	0.61	0.20	359	0.35	0.08	0.07	0.02
2.00	0.3003	1.00	16013	2440	0.15	2932	0.18	1927	0.20	0.79	0.66	0.12	204	0.20	0.08	0.07	0.01
4.00	0.6006	0.00	16013	12885	0.80	11663	0.73	6004	1.00	0.47	0.51	0.37	804	1.00	0.06	0.07	0.05
4.00	0.6006	0.10	16013	9398	0.59	8763	0.55	4685	0.78	0.50	0.53	0.29	599	0.74	0.06	0.07	0.03
4.00	0.6006	0.25	16013	6444	0.40	6437	0.40	3441	0.57	0.53	0.53	0.21	437	0.54	0.07	0.07	0.02
4.00	0.6006	0.50	16013	4051	0.25	4348	0.27	2325	0.39	0.57	0.53	0.14	292	0.36	0.07	0.07	0.01
4.00	0.6006	1.00	16013	2261	0.14	2588	0.16	1413	0.24	0.62	0.55	0.08	172	0.21	0.08	0.07	0.01
6.00	0.9009	0.00	16013	9975	0.62	8556	0.53	3988	1.00	0.40	0.47	0.24	592	1.00	0.06	0.07	0.03
6.00	0.9009	0.10	16013	7276	0.45	6395	0.40	3191	0.80	0.44	0.50	0.19	439	0.74	0.06	0.07	0.02
6.00	0.9009	0.25	16013	5174	0.32	4898	0.31	2487	0.62	0.48	0.51	0.15	333	0.56	0.06	0.07	0.02
6.00	0.9009	0.50	16013	3446	0.22	3499	0.22	1808	0.45	0.52	0.52	0.11	237	0.40	0.07	0.07	0.01
6.00	0.9009	1.00	16013	2053	0.13	2222	0.14	1166	0.29	0.57	0.52	0.07	150	0.25	0.07	0.07	0.00
8.00	1.2012	0.00	16013	7006	0.44	6212	0.39	2717	1.00	0.39	0.44	0.16	435	1.00	0.06	0.07	0.02
8.00	1.2012	0.10	16013	5417	0.34	4701	0.29	2262	0.83	0.42	0.48	0.14	327	0.75	0.06	0.07	0.02
8.00	1.2012	0.25	16013	4077	0.25	3748	0.23	1870	0.69	0.46	0.50	0.11	258	0.59	0.06	0.07	0.01
8.00	1.2012	0.50	16013	2893	0.18	2856	0.18	1425	0.52	0.49	0.50	0.08	194	0.45	0.07	0.07	0.01
8.00	1.2012	1.00	16013	1836	0.11	1924	0.12	977	0.36	0.53	0.51	0.06	130	0.30	0.07	0.07	0.00

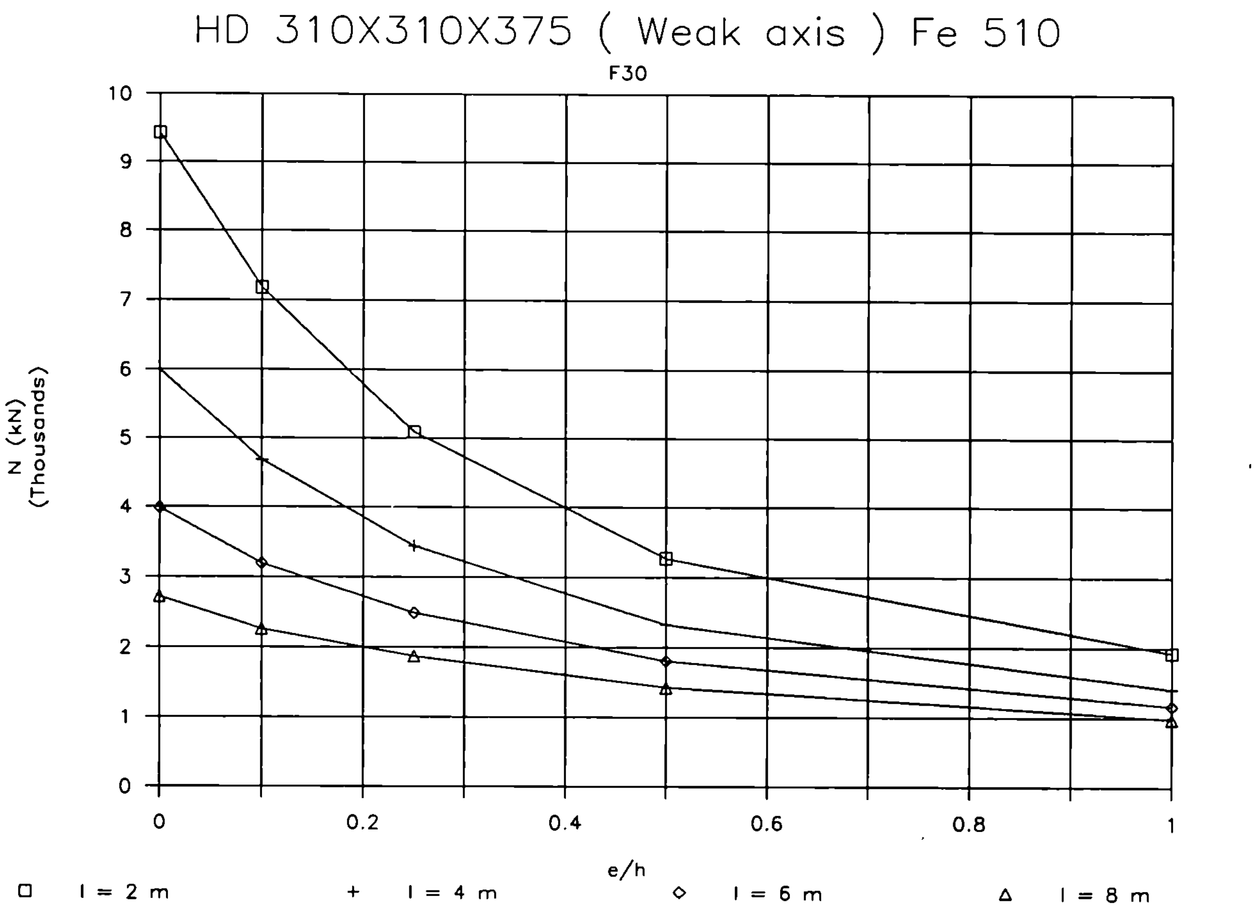
HD 310X310X375 (Weak axis) Fe 510
F30
N (kN) (Thousands)
e/h
l = 2 m
l = 4 m
l = 6 m
l = 8 m

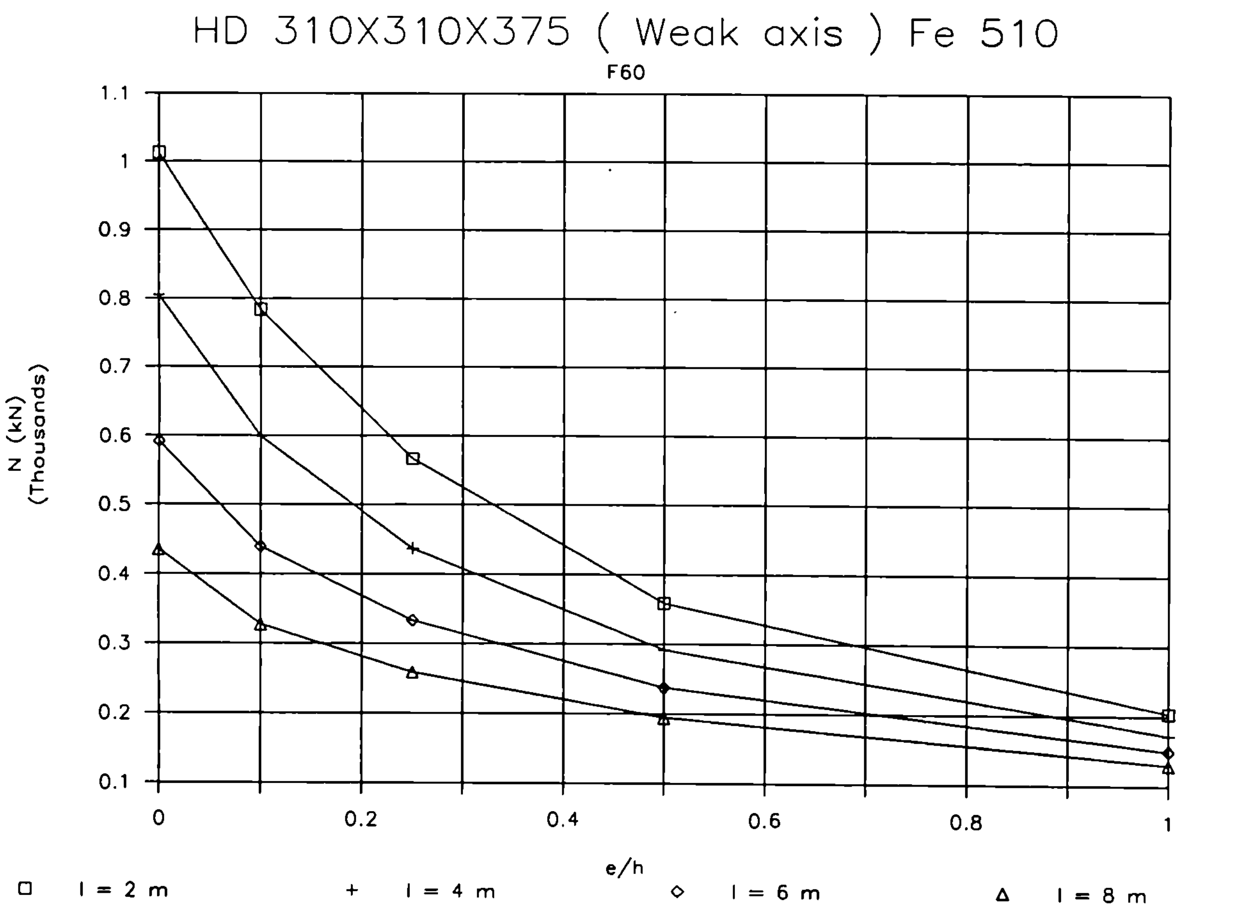
HD 310X310X375 (Weak axis) Fe 510
F60
N (kN) (Thousands)
e/h
l = 2 m
l = 4 m
l = 6 m
l = 8 m

HD 310X310X500 (Weak axis) Sigma yield = 325 N/mm2 ; U/A = 33 ; t = 75 mm

l (m)	Lambda Bar	e/h	Npl (kN)	F0				F30					F60				
				N(EC3) (kN)	N(EC3)/Npl	N(CEF) (kN)	N(CEF)/Npl	N(F30) (kN)	N/Nc	N/N(F0,EC3)	N/N(F0,CEF)	N/Npl	N(F60) (kN)	N/Nc	N/N(F0,EC3)	N/N(F0,CEF)	N/Npl
2.00	0.2844	0.00	20721	19102	0.92	19573	0.94	15052	1.00	0.79	0.77	0.72	1920	1.00	0.10	0.10	0.09
2.00	0.2844	0.10	20721	14570	0.70	15178	0.73	11672	0.78	0.80	0.77	0.56	1462	0.76	0.10	0.10	0.07
2.00	0.2844	0.25	20721	9997	0.48	11022	0.53	8281	0.55	0.83	0.75	0.39	1040	0.54	0.10	0.09	0.05
2.00	0.2844	0.50	20721	6075	0.29	7060	0.34	5140	0.34	0.85	0.73	0.24	655	0.34	0.11	0.09	0.03
2.00	0.2844	1.00	20721	3207	0.15	3915	0.19	3010	0.20	0.94	0.77	0.14	361	0.19	0.11	0.09	0.01
4.00	0.5689	0.00	20721	16899	0.82	16466	0.79	10096	1.00	0.60	0.61	0.48	1602	1.00	0.09	0.10	0.07
4.00	0.5689	0.10	20721	12392	0.60	12073	0.58	7968	0.79	0.64	0.66	0.38	1160	0.72	0.09	0.10	0.05
4.00	0.5689	0.25	20721	8526	0.41	8836	0.43	5892	0.58	0.69	0.67	0.28	822	0.51	0.10	0.09	0.03
4.00	0.5689	0.50	20721	5372	0.26	5880	0.28	3921	0.39	0.73	0.67	0.18	539	0.34	0.10	0.09	0.02
4.00	0.5689	1.00	20721	2987	0.14	3465	0.17	2412	0.24	0.81	0.70	0.11	316	0.20	0.11	0.09	0.01
6.00	0.8533	0.00	20721	13458	0.65	12709	0.61	6965	1.00	0.52	0.55	0.33	1202	1.00	0.09	0.09	0.05
6.00	0.8533	0.10	20721	9812	0.47	9112	0.44	5587	0.80	0.57	0.61	0.26	871	0.72	0.09	0.10	0.04
6.00	0.8533	0.25	20721	6959	0.34	6859	0.33	4329	0.62	0.62	0.63	0.20	641	0.53	0.09	0.09	0.03
6.00	0.8533	0.50	20721	4620	0.22	4834	0.23	3081	0.44	0.67	0.64	0.14	446	0.37	0.10	0.09	0.02
6.00	0.8533	1.00	20721	2731	0.13	3026	0.15	1947	0.28	0.71	0.64	0.09	277	0.23	0.10	0.09	0.01
8.00	1.1377	0.00	20721	9718	0.47	9356	0.45	4901	1.00	0.50	0.52	0.23	891	1.00	0.09	0.10	0.04
8.00	1.1377	0.10	20721	7450	0.36	6969	0.34	4035	0.82	0.54	0.58	0.19	661	0.74	0.09	0.09	0.03
8.00	1.1377	0.25	20721	5563	0.27	5432	0.26	3258	0.66	0.59	0.60	0.15	509	0.57	0.09	0.09	0.02
8.00	1.1377	0.50	20721	3911	0.19	3988	0.19	2468	0.50	0.63	0.62	0.11	374	0.42	0.10	0.09	0.01
8.00	1.1377	1.00	20721	2460	0.12	2636	0.13	1661	0.34	0.68	0.63	0.08	243	0.27	0.10	0.09	0.01

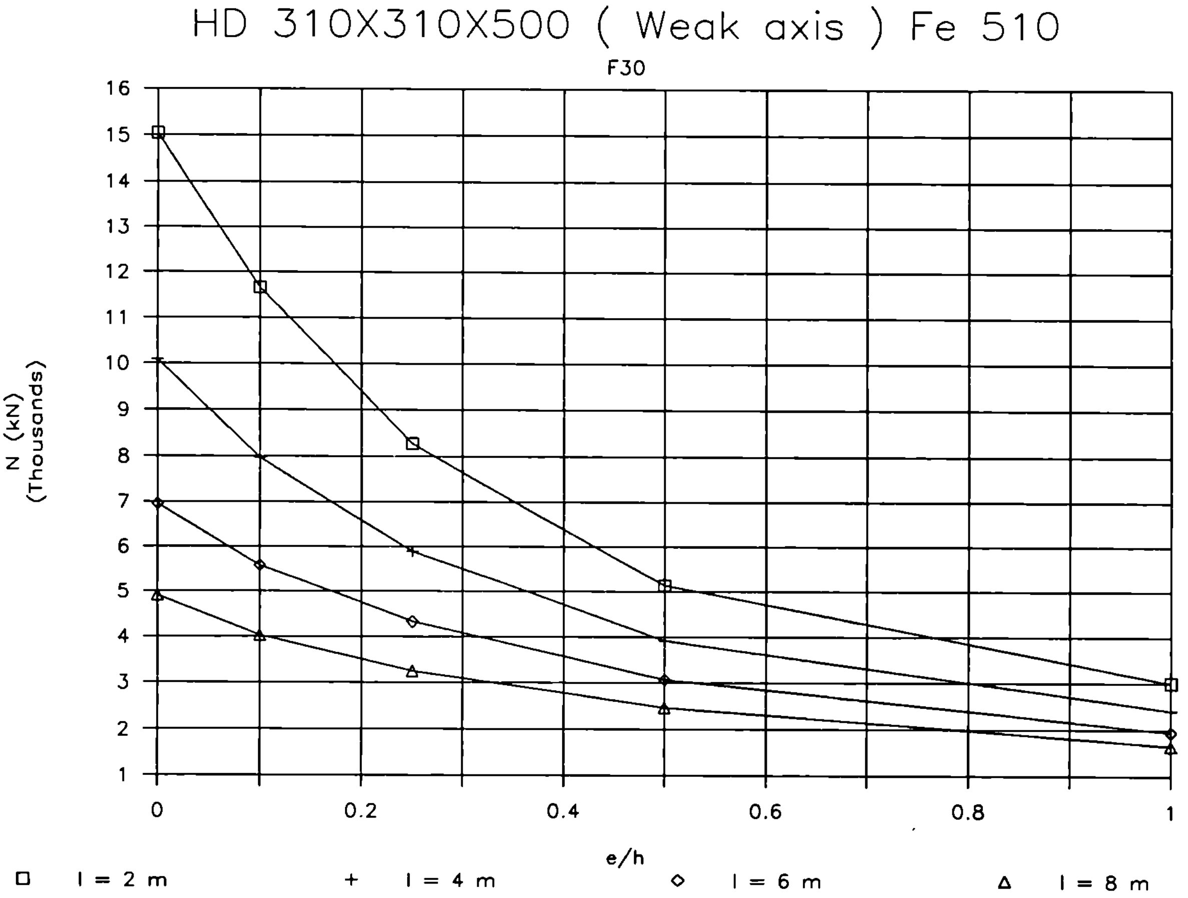
HD 310X310X500 (Weak axis) Fe 510
F30
N (kN)
(Thousands)
e/h
l = 2 m
l = 4 m
l = 6 m
l = 8 m

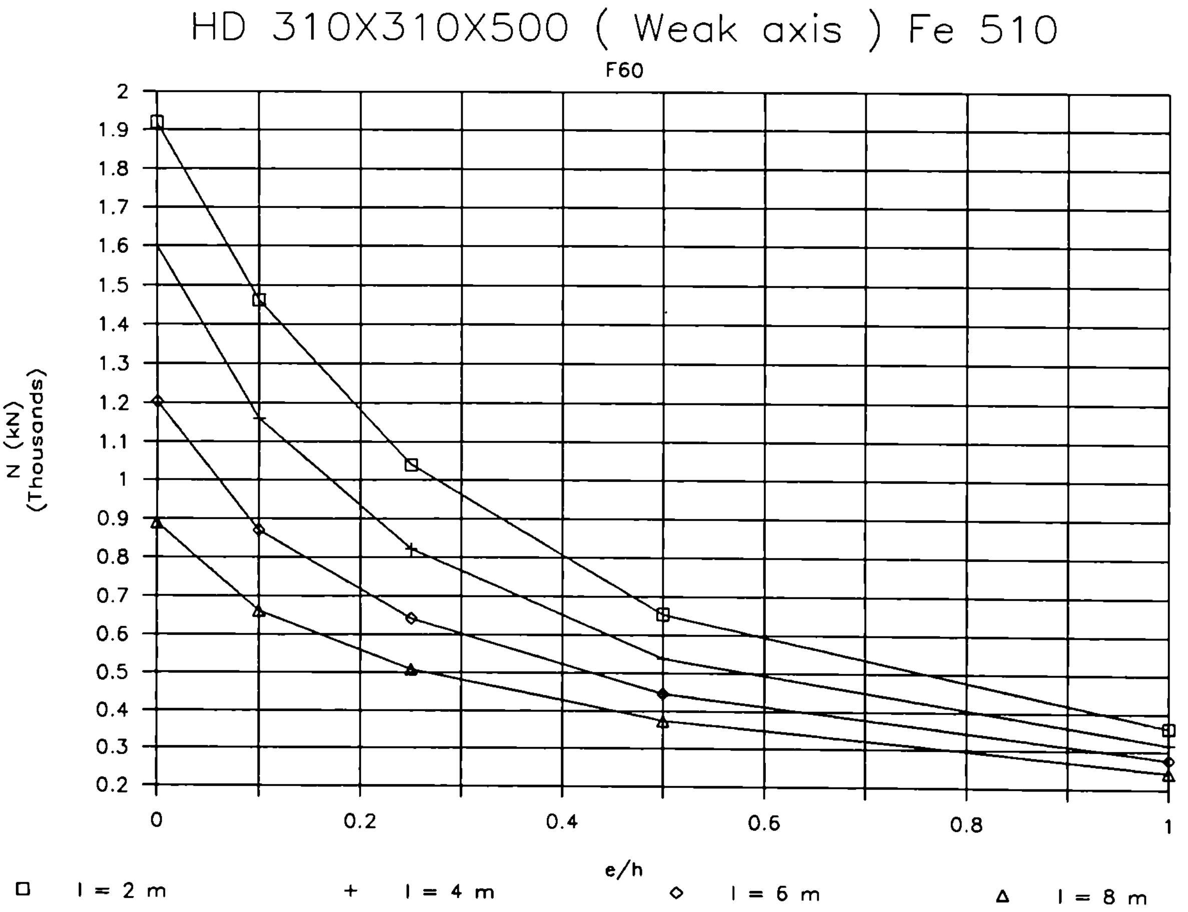
HD 310X310X500 (Weak axis) Fe 510
F60
N (kN)
(Thousands)
e/h
l = 2 m
l = 4 m
l = 6 m
l = 8 m

HD 400X400X314 (Weak axis) Sigma yield = 345 N/mm2 ; U/A = 58 ; t = 40 mm

l (m)	Lambda Bar	e/h	Npl (kN)	F0				F30					F60				
				N(EC3) (kN)	N(EC3)/Npl	N(CEF) (kN)	N(CEF)/Npl	N(F30) (kN)	N/Nc	N/N(F0,EC3)	N/N(F0,CEF)	N/Npl	N(F60) (kN)	N/Nc	N/N(F0,EC3)	N/N(F0,CEF)	N/Npl
2.00	0.2498	0.00	13800	12940	0.94	13099	0.95	4668	1.00	0.36	0.36	0.33	757	1.00	0.06	0.06	0.05
2.00	0.2498	0.10	13800	9940	0.72	10157	0.74	3620	0.78	0.36	0.36	0.26	597	0.79	0.06	0.06	0.04
2.00	0.2498	0.25	13800	6853	0.50	7498	0.54	2551	0.55	0.37	0.34	0.18	431	0.57	0.06	0.06	0.03
2.00	0.2498	0.50	13800	4154	0.30	4796	0.35	1667	0.36	0.40	0.35	0.12	277	0.37	0.07	0.06	0.02
2.00	0.2498	1.00	13800	2183	0.16	2614	0.19	970	0.21	0.44	0.37	0.07	177	0.23	0.08	0.07	0.01
4.00	0.4996	0.00	13800	11786	0.85	11073	0.80	3666	1.00	0.31	0.33	0.26	620	1.00	0.05	0.06	0.04
4.00	0.4996	0.10	13800	8752	0.63	8380	0.61	2715	0.74	0.31	0.32	0.19	470	0.76	0.05	0.06	0.03
4.00	0.4996	0.25	13800	6020	0.44	6124	0.44	2001	0.55	0.33	0.33	0.14	346	0.56	0.06	0.06	0.02
4.00	0.4996	0.50	13800	3757	0.27	4035	0.29	1340	0.37	0.36	0.33	0.09	230	0.37	0.06	0.06	0.01
4.00	0.4996	1.00	13800	2059	0.15	2354	0.17	782	0.21	0.38	0.33	0.05	133	0.21	0.06	0.06	0.00
6.00	0.7494	0.00	13800	10031	0.73	8645	0.63	2661	1.00	0.27	0.31	0.19	478	1.00	0.05	0.06	0.03
6.00	0.7494	0.10	13800	7275	0.53	6444	0.47	2057	0.77	0.28	0.32	0.14	365	0.76	0.05	0.06	0.02
6.00	0.7494	0.25	13800	5084	0.37	4850	0.35	1549	0.58	0.30	0.32	0.11	276	0.58	0.05	0.06	0.02
6.00	0.7494	0.50	13800	3306	0.24	3402	0.25	1111	0.42	0.34	0.33	0.08	193	0.40	0.06	0.06	0.01
6.00	0.7494	1.00	13800	1910	0.14	2097	0.15	685	0.26	0.36	0.33	0.04	118	0.25	0.06	0.06	0.00
8.00	0.9992	0.00	13800	7768	0.56	6616	0.48	2021	1.00	0.26	0.31	0.14	364	1.00	0.05	0.06	0.02
8.00	0.9992	0.10	13800	5777	0.42	4978	0.36	1552	0.77	0.27	0.31	0.11	283	0.78	0.05	0.06	0.02
8.00	0.9992	0.25	13800	4201	0.30	3880	0.28	1239	0.61	0.29	0.32	0.08	221	0.61	0.05	0.06	0.01
8.00	0.9992	0.50	13800	2870	0.21	2835	0.21	919	0.45	0.32	0.32	0.06	162	0.44	0.06	0.06	0.01
8.00	0.9992	1.00	13800	1750	0.13	1845	0.13	603	0.30	0.34	0.33	0.04	105	0.29	0.06	0.06	0.00

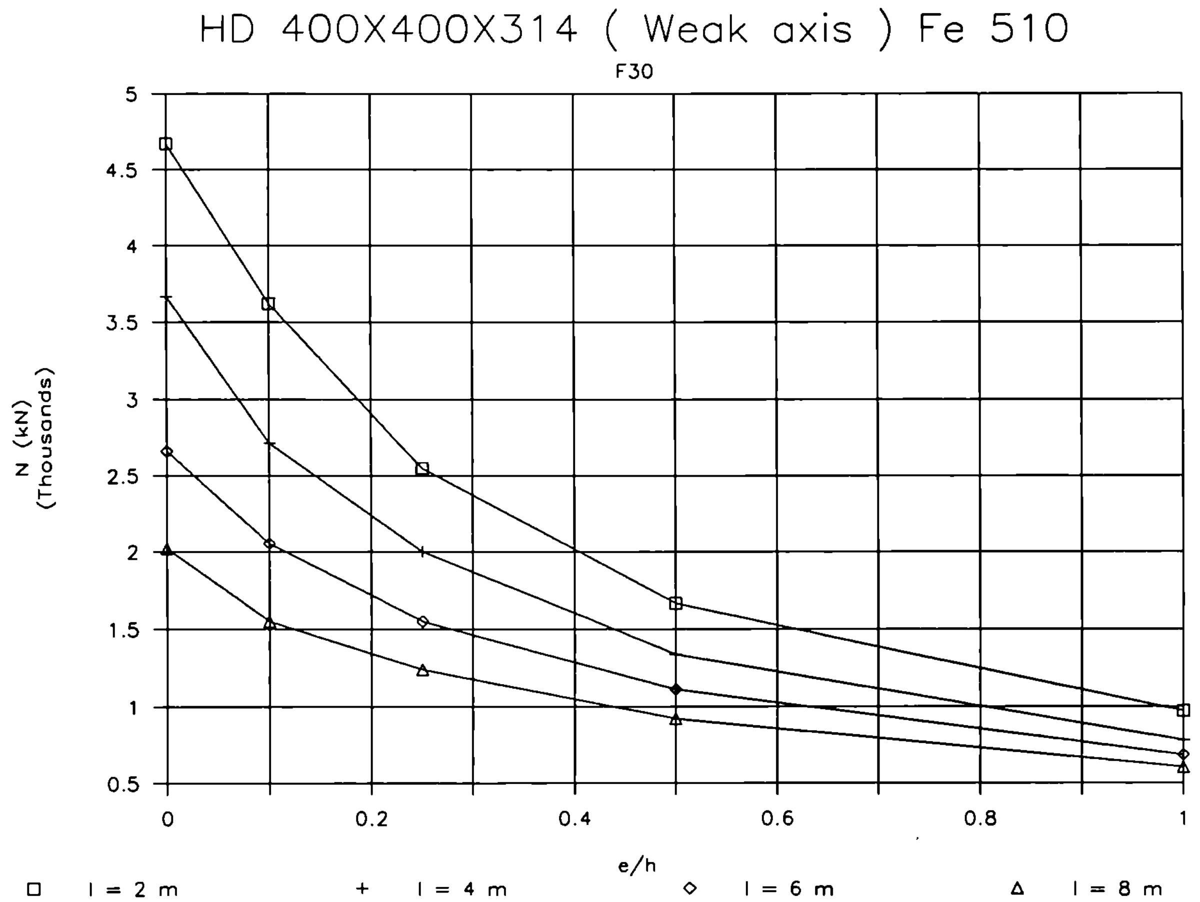
HD 400X400X314 (Weak axis) Fe 510
F30
N (kN)
(Thousands)
5
4.5
4
3.5
3
2.5
2
1.5
1
0.5
0
0.2
0.4
0.6
0.8
1
e/h
□ l = 2 m
+ l = 4 m
◇ l = 6 m
Δ l = 8 m

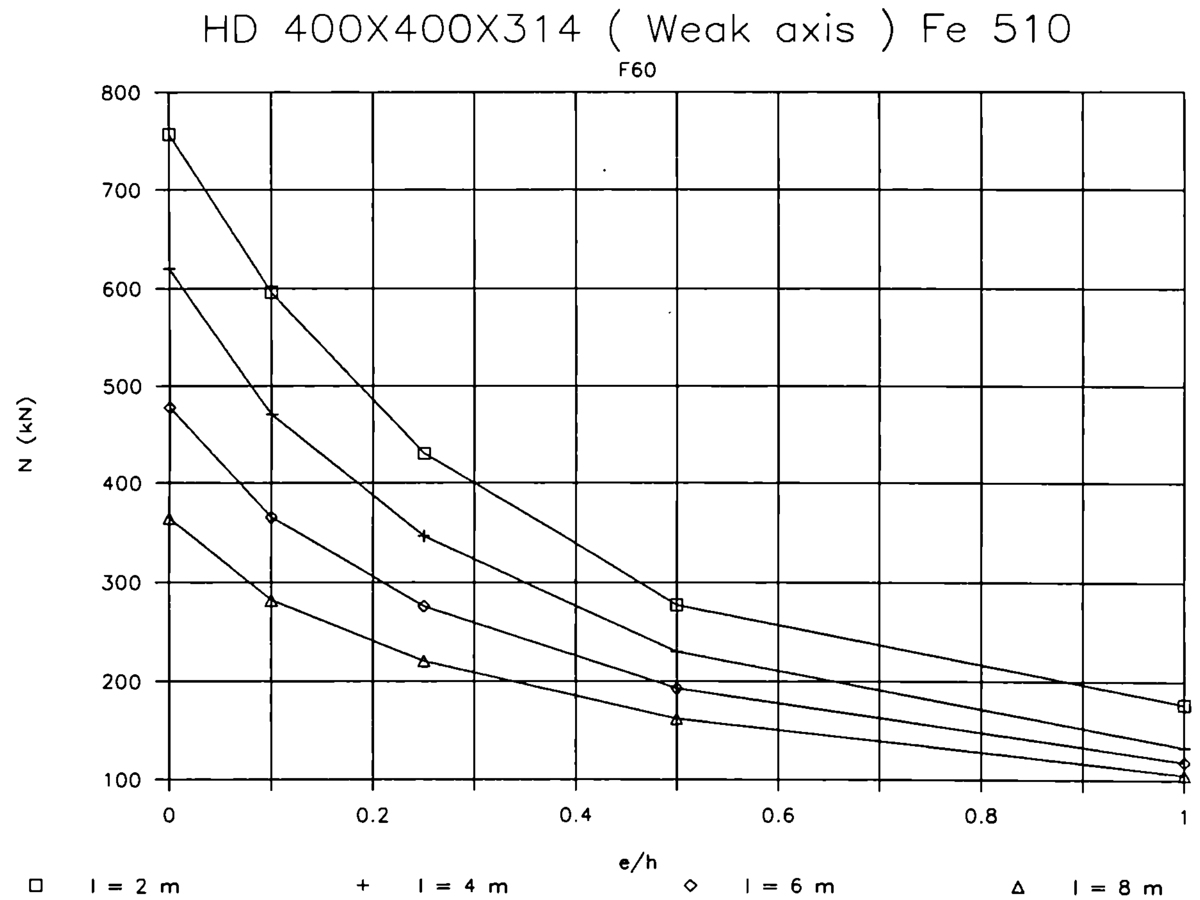
HD 400X400X314 (Weak axis) Fe 510
F60
N (kN)
800
700
600
500
400
300
200
100
0
0.2
0.4
0.6
0.8
1
e/h
□ l = 2 m
+ l = 4 m
◇ l = 6 m
Δ l = 8 m

HD 400X400X678 (Weak axis) Sigma yield = 315 N/mm2 ; U/A = 30 ; t = 82 mm

l (m)	Lambda Bar	e/h	Npl (kN)	F0 N(EC3) (kN)	F0 N(EC3)/Npl	F0 N(CEF) (kN)	F0 N(CEF)/Npl	F30 N(F30) (kN)	F30 N/Nc	F30 N/N(F0,EC3)	F30 N/N(F0,CEF)	F30 N/Npl	F60 N(F60) (kN)	F60 N/Nc	F60 N/N(F0,EC3)	F60 N/N(F0,CEF)	F60 N/Npl
2.00	0.2218	0.00	27216	25611	0.94	26100	0.96	25859	1.00	1.01	0.99	0.95	3302	1.00	0.13	0.13	0.12
2.00	0.2218	0.10	27216	19690	0.72	20543	0.75	20341	0.79	1.03	0.99	0.74	2532	0.77	0.13	0.12	0.09
2.00	0.2218	0.25	27216	13594	0.50	15068	0.55	14511	0.56	1.07	0.96	0.53	1812	0.55	0.13	0.12	0.06
2.00	0.2218	0.50	27216	8250	0.30	9750	0.36	9545	0.37	1.16	0.98	0.35	1129	0.34	0.14	0.12	0.04
2.00	0.2218	1.00	27216	4340	0.16	5352	0.20	5300	0.20	1.22	0.99	0.19	655	0.20	0.15	0.12	0.02
4.00	0.4436	0.00	27216	23622	0.87	22738	0.84	17221	1.00	0.73	0.76	0.63	2778	1.00	0.12	0.12	0.10
4.00	0.4436	0.10	27216	17674	0.65	17357	0.64	13403	0.78	0.76	0.77	0.49	2036	0.73	0.12	0.12	0.07
4.00	0.4436	0.25	27216	12163	0.45	12659	0.47	9700	0.56	0.80	0.77	0.35	1485	0.53	0.12	0.12	0.05
4.00	0.4436	0.50	27216	7570	0.28	8345	0.31	6635	0.39	0.88	0.80	0.24	967	0.35	0.13	0.12	0.03
4.00	0.4436	1.00	27216	4129	0.15	4854	0.18	4238	0.25	1.03	0.87	0.15	555	0.20	0.13	0.11	0.02
6.00	0.6654	0.00	27216	20791	0.76	18544	0.68	11910	1.00	0.57	0.64	0.43	2130	1.00	0.10	0.11	0.07
6.00	0.6654	0.10	27216	15164	0.56	13866	0.51	9494	0.80	0.63	0.68	0.34	1588	0.75	0.10	0.11	0.05
6.00	0.6654	0.25	27216	10560	0.39	10339	0.38	7165	0.60	0.68	0.69	0.26	1184	0.56	0.11	0.11	0.04
6.00	0.6654	0.50	27216	6797	0.25	7163	0.26	4999	0.42	0.74	0.70	0.18	821	0.39	0.12	0.11	0.03
6.00	0.6654	1.00	27216	3876	0.14	4327	0.16	3250	0.27	0.84	0.75	0.11	501	0.24	0.13	0.12	0.01
8.00	0.8872	0.00	27216	17017	0.63	14744	0.54	8682	1.00	0.51	0.59	0.31	1620	1.00	0.10	0.11	0.05
8.00	0.8872	0.10	27216	12498	0.46	11020	0.40	7096	0.82	0.57	0.64	0.26	1227	0.76	0.10	0.11	0.04
8.00	0.8872	0.25	27216	8957	0.33	8439	0.31	5586	0.64	0.62	0.66	0.20	956	0.59	0.11	0.11	0.03
8.00	0.8872	0.50	27216	6016	0.22	6090	0.22	4097	0.47	0.68	0.67	0.15	696	0.43	0.12	0.11	0.02
8.00	0.8872	1.00	27216	3595	0.13	3895	0.14	2667	0.31	0.74	0.68	0.09	446	0.28	0.12	0.11	0.01

HD 400X400X678 (Weak axis) Fe 510

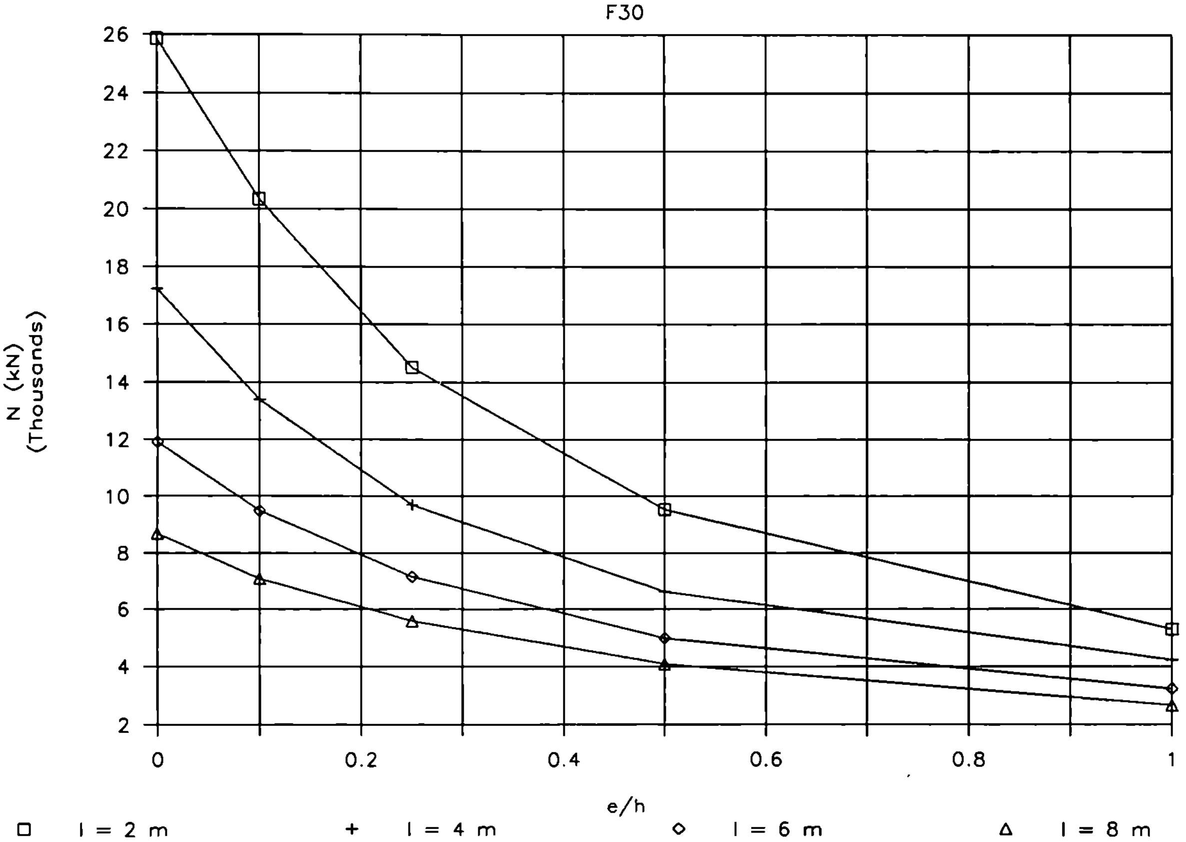

HD 400X400X678 (Weak axis) Fe 510

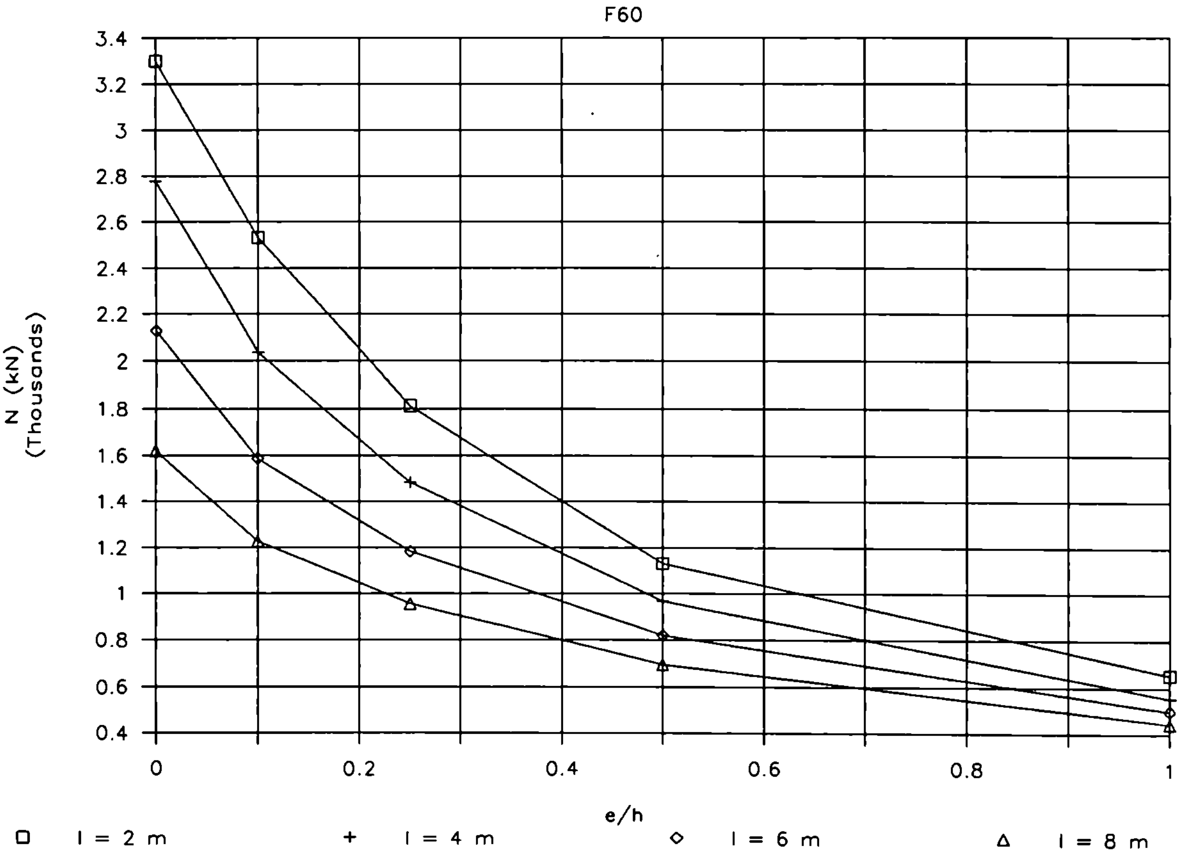

HD 400X400X1086 (Weak axis) Sigma yield = 305 N/mm2 ; U/A = 20 ; t = 125 mm

l (m)	Lambda Bar	e/h	Npl (kN)	F0 N(EC3) (kN)	F0 N(EC3)/Npl	F0 N(CEF) (kN)	F0 N(CEF)/Npl	F30 N(F30) (kN)	F30 N/Nc	F30 N/N(F0,EC3)	F30 N/N(F0,CEF)	F30 N/Npl	F60 N(F60) (kN)	F60 N/Nc	F60 N/N(F0,EC3)	F60 N/N(F0,CEF)	F60 N/Npl
2.00	0.2039	0.00	42273	38937	0.92	40850	0.97	40260	1.00	1.03	0.99	0.95	14400	1.00	0.37	0.35	0.34
2.00	0.2039	0.10	42273	29964	0.71	32524	0.77	32278	0.80	1.08	0.99	0.76	10739	0.75	0.36	0.33	0.25
2.00	0.2039	0.25	42273	20742	0.49	23800	0.56	23615	0.59	1.14	0.99	0.55	7289	0.51	0.35	0.31	0.17
2.00	0.2039	0.50	42273	12690	0.30	15347	0.36	15228	0.38	1.20	0.99	0.36	4649	0.32	0.37	0.30	0.10
2.00	0.2039	1.00	42273	6722	0.16	8468	0.20	8405	0.21	1.25	0.99	0.19	2829	0.20	0.42	0.33	0.06
4.00	0.4078	0.00	42273	35149	0.83	37659	0.89	31957	1.00	0.91	0.85	0.75	10865	1.00	0.31	0.29	0.25
4.00	0.4078	0.10	42273	26543	0.63	28335	0.67	25078	0.78	0.94	0.89	0.59	8079	0.74	0.30	0.29	0.19
4.00	0.4078	0.25	42273	18445	0.44	20576	0.49	18268	0.57	0.99	0.89	0.43	5683	0.52	0.31	0.28	0.13
4.00	0.4078	0.50	42273	11582	0.27	13448	0.32	12611	0.39	1.09	0.94	0.29	3655	0.34	0.32	0.27	0.08
4.00	0.4078	1.00	42273	6377	0.15	7762	0.18	7694	0.24	1.21	0.99	0.18	2075	0.19	0.33	0.27	0.04
6.00	0.6117	0.00	42273	30424	0.72	32400	0.77	22627	1.00	0.74	0.70	0.53	8179	1.00	0.27	0.25	0.19
6.00	0.6117	0.10	42273	22684	0.54	23701	0.56	17950	0.79	0.79	0.76	0.42	6117	0.75	0.27	0.26	0.14
6.00	0.6117	0.25	42273	16013	0.38	17460	0.41	13396	0.59	0.84	0.77	0.31	4506	0.55	0.28	0.26	0.10
6.00	0.6117	0.50	42273	10418	0.25	11744	0.28	9287	0.41	0.89	0.79	0.21	3102	0.38	0.30	0.26	0.07
6.00	0.6117	1.00	42273	5978	0.14	7057	0.17	6263	0.28	1.05	0.89	0.14	1864	0.23	0.31	0.26	0.04
8.00	0.8156	0.00	42273	24988	0.59	26897	0.64	17028	1.00	0.68	0.63	0.40	6115	1.00	0.24	0.23	0.14
8.00	0.8156	0.10	42273	18824	0.45	19319	0.46	13771	0.81	0.73	0.71	0.32	4705	0.77	0.25	0.24	0.11
8.00	0.8156	0.25	42273	13658	0.32	14550	0.34	10687	0.63	0.78	0.73	0.25	3621	0.59	0.27	0.25	0.08
8.00	0.8156	0.50	42273	9260	0.22	10231	0.24	7687	0.45	0.83	0.75	0.18	2609	0.43	0.28	0.26	0.06
8.00	0.8156	1.00	42273	5563	0.13	6400	0.15	4942	0.29	0.89	0.77	0.11	1670	0.27	0.30	0.26	0.03

HD 400X400X1086 (Weak axis) Fe 510

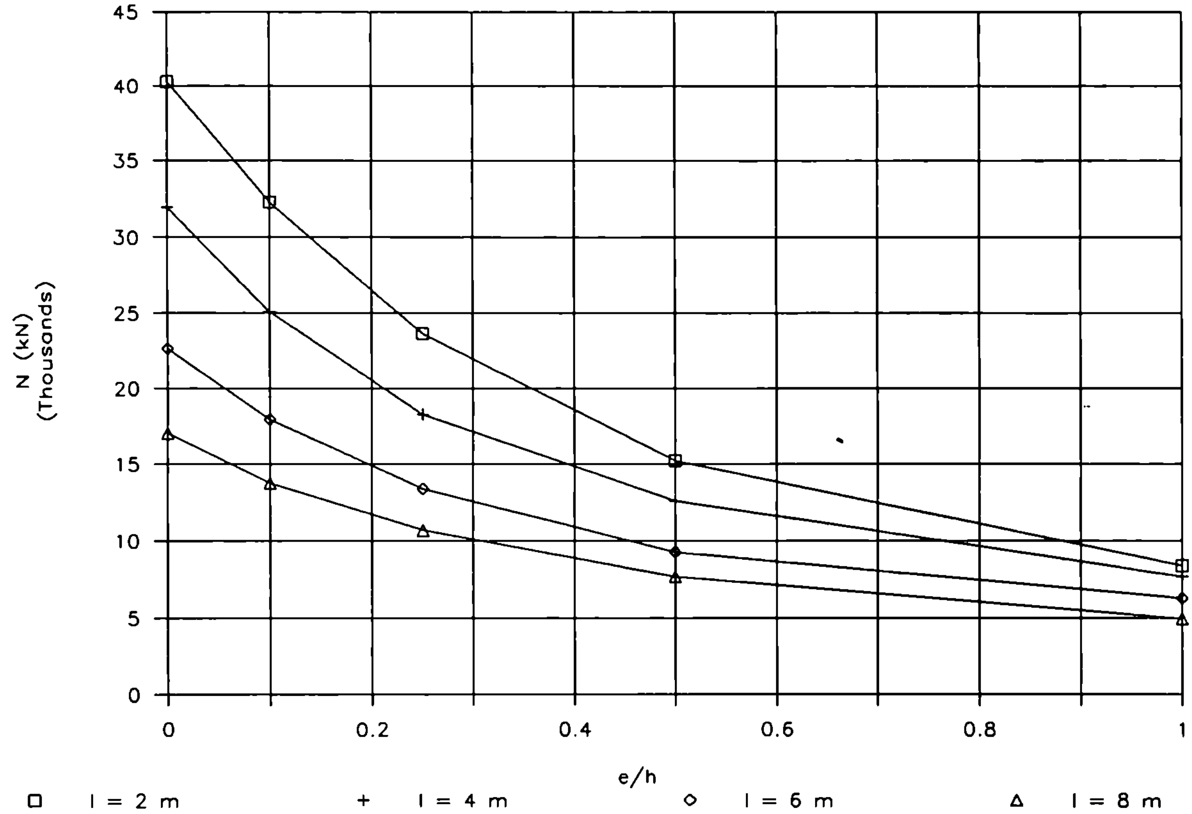

HD 400X400X1086 (Weak axis) Fe 510

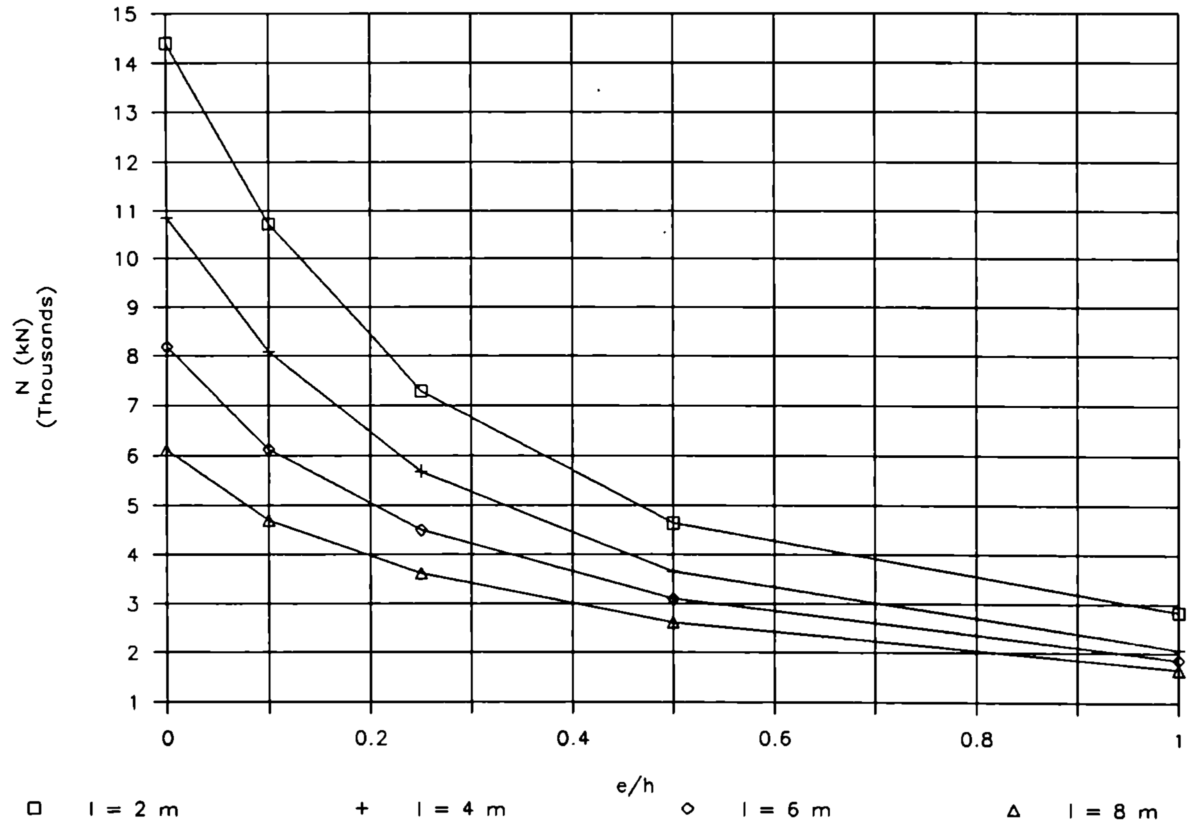

HE 550 M (Weak axis) Sigma yield = 450 N/mm2 ; U/A = 64 ; t = 40 mm

l (m)	Lambda Bar	e/h	Npl (kN)	F0				F30					F60				
				N(EC3) (kN)	N(EC3)/Npl	N(CEF) (kN)	N(CEF)/Npl	N(F30) (kN)	N/Nc	N/N(F0,EC3)	N/N(F0,CEF)	N/Npl	N(F60) (kN)	N/Nc	N/N(F0,EC3)	N/N(F0,CEF)	N/Npl
2.00	0.4008	0.00	15930	14473	0.91	14261	0.90	3927	1.00	0.27	0.28	0.24	757	1.00	0.05	0.05	0.04
2.00	0.4008	0.10	15930	10675	0.67	10751	0.67	2970	0.76	0.28	0.28	0.18	578	0.76	0.05	0.05	0.03
2.00	0.4008	0.25	15930	6965	0.44	7496	0.47	2186	0.56	0.31	0.29	0.13	411	0.54	0.06	0.05	0.02
2.00	0.4008	0.50	15930	3977	0.25	4572	0.29	1371	0.35	0.34	0.30	0.08	254	0.34	0.06	0.06	0.01
2.00	0.4008	1.00	15930	2099	0.13	2510	0.16	773	0.20	0.37	0.31	0.04	139	0.18	0.07	0.06	0.00
4.00	0.8016	0.00	15930	11533	0.72	10392	0.65	2862	1.00	0.25	0.28	0.17	565	1.00	0.05	0.05	0.03
4.00	0.8016	0.10	15930	7996	0.50	7377	0.46	2091	0.73	0.26	0.28	0.13	416	0.74	0.05	0.06	0.02
4.00	0.8016	0.25	15930	5314	0.33	5280	0.33	1568	0.55	0.30	0.30	0.09	300	0.53	0.06	0.06	0.01
4.00	0.8016	0.50	15930	3312	0.21	3534	0.22	1076	0.38	0.32	0.30	0.06	200	0.35	0.06	0.06	0.01
4.00	0.8016	1.00	15930	1895	0.12	2133	0.13	649	0.23	0.34	0.30	0.04	118	0.21	0.06	0.06	0.00
6.00	1.2024	0.00	15930	7259	0.46	6816	0.43	1923	1.00	0.26	0.28	0.12	385	1.00	0.05	0.06	0.02
6.00	1.2024	0.10	15930	5379	0.34	4915	0.31	1460	0.76	0.27	0.30	0.09	285	0.74	0.05	0.06	0.01
6.00	1.2024	0.25	15930	3886	0.24	3786	0.24	1135	0.59	0.29	0.30	0.07	219	0.57	0.06	0.06	0.01
6.00	1.2024	0.50	15930	2680	0.17	2743	0.17	835	0.43	0.31	0.30	0.05	156	0.41	0.06	0.06	0.00
6.00	1.2024	1.00	15930	1665	0.10	1781	0.11	542	0.28	0.33	0.30	0.03	101	0.26	0.06	0.06	0.00
8.00	1.6032	0.00	15930	4520	0.28	4499	0.28	1303	1.00	0.29	0.29	0.08	260	1.00	0.06	0.06	0.01
8.00	1.6032	0.10	15930	3667	0.23	3470	0.22	1031	0.79	0.28	0.30	0.06	202	0.78	0.06	0.06	0.01
8.00	1.6032	0.25	15930	2888	0.18	2776	0.17	845	0.65	0.29	0.30	0.05	163	0.63	0.06	0.06	0.01
8.00	1.6032	0.50	15930	2152	0.14	2152	0.14	655	0.50	0.30	0.30	0.04	124	0.48	0.06	0.06	0.00
8.00	1.6032	1.00	15930	1439	0.09	1506	0.09	451	0.35	0.31	0.30	0.02	85	0.33	0.06	0.06	0.00

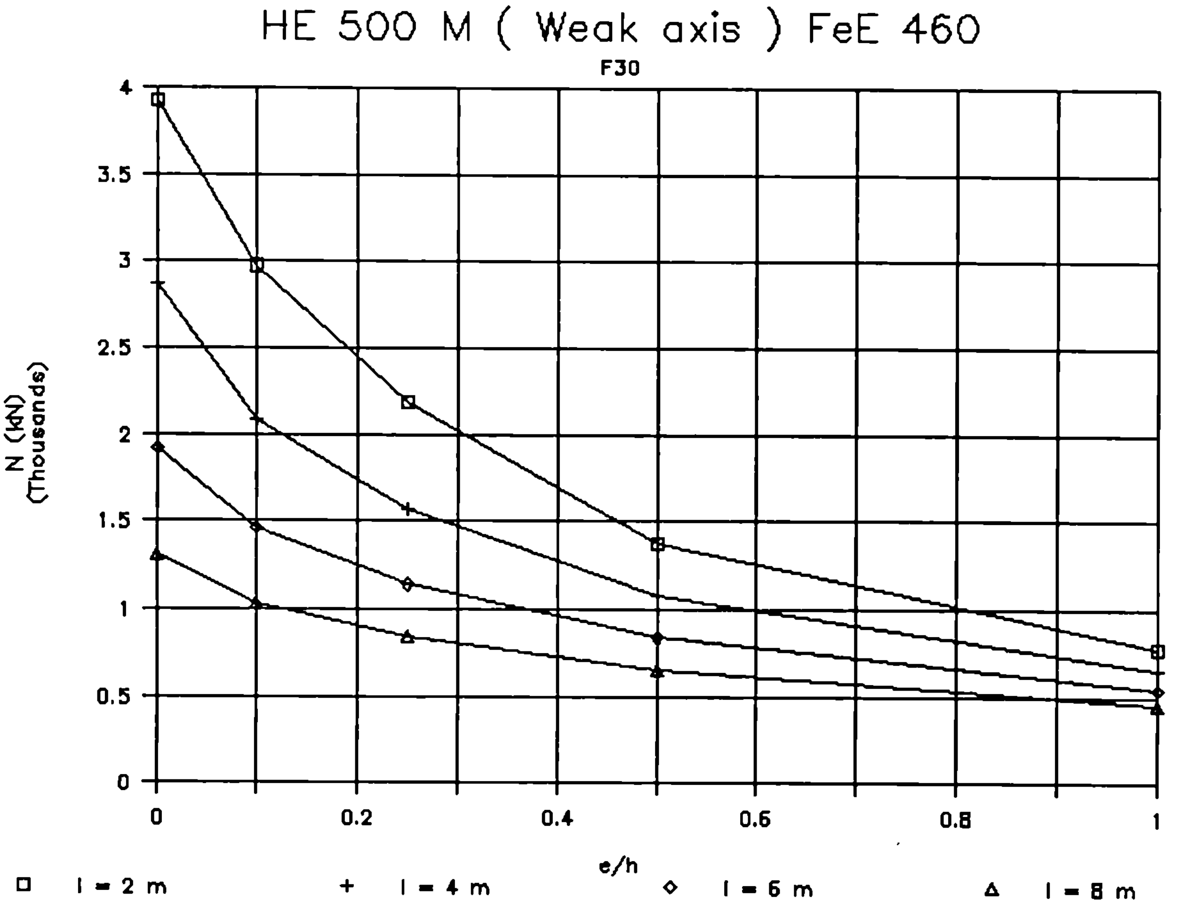
HE 500 M (Weak axis) FeE 460
F30
N (kN)
(Thousands)
e/h
□ l = 2 m
+ l = 4 m
◇ l = 6 m
△ l = 8 m

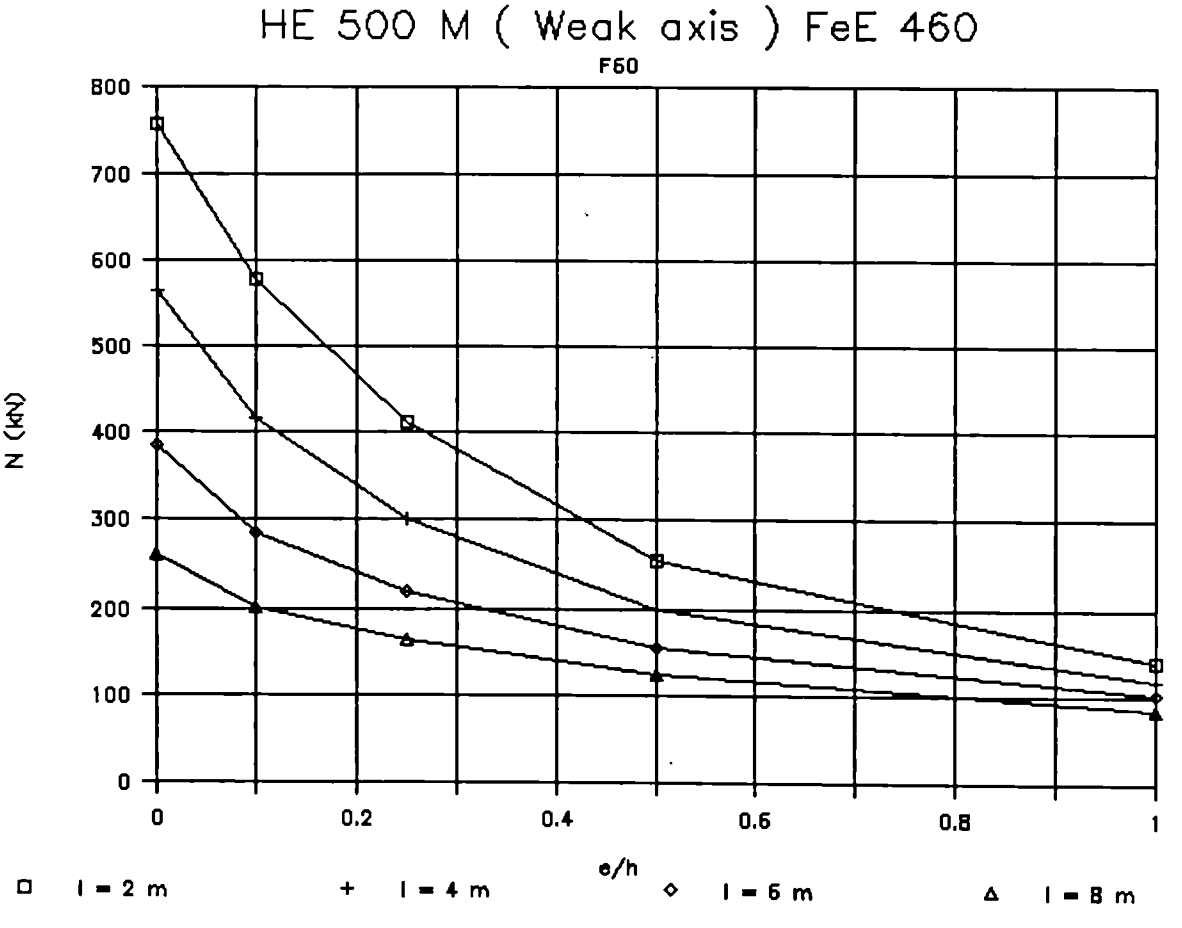
HE 500 M (Weak axis) FeE 460
F60
N (kN)
e/h
□ l = 2 m
+ l = 4 m
◇ l = 6 m
△ l = 8 m

HD 400X400X314 (Weak axis) Sigma yield = 450 N/mm2 ; U/A = 58 ; t = 40 mm

l (m)	Lambda Bar	e/h	Npl (kN)	F0				F30					F60				
				N(EC3) (kN)	N(EC3)/Npl	N(CEF) (kN)	N(CEF)/Npl	N(F30) (kN)	N/Nc	N/N(F0,EC3)	N/N(F0,CEF)	N/Npl	N(F60) (kN)	N/Nc	N/N(F0,EC3)	N/N(F0,CEF)	N/Npl
2.00	0.2853	0.00	18000	16853	0.94	16929	0.94	5759	1.00	0.34	0.34	0.31	951	1.00	0.06	0.06	0.05
2.00	0.2853	0.10	18000	12890	0.72	12929	0.72	4503	0.78	0.35	0.35	0.25	750	0.79	0.06	0.06	0.04
2.00	0.2853	0.25	18000	8864	0.49	9593	0.53	3264	0.57	0.37	0.34	0.18	546	0.57	0.06	0.06	0.03
2.00	0.2853	0.50	18000	5377	0.30	6136	0.34	2088	0.36	0.39	0.34	0.11	350	0.37	0.07	0.06	0.01
2.00	0.2853	1.00	18000	2838	0.16	3386	0.19	1177	0.20	0.41	0.35	0.06	207	0.22	0.07	0.06	0.01
4.00	0.5706	0.00	18000	15166	0.84	13680	0.76	4440	1.00	0.29	0.32	0.24	762	1.00	0.05	0.06	0.04
4.00	0.5706	0.10	18000	11111	0.62	10299	0.57	3337	0.75	0.30	0.32	0.18	578	0.76	0.05	0.06	0.03
4.00	0.5706	0.25	18000	7620	0.42	7526	0.42	2459	0.55	0.32	0.33	0.13	428	0.56	0.06	0.06	0.02
4.00	0.5706	0.50	18000	4783	0.27	5059	0.28	1653	0.37	0.35	0.33	0.09	286	0.38	0.06	0.06	0.01
4.00	0.5706	1.00	18000	2652	0.15	2980	0.17	973	0.22	0.37	0.33	0.05	168	0.22	0.06	0.06	0.00
6.00	0.8559	0.00	18000	12318	0.68	10310	0.57	3139	1.00	0.25	0.30	0.17	566	1.00	0.05	0.05	0.03
6.00	0.8559	0.10	18000	8868	0.49	7571	0.42	2417	0.77	0.27	0.32	0.13	430	0.76	0.05	0.06	0.02
6.00	0.8559	0.25	18000	6249	0.35	5814	0.32	1856	0.59	0.30	0.32	0.10	330	0.58	0.05	0.06	0.01
6.00	0.8559	0.50	18000	4129	0.23	4130	0.23	1349	0.43	0.33	0.33	0.07	235	0.42	0.06	0.06	0.01
6.00	0.8559	1.00	18000	2425	0.13	2602	0.14	850	0.27	0.35	0.33	0.04	147	0.26	0.06	0.06	0.00
8.00	1.1412	0.00	18000	8915	0.50	7655	0.43	2274	1.00	0.26	0.30	0.12	419	1.00	0.05	0.05	0.02
8.00	1.1412	0.10	18000	6745	0.37	5718	0.32	1783	0.78	0.26	0.31	0.09	325	0.78	0.05	0.06	0.01
8.00	1.1412	0.25	18000	5002	0.28	4516	0.25	1442	0.63	0.29	0.32	0.08	258	0.62	0.05	0.06	0.01
8.00	1.1412	0.50	18000	3498	0.19	3381	0.19	1079	0.47	0.31	0.32	0.05	193	0.46	0.06	0.06	0.01
8.00	1.1412	1.00	18000	2185	0.12	2257	0.13	737	0.32	0.34	0.33	0.04	129	0.31	0.06	0.06	0.00

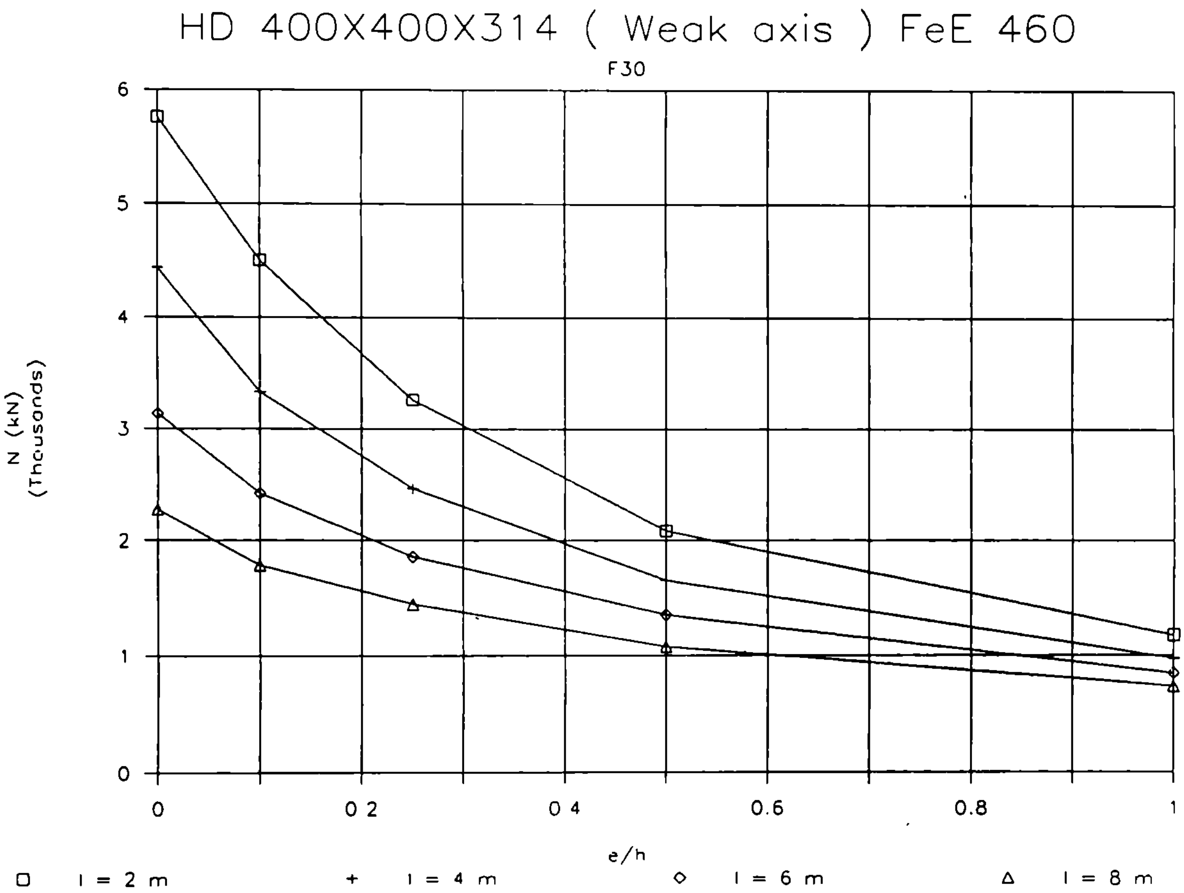
HD 400X400X314 (Weak axis) FeE 460
F30
N (kN)
(Thousands)
e/h
□ l = 2 m
+ l = 4 m
◇ l = 6 m
△ l = 8 m

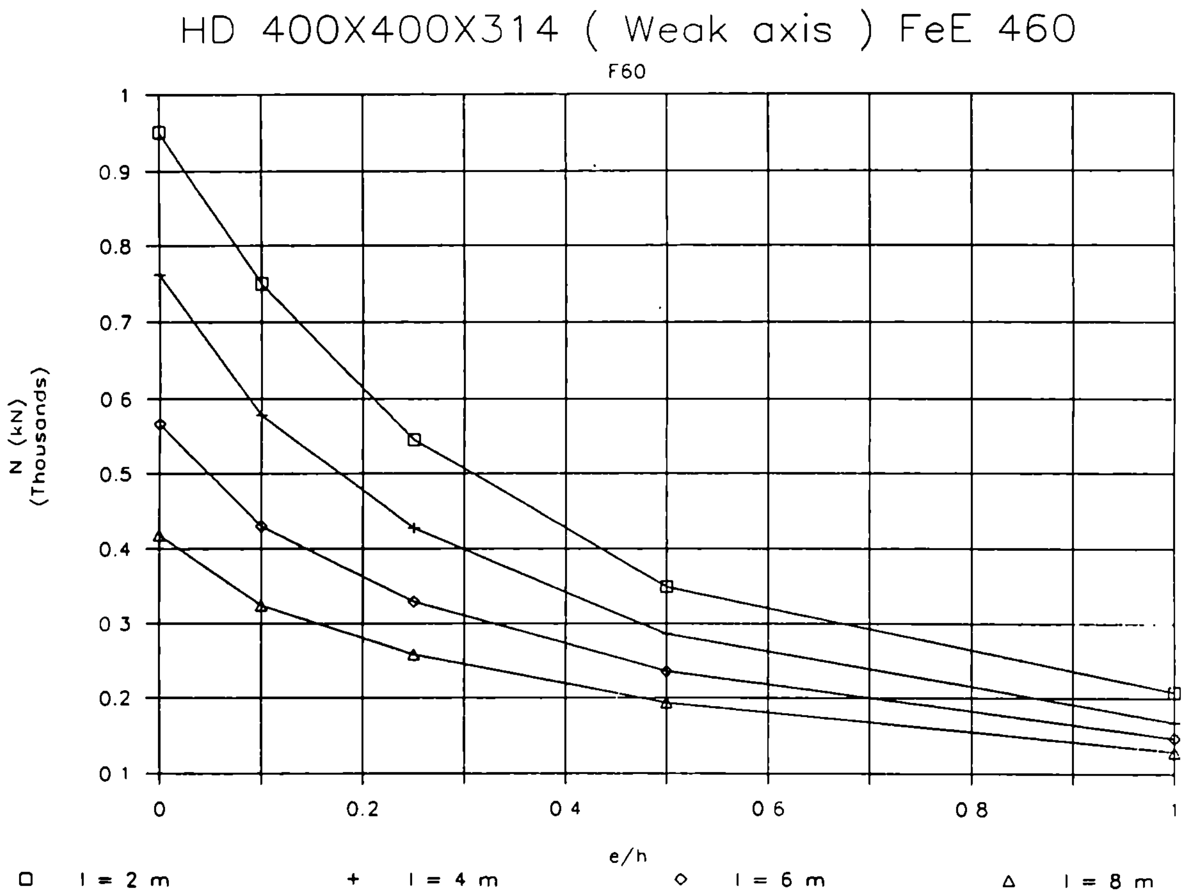
HD 400X400X314 (Weak axis) FeE 460
F60
N (kN)
(Thousands)
e/h
□ l = 2 m
+ l = 4 m
◇ l = 6 m
△ l = 8 m

PART III

TESTS

CONTENTS OF PART III: TESTS

	Pages
Appendix A: Transient state beam tests	**A1 to A60**
Appendix B: Six full scale steel column fire tests	
Test 1: HD 210x210x198	1.1 to 1.15
Test 2: HD 310x310x500	2.1 to 2.15
Test 3: HD 310x310x500	3.1 to 3.15
Test 4: HD 400x400x1086	4.1 to 4.15
Test 5: W 360x410x314	5.1 to 5.14
Test 6: W 360x410x314	6.1 to 6.14

PART III

APPENDIX A

Transient state beam tests

KRUPP TESTS 1988 FOR ARBED

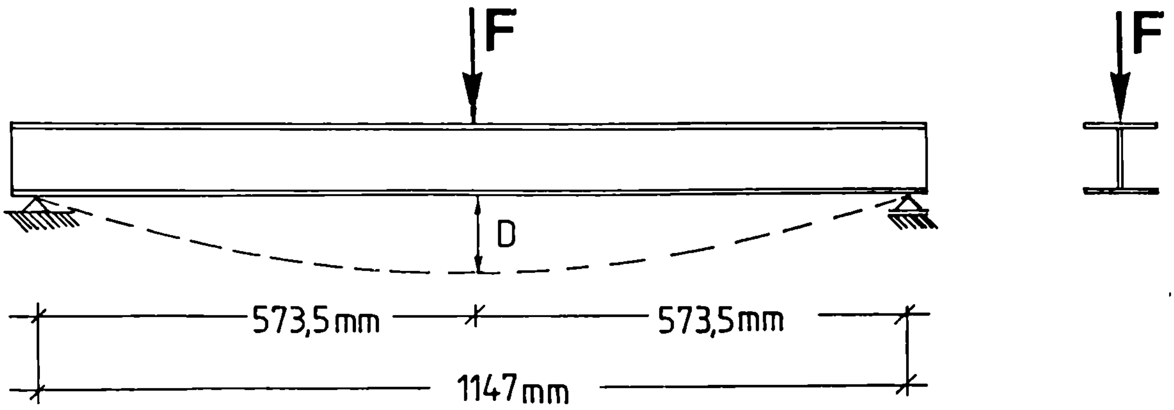

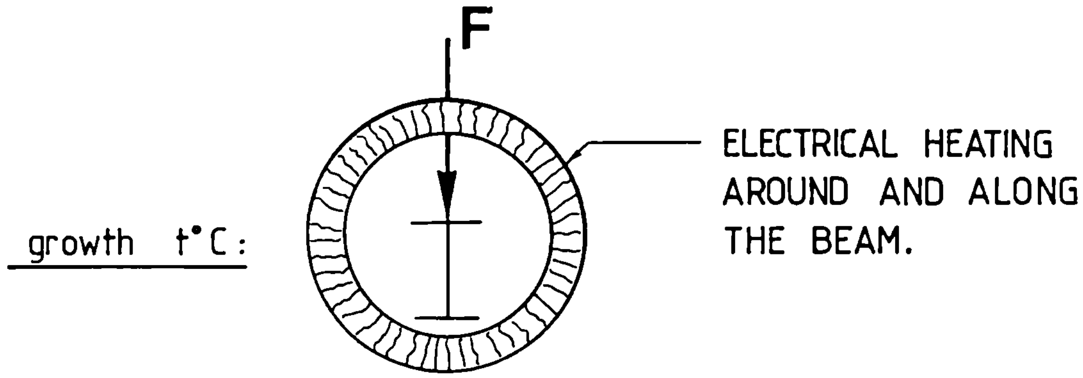

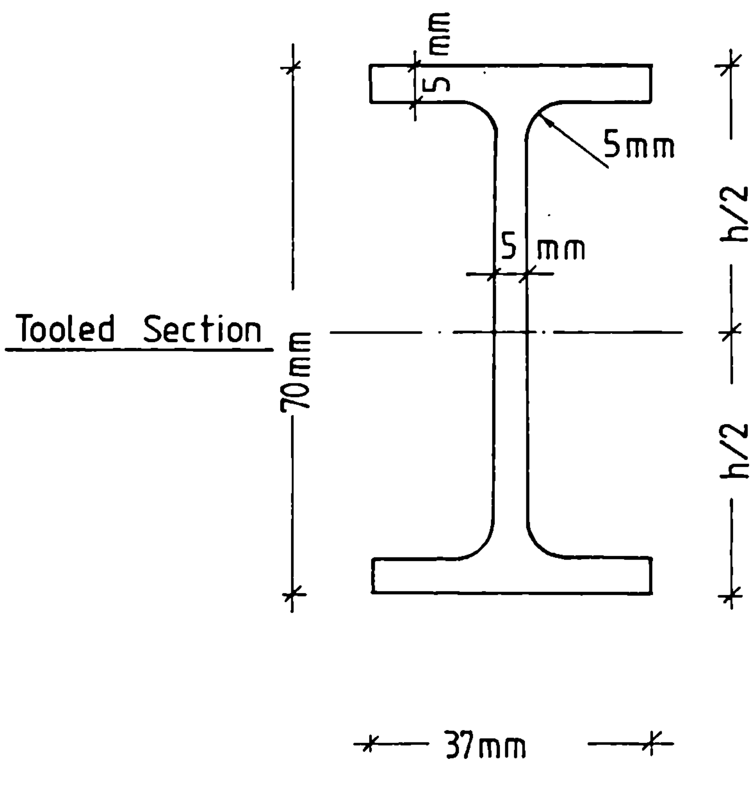

TOOLING OF I-BEAMS 70x40x5x5

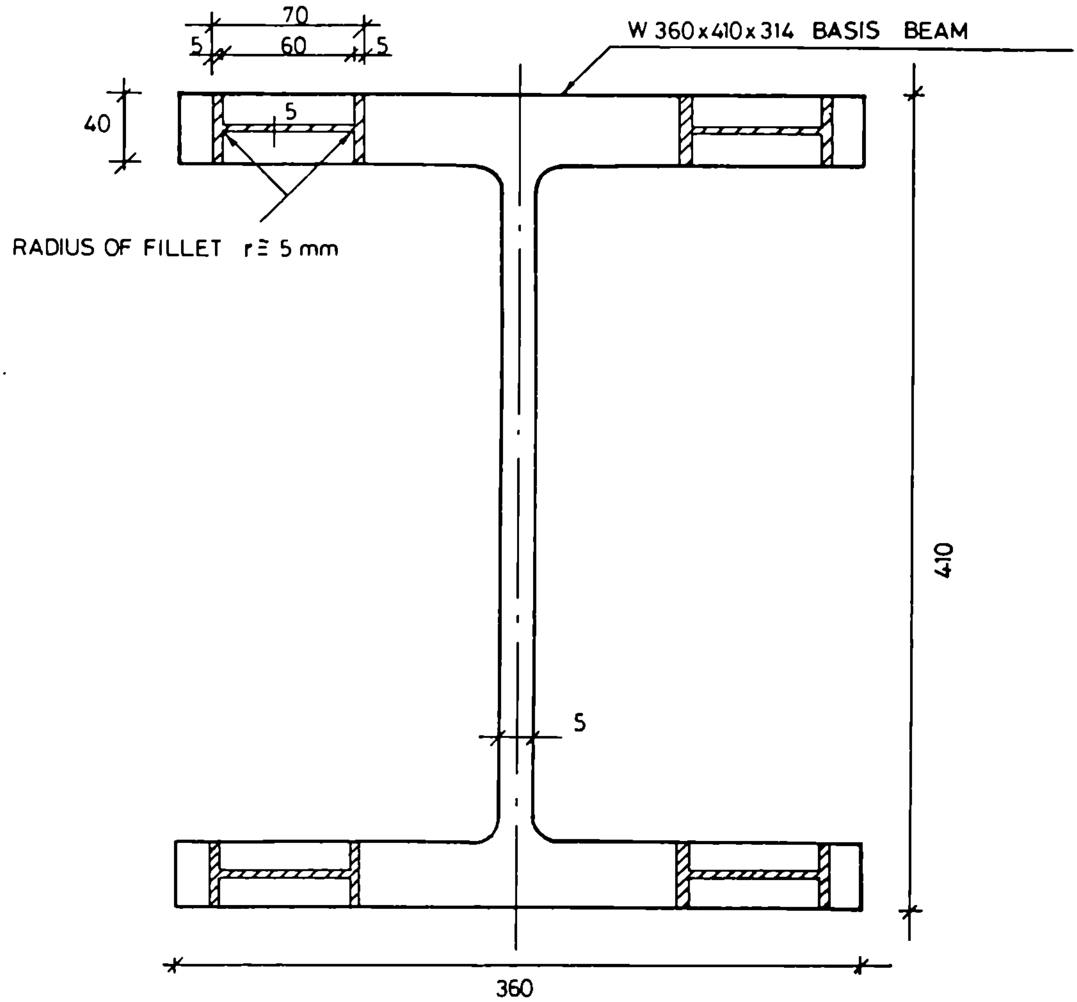

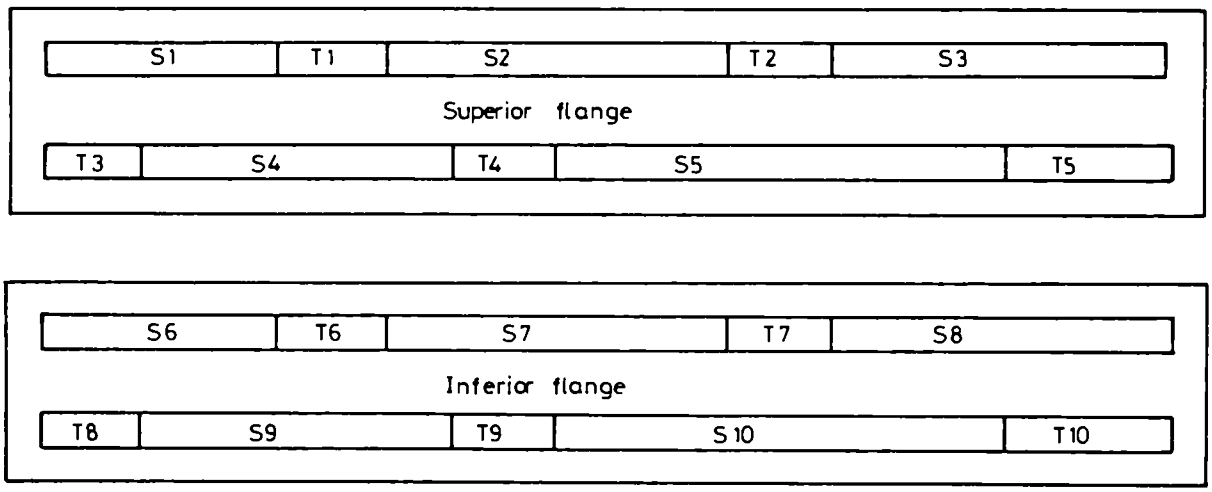

Positions of test pieces

S= beams for transient state bending tests
T= bars for tensile tests

ARBED BEAM TEST

Position of Thermoelements : Specimen S1 - S10

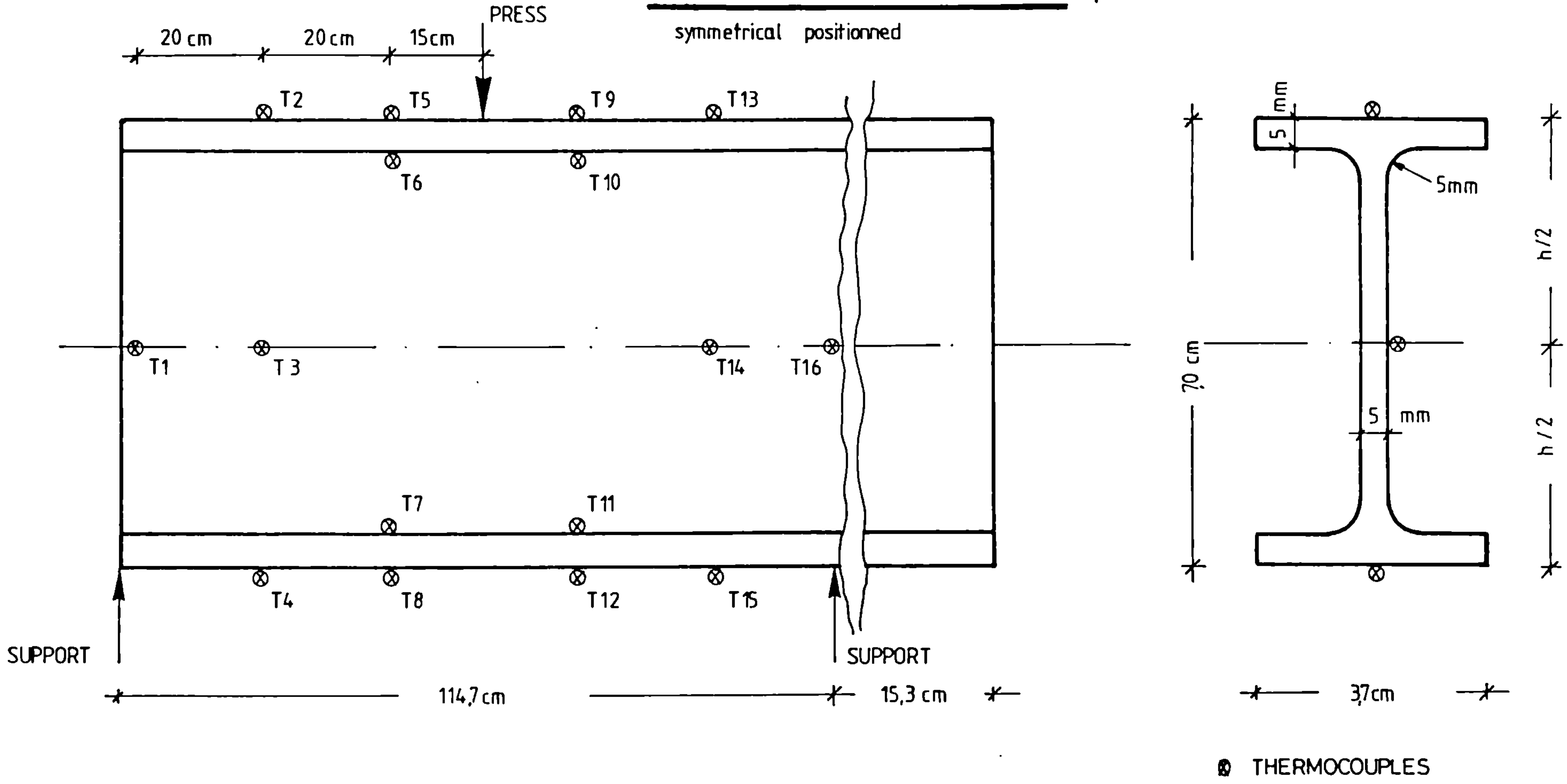

ARBED-TEST BEAM

BEAM S6

DATE: 10-3-1988

EXTREMA VALUES OF THE PROFILE TEMPERATURES CAPTED WITH THERMOCOUPLES

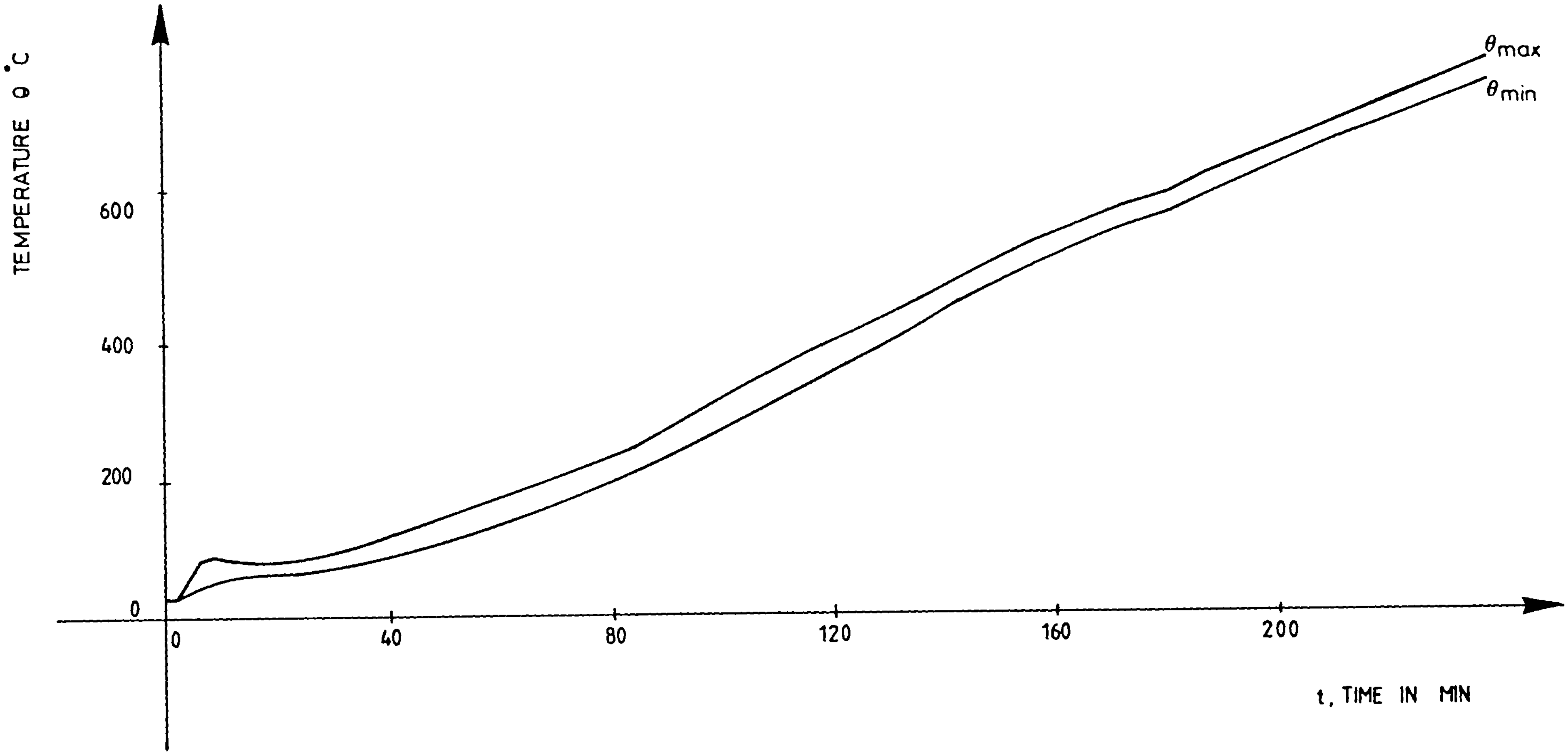

MEASURED VERTICAL DISPLACEMENTS (MM) AT THE MIDDLE OF THE BEAM
IN FUNCTION OF THE TEMPERATURE (C)

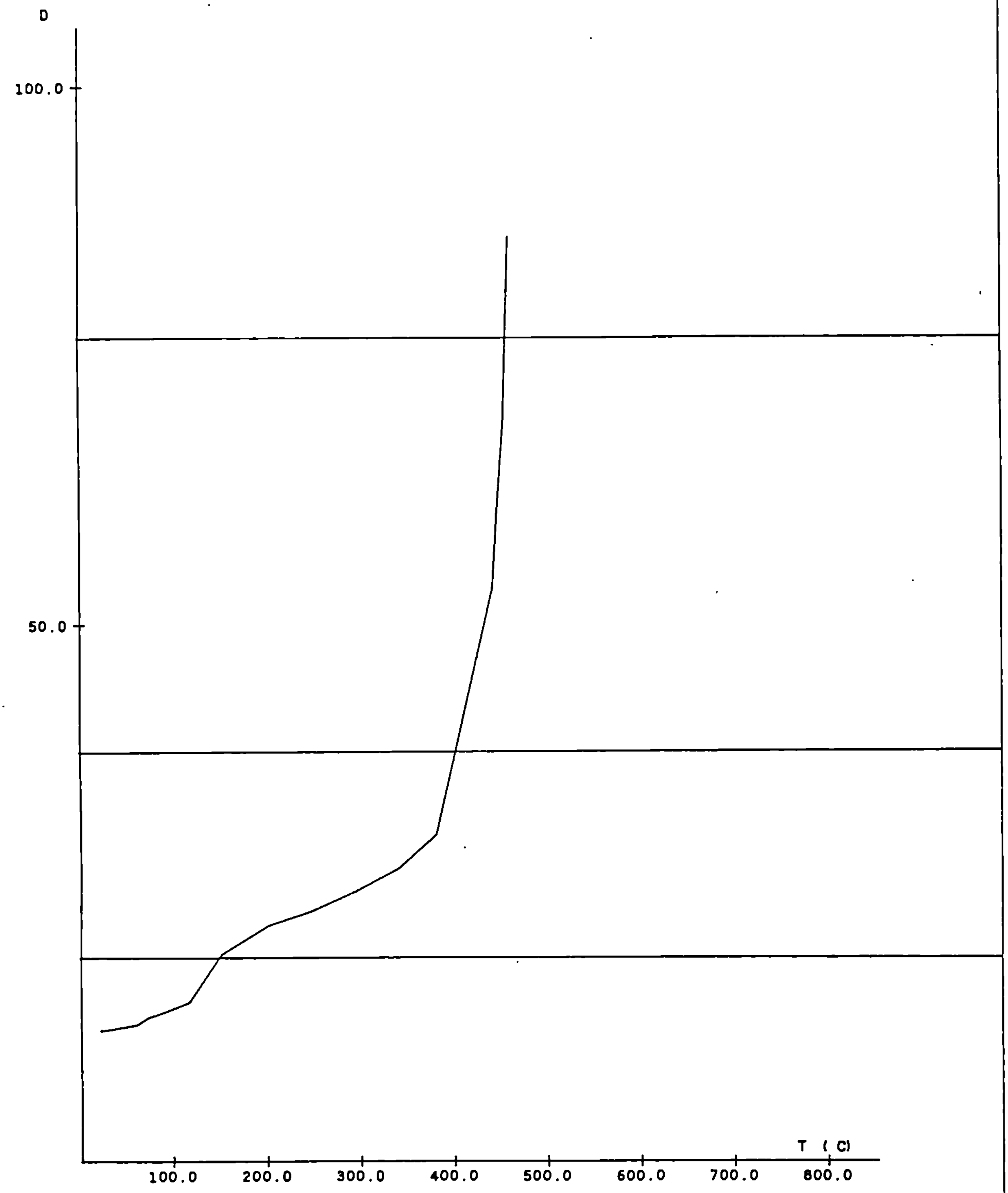

ARBED-RECHERCHES / RPS DEPARTMENT	CEFICOSS Analysis / CEF7DP1	
PROJECT TITLE TEST NR. S 1 -STE 460 $F/F_{p\,COLD} = 1.0$	PROJECT NUMBER REFAO III	
	ESCH/ALZETTE : 16-AUG-1988	SHEET :

MEASURED VERTICAL DISPLACEMENTS (MM) AT THE MIDDLE OF THE BEAM
IN FUNCTION OF THE TEMPERATURE (C)

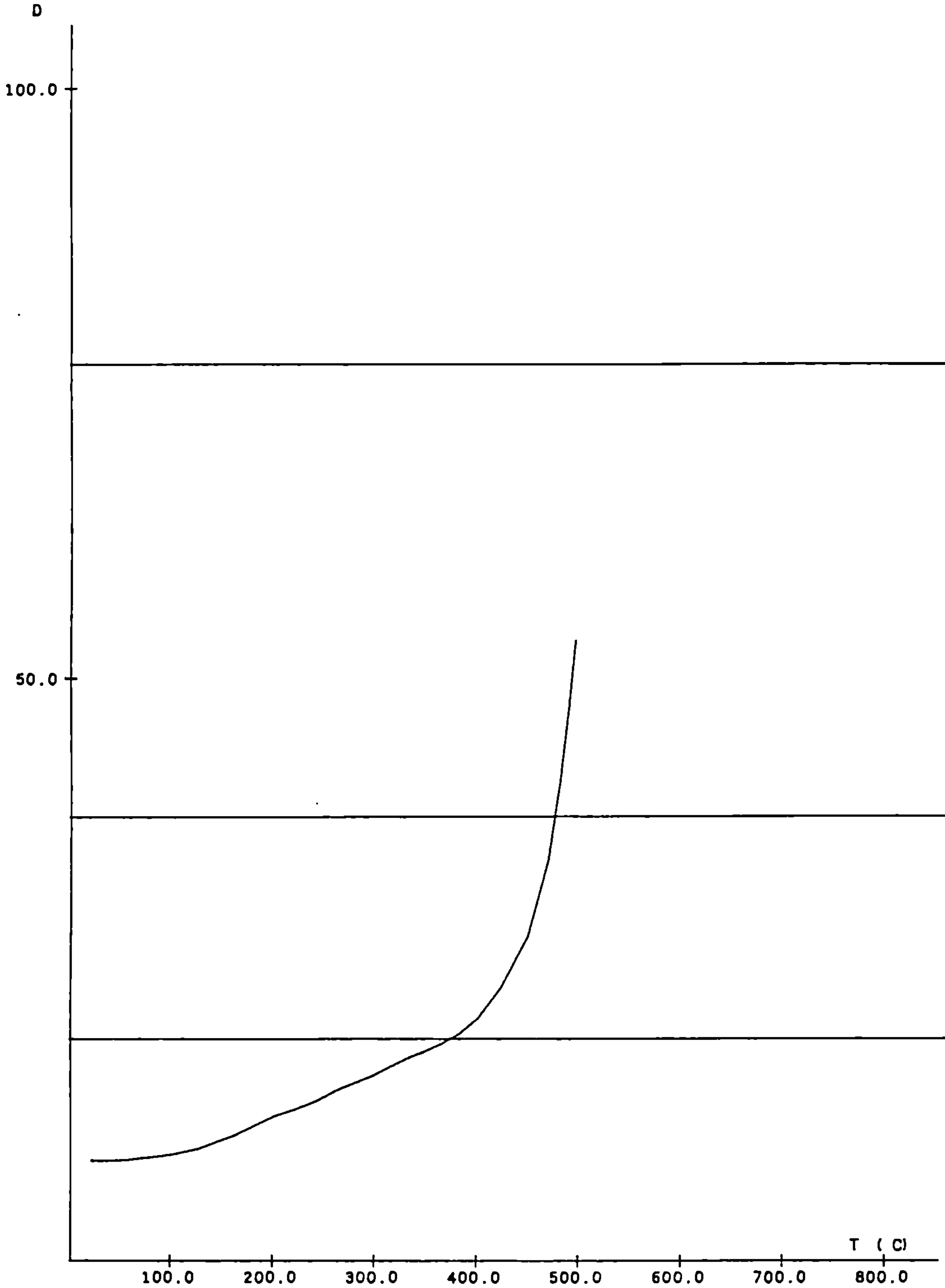

ARBED-RECHERCHES / RPS DEPARTMENT	CEFICOSS Analysis / CEF7DP1
PROJECT TITLE TEST NR. S 3 -STE 460 $F/F_{PCOLD}=0.85$	PROJECT NUMBER REFAO III ESCH/ALZETTE : 16-AUG-1988 SHEET :

MEASURED VERTICAL DISPLACEMENTS (MM) AT THE MIDDLE OF THE BEAM
IN FUNCTION OF THE TEMPERATURE (C)

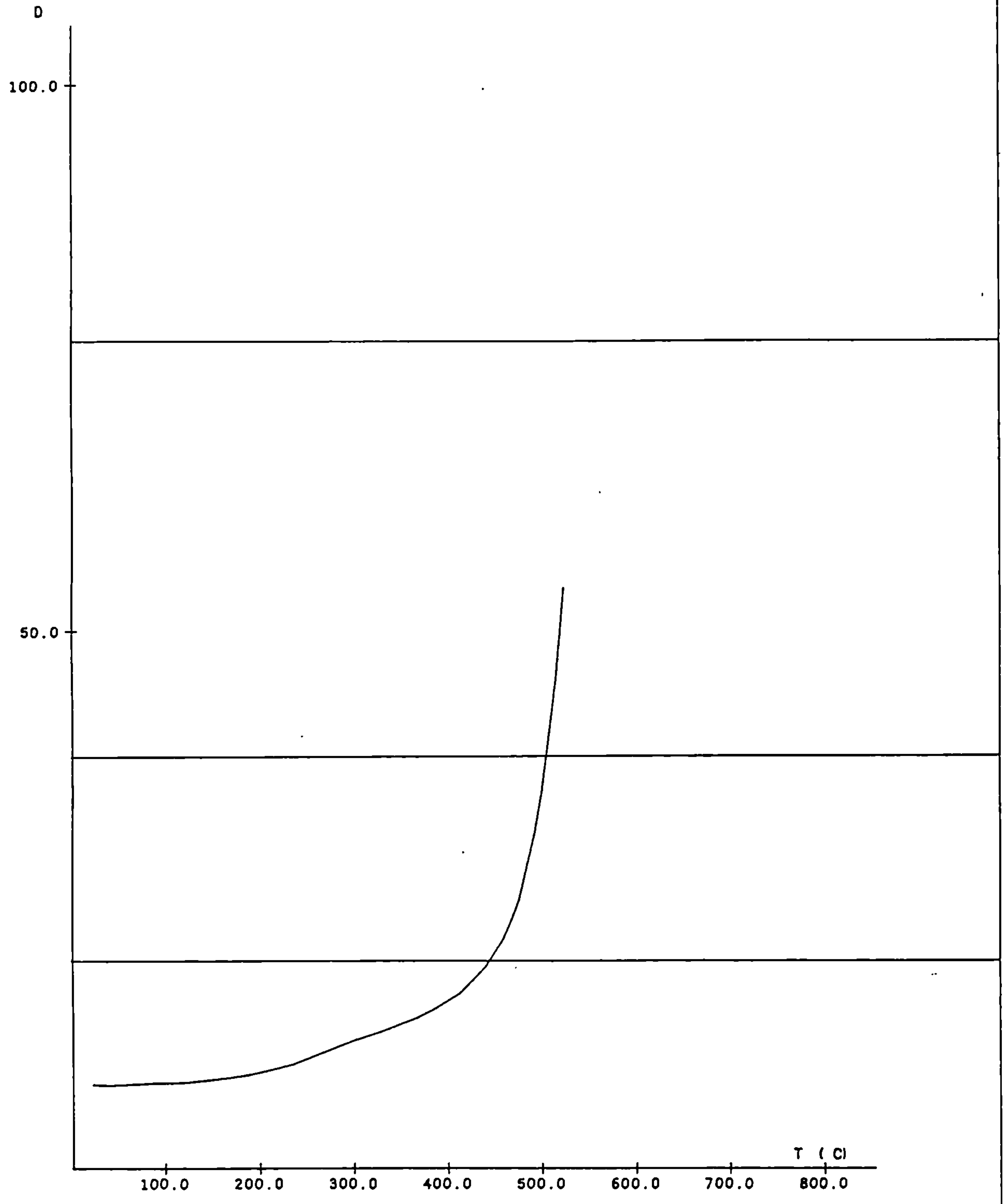

ARBED-RECHERCHES / RPS DEPARTMENT	CEFICOSS Analysis / CEF7DP1
PROJECT TITLE TEST NR. S 2 -STE 460 F/F_{PCOLD} =0.75	PROJECT NUMBER REFAO III ESCH/ALZETTE : 16-AUG-1988 SHEET :

MEASURED VERTICAL DISPLACEMENTS (MM) AT THE MIDDLE OF THE BEAM
IN FUNCTION OF THE TEMPERATURE (C)

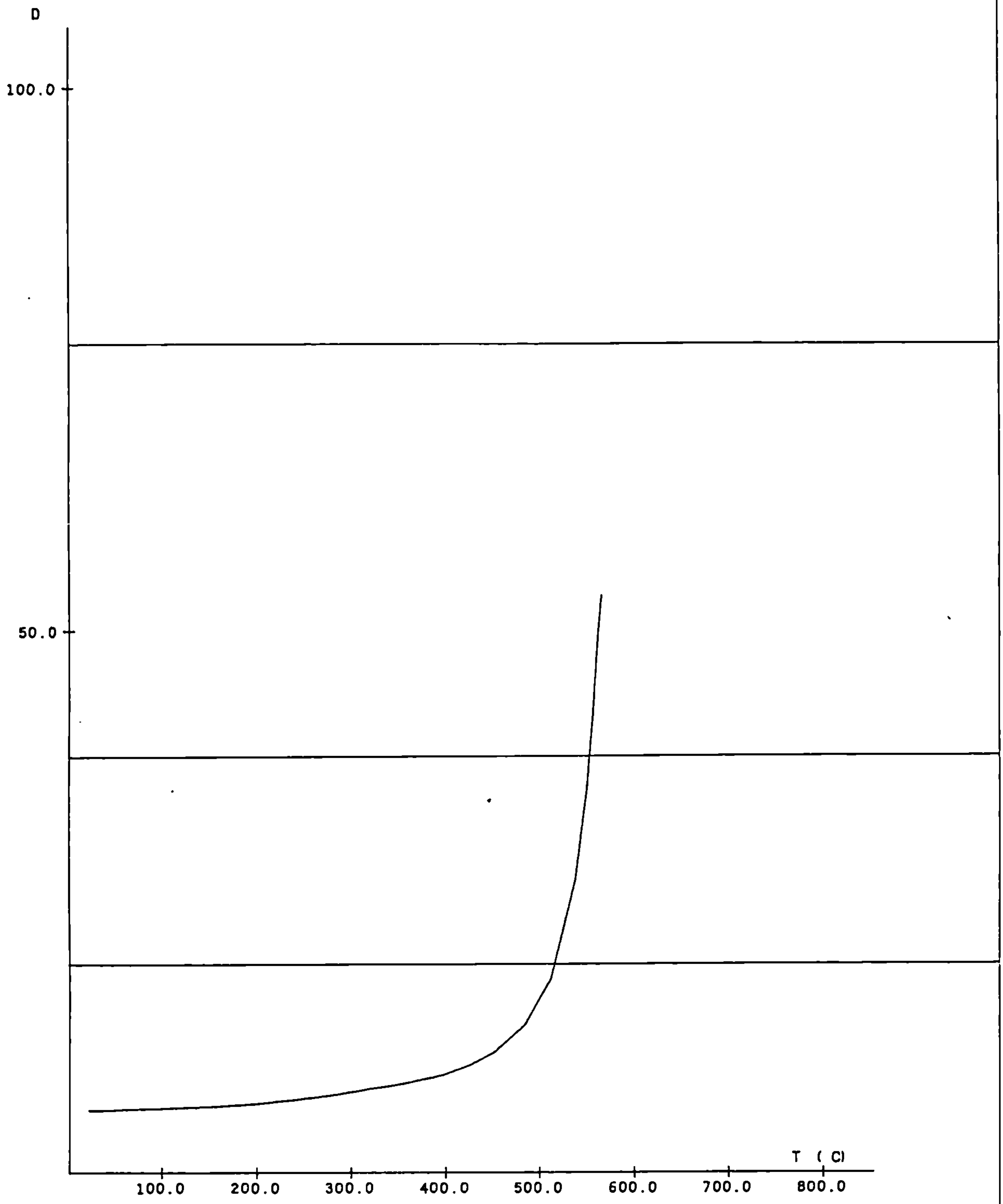

ARBED-RECHERCHES / RPS DEPARTMENT	CEFICOSS Analysis / CEF7DP1
PROJECT TITLE	PROJECT NUMBER
TEST NR. S 4 -STE 460	REFAO III
$F/F_{PCOLD}=0.60$	ESCH/ALZETTE : 16-AUG-1988 · SHEET :

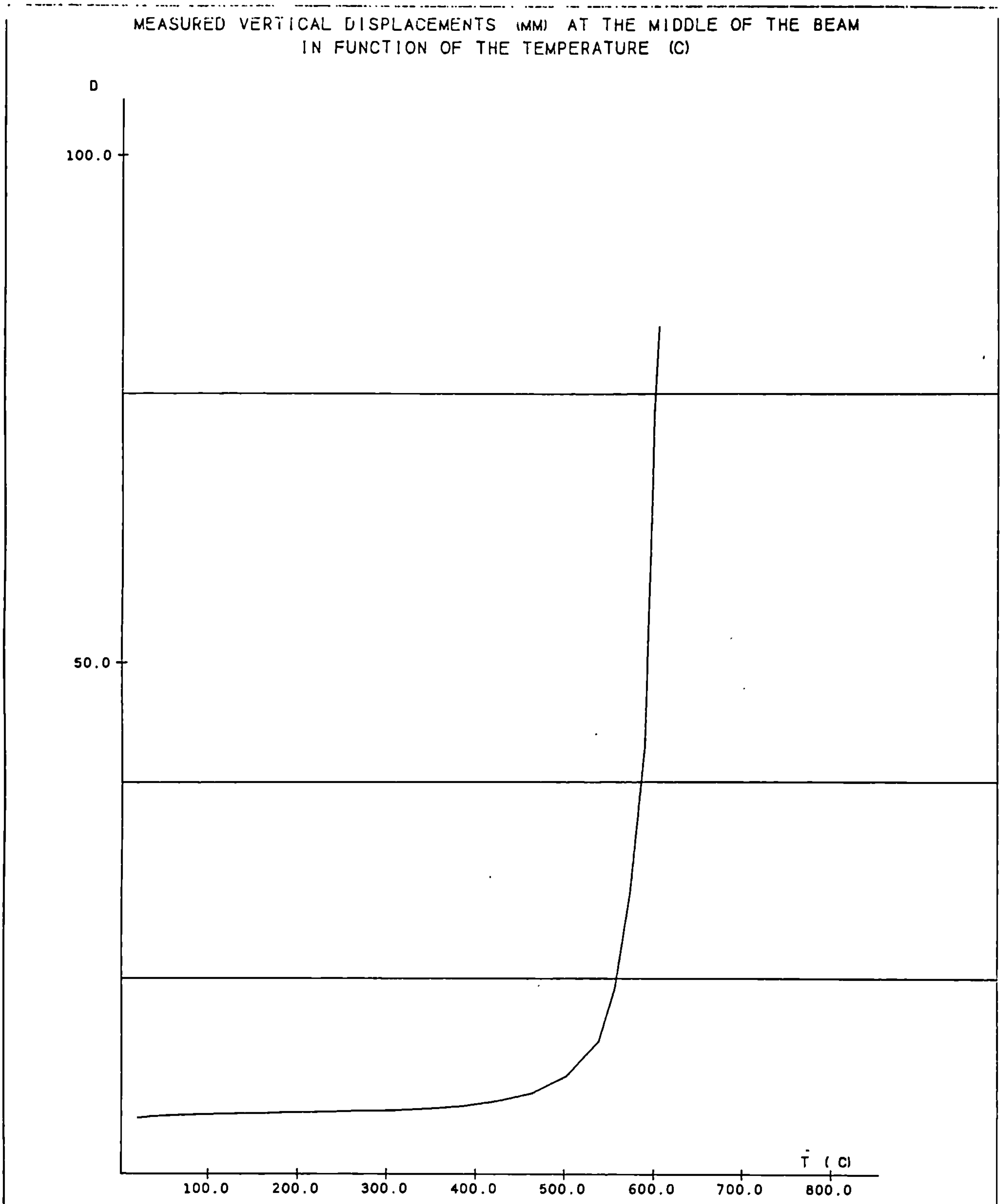

ARBED-RECHERCHES / RPS DEPARTMENT	CEFICOSS Analysis / CEF7DP1
PROJECT TITLE TEST NR. S10 -STE 460 F/F_{PCOLD}=0.50	PROJECT NUMBER REFAO III ESCH/ALZETTE : 16-AUG-1988 SHEET :

MEASURED VERTICAL DISPLACEMENTS (MM) AT THE MIDDLE OF THE BEAM
IN FUNCTION OF THE TEMPERATURE (C)

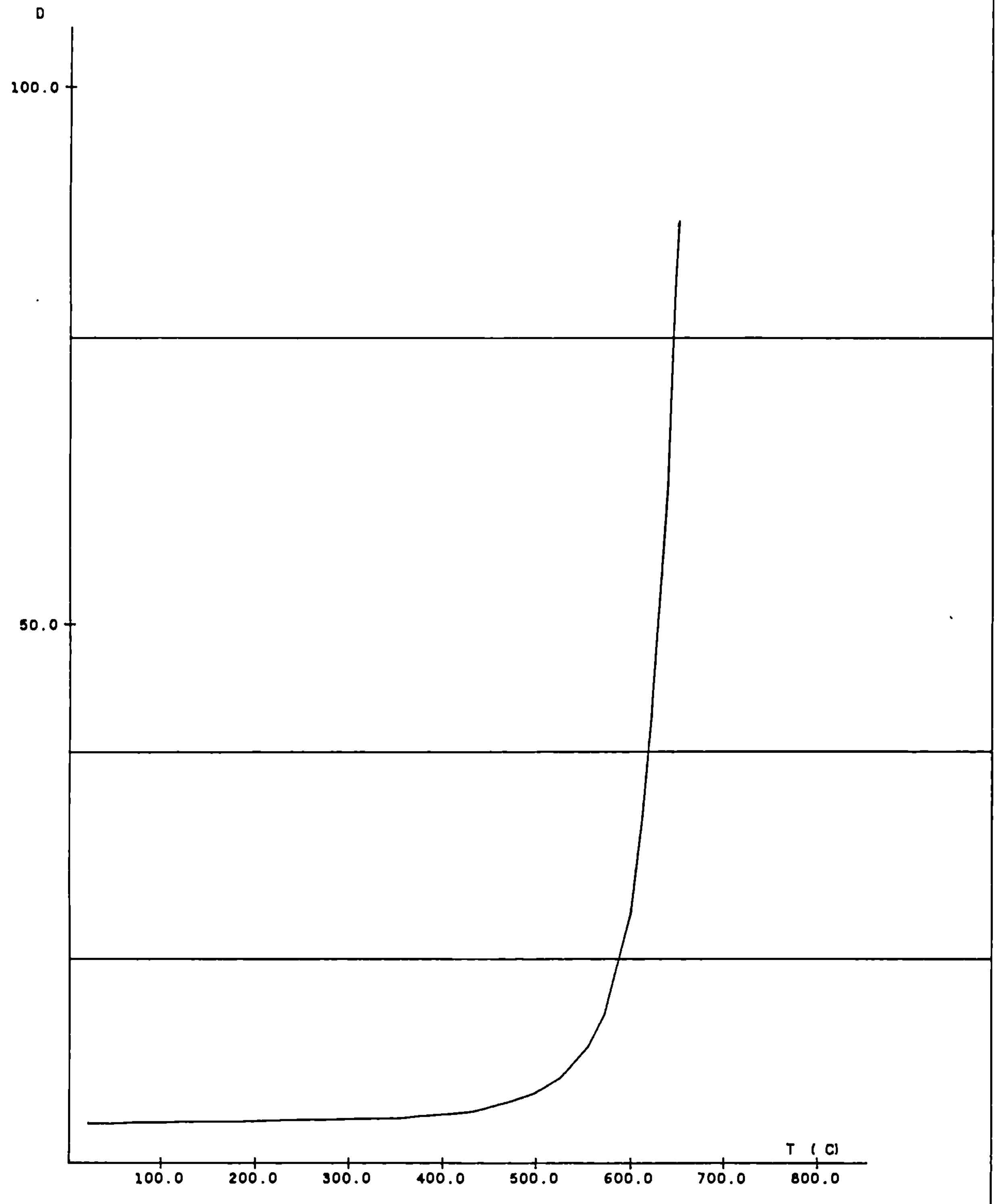

ARBED-RECHERCHES / RPS DEPARTMENT	CEFICOSS Analysis / CEF7DP1
PROJECT TITLE TEST NR. S 5 -STE 460 $F/F_{PCOLD} = 0.40$	PROJECT NUMBER REFAO III ESCH/ALZETTE : 16-AUG-1988 SHEET :

MEASURED VERTICAL DISPLACEMENTS (MM) AT THE MIDDLE OF THE BEAM
IN FUNCTION OF THE TEMPERATURE (C)

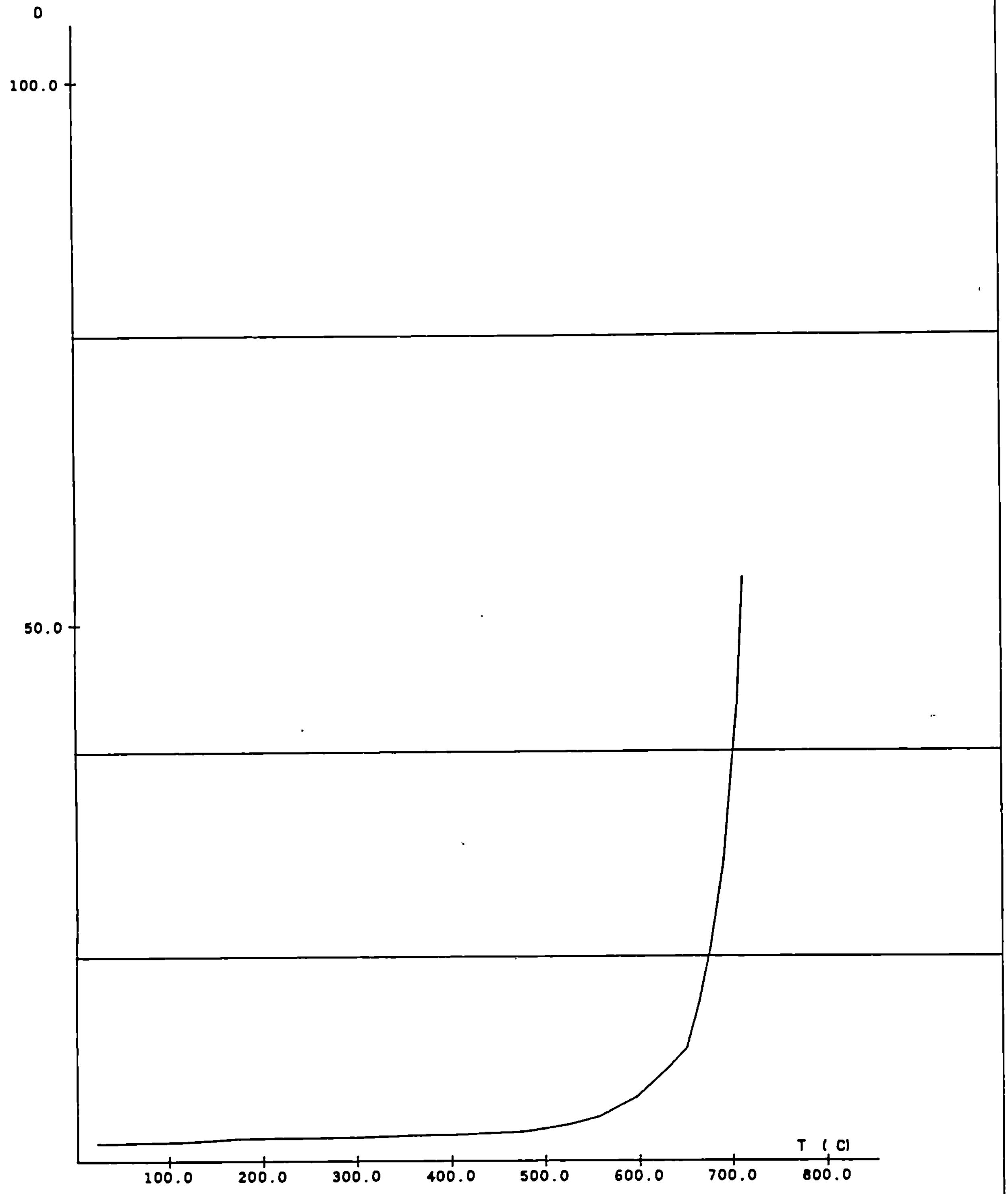

ARBED-RECHERCHES / RPS DEPARTMENT	CEFICOSS Analysis / CEF7DP1
PROJECT TITLE TEST NR. S 9 -STE 460 $F/F_{PCOLD} = 0.20$	PROJECT NUMBER REFAO III ESCH/ALZETTE : 16-AUG-1988 — SHEET :

MEASURED VERTICAL DISPLACEMENTS (MM) AT THE MIDDLE OF THE BEAM
IN FUNCTION OF THE TEMPERATURE (C)

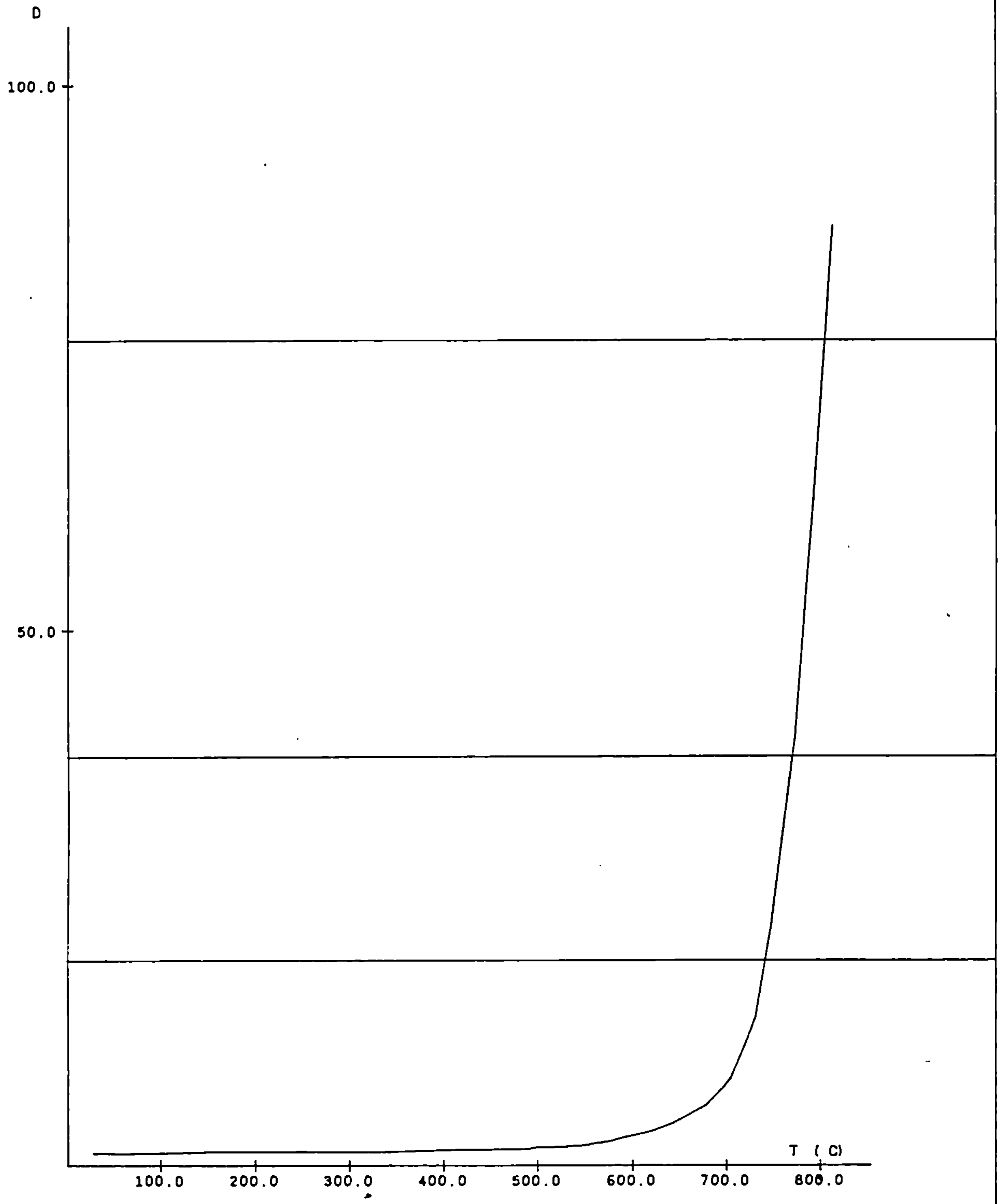

ARBED-RECHERCHES / RPS DEPARTMENT	CEFICOSS Analysis / CEF7DP1
PROJECT TITLE TEST NR. S 7 -STE 460 $F/F_{PCOLD} = 0.10$	PROJECT NUMBER REFAO III ESCH/ALZETTE : 16-AUG-1988 — SHEET :

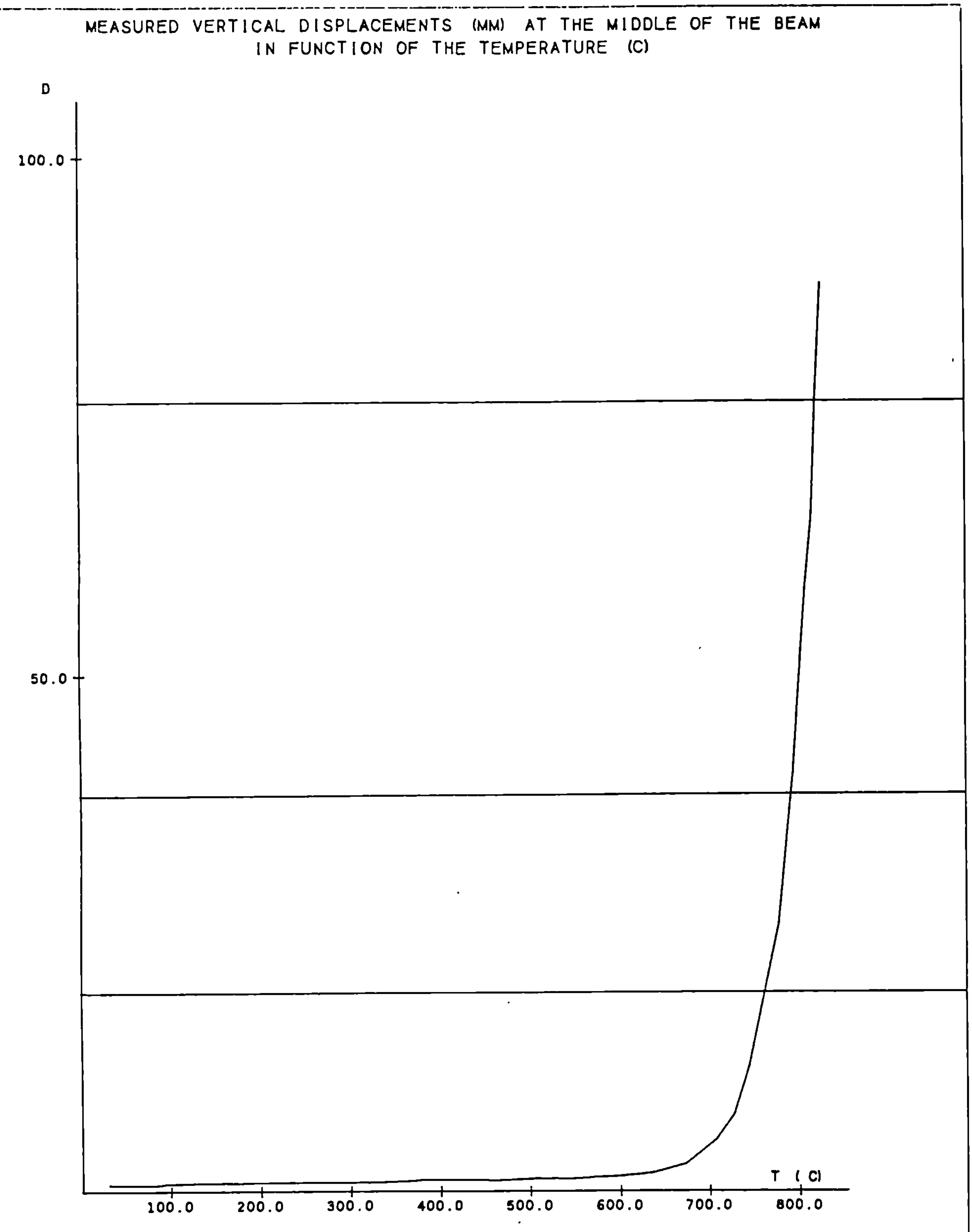

ARBED-RECHERCHES / RPS DEPARTMENT	CEFICOSS Analysis / CEF7DP1
PROJECT TITLE TEST NR. S 6 -STE 460 F/F_{PCOLD}=0.075	PROJECT NUMBER REFAO III ESCH/ALZETTE : 16-AUG-1988 SHEET :

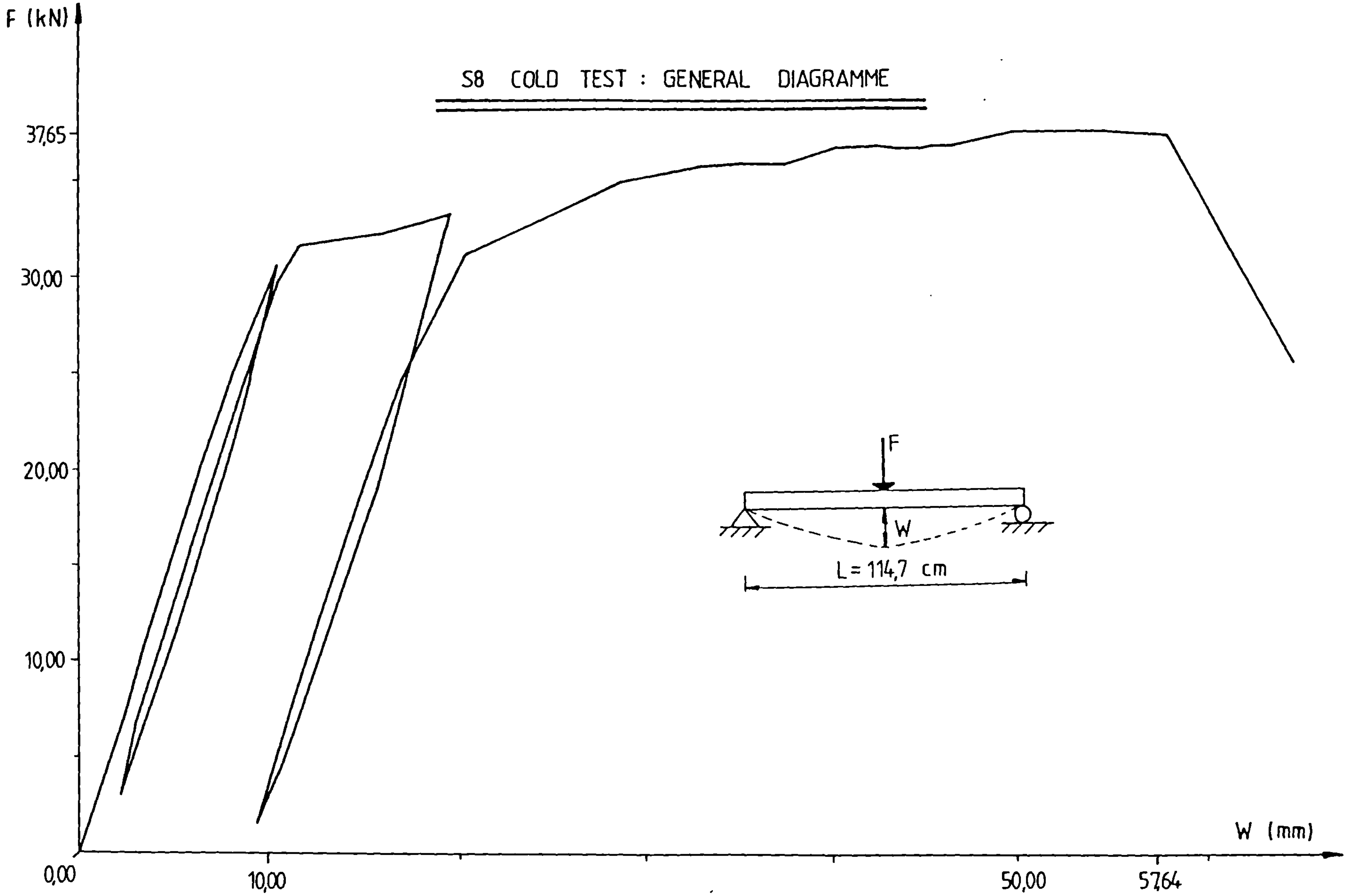
S8 COLD TEST : GENERAL DIAGRAMME
F (kN)
37,65
30,00
20,00
10,00
0,00
10,00
50,00
57,64
W (mm)
F
W
L = 114,7 cm

Krupp transient state beam tests parameters (S1 to S10)

TEST	R_{eH} [N/mm²]	F_{PCOLD} [kN]	F [kN]	F/F_{PCOLD}	$\dot{\theta}_m$ [K/min]	θ_{init} [°C]	$(\theta_m)_{max}$ [°C]	$(D_{mes.})_{max}$ [mm]	$(t_{test})_{max}$ [min]	
S1	502	30,0	30,0	1,00	3,6	22,1	461	85,8	121	(1)
S2	504,5	30,2	22,7	0,75	3,4	22,5	525	53,9	146	(2)
S3	507	30,3	25,8	0,85	3,5	21,7	497	53,2	137	(2)
S4	516	30,8	18,5	0,60	3,5	21.4	566	53,1	155	(2)
S5	513	30.7	12,3	0,40	3,5	21.0	651	87.5	182	(2)
S6	53[illegible]	31,6	2,4	0,075	3,4	31,2	828	87,8	235	(2)
S7	526	31,4	3,2	0,10	3,5	28	813	86,9	227	(2)
S8	523	31,3	37,65	1,20	/	/	/	75,0	/	(3)
S9	523,5	31,3	6,3	0,20	3,5	22,4	713	54,1	198	(2)
S10	522,5	31,2	15,6	0,50	3,4	20,1	605	83,2	175	(2)

REMARKS: (1) after cold loading before the heating the middle-span section is already fully plastified
(2) after cold loading before the heating the middle-span section is partially plastified or still elastic
(3) only cold loadings – unloadings

INFLUENCE OF THE TOOLING TOLERANCE GEOMETRICAL AND MECHANICAL CHARACTERISTICS DIMENSIONS

			SUPPOSED VALUES			
meaning of notations		dimensions	-1/10mm	exact	+1/10mmm	max/min in %
depth of section	h	mm	69,90	70,0	70,1	±0,14
width of flange	b	mm	36,9	37,0	37,1	±0,27
thickness of web and flange	t,e	mm	4,9	5,0	5,1	±2,00
radius of fillet	r	mm	4,9	5,0	5,1	±2,00
cross-section area	A	cm²	6,77	6,91	7,06	±2,17
moment of inertia	I_{xx}	cm	48,86	49,95	51,04	±2,18
elastic section modulus	W_{xx}	cm³	13,98	14,27	14,56	±2,03
plastic section modulus	W_{xxpl}	cm³	16,77	17,14	17,52	±2,22
(W_{xxpl}/W_{xx})factor	α_{pl}	/	1,20	1,20	1,20	/

Values: * exactly : all the cross-section values are nominal

* -1/10mm : all the cross-section values are situated on the minimal tolerance

* +1/10mm : all the cross-section values are situated on the maximal tolerance

MODELISATION OF THE SECTION

SCALE : 5/1

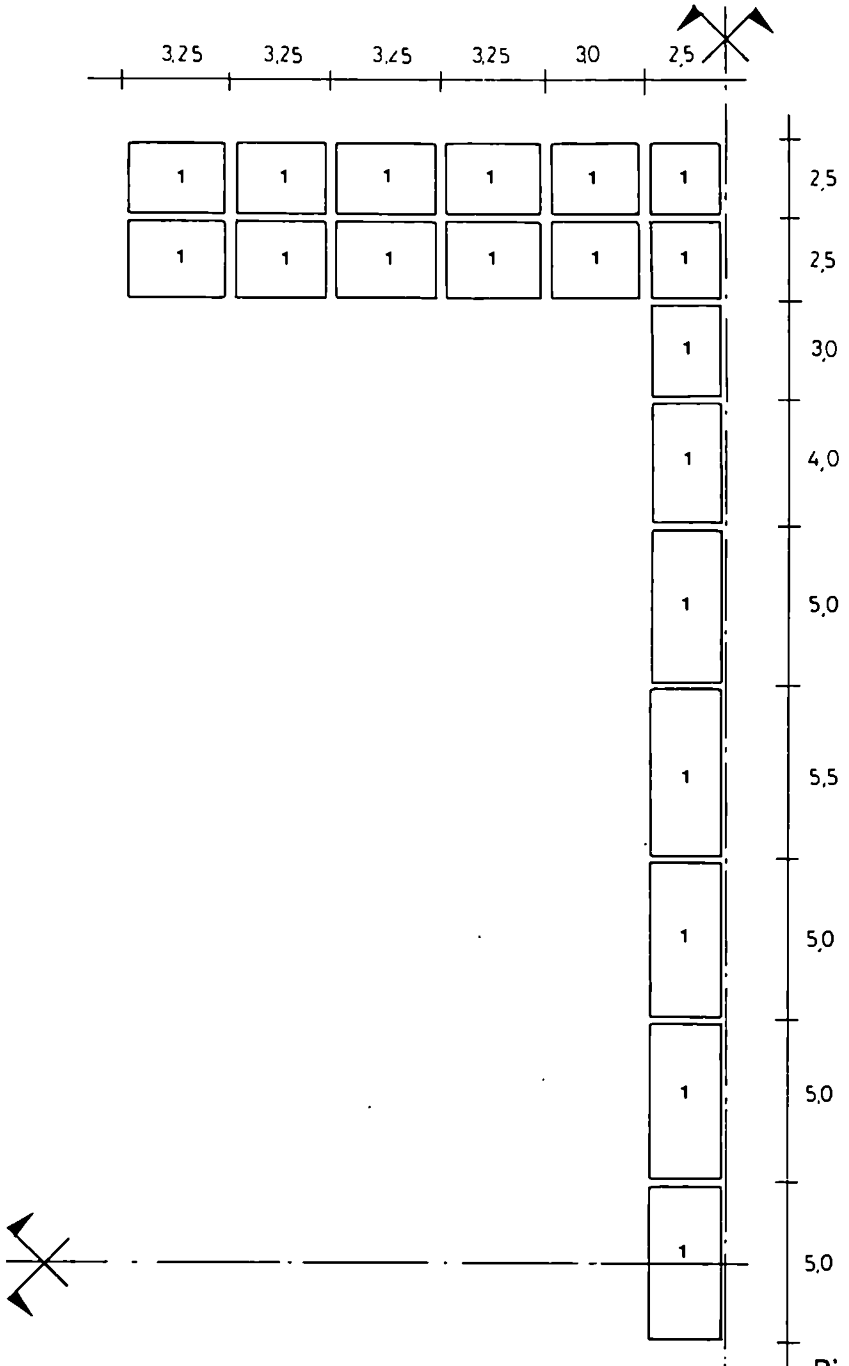

Dimensions in [mm]

ARBED-RECHERCHES / RPS DEPARTMENT	CEFICOSS A / CEF7DP1
PROJECT TITLE TESTS S 1 TO S 10 - STE 460	PROJECT NUMBER REFAO III
	ESCH/ALZETTE : 17-AUG-1988 SHEET :

TEMPERATURE IN THE FLANGE OF THE SECTION

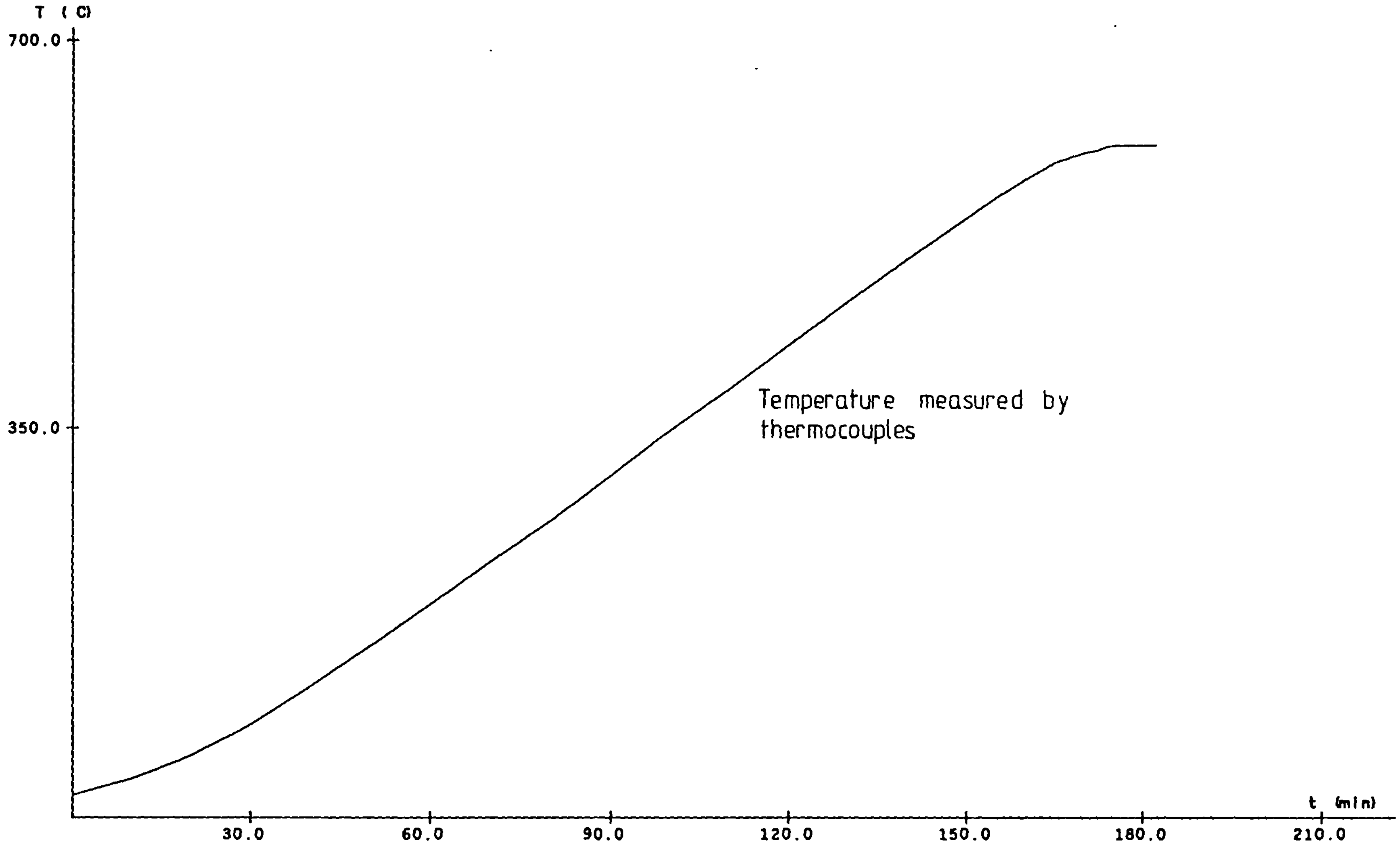

ARBED-RECHERCHES / RPS DEPARTMENT	CEFICOSS Analysis / CEF7DP1
PROJECT TITLE TEST S 10 - STE 460	PROJECT NUMBER REFAO III
	ESCH/ALZETTE : 22-AUG-1988 | SHEET :

TEMPERATURE IN THE WEB OF THE SECTION

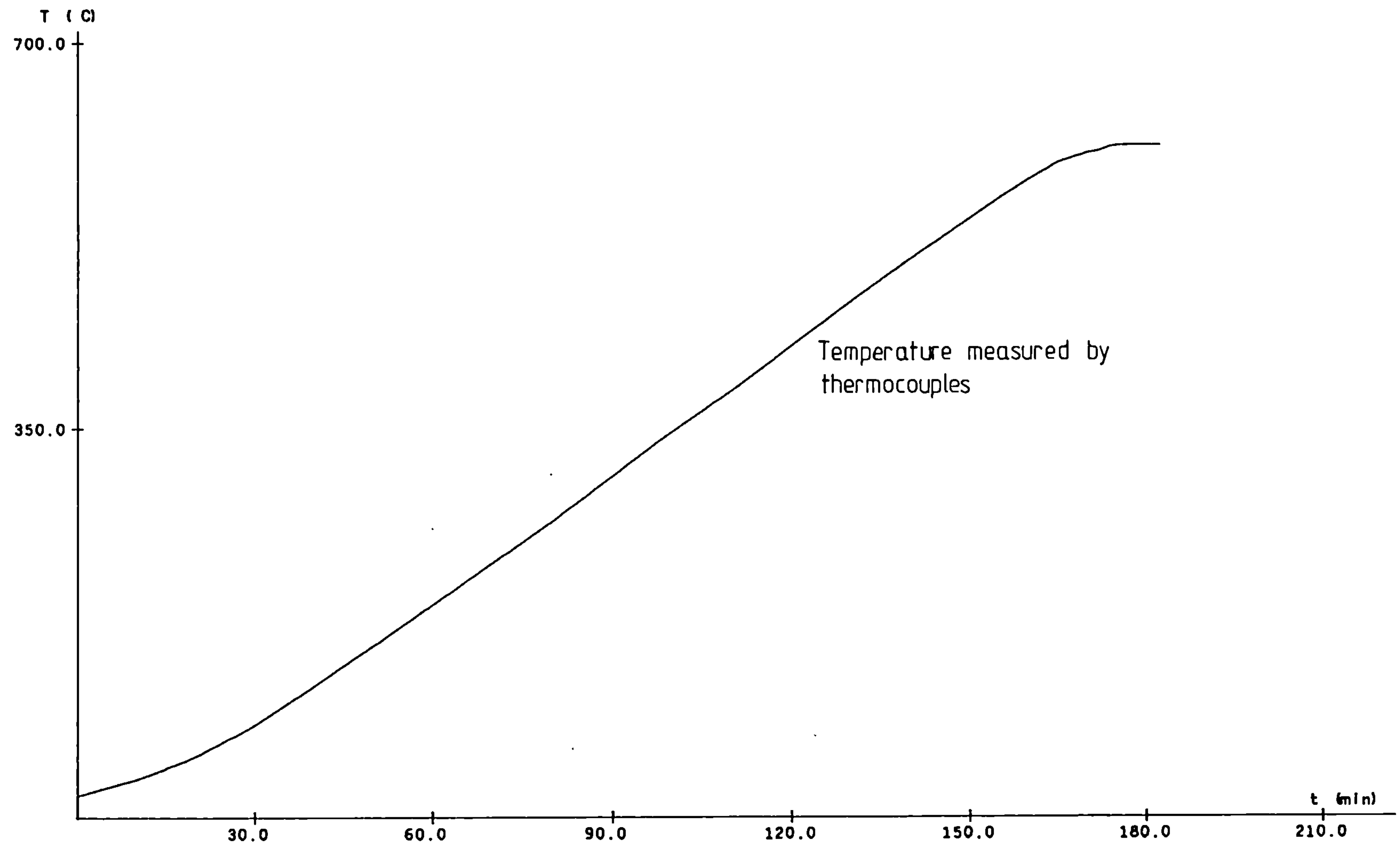

ARBED-RECHERCHES / RPS DEPARTMENT	CEFICOSS Analysis / CEF7DP1
PROJECT TITLE TEST S 10 - STE 460	PROJECT NUMBER REFAO III
	ESCH/ALZETTE : 22-AUG-1988 — SHEET :

VERTICAL DISPLACEMENTS LAW AT THE MIDDLE OF THE SEAM
IN FUNCTION OF THE TEMPERATURE (C)

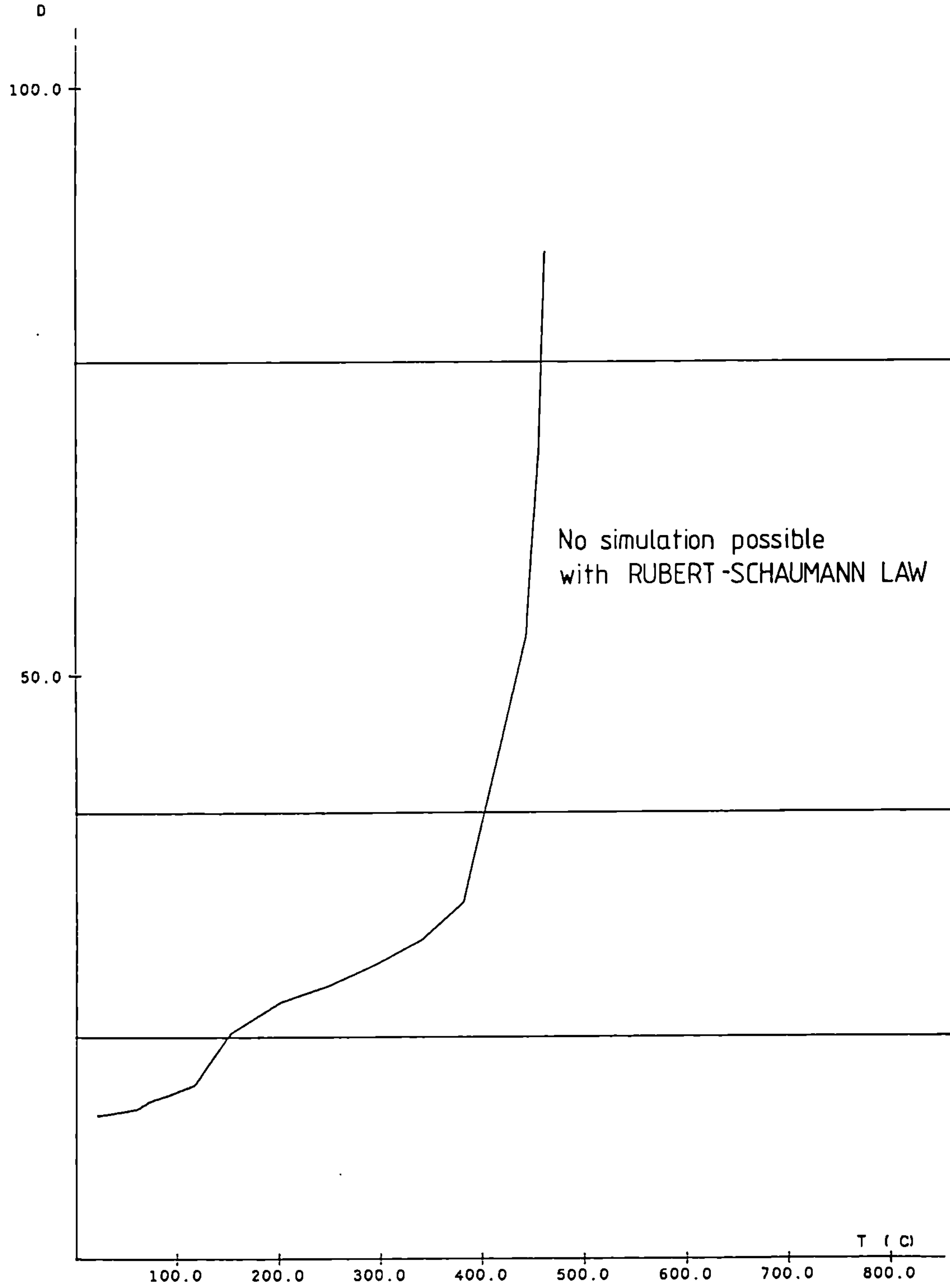

ARBED-RECHERCHES / RPS DEPARTMENT	CEFICOSS Analysis / CEF7DP1
PROJECT TITLE TEST NR. S 1 -STE 460 F/F_{PCOLD} = 1.0	PROJECT NUMBER REFAO III ESCH/ALZETTE : 16-AUG-1988 — SHEET :

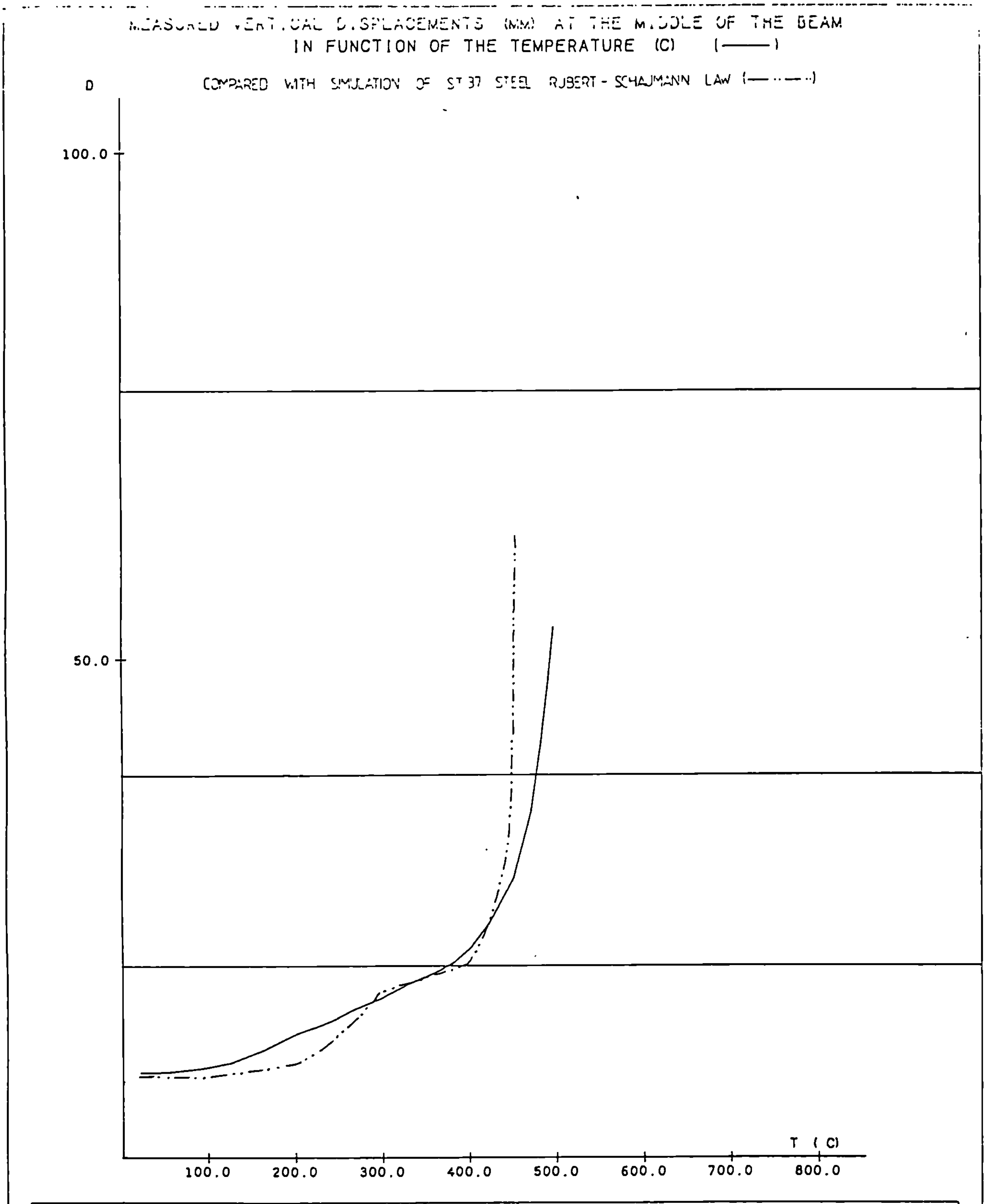

ARBED-RECHERCHES / RPS DEPARTMENT	CEFICOSS Analysis / CEF7DP1	
PROJECT TITLE	PROJECT NUMBER	
TEST NR. S 3 -STE 460 $F/F_{PCOLD} = 0.85$	REFAO 111	
	ESCH/ALZETTE : 16-AUG-1988	SHEET :

MEASURED VERTICAL DISPLACEMENTS (MM) AT THE MIDDLE OF THE BEAM
IN FUNCTION OF THE TEMPERATURE (C) (——)

COMPARED WITH SIMULATION OF ST 37 STEEL RUBERT - SCHAUMANN LAW (—··—·)

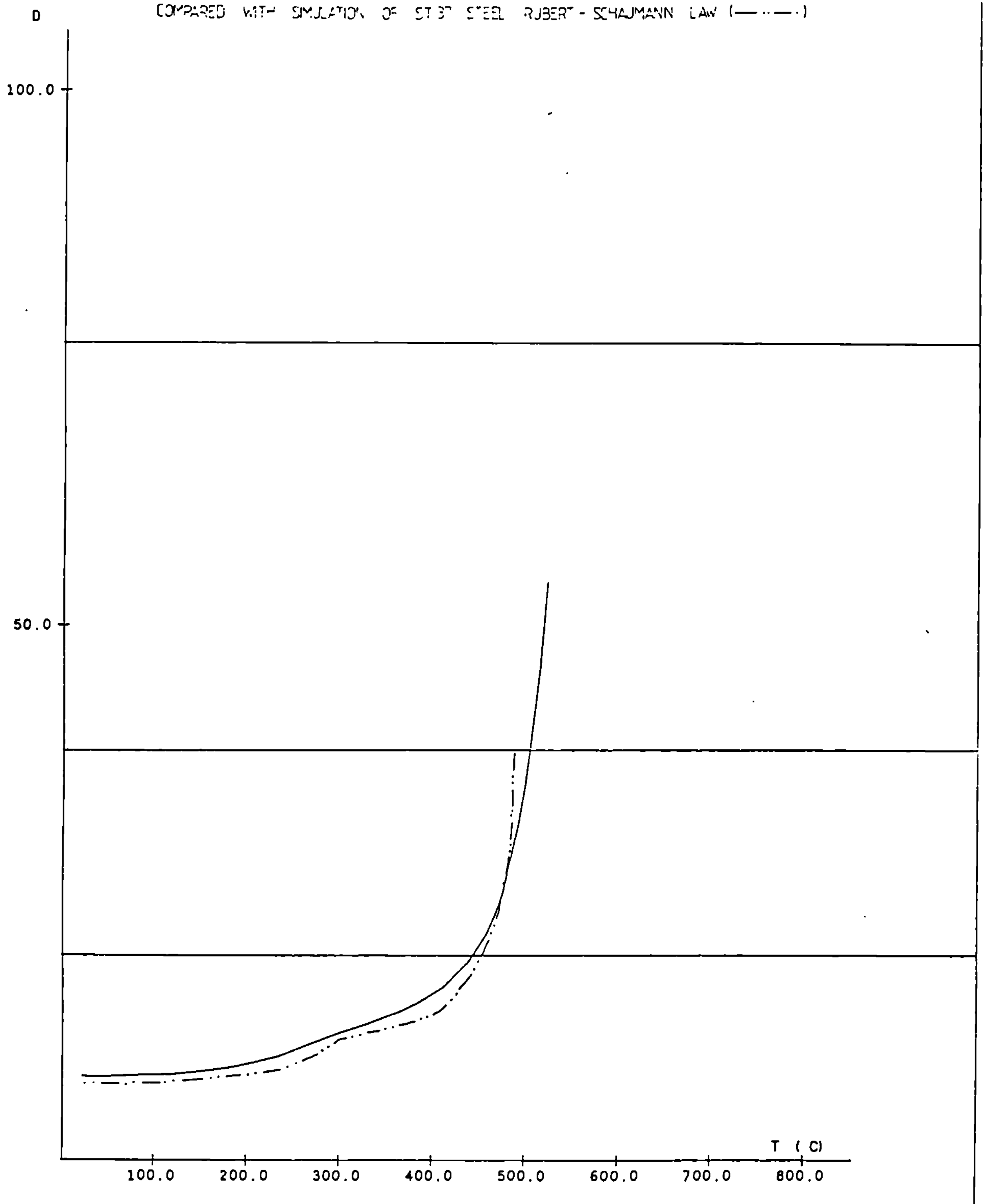

ARBED-RECHERCHES / RPS DEPARTMENT	CEFICOSS Analysis / CEF7DP1
PROJECT TITLE TEST NR. S 2 -STE 460 $F/F_{PCOLD} = 0.75$	PROJECT NUMBER REFAO III ESCH/ALZETTE : 16-AUG-1988 — SHEET :

MEASURED VERTICAL DISPLACEMENTS (MM) AT THE MIDDLE OF THE BEAM
IN FUNCTION OF THE TEMPERATURE (C) (——)

COMPARED WITH SIMULATION OF ST 37 STEEL RUBERT - SCHAUMANN LAW (—··—·)

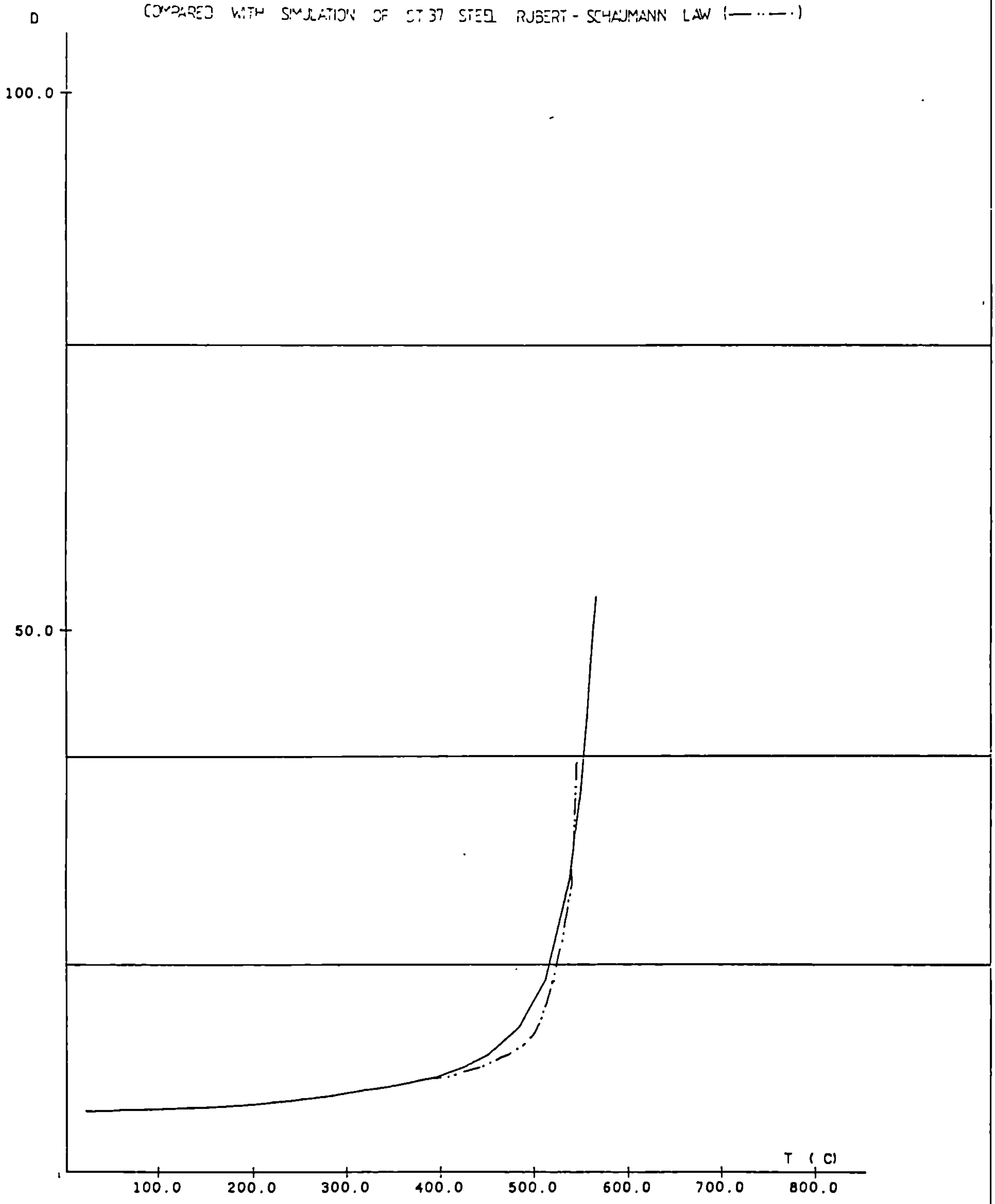

ARBED-RECHERCHES / RPS DEPARTMENT	CEFICOSS Analysis / CEF7DP1
PROJECT TITLE TEST NR. S 4 -STE 460 $F/F_{PCOLD} = 0.60$	PROJECT NUMBER REFAO III ESCH/ALZETTE : 16-AUG-1988 — SHEET :

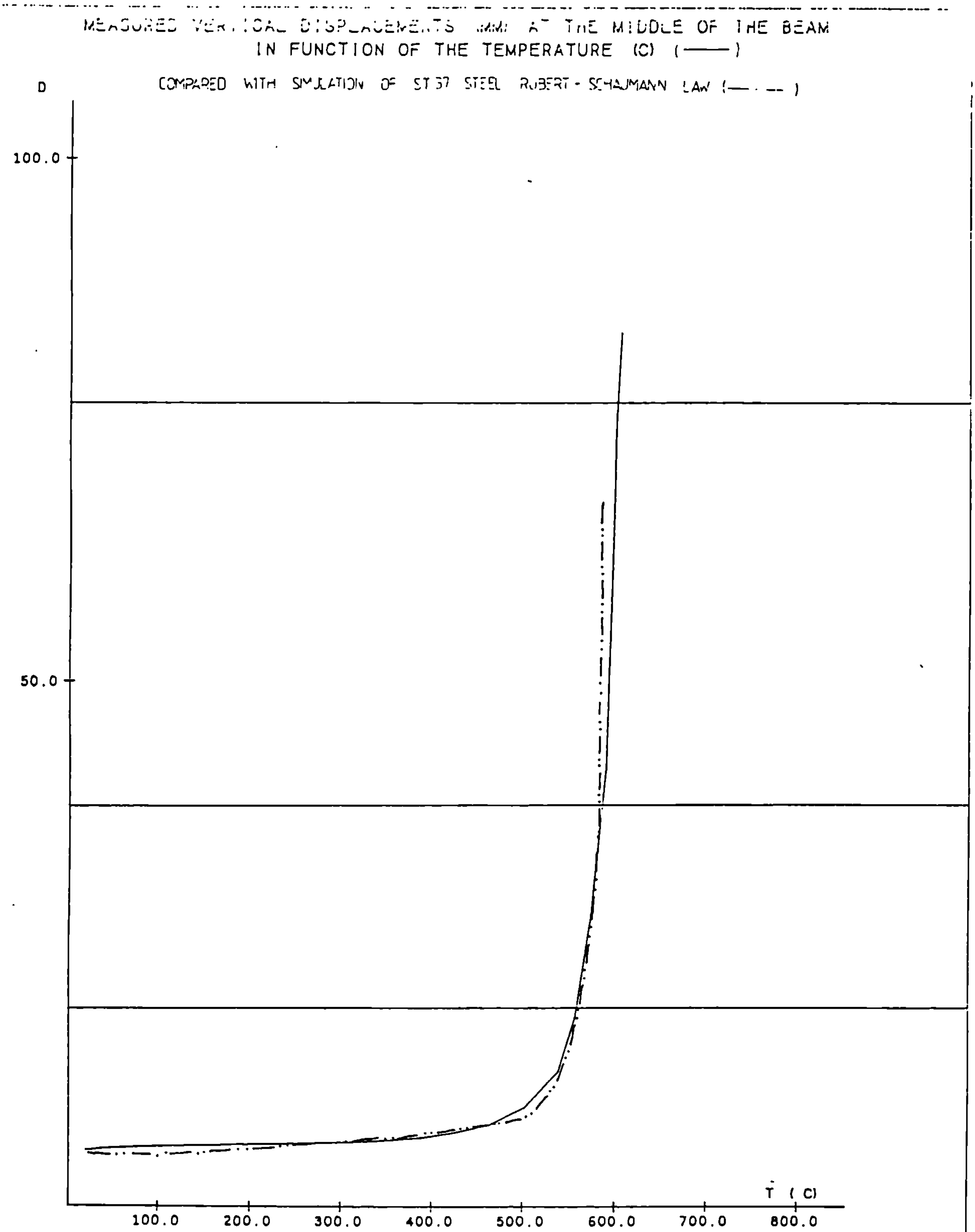

ARBED-RECHERCHES / RPS DEPARTMENT	CEFICOSS Analysis / CEF7DP1
PROJECT TITLE TEST NR. S10 -STE 460 F/F_{PCOLD} =0.50	PROJECT NUMBER REFAO III ESCH/ALZETTE : 16-AUG-1988 SHEET :

MEASURED VERTICAL DISPLACEMENTS (MM) AT THE MIDDLE OF THE BEAM
IN FUNCTION OF THE TEMPERATURE (C) (——)

COMPARED WITH SIMULATION OF ST 37 STEEL RUBERT-SCHAUMANN LAW (—··—·)

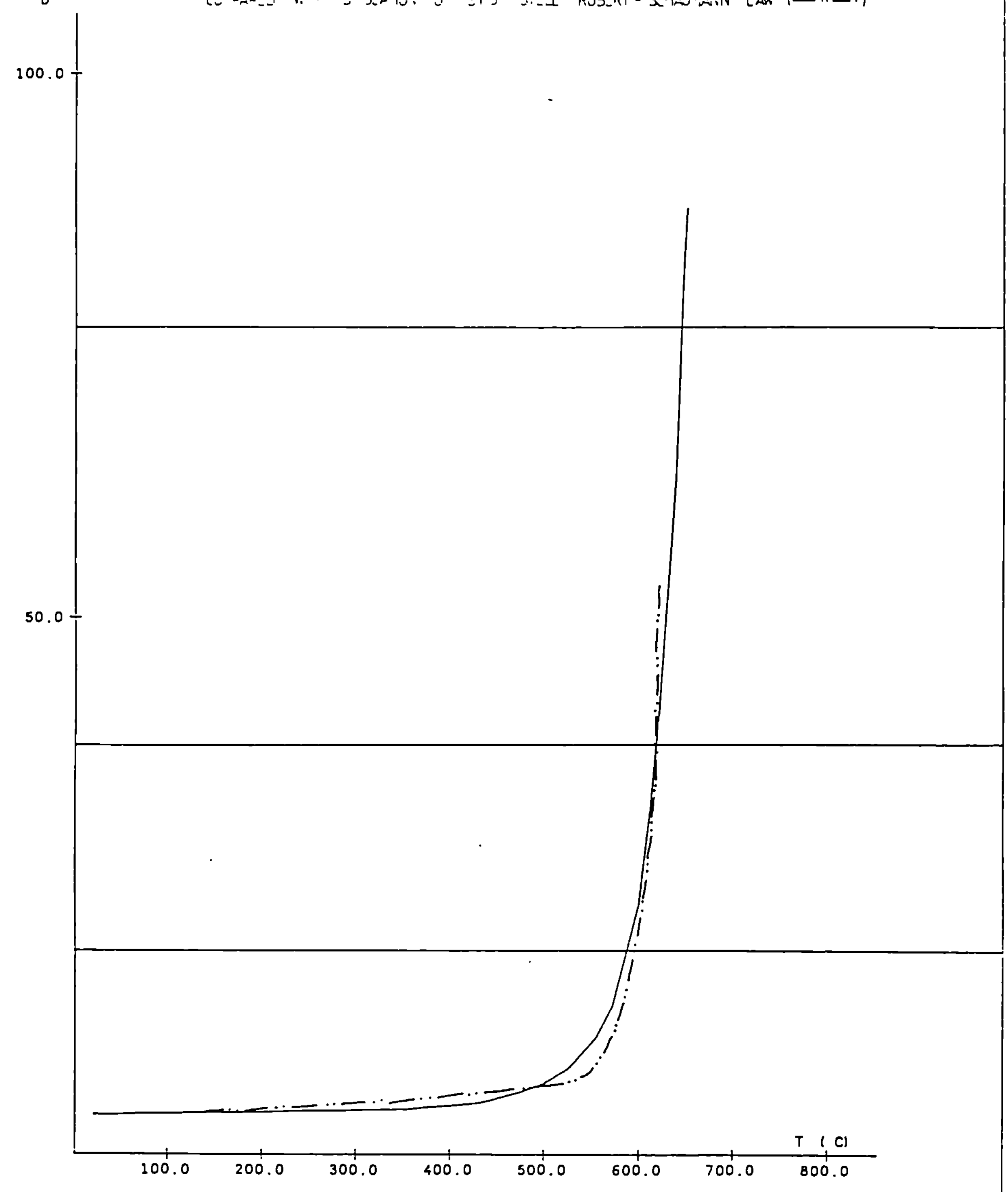

ARBED-RECHERCHES / RPS DEPARTMENT	CEFICOSS Analysis / CEF7DP1
PROJECT TITLE TEST NR. S 5 -STE 460 $F/F_{PCOLD} = 0.40$	PROJECT NUMBER REFAO III
	ESCH/ALZETTE : 16-AUG-1988 — SHEET :

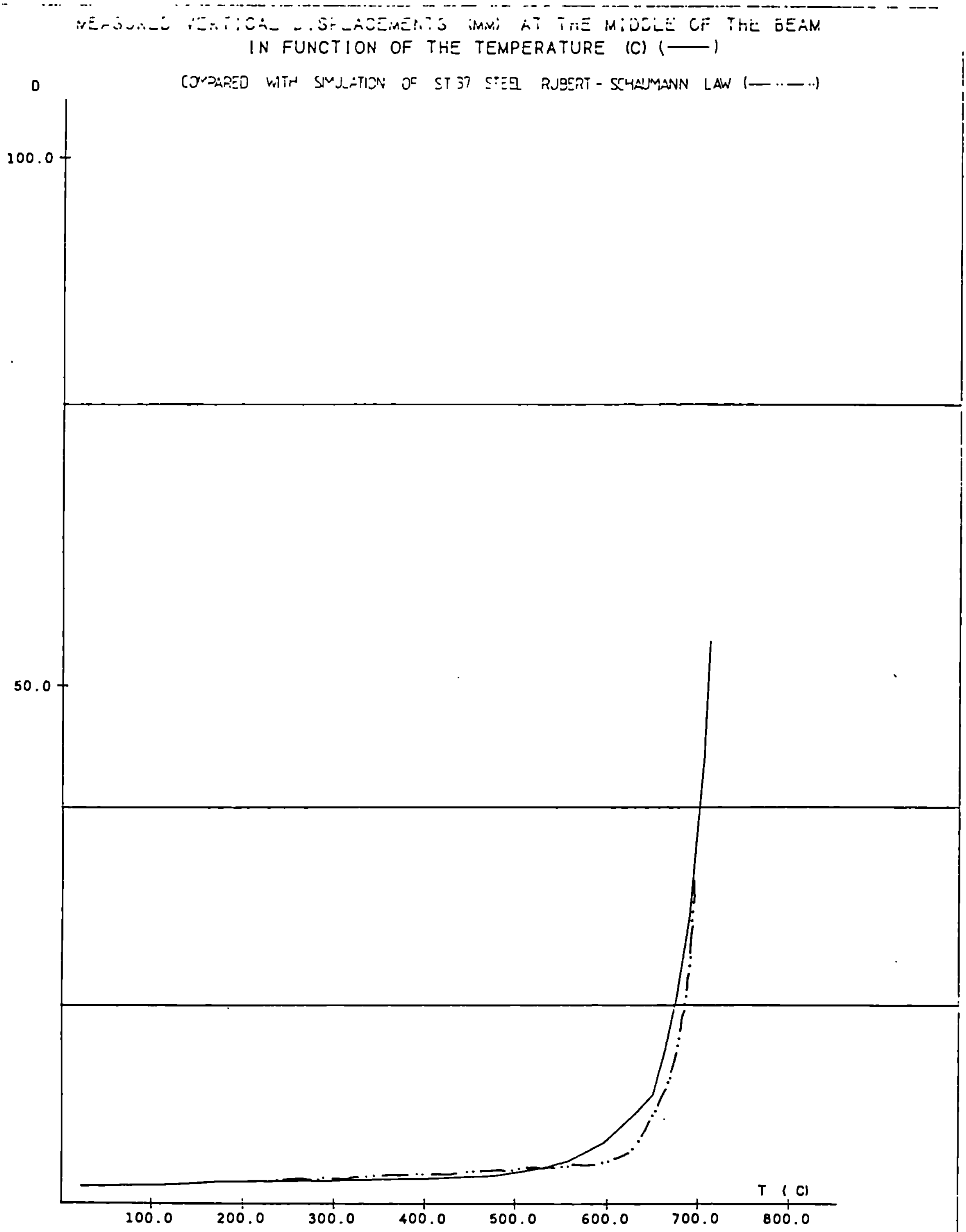

ARBED-RECHERCHES / RPS DEPARTMENT	CEFICOSS Analysis / CEF7DP1
PROJECT TITLE TEST NR. S 9 -STE 460 $F/F_{PCOLD} = 0.20$	PROJECT NUMBER REFAO III ESCH/ALZETTE : 16-AUG-1988 — SHEET :

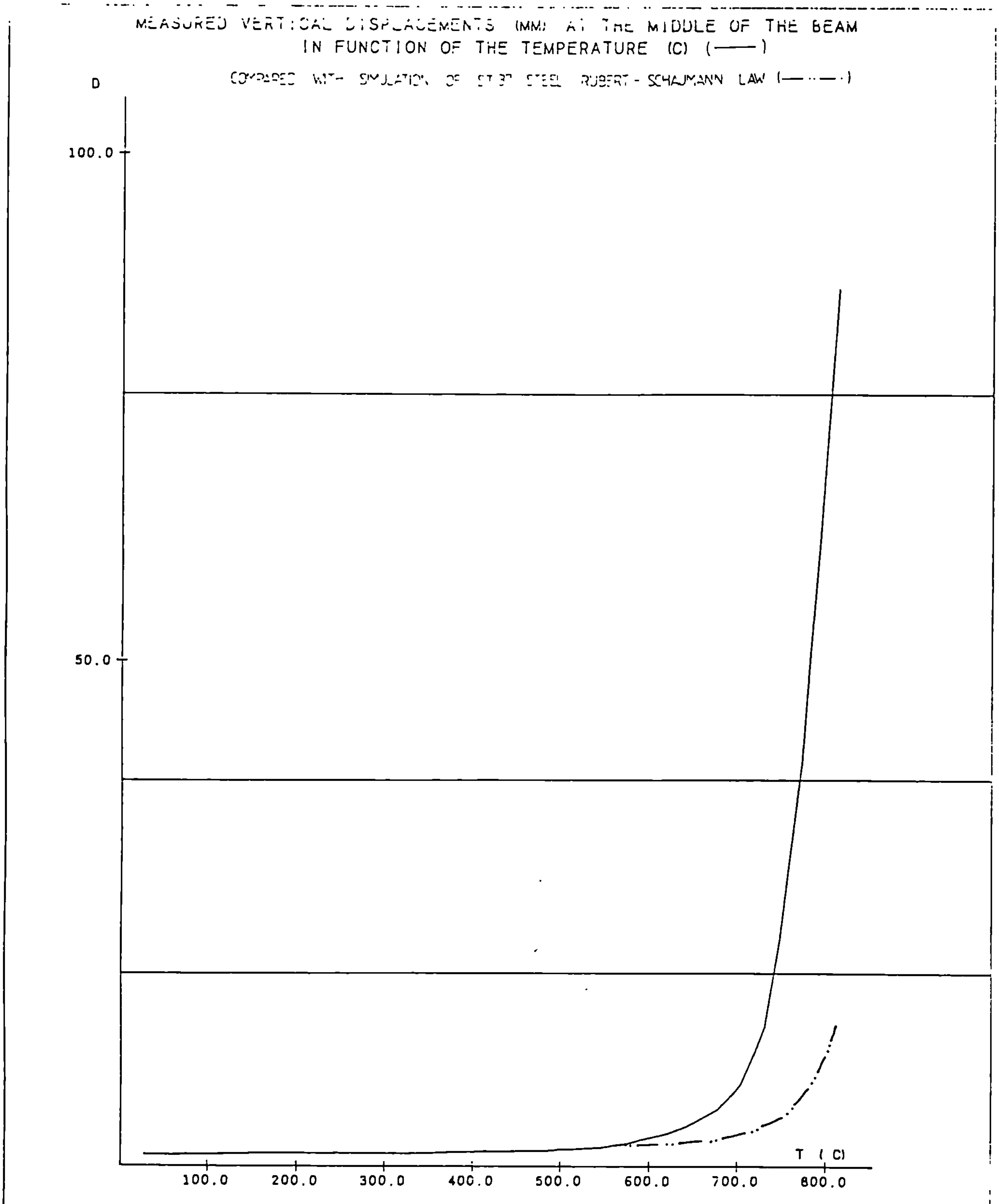

ARBED-RECHERCHES / RPS DEPARTMENT	CEFICOSS Analysis / CEF7DP1
PROJECT TITLE TEST NR. S 7 -STE 460 $F/F_{PCOLD} = 0.10$	PROJECT NUMBER REFAO III ESCH/ALZETTE : 16-AUG-1988 — SHEET :

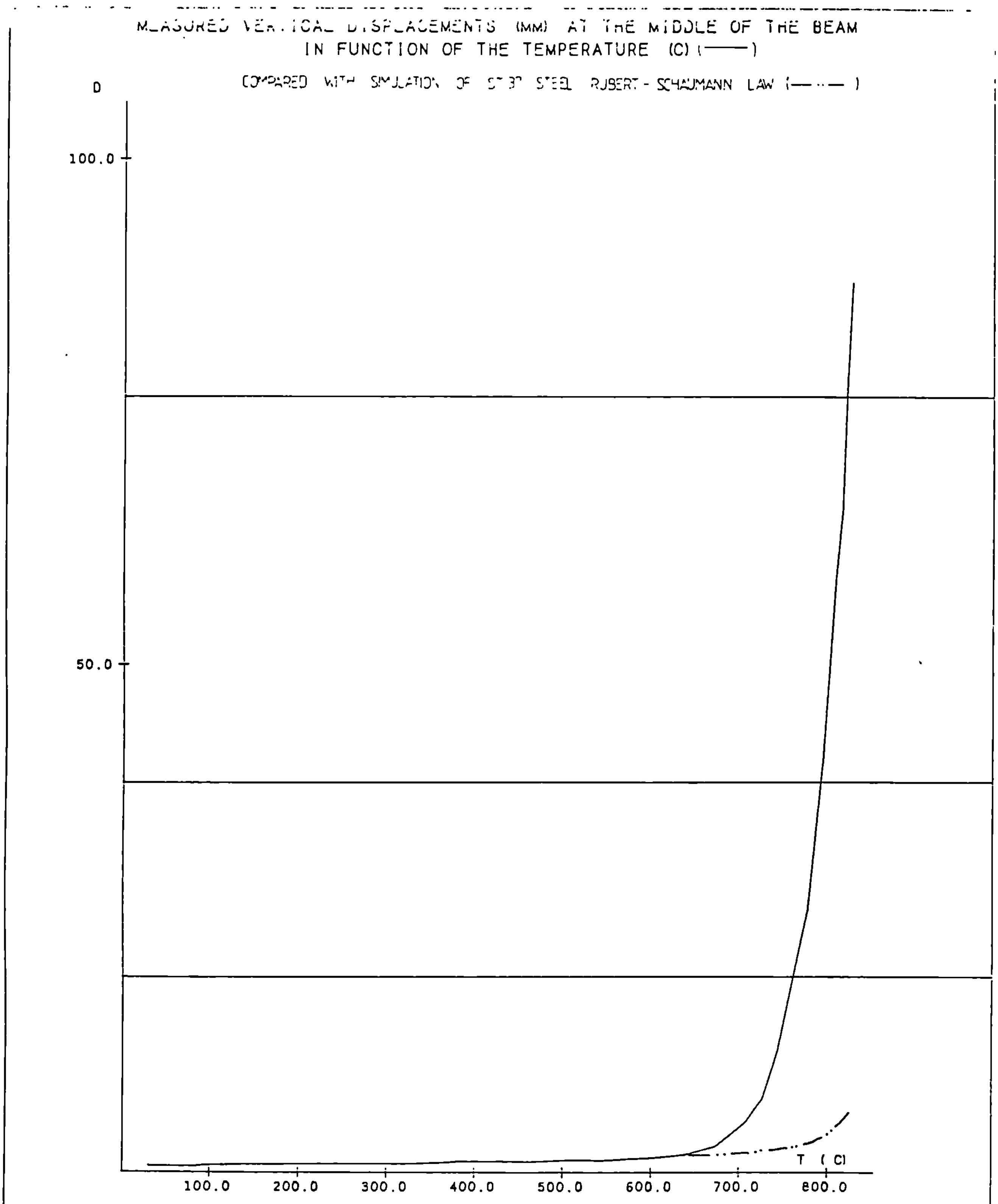

ARBED-RECHERCHES / RPS DEPARTMENT	CEFICOSS Analysis / CEF7DP1
PROJECT TITLE TEST NR. S 6 -STE 460 F/F_{PCOLD} =0.075	PROJECT NUMBER REFAO III ESCH/ALZETTE : 16-AUG-1988 SHEET :

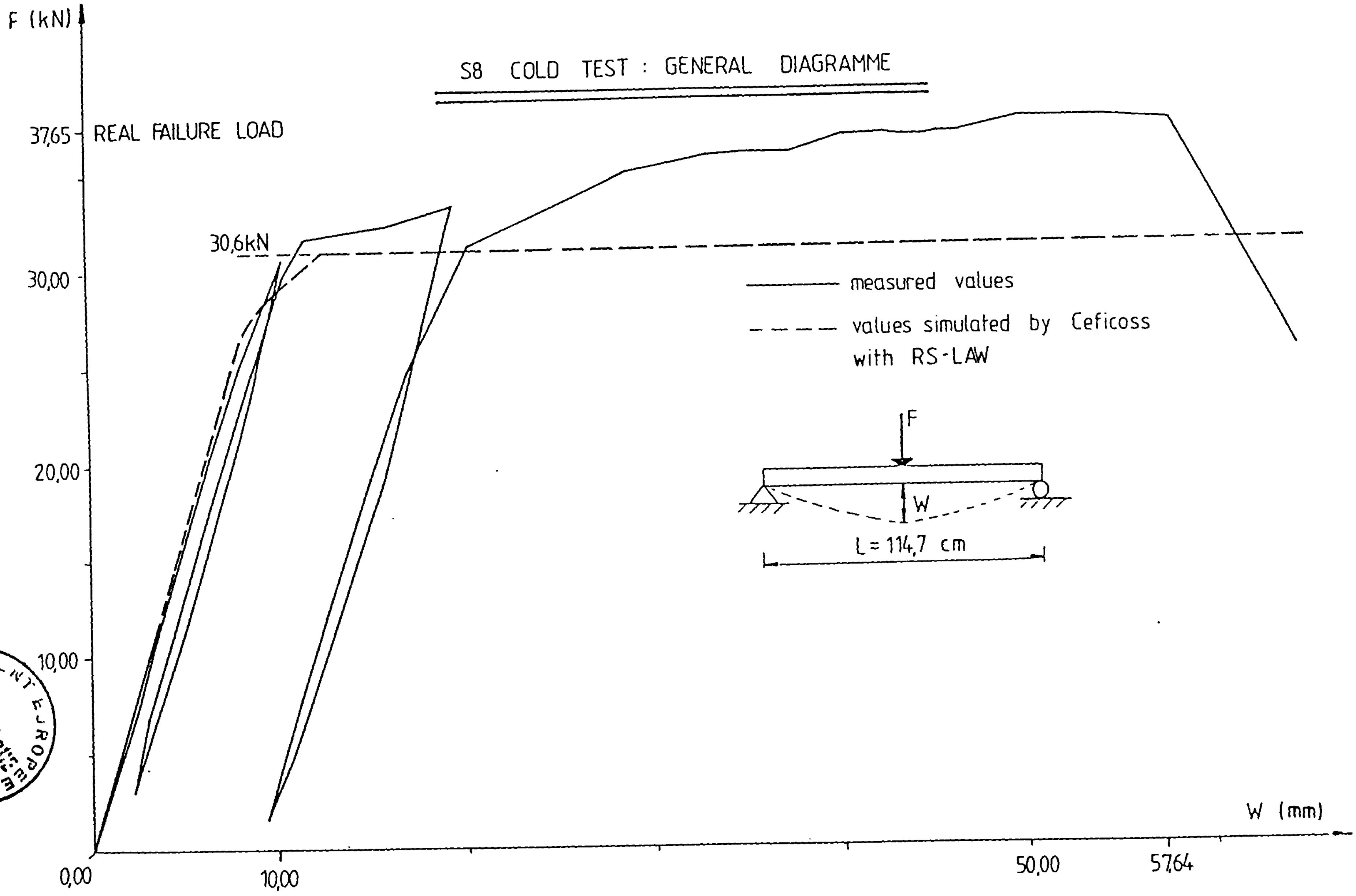
S8 COLD TEST : GENERAL DIAGRAMME
F (kN)
37,65
REAL FAILURE LOAD
30,6kN
30,00
20,00
10,00
0,00
10,00
50,00
57,64
W (mm)
measured values
values simulated by Ceficoss with RS-LAW
F
W
L = 114,7 cm

KRUPP TESTS 1988 FOR ARBED

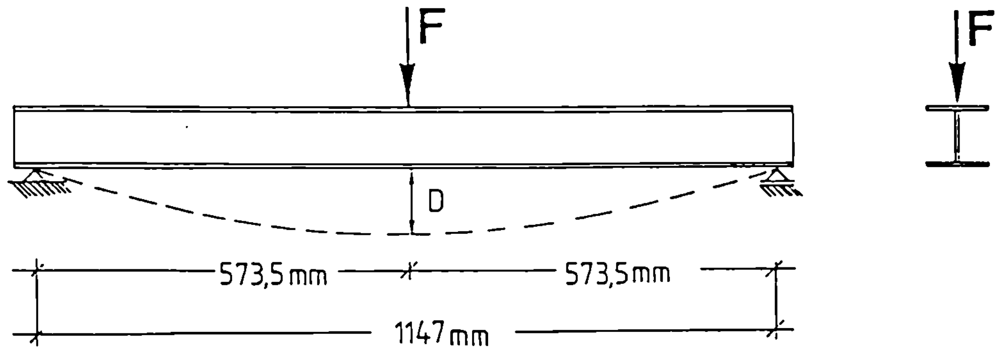

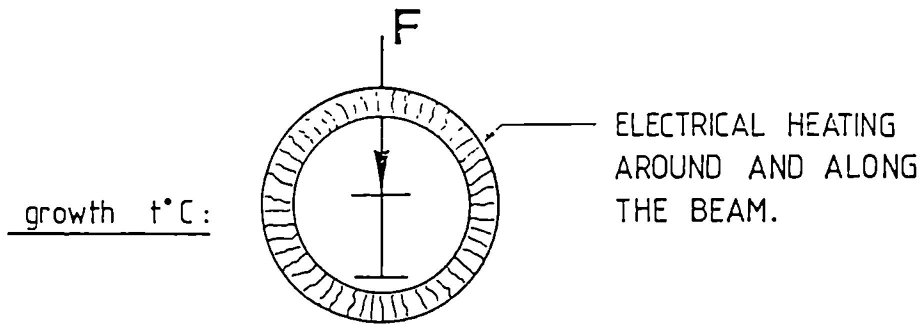

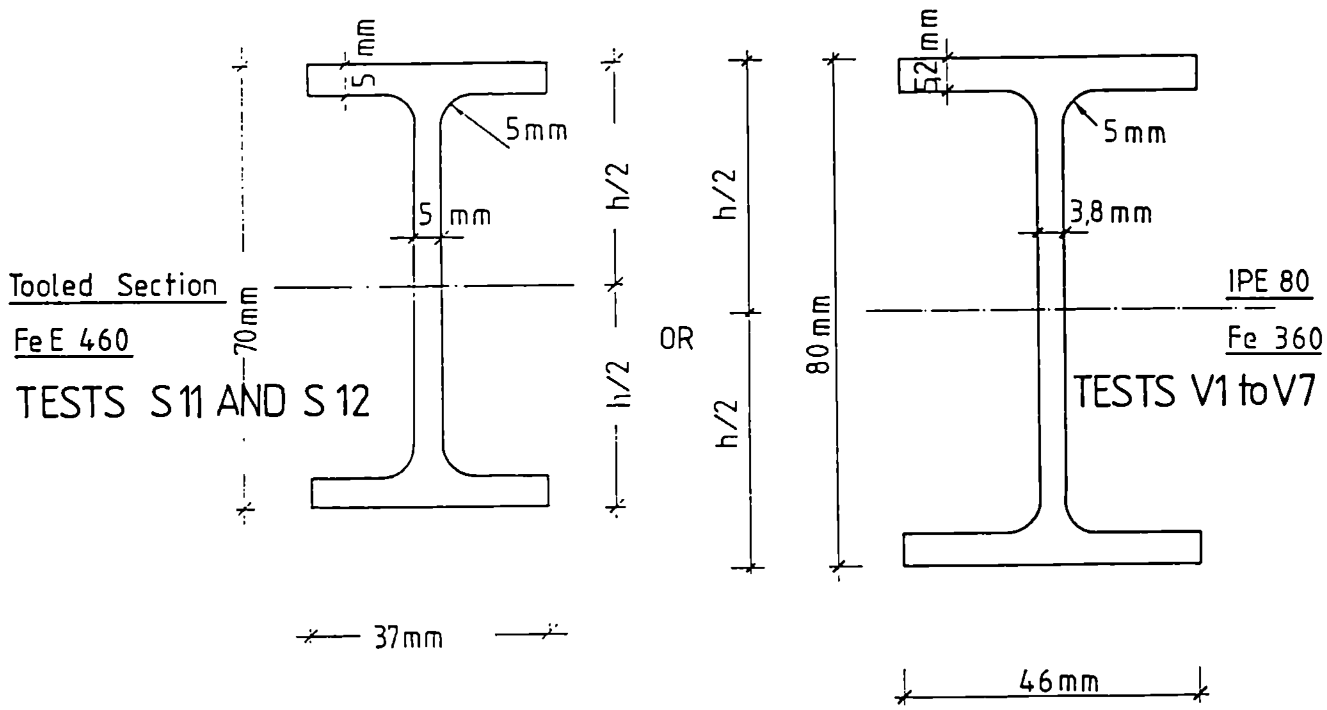

TOOLING OF I-BEAMS 70x40x5x5

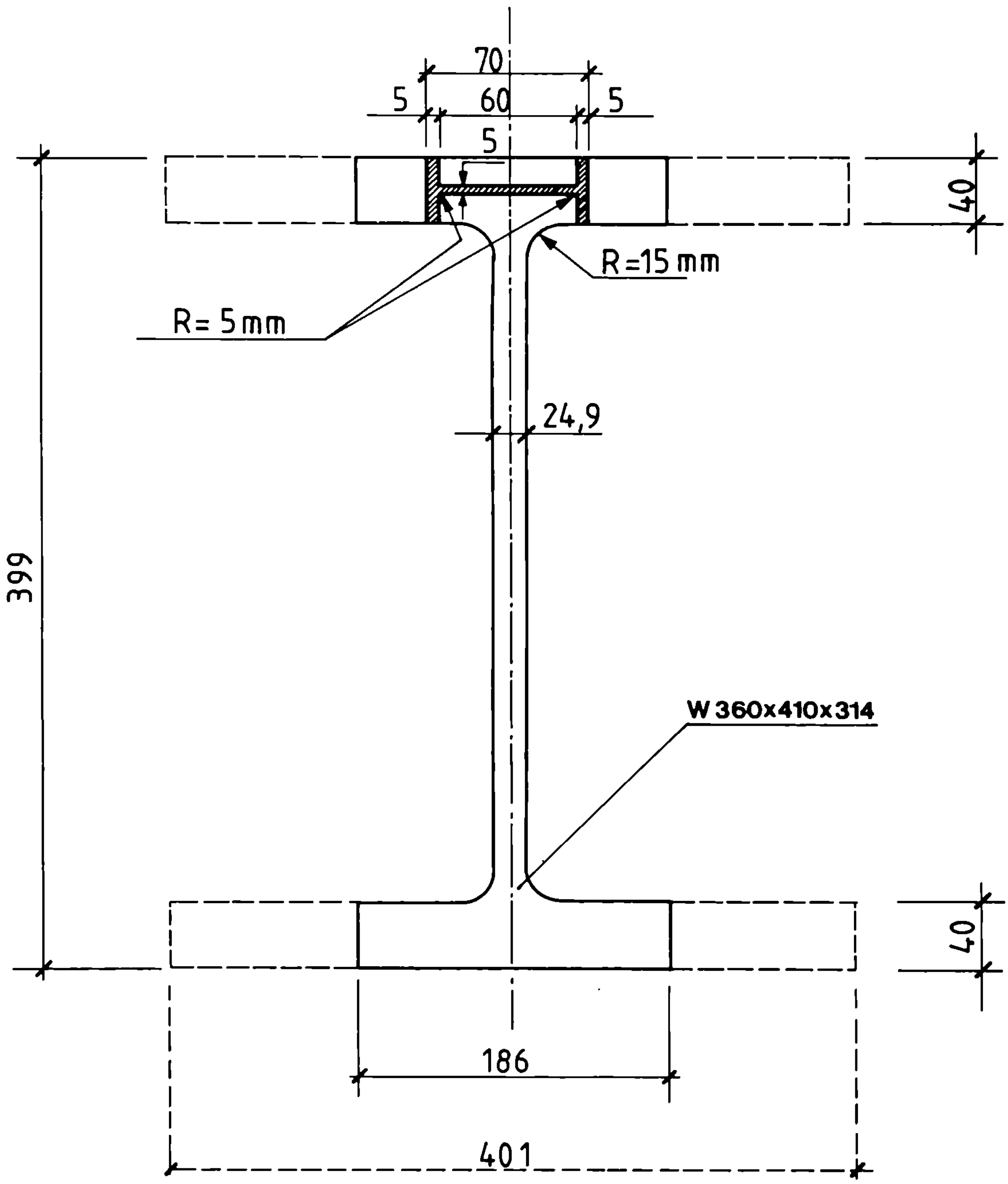

TRUNCATED BASIS BEAM

POSITION OF TESTPIECES S,V,T,P

S,V: BEAMS FOR TRANSIENT STATE BENDING TESTS

T,P: BARS FOR TENSILE TESTS

A. FeE 460

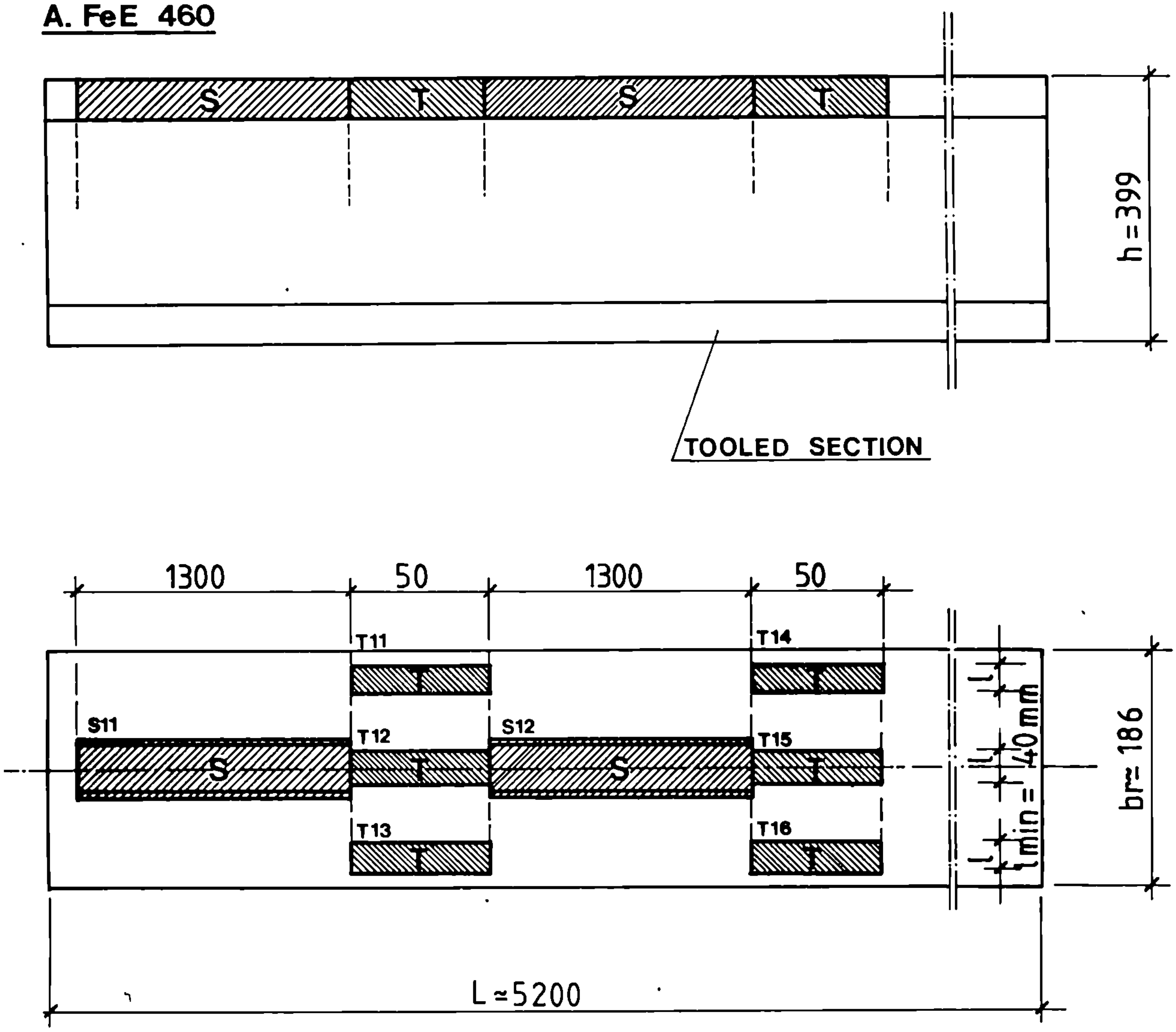

B. Fe 360

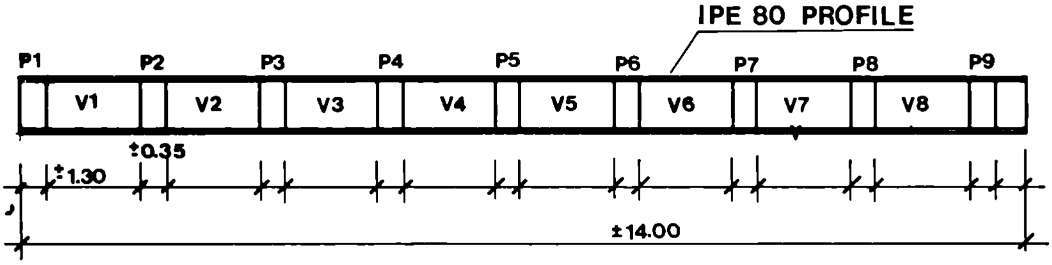

ARBED BEAM TEST : POSITION OF THERMOCOUPLES (SPECIMEN S11,S12,V1-V6)

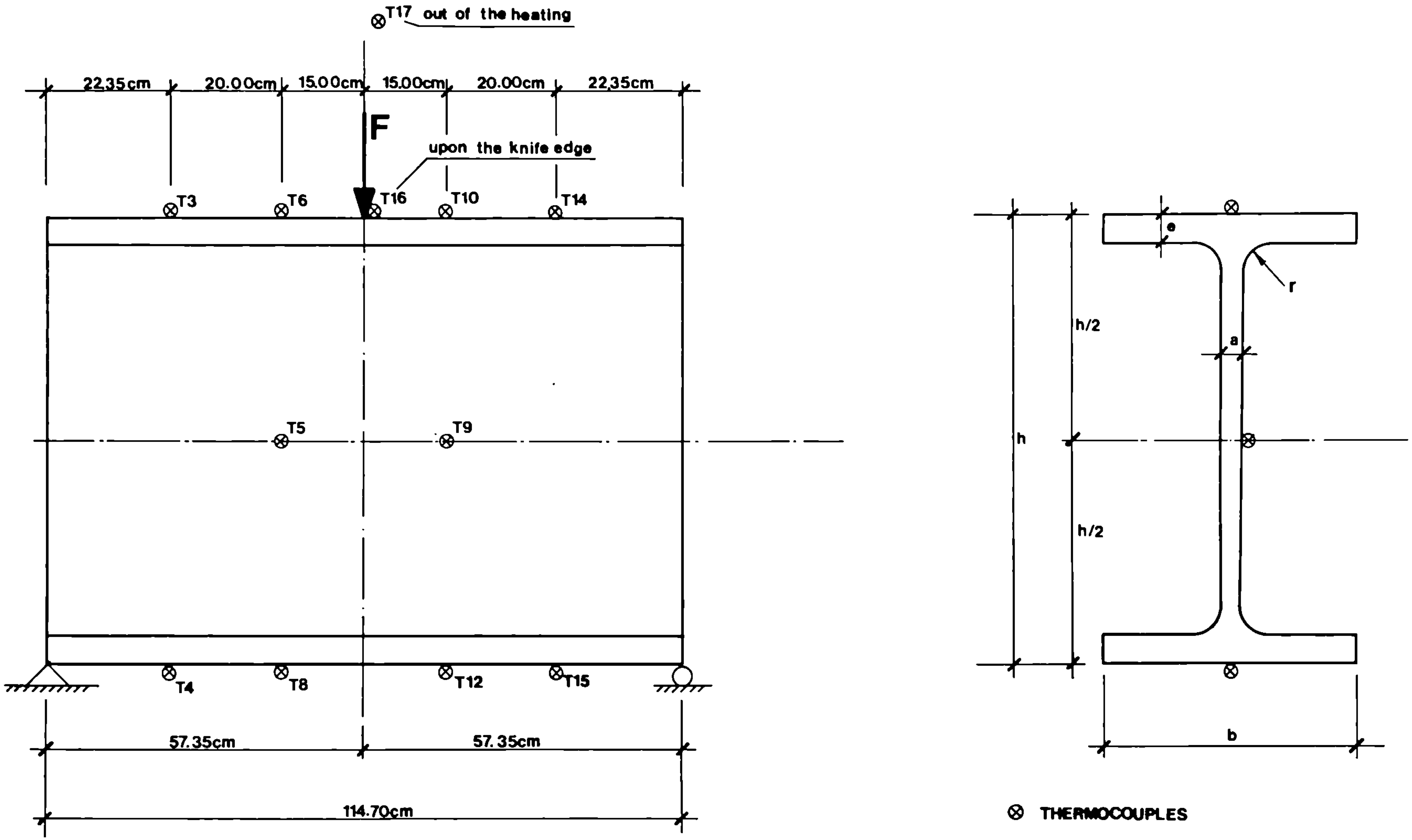

EXTREMA VALUES OF THE PROFILE TEMPERATURES CAPTED WITH THERMOCOUPLES

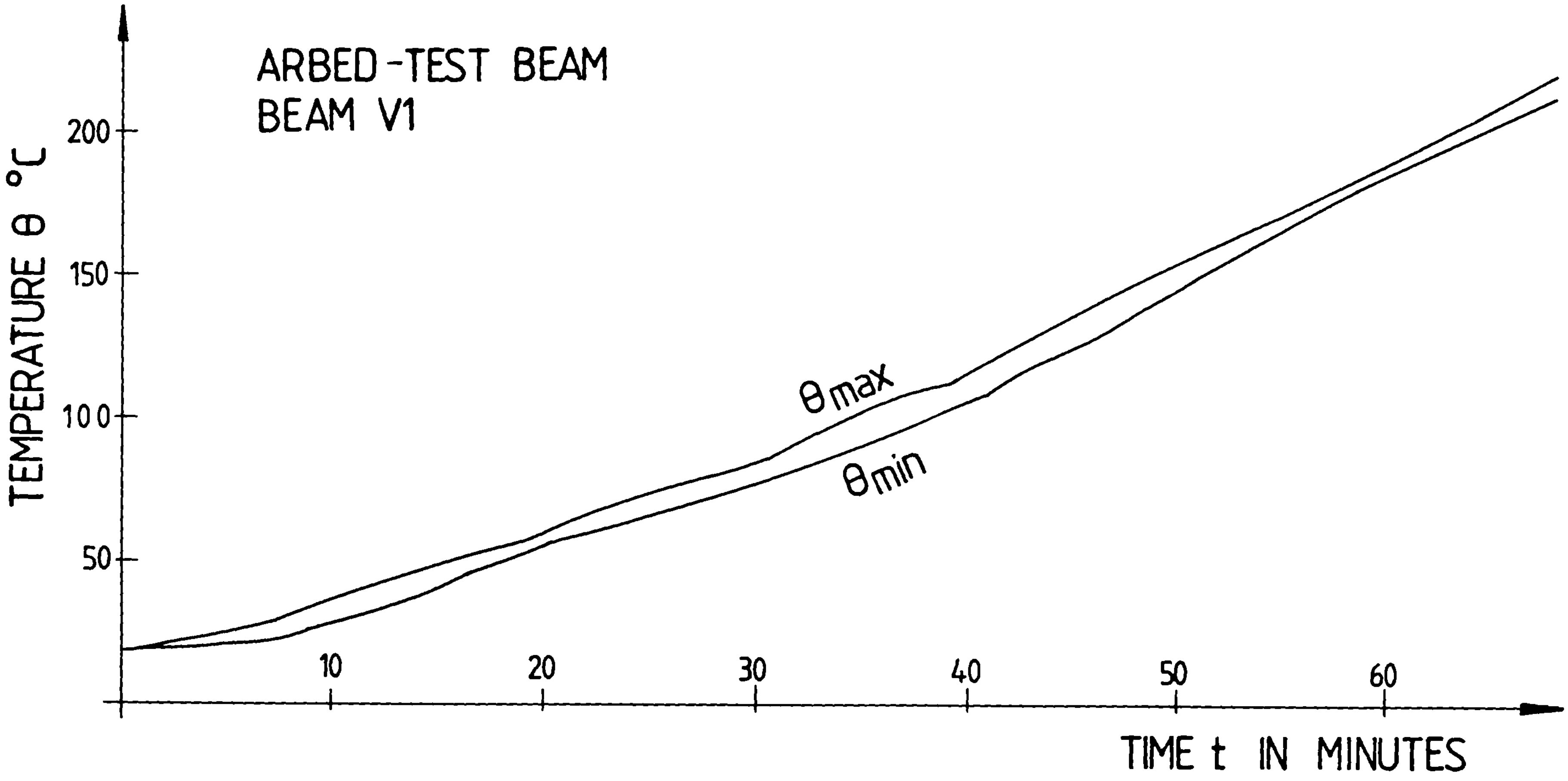

STIFFENING AGAINST BUCKLING (S12 and V2 Tests)

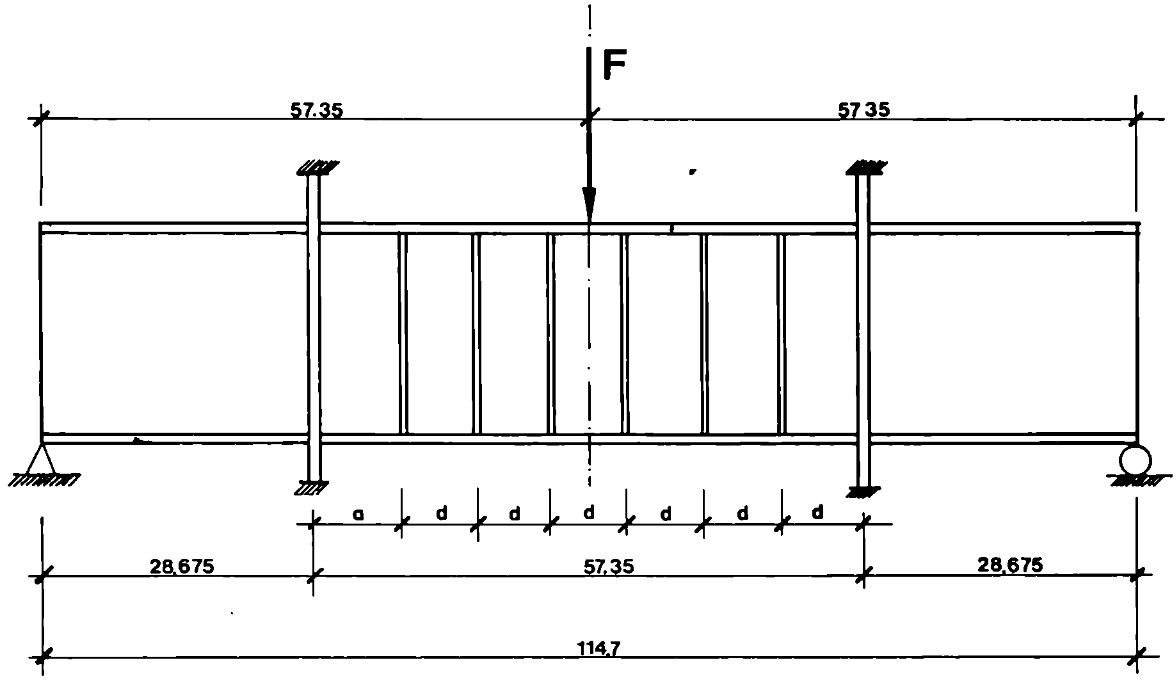

d=8.2cm

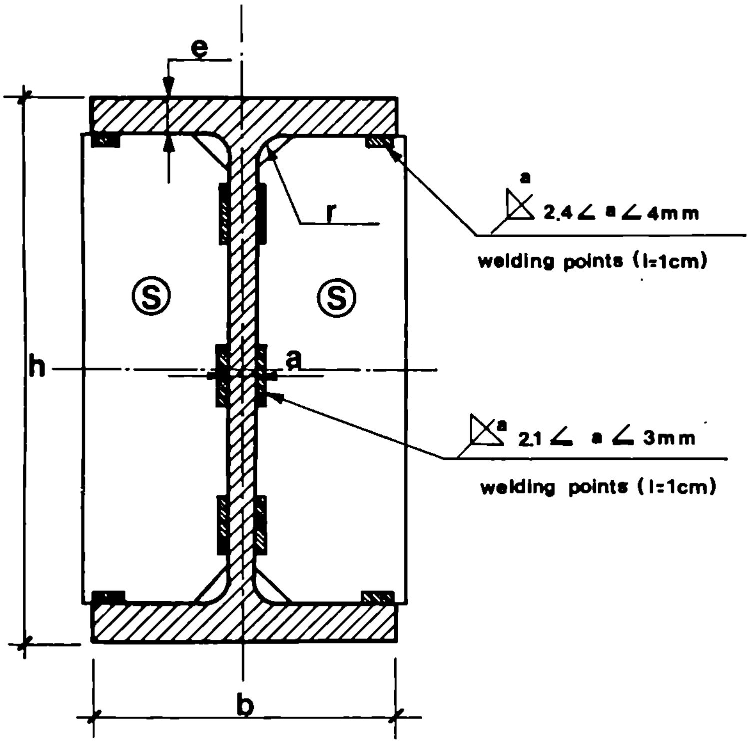

IPE 80 PROFILE (Fe360)

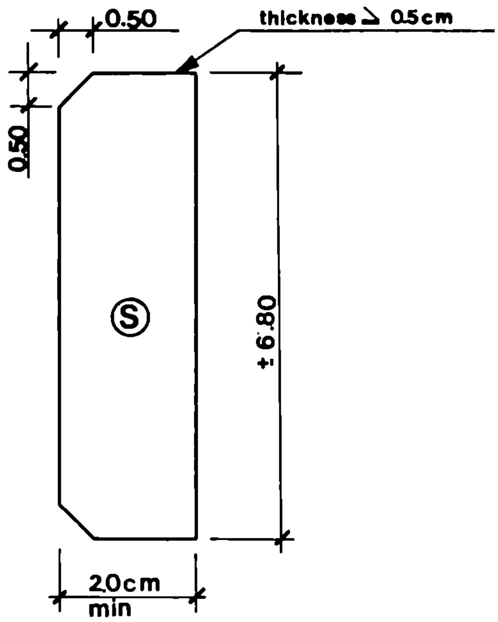

12 STIFFENERS (Fe360)

KRUPP TRANSIENT STATE BEAM TEST PARAMETERS (S11,S12 ; V1 TO V7)

Geometrical characteristics

Variables [mm]	Measures of test specimens: Tooled profile Fe E 460 steel		IPE 80 profile Fe 360 steel						
	S 11	S 12	V 1	V 2	V 3	V 4	V 5	V 6	V 7
h	70.00	70.00	80.20	80.40	80.20	80.30	80.30	80.30	80.30
b	38.00	38.00	44.50	45.30	45.00	45.00	45.00	45.00	45.00
a	5.00	5.10	4.30	4.30	4.30	4.30	4.40	4.30	4.30
e	5.00	5.10	5.50	5.80	5.70	5.80	5.70	5.80	5.80
r	5.00	5.00	5.00	4.50	4.50	4.50	4.50	4.50	4.50
F [cm2]	7.01	7.14	8.09	8.39	8.26	8.35	8.34	8.35	8.35
Wplx [cm3]	17.47	17.75	24.15	25.27	24.78	25.10	24.94	25.10	25.10

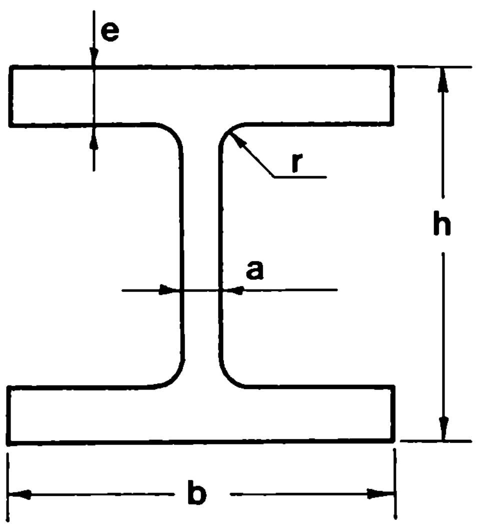

Evolution of the forces in function of the temperature (S 11 test ; Fe E 460)

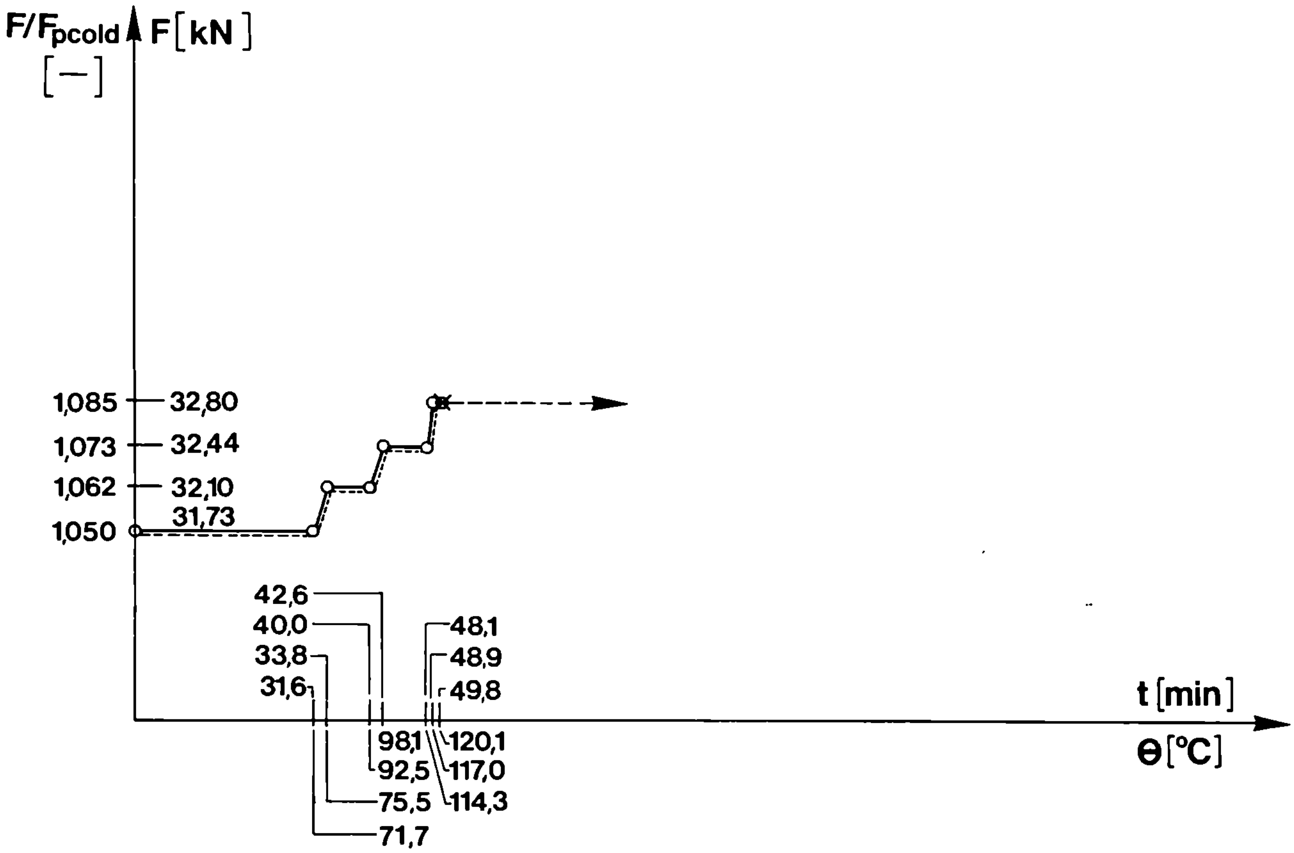

——: evolution of the test data

⌧ : failure of the beam test

----: evolution of the simulation data

failure temperature of the simulation : **460,0 °C**

Evolution of the forces in function of the temperature (S 12 test ; Fe E 460)

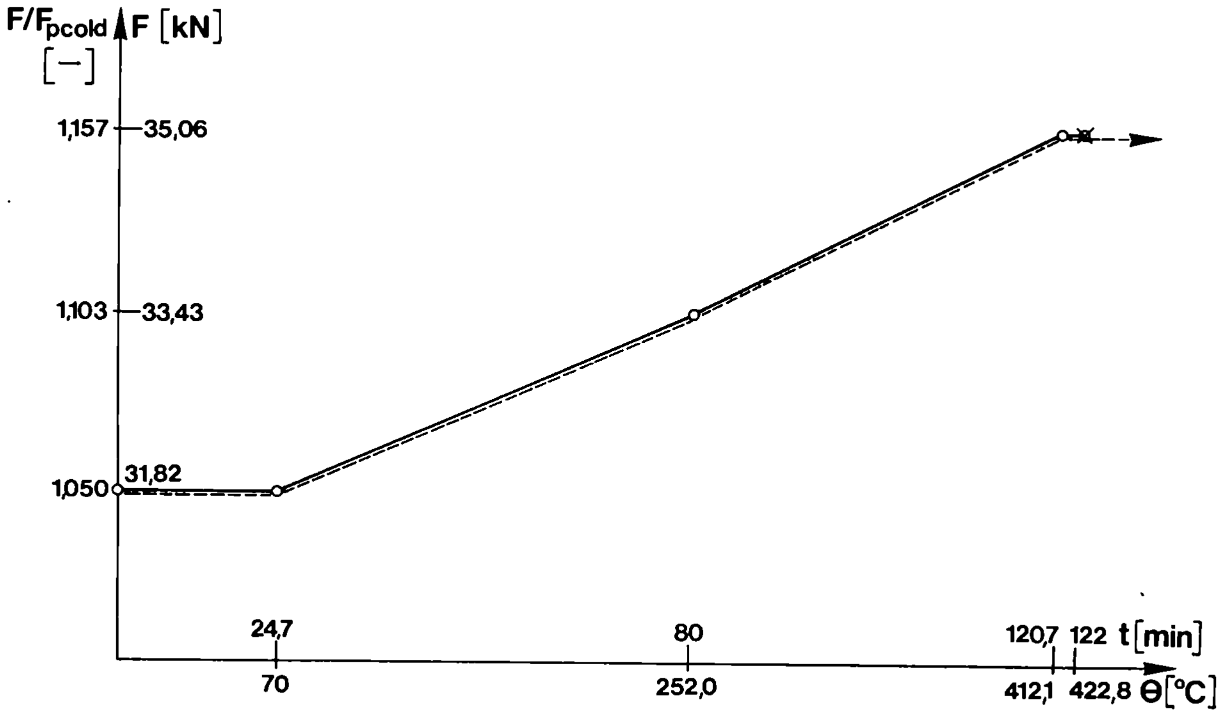

—— : evolution of the test data

✱ : failure of the beam test

----: evolution of the simulation data

failure temperature of the simulation : **440,0 °C**

KRUPP TRANSIENT STATE BEAM TEST PARAMETERS (S1 TO S10) COMPARED TO QL-LAW SIMULATIONS

STEEL QUALITY : Fe E 460

TEST	Sig y	Sig t	St/Sy	Fpcold	F	F/Fpcold	Tm	Tinit	(Tmeas.)max	(Tsim.)max	Dmeas.-sim.	(Wmeas.)max	(Wsim.)max	(Ɛsim.)max	
	[N/mm2]	[N/mm2]		[kN]	[kN]		[°C/min]	[°C]	[°C]	[°C]	[%]	[mm]	[mm]	[%]	
S1	502.00	653.00	1.30	30.00	30.00	1.000	3.60	22.10	461.00	428.00	-7.2	85.80	64.40	4.75	(1)
S3	507.00	655.00	1.29	30.30	25.80	0.850	3.50	21.70	497.00	467.00	-6.0	53.20	44.80	2.96	(2)
S2	504.50	654.00	1.30	30.20	22.70	0.750	3.40	22.50	525.00	497.00	-5.3	53.90	39.30	2.79	(2)
S4	516.00	658.00	1.28	30.80	18.50	0.600	3.50	21.40	566.00	543.00	-4.1	53.10	39.70	2.86	(2)
S10	522.50	650.00	1.24	31.20	15.60	0.500	3.40	20.10	605.00	574.00	-5.1	83.20	73.80	7.12	(2)
S5	513.00	658.00	1.28	30.70	12.30	0.400	3.50	21.00	651.00	613.00	-5.8	87.50	89.90	7.96	(2)
S9	523.50	648.00	1.24	31.30	6.30	0.200	3.50	22.40	713.00	693.00	-2.8	54.10	108.60	10.14	(2)
S7	526.00	652.00	1.24	31.40	3.20	0.100	3.50	28.00	813.00	813.00	0.0	86.90	135.90	7.78	(2)
S6	529.00	655.00	1.24	31.60	2.40	0.075	3.40	31.20	828.00	827.00	-0.1	87.80	41.10	3.13	(2)
S8	523.00	649.00	1.24	31.30	37.65	1.200	(Fmeas.)max=37.65 kN ; (Fsim.)max = 36 kN ; Dmax = -4.3 %					75.00	74.50	7.13	(3)

Remarks :

(1) after cold loading before the heating the middle-span section is already fully plastified

(2) after cold loading before the heating the middle-span section is already partially plastified or still elastic

(3) only cold loadings - unloadings

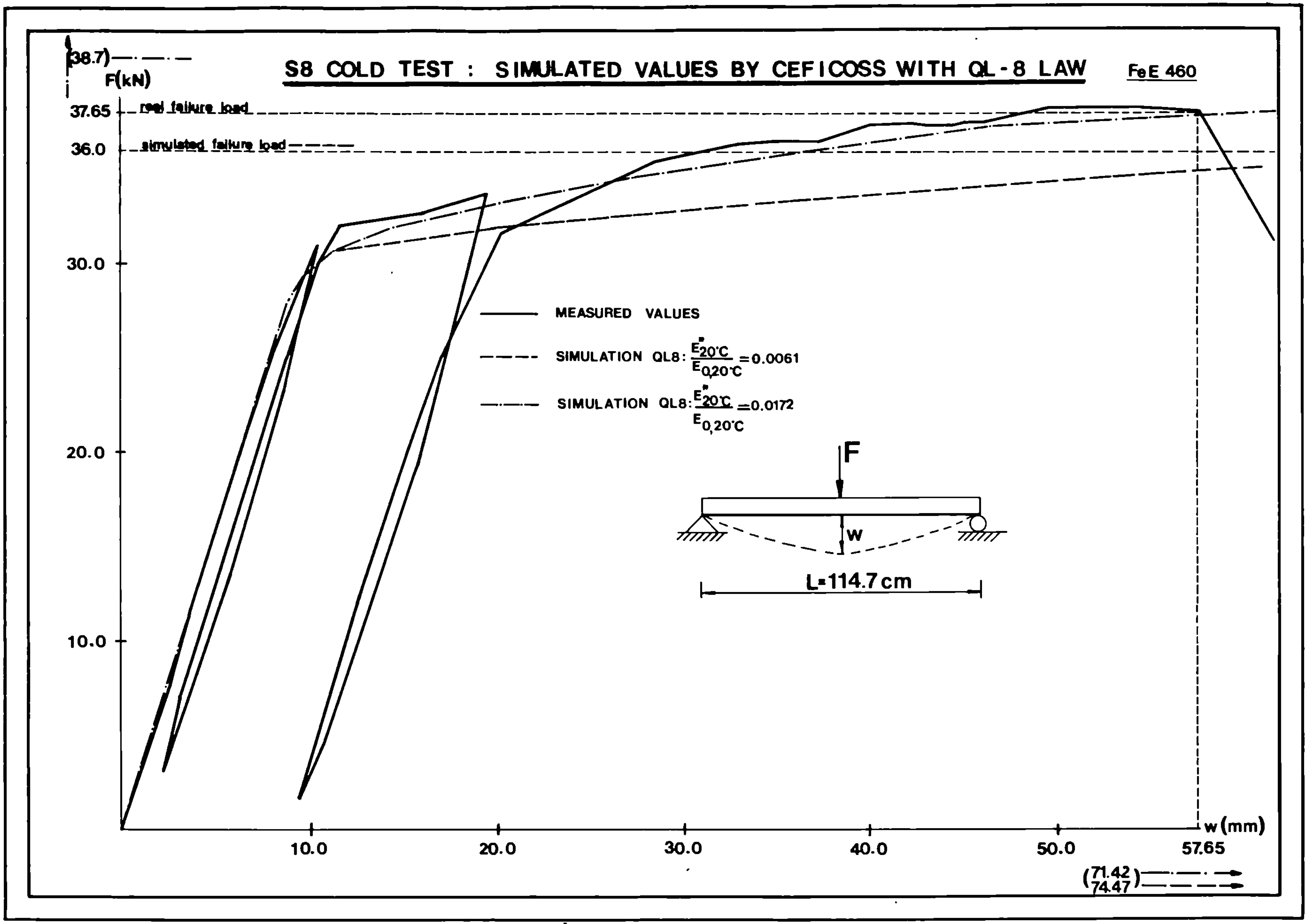
S8 COLD TEST : SIMULATED VALUES BY CEFICOSS WITH QL-8 LAW
FeE 460
F(kN)
(38.7)
37.65
real failure load
36.0
simulated failure load
30.0
20.0
10.0
10.0
20.0
30.0
40.0
50.0
57.65
w (mm)
(71.42)
(74.47)
MEASURED VALUES
SIMULATION QL8: $\frac{E^{*}_{20°C}}{E_{0,20°C}} = 0.0061$
SIMULATION QL8: $\frac{E^{*}_{20°C}}{E_{0,20°C}} = 0.0172$
F
w
L=114.7 cm

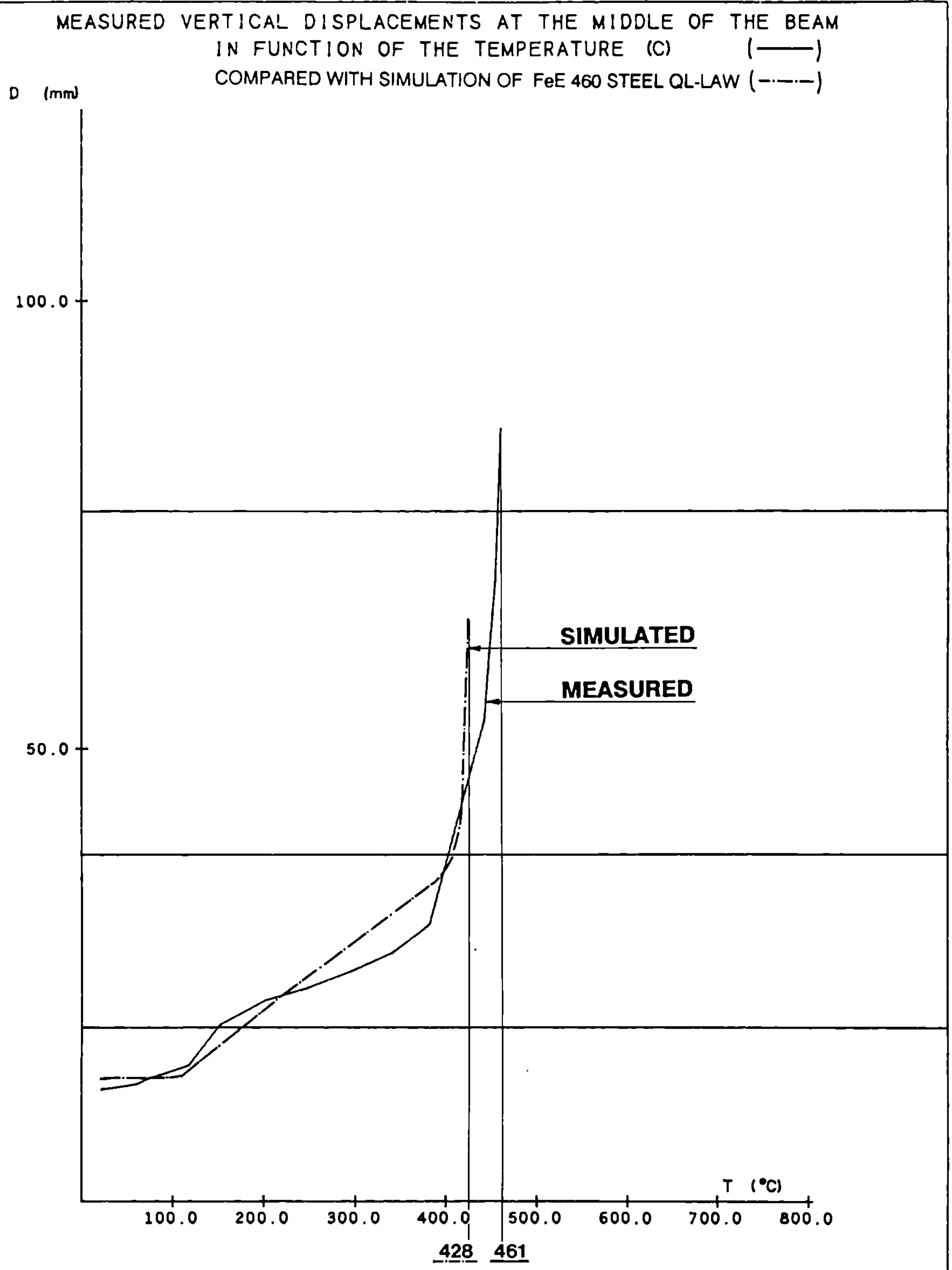

ARBED-RECHERCHES / RPS DEPARTMENT	CEFICOSS Analysis / CEF7DP1
PROJECT TITLE TEST NR. S 1- STE 460 F / FPCOLD = 1.000	PROJECT NUMBER REFAO III ESCH/ALZETTE : 28-OCT-1988 — SHEET :

MEASURED VERTICAL DISPLACEMENTS AT THE MIDDLE OF THE BEAM
IN FUNCTION OF THE TEMPERATURE (C) (———)
COMPARED WITH SIMULATION OF FeE 460 STEEL QL-LAW (-·-·-)

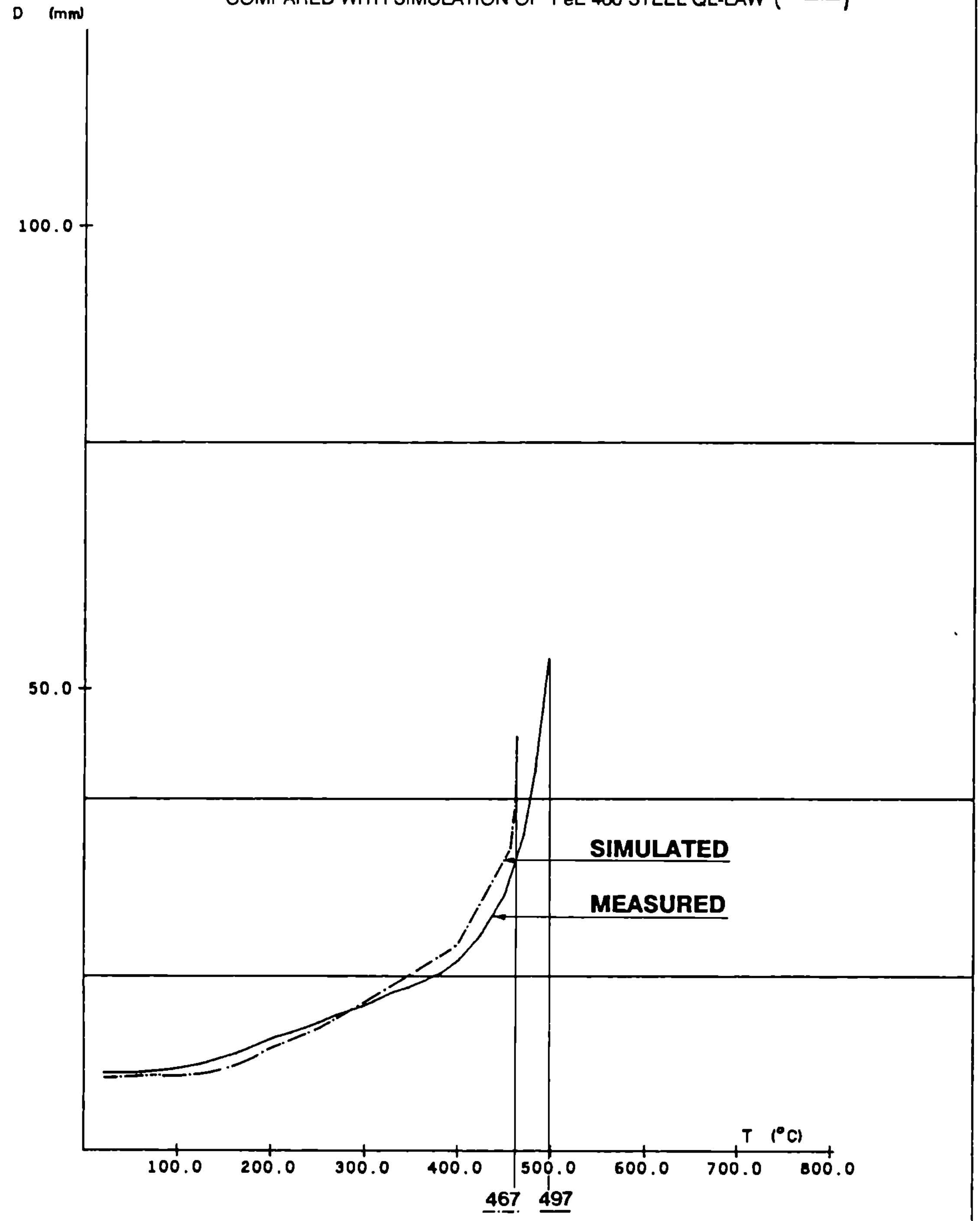

ARBED-RECHERCHES / RPS DEPARTMENT	CEFICOSS Analysis / CEF7DP1
PROJECT TITLE	PROJECT NUMBER
TEST NR. S 3- STE 460 F / FPCOLD = 0.850	REFAO III
	ESCH/ALZETTE : 28-OCT-1988 SHEET :

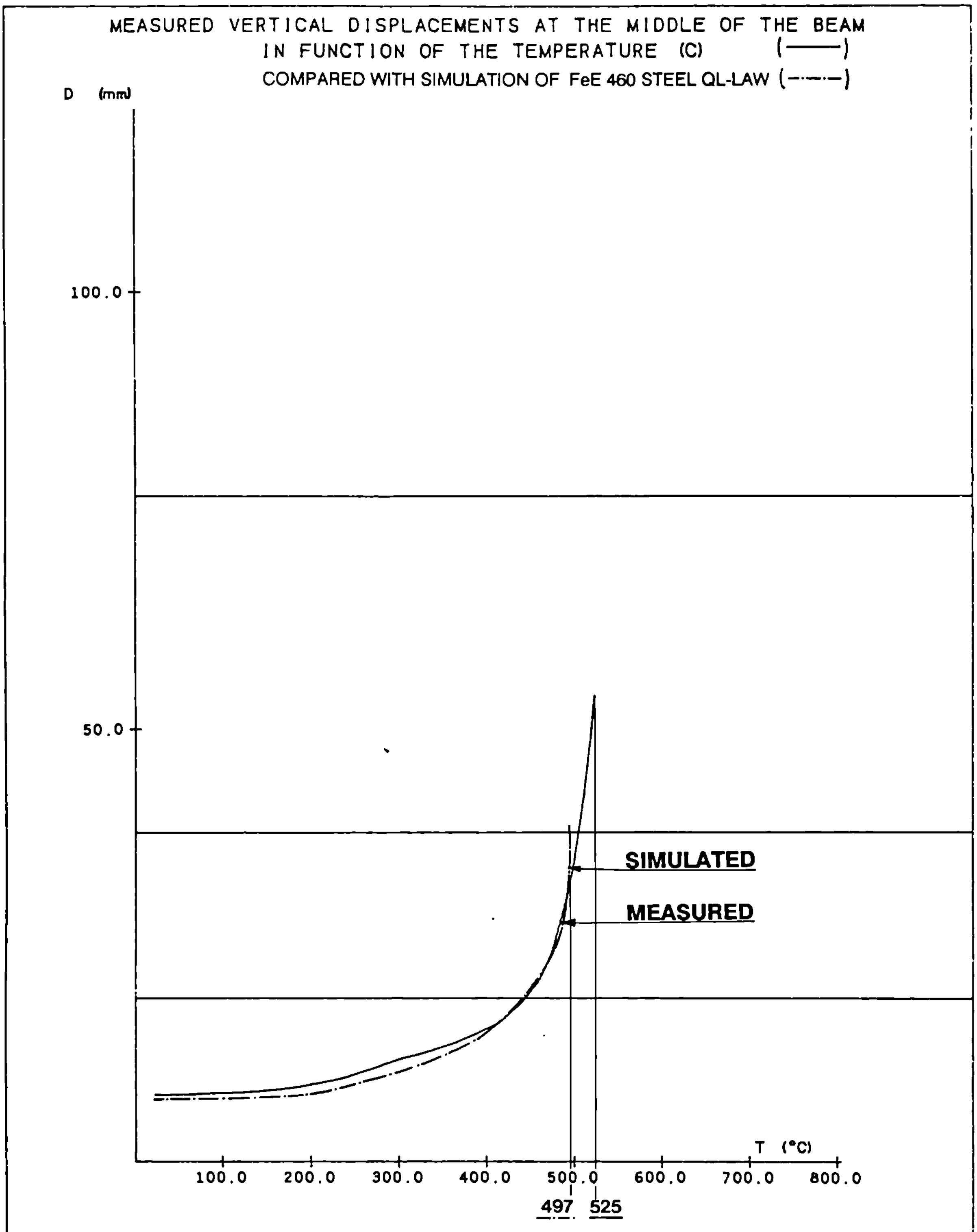

ARBED-RECHERCHES / RPS DEPARTMENT	CEFICOSS Analysis / CEF7DP1
PROJECT TITLE	PROJECT NUMBER
TEST NR. S 2- STE 460 F / FPCOLD = 0.750	REFAO III
	ESCH/ALZETTE : 28-OCT-1988 — SHEET :

MEASURED VERTICAL DISPLACEMENTS AT THE MIDDLE OF THE BEAM
IN FUNCTION OF THE TEMPERATURE (C) (———)
COMPARED WITH SIMULATION OF FeE 460 STEEL QL-LAW (—·—·—)

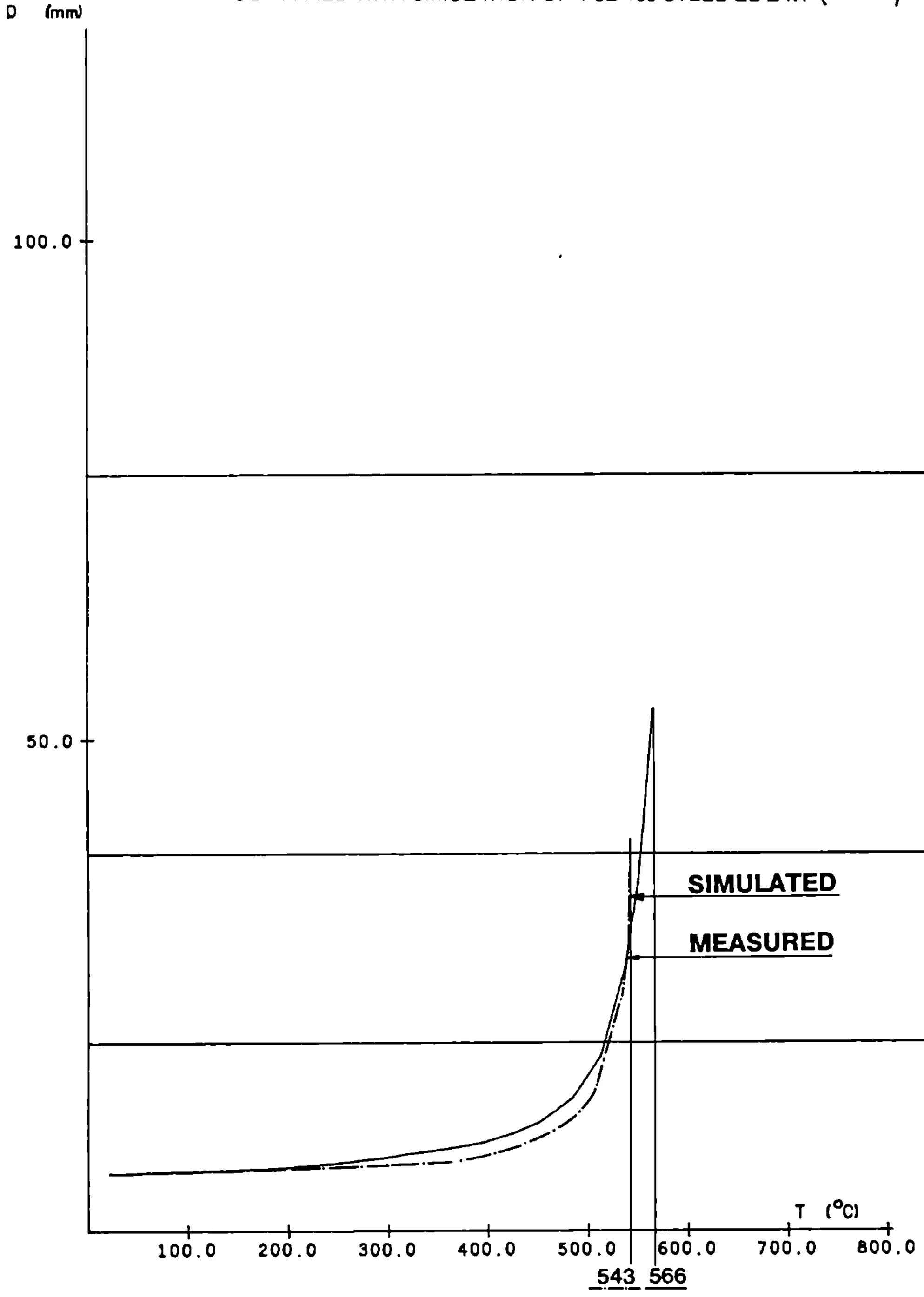

ARBED-RECHERCHES / RPS DEPARTMENT	CEFICOSS Analysis / CEF7DP1
PROJECT TITLE TEST NR. S 4- STE 460 F / FPCOLD = 0.600	PROJECT NUMBER REFAO III ESCH/ALZETTE : 28-OCT-1988 · SHEET :

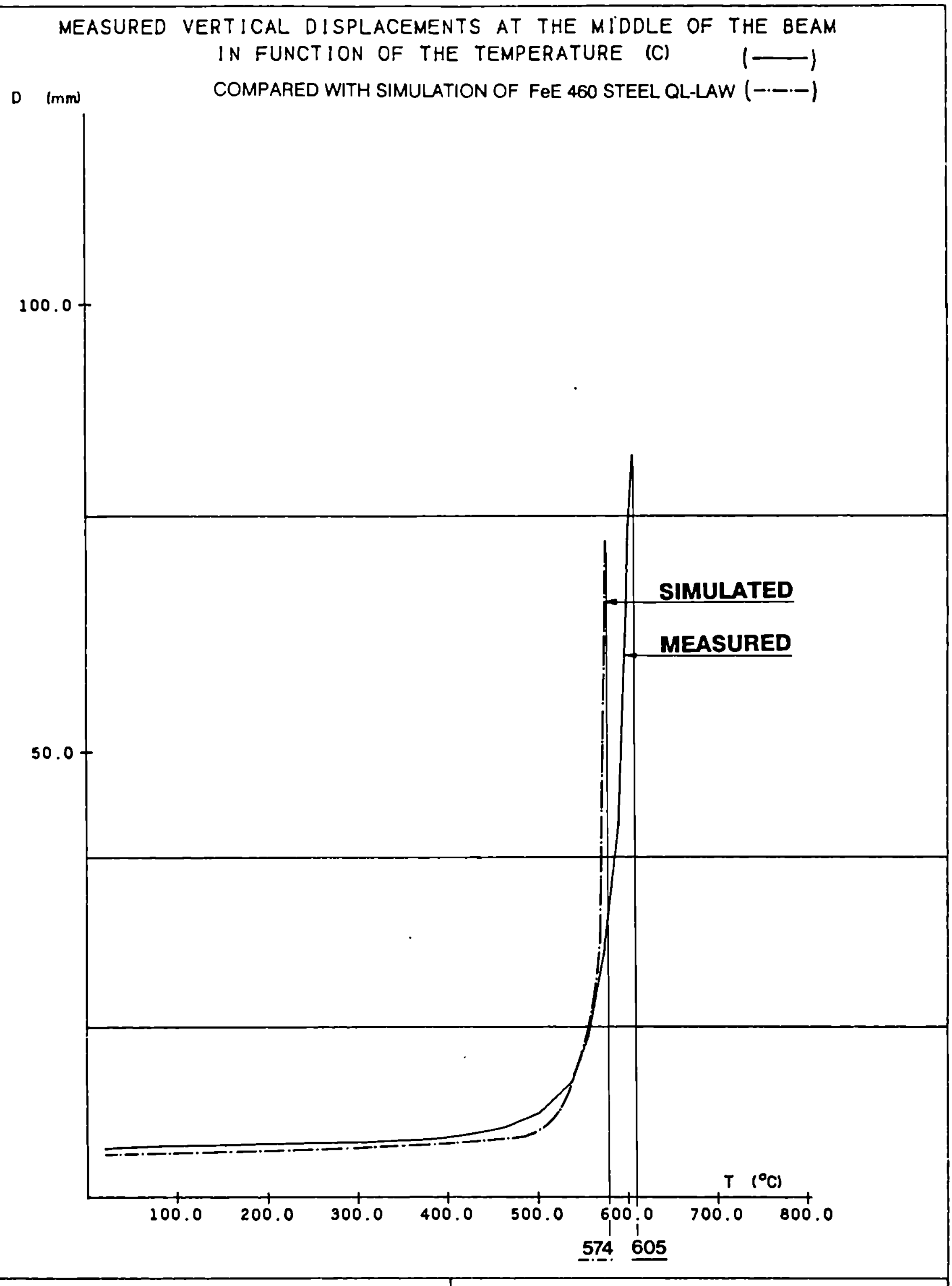

ARBED-RECHERCHES / RPS DEPARTMENT	CEFICOSS Analysis / CEF7DP1
PROJECT TITLE TEST NR. S10- STE 460 F / FPCOLD = 0.500	PROJECT NUMBER REFAO III ESCH/ALZETTE : 28-OCT-1988 | SHEET :

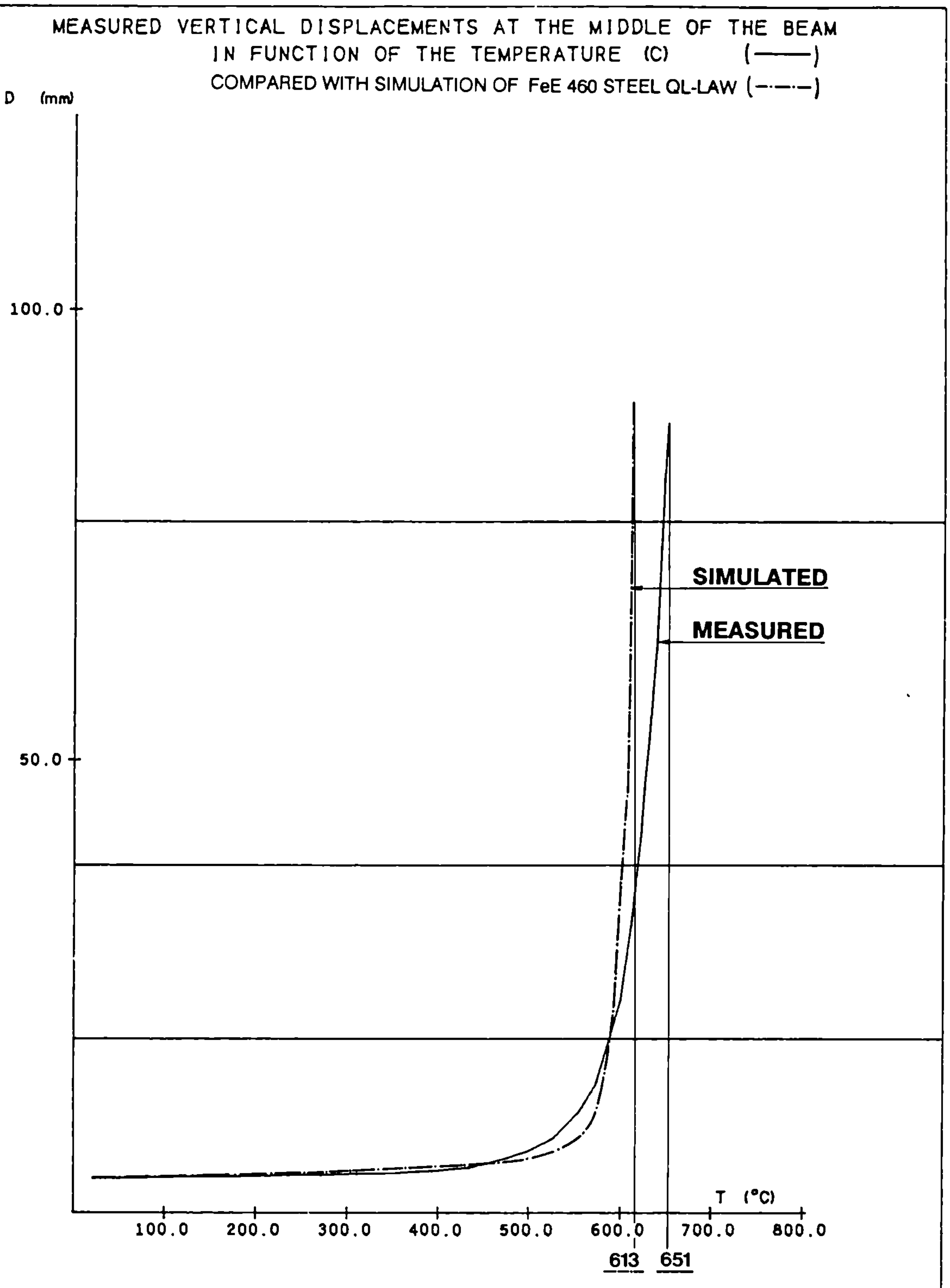

ARBED-RECHERCHES / RPS DEPARTMENT	CEFICOSS Analysis / CEF7DP1
PROJECT TITLE TEST NR. S 5- STE 460 F / FPCOLD = 0.400	PROJECT NUMBER REFAO III ESCH/ALZETTE : 28-OCT-1988 SHEET :

MEASURED VERTICAL DISPLACEMENTS AT THE MIDDLE OF THE BEAM
IN FUNCTION OF THE TEMPERATURE (C) (——)
COMPARED WITH SIMULATION OF FeE 460 STEEL QL-LAW (—·—·—)

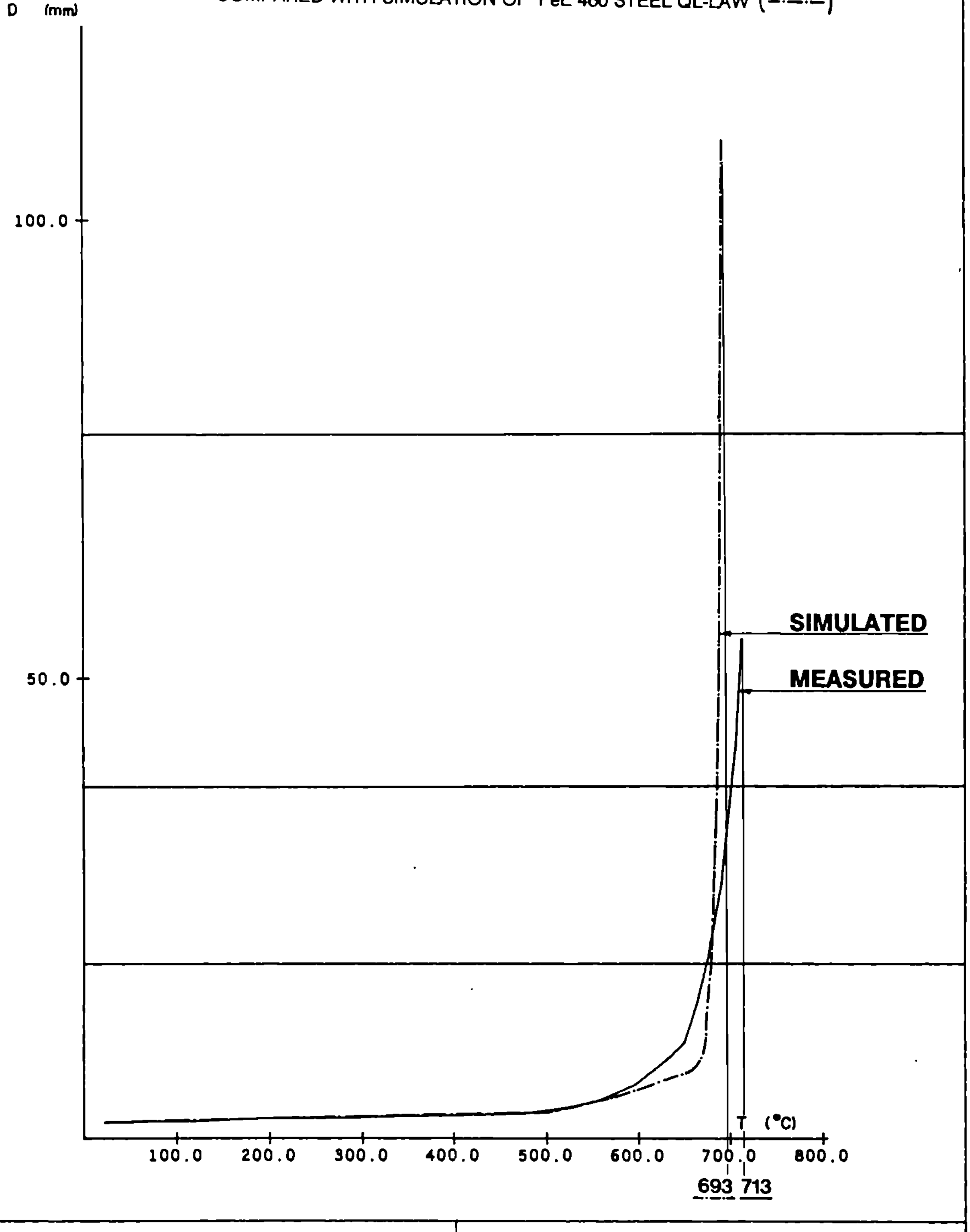

ARBED-RECHERCHES / RPS DEPARTMENT	CEFICOSS Analysis / CEF7DP1
PROJECT TITLE TEST NR. S 9- STE 460 F / FPCOLD = 0.200	PROJECT NUMBER REFAO III ESCH/ALZETTE : 28-OCT-1988 | SHEET :

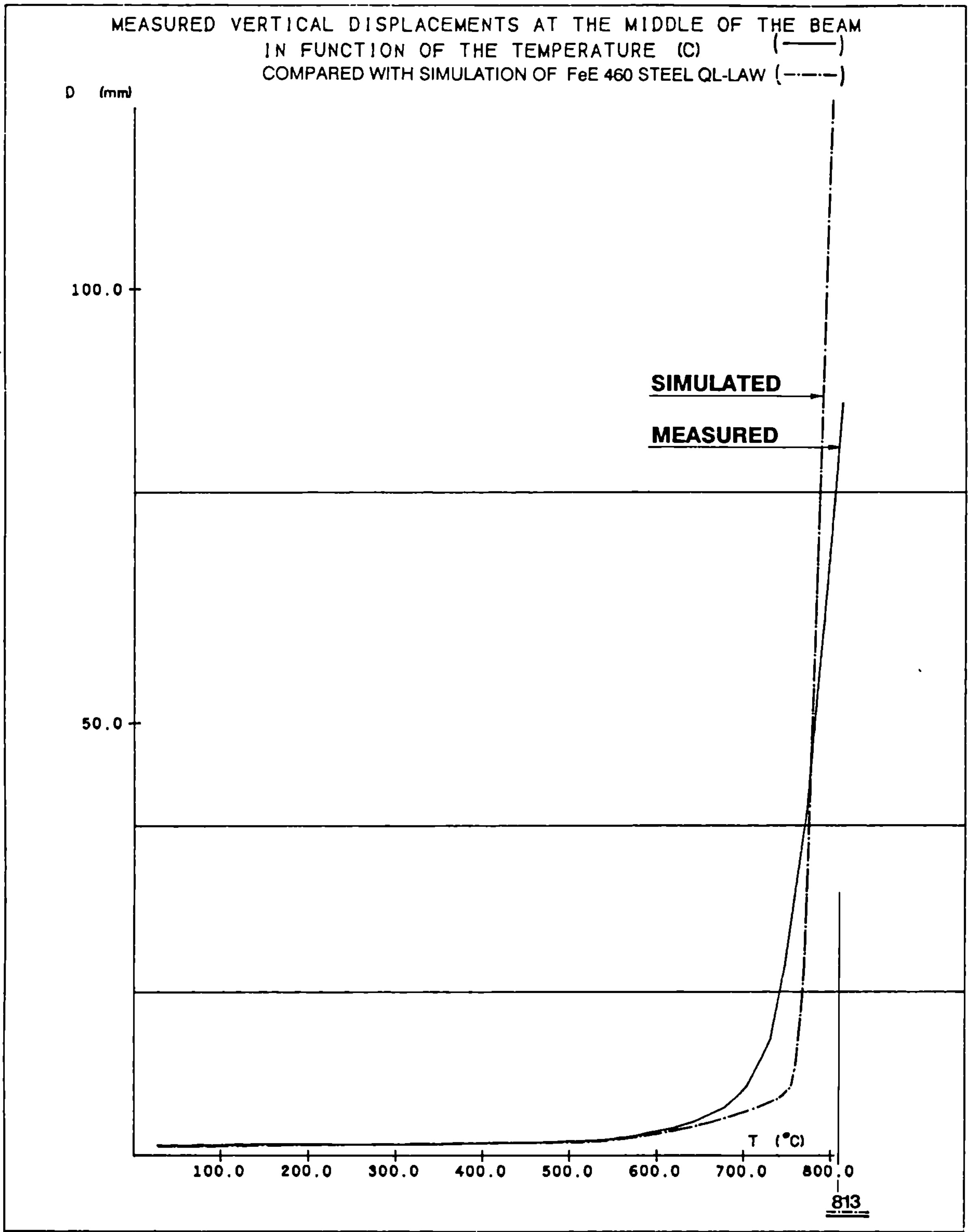

ARBED-RECHERCHES / RPS DEPARTMENT	CEFICOSS Analysis / CEF7DP1
PROJECT TITLE TEST NR. S 7- STE 460 F / FPCOLD = 0.100	PROJECT NUMBER REFAO III ESCH/ALZETTE : 28-OCT-1988 SHEET :

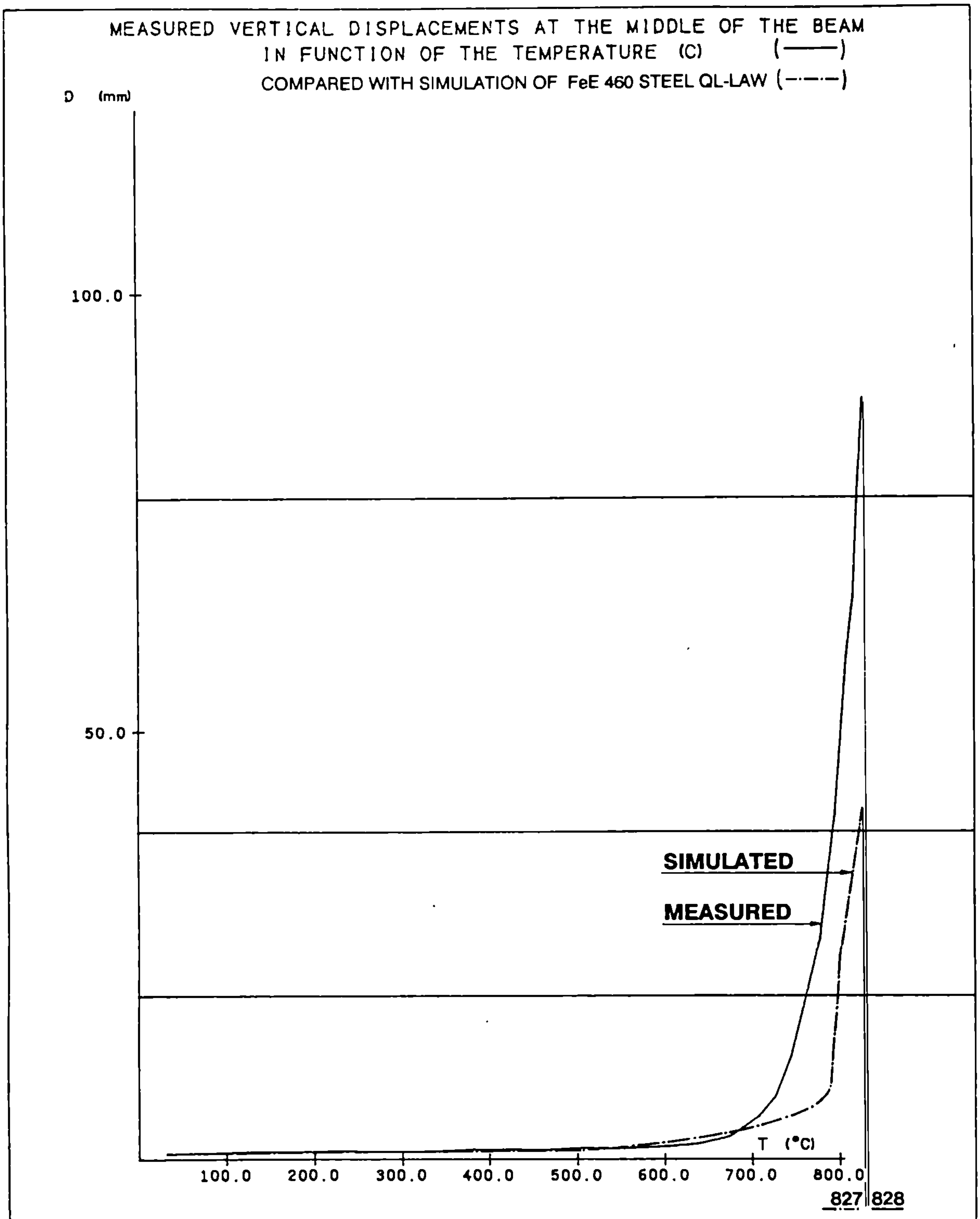

ARBED-RECHERCHES / RPS DE'4'ARTMENT | CEFICOSS Analysis / CEF7DP1

PROJECT TITLE

TEST NR. S 6- STE 460
F / FPCOLD = 0.075

PROJECT NUMBER

REFAO III

ESCH/ALZETTE : 28-OCT-1988 | SHEET :

KRUPP TRANSIENT STATE BEAM TEST PARAMETERS (S11,S12 ; V1 TO V7) COMPARED TO QL-LAW SIMULATIONS

STEEL QUALITY	TEST	PROFILES	Sig y [N/mm2]	Sig t [N/mm2]	St/Sy	Wplx [cm3]	Fpcold (1) [kN]	F [kN]	F/Fpcold	(Tmeas.)max (7) [°C]	(Tsim.)max [°C]	Dmeas.-sim. [%]	(Wmeas.)max [mm]	(Wsim.)max [mm]	(Esim.)max [%]	(Fmeas.)max [kN]	(F/Fpcold)max measured	
Fe E 460	S11	TOOLED PROFILES	496.00	758.00	1.53	17.470	30.22	31.73	1.05	120.10	460.0	(8)	21.34	135.20	12.43	32.80	1.085	(2),(6)
	S12		489.50	744.50	1.52	17.750	30.30	31.82	1.05	422.80	440.0	4.07	54.70	98.00	7.41	35.06	1.157	(2),(5)
Fe 360	V1	IPE 80	321.80	508.30	1.58	24.150	27.10	29.81	1.10	217.80	440.0	(8)	37.90	84.00	8.67	32.41	1.196	(2),(6)
	V2		315.00	505.30	1.60	25.270	27.76	30.54	1.10	336.90	440.0	(8)	58.90	63.70	5.68	33.36	1.202	(2),(5)
	V3		310.00	501.50	1.62	24.780	26.79	22.77	0.85	530.00	530.0	0.00	95.30	57.10	5.27			(3)
	V4		308.00	503.30	1.63	25.100	26.96	16.18	0.60	600.00	595.0	-0.83	90.66	90.10	7.75			(3)
	V5		310.00	505.30	1.63	24.940	26.96	13.48	0.50	630.00	625.0	-0.79	78.60	105.20	8.22			(3)
	V6		312.00	506.00	1.62	25.100	27.31	2.73	0.10	921.00	900.0	-2.28	78.40	242.10	14.66			(3)
	V7		311.80	504.30	1.62	25.100	27.29	33.02	1.21	(Fmeas.)max=33.02 kN; (Fsim.)max=32.3 kN;Dmax=-2.2%			67.10	44.90	4.69	33.02	1.210	(4)

REMARKS ON THE KRUPP TRANSIENT BEAM TEST PARAMETERS (S11,S12;V1 TO V7)

(1) Fpcold, the theoretical necessary applied force to obtain the middle-span section fully plastified (plastic hinge) with a bi-rectangular stress distribution (rigid-plastic theory) = 4*Sigy*Wplx/L (for a simply-supported beam, with a mid-span concentrated load)

(2) Testing procedure (plastic domain) :

a) cold loading till F/Fpcold level
b) heating with constant load
c) heating and load increasing together till collapse

(3) Testing procedure (elasto-plastic domain) :

a) cold loading till F/Fpcold level
b) heating with constant load F till collapse

(4) Testing procedure (cold test) :

cold loading till collapse with unloading

(5) Specimens with stiffeners welded by points like shown on figure 2.6

(6) The load is applied to these beams (V1;S11) via a ball (between the plunger of the actuator and the upper flange) instead of a kind of knife edge for the other beams (V2 to V7;S12) better against buckling

(7) Mean value of the temperature measured with numbers 6, 8, 10 and 12 thermocouples

(8) Early lateral-torsional buckling failure problem

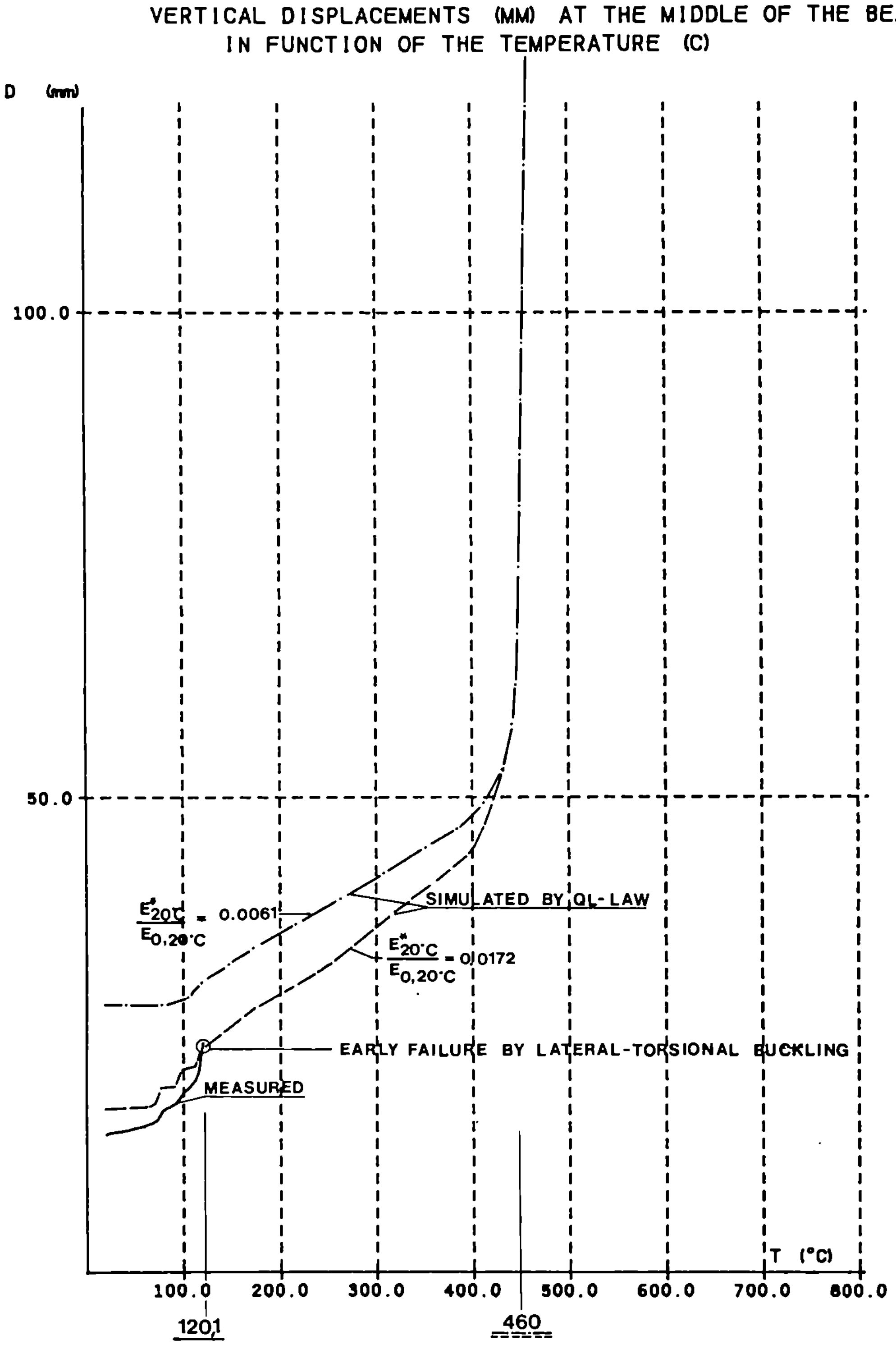

ARBED-RECHERCHES / RPS DEPARTMENT	CEFICOSS Analysis / CEF8.1
PROJECT TITLE	PROJECT NUMBER
TEST NR. S11 - Fe E 460 F/FPcold = 1.05 (+ variable loads)	REFAO III ESCH/ALZETTE : 6-MAR-1989 SHEET :

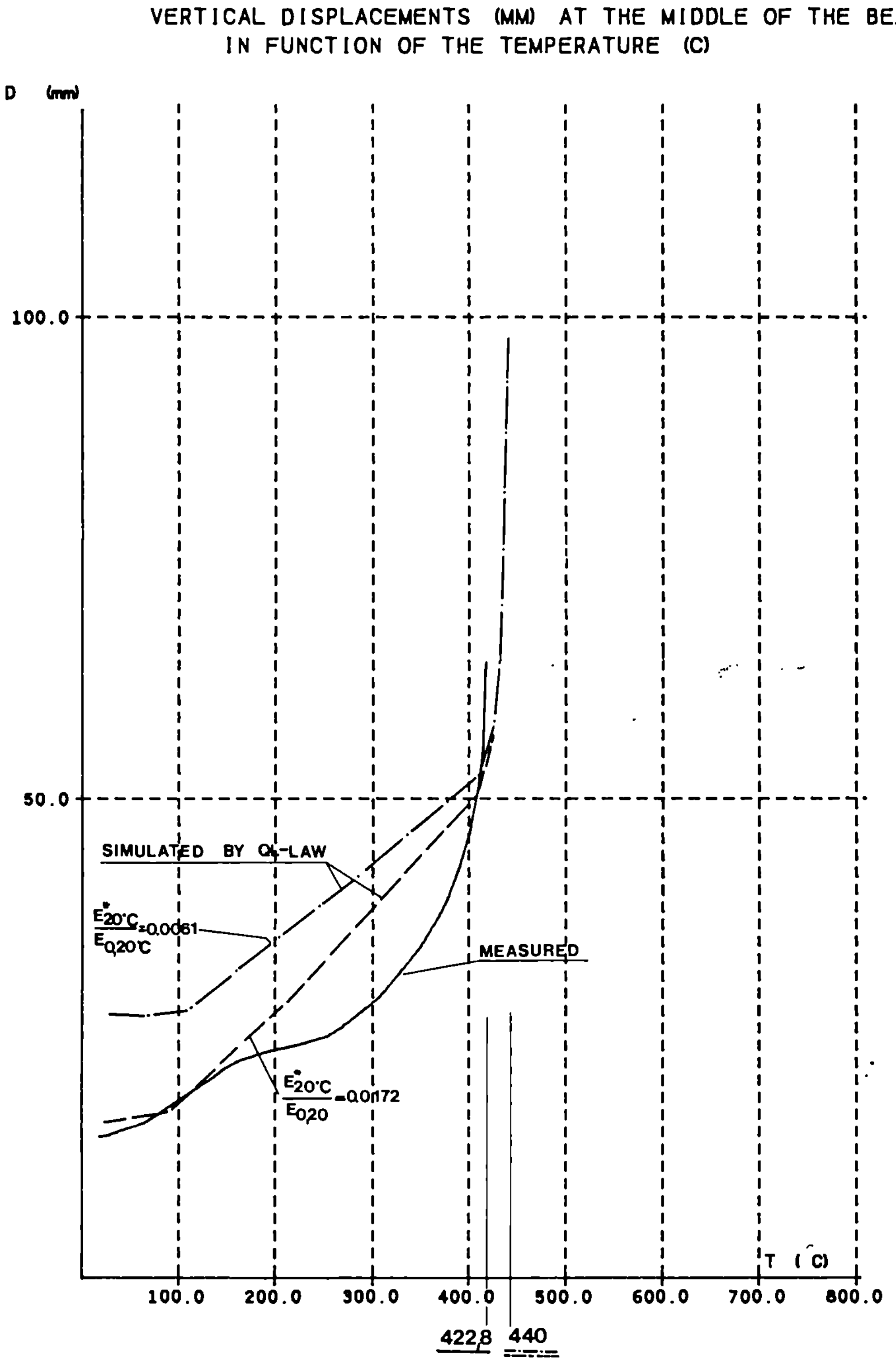

ARBED-RECHERCHES / RPS DEPARTMENT	CEFICOSS Analysis / CEF8.1
PROJECT TITLE TEST NR. S12 - Fe E 460 F/FPcold = 1.05 (+ variable loads)	**PROJECT NUMBER** REFAO III ESCH/ALZETTE : 6-MAR-1989	SHEET :

VERTICAL DISPLACEMENTS (MM) AT THE MIDDLE OF THE BEAM
IN FUNCTION OF THE TEMPERATURE (C)

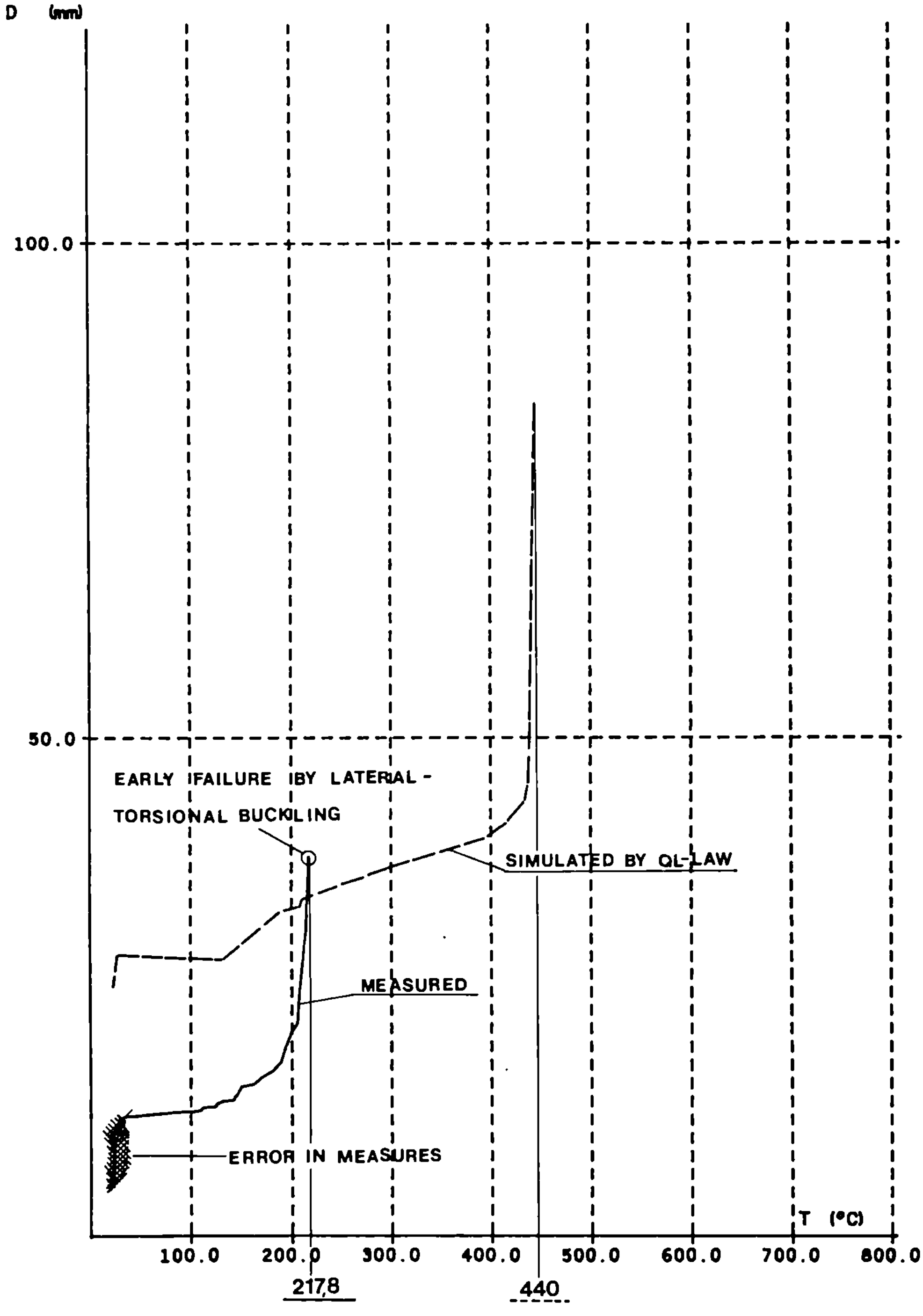

ARBED-RECHERCHES / RPS DEPARTMENT	CEFICOSS Analysis / CEF8.1
PROJECT TITLE TEST NR. V 1 - Fe 360 F/FPcold = 1.10 (+ variable loads)	PROJECT NUMBER REFAO III ESCH/ALZETTE : 6-MAR-1989 SHEET :

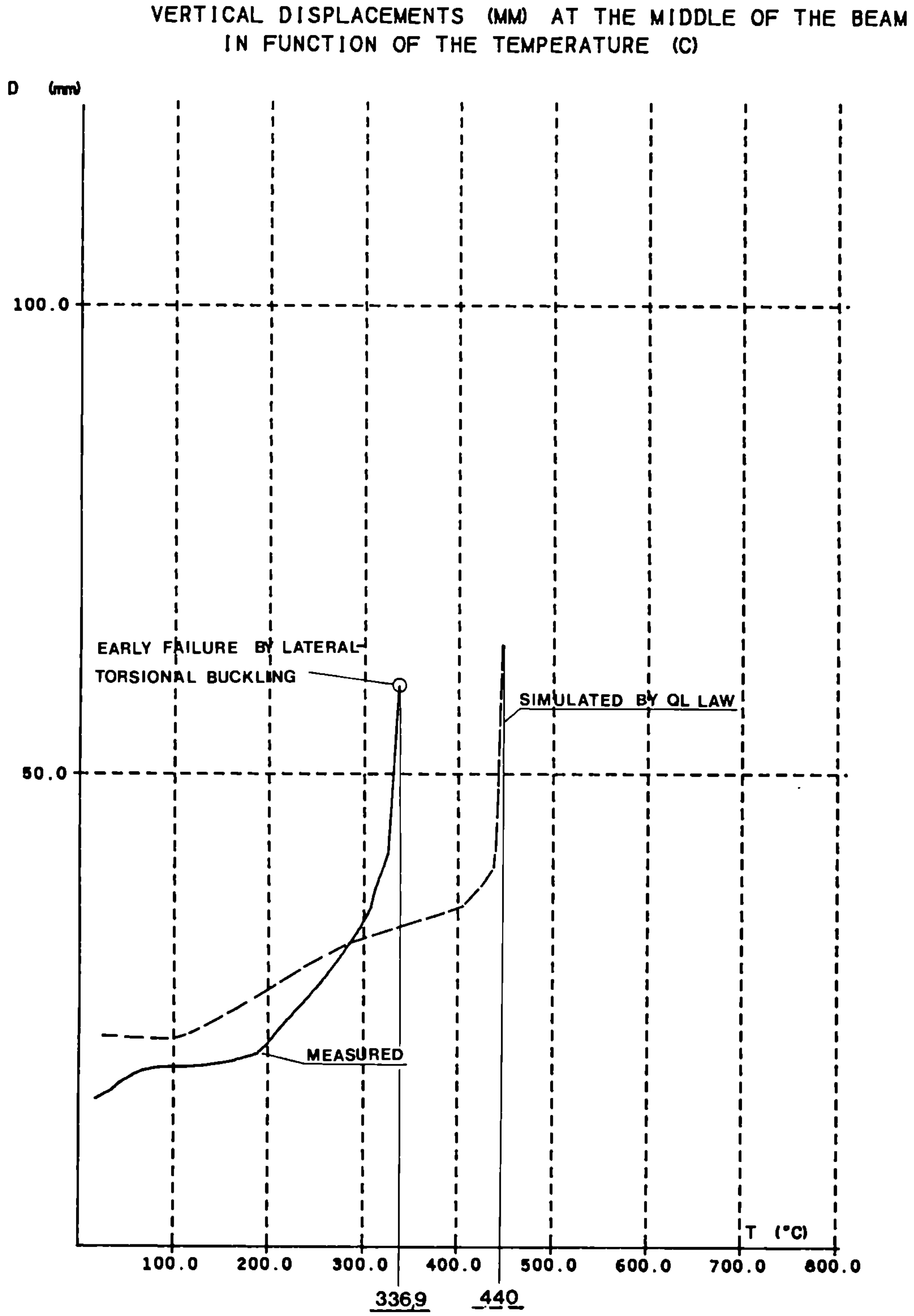

ARBED-RECHERCHES / RPS DEPARTMENT	CEFICOSS Analysis / CEF8.1
PROJECT TITLE TEST NR. V 2 - Fe 360 F/FPcold = 1.10 (+ variable loads)	PROJECT NUMBER REFAO III ESCH/ALZETTE : 6-MAR-1989	SHEET :

VERTICAL DISPLACEMENTS (MM) AT THE MIDDLE OF THE BEAM
IN FUNCTION OF THE TEMPERATURE (C)

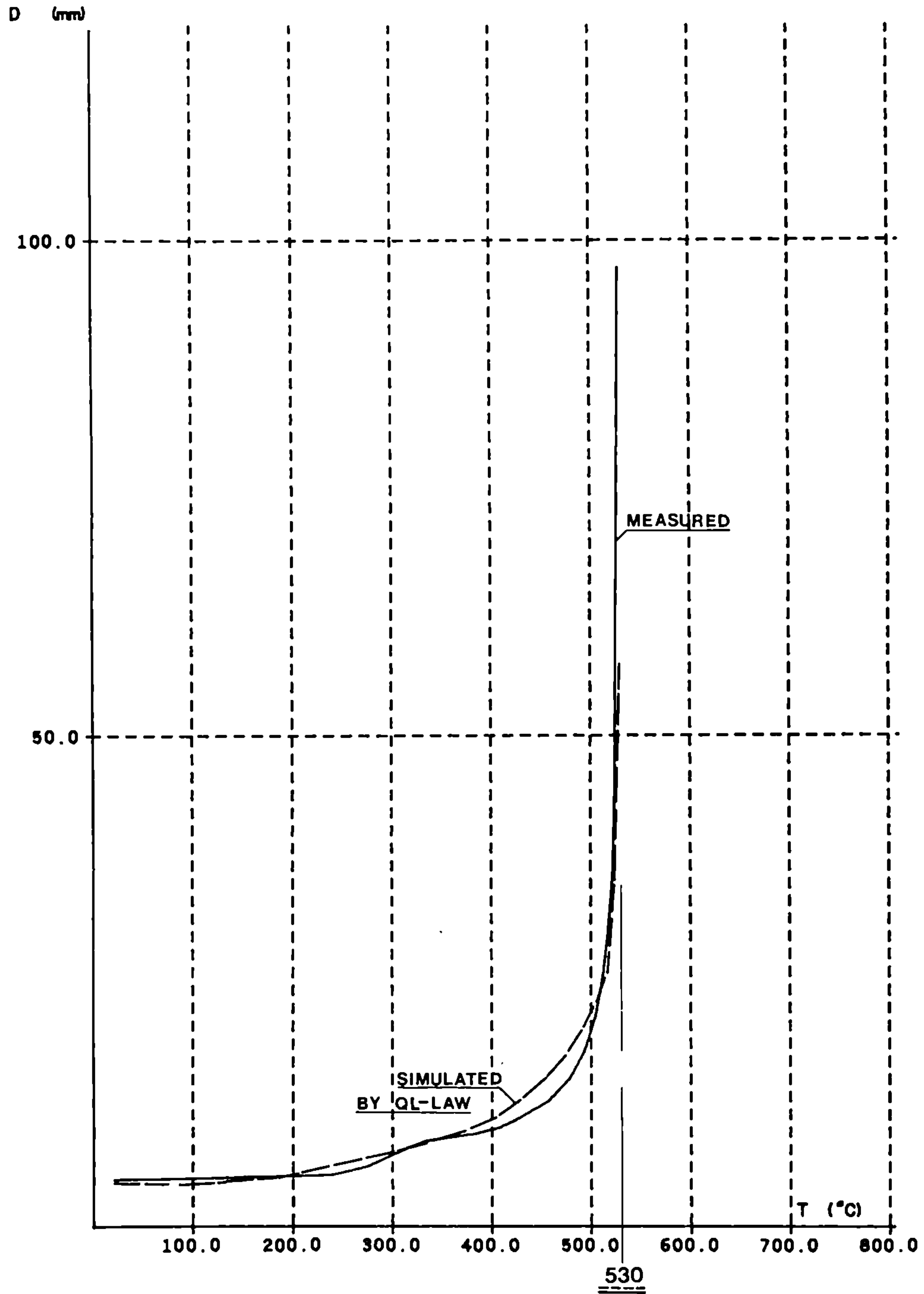

ARBED-RECHERCHES / RPS DEPARTMENT	CEFICOSS Analysis / CEF8.1
PROJECT TITLE	**PROJECT NUMBER**
TEST NR. V 3 - Fe 360 F/FPcold = 0.85	REFAO III
	ESCH/ALZETTE : 6-MAR-1989 SHEET :

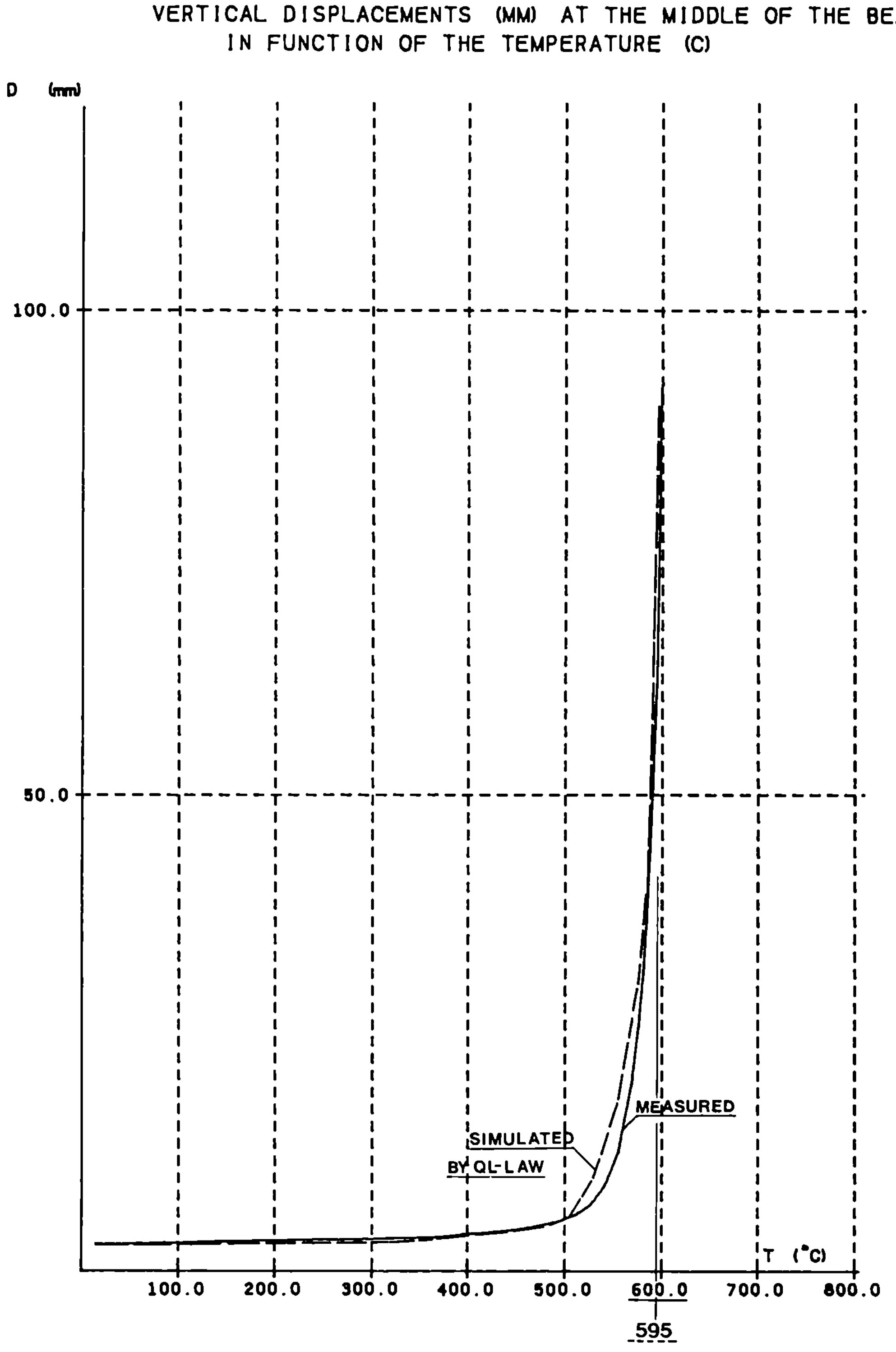

ARBED-RECHERCHES / RPS DEPARTMENT	CEFICOSS Analysis / CEF8.1
PROJECT TITLE TEST NR. V 4 - Fe 360 F/FPcold = 0.60	PROJECT NUMBER REFAO III ESCH/ALZETTE : 6-MAR-1989 SHEET :

VERTICAL DISPLACEMENTS (MM) AT THE MIDDLE OF THE BEAM
IN FUNCTION OF THE TEMPERATURE (C)

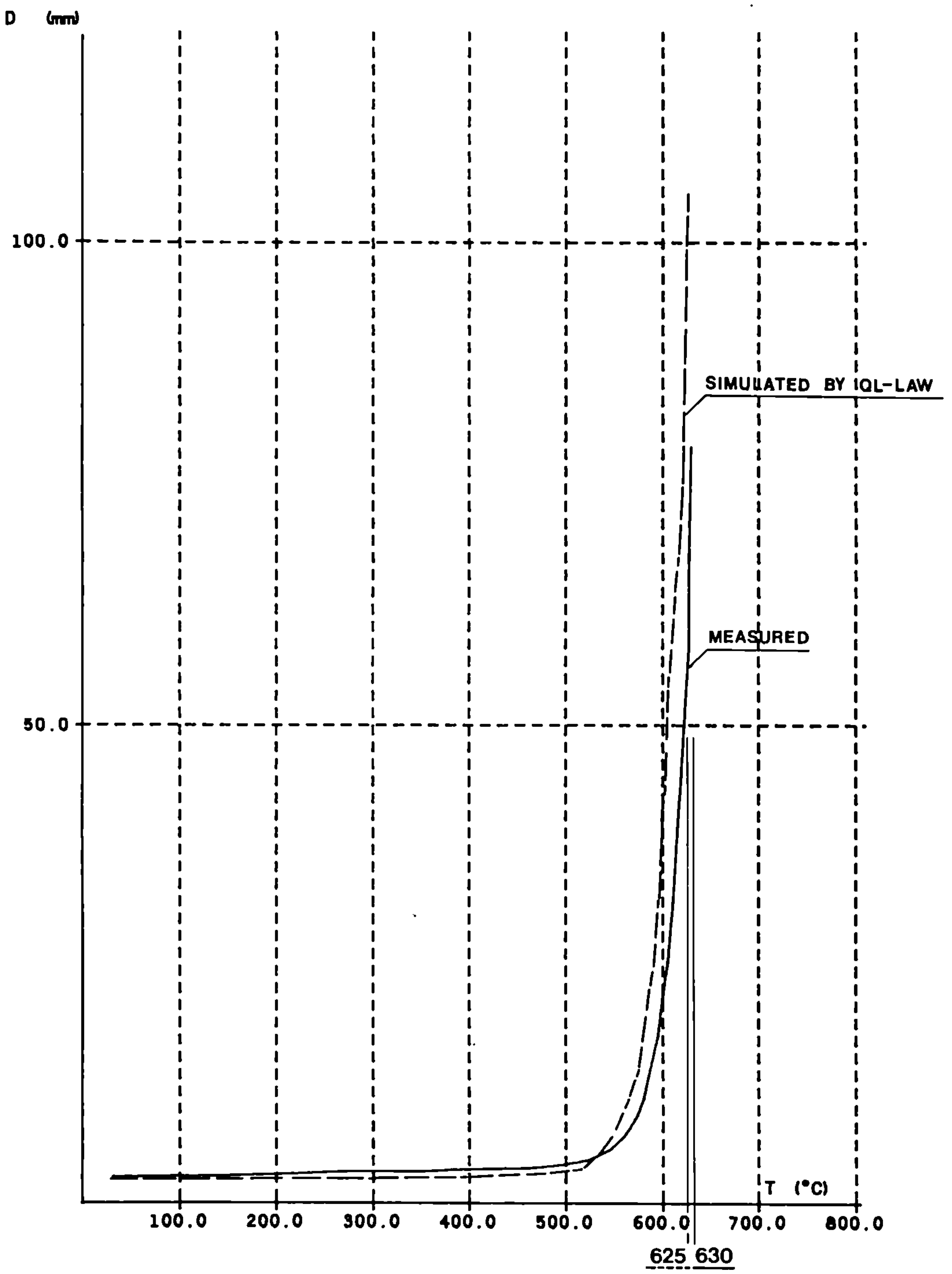

ARBED-RECHERCHES / RPS DEPARTMENT	CEFICOSS Analysis / CEF8.1
PROJECT TITLE TEST NR. V 5 - Fe 360 F/FPcold = 0.50	PROJECT NUMBER REFAO III ESCH/ALZETTE : 6-MAR-1989 SHEET :

VERTICAL DISPLACEMENTS (MM) AT THE MIDDLE OF THE BEAM
IN FUNCTION OF THE TEMPERATURE (C)

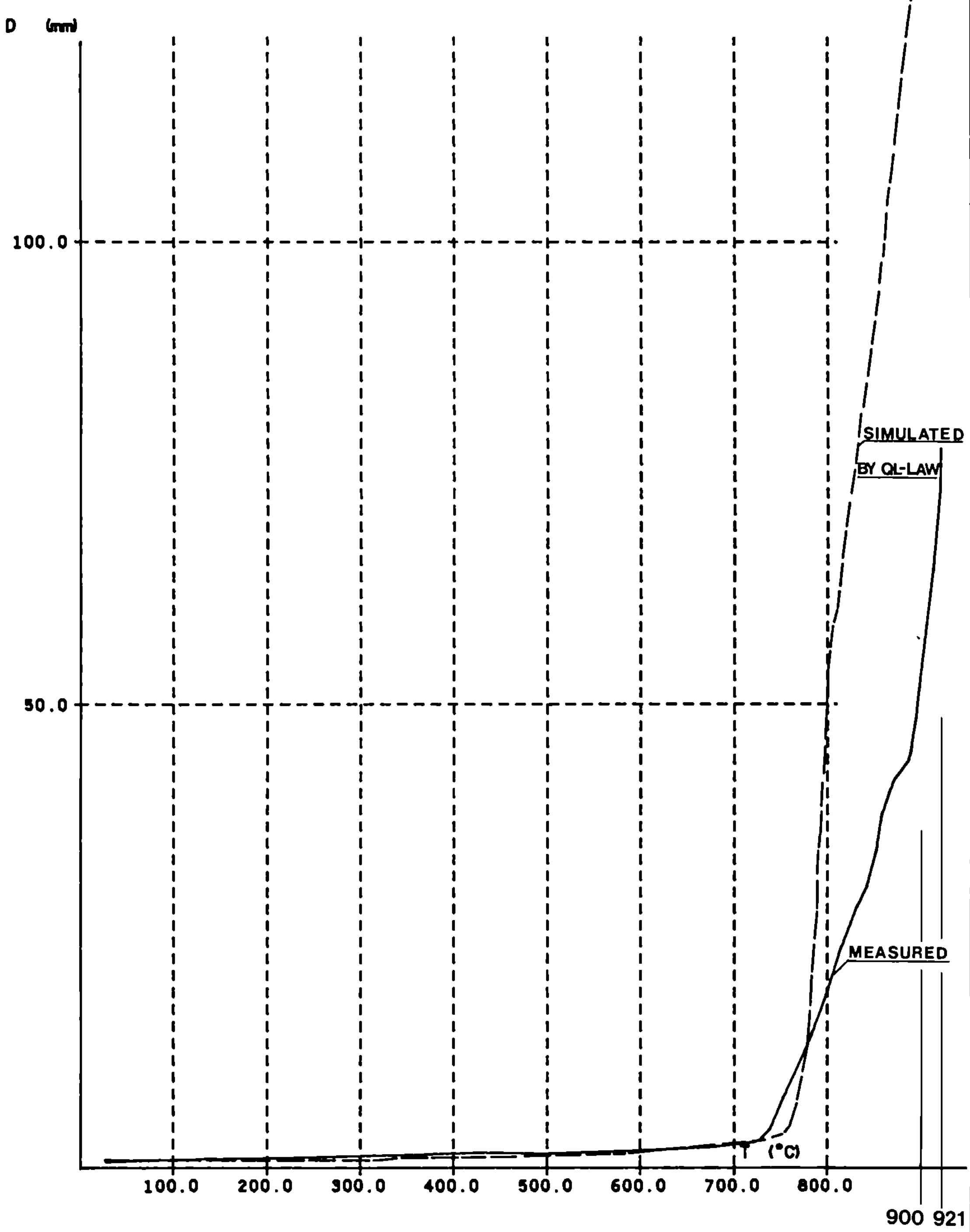

ARBED-RECHERCHES / RPS DEPARTMENT	CEFICOSS Analysis / CEF8.1
PROJECT TITLE	PROJECT NUMBER
TEST NR. V 6 - Fe 360 F/FPcold = 0.10	REFAO III
	ESCH/ALZETTE : 6-MAR-1989 | SHEET :

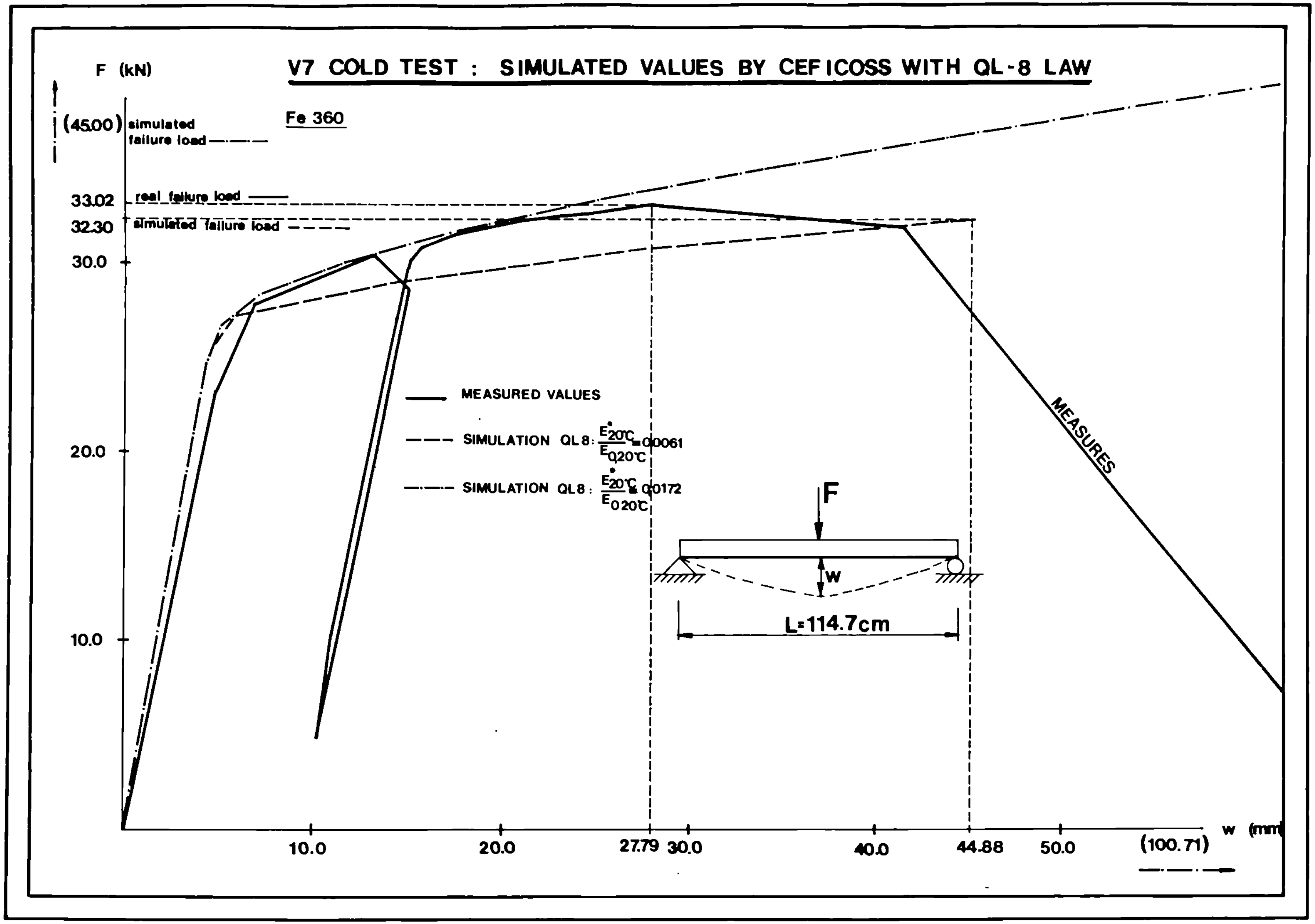
V7 COLD TEST : SIMULATED VALUES BY CEFICOSS WITH QL-8 LAW
F (kN)
Fe 360
(45.00) simulated failure load
real failure load
simulated failure load
33.02
32.30
30.0
20.0
10.0
MEASURED VALUES
SIMULATION QL8: E°20°C / E0.20°C = 0.0061
SIMULATION QL8: E°20°C / E0.20°C = 0.0172
MEASURES
F
w
L=114.7cm
10.0
20.0
27.79
30.0
40.0
44.88
50.0
(100.71)
w (mm)

PART III

APPENDIX B

SIX FULL SCALE STEEL COLUMN FIRE TESTS

TEST 1

COLUMN HD 210X210X198 - Fe 510

BUCKLING LENGTH 5.7 m

TEST PERFORMED IN BRAUNSCHWEIG

TEST Nr 1

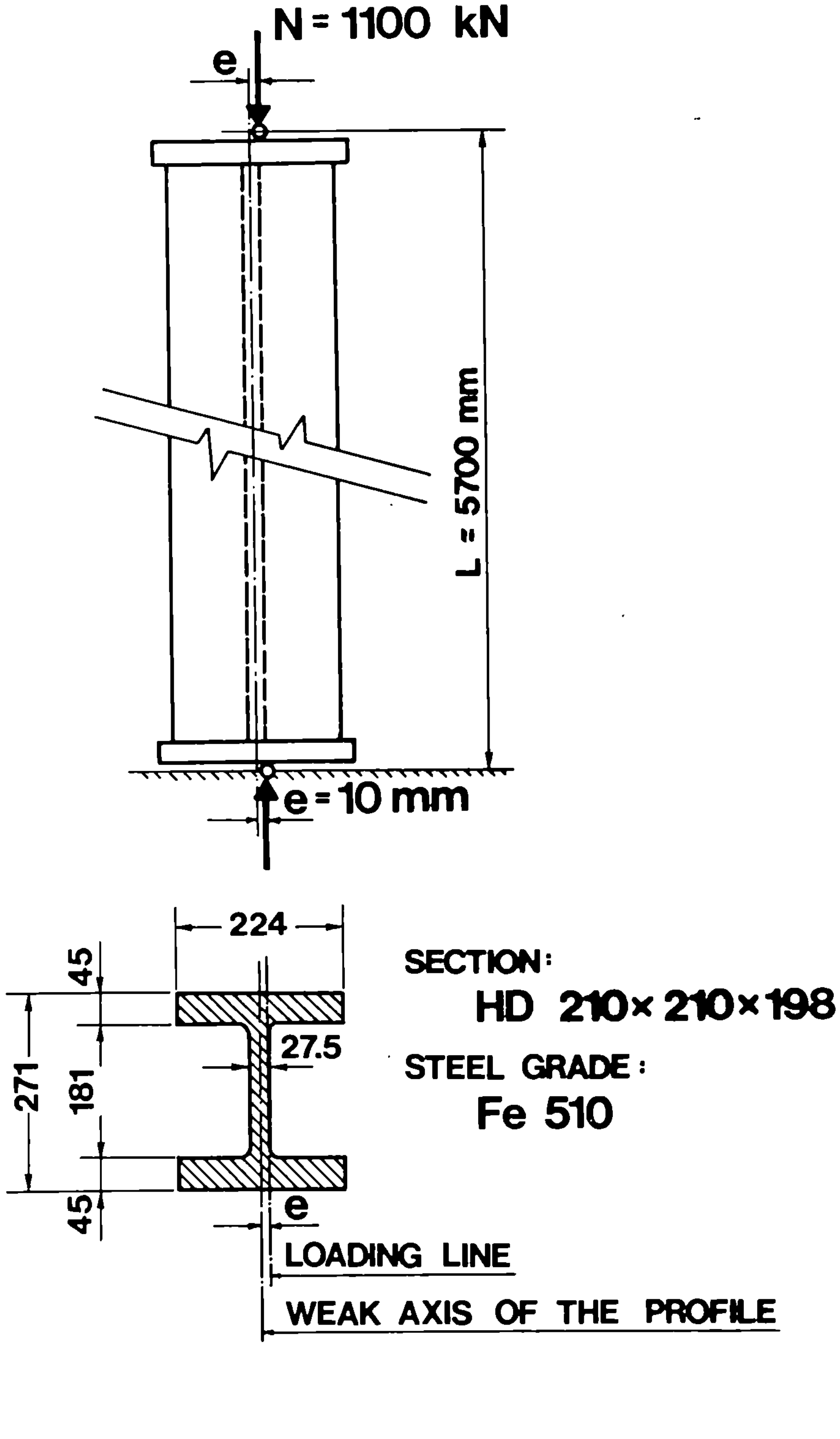

N = 1100 kN
e
L = 5700 mm
e = 10 mm
224
45
271
181
27.5
45
e
LOADING LINE
WEAK AXIS OF THE PROFILE
SECTION:
HD 210× 210×198
STEEL GRADE:
Fe 510

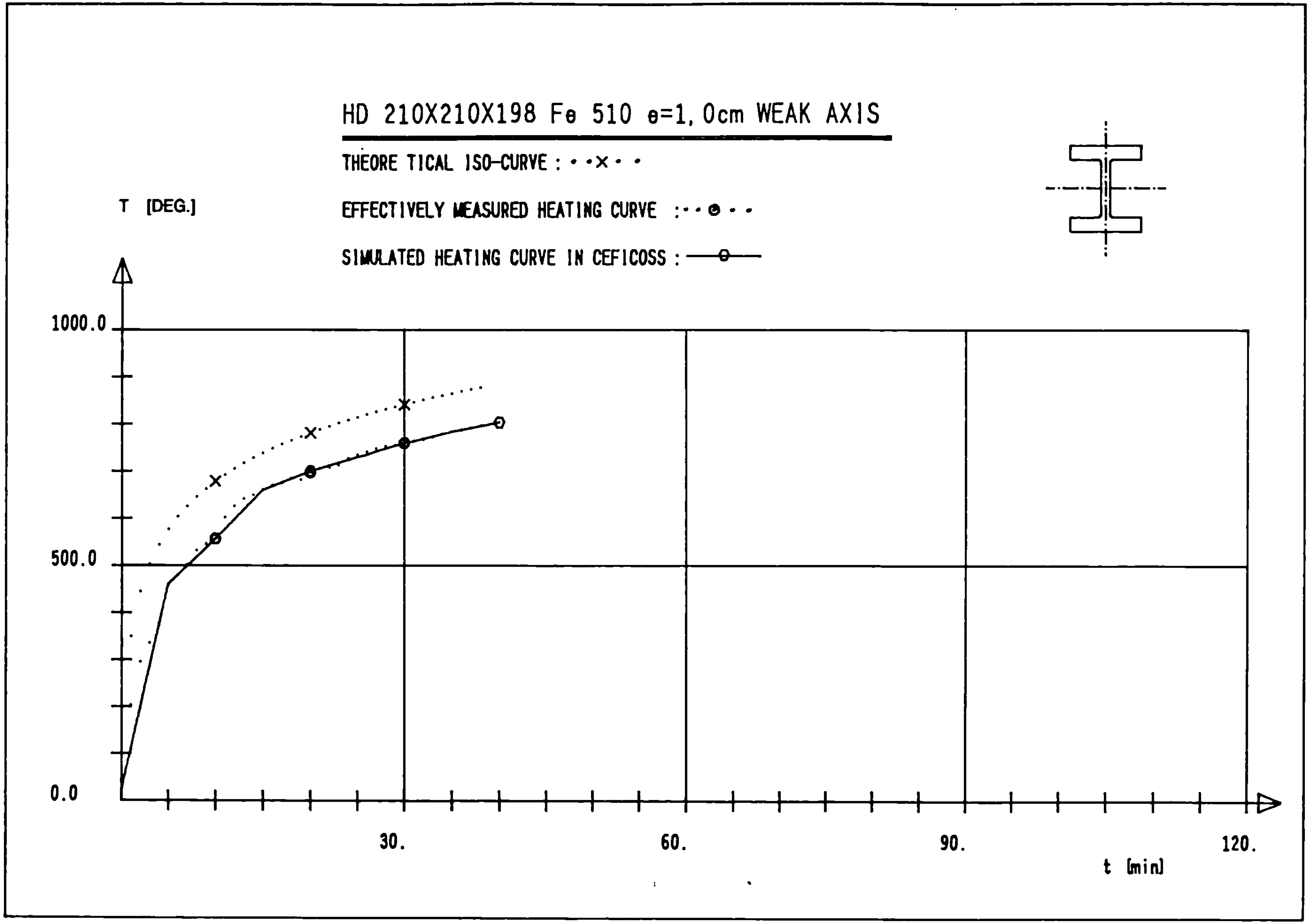
HD 210X210X198 Fe 510 e=1,0cm WEAK AXIS
THEORE TICAL ISO-CURVE : • •X• •
EFFECTIVELY MEASURED HEATING CURVE :• • ⊗ • •
SIMULATED HEATING CURVE IN CEFICOSS : —⊖—
T [DEG.]
1000.0
500.0
0.0
30.
60.
90.
120.
t [min]

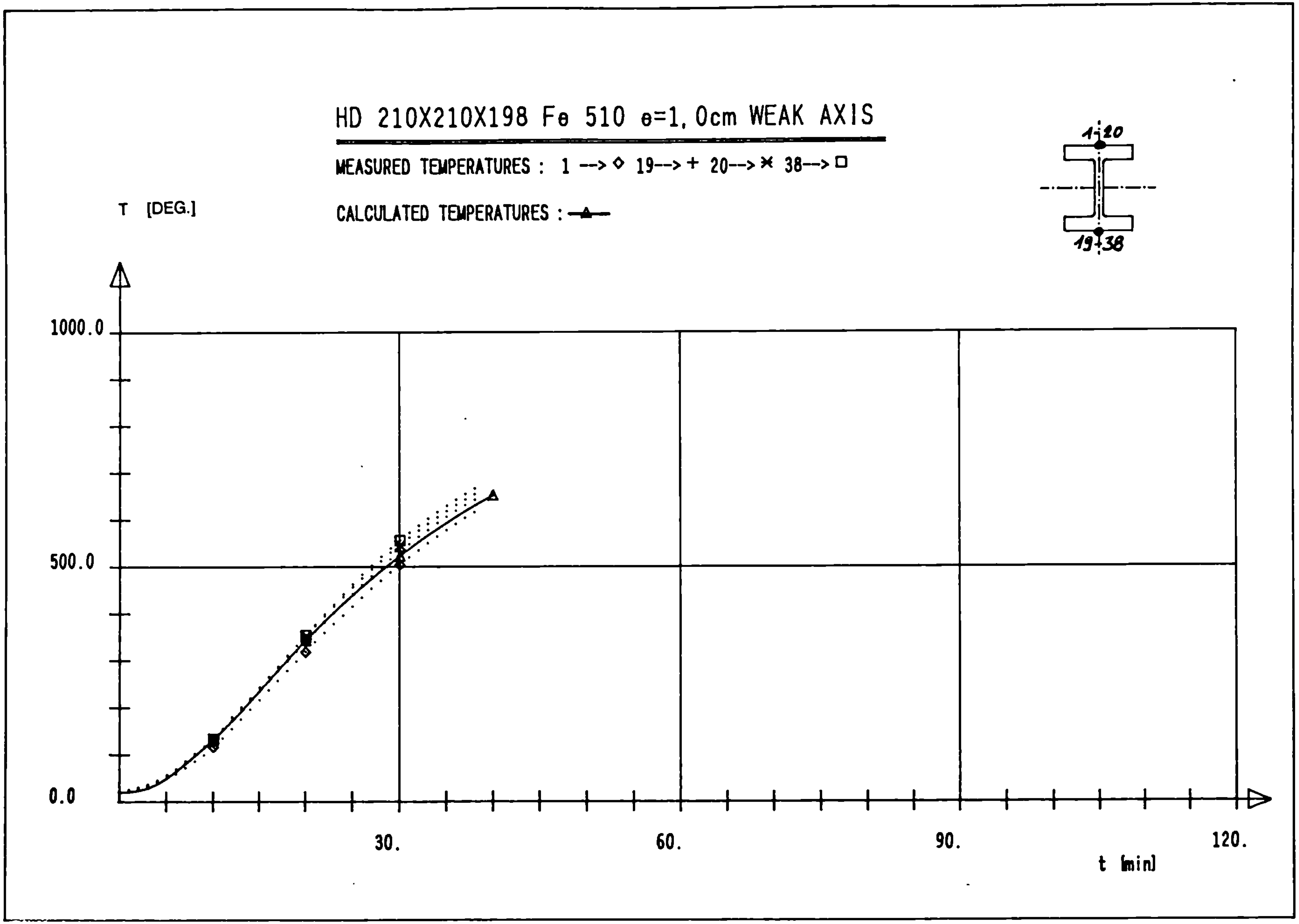

HD 210X210X198 Fe 510 e=1,0cm WEAK AXIS
MEASURED TEMPERATURES : 1 --> ◇ 19--> + 20--> ✕ 38--> □
CALCULATED TEMPERATURES : —△—
T [DEG.]
1000.0
500.0
0.0
30.
60.
90.
120.
t [min]
1-20
19-38

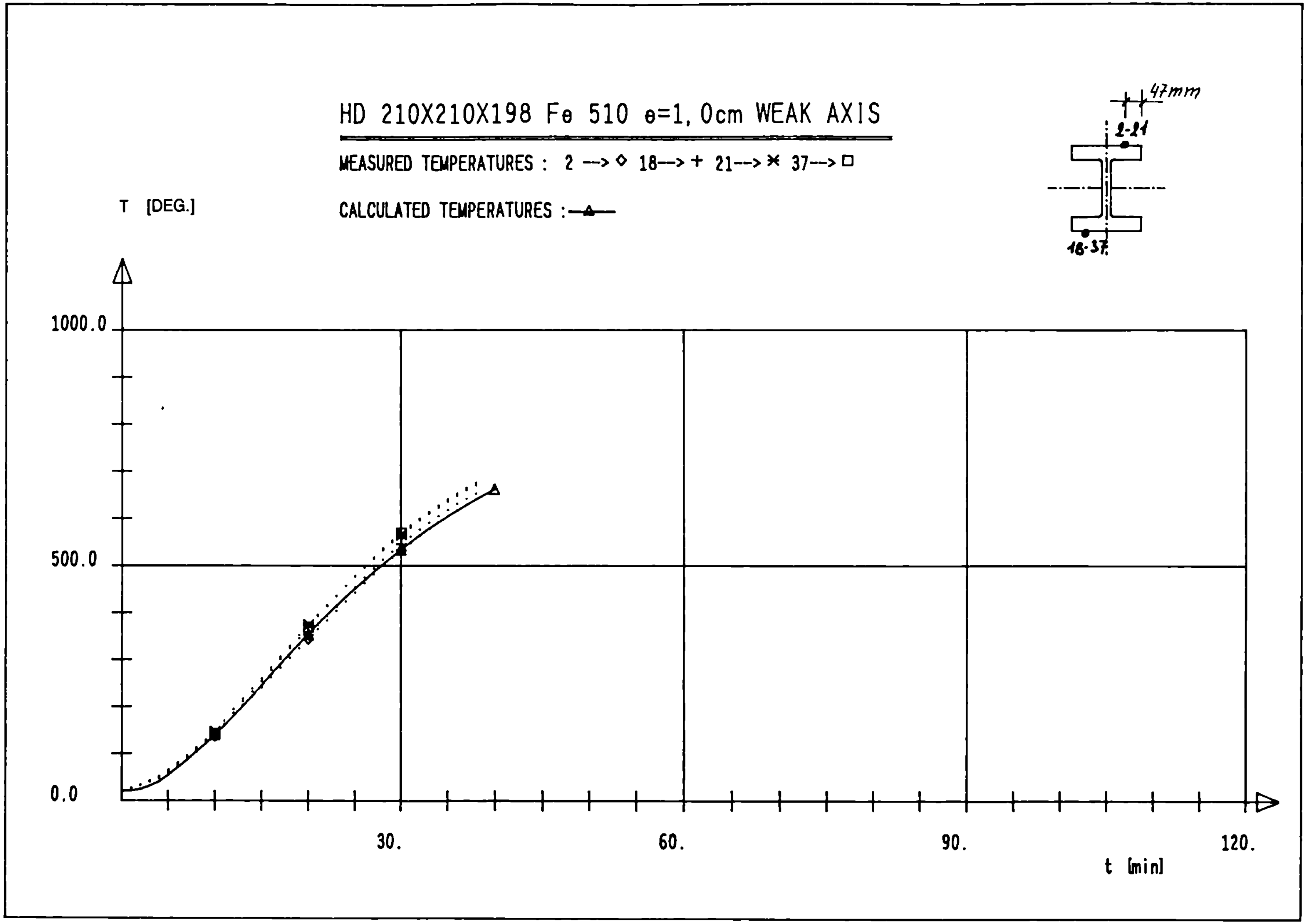

HD 210X210X198 Fe 510 e=1,0cm WEAK AXIS
MEASURED TEMPERATURES : 2 ---> ◇ 18---> + 21---> ✕ 37---> □
CALCULATED TEMPERATURES :—△—
T [DEG.]
1000.0
500.0
0.0
30.
60.
90.
120.
t [min]
47mm
2-21
18-37

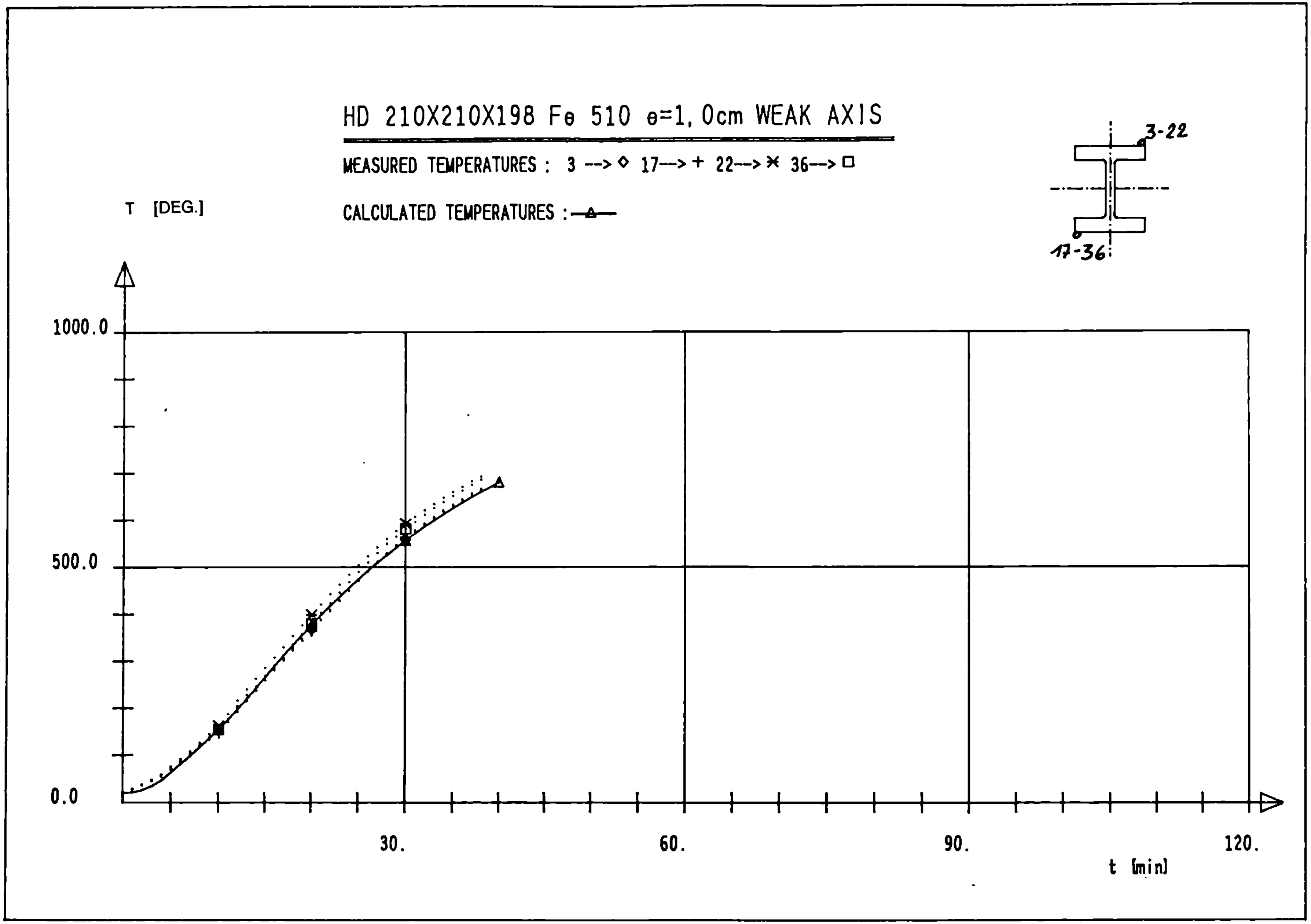
HD 210X210X198 Fe 510 e=1,0cm WEAK AXIS
MEASURED TEMPERATURES : 3 --> ◇ 17--> + 22--> ✕ 36--> □
CALCULATED TEMPERATURES : —△—
T [DEG.]
3-22
17-36
1000.0
500.0
0.0
30.
60.
90.
120.
t [min]

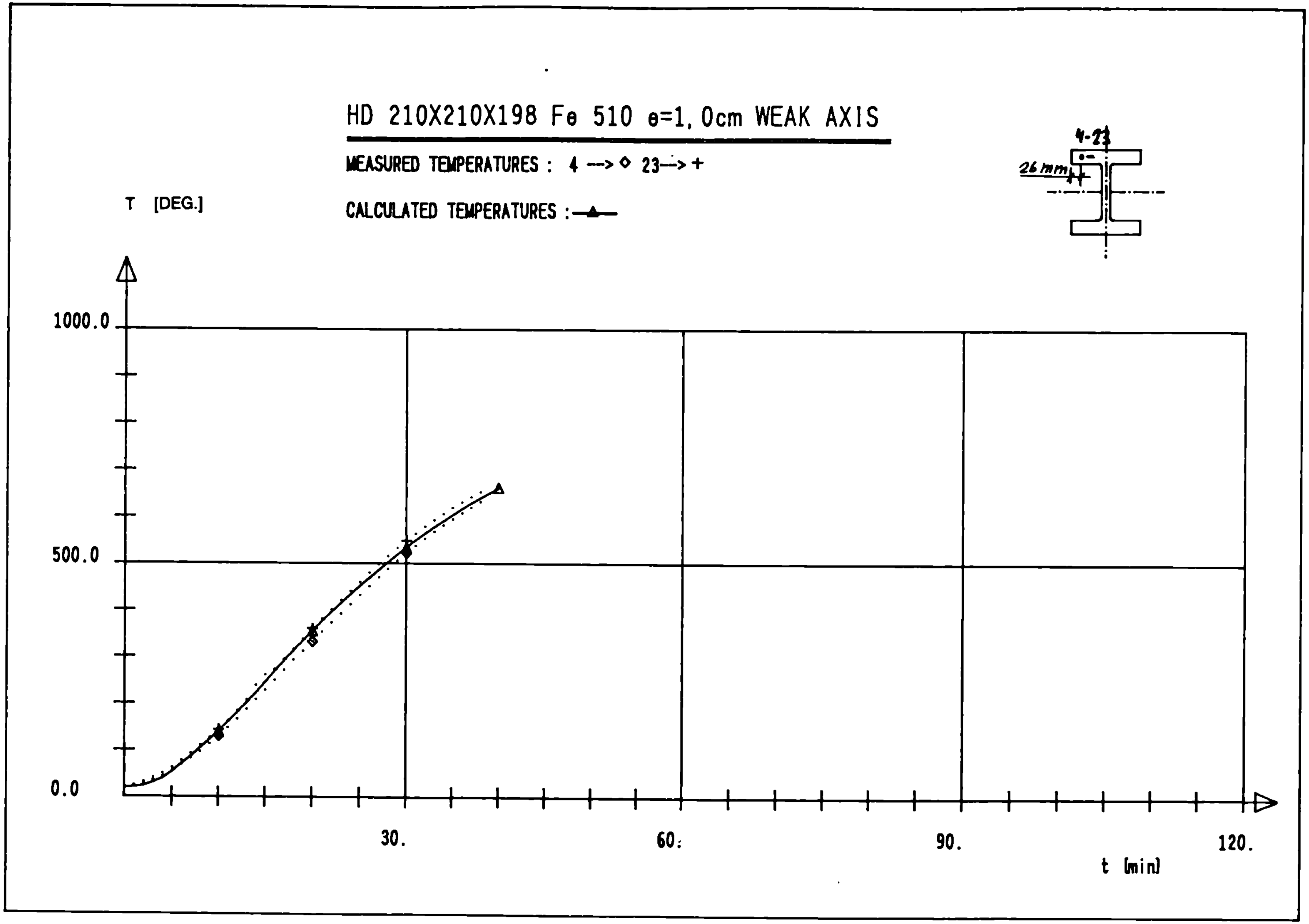
HD 210X210X198 Fe 510 e=1,0cm WEAK AXIS
MEASURED TEMPERATURES : 4 —> ◇ 23—> +
CALCULATED TEMPERATURES :—▲—
T [DEG.]
1000.0
500.0
0.0
30.
60.
90.
120.
t [min]
4-23
26 mm

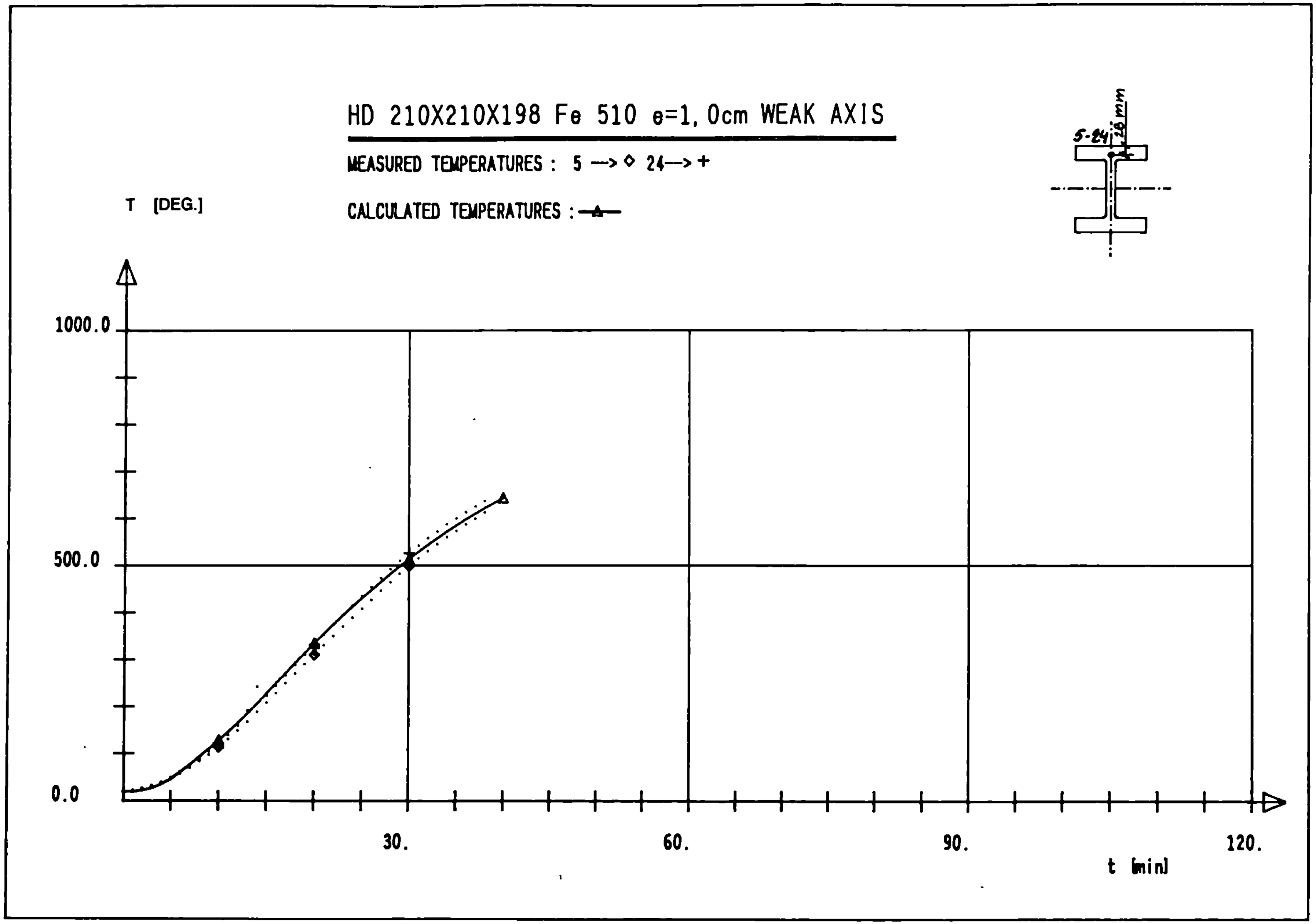
HD 210X210X198 Fe 510 e=1,0cm WEAK AXIS
MEASURED TEMPERATURES : 5 —> ◇ 24—> +
CALCULATED TEMPERATURES : —△—
T [DEG.]
1000.0
500.0
0.0
30.
60.
90.
120.
t [min]
5-24
26 mm

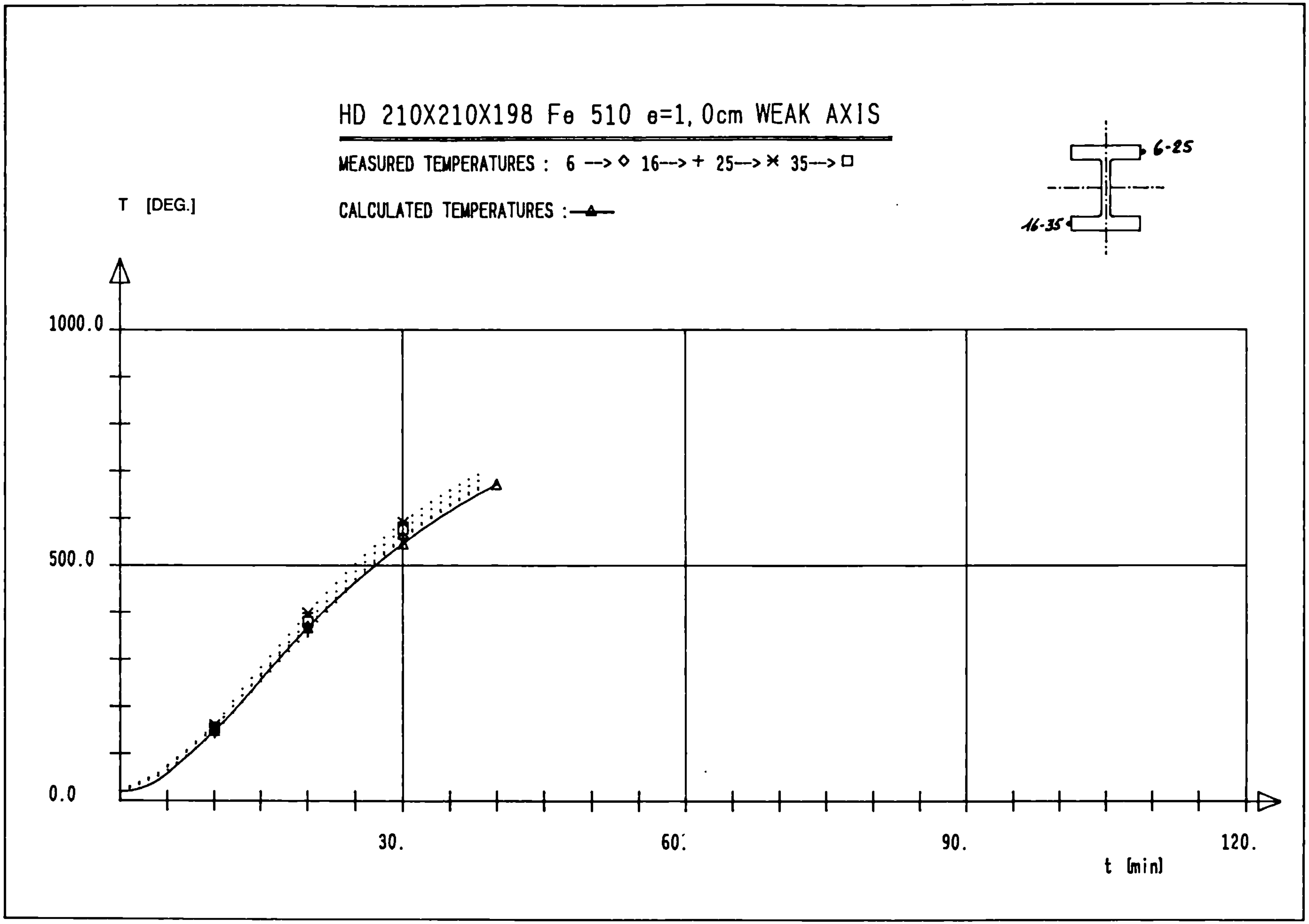
HD 210X210X198 Fe 510 e=1,0cm WEAK AXIS
MEASURED TEMPERATURES : 6 --> ◇ 16--> + 25--> ✕ 35--> □
CALCULATED TEMPERATURES : —△—
T [DEG.]
6-25
16-35
1000.0
500.0
0.0
30.
60.
90.
120.
t [min]

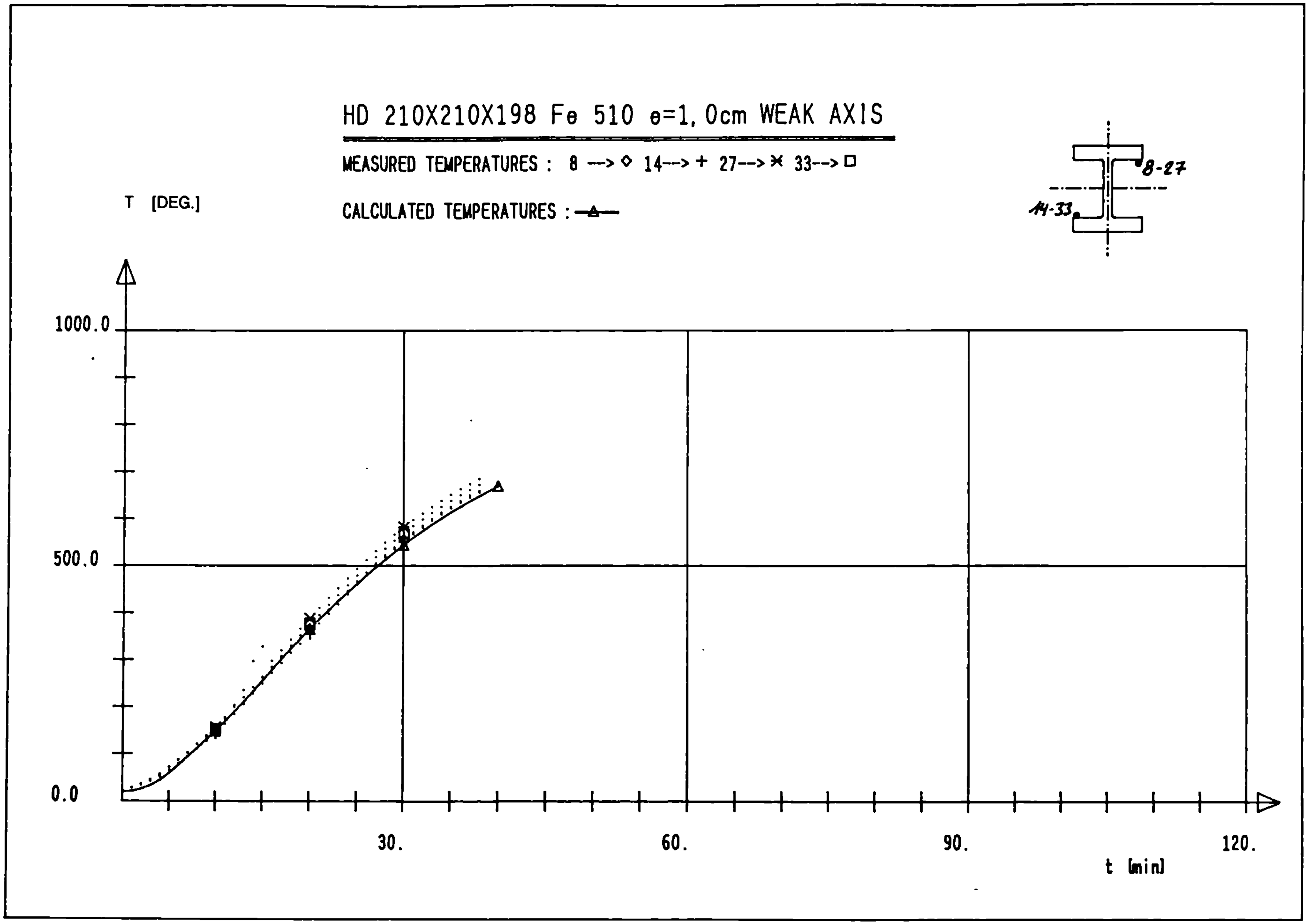
HD 210X210X198 Fe 510 e=1,0cm WEAK AXIS
MEASURED TEMPERATURES : 8 ---> ◇ 14---> + 27---> ✕ 33---> □
CALCULATED TEMPERATURES : —△—
T [DEG.]
8-27
14-33
1000.0
500.0
0.0
30.
60.
90.
120.
t [min]

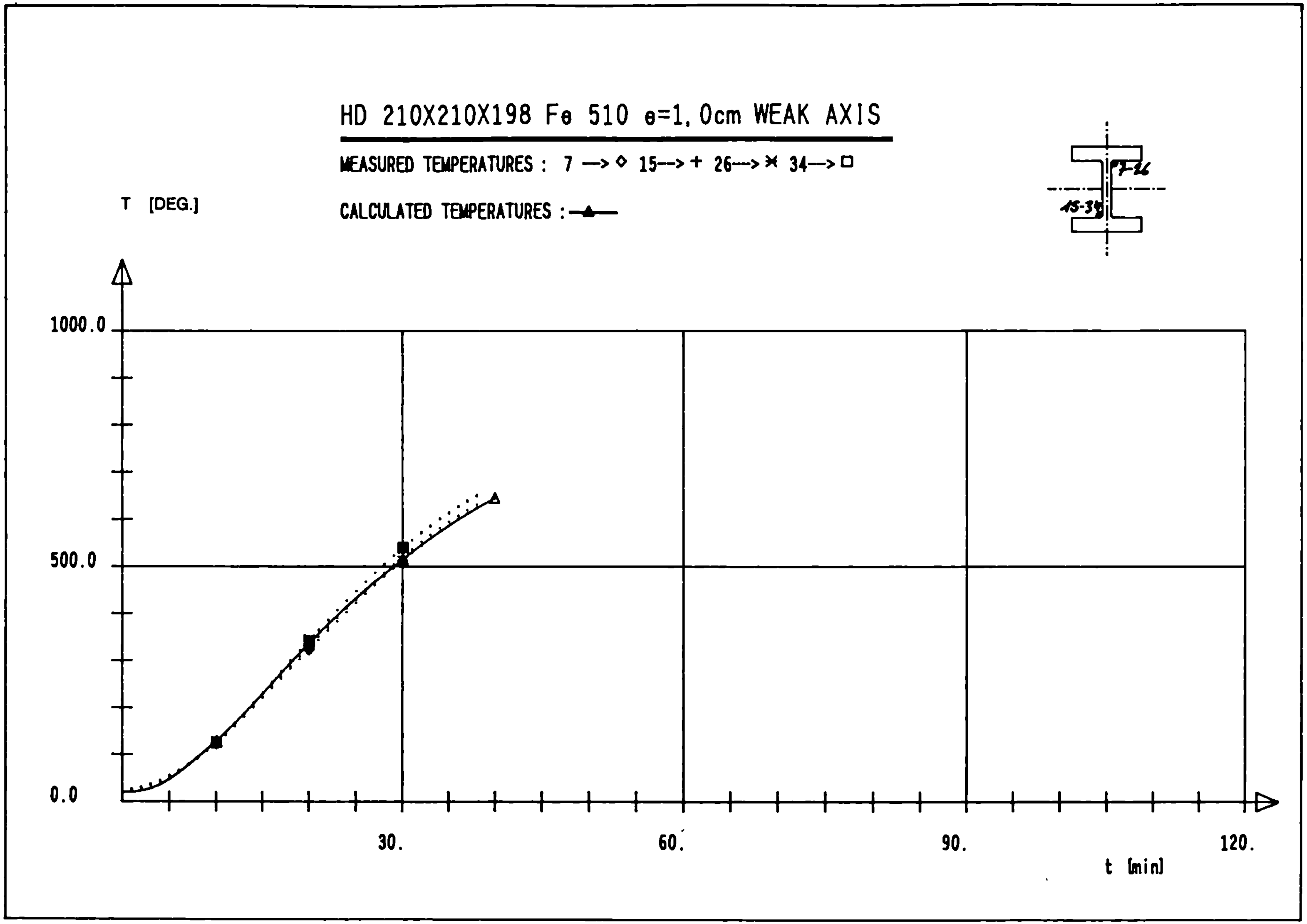
HD 210X210X198 Fe 510 e=1,0cm WEAK AXIS
MEASURED TEMPERATURES : 7 —> ◇ 15—> + 26—> ✕ 34—> □
CALCULATED TEMPERATURES : —▲—
T [DEG.]
1000.0
500.0
0.0
30.
60.
90.
120.
t [min]
7-26
15-34

1.10

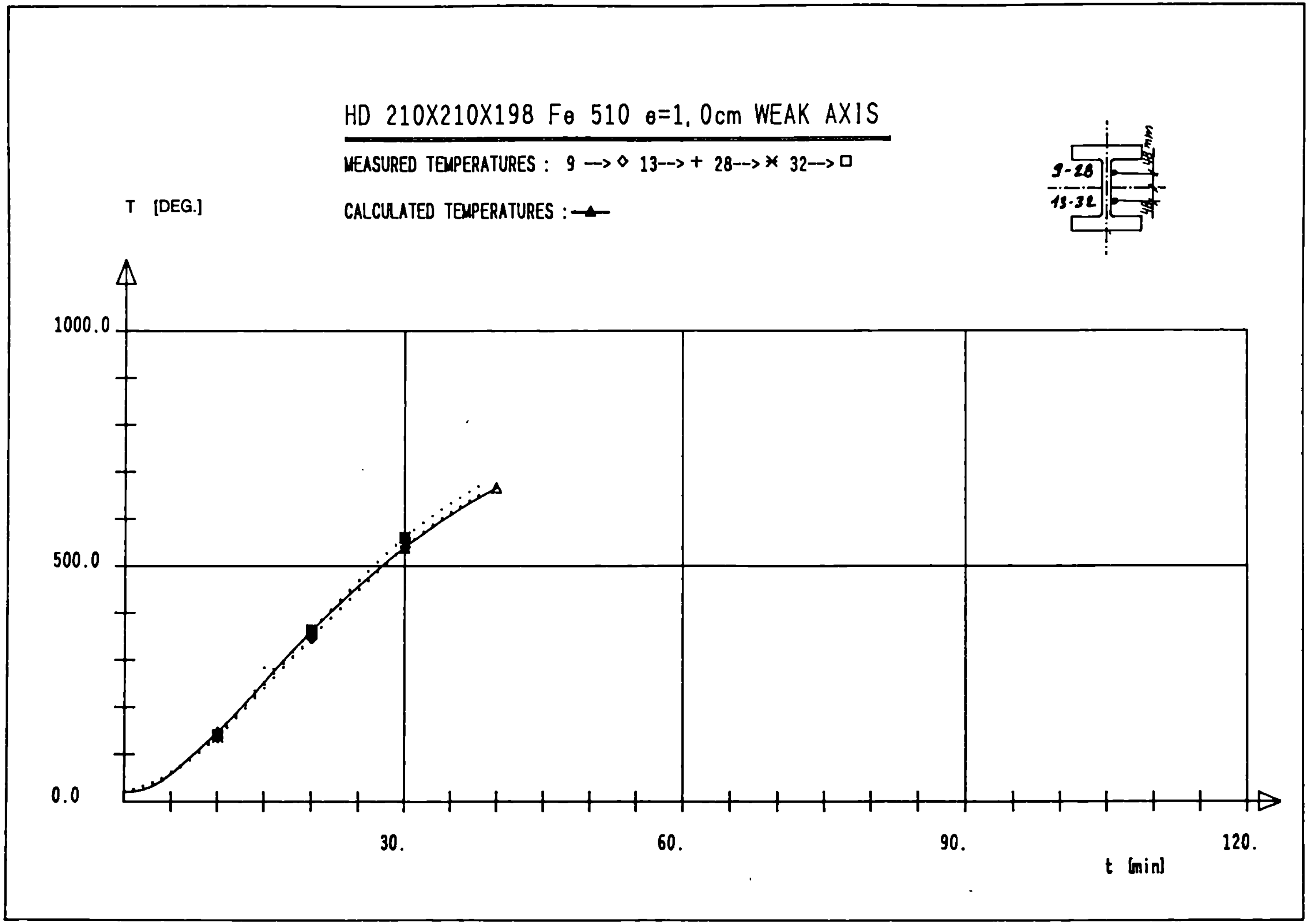
HD 210X210X198 Fe 510 e=1,0cm WEAK AXIS
MEASURED TEMPERATURES : 9 --> ◇ 13--> + 28--> ✕ 32--> □
CALCULATED TEMPERATURES :
T [DEG.]
1000.0
500.0
0.0
30.
60.
90.
120.
t [min]
9-28
13-32

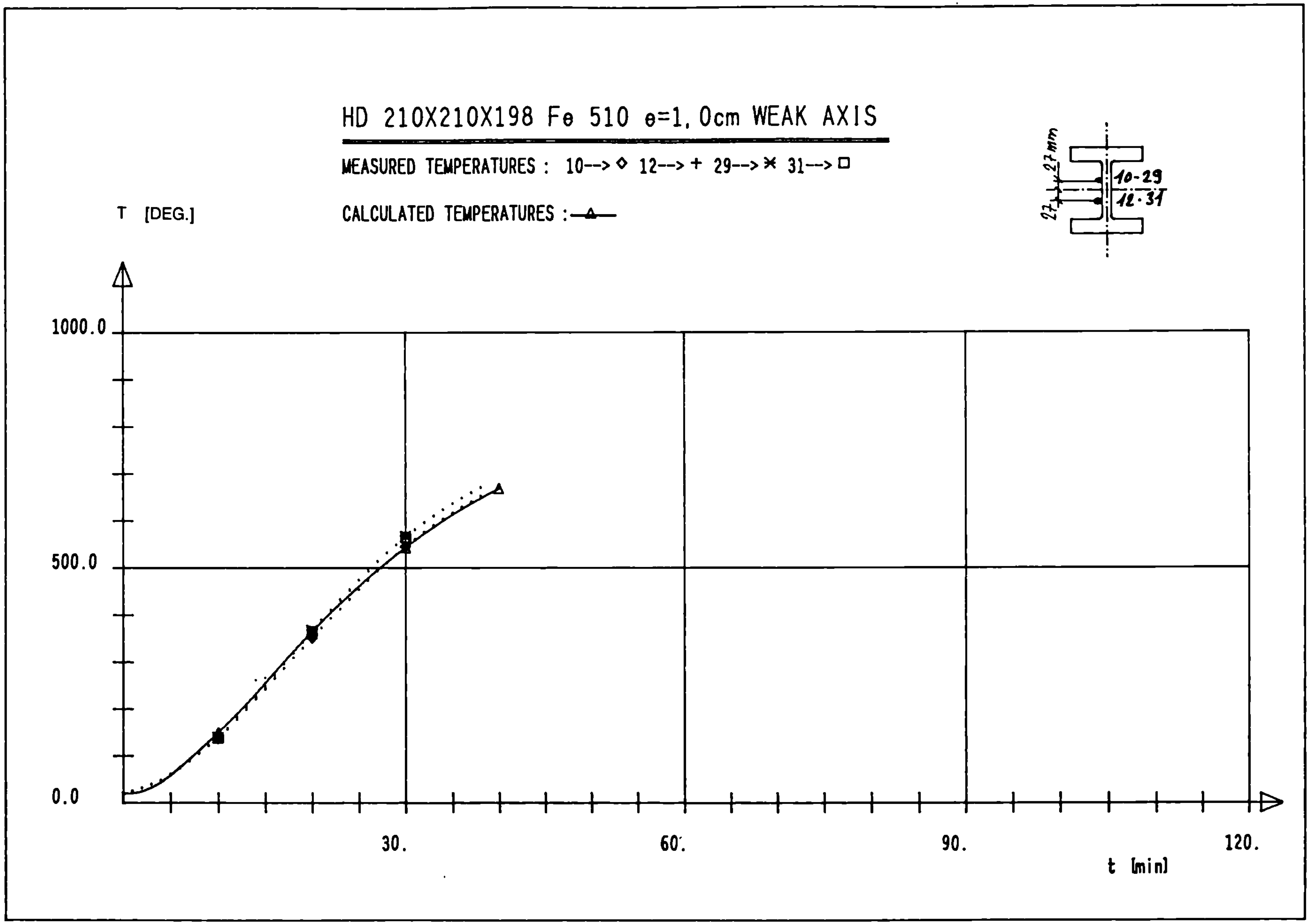
HD 210X210X198 Fe 510 e=1,0cm WEAK AXIS
MEASURED TEMPERATURES : 10--> ◇ 12--> + 29--> ✳ 31--> □
CALCULATED TEMPERATURES : —△—
T [DEG.]
1000.0
500.0
0.0
30.
60.
90.
120.
t [min]
27mm
27
10-29
12-31

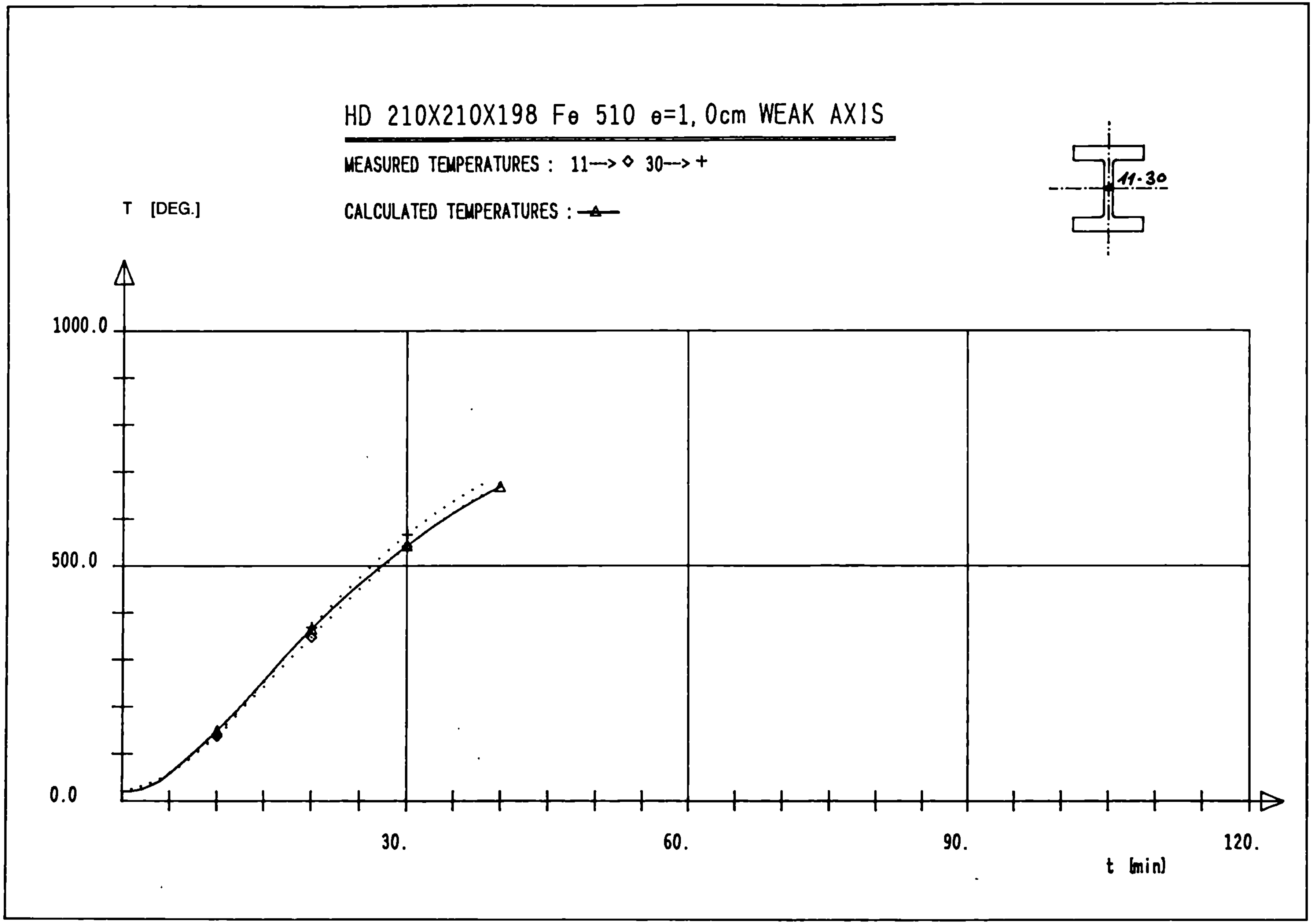
HD 210X210X198 Fe 510 e=1,0cm WEAK AXIS
MEASURED TEMPERATURES : 11—> ◇ 30—> +
CALCULATED TEMPERATURES : —△—
T [DEG.]
1000.0
500.0
0.0
30.
60.
90.
120.
t (min)
11-30

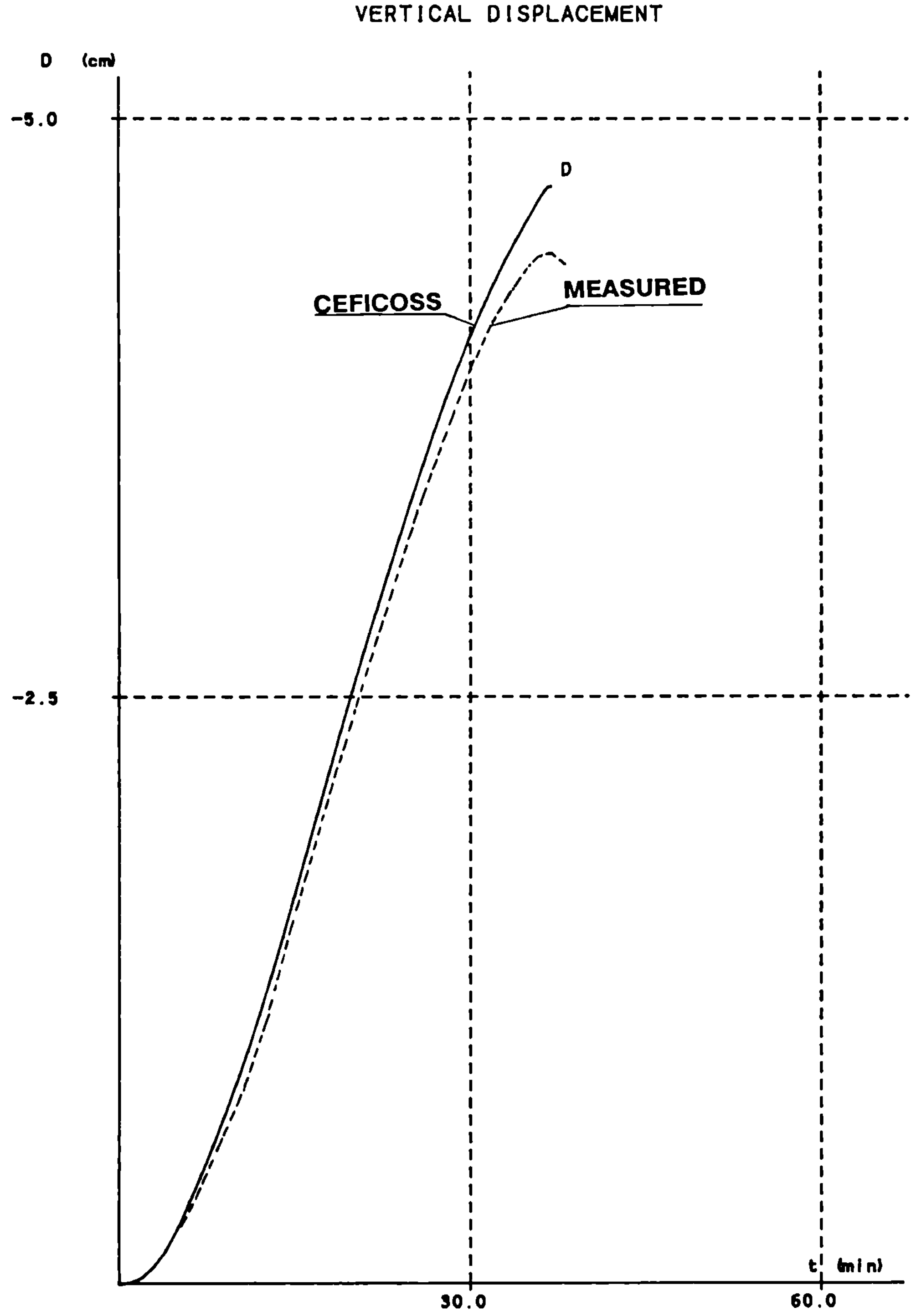

ARBED-RECHERCHES / RPS DEPARTMENT	CEFICOSS Analysis / CEF81
PROJECT TITLE TEST 1 HD 210X210X198 / Fe 510 / WEAK AXIS	PROJECT NUMBER REFAO III ESCH/ALZETTE : 20-FEB-1989 — SHEET : 1.14

TEST 1 : HD 210X210X198 / SIMULATION BRAUNSCHWEIG

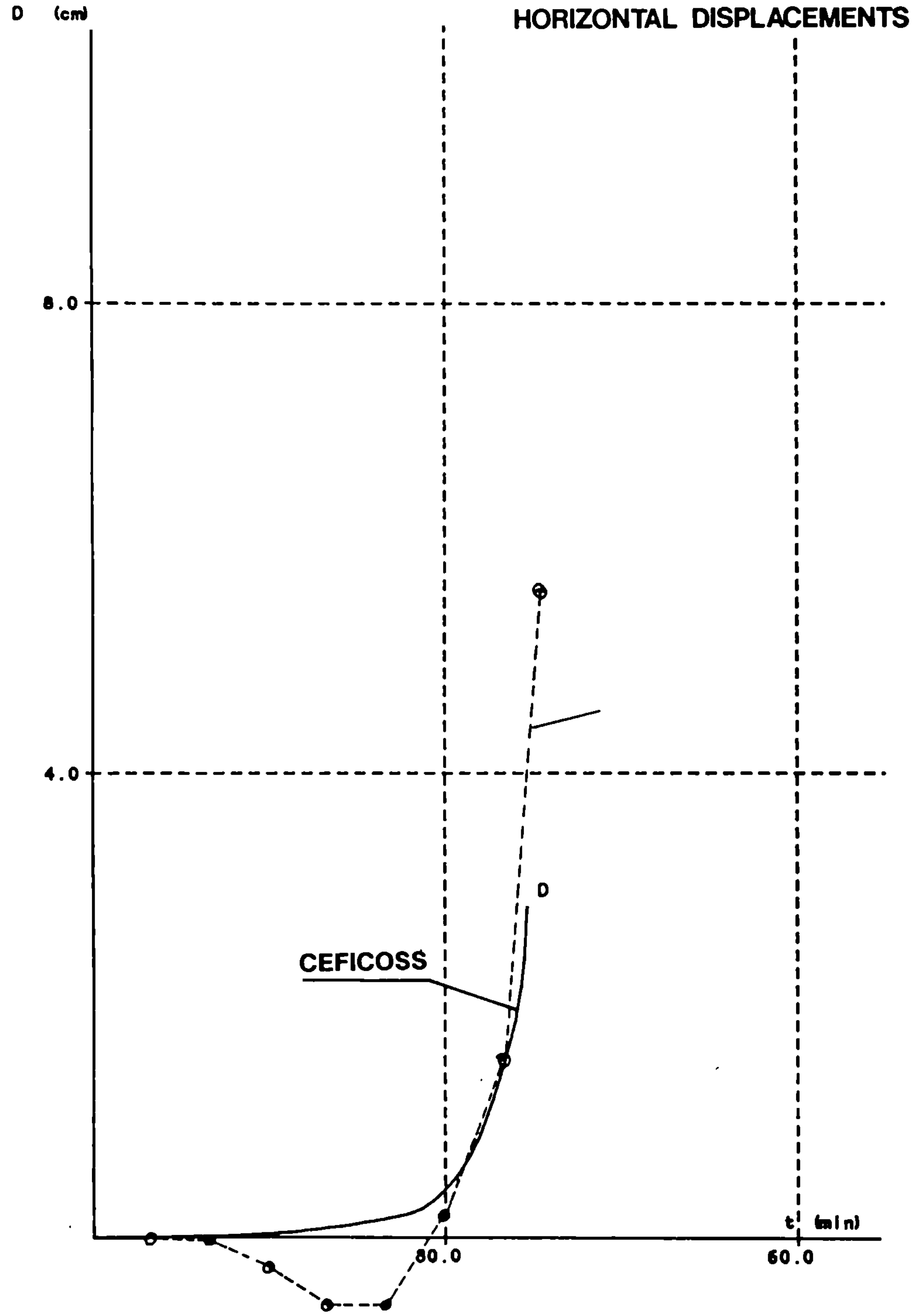

ARBED-RECHERCHES / RPS DEPARTMENT	CEFICOSS Analysis / CEF81
PROJECT TITLE TEST 1 HD 210X210X198 / Fe 510 / WEAK AXIS	PROJECT NUMBER REFAO III ESCH/ALZETTE : 20-FEB-1989 — SHEET : 1.15

TEST 2

COLUMN HD 310x310x500 - Fe 510

BUCKLING LENGTH 4.14 m

TEST PERFORMED IN GAND

TEST Nr 2

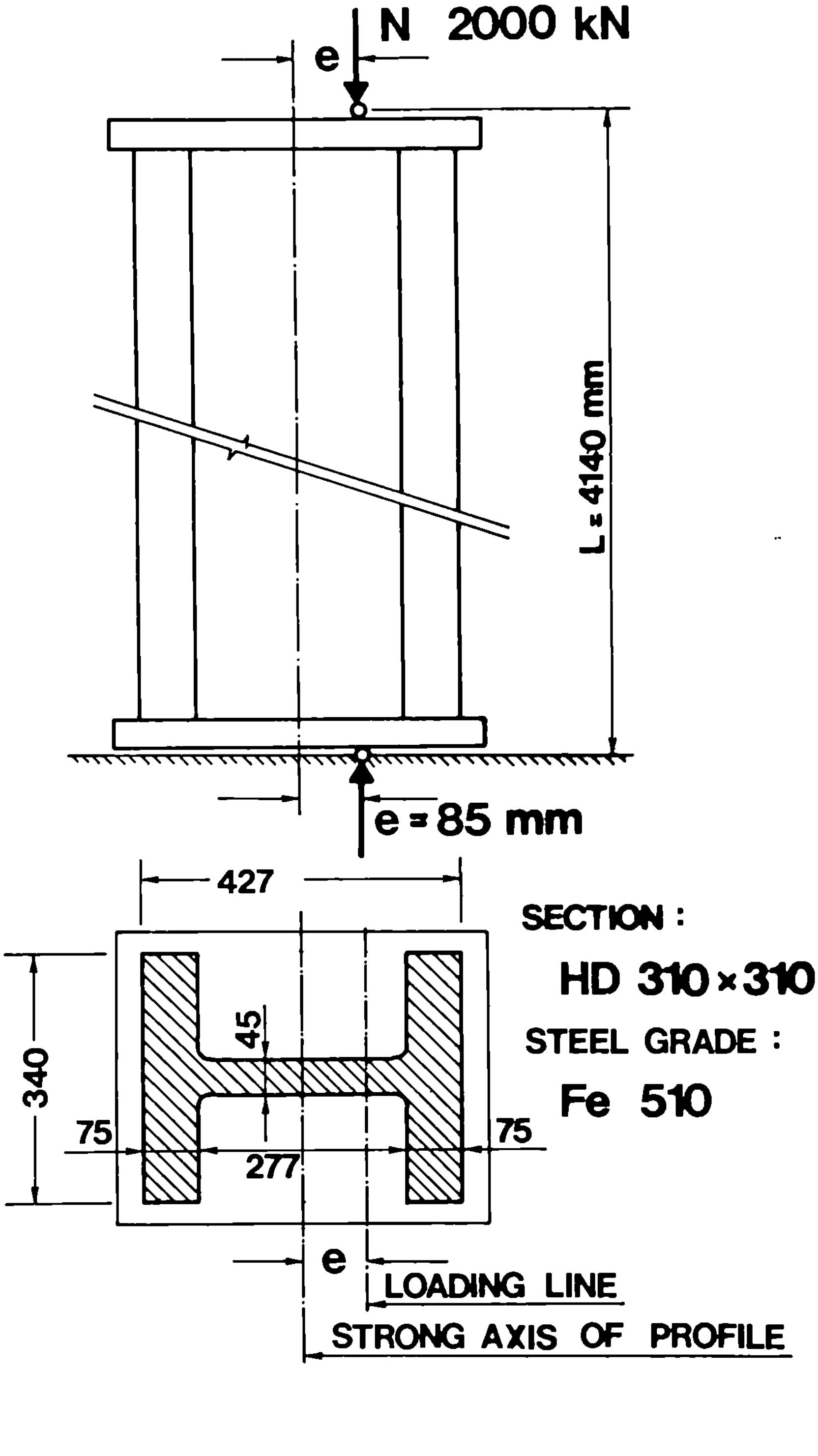

SECTION :

HD 310×310×500

STEEL GRADE :

Fe 510

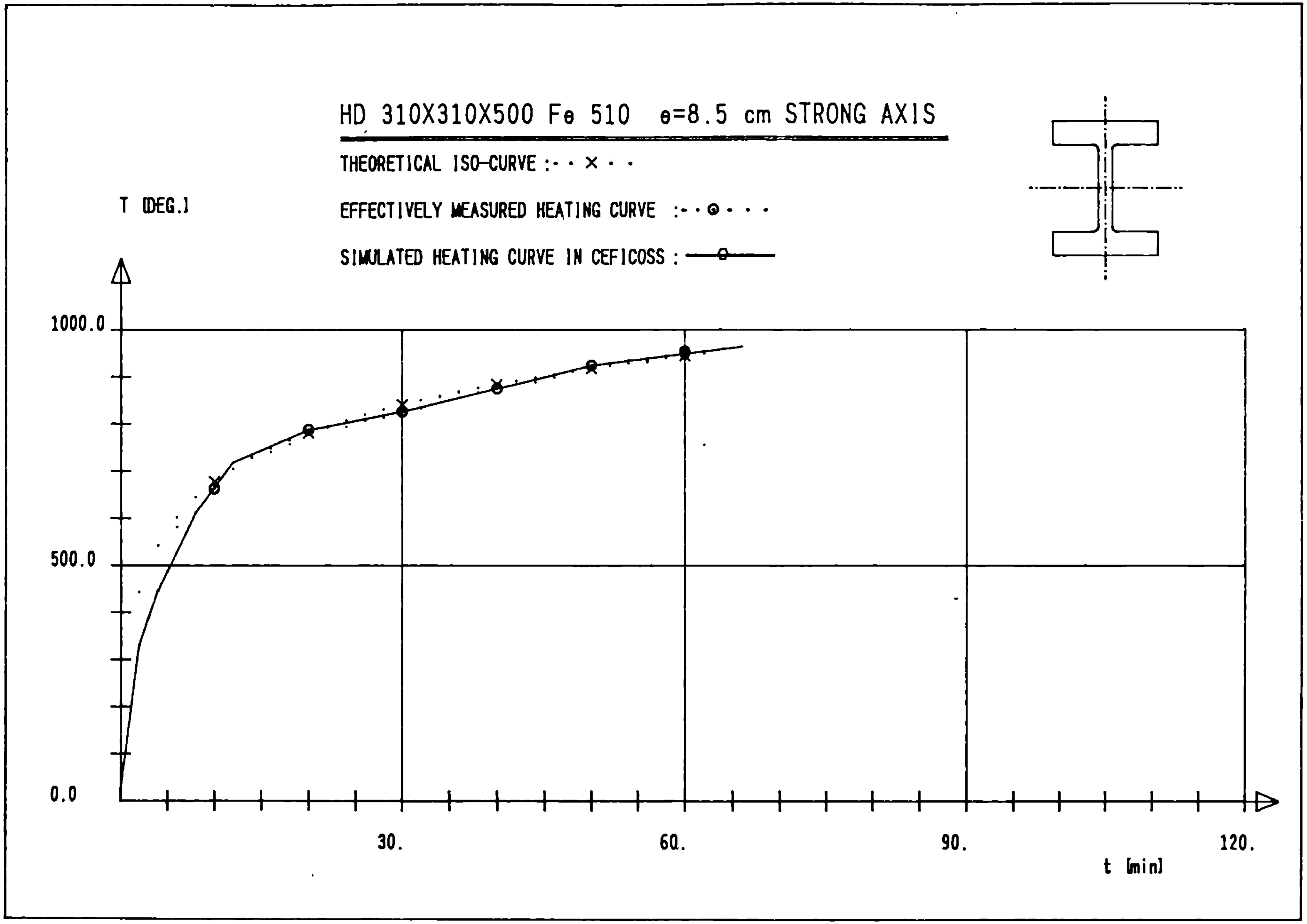

HD 310X310X500 Fe 510 e=8.5 cm STRONG AXIS
THEORETICAL ISO-CURVE :· · × · ·
EFFECTIVELY MEASURED HEATING CURVE :· · ⊙ · · ·
SIMULATED HEATING CURVE IN CEFICOSS : —o—
T [DEG.]
1000.0
500.0
0.0
30.
60.
90.
120.
t [min]

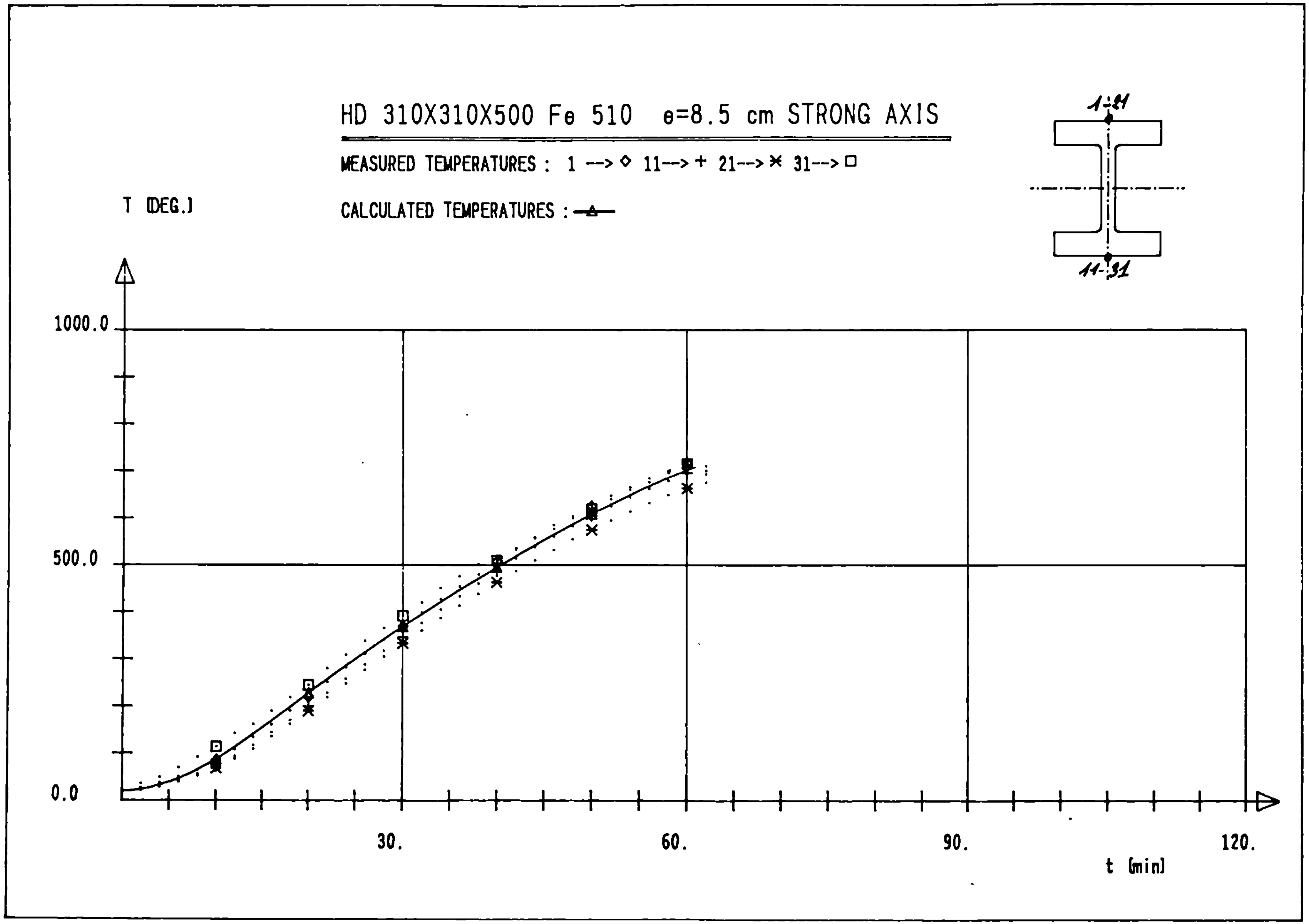
HD 310X310X500 Fe 510 e=8.5 cm STRONG AXIS
MEASURED TEMPERATURES : 1 --> ◇ 11--> + 21--> ✳ 31--> □
CALCULATED TEMPERATURES : —△—
T [DEG.]
1000.0
500.0
0.0
30.
60.
90.
120.
t [min]
1-21
11-31

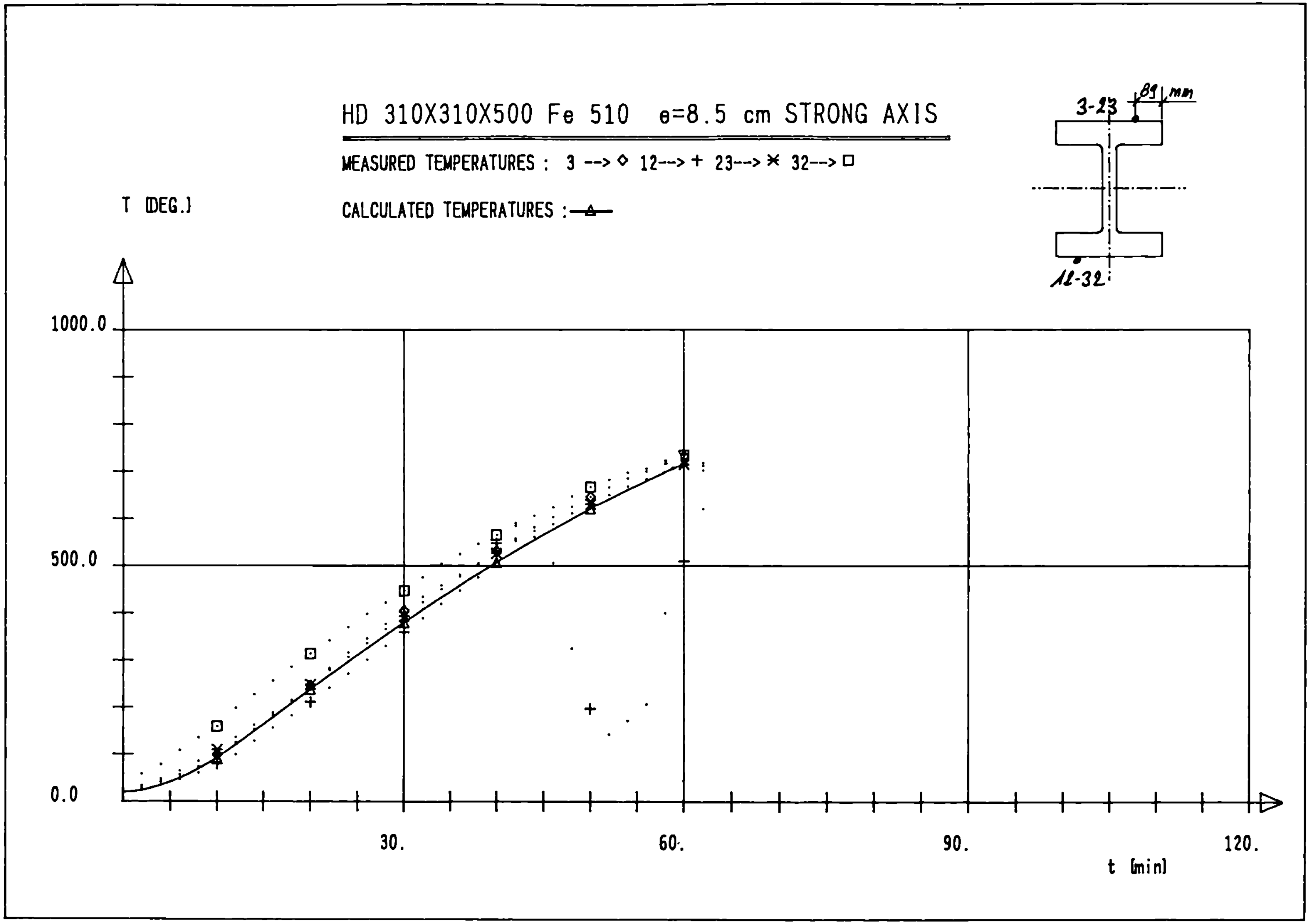

HD 310X310X500 Fe 510 e=8.5 cm STRONG AXIS
MEASURED TEMPERATURES : 3 --> ◇ 12--> + 23--> ✕ 32--> □
CALCULATED TEMPERATURES : —△—
T [DEG.]
1000.0
500.0
0.0
30.
60.
90.
120.
t [min]
3-23
89 mm
12-32

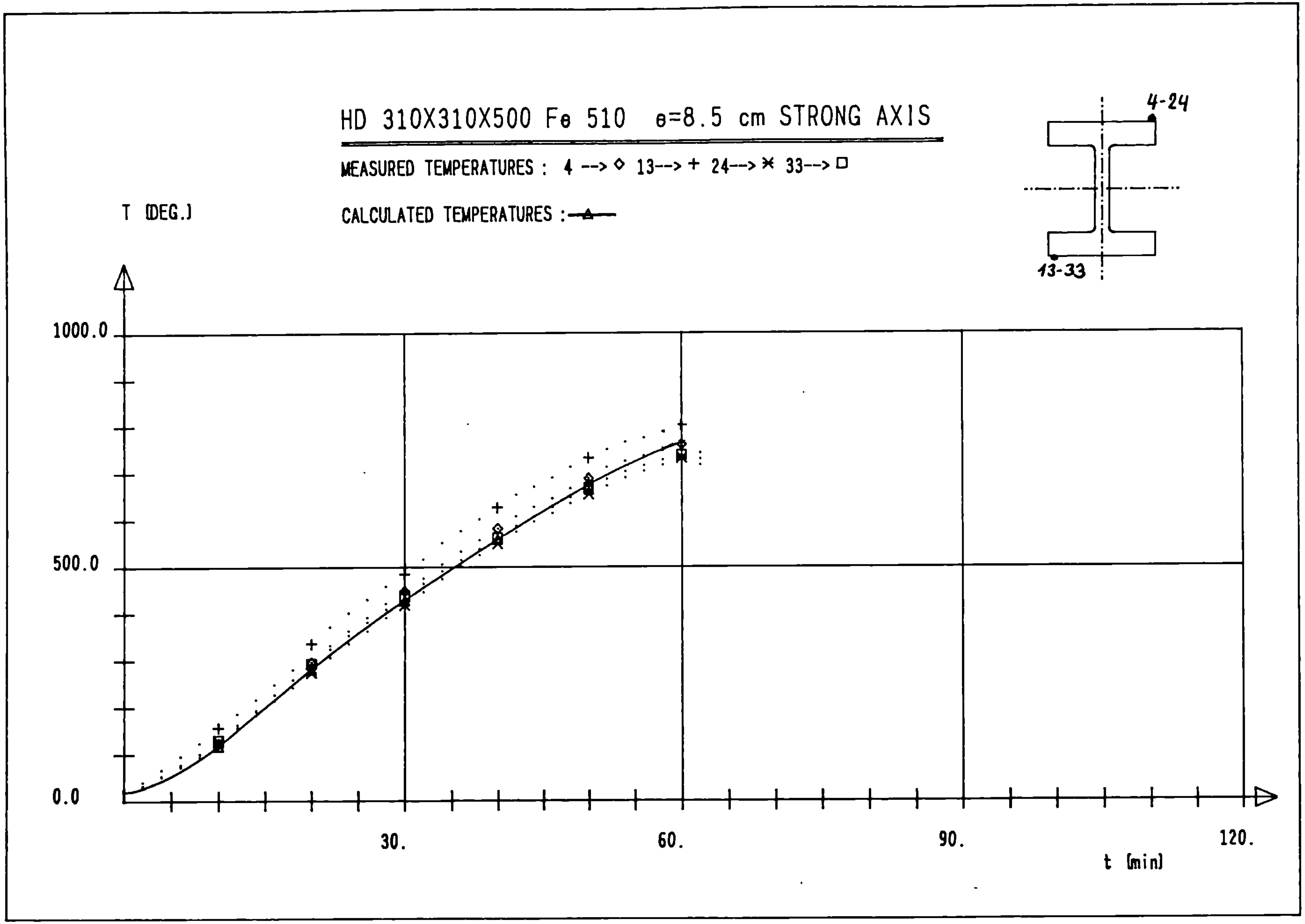
HD 310X310X500 Fe 510 e=8.5 cm STRONG AXIS
MEASURED TEMPERATURES : 4 --> ◇ 13--> + 24--> ✳ 33--> □
CALCULATED TEMPERATURES :
T (DEG.)
1000.0
500.0
0.0
30.
60.
90.
120.
t (min)
4-24
13-33

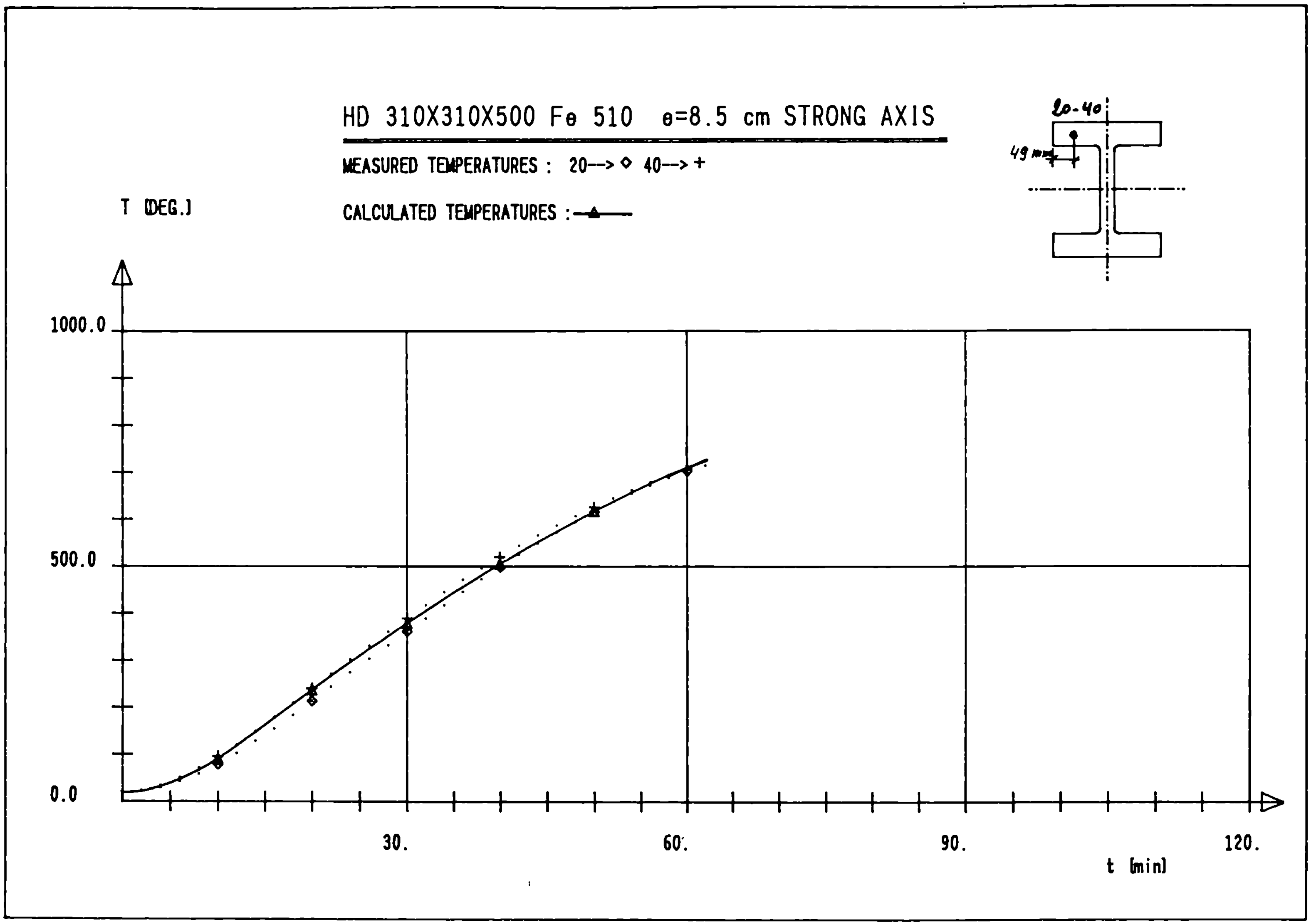
HD 310X310X500 Fe 510 e=8.5 cm STRONG AXIS
MEASURED TEMPERATURES : 20--> ◇ 40--> +
CALCULATED TEMPERATURES :
T [DEG.]
1000.0
500.0
0.0
30.
60.
90.
120.
t [min]
20-40
49 mm

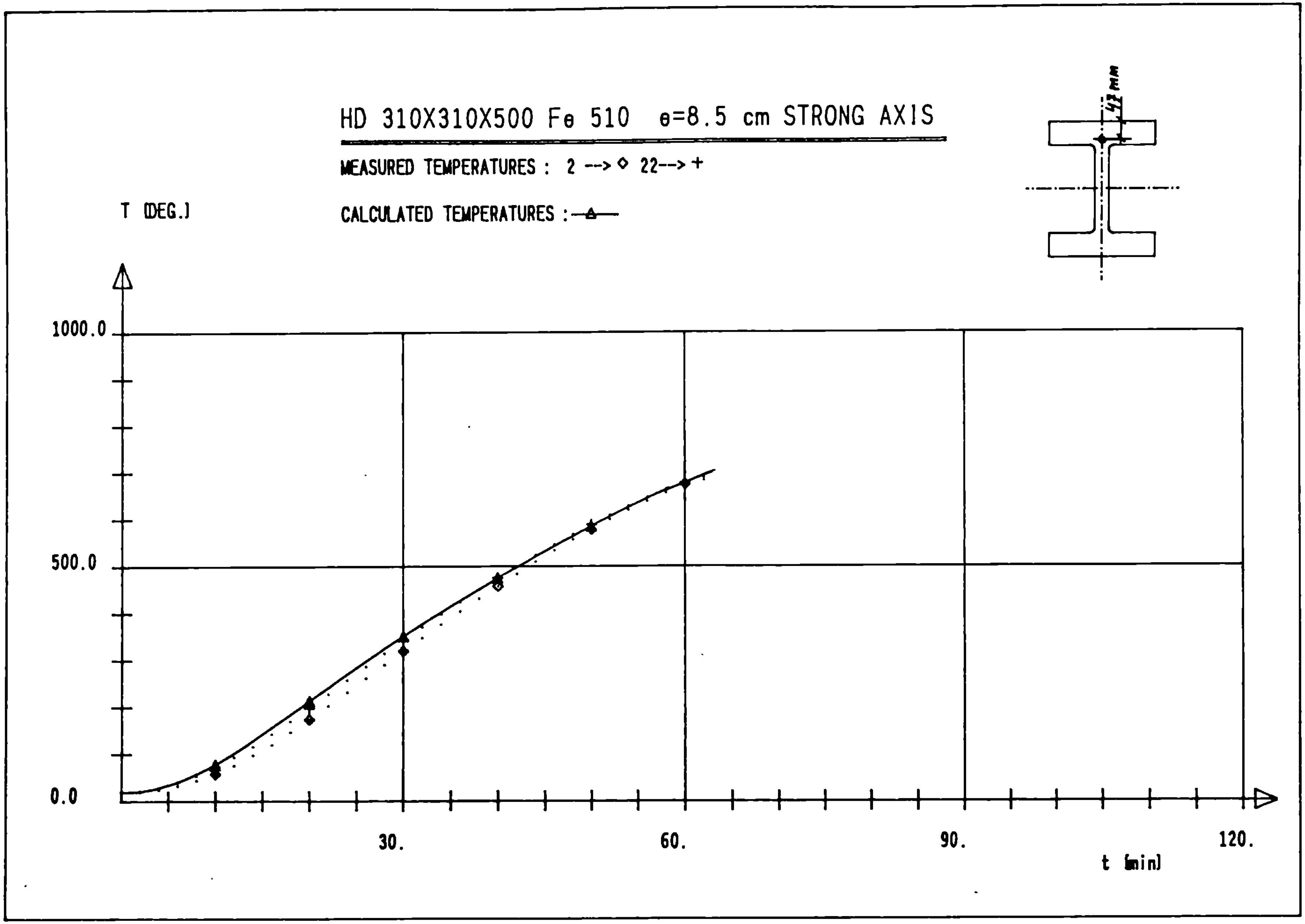
HD 310X310X500 Fe 510 e=8.5 cm STRONG AXIS
MEASURED TEMPERATURES : 2 --> ◇ 22--> +
CALCULATED TEMPERATURES : —△—
T (DEG.]
1000.0
500.0
0.0
30.
60.
90.
120.
t (min]
43 mm

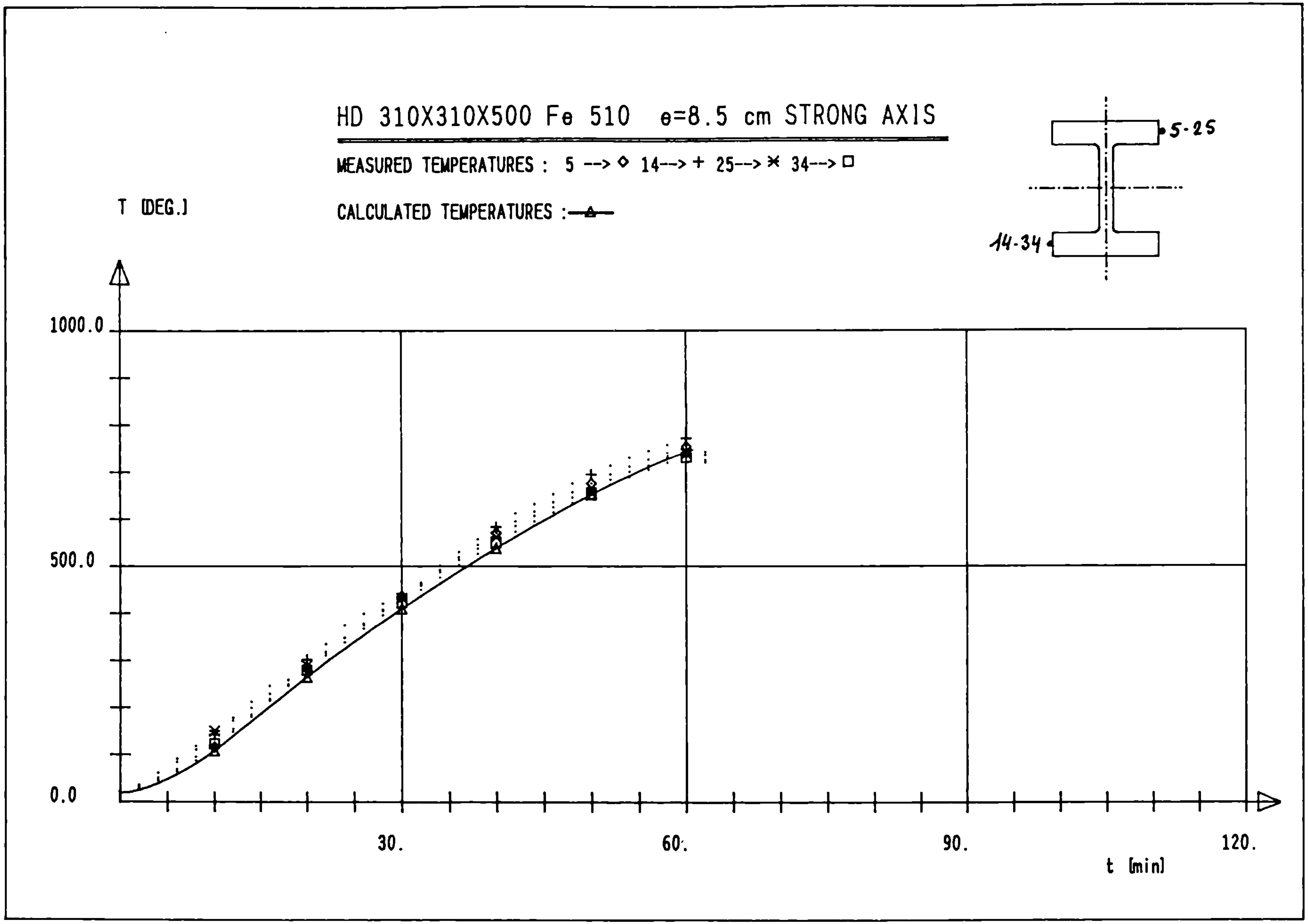
HD 310X310X500 Fe 510 e=8.5 cm STRONG AXIS
MEASURED TEMPERATURES : 5 --> ◇ 14--> + 25--> ✳ 34--> □
CALCULATED TEMPERATURES :
T [DEG.]
1000.0
500.0
0.0
30.
60.
90.
120.
t [min]
5-25
14-34

2.9

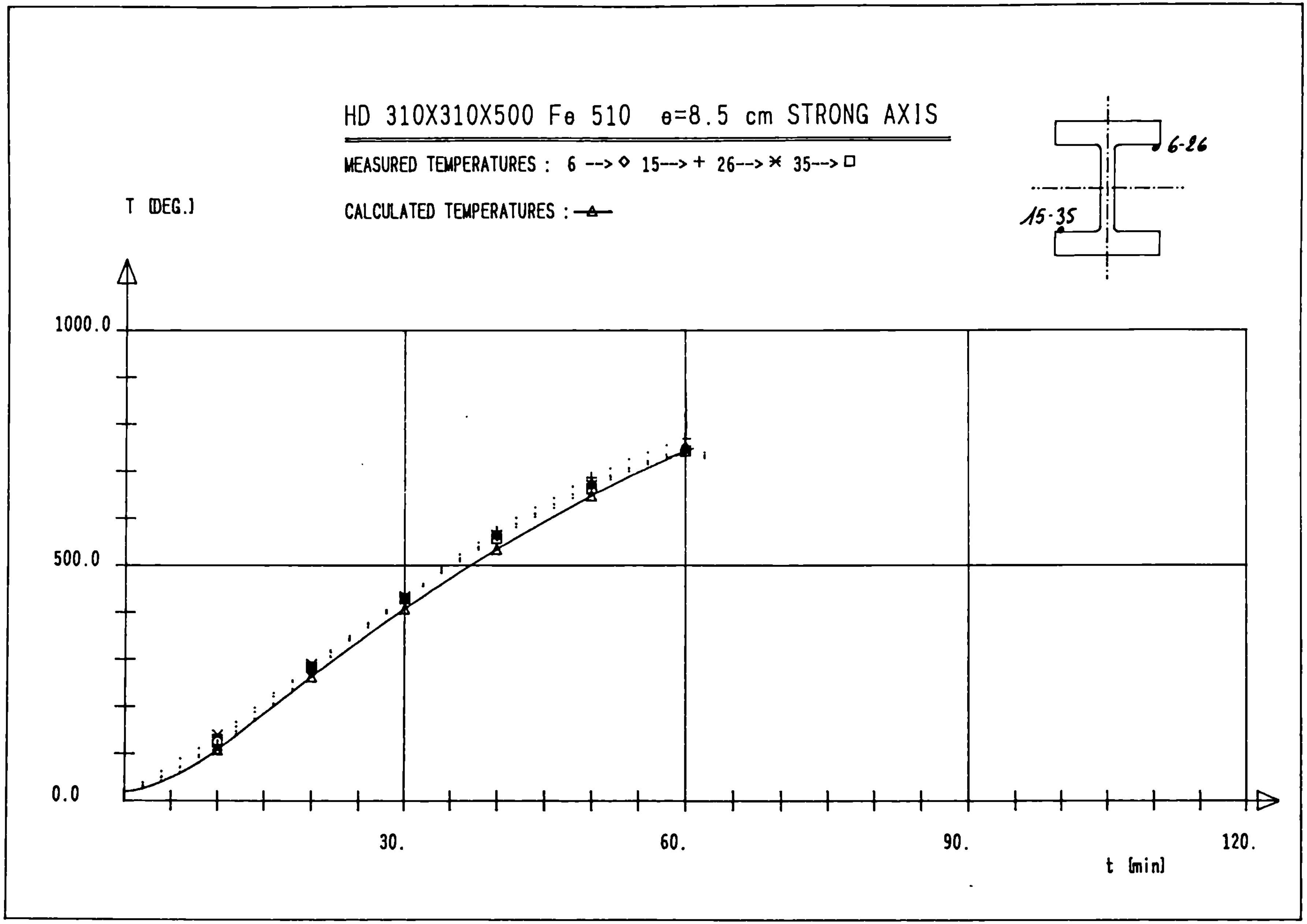
HD 310X310X500 Fe 510 e=8.5 cm STRONG AXIS
MEASURED TEMPERATURES : 6 --> ◇ 15--> + 26--> ✕ 35--> □
CALCULATED TEMPERATURES : —△—
T (DEG.)
1000.0
500.0
0.0
30.
60.
90.
120.
t [min]
6-26
15-35

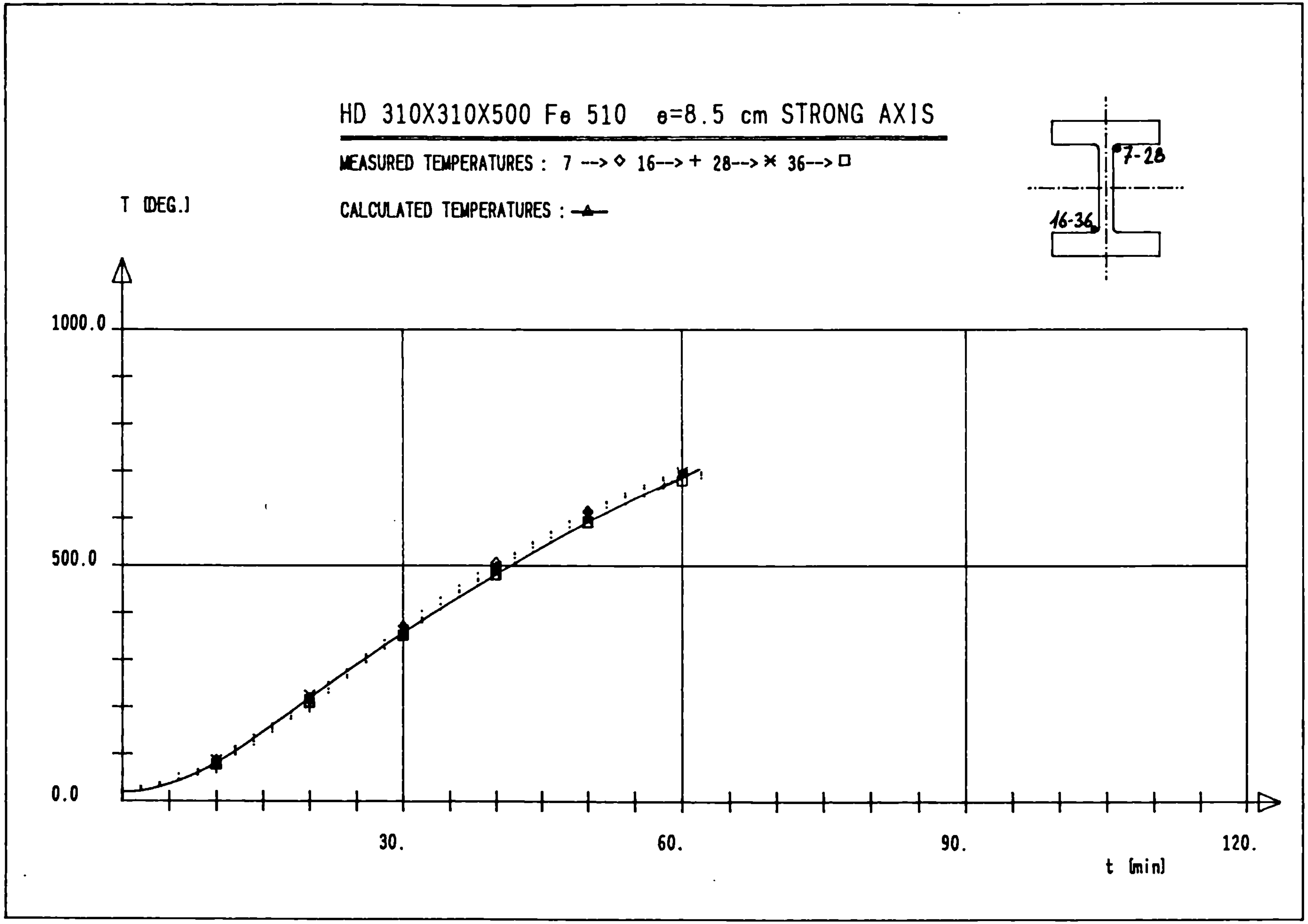
HD 310X310X500 Fe 510 e=8.5 cm STRONG AXIS
MEASURED TEMPERATURES : 7 --> ◇ 16--> + 28--> ✕ 36--> □
CALCULATED TEMPERATURES :
T [DEG.]
1000.0
500.0
0.0
30.
60.
90.
120.
t [min]
7-28
16-36

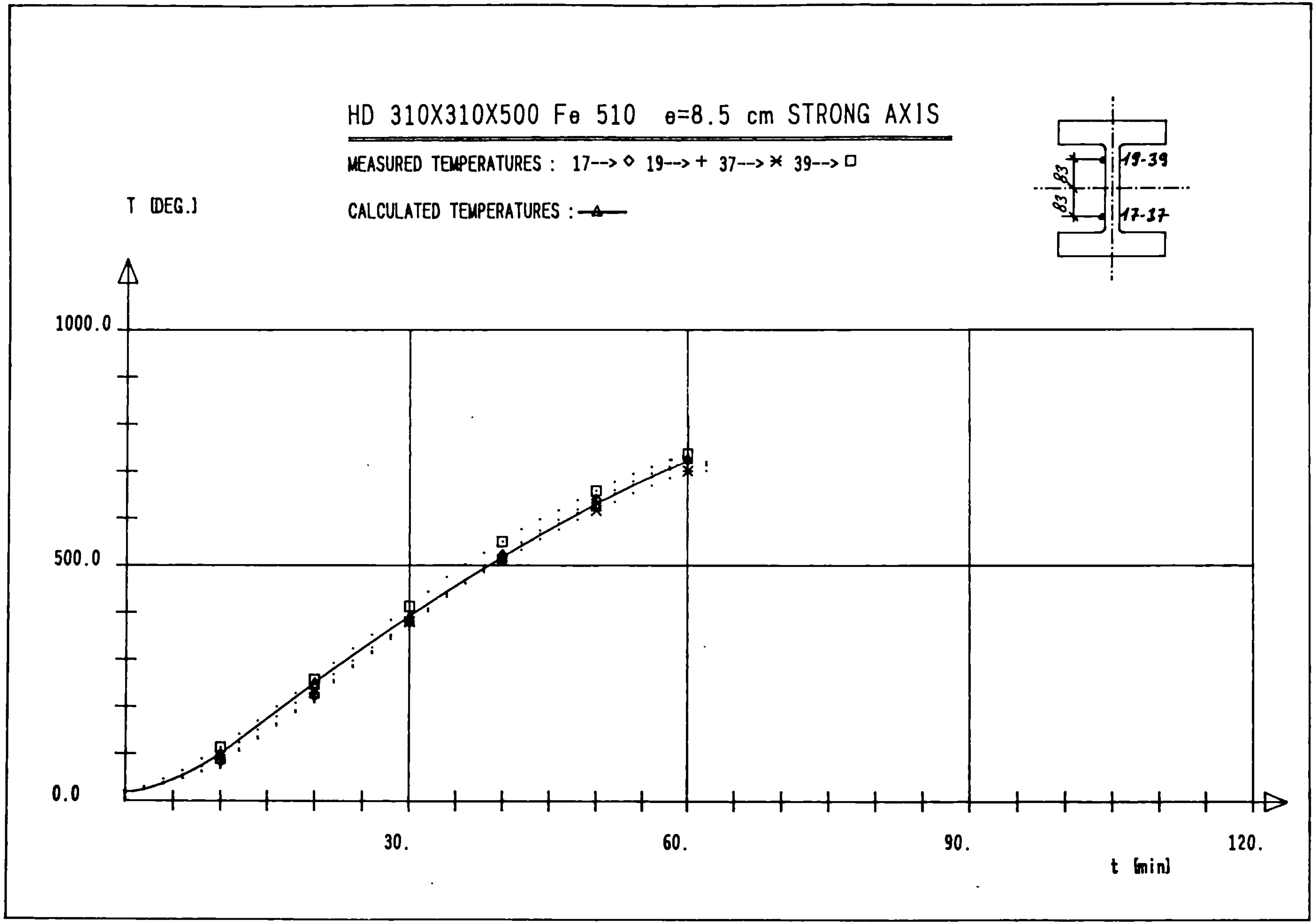
HD 310X310X500 Fe 510 e=8.5 cm STRONG AXIS
MEASURED TEMPERATURES : 17--> ◇ 19--> + 37--> ✱ 39--> □
CALCULATED TEMPERATURES :
T (DEG.)
1000.0
500.0
0.0
30.
60.
90.
120.
t (min)
19-39
17-37
83
83
83

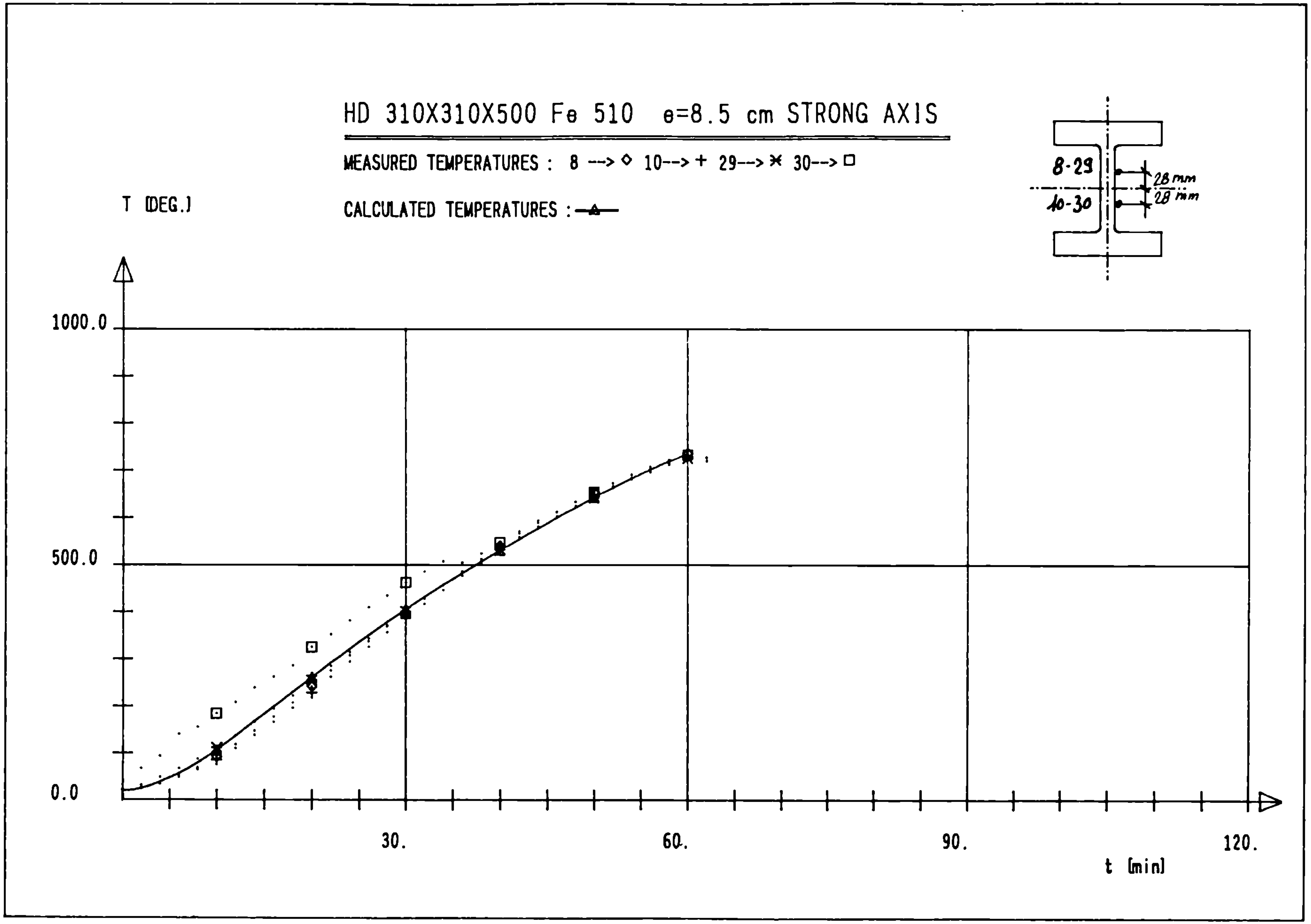
HD 310X310X500 Fe 510 e=8.5 cm STRONG AXIS
MEASURED TEMPERATURES : 8 --> ◇ 10--> + 29--> ✳ 30--> □
CALCULATED TEMPERATURES :
T [DEG.]
1000.0
500.0
0.0
30.
60.
90.
120.
t [min]
8-29
10-30
28 mm
28 mm

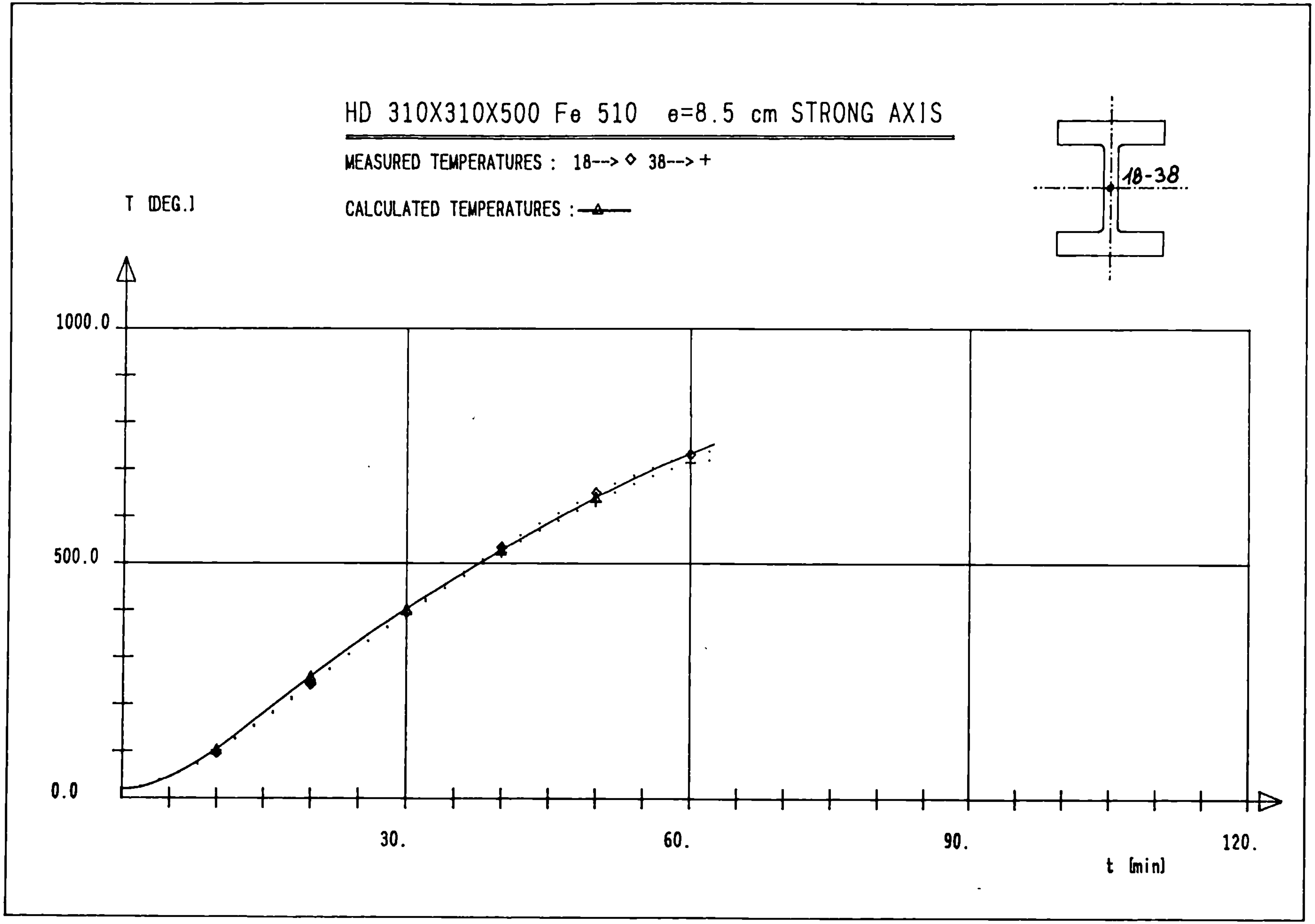
HD 310X310X500 Fe 510 e=8.5 cm STRONG AXIS
MEASURED TEMPERATURES : 18--> ◇ 38--> +
CALCULATED TEMPERATURES :
18-38
T [DEG.]
1000.0
500.0
0.0
30.
60.
90.
120.
t [min]

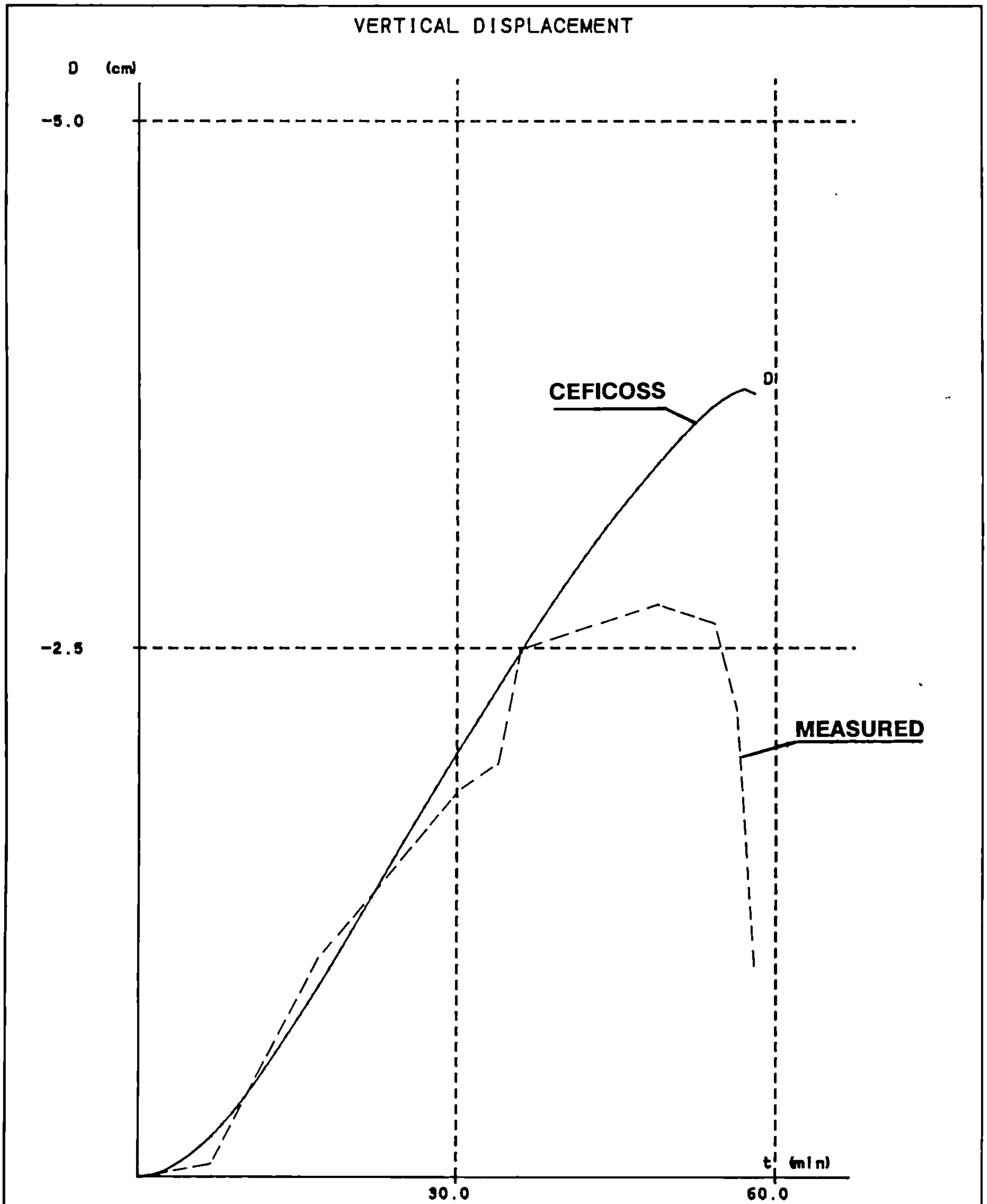

ARBED-RECHERCHES / RPS DEPARTMENT	CEFICOSS Analysis / CEF8.1
PROJECT TITLE TEST 2 HD 310X310X500 / Fe 510 / STRONG AXIS	PROJECT NUMBER REFAO III ESCH/ALZETTE : 28-FEB-1989 SHEET : 2.14

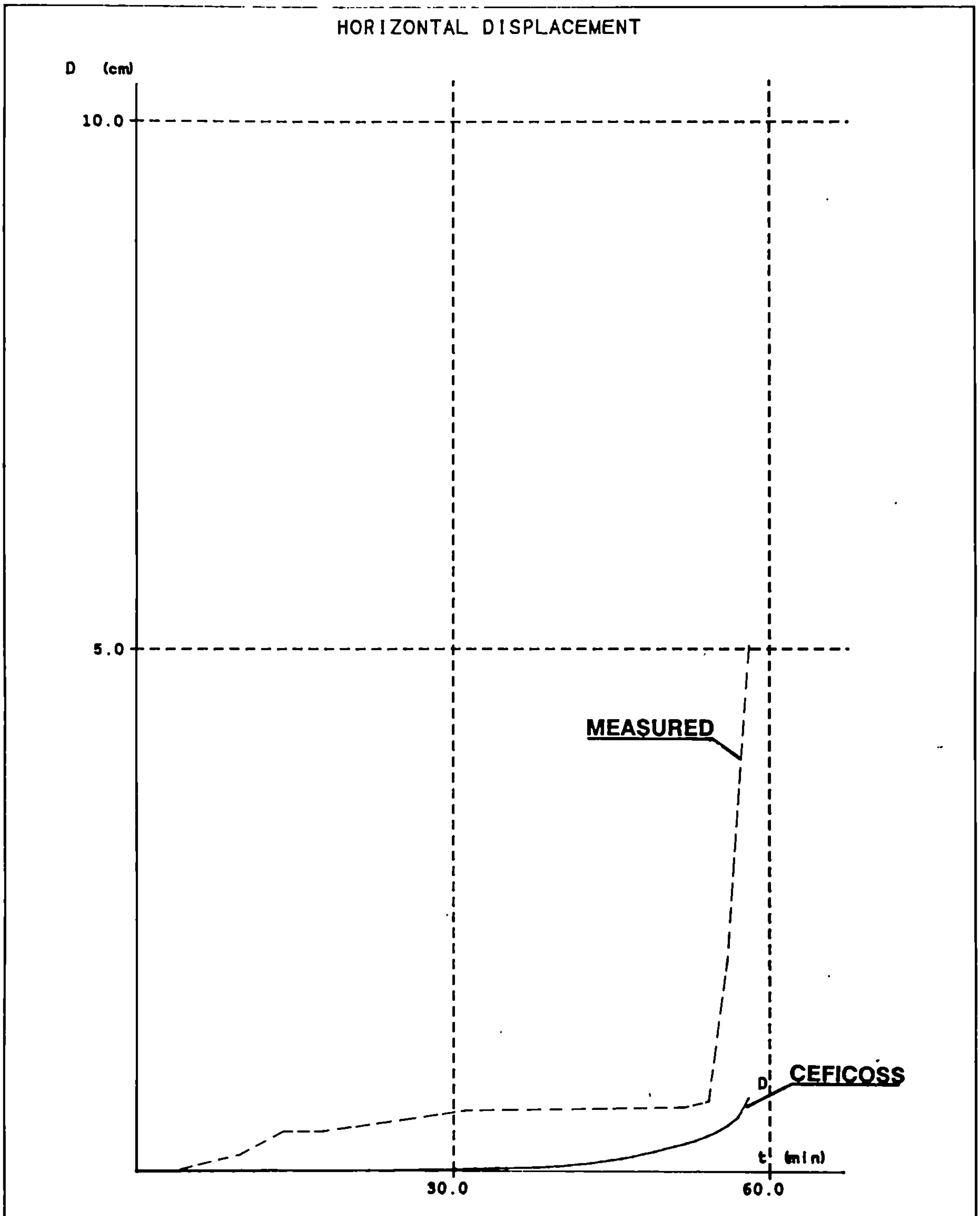

ARBED-RECHERCHES / RPS DEPARTMENT	CEFICOSS Analysis / CEF8.1
PROJECT TITLE TEST 2 HD 310X310X500 / Fe 510 / STRONG AXIS	PROJECT NUMBER REFAO III ESCH/ALZETTE : 28-FEB-1989 SHEET : 2.15

TEST 3

COLUMN HD 310x310x500 - Fe 510

BUCKLING LENGTH 5.70 m

TEST PERFORMED IN BRAUNSCHWEIG

TEST Nr 3

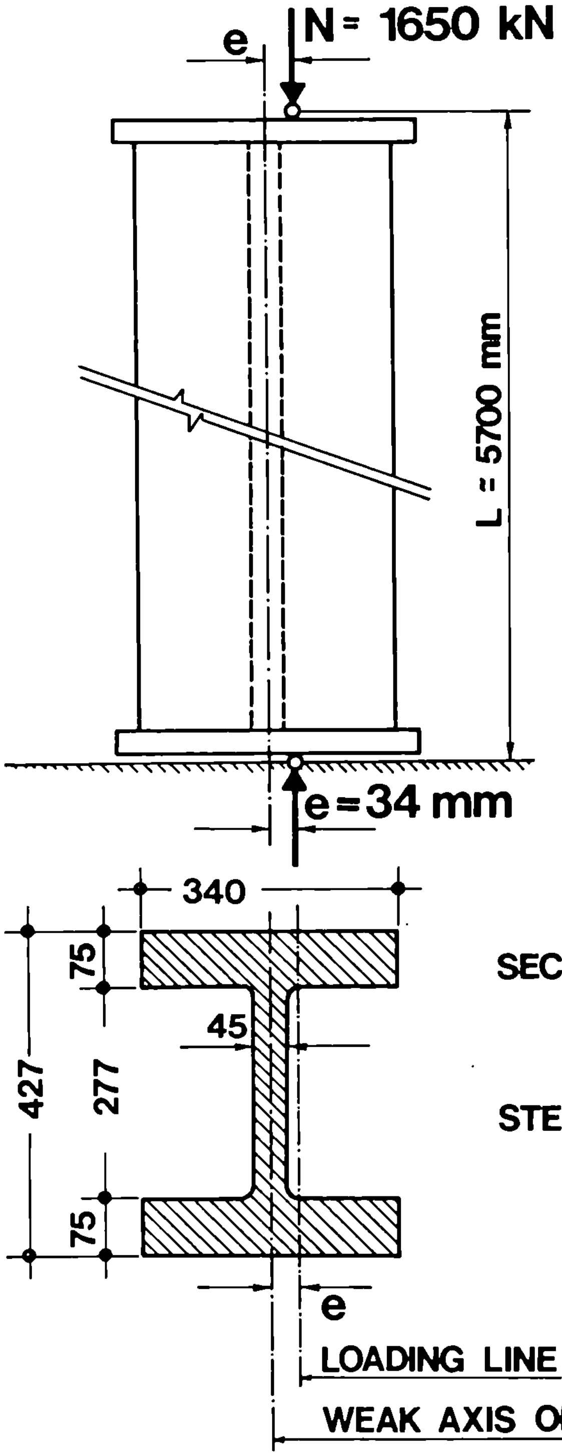

SECTION :

HD 310×310×500

STEEL GRADE :

Fe 510

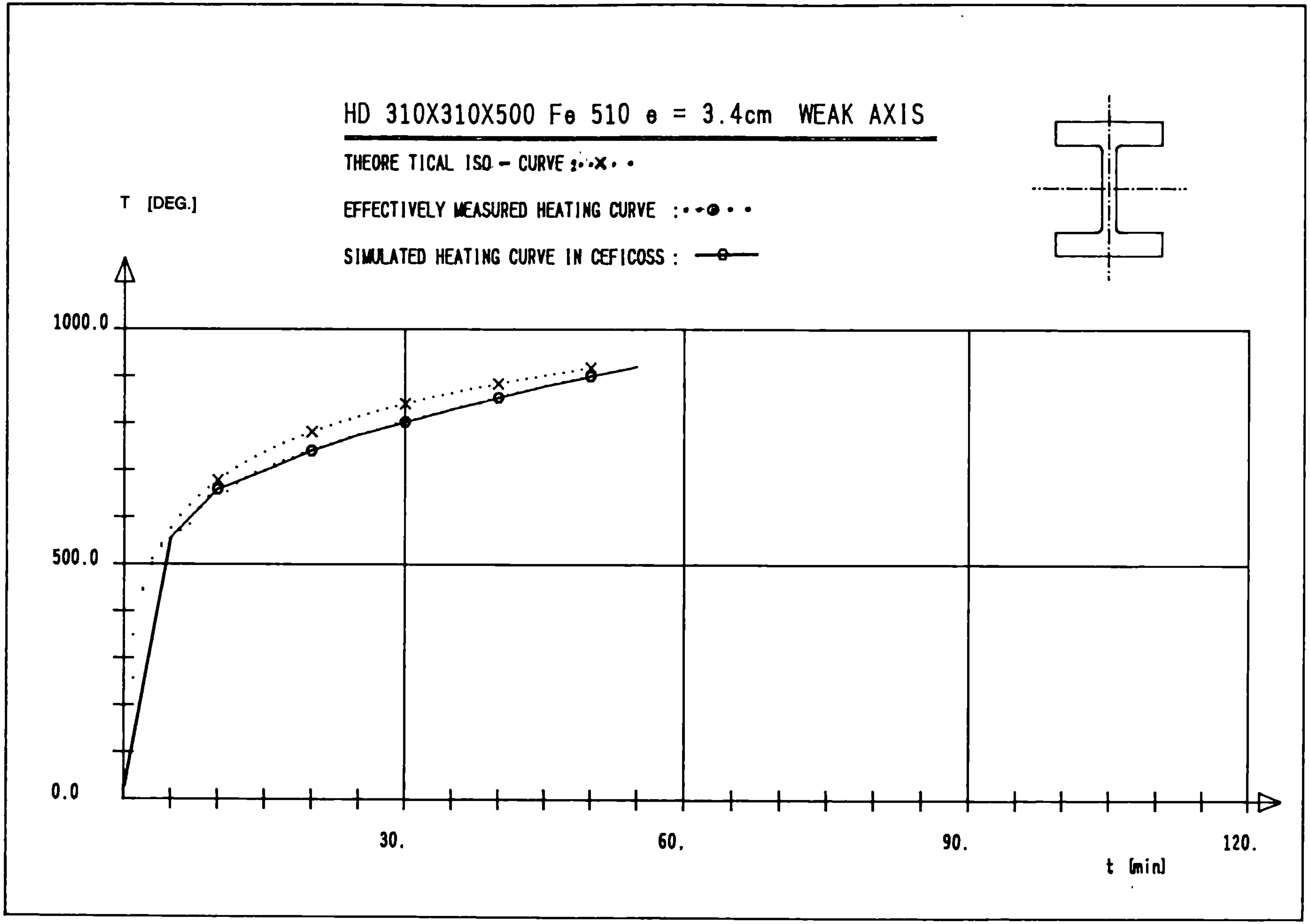
HD 310X310X500 Fe 510 e = 3.4cm WEAK AXIS
THEORE TICAL ISO - CURVE : · · X · ·
EFFECTIVELY MEASURED HEATING CURVE : · · ⊙ · ·
SIMULATED HEATING CURVE IN CEFICOSS :
T [DEG.]
1000.0
500.0
0.0
30.
60.
90.
120.
t [min]

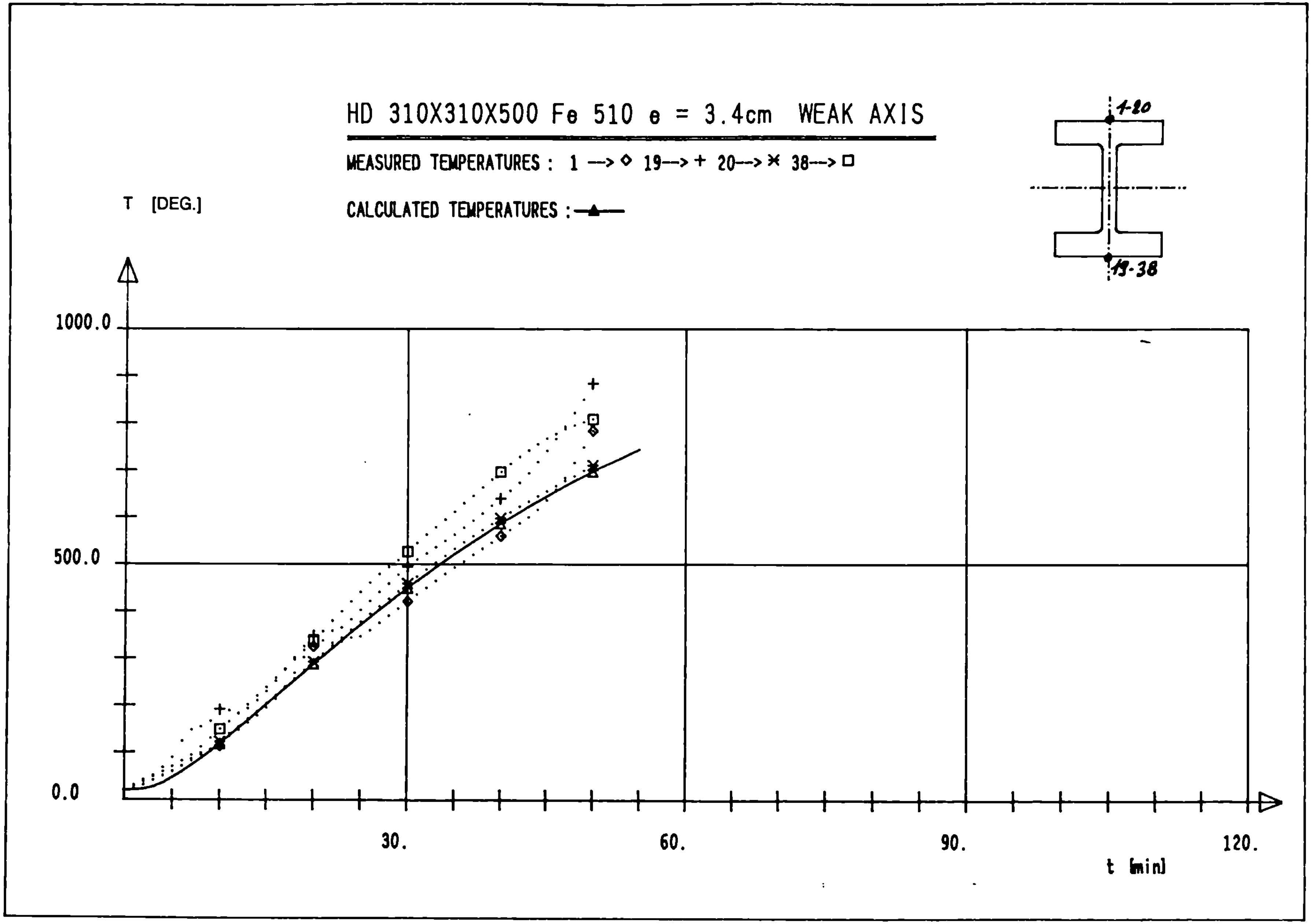
HD 310X310X500 Fe 510 e = 3.4cm WEAK AXIS
MEASURED TEMPERATURES : 1 ---> ◇ 19---> + 20---> ✕ 38---> □
CALCULATED TEMPERATURES :
T [DEG.]
1000.0
500.0
0.0
30.
60.
90.
120.
t [min]
1-20
19-38

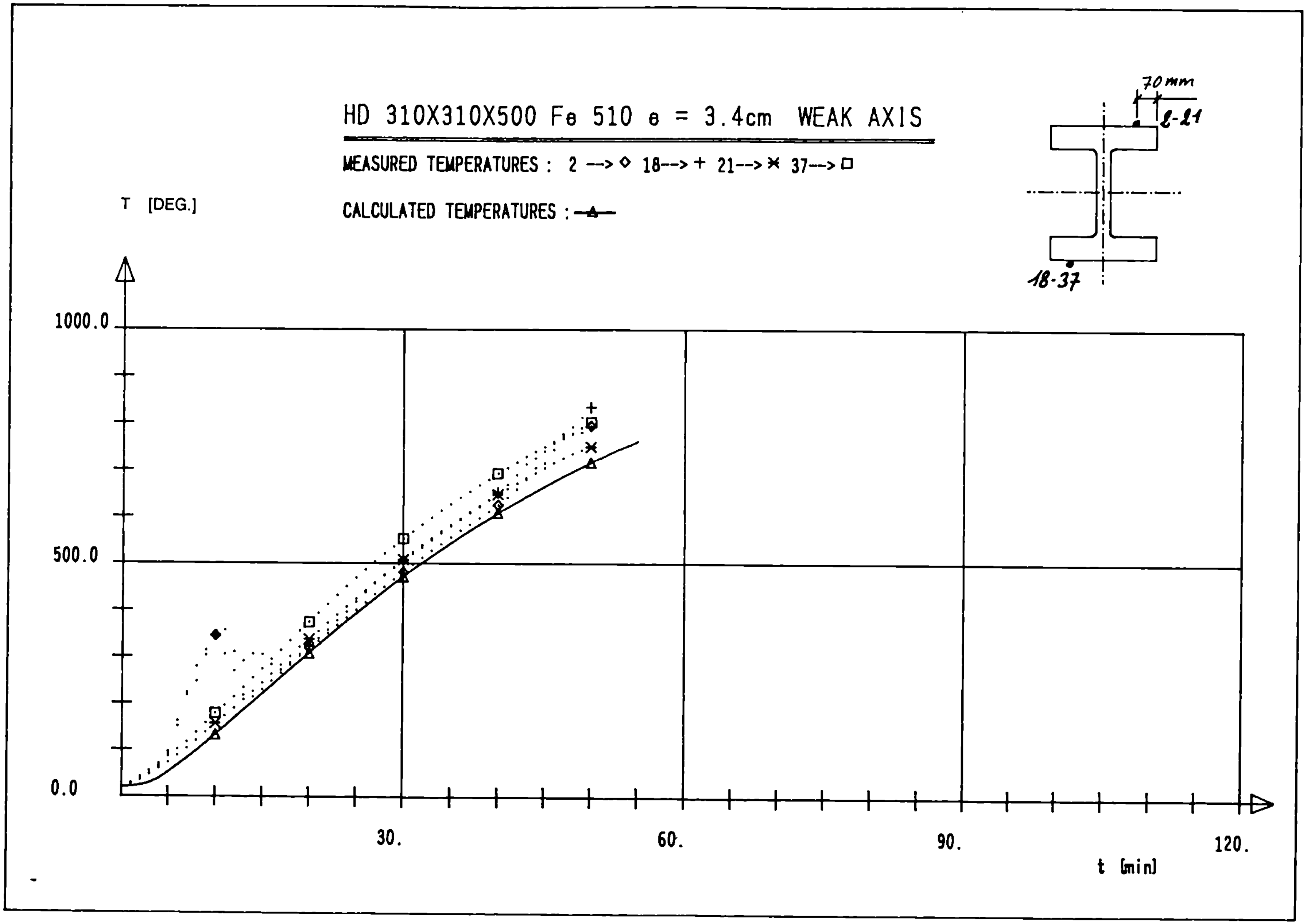
HD 310X310X500 Fe 510 e = 3.4cm WEAK AXIS
MEASURED TEMPERATURES : 2 --> ◇ 18--> + 21--> ✕ 37--> □
CALCULATED TEMPERATURES : —△—
T [DEG.]
1000.0
500.0
0.0
30.
60.
90.
120.
t [min]
70 mm
2-21
18-37

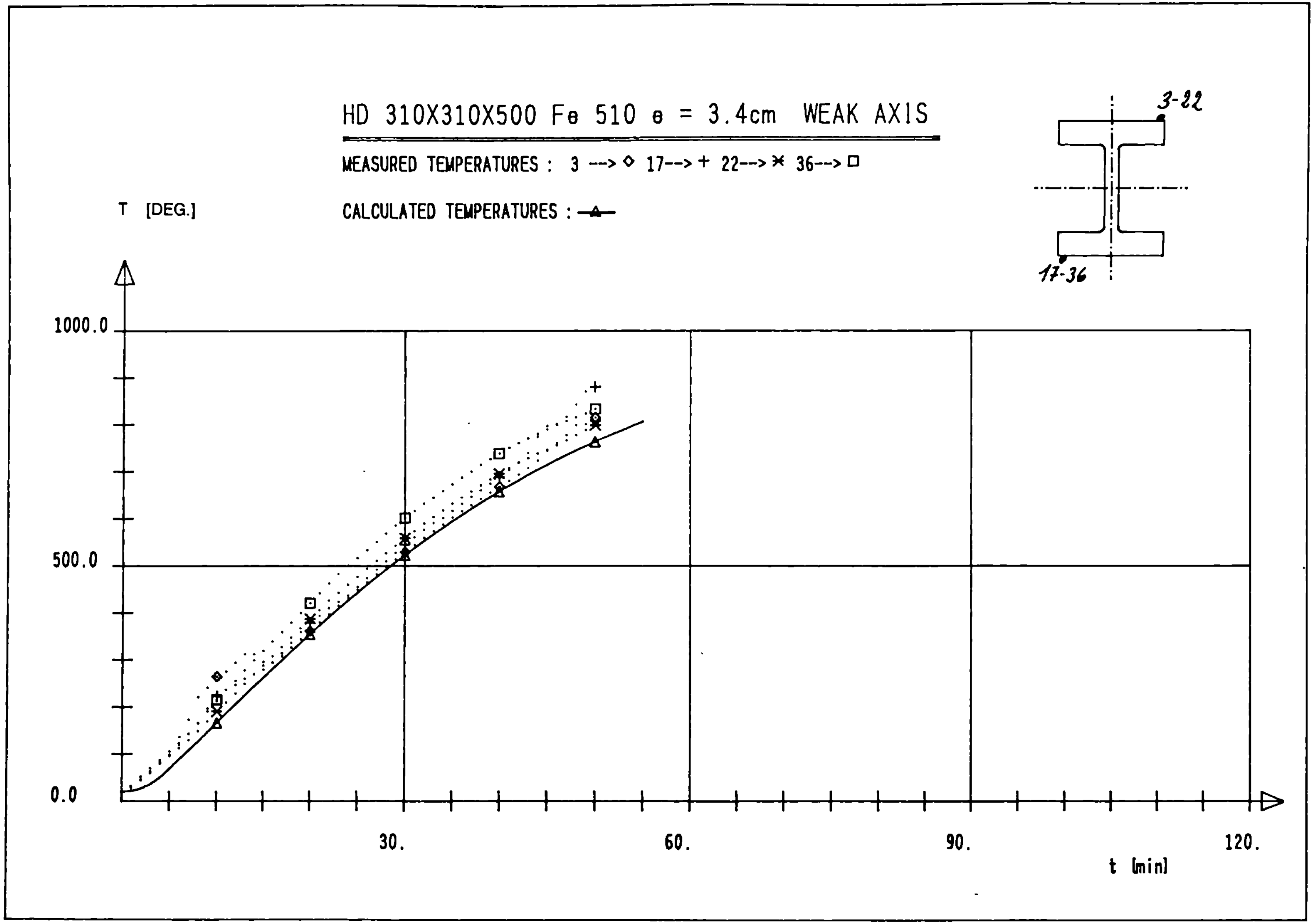

HD 310X310X500 Fe 510 e = 3.4cm WEAK AXIS
MEASURED TEMPERATURES : 3 --> ◇ 17--> + 22--> ✕ 36--> □
CALCULATED TEMPERATURES : —△—
T [DEG.]
1000.0
500.0
0.0
30.
60.
90.
120.
t [min]
3-22
17-36

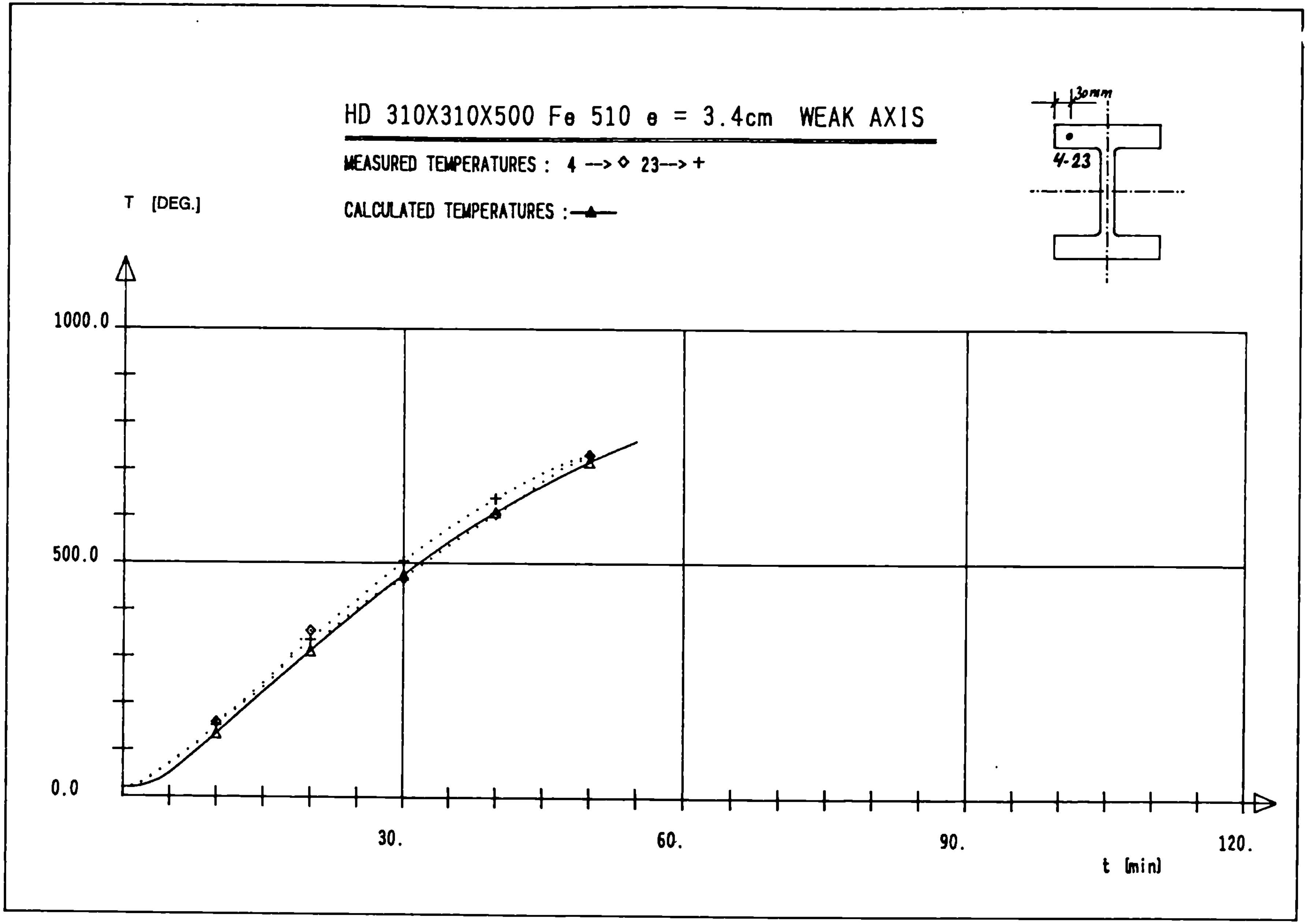
HD 310X310X500 Fe 510 e = 3.4cm WEAK AXIS
MEASURED TEMPERATURES : 4 —> ◇ 23—> +
CALCULATED TEMPERATURES :
T [DEG.]
1000.0
500.0
0.0
30.
60.
90.
120.
t (min)
30mm
4-23

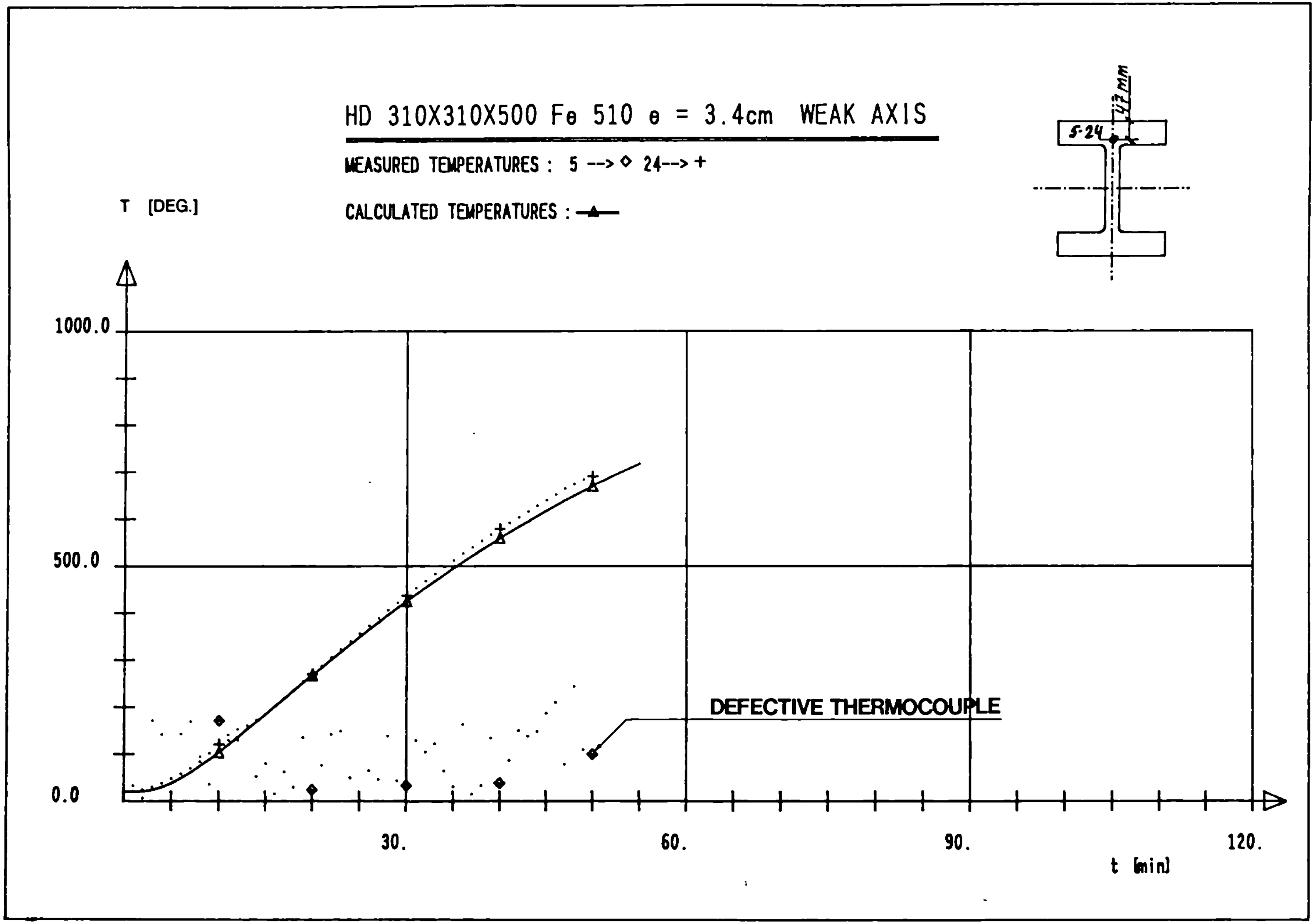
HD 310X310X500 Fe 510 e = 3.4cm WEAK AXIS
MEASURED TEMPERATURES : 5 --> ◇ 24--> +
CALCULATED TEMPERATURES : —▲—
T [DEG.]
1000.0
500.0
0.0
30.
60.
90.
120.
t [min]
DEFECTIVE THERMOCOUPLE
5-24
47mm

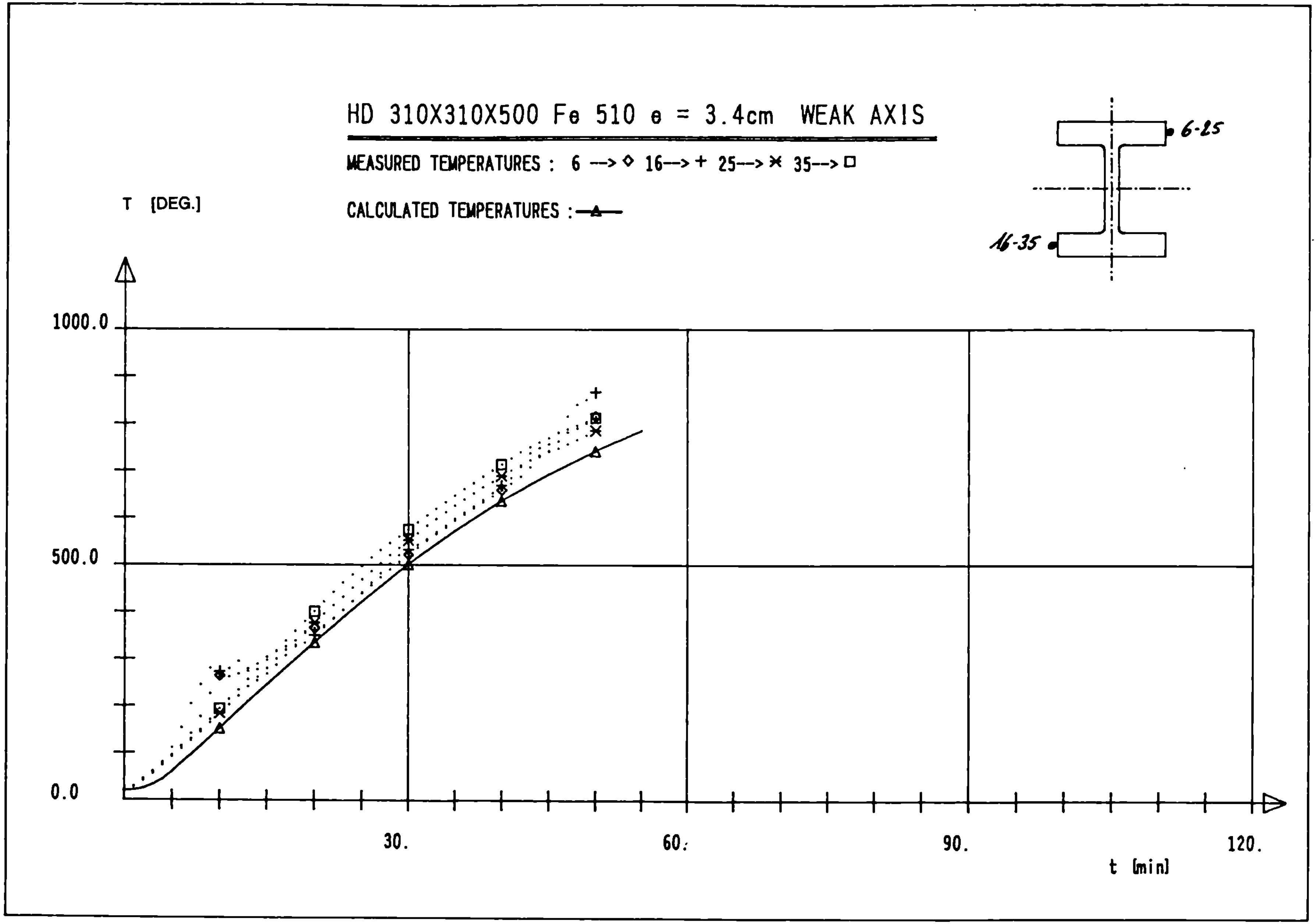
HD 310X310X500 Fe 510 e = 3.4cm WEAK AXIS
MEASURED TEMPERATURES : 6 ---> ◇ 16---> + 25---> ✕ 35---> □
CALCULATED TEMPERATURES : —△—
T [DEG.]
1000.0
500.0
0.0
30.
60.
90.
120.
t [min]
6-25
16-35

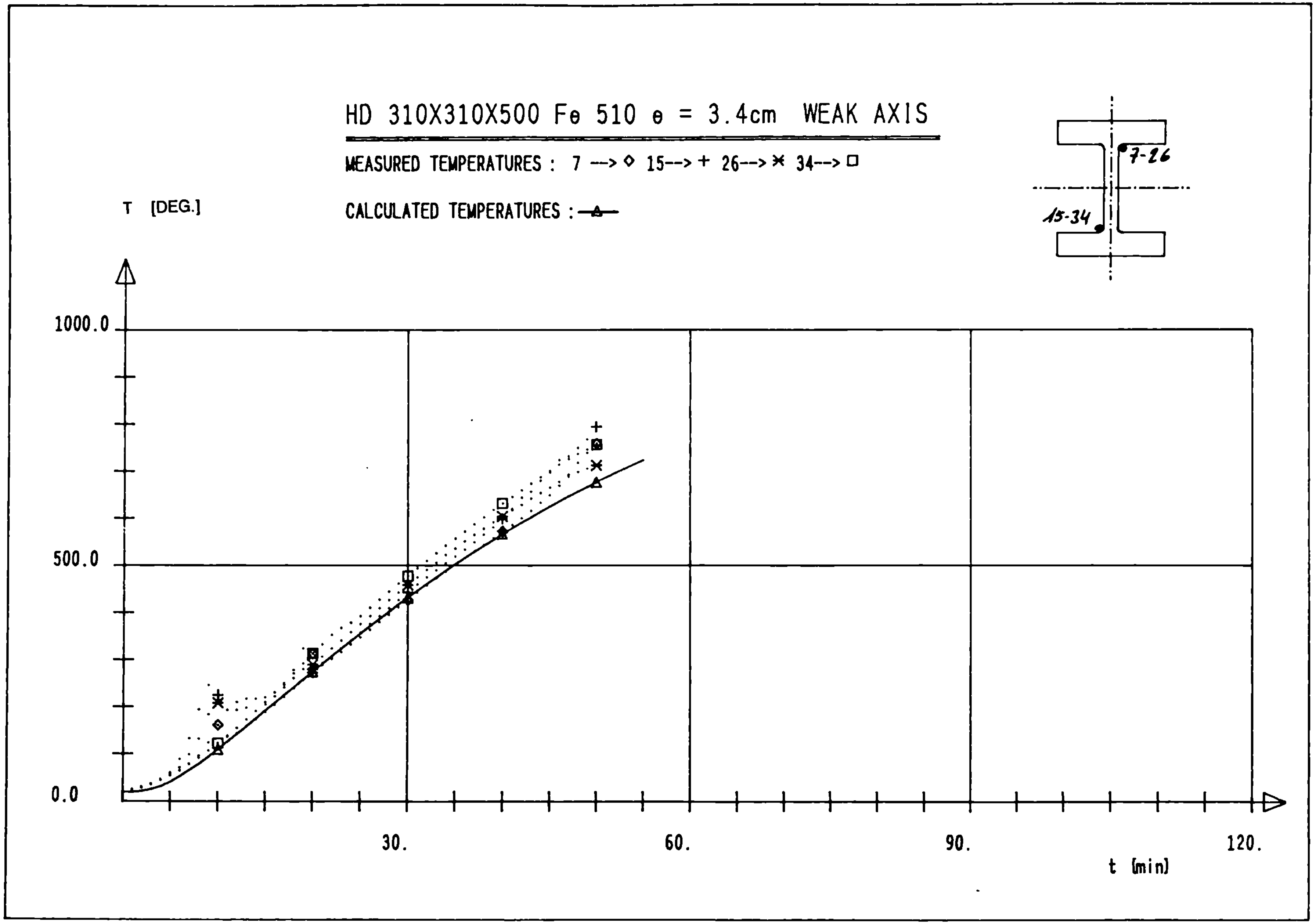
HD 310X310X500 Fe 510 e = 3.4cm WEAK AXIS
MEASURED TEMPERATURES : 7 ---> ◇ 15---> + 26---> ✳ 34---> □
CALCULATED TEMPERATURES : —△—
T [DEG.]
1000.0
500.0
0.0
30.
60.
90.
120.
t (min)
7-26
15-34

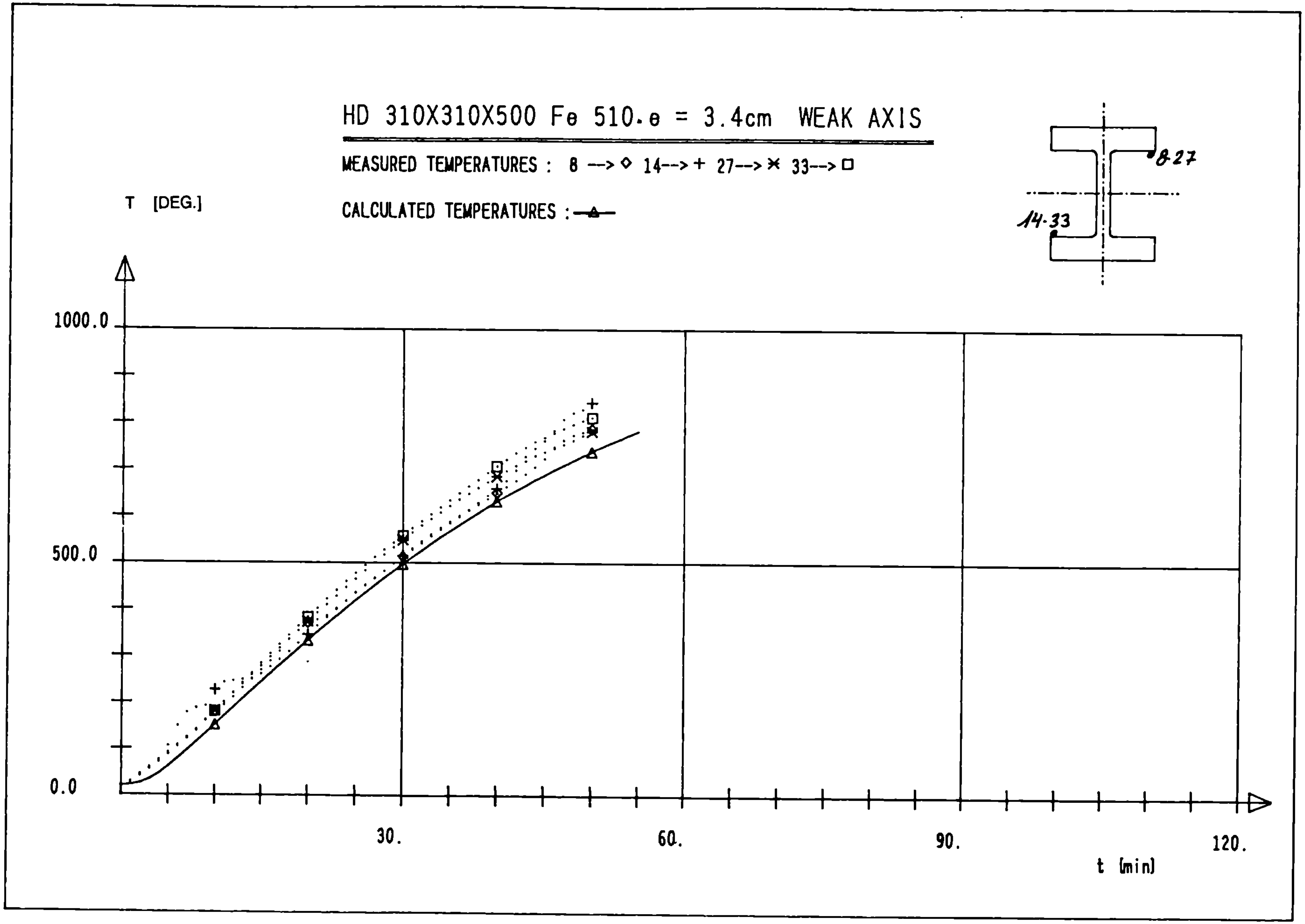
HD 310X310X500 Fe 510. e = 3.4cm WEAK AXIS
MEASURED TEMPERATURES : 8 --> ◇ 14--> + 27--> ✕ 33--> □
CALCULATED TEMPERATURES : —△—
T [DEG.]
1000.0
500.0
0.0
30.
60.
90.
120.
t (min)
8·27
14·33

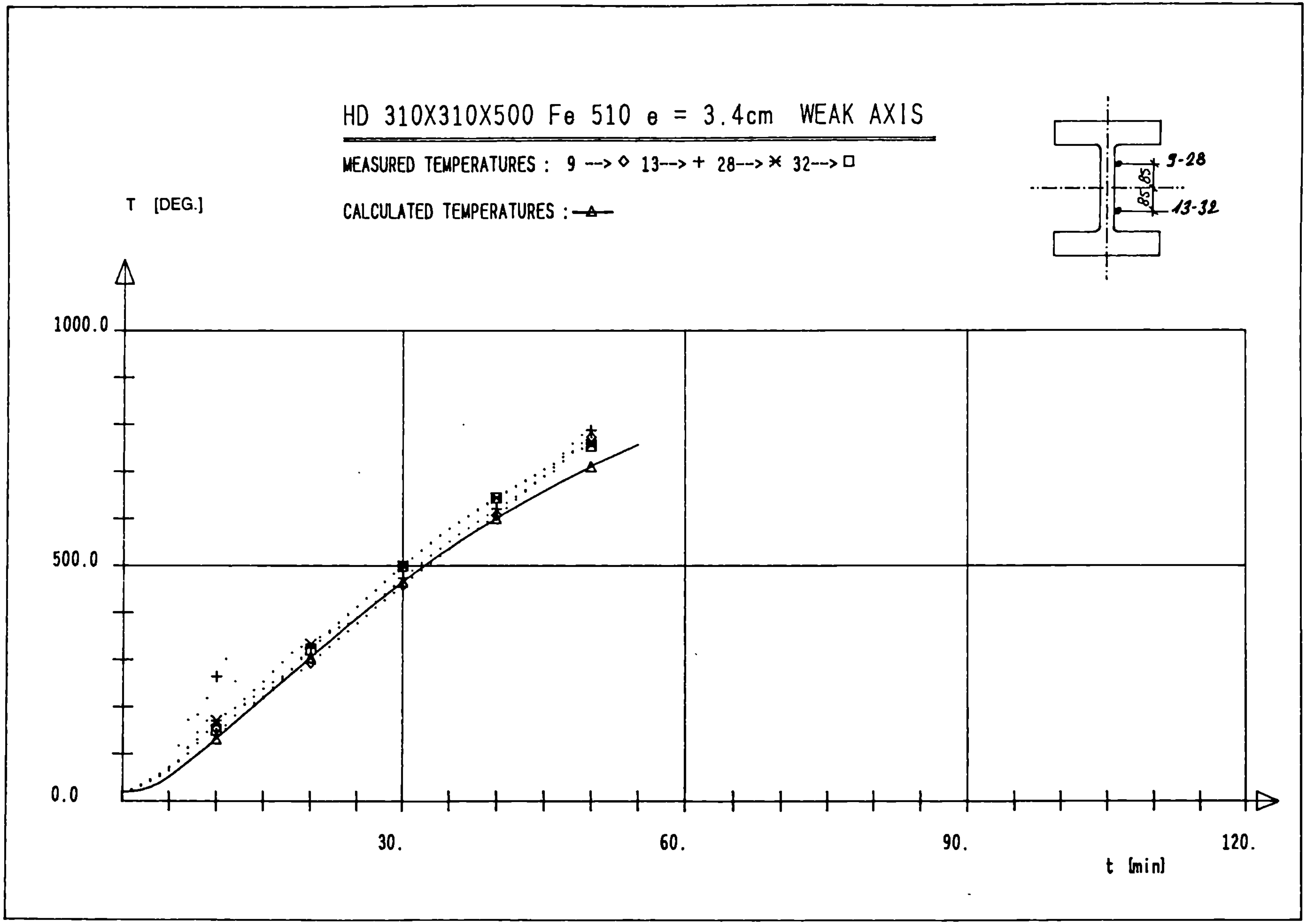
HD 310X310X500 Fe 510 e = 3.4cm WEAK AXIS
MEASURED TEMPERATURES : 9 ---> ◇ 13---> + 28---> ✱ 32---> □
CALCULATED TEMPERATURES : —△—
T [DEG.]
1000.0
500.0
0.0
30.
60.
90.
120.
t [min]
9-28
13-32
85
85

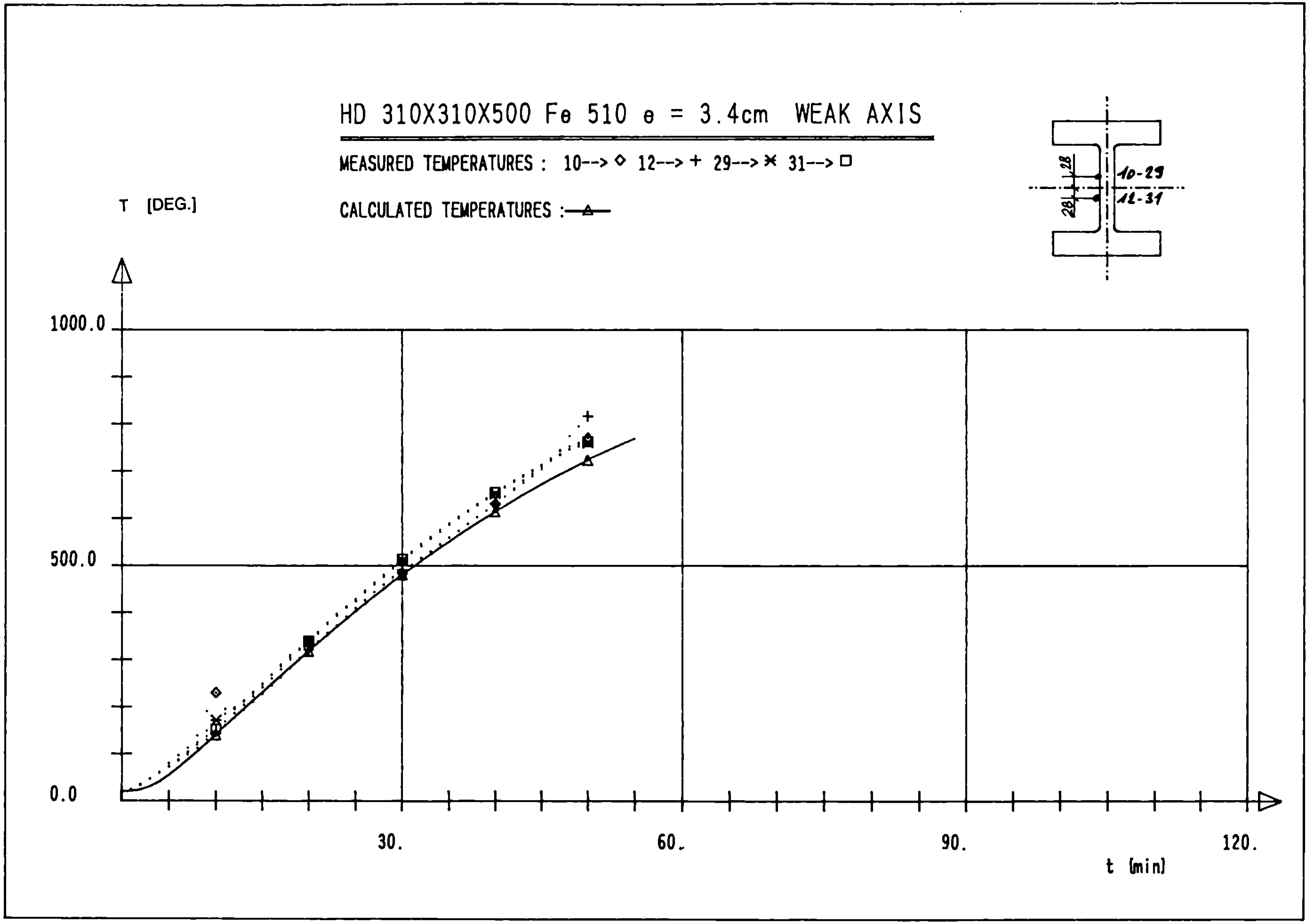
HD 310X310X500 Fe 510 e = 3.4cm WEAK AXIS
MEASURED TEMPERATURES : 10--> ◇ 12--> + 29--> ✕ 31--> □
CALCULATED TEMPERATURES :—△—
T [DEG.]
1000.0
500.0
0.0
30.
60.
90.
120.
t (min)
28
28
10-29
12-31

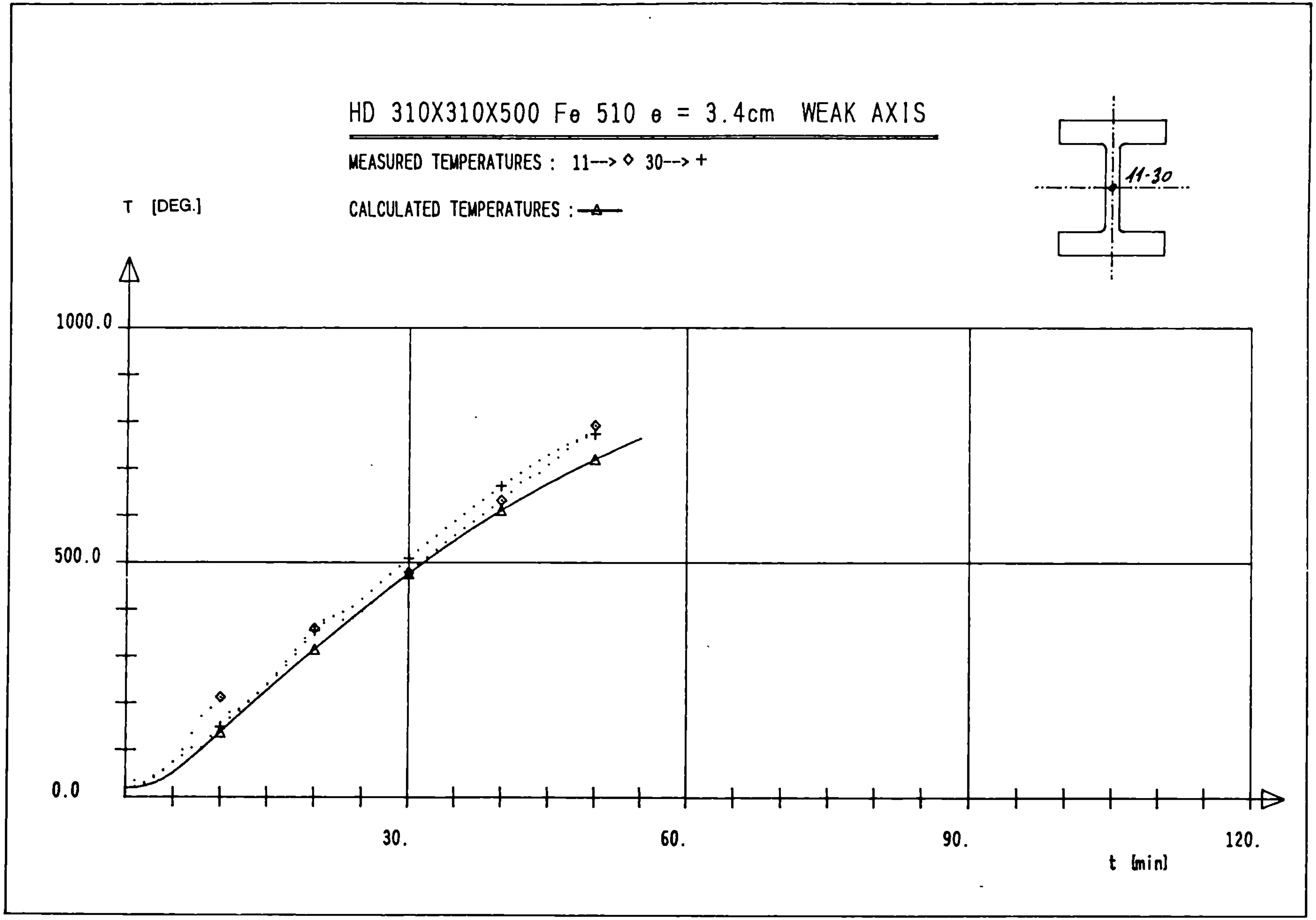
HD 310X310X500 Fe 510 e = 3.4cm WEAK AXIS
MEASURED TEMPERATURES : 11--> ◇ 30--> +
CALCULATED TEMPERATURES : —△—
T [DEG.]
1000.0
500.0
0.0
30.
60.
90.
120.
t [min]
11-30

VERTICAL DISPLACEMENT

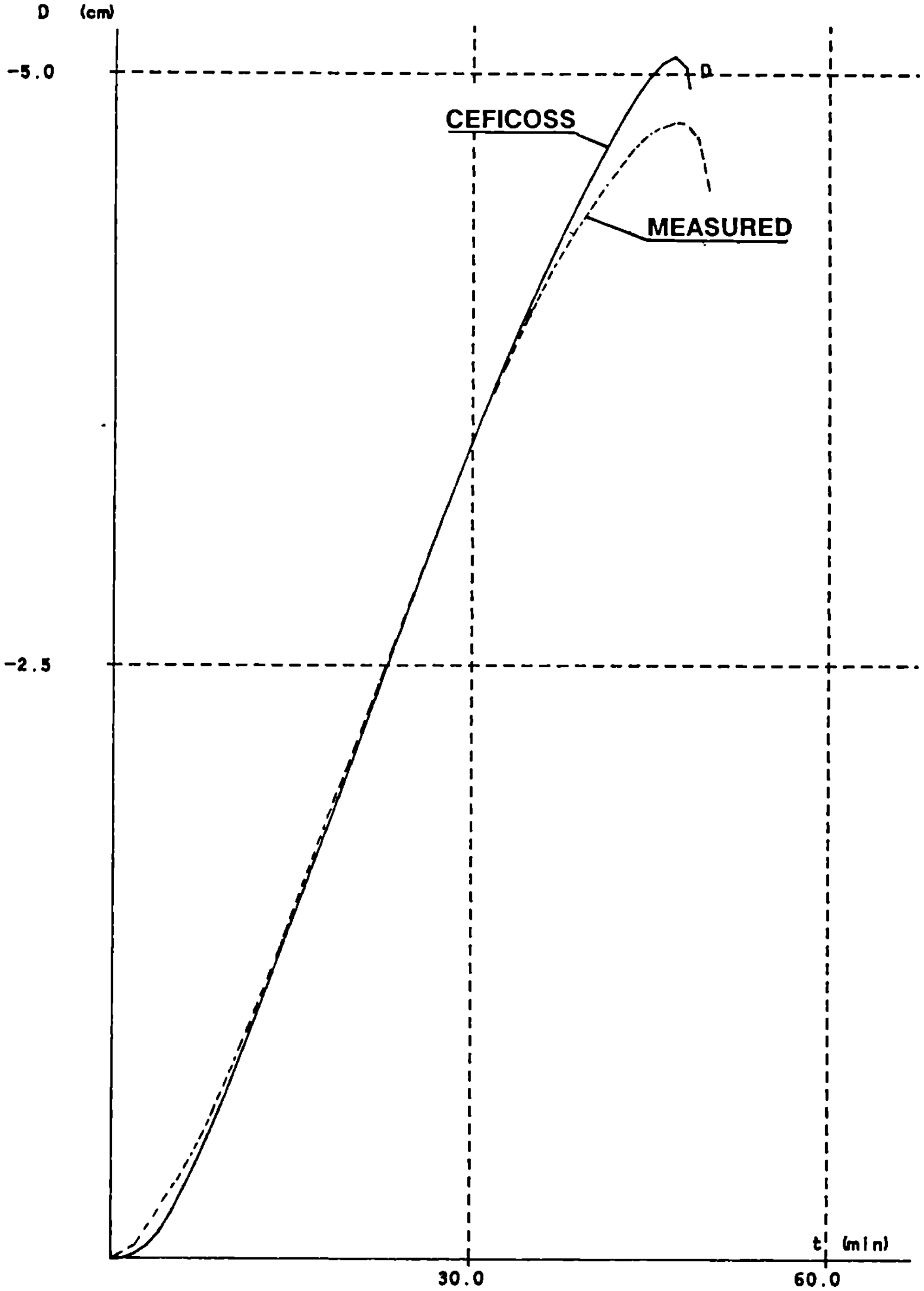

ARBED-RECHERCHES / RPS DEPARTMENT	CEFICOSS Analysis / CEF81
PROJECT TITLE TEST 3 HE 310X310X500 / Fe 510 / WEAK AXIS	PROJECT NUMBER REFAO III ESCH/ALZETTE : 22-FEB-1989 SHEET : 3.14

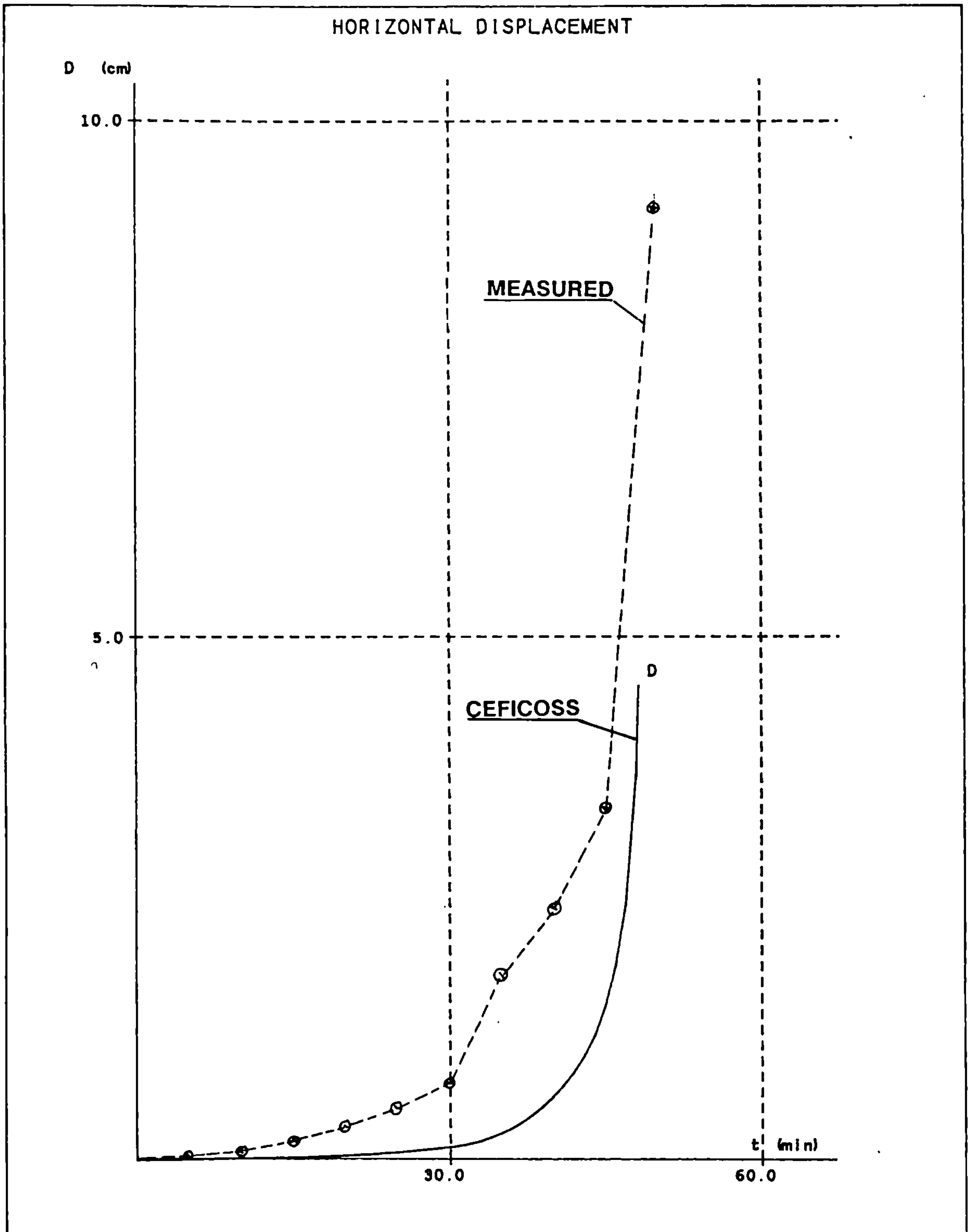

ARBED-RECHERCHES / RPS DEPARTMENT	CEFICOSS Analysis / CEF81
PROJECT TITLE TEST 3 HE 310X310X500 / Fe 510 / WEAK AXIS	PROJECT NUMBER REFAO III ESCH/ALZETTE : 22-FEB-1989 — SHEET : 3.15

TEST 4

COLUMN HD 400x400x1086 - Fe 510

BUCKLING LENGTH 4.14 m

TEST PERFORMED IN GAND

TEST Nr 4

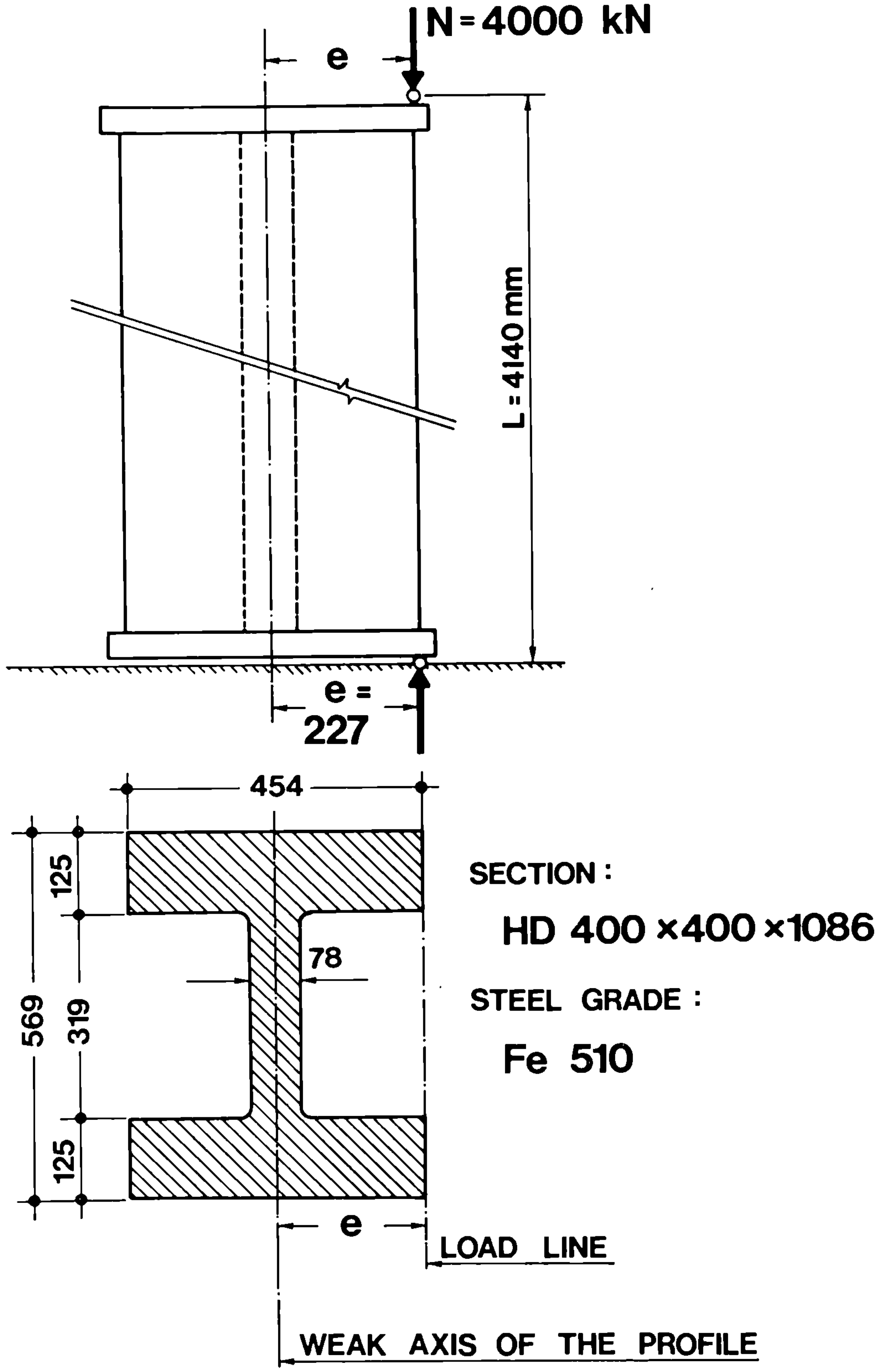

N = 4000 kN
e
L = 4140 mm
e = 227
454
125
319
569
125
78
SECTION :
HD 400 ×400 ×1086
STEEL GRADE :
Fe 510
e
LOAD LINE
WEAK AXIS OF THE PROFILE

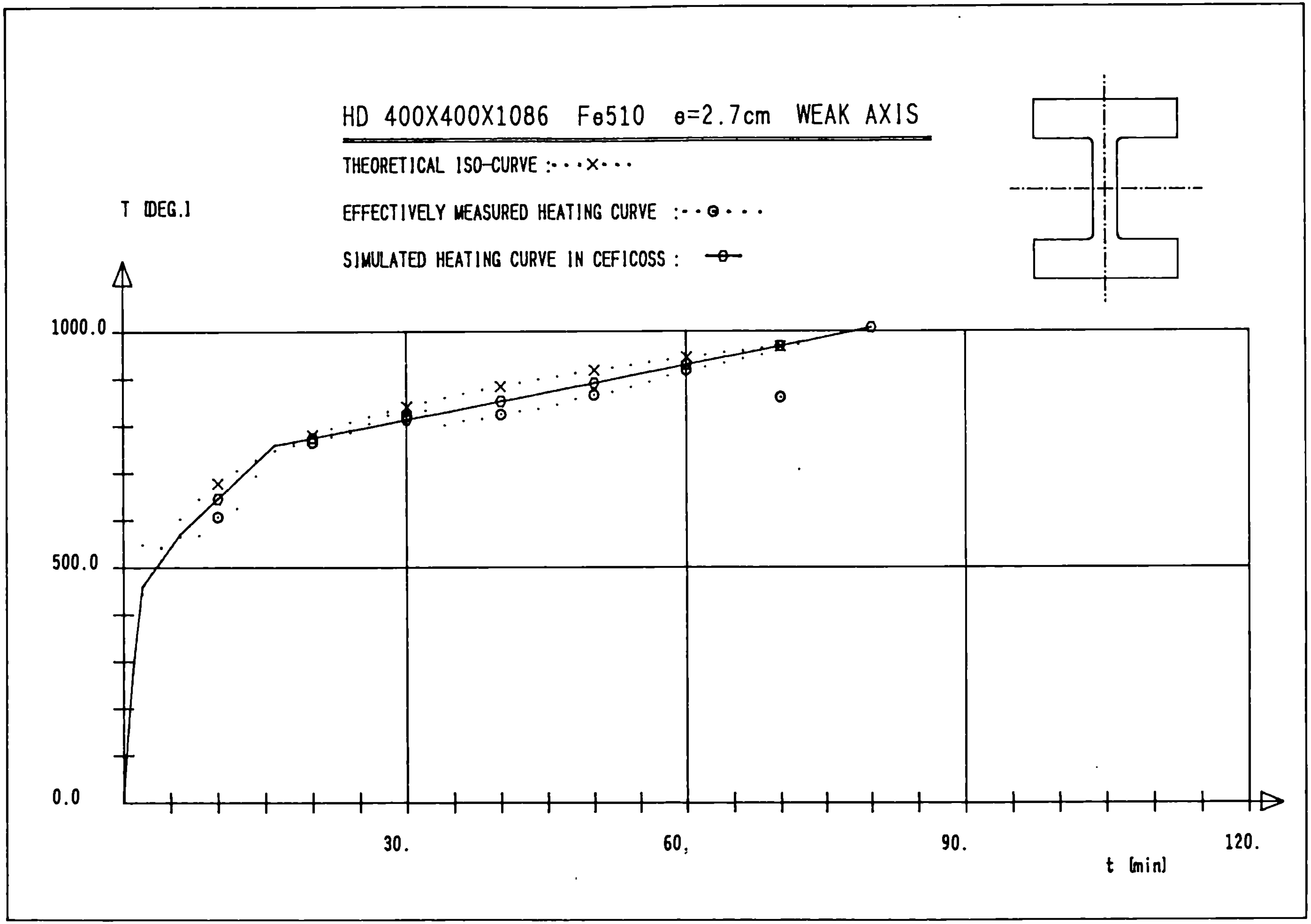
HD 400X400X1086 Fe510 e=2.7cm WEAK AXIS
THEORETICAL ISO-CURVE :
EFFECTIVELY MEASURED HEATING CURVE :
SIMULATED HEATING CURVE IN CEFICOSS :
T [DEG.]
1000.0
500.0
0.0
30.
60.
90.
120.
t [min]

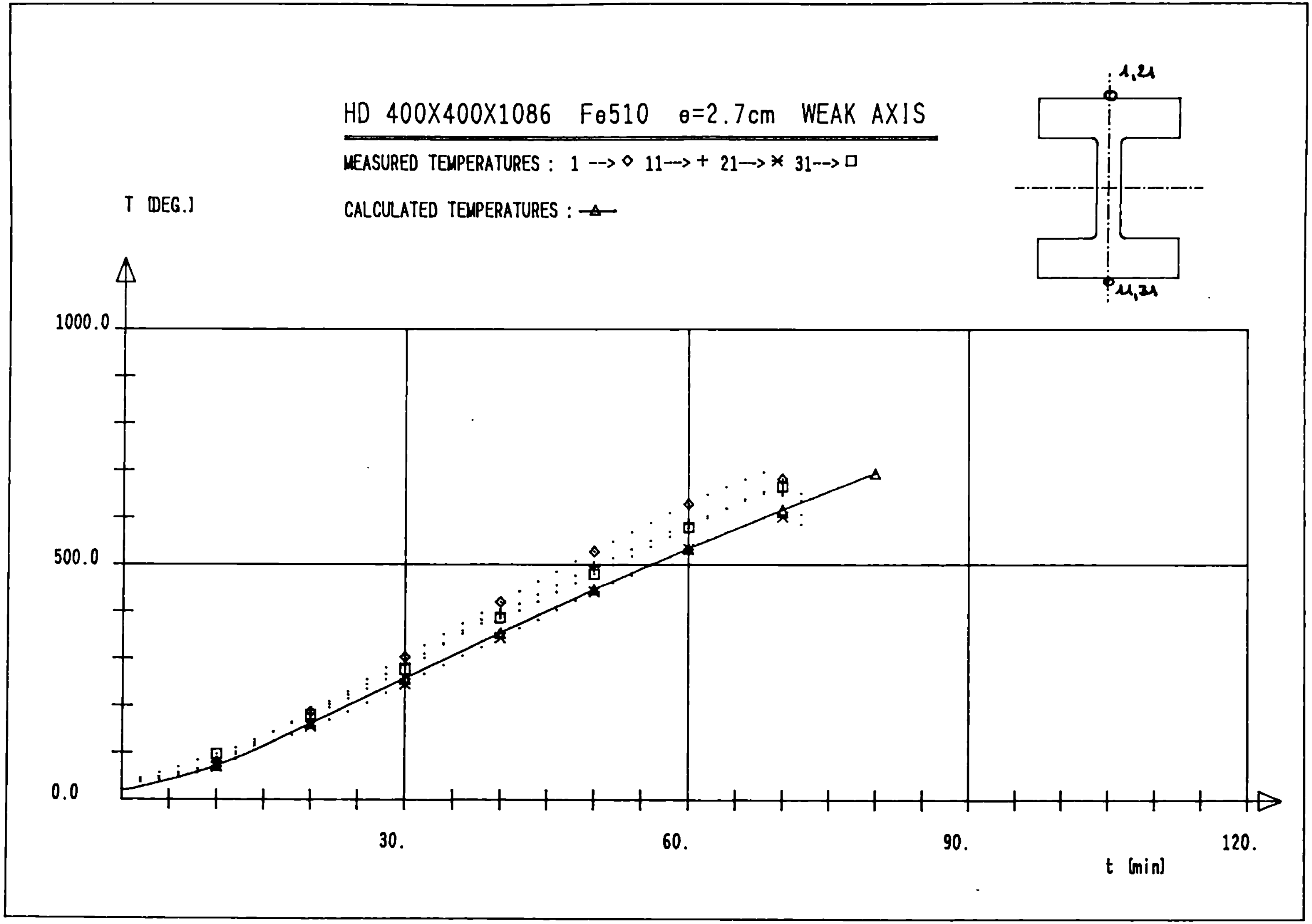
HD 400X400X1086 Fe510 e=2.7cm WEAK AXIS
MEASURED TEMPERATURES : 1 --> ◇ 11--> + 21--> ✱ 31--> □
CALCULATED TEMPERATURES : —△—
T [DEG.]
1000.0
500.0
0.0
30.
60.
90.
120.
t [min]
1,21
11,31

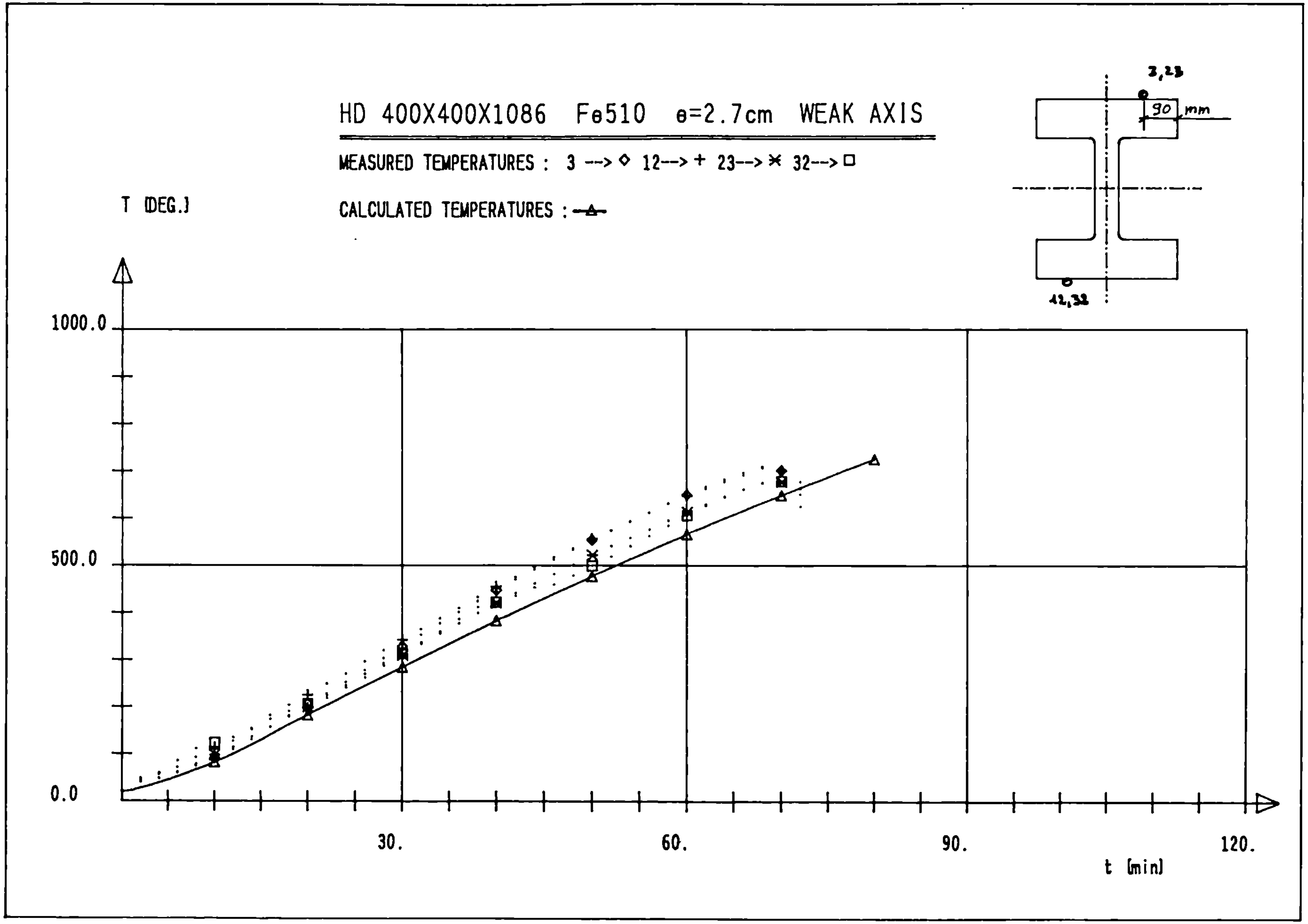
HD 400X400X1086 Fe510 e=2.7cm WEAK AXIS
MEASURED TEMPERATURES : 3 --> ◇ 12--> + 23--> ✕ 32--> □
CALCULATED TEMPERATURES : —△—
T (DEG.)
1000.0
500.0
0.0
30.
60.
90.
120.
t (min)
3,23
90 mm
12,32

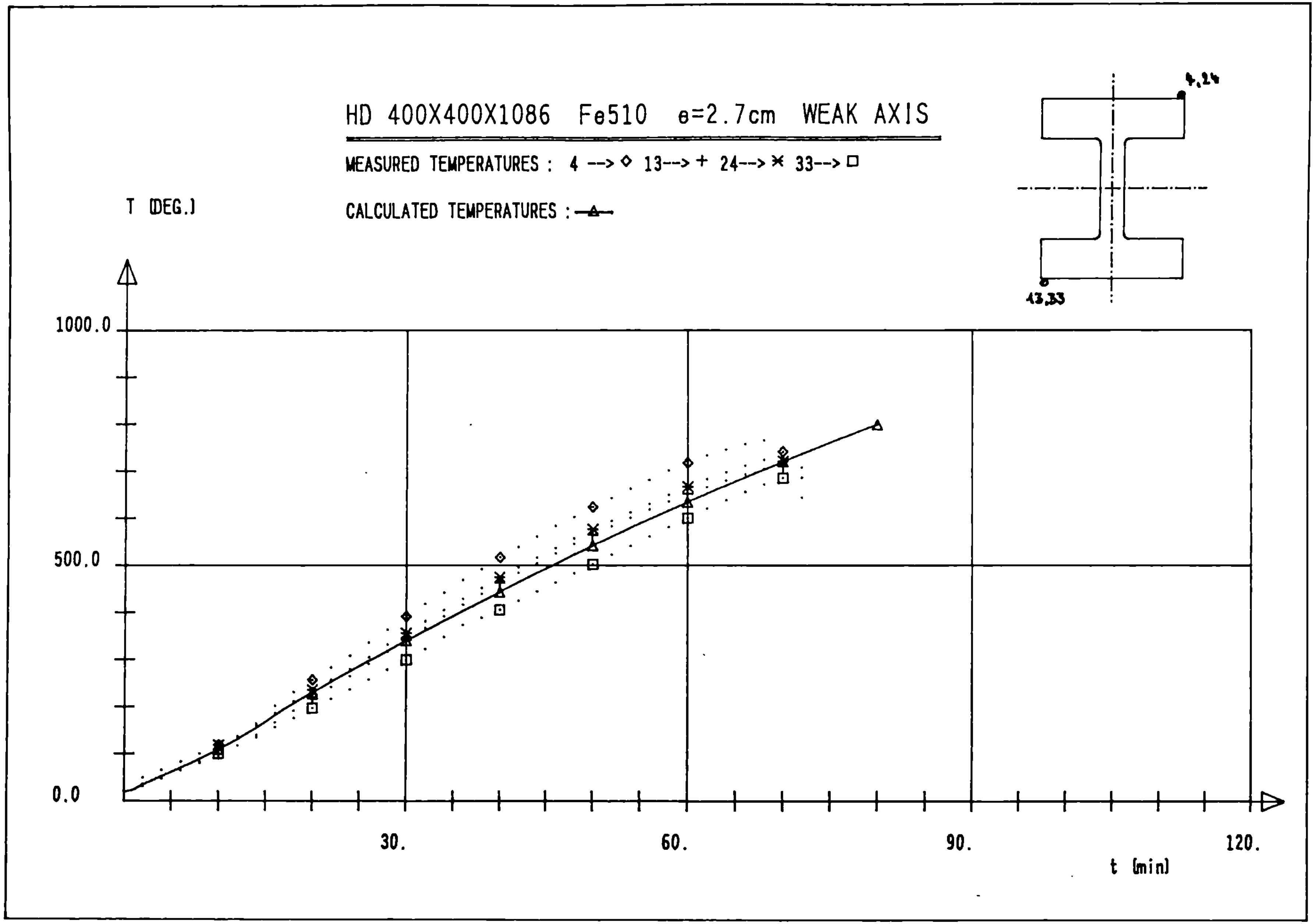
HD 400X400X1086 Fe510 e=2.7cm WEAK AXIS
MEASURED TEMPERATURES : 4 --> ◇ 13--> + 24--> ✕ 33--> □
CALCULATED TEMPERATURES : —△—
T (DEG.)
1000.0
500.0
0.0
30.
60.
90.
120.
t (min)
4,24
13,33

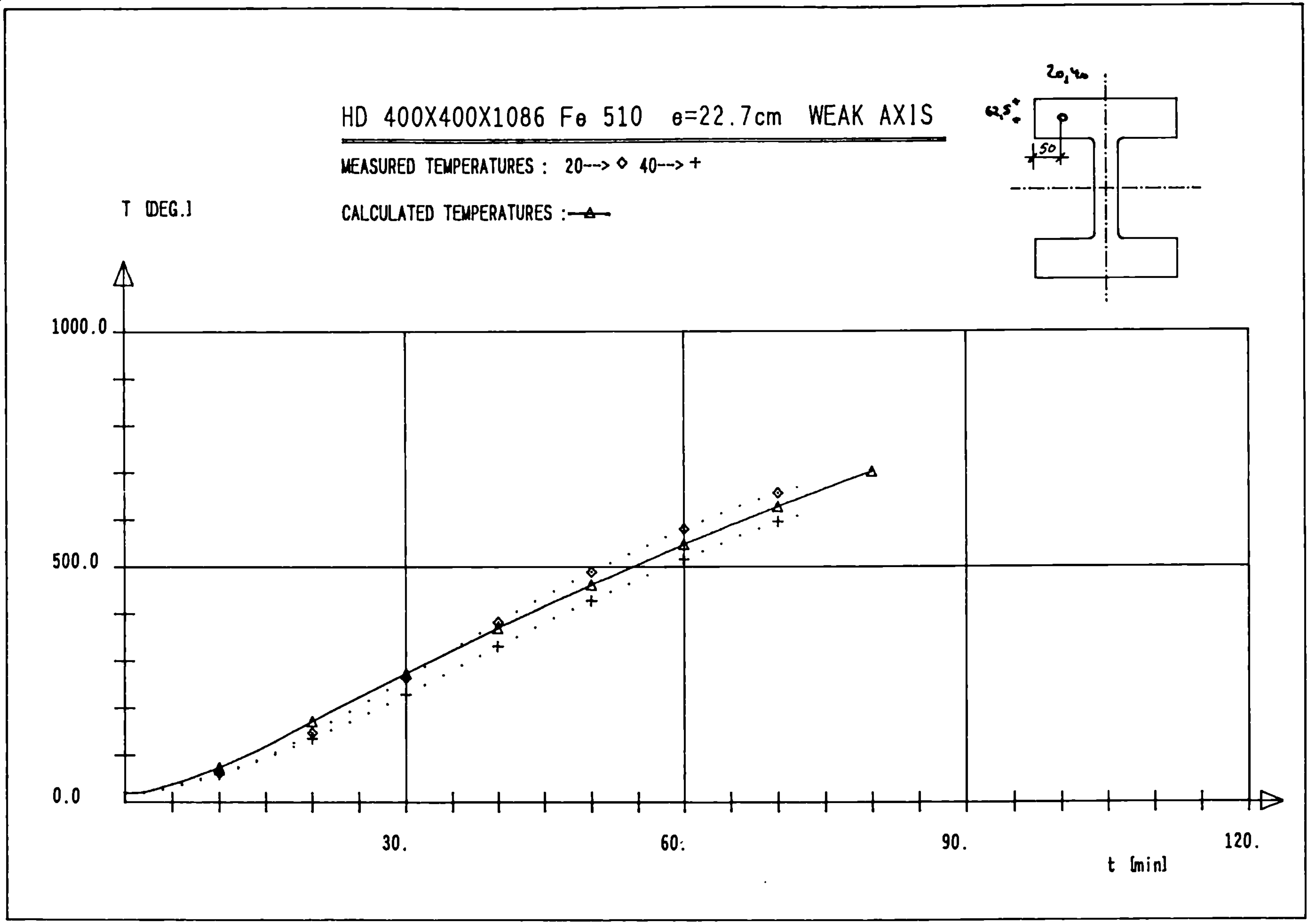
HD 400X400X1086 Fe 510 e=22.7cm WEAK AXIS
MEASURED TEMPERATURES : 20--> ◇ 40--> +
CALCULATED TEMPERATURES :—△—
T [DEG.]
1000.0
500.0
0.0
30.
60.
90.
120.
t [min]
50

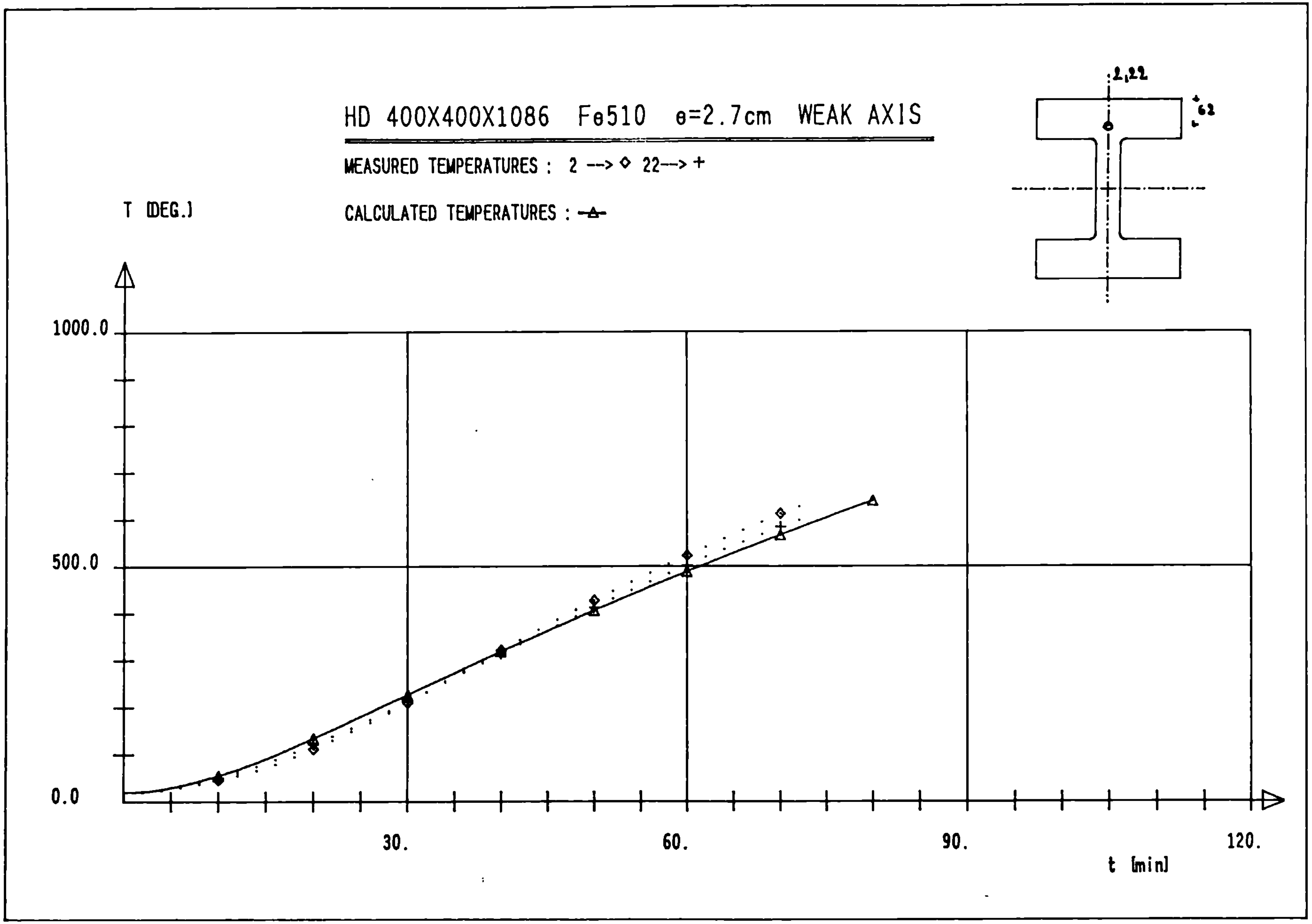
HD 400X400X1086 Fe510 e=2.7cm WEAK AXIS
MEASURED TEMPERATURES : 2 --> ◇ 22--> +
CALCULATED TEMPERATURES : -△-
T (DEG.)
1000.0
500.0
0.0
30.
60.
90.
120.
t [min]
2,22
62

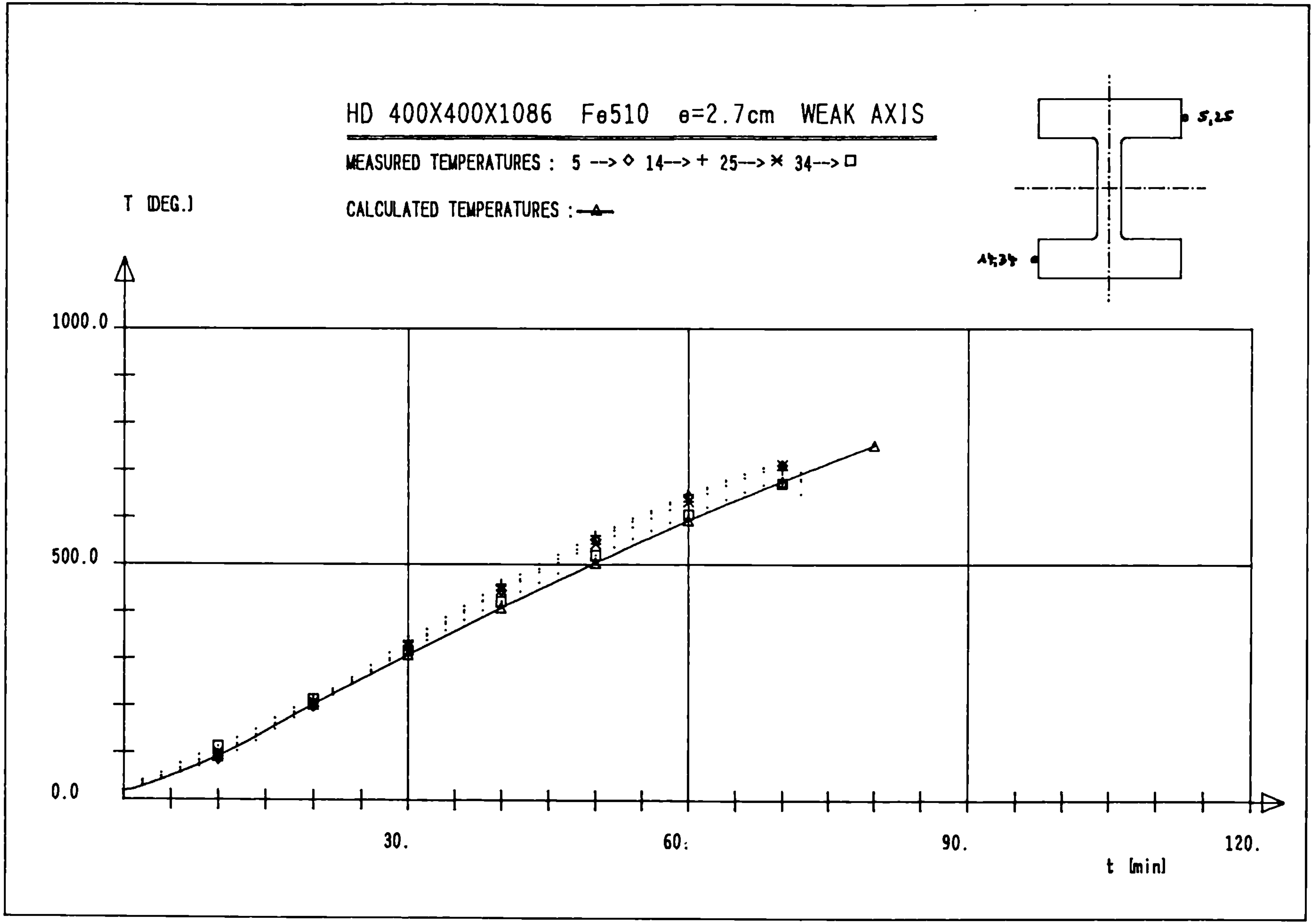

HD 400X400X1086 Fe510 e=2.7cm WEAK AXIS
MEASURED TEMPERATURES : 5 --> ◇ 14--> + 25--> ✕ 34--> □
CALCULATED TEMPERATURES : —△—
T (DEG.)
1000.0
500.0
0.0
30.
60.
90.
120.
t [min]
5,25
14,34

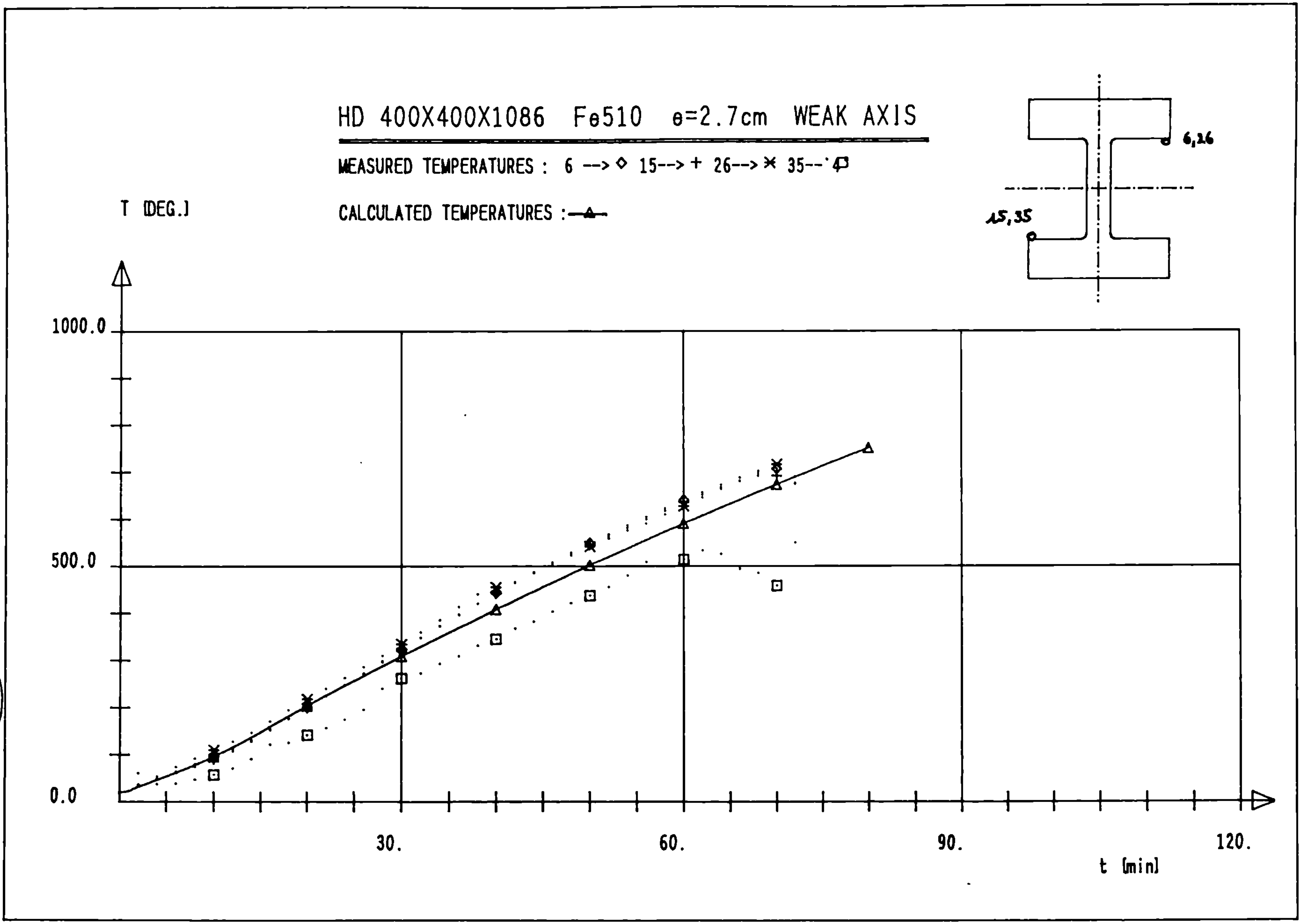
HD 400X400X1086 Fe510 e=2.7cm WEAK AXIS
MEASURED TEMPERATURES : 6 --> ◇ 15--> + 26--> ✕ 35--> □
CALCULATED TEMPERATURES : —△—
T [DEG.]
1000.0
500.0
0.0
30.
60.
90.
120.
t [min]
6,26
15,35

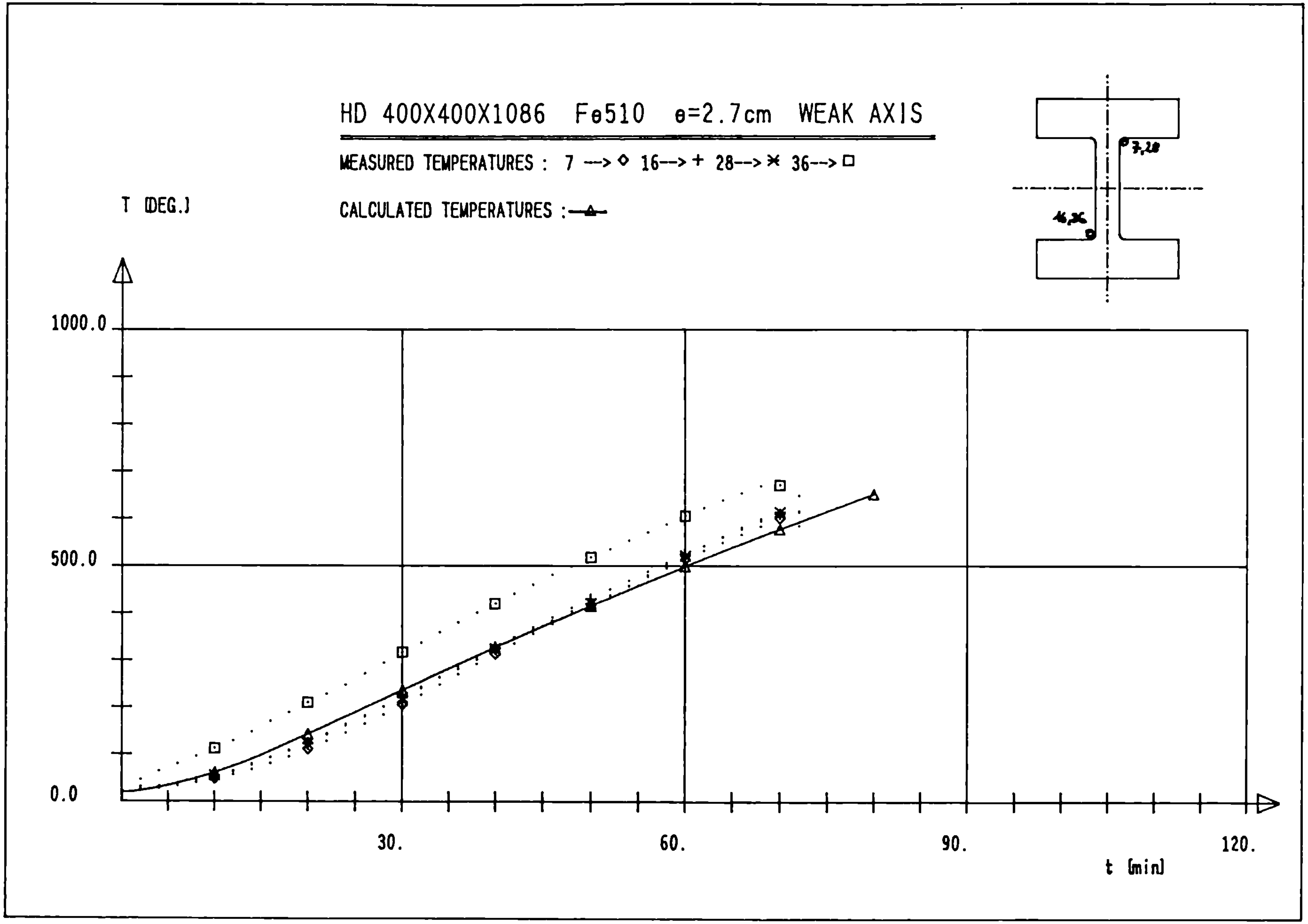

HD 400X400X1086 Fe510 e=2.7cm WEAK AXIS
MEASURED TEMPERATURES : 7 --> ◇ 16--> + 28--> ✶ 36--> □
CALCULATED TEMPERATURES : —△—
T (DEG.)
1000.0
500.0
0.0
30.
60.
90.
120.
t (min)
7,28
16,36

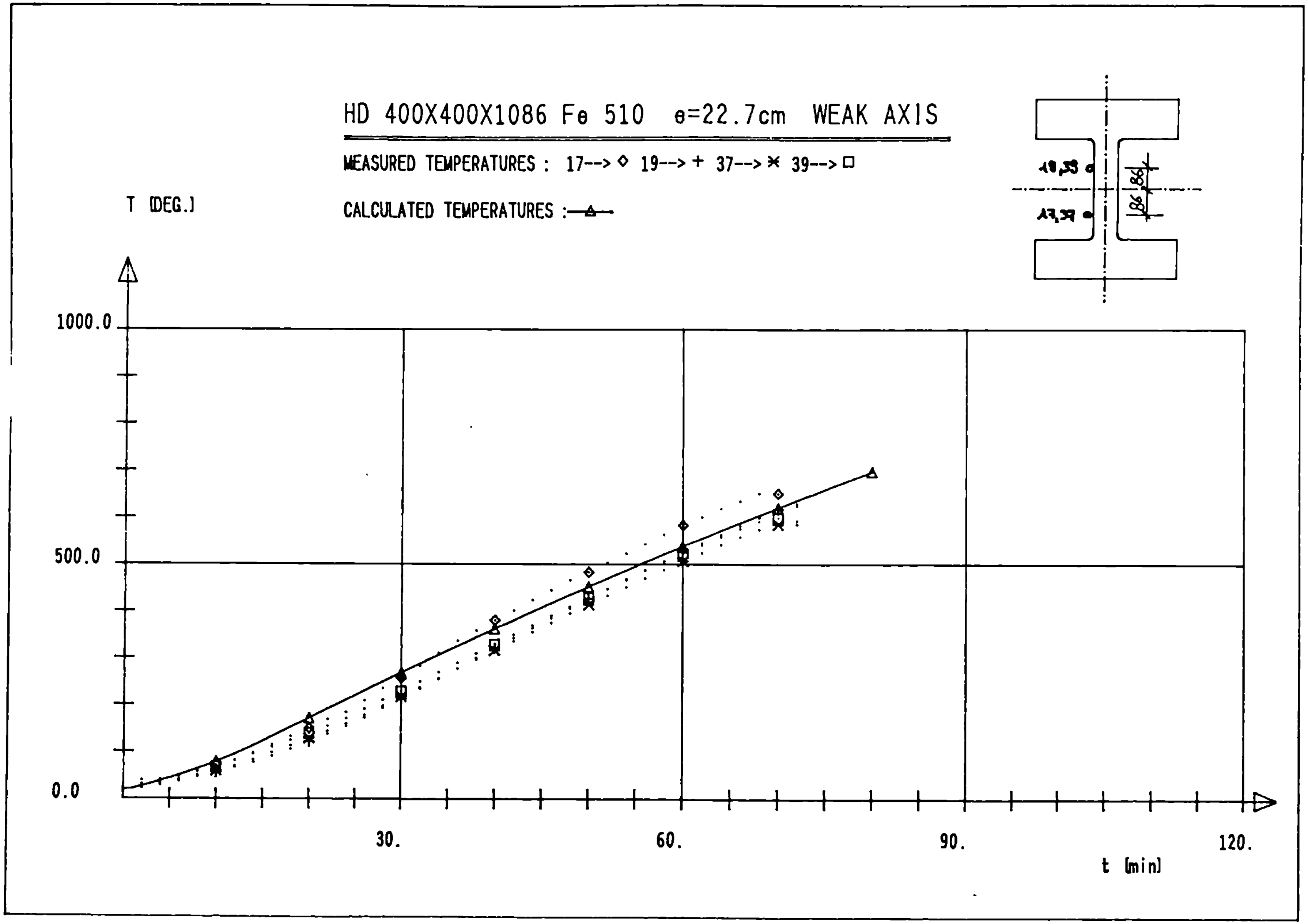
HD 400X400X1086 Fe 510 e=22.7cm WEAK AXIS
MEASURED TEMPERATURES : 17--> ◇ 19--> + 37--> ✕ 39--> □
CALCULATED TEMPERATURES :—△—
T (DEG.)
1000.0
500.0
0.0
30.
60.
90.
120.
t (min)

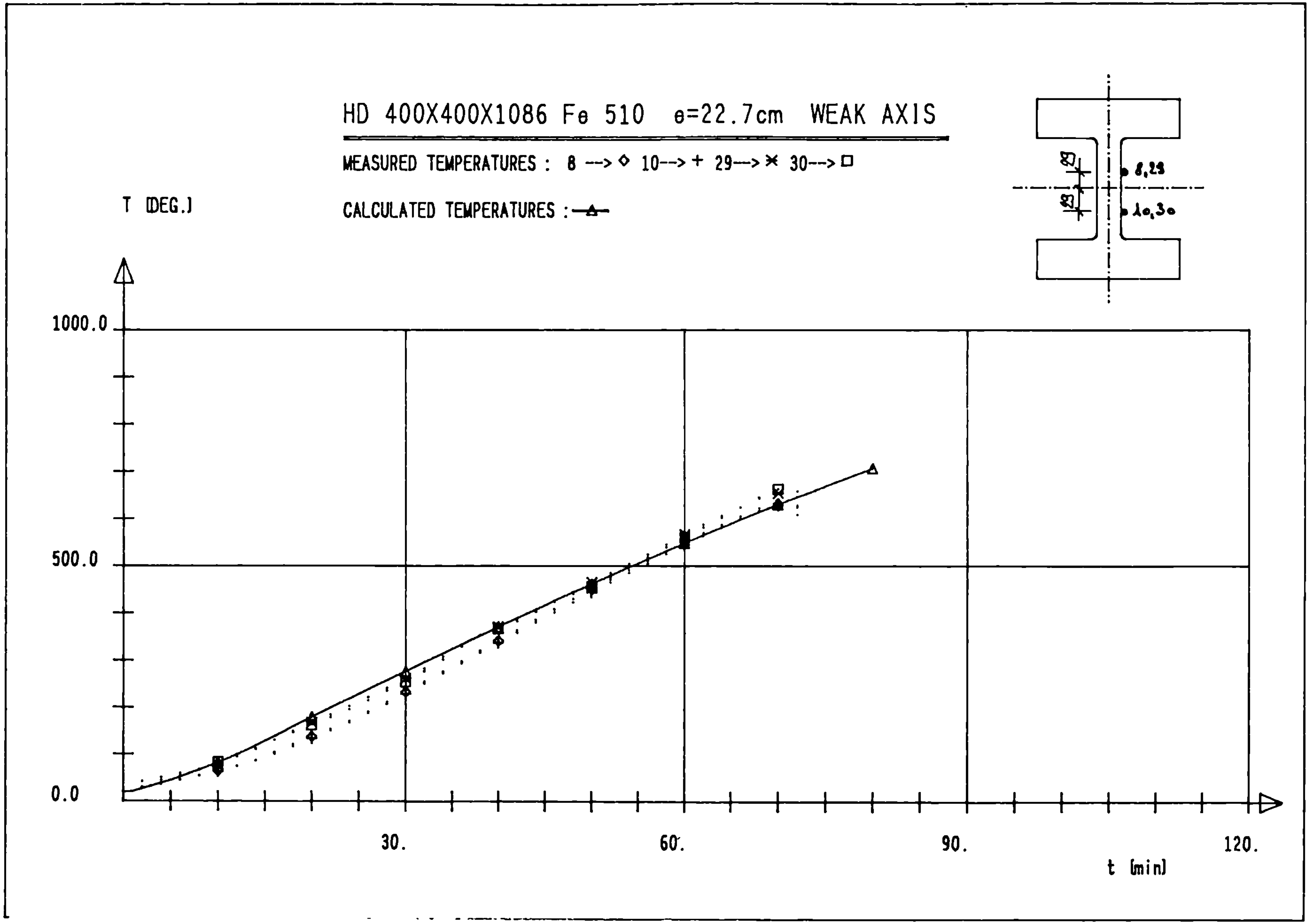
HD 400X400X1086 Fe 510 e=22.7cm WEAK AXIS
MEASURED TEMPERATURES : 8 ---> ◇ 10---> + 29---> ✕ 30---> □
CALCULATED TEMPERATURES : —△—
T (DEG.)
1000.0
500.0
0.0
30.
60.
90.
120.
t (min)

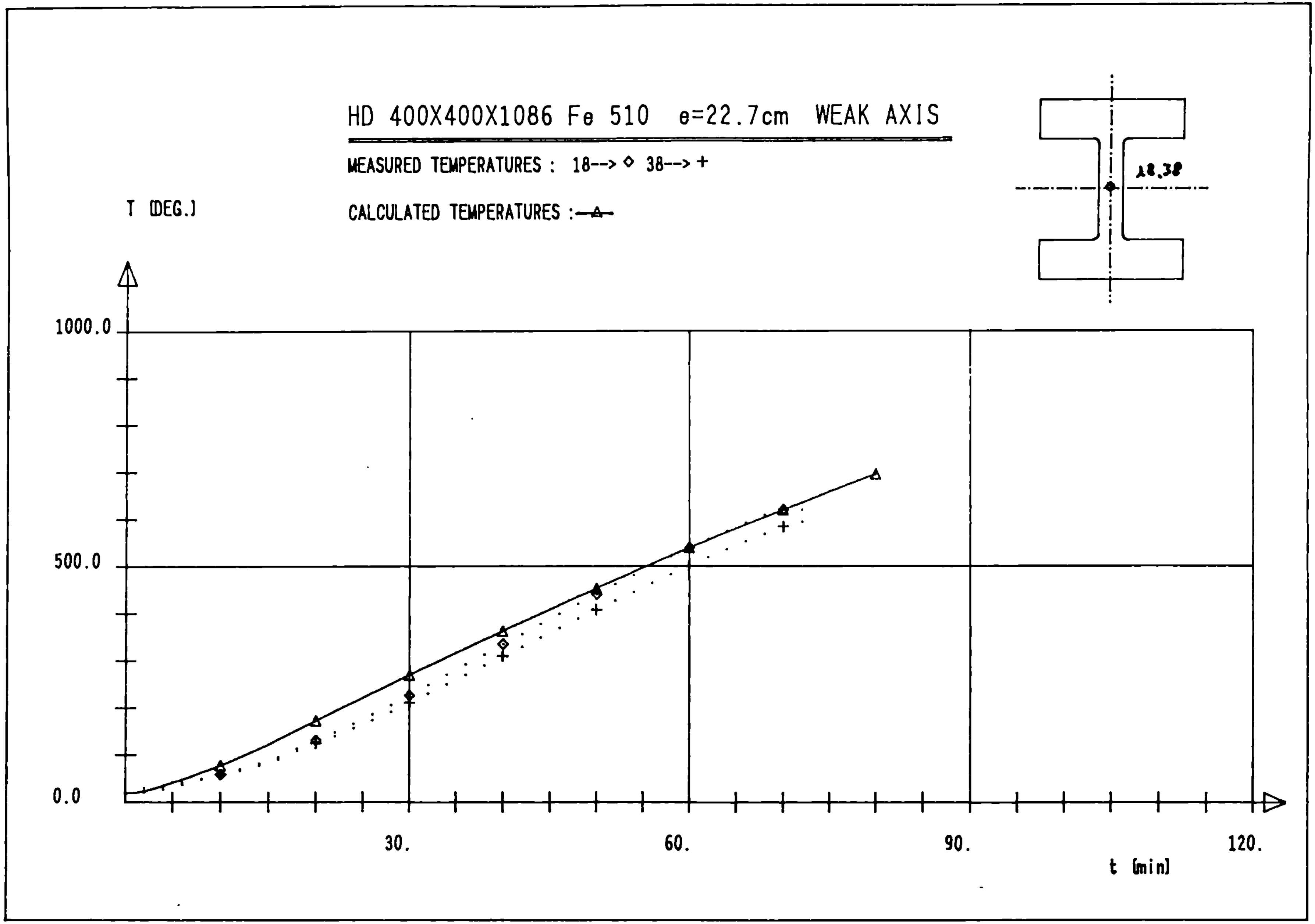
HD 400X400X1086 Fe 510 e=22.7cm WEAK AXIS
MEASURED TEMPERATURES : 18--> ◇ 38--> +
CALCULATED TEMPERATURES :—△—
T [DEG.]
1000.0
500.0
0.0
30.
60.
90.
120.
t [min]
18,38

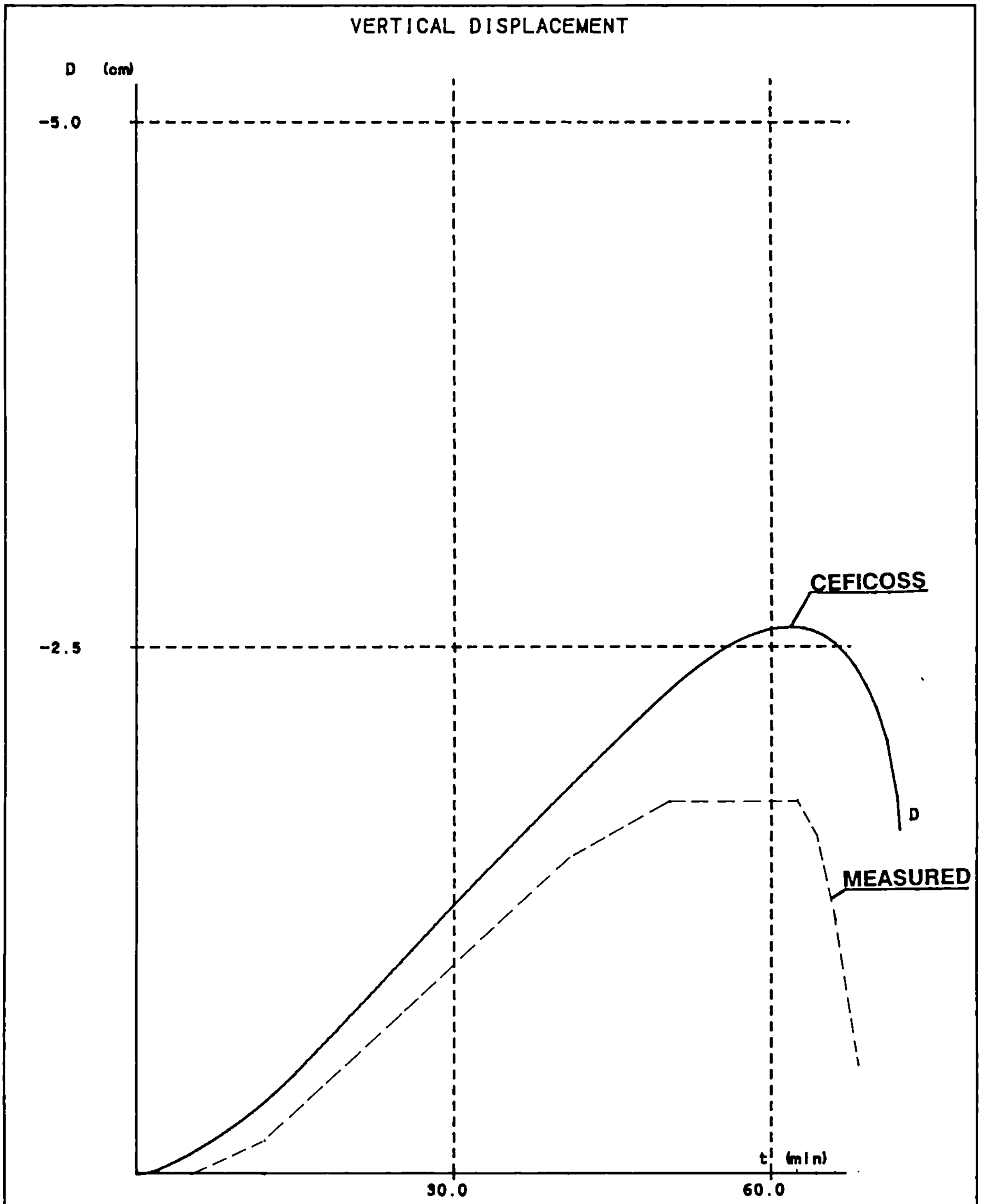

ARBED-RECHERCHES / RPS DEPARTMENT	CEFICOSS Analysis / CEF8.1
PROJECT TITLE TEST 4 HD 400X400X1086 / Fe 510 / WEAK AXIS	PROJECT NUMBER REFAO III ESCH/ALZETTE : 2-MAR-1989 SHEET : 4.14

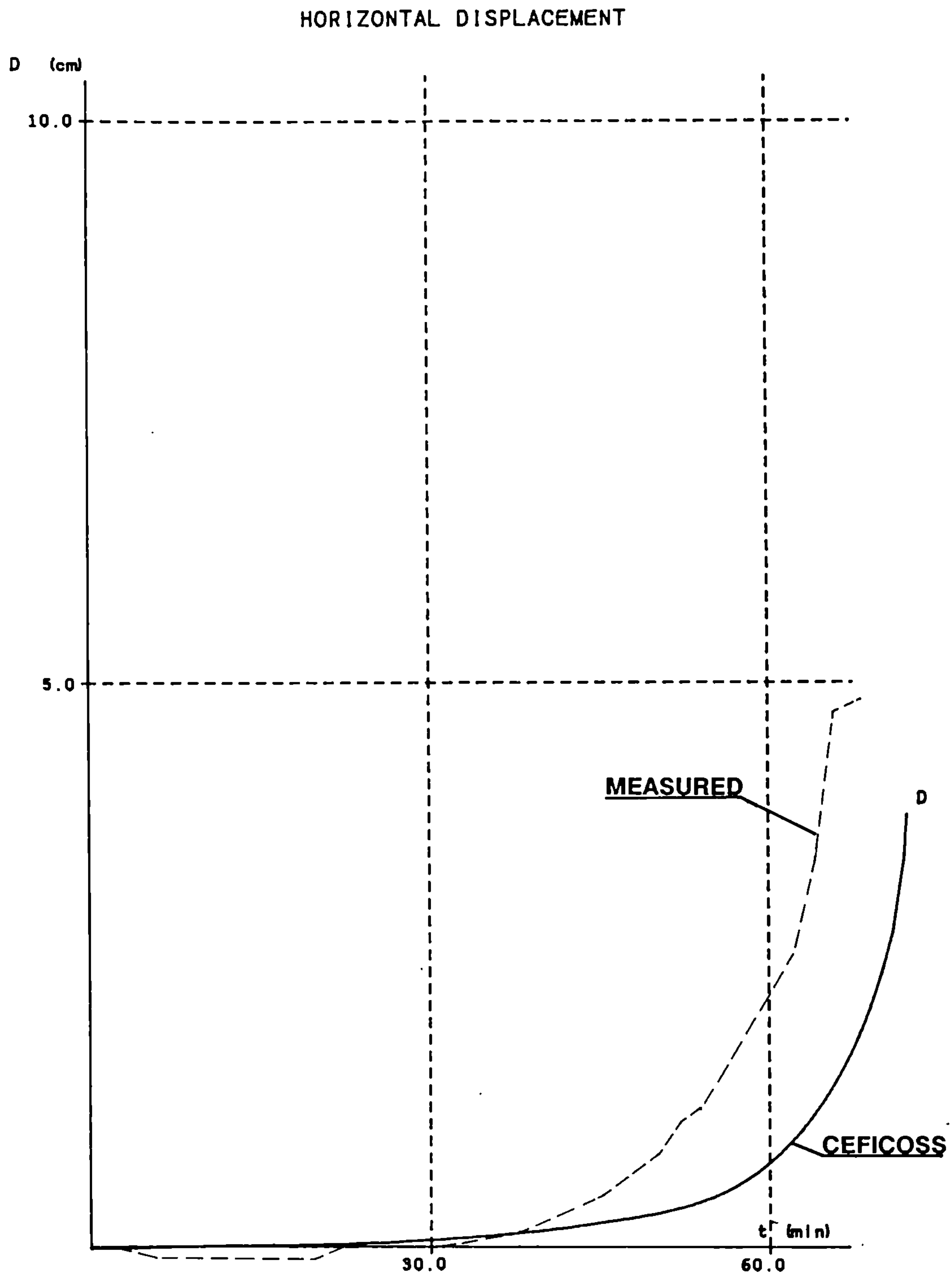

ARBED-RECHERCHES / RPS DEPARTMENT	CEFICOSS Analysis / CEF8.1
PROJECT TITLE TEST 4 HD 400X400X1086 / Fe 510 / WEAK AXIS	PROJECT NUMBER REFAO III ESCH/ALZETTE : 2-MAR-1989 SHEET : 4.15

TEST 5

COLUMN W 360x410x314 - Fe 510

BUCKLING LENGTH 4.14 m

TEST PERFORMED IN GAND

TEST Nr 5

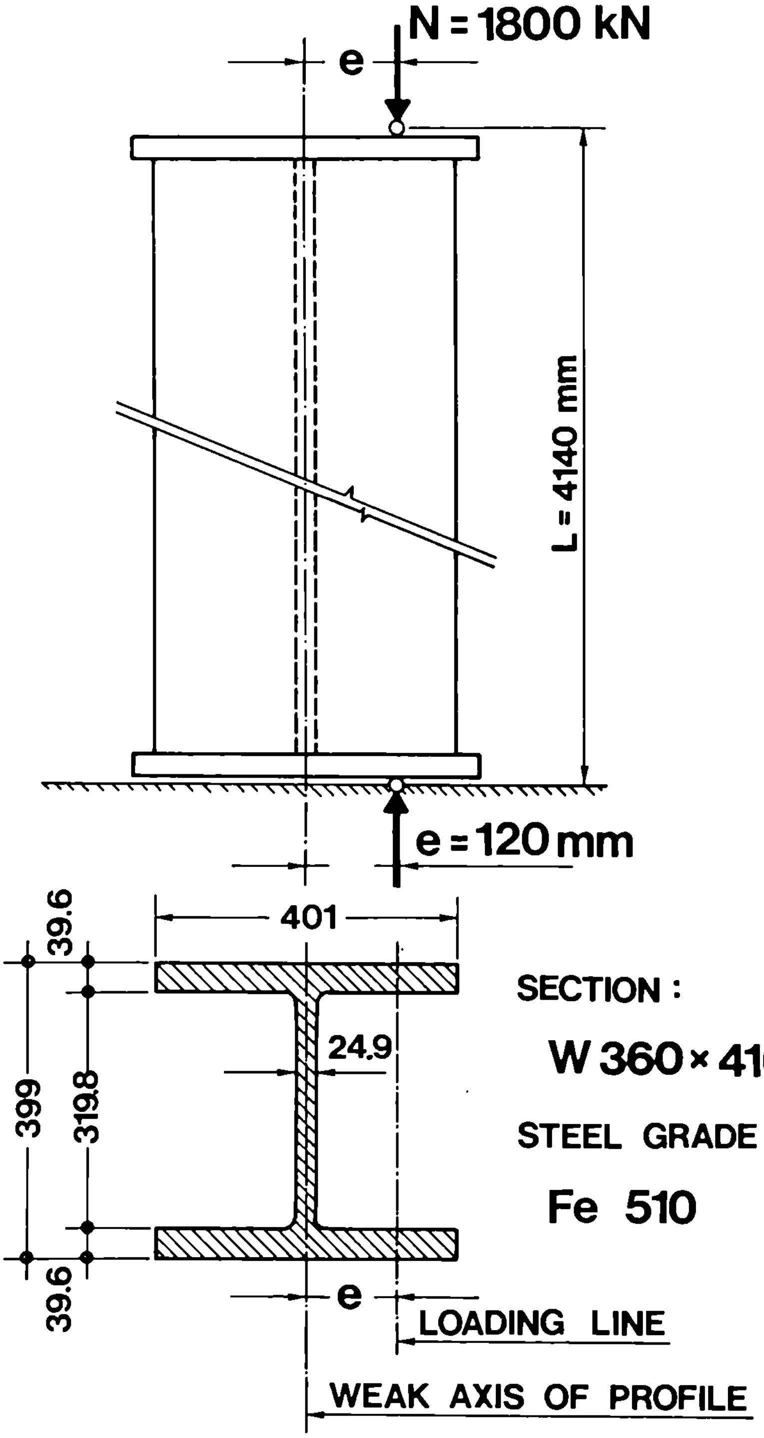

SECTION :

W 360 × 410 × 314

STEEL GRADE :

Fe 510

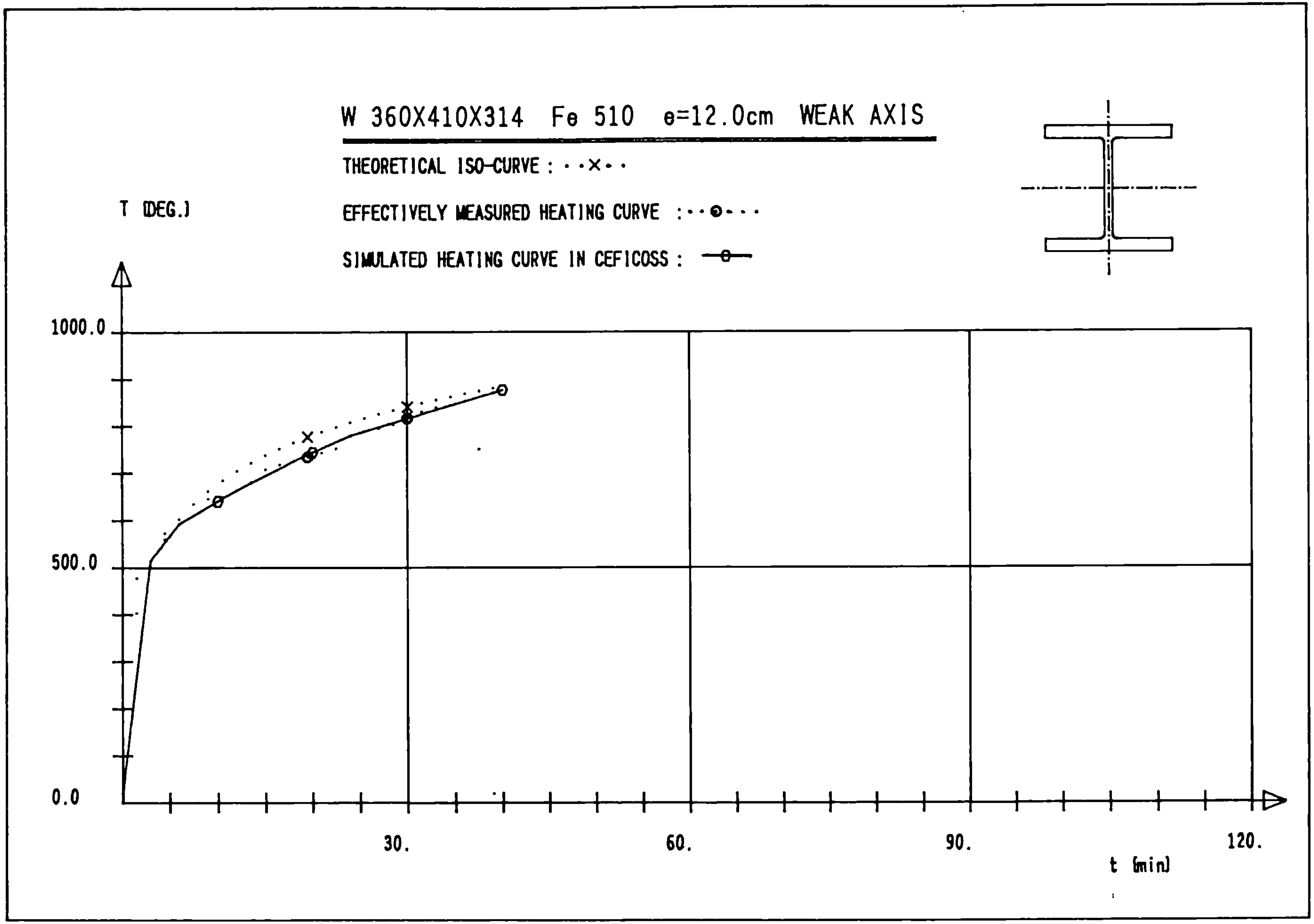
W 360X410X314 Fe 510 e=12.0cm WEAK AXIS
THEORETICAL ISO-CURVE : · · X · ·
EFFECTIVELY MEASURED HEATING CURVE : · · ⊙ · · ·
SIMULATED HEATING CURVE IN CEFICOSS :
T (DEG.)
1000.0
500.0
0.0
30.
60.
90.
120.
t (min)

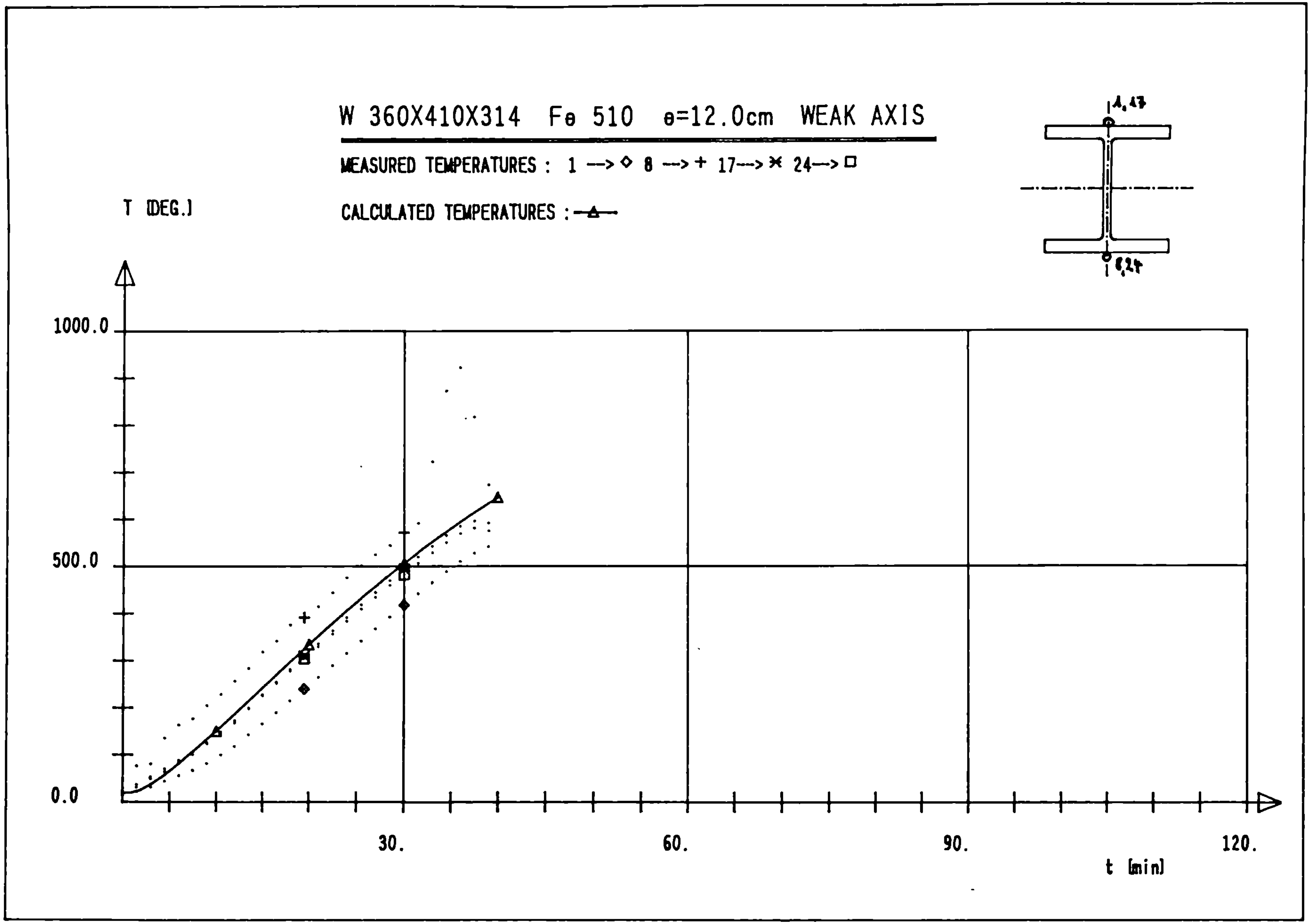
W 360X410X314 Fe 510 e=12.0cm WEAK AXIS
MEASURED TEMPERATURES : 1 —> ◇ 8 —> + 17—> ✕ 24—> □
CALCULATED TEMPERATURES : —△—
T [DEG.]
1000.0
500.0
0.0
30.
60.
90.
120.
t [min]
1,17
8,24

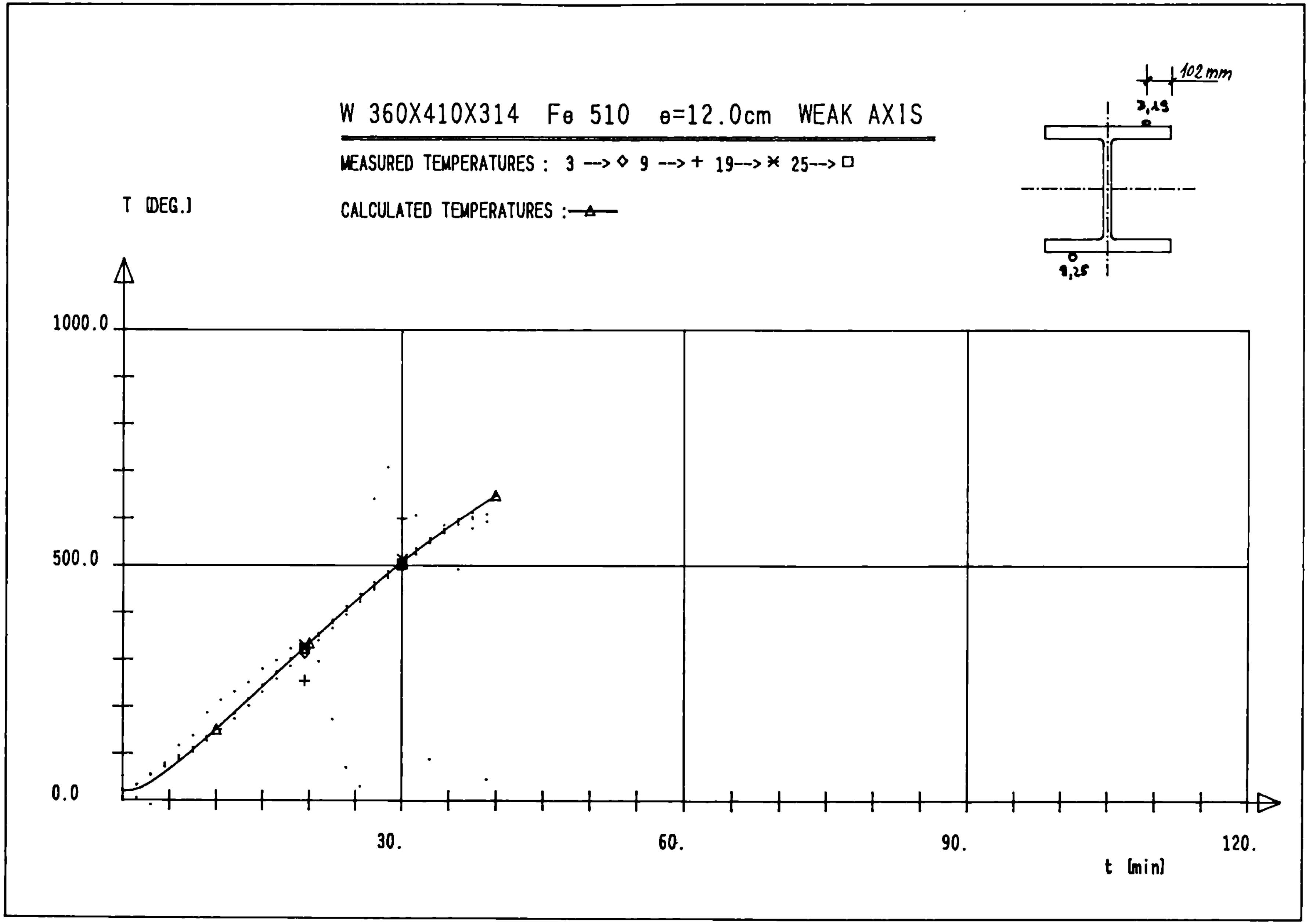
W 360X410X314 Fe 510 e=12.0cm WEAK AXIS
MEASURED TEMPERATURES : 3 --> ◇ 9 --> + 19--> ✕ 25--> □
CALCULATED TEMPERATURES :—△—
T [DEG.]
1000.0
500.0
0.0
30.
60.
90.
120.
t [min]
102 mm
3,19
9,25

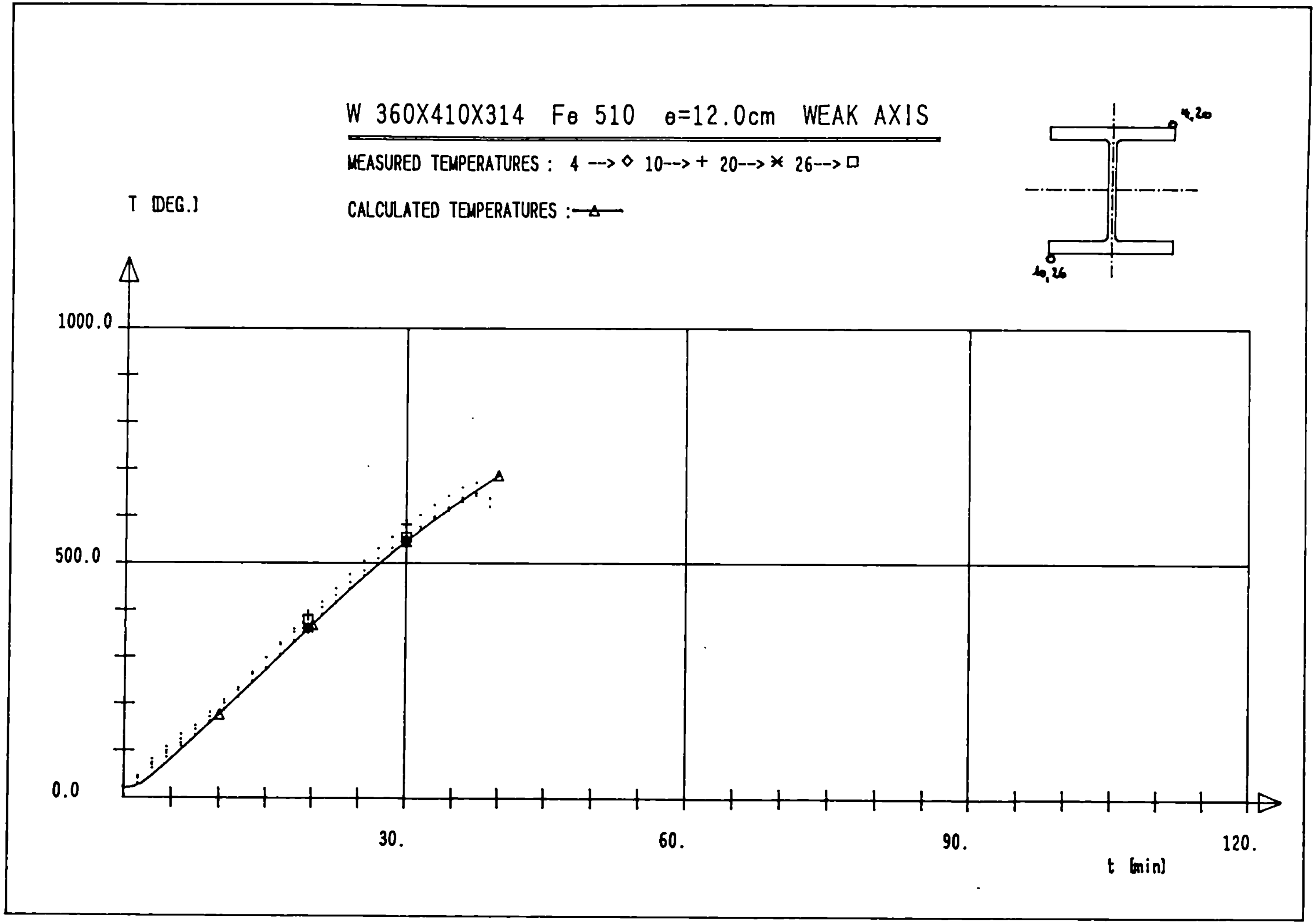
W 360X410X314 Fe 510 e=12.0cm WEAK AXIS
MEASURED TEMPERATURES : 4 --> ◇ 10--> + 20--> ✕ 26--> □
CALCULATED TEMPERATURES :—△—
T (DEG.)
1000.0
500.0
0.0
30.
60.
90.
120.
t (min)
4,20
10,26

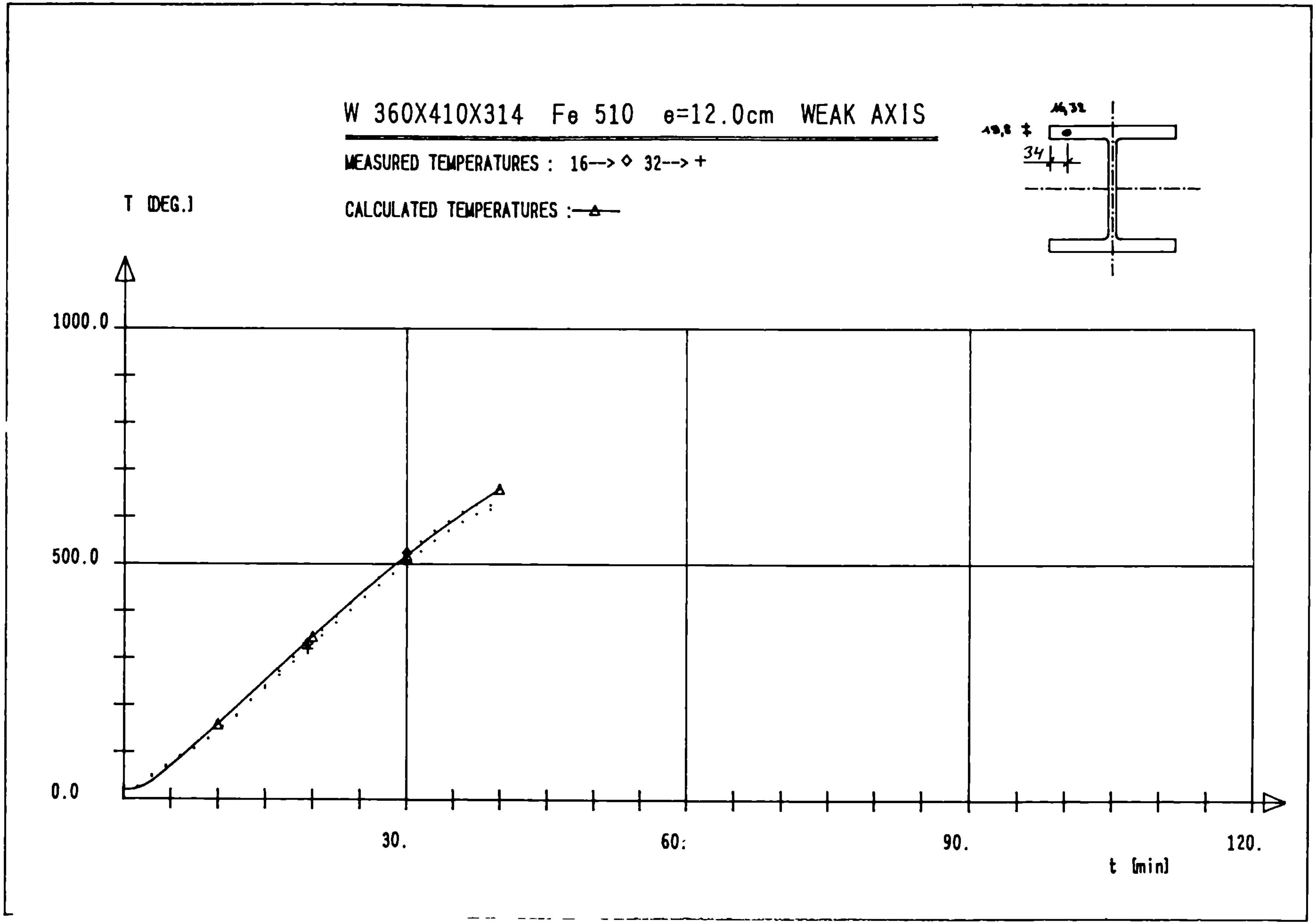
W 360X410X314 Fe 510 e=12.0cm WEAK AXIS
MEASURED TEMPERATURES : 16--> ◇ 32--> +
CALCULATED TEMPERATURES :—△—
T [DEG.]
1000.0
500.0
0.0
30.
60.
90.
120.
t [min]
34

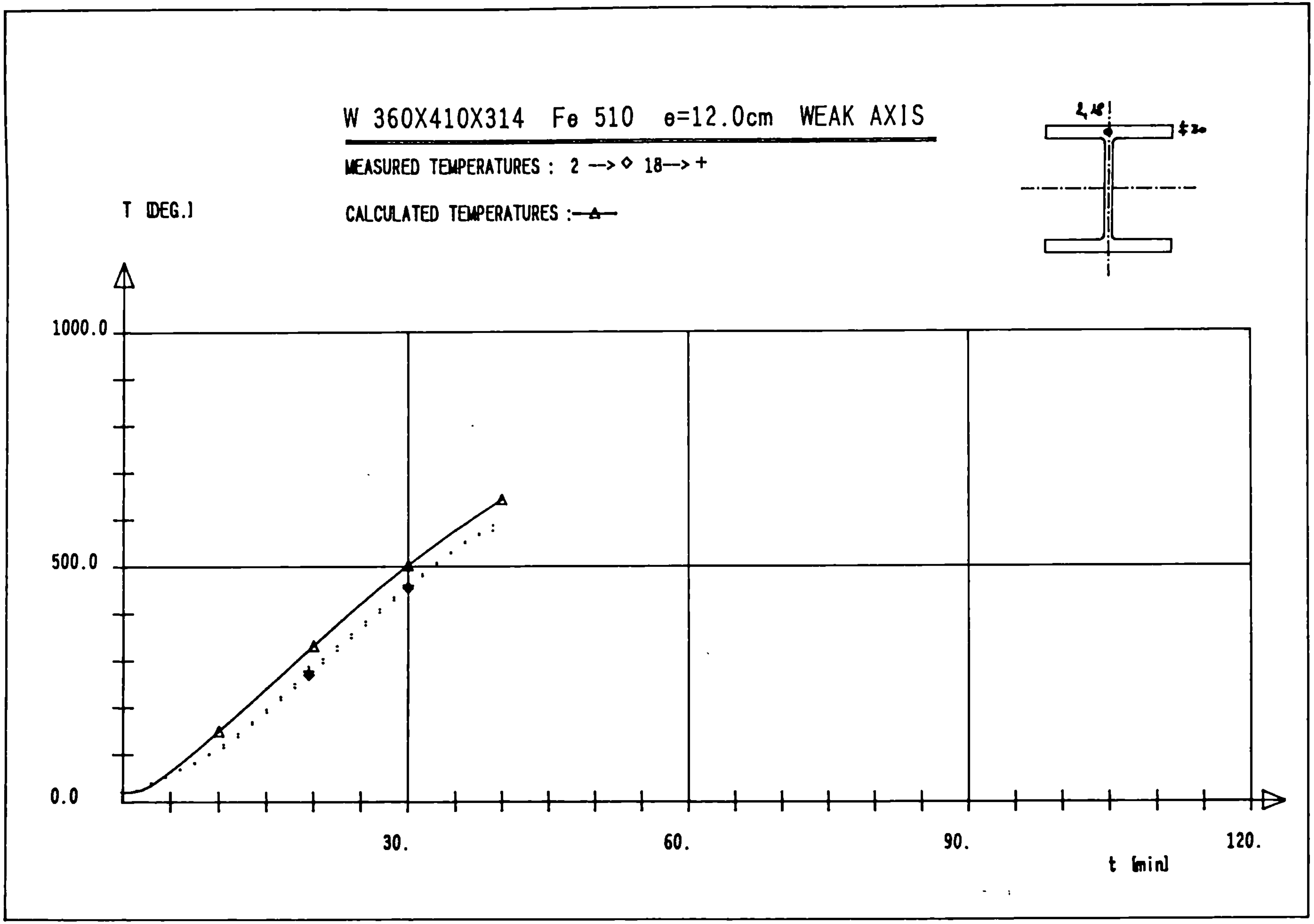
W 360X410X314 Fe 510 e=12.0cm WEAK AXIS
MEASURED TEMPERATURES : 2 --> ◇ 18--> +
CALCULATED TEMPERATURES :—△—
T [DEG.]
1000.0
500.0
0.0
30.
60.
90.
120.
t [min]

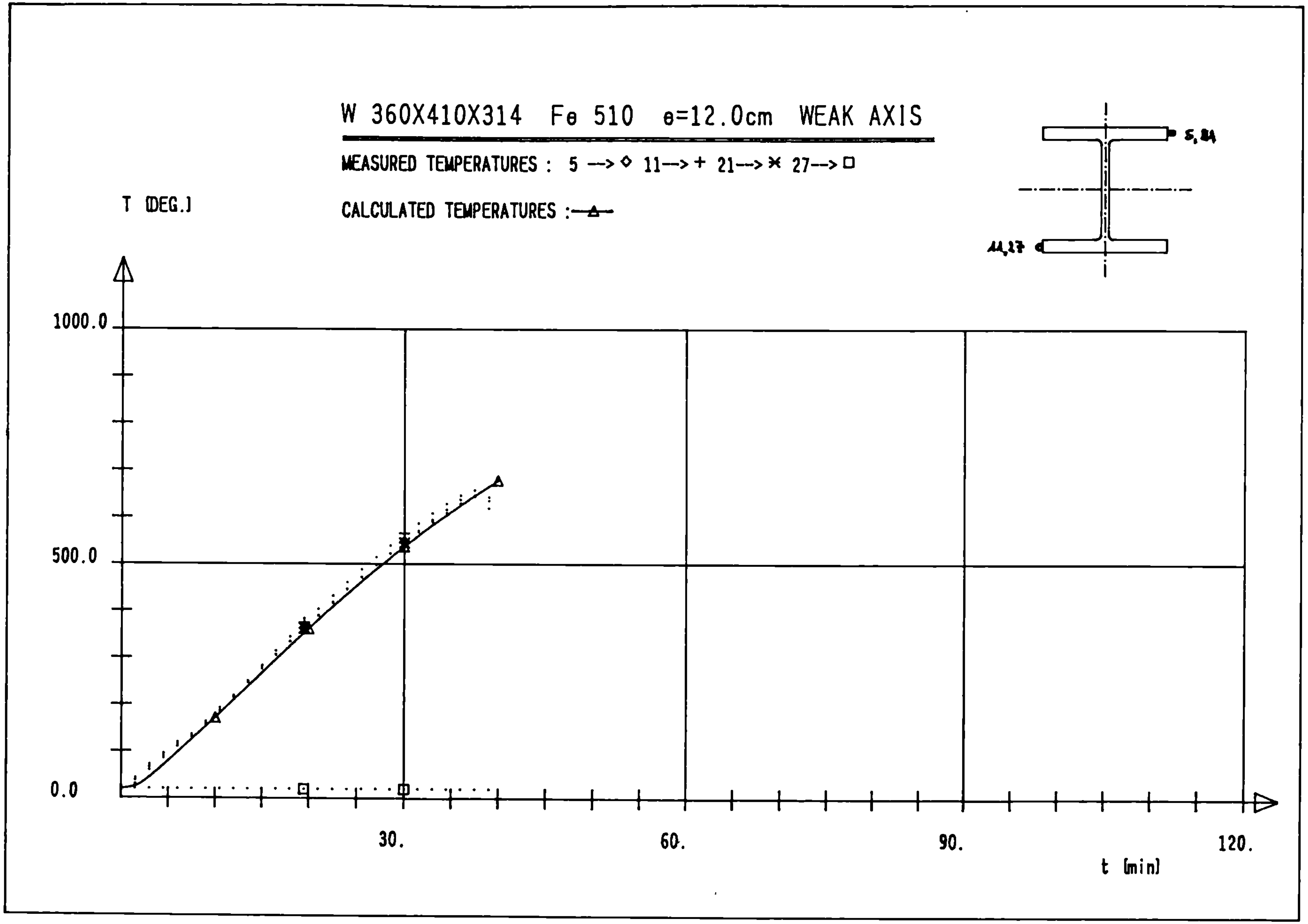
W 360X410X314 Fe 510 e=12.0cm WEAK AXIS
MEASURED TEMPERATURES : 5 —> ◇ 11—> + 21—> ✳ 27—> □
CALCULATED TEMPERATURES :—△—
T (DEG.)
1000.0
500.0
0.0
30.
60.
90.
120.
t (min)

5.9

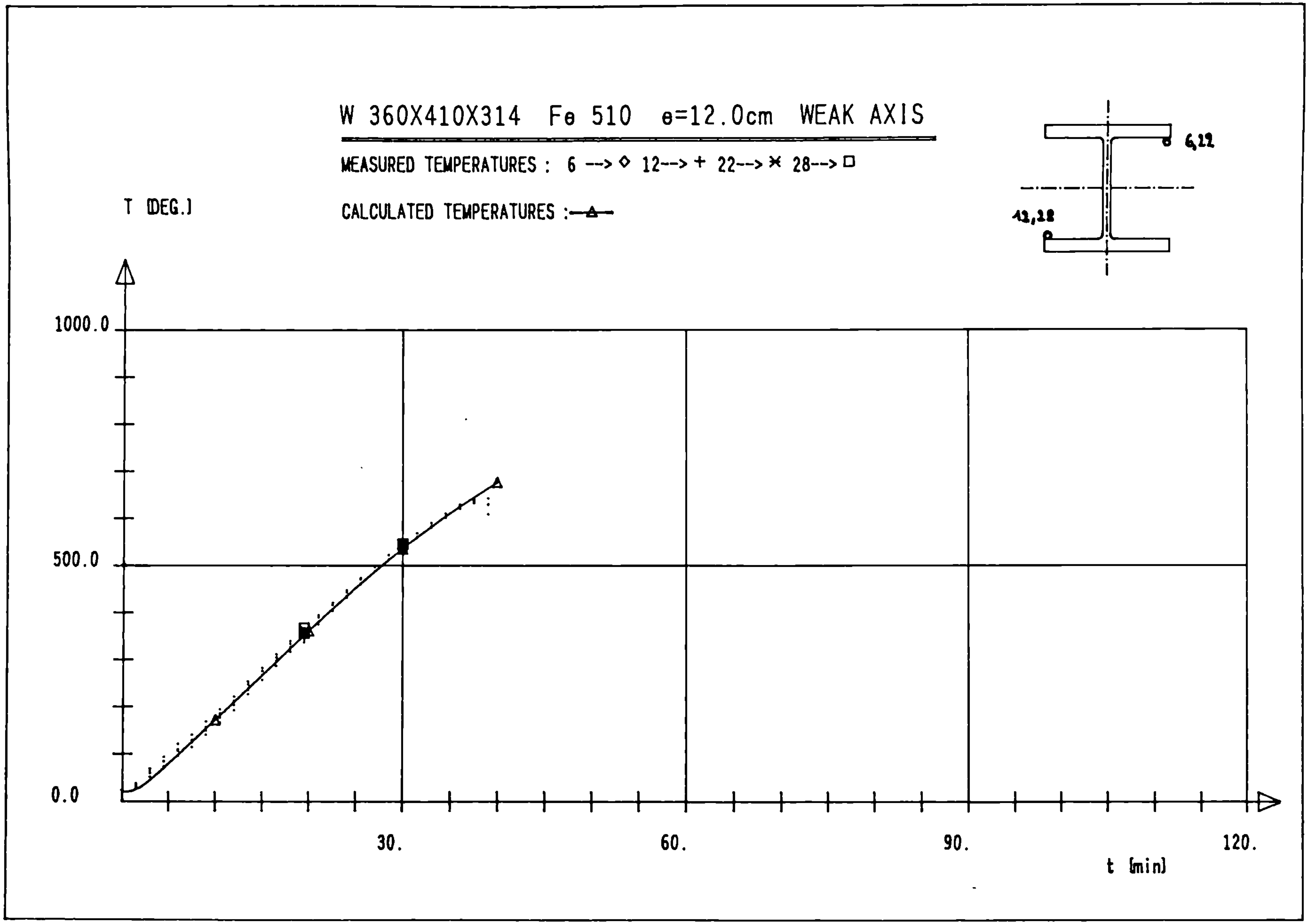
W 360X410X314 Fe 510 e=12.0cm WEAK AXIS
MEASURED TEMPERATURES : 6 --> ◇ 12--> + 22--> × 28--> □
CALCULATED TEMPERATURES :—△—
T [DEG.]
1000.0
500.0
0.0
30.
60.
90.
120.
t [min]
6,22
12,28

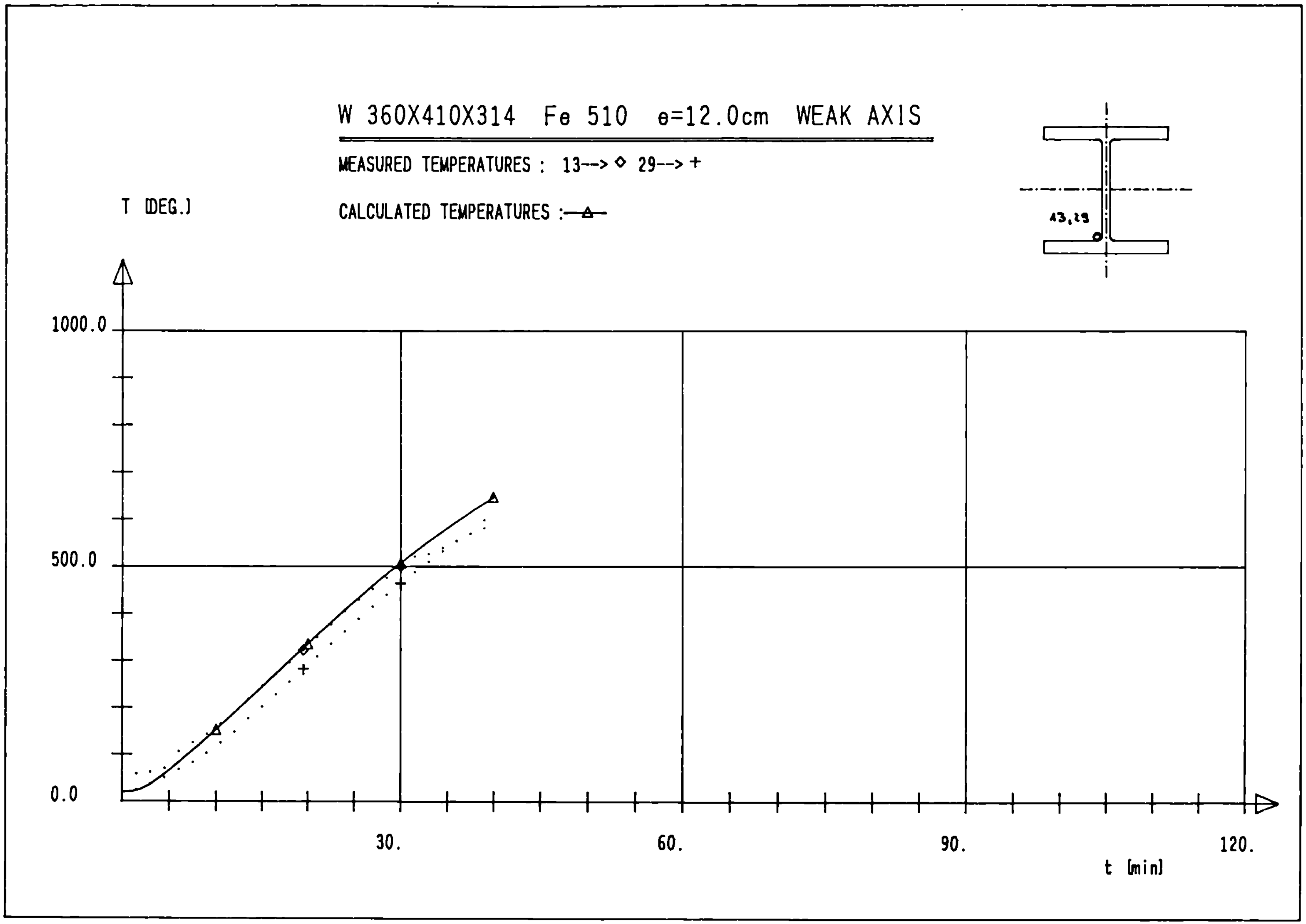
W 360X410X314 Fe 510 e=12.0cm WEAK AXIS
MEASURED TEMPERATURES : 13--> ◇ 29--> +
CALCULATED TEMPERATURES :—△—
T (DEG.)
43,29
1000.0
500.0
0.0
30.
60.
90.
120.
t (min)

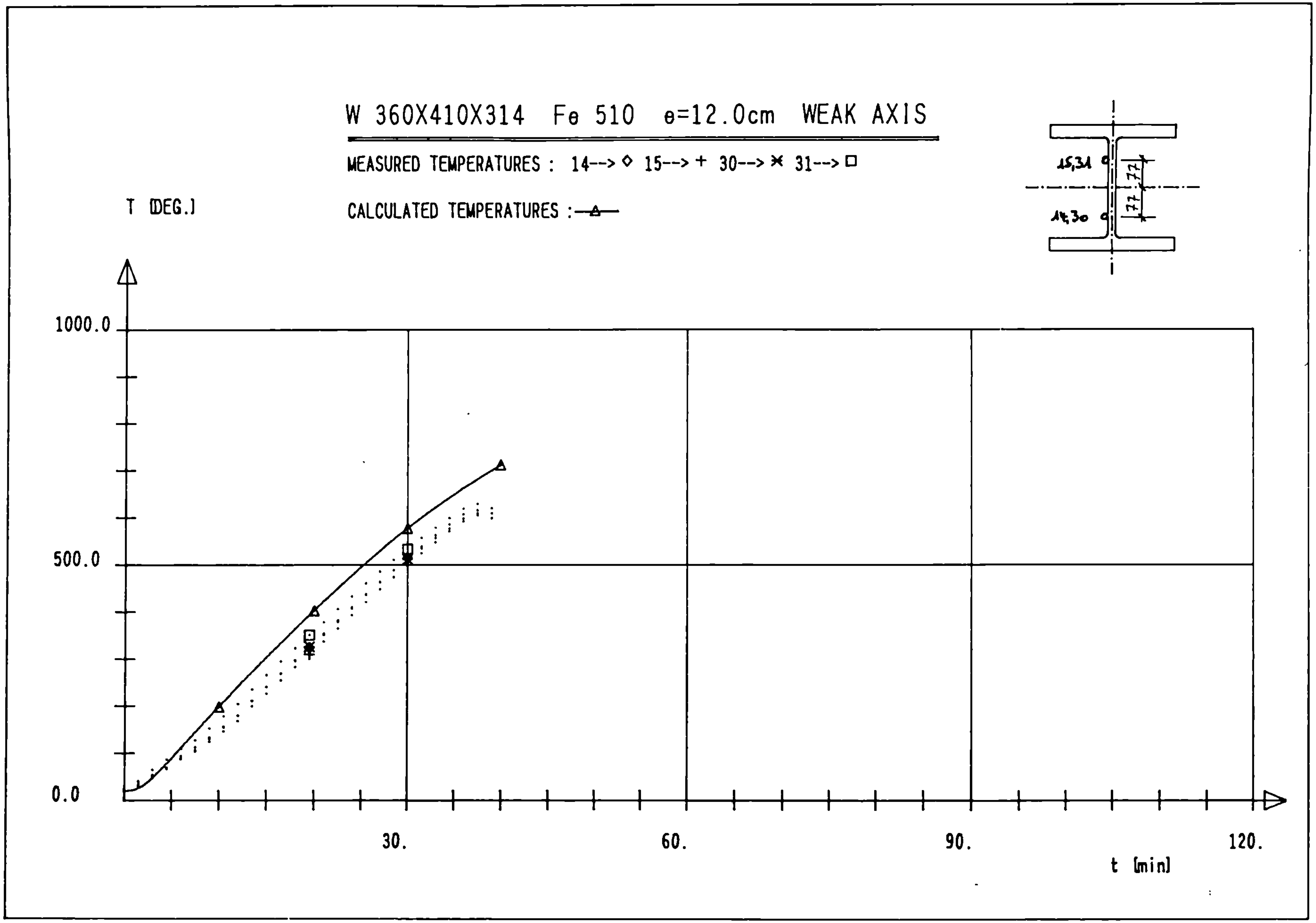
W 360X410X314 Fe 510 e=12.0cm WEAK AXIS
MEASURED TEMPERATURES : 14--> ◇ 15--> + 30--> ✱ 31--> □
CALCULATED TEMPERATURES : —△—
T [DEG.]
1000.0
500.0
0.0
30.
60.
90.
120.
t [min]
15,31
14,30
77
77

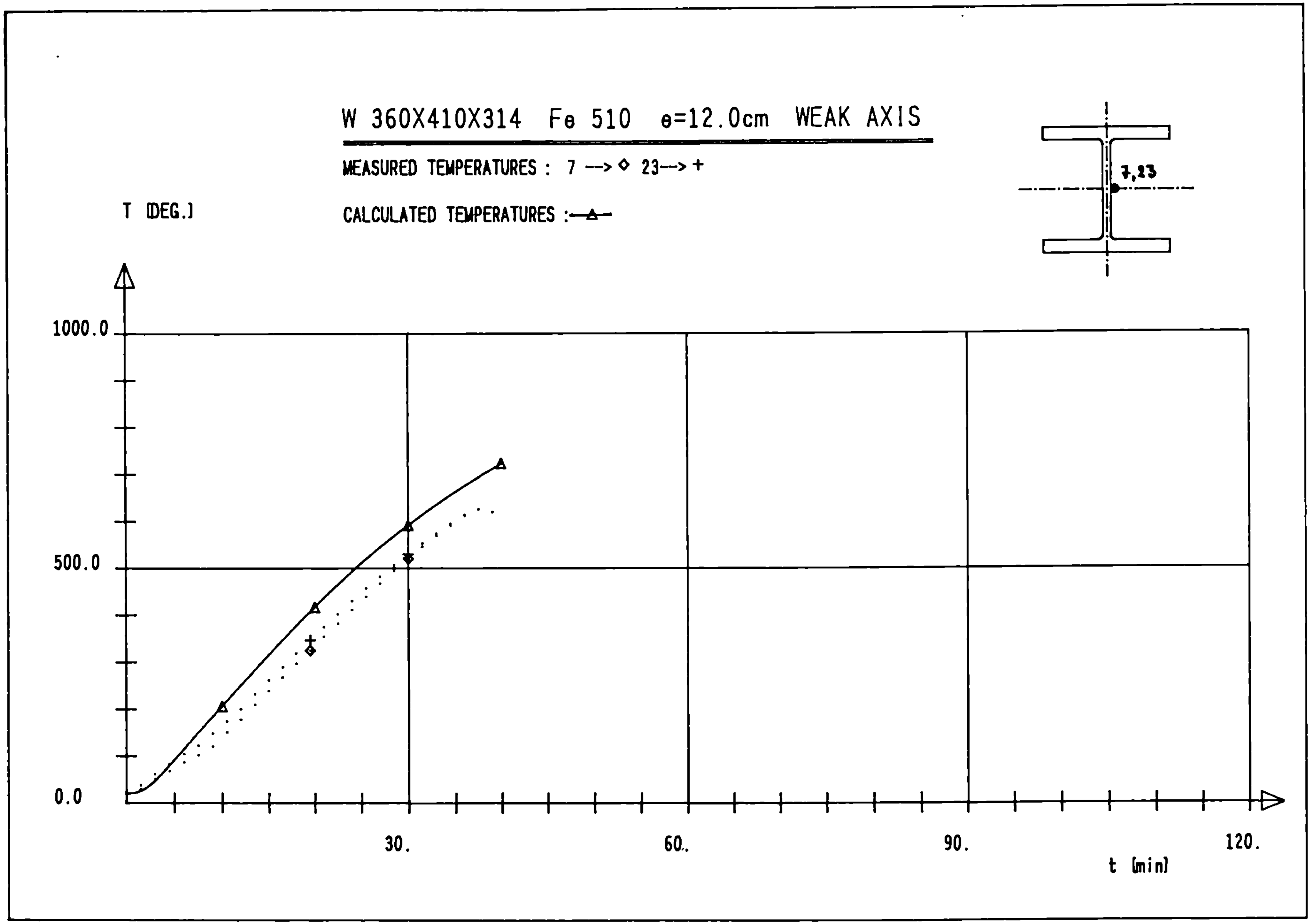
W 360X410X314 Fe 510 e=12.0cm WEAK AXIS
MEASURED TEMPERATURES : 7 --> ◇ 23--> +
CALCULATED TEMPERATURES :—Δ—
T [DEG.]
1000.0
500.0
0.0
30.
60.
90.
120.
t [min]
7,23

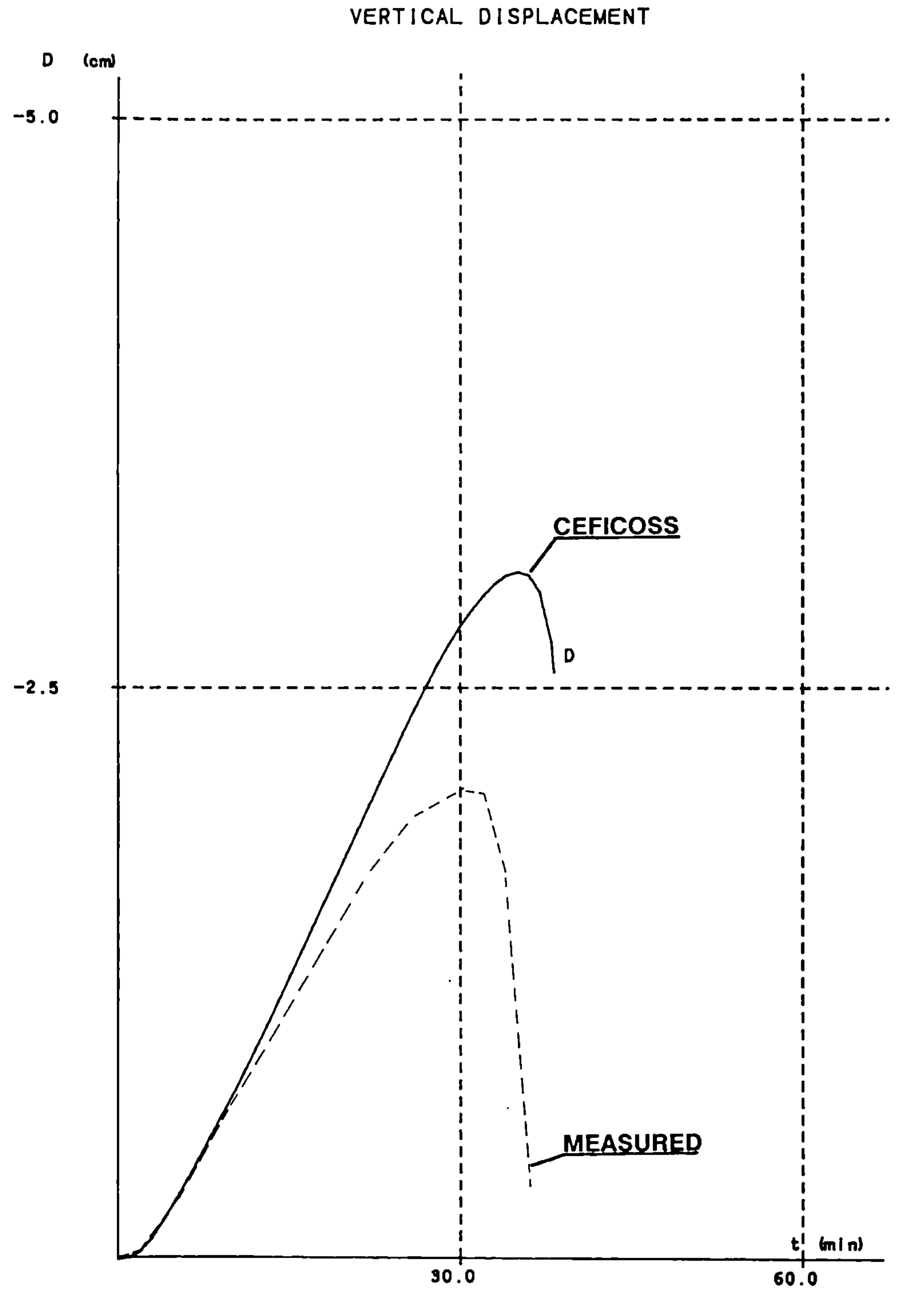

ARBED-RECHERCHES / RPS DEPARTMENT	CEFICOSS Analysis / CEF8.1
PROJECT TITLE TEST 5 W 360X410X314 / Fe 510 / WEAK AXIS	PROJECT NUMBER REFAO III ESCH/ALZETTE : 28-FEB-1989 SHEET :5.13

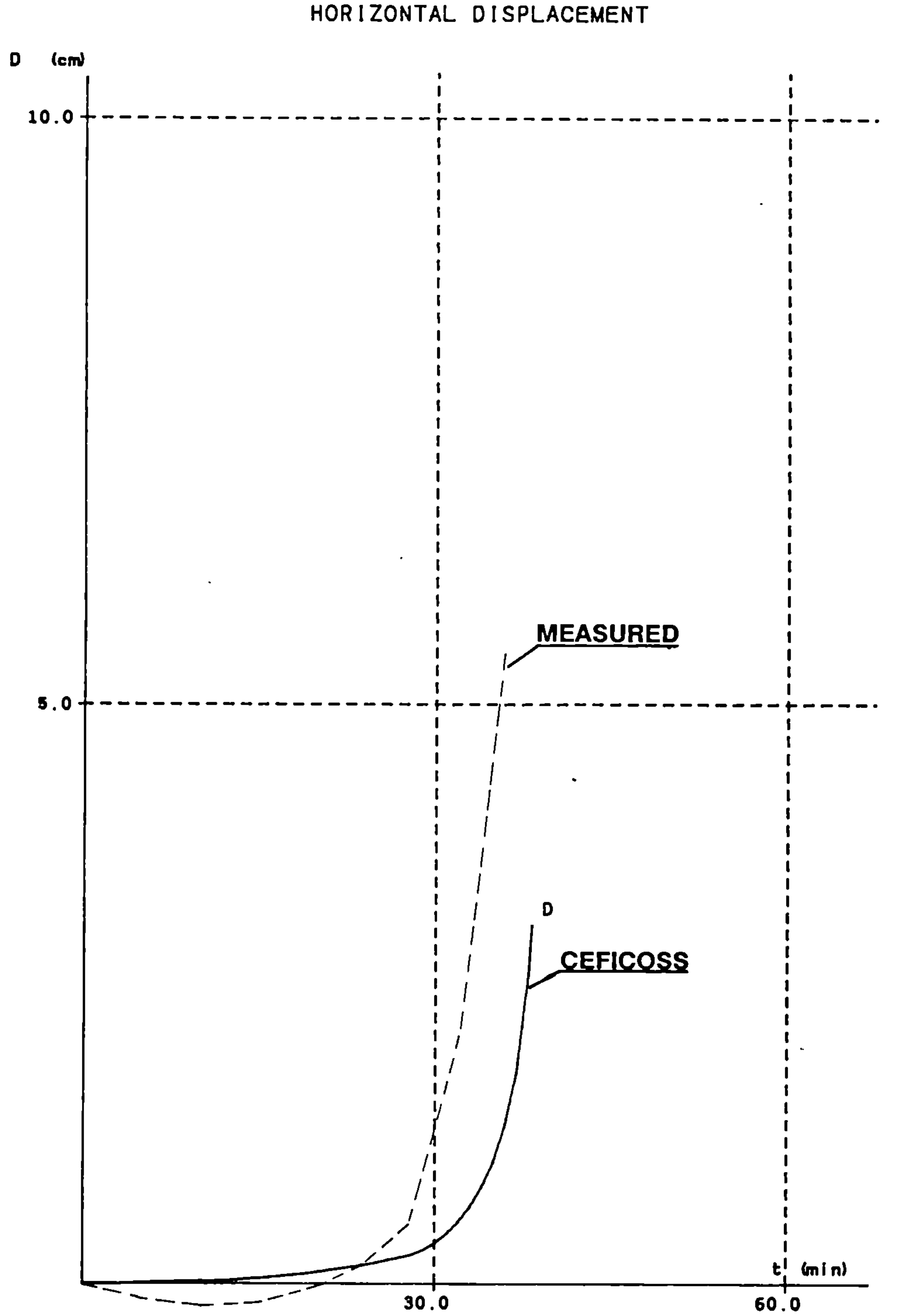

ARBED-RECHERCHES / RPS DEPARTMENT

CEFICOSS Analysis / CEF8.1

PROJECT TITLE

TEST 5

W 360X410X314 / Fe 510 / WEAK AXIS

PROJECT NUMBER

REFAO III

ESCH/ALZETTE : 28-FEB-1989

SHEET : 5.14

TEST 6

COLUMN W 360x410x314 - FeE 460

BUCKLING LENGTH 4.14 m

TEST PERFORMED IN GAND

TEST Nr 6

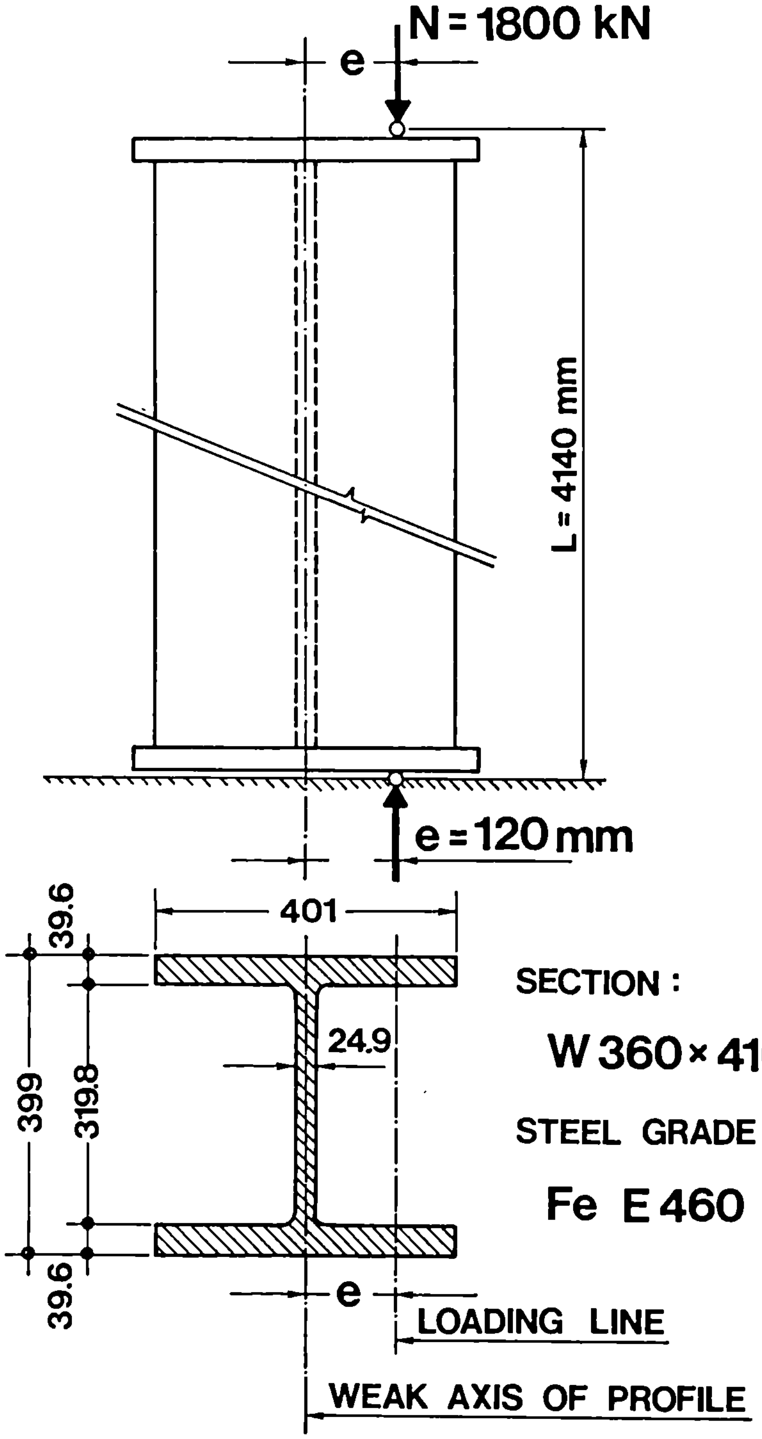

SECTION :

W 360 × 410 × 314

STEEL GRADE :

Fe E 460

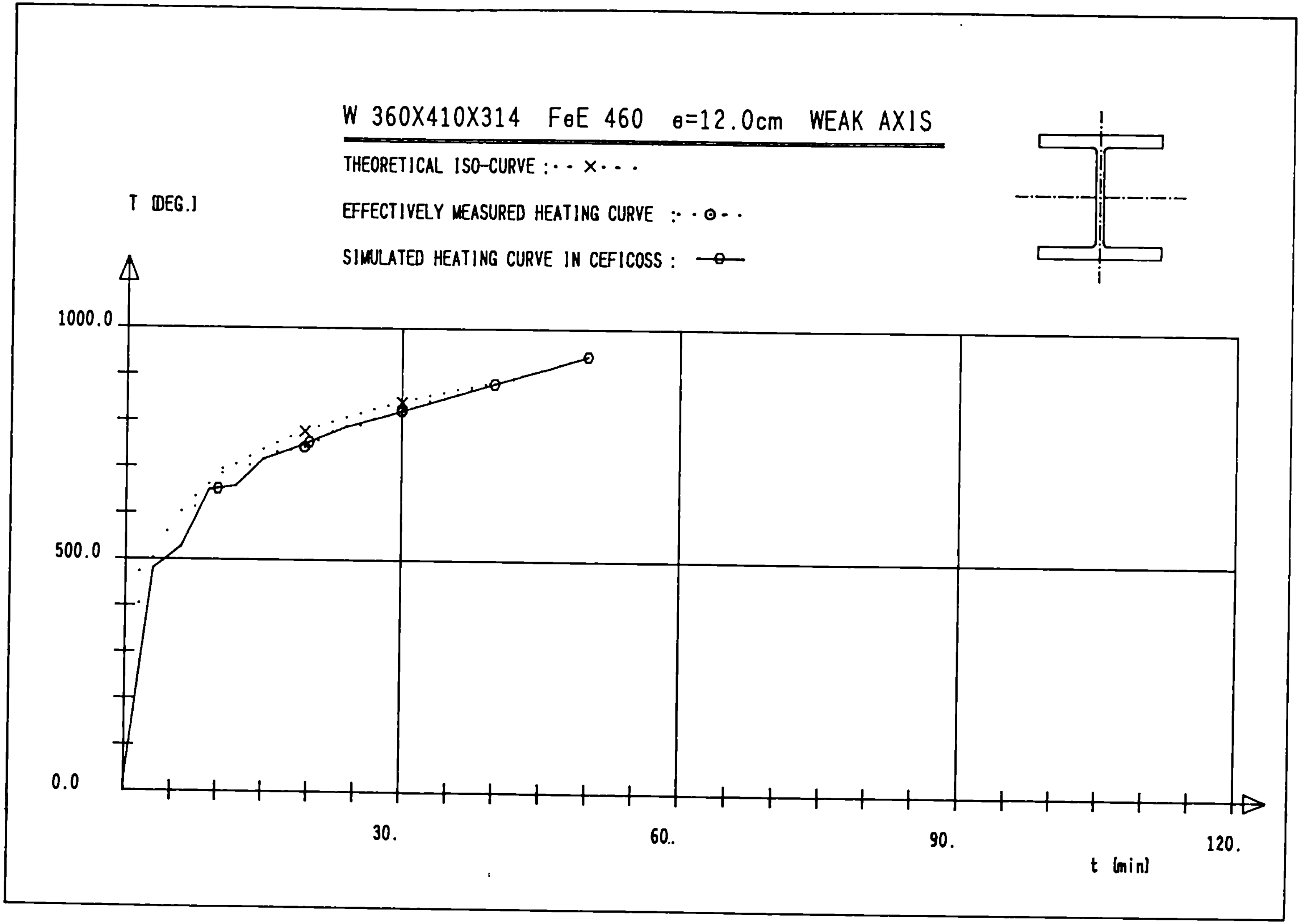

W 360X410X314 FeE 460 e=12.0cm WEAK AXIS
THEORETICAL ISO-CURVE : · · X · · ·
EFFECTIVELY MEASURED HEATING CURVE : · · ⊙ · ·
SIMULATED HEATING CURVE IN CEFICOSS : —o—
T [DEG.]
1000.0
500.0
0.0
30.
60.
90.
120.
t [min]

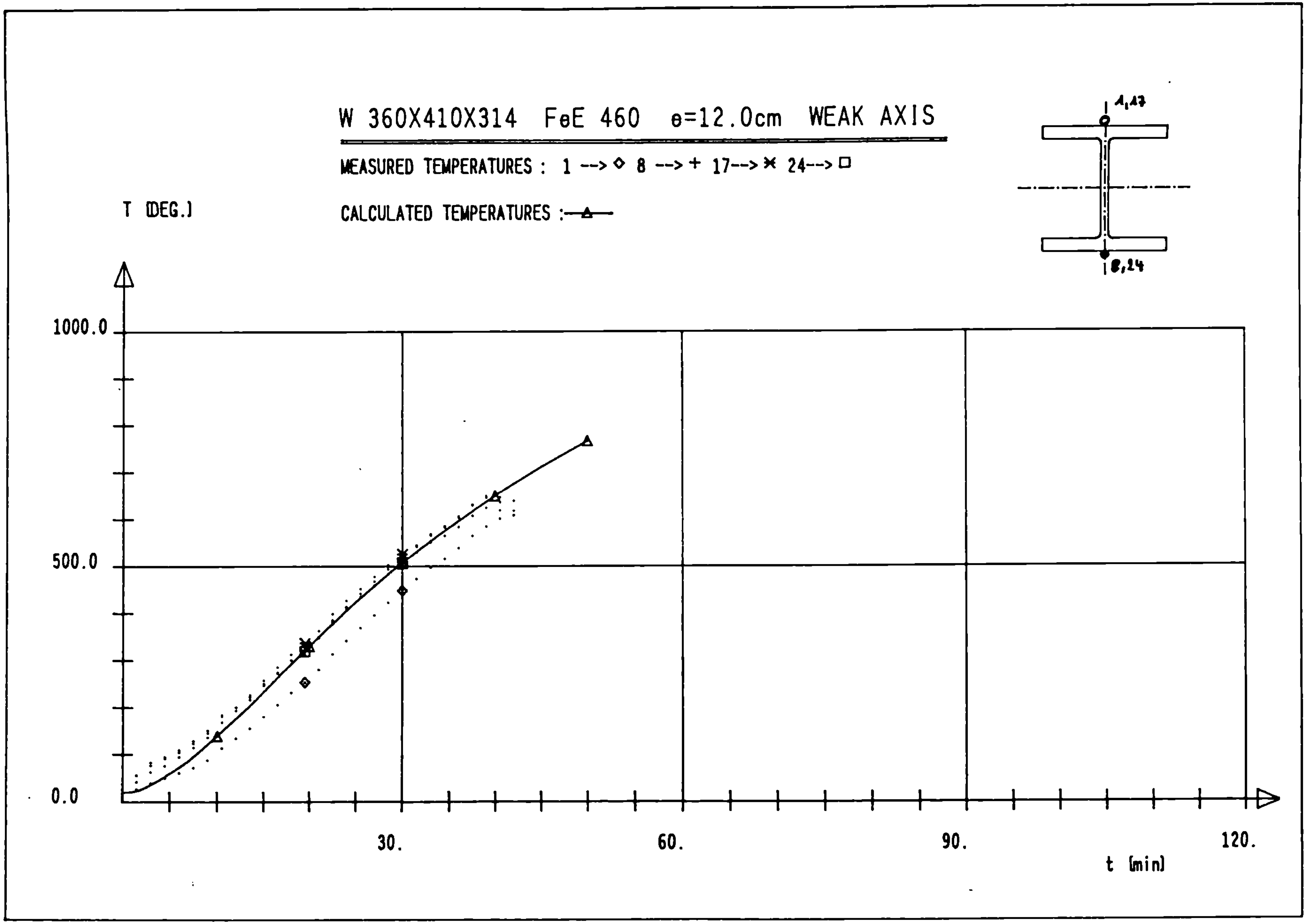
W 360X410X314 FeE 460 e=12.0cm WEAK AXIS
MEASURED TEMPERATURES : 1 --> ◇ 8 --> + 17--> ✕ 24--> □
CALCULATED TEMPERATURES :—△—
T (DEG.)
1000.0
500.0
0.0
30.
60.
90.
120.
t (min)
A,17
B,24

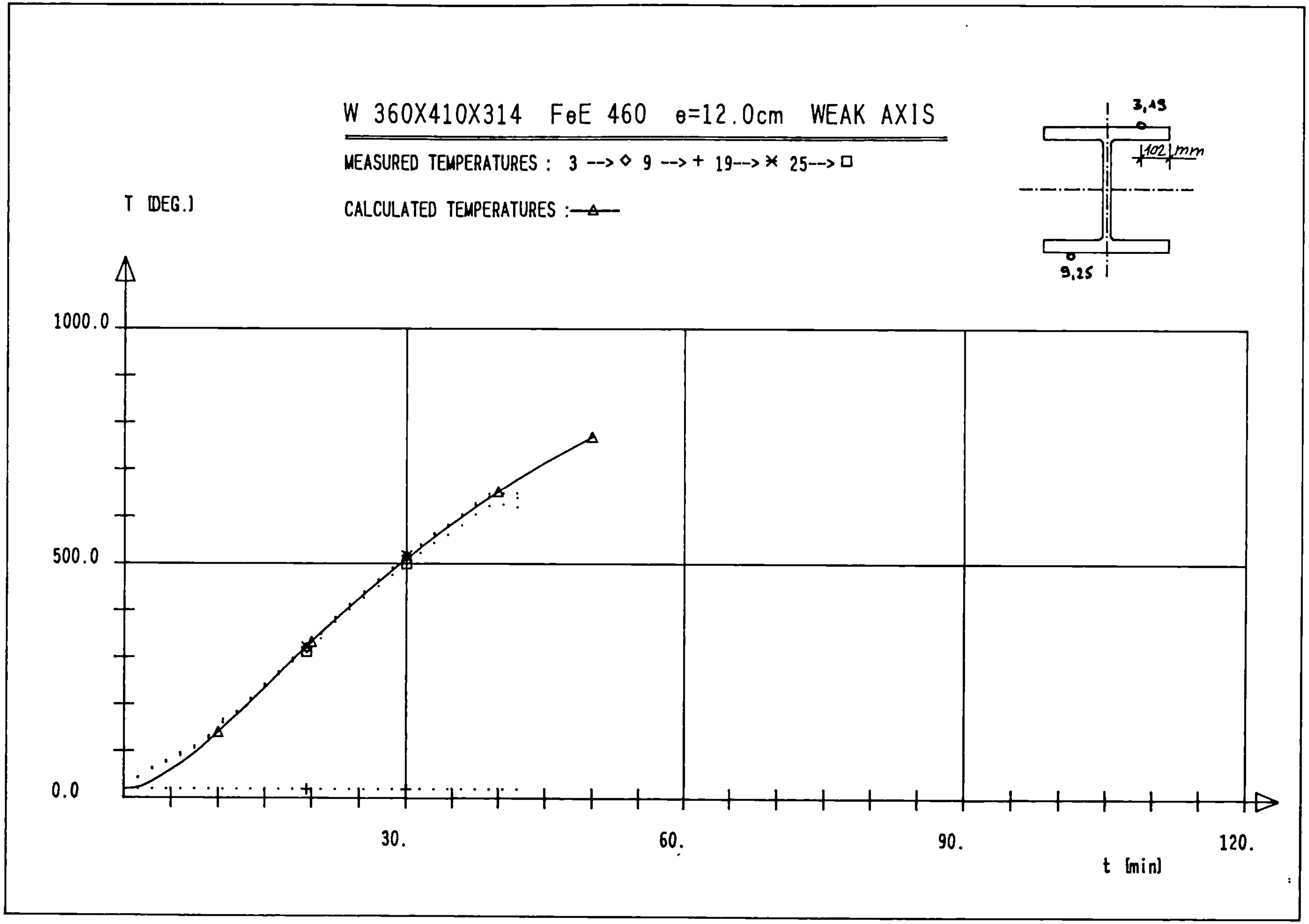
W 360X410X314 FeE 460 e=12.0cm WEAK AXIS
MEASURED TEMPERATURES : 3 --> ◇ 9 --> + 19--> ✕ 25--> □
CALCULATED TEMPERATURES :—△—
T [DEG.]
1000.0
500.0
0.0
30.
60.
90.
120.
t [min]
3,13
102 mm
9,25

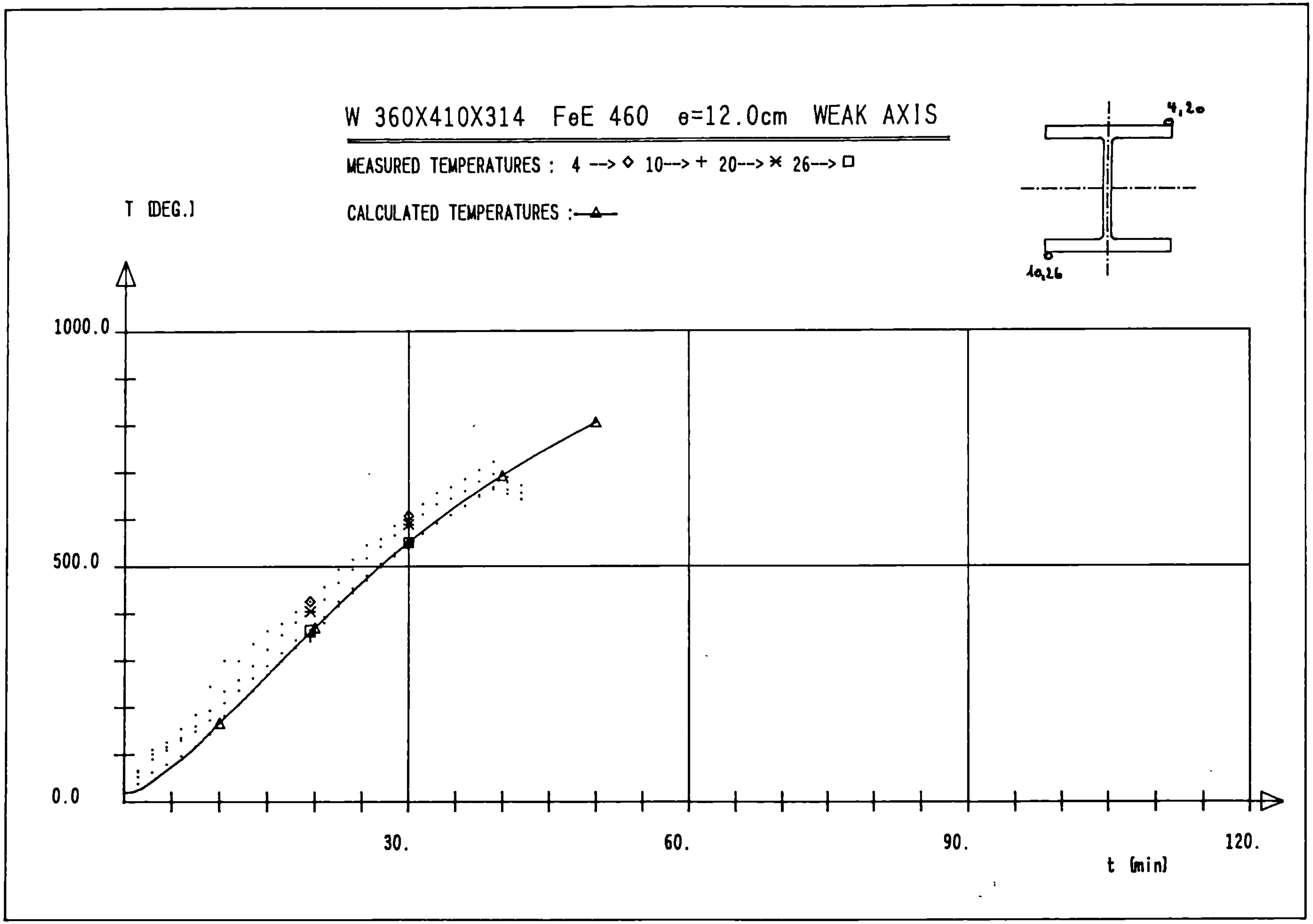
W 360X410X314 FeE 460 e=12.0cm WEAK AXIS
MEASURED TEMPERATURES : 4 --> ◇ 10--> + 20--> ✳ 26--> □
CALCULATED TEMPERATURES :—△—
T (DEG.)
1000.0
500.0
0.0
30.
60.
90.
120.
t (min)
4,20
10,26

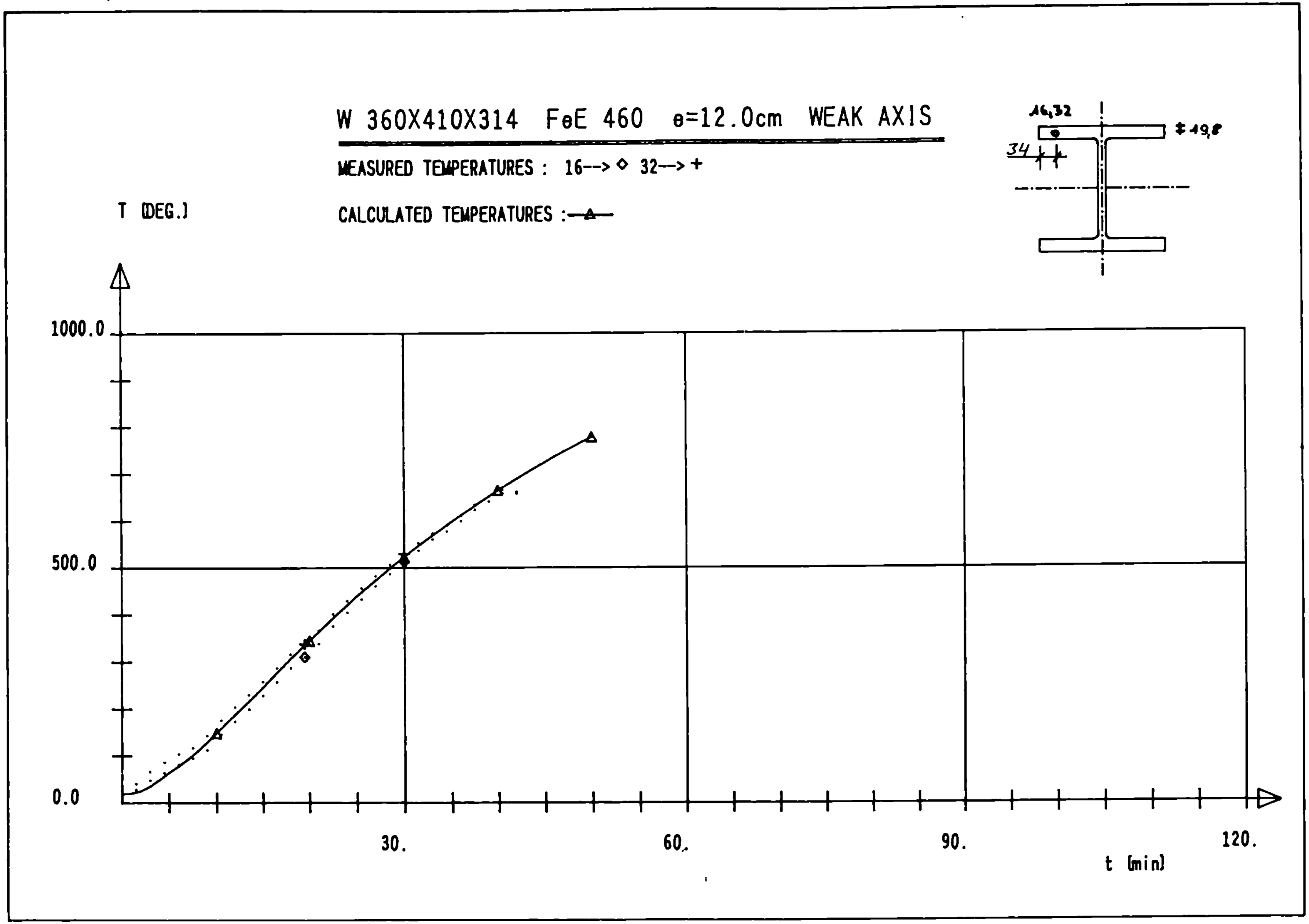
W 360X410X314 FeE 460 e=12.0cm WEAK AXIS
MEASURED TEMPERATURES : 16--> ◇ 32--> +
CALCULATED TEMPERATURES :—△—
T (DEG.)
1000.0
500.0
0.0
30.
60.
90.
120.
t (min)
16,32
19,8
34

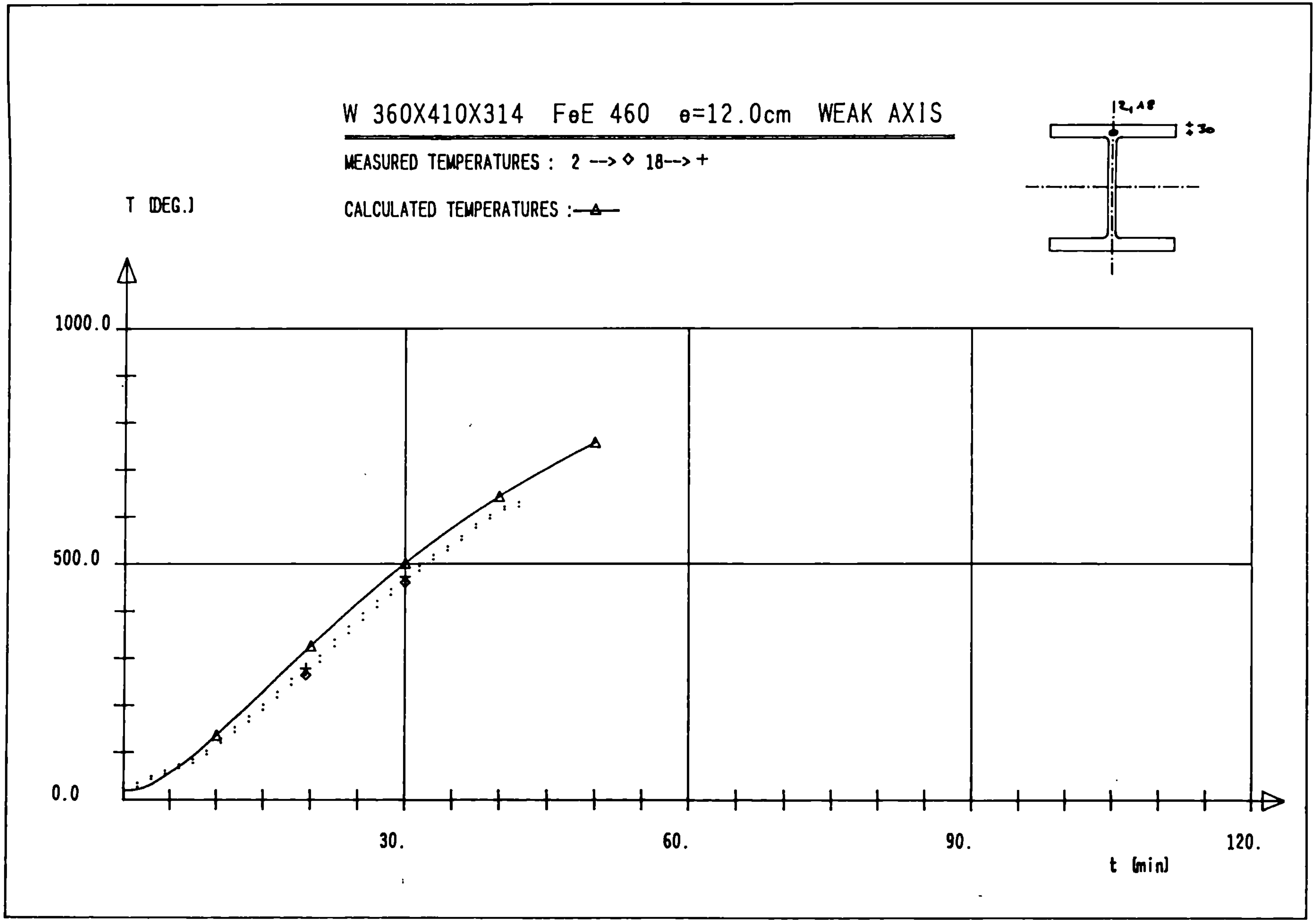
W 360X410X314 FeE 460 e=12.0cm WEAK AXIS
MEASURED TEMPERATURES : 2 --> ◇ 18--> +
CALCULATED TEMPERATURES :—△—
T (DEG.)
1000.0
500.0
0.0
30.
60.
90.
120.
t (min)

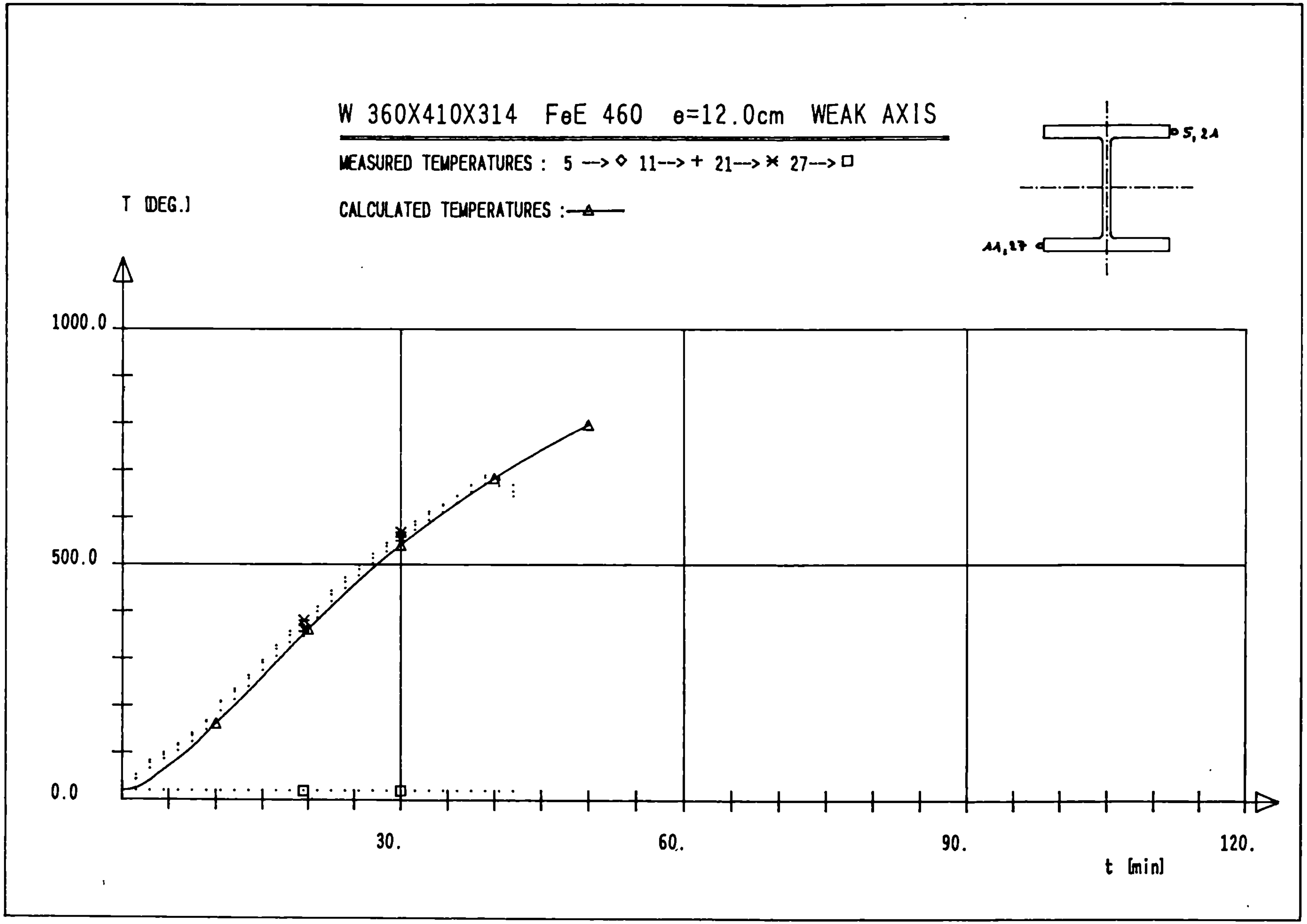
W 360X410X314 FeE 460 e=12.0cm WEAK AXIS
MEASURED TEMPERATURES : 5 --> ◇ 11--> + 21--> ✕ 27--> □
CALCULATED TEMPERATURES :—△—
T [DEG.]
1000.0
500.0
0.0
30.
60.
90.
120.
t [min]
5, 21
11, 27

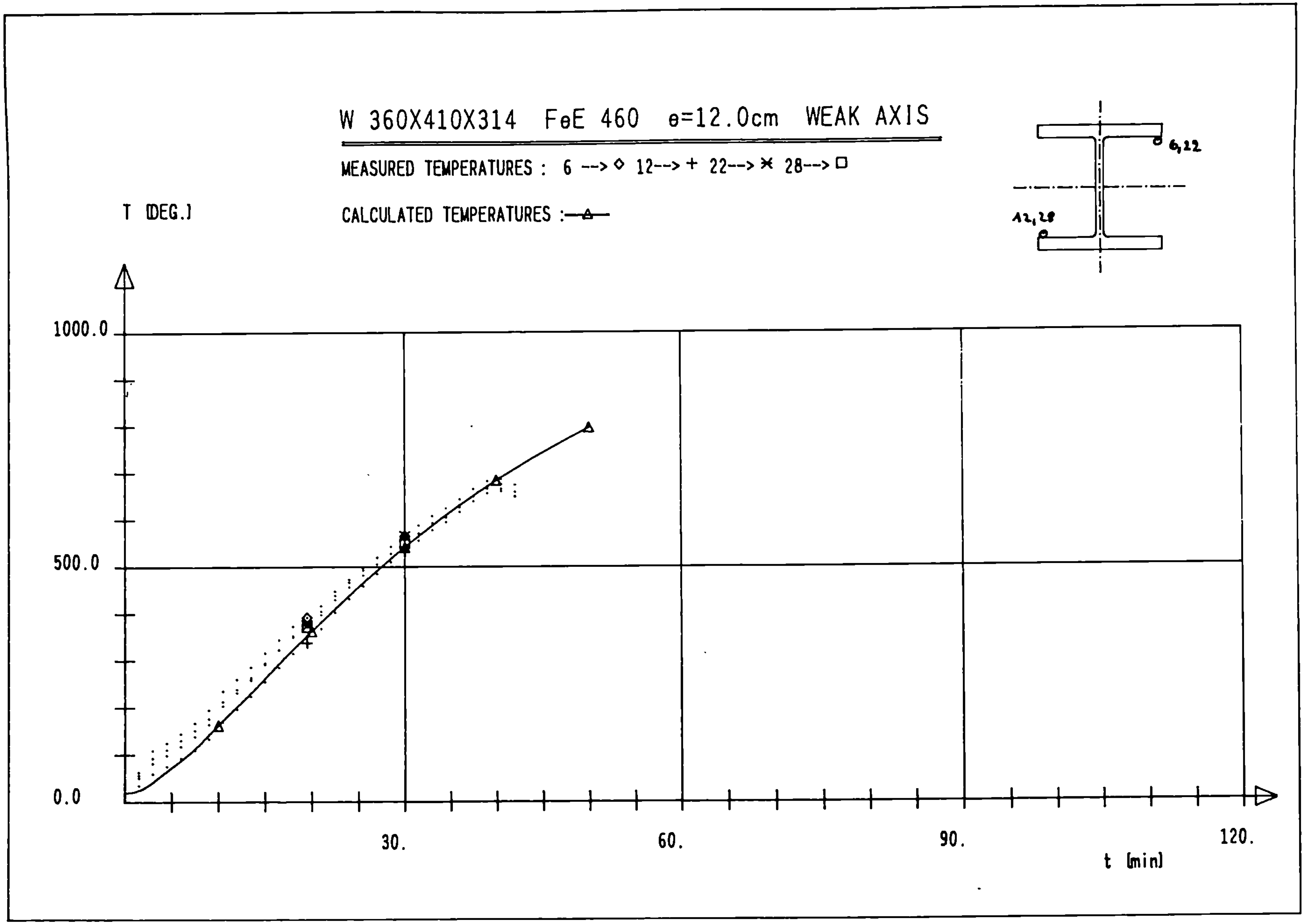
W 360X410X314 FeE 460 e=12.0cm WEAK AXIS
MEASURED TEMPERATURES : 6 --> ◇ 12--> + 22--> ✕ 28--> □
CALCULATED TEMPERATURES :—△—
T [DEG.]
6,22
12,28
1000.0
500.0
0.0
30.
60.
90.
120.
t [min]

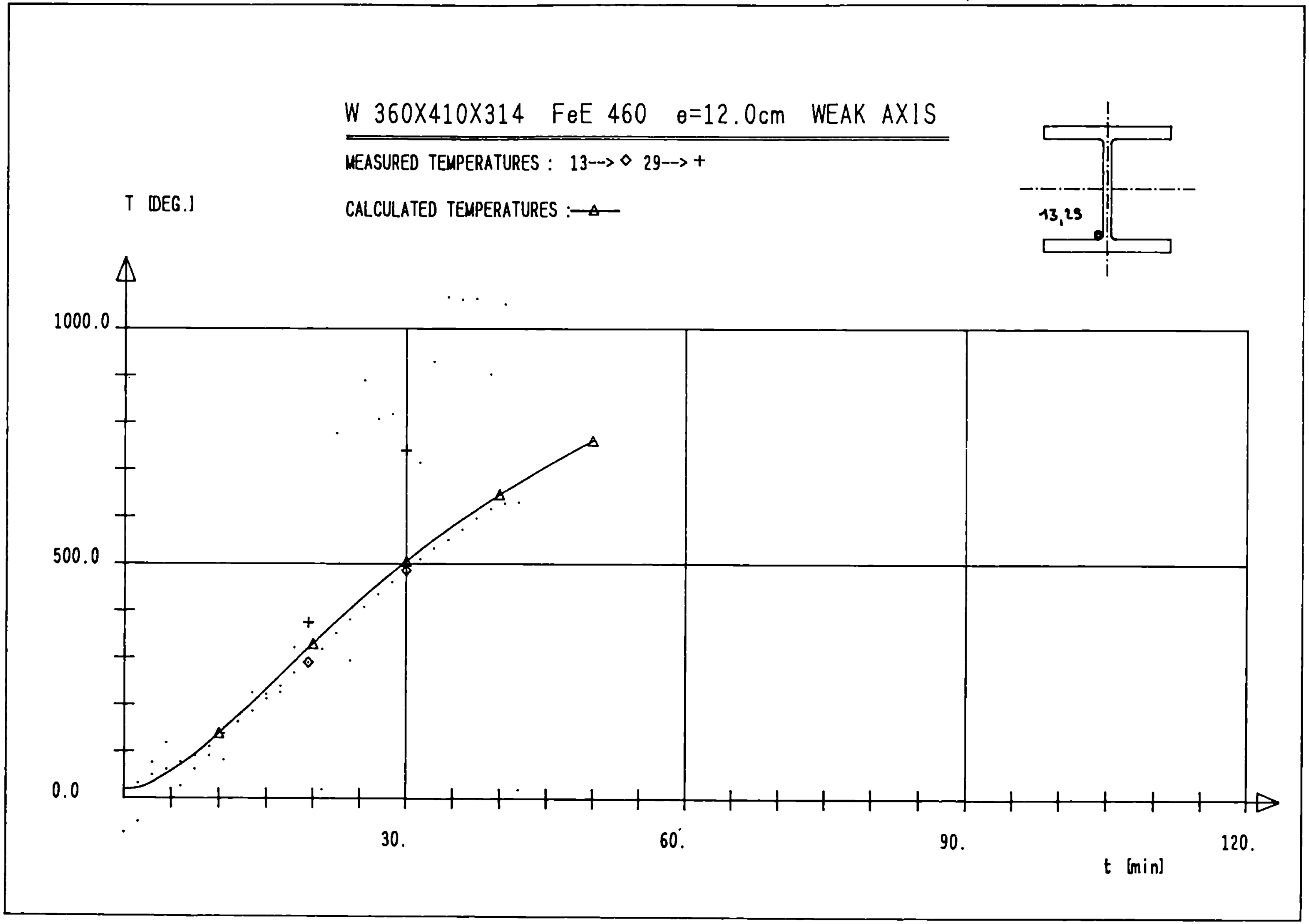
W 360X410X314 FeE 460 e=12.0cm WEAK AXIS
MEASURED TEMPERATURES : 13--> ◇ 29--> +
CALCULATED TEMPERATURES :—△—
T [DEG.]
1000.0
500.0
0.0
30.
60.
90.
120.
t [min]
13,29

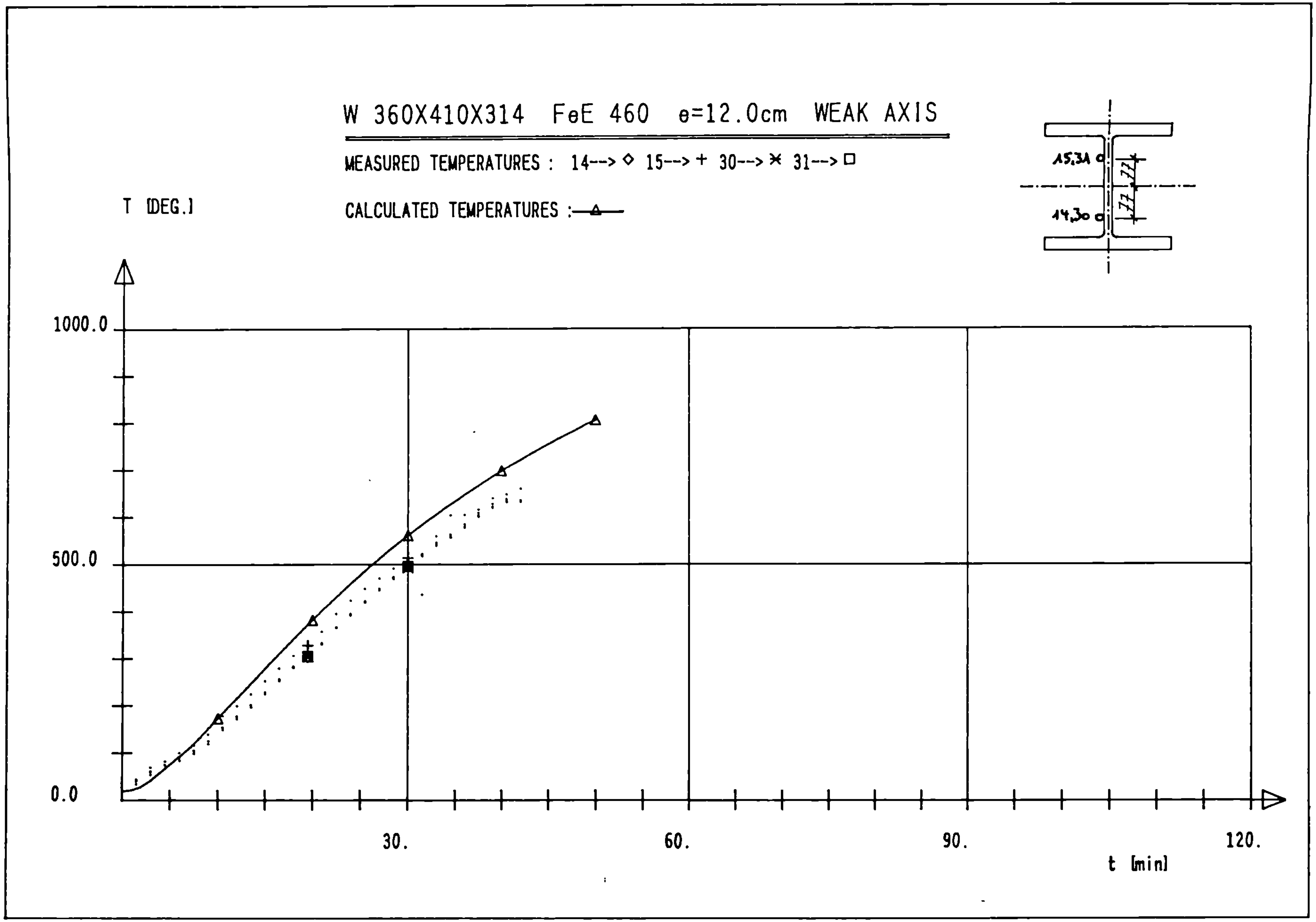
W 360X410X314 FeE 460 e=12.0cm WEAK AXIS
MEASURED TEMPERATURES : 14--> ◇ 15--> + 30--> ✕ 31--> □
CALCULATED TEMPERATURES :—△—
T [DEG.]
1000.0
500.0
0.0
30.
60.
90.
120.
t [min]
15,31
14,30
7,7
7,7

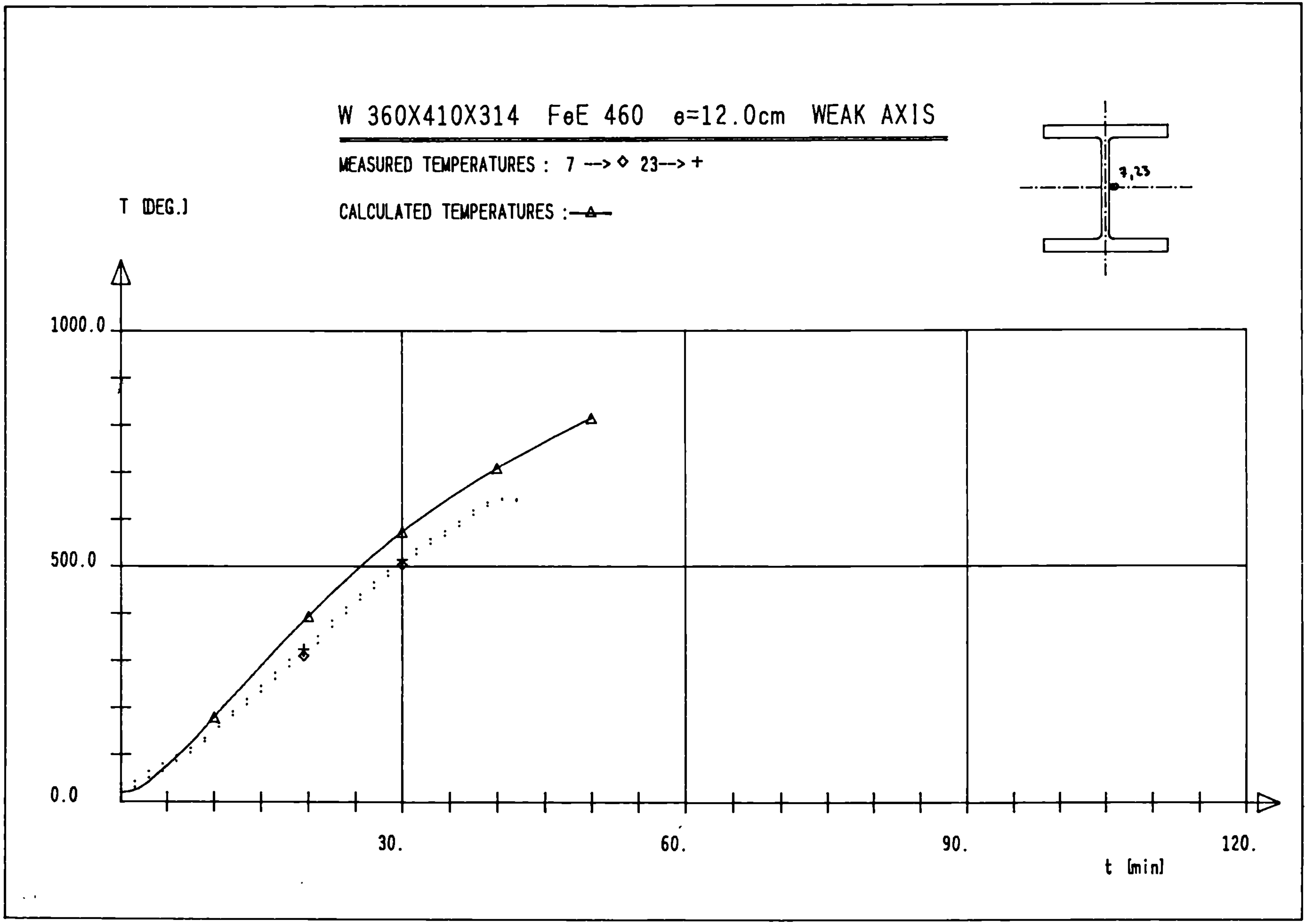

W 360X410X314 FeE 460 e=12.0cm WEAK AXIS
MEASURED TEMPERATURES : 7 --> ◇ 23--> +
CALCULATED TEMPERATURES :—△—
T [DEG.]
1000.0
500.0
0.0
30.
60.
90.
120.
t [min]
7,23

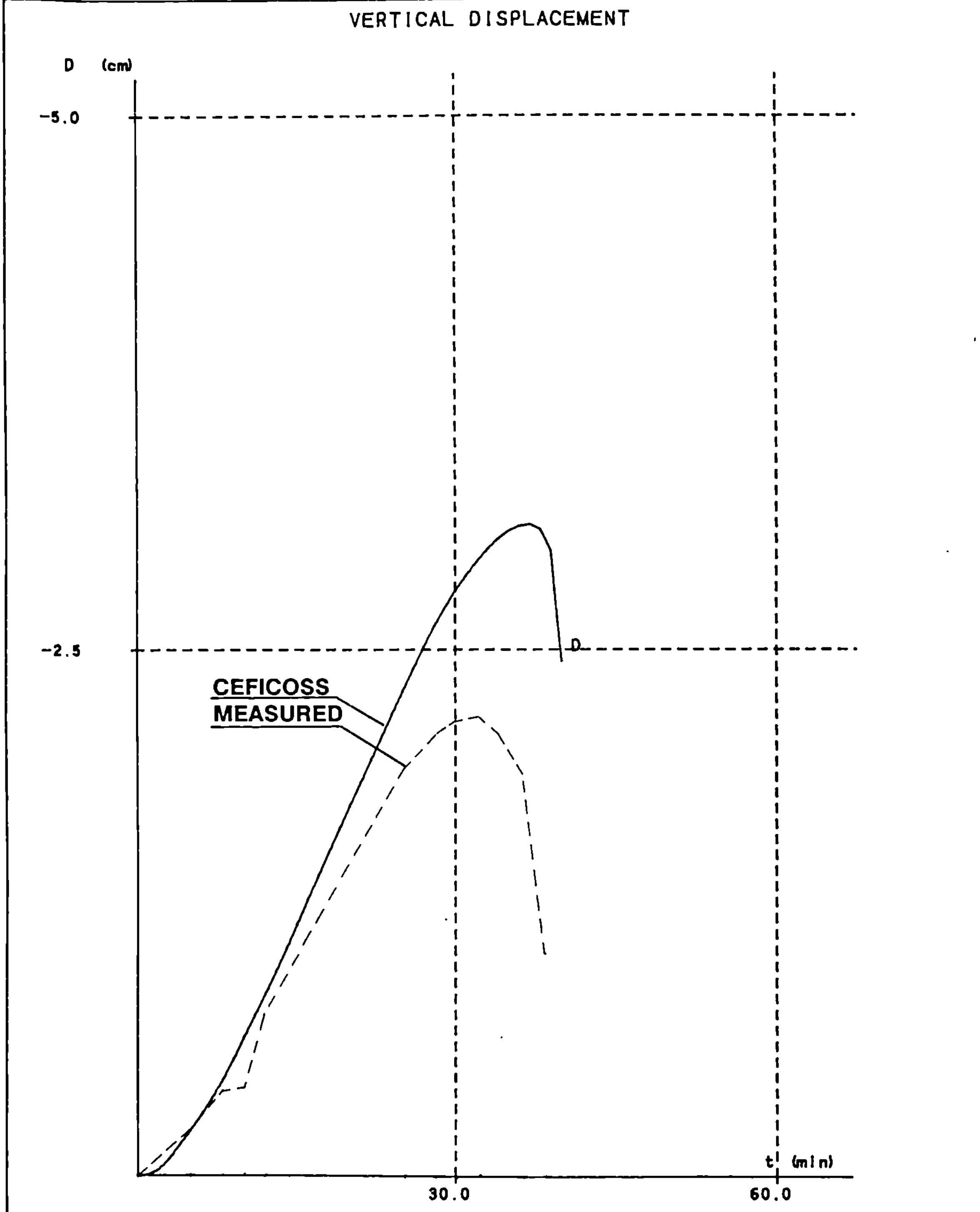

ARBED-RECHERCHES / RPS DEPARTMENT	CEFICOSS Analysis / CEF8.1
PROJECT TITLE TEST 6 W 360X410X314 / FeE 460 / WEAK AXIS	PROJECT NUMBER REFAO III ESCH/ALZETTE : 28-FEB-1989 — SHEET : 6.13

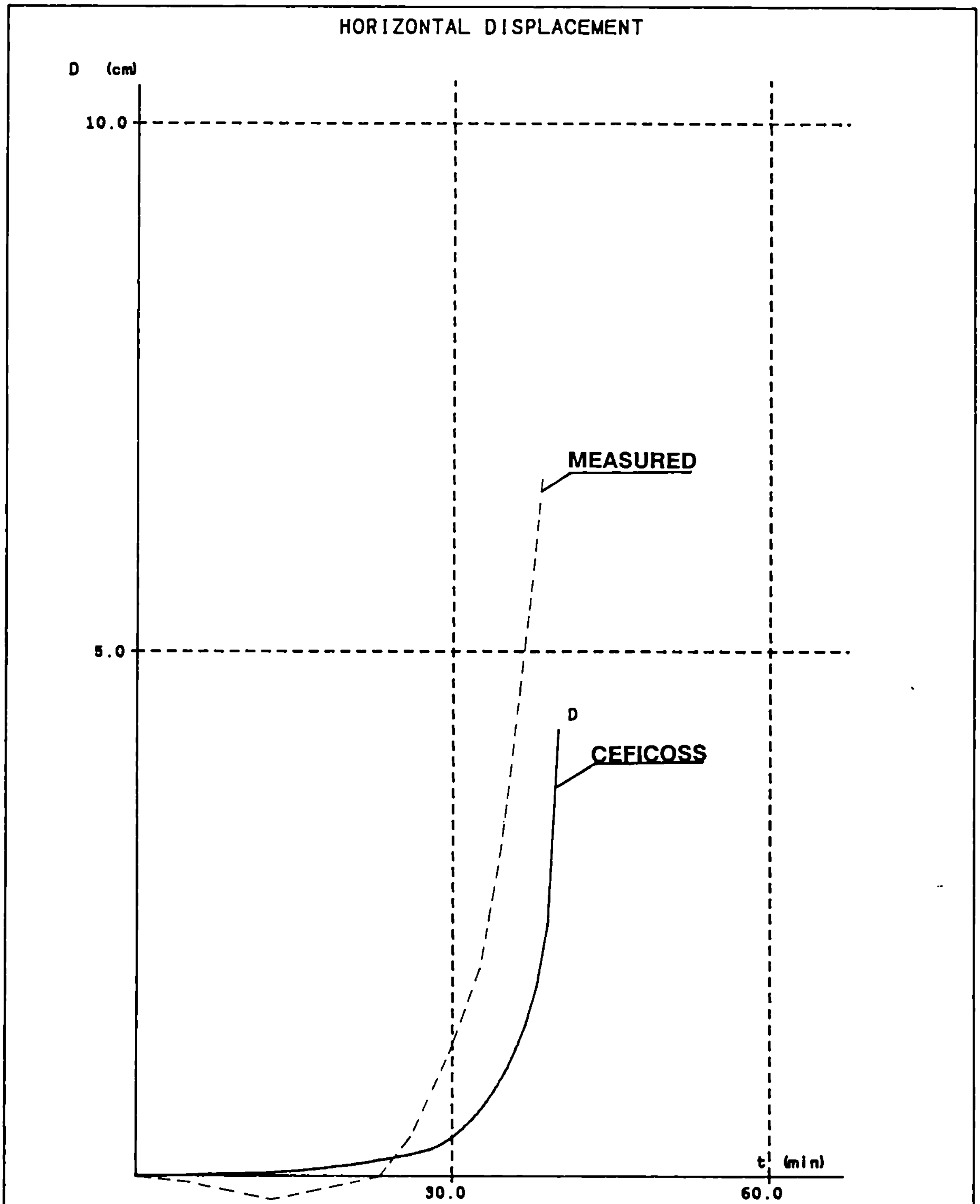

ARBED-RECHERCHES / RPS DEPARTMENT	CEFICOSS Analysis / CEF8.1
PROJECT TITLE	PROJECT NUMBER
TEST 6	REFAO III
W 360X410X314 / FeE 460 / WEAK AXIS	ESCH/ALZETTE : 28-FEB-1989 SHEET : 6.14

European Communities – Commission

EUR 14348 – Practical design tools for unprotected steel columns submitted to ISO-Fire — Refao III

Luxembourg: Office for Official Publications of the European Communities

1993 – XV, 316 pp., num. tab., fig. – 21.0 x 29.7 cm

Technical steel research series

ISBN 92-826-4938-5

Price (excluding VAT) in Luxembourg: ECU 33

The main parameters to be considered in this research programme, i.e. the geometrical factors (shapes, buckling lengths), steel qualities and coefficients governing the heat exchanges, are presented first.

The temperature-dependent stress-strain relationships of steel as initially existing in the programme Ceficoss have been tested by a simulation of bending tests as described in the literature. It has shown the necessity of improving these laws when pure steel elements have to be calculated.

New improved stress-strain relationships of steel have been carried out and calibrated thanks to transient-state beam tests performed on small, simply supported, steel beams, subjected to a concentrated constant load, and submitted to a controlled temperature increase. These new laws have been established as well for commonly used construction steels and for high-strength steel FeE 460.

The validity of these improved relationships has next been verified by efficiently simulating six full-scale fire tests performed on unprotected steel columns in the laboratories of Braunschweig and Ghent.

The possibility of taking into account a distribution of residual stresses has been introduced in Ceficoss. The simulation of the six column tests showed that residual stresses have quite a small influence on the fire-resistance time of columns. It has been decided, however, to consider systematically a distribution of residual stresses in the calculations.

Practical design tools have finally been implemented and are proposed here in the form of tables as well as diagrams.

Venta y suscripciones • Salg og abonnement • Verkauf und Abonnement • Πωλήσεις και συνδρομές
Sales and subscriptions • Vente et abonnements • Vendita e abbonamenti
Verkoop en abonnementen • Venda e assinaturas

BELGIQUE / BELGIË

Moniteur belge / Belgisch Staatsblad
Rue de Louvain 42 / Leuvenseweg 42
B-1000 Bruxelles / B-1000 Brussel
Tél. (02) 512 00 26
Fax (02) 511 01 84

Autres distributeurs / Overige verkooppunten

Librairie européenne/ Europese boekhandel
Rue de la Loi 244/Wetstraat 244
B-1040 Bruxelles / B-1040 Brussel
Tél. (02) 231 04 35
Fax (02) 735 08 60

Jean De Lannoy
Avenue du Roi 202 /Koningslaan 202
B-1060 Bruxelles / B-1060 Brussel
Tél. (02) 538 51 69
Télex 63220 UNBOOK B
Fax (02) 538 08 41

Document delivery:

Credoc
Rue de la Montagne 34 / Bergstraat 34
Bte 11 / Bus 11
B-1000 Bruxelles / B-1000 Brussel
Tél. (02) 511 69 41
Fax (02) 513 31 95

DANMARK

J. H. Schultz Information A/S
Herstedvang 10-12
DK-2620 Albertslund
Tlf. (45) 43 63 23 00
Fax (Sales) (45) 43 63 19 69
Fax (Management) (45) 43 63 19 49

DEUTSCHLAND

Bundesanzeiger Verlag
Breite Straße
Postfach 10 80 06
D-W-5000 Köln 1
Tel. (02 21) 20 29-0
Telex ANZEIGER BONN 8 882 595
Fax 2 02 92 78

GREECE/ΕΛΛΑΔΑ

G.C. Eleftheroudakis SA
International Bookstore
Nikis Street 4
GR-10563 Athens
Tel. (01) 322 63 23
Telex 219410 ELEF
Fax 323 98 21

ESPAÑA

Boletín Oficial del Estado
Trafalgar, 29
E-28071 Madrid
Tel. (91) 538 22 95
Fax (91) 538 23 49

Mundi-Prensa Libros, SA
Castelló, 37
E-28001 Madrid
Tel. (91) 431 33 99 (Libros)
431 32 22 (Suscripciones)
435 36 37 (Dirección)
Télex 49370-MPLI-E
Fax (91) 575 39 98

Sucursal:

Librería Internacional AEDOS
Consejo de Ciento, 391
E-08009 Barcelona
Tel. (93) 488 34 92
Fax (93) 487 76 59

Llibreria de la Generalitat de Catalunya
Rambla dels Estudis, 118 (Palau Moja)
E-08002 Barcelona
Tel. (93) 302 68 35
302 64 62
Fax (93) 302 12 99

FRANCE

**Journal officiel
Service des publications des Communautés européennes**
26, rue Desaix
F-75727 Paris Cedex 15
Tél. (1) 40 58 75 00
Fax (1) 40 58 77 00

IRELAND

Government Supplies Agency
4-5 Harcourt Road
Dublin 2
Tel. (1) 61 31 11
Fax (1) 78 06 45

ITALIA

Licosa SpA
Via Duca di Calabria, 1/1
Casella postale 552
I-50125 Firenze
Tel. (055) 64 54 15
Fax 64 12 57
Telex 570466 LICOSA I

GRAND-DUCHÉ DE LUXEMBOURG

Messageries Paul Kraus
11, rue Christophe Plantin
L-2339 Luxembourg
Tél. 499 88 88
Télex 2515
Fax 499 88 84 44

NEDERLAND

SDU Overheidsinformatie
Externe Fondsen
Postbus 20014
2500 EA 's-Gravenhage
Tel. (070) 37 89 911
Fax (070) 34 75 778

PORTUGAL

Imprensa Nacional
Casa da Moeda, EP
Rua D. Francisco Manuel de Melo, 5
P-1092 Lisboa Codex
Tel. (01) 69 34 14

Distribuidora de Livros Bertrand, Ld.ª

Grupo Bertrand, SA
Rua das Terras dos Vales, 4-A
Apartado 37
P-2700 Amadora Codex
Tel. (01) 49 59 050
Telex 15798 BERDIS
Fax 49 60 255

UNITED KINGDOM

HMSO Books (Agency section)
HMSO Publications Centre
51 Nine Elms Lane
London SW8 5DR
Tel. (071) 873 9090
Fax 873 8463
Telex 29 71 138

ÖSTERREICH

Manz'sche Verlags- und Universitätsbuchhandlung
Kohlmarkt 16
A-1014 Wien
Tel. (0222) 531 61-0
Telex 112 500 BOX A
Fax (0222) 531 61-39

SUOMI

Akateeminen Kirjakauppa
Keskuskatu 1
PO Box 128
SF-00101 Helsinki
Tel. (0) 121 41
Fax (0) 121 44 41

NORGE

Narvesen information center
Bertrand Narvesens vei 2
PO Box 6125 Etterstad
N-0602 Oslo 6
Tel. (2) 57 33 00
Telex 79668 NIC N
Fax (2) 68 19 01

SVERIGE

BTJ
Tryck Traktorwägen 13
S-222 60 Lund
Tel. (046) 18 00 00
Fax (046) 18 01 25

SCHWEIZ / SUISSE / SVIZZERA

OSEC
Stampfenbachstraße 85
CH-8035 Zürich
Tel. (01) 365 54 49
Fax (01) 365 54 11

CESKOSLOVENSKO

NIS
Havelkova 22
13000 Praha 3
Tel. (02) 235 84 46
Fax 42-2-264775

MAGYARORSZÁG

Euro-Info-Service
Pf. 1271
H-1464 Budapest
Tel./Fax (1) 111 60 61/111 62 16

POLSKA

Business Foundation
ul. Krucza 38/42
00-512 Warszawa
Tel. (22) 21 99 93, 628-28-82
International Fax&Phone
(0-39) 12-00-77

ROUMANIE

Euromedia
65, Strada Dionisie Lupu
70184 Bucuresti
Tel./Fax 0 12 96 46

BULGARIE

D.J.B.
59, bd Vitocha
1000 Sofia
Tel./Fax 2 810158

RUSSIA

CCEC (Centre for Cooperation with the European Communities)
9, Prospekt 60-let Oktyabria
117312 Moscow
Tel. 095 135 52 87
Fax 095 420 21 44

CYPRUS

Cyprus Chamber of Commerce and Industry
Chamber Building
38 Grivas Dhigenis Ave
3 Deligiorgis Street
PO Box 1455
Nicosia
Tel. (2) 449500/462312
Fax (2) 458630

TÜRKIYE

Pres Gazete Kitap Dergi Pazarlama Dağitim Ticaret ve sanayi AŞ
Narlibahçe Sokak N. 15
Istanbul-Cağaloğlu
Tel. (1) 520 92 96 - 528 55 66
Fax 520 64 57
Telex 23822 DSVO-TR

ISRAEL

ROY International
PO Box 13056
41 Mishmar Hayarden Street
Tel Aviv 61130
Tel. 3 496 108
Fax 3 544 60 39

CANADA

Renouf Publishing Co. Ltd
Mail orders — Head Office:
1294 Algoma Road
Ottawa, Ontario K1B 3W8
Tel. (613) 741 43 33
Fax (613) 741 54 39
Telex 0534783

Ottawa Store:
61 Sparks Street
Tel. (613) 238 89 85

Toronto Store:
211 Yonge Street
Tel. (416) 363 31 71

UNITED STATES OF AMERICA

UNIPUB
4611-F Assembly Drive
Lanham, MD 20706-4391
Tel. Toll Free (800) 274 4888
Fax (301) 459 0056

AUSTRALIA

Hunter Publications
58A Gipps Street
Collingwood
Victoria 3066
Tel. (3) 417 5361
Fax (3) 419 7154

JAPAN

Kinokuniya Company Ltd
17-7 Shinjuku 3-Chome
Shinjuku-ku
Tokyo 160-91
Tel. (03) 3439-0121

Journal Department
PO Box 55 Chitose
Tokyo 156
Tel. (03) 3439-0124

SINGAPORE

Legal Library Services Ltd
STK Agency
Robinson Road
PO Box 1817
Singapore 9036

AUTRES PAYS
OTHER COUNTRIES
ANDERE LÄNDER

Office des publications officielles des Communautés européennes
2, rue Mercier
L-2985 Luxembourg
Tél. 499 28 1
Télex PUBOF LU 1324 b
Fax 48 85 73/48 68 17

5 426709 41 066 26

10/92

CG-NA-14348-EN-C

NOTICE TO THE READER

All scientific and technical reports published by the Commission of the European Communities are announced in the monthly periodical **'euro abstracts'**. For subscription (1 year: ECU 118) please write to the address below.

Price (excluding VAT) in Luxembourg: ECU 33

ISBN 92-826-4938-5

OFFICE FOR OFFICIAL PUBLICATIONS
OF THE EUROPEAN COMMUNITIES

L-2985 Luxembourg

9 789282 649381